Author:
Van Veen, Branca C

Title:
Conformationally-Directed Nucleophilic Substitutions at Vinylic Carbons

Conformationally-Directed Nucleophilic Substitutions at Vinylic Carbons

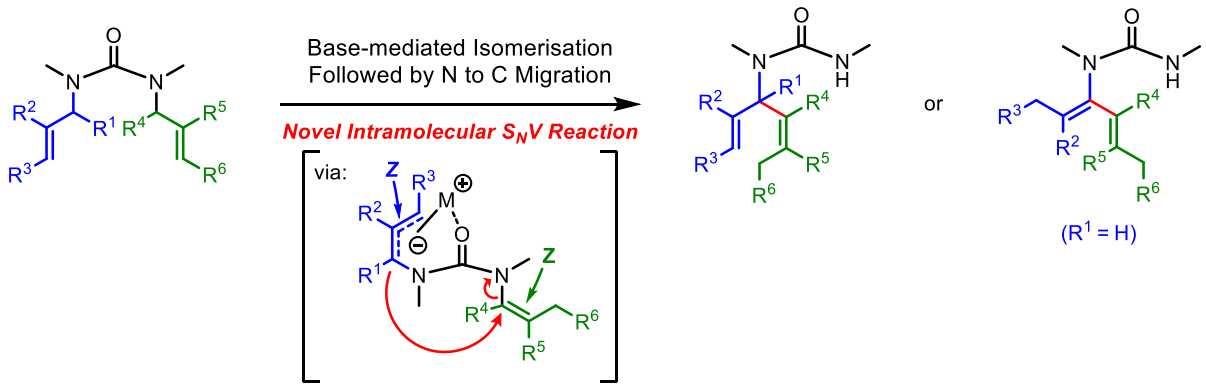

Branca C. van Veen

Supervisor: Jonathan Clayden

A dissertation submitted to the University of Bristol in accordance with the requirements for award of the degree of Doctor of Philosophy in the Faculty of Science, School of Chemistry, September 2022.

Word Count: 91767

I. Abstract

A reaction in which a nucleophile displaces a leaving group at an sp^2-hybridised vinylic carbon is recognised as a nucleophilic vinylic substitution (S_NV). Although inter- and intramolecular S_NV reactions have been the subject of some study, the use of carbon nucleophiles is rare, and all intramolecular S_NV reactions result in cyclised products. However, formation of non-cyclised products could be achieved if the incoming nucleophile is tethered to the leaving group; this approach has been pioneered by Clayden and co-workers with the N→C vinyl migration in *N*-benzyl, and amino-acid and aminonitrile derived ureas.

This thesis reports the development of a novel intramolecular S_NV reaction where a vinyl group undergoes N→C migration on treatment of *N*,*N*'-diallyl ureas with base, enabling access to a wider range of non-cyclised alkenes. Key to the success of this reaction is the conformational restriction of the urea, which brings the unsaturated coupling partners in close proximity to allow for this unusual reaction at unactivated sp^2-hybridised carbons.

A practical method was developed to access a broad range of *N*-methyl allylamines – generally volatile and have limited commercial availability – as their hydrochloride salts.[1] These enabled facile access to the starting ureas via chloroformylation and subsequent amine-coupling.

The N→C vinyl migration was optimised and then performed on a range of highly substituted symmetrical and unsymmetrical diallyl ureas. Despite the complex tandem sequence of isomerisations and substitution, the starting ureas are cleanly converted to the desired rearranged products in good yields. Interestingly, mechanistic studies confirmed that the S_NV reaction is stereospecific and complete regioselectivity is induced by incorporation of a β-substituent on one of the allyl chains, or by introduction of an *E*-vinyl chain on one side of the urea. Finally, the synthetic applicability of the rearranged products was demonstrated by transformation to an *N*-methyl alkylamine and through participation in Diels-Alder reactions.

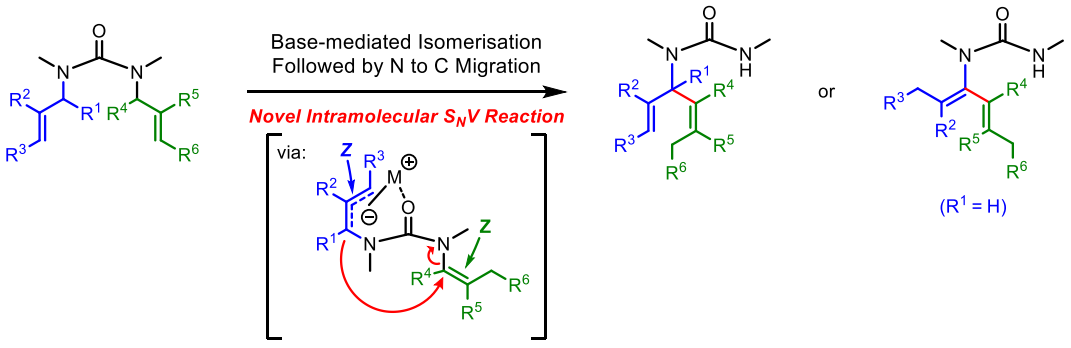

II. Contents

III. Acknowledgements

Firstly, I would like to thank Professor Jonathan Clayden for giving me the opportunity to do my PhD in his group on such an exciting, yet very challenging, project and for his advice and help throughout the years. It has been a privilege to return to his group after my Erasmus+ internship.

Secondly, thanks to the whole Clayden group, past and present members, you guys are amazing and made my time in- and outside of the lab very enjoyable. Matthew, Makenzie, Dan, Mo, Louise, Mary, Frank, Rakesh, Mark, Maria, James, Katie, JP, Rajendra, Jordan, Olivia, Matej, Helge, Ömer, Xiyue and Theo – thank you all. A special mention to: David, it was a pleasure working next to you since the start and even though you left quite soon into my PhD, I enjoyed your surprise messages on my fumehood; for now, I must say: see you later alligator… Roman, from internship supervisor to playing beach volleyball in Tarragona, you are a great chemist and person. Dabs, it was a pleasure to work and play board-games with such a clever person and chemist. Steve, my personal moving man, it has been very nice to have you there for almost my whole PhD, your chemistry knowledge is infinite and has helped my development enormously. Javier, thanks for being the fellow foreigner to spend time with while we could not go home in those crazy times. Ellie, my victim for playing board-games whether you liked it or not, I always enjoyed your company. Mehul, together Buurman and Buurman, thank you for just accepting my big queue at Bianca, listening to my stress rants, and always making me laugh – init bruv...

A big thank you to Paul Lawrence for assisting me with the mechanistic NMR experiments and to Steve, Ellie, Maria, Mehul, and Riccardo for proofreading this thesis.

Finally, a special thank you to Riccardo, my parents and my sister who have always been there for me during the PhD, by making me feel so supported and loved even with a big sea between us.

IV. Author’s Declaration

I declare that the work in this dissertation was carried out in accordance with the requirements of the University's Regulations and Code of Practice for Research Degree Programmes and that it has not been submitted for any other academic award. Except where indicated by specific reference in the text, the work is the candidate's own work. Work done in collaboration with, or with the assistance of, others, is indicated as such. Any views expressed in the dissertation are those of the author.

SIGNED: Branca Catharina van Veen DATE: 05/09/2022

V. Abbreviations and Acronyms

ADDP	1,1'-(Azodicarbonyl)dipiperidine
Aq.	Aqueous
Boc	*tert*-Butyloxycarbonyl
BRSM	Based on Recovered Starting Material
***n*-BuLi**	*n*-Butyllithium
***s*-BuLi**	*sec*-Butyllithium
COSY	Correlation Spectroscopy
d.r.	Diastereomeric Ratio
DBU	1,8-Diazabicyclo[5.4.0]undec-7-ene
DCE	1,2-Dichloroethane
DEAD	Diethyl Azodicarboxylate
DEAD-H_2	Diethyl 1,2-Hydrazinedicarboxylate
DIAD	Diisopropyl Azodicarboxylate
DIPA	Diisopropylamine
DIPEA	Diisopropylethylamine
DMF	Dimethylformamide
DMI	1,3-Dimethyl-2-imidazolidinone
DMPU	1,3-Dimethyl-3,4,5,6-tetrahydro-2(1H)-pyrimidinone
equiv.	Equivalents
ESI	Electrospray Ionisation
HMDS	Bis(trimethylsilyl)amine
HRMS	High-Resolution Mass Spectrometry
HSQC	Heteronuclear Single Quantum Correlation
IR	Infrared
KHMDS	Potassium Bis(trimethylsilyl)amide
KIE	Kinetic Isotope Effect
LDA	Lithium Diisopropylamide
LiHMDS	Lithium Bis(trimethylsilyl)amide

LG	Leaving Group
MP	Melting Point
NaHMDS	Sodium Bis(trimethylsilyl)amide
NMR	Nuclear Magnetic Resonance
NOE	Nuclear Overhauser Effect
Nu	Nucleophile
PTC	Phase-Transfer Catalyst
ppm	Parts Per Million
quant.	Quantitative
r.t.	Room Temperature
sat.	Saturated
S_NV	Nucleophilic Vinylic Substitution
t	Time
T	Temperature
TBAB	Tetrabutylammonium Bromide
TBS	*tert*-Butyldimethylsilyl
TFA	Trifluoroacetic acid
THF	Tetrahydrofuran
TLC	Thin-Layer Chromatography
TMS	Trimethylsilyl
TS	Transition State
UV	Ultraviolet
VT	Variable Temperature
wt%	Weight Percent
µW	Microwave
ZPE	Zero-Point Energy

1.0 Introduction

1.1 Nucleophilic Vinylic Substitution (S_NV)

Nucleophilic vinylic substitution (S_NV) is a reaction in which a leaving group gets displaced by a nucleophile at an sp^2-hybridised vinylic carbon. Since the late 1950s the S_NV reaction has been explored by various research groups, but has been less well-recognised than nucleophilic substitution reactions at saturated sp^3-hybridised carbons[2] and sp^2-hybridised carbons in aromatic systems (S_NAr reactions).[3,4] This is due to the fact that, for some time, the reputation of being challenging to conduct was associated with the S_NV reaction.[5,6] Unactivated or slightly activated vinyl halides were believed to lack reactivity because of the partial double-bond character between the leaving group (halide) and the alkene.[5,7] However, more recently, nucleophilic substitution at an sp^2-hybridised vinylic carbon has become apparent as a powerful method for the generation of substituted carbon-carbon double-bonds and thus has been utilised in the synthesis of various vinyl ethers, endocyclic alkenes and unsaturated carbon frameworks.

1.1.1 Mechanism

The mechanism of the S_NV reaction has been extensively studied and a wide array of mechanistic routes have been proposed, including over 30 variants described by Rappoport.[5,7] In this thesis, three key mechanisms – an addition-elimination pathway and concerted mechanisms via in-plane σ* or out-of-plane π* orbital attack – will be reviewed (Scheme 1). The addition-elimination (Ad_N-E) route is initiated by a nucleophilic attack on the sp^2-hybridised α-carbon of a vinyl halide (**1**), approaching the carbon-carbon double-bond perpendicular to its plane (out-of-plane), and involves the generation of a carbanion intermediate **2** (Scheme 1). However, in vinylic systems with good or excellent leaving groups 'LG' ($–I^+Ph$, –OTf), this perpendicular nucleophilic attack on the π* orbital of a vinylic carbon can occur via a concerted addition-elimination mechanism and is referred to as $S_NVπ$ (**3**, Scheme 1).[7] A concerted nucleophilic vinylic substitution can also take place via an in-plane attack of the nucleophile at the σ* orbital of the leaving group–carbon bond and is then designated as $S_NVσ$ (**4**, Scheme 1).[8] In contrast to $S_NVπ$ that leads to retention of stereochemistry (**6**), the in-plane attack ($S_NVσ$) results in vinylic substitution with inversion of stereochemistry (**7**).[9,10]

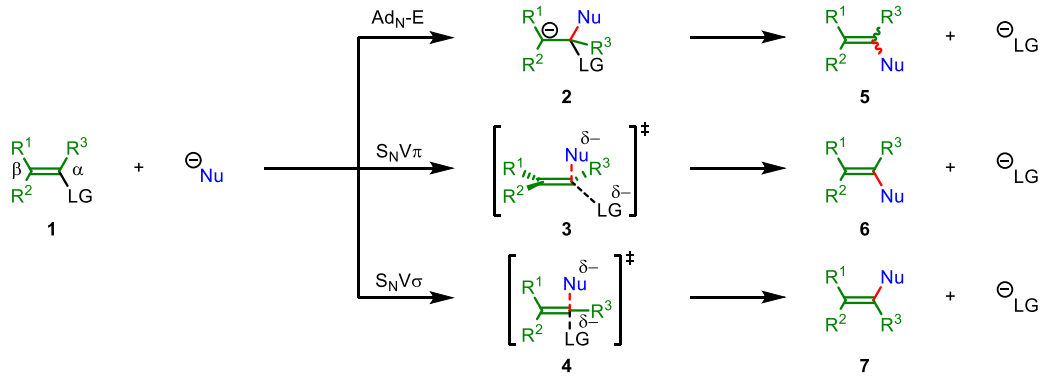

Scheme 1. Three key mechanisms of nucleophilic vinylic substitution. Blue represents the nucleophile. Green represents the electrophile. Red represents the new bonds formed.

For carbanion intermediate **2** to form in the Ad$_N$-E reaction, a poor leaving group (LG = SR, CN, OR) is required in most vinylic systems and a good leaving group (LG = Cl, Br, SO_3R, OTs) in vinylic systems that are highly activated by the presence of electron-withdrawing groups at the β-position due to their capability of delocalising a negative charge by resonance.[5,7] Finally, elimination of the leaving group results in the formation of substitution product **5** (Scheme 1). The rate-determining step is the nucleophilic attack and is facilitated by electron-withdrawing β-carbon substituents, but limited by bulky α-carbon substituents.[5,7,11] The stereochemical outcome of the Ad$_N$-E pathway can either be retention or inversion of configuration and is dependent on the intermediate carbanion's lifetime.[12,13] With a long-lived carbanion formed in a highly activated vinylic system accompanied by a poor or good leaving group, expulsion of the leaving group is slower than internal 60° and 120° rotation of the carbanion, and thus isomers **9** and **10**, both formed from **8**, will completely or partially equilibrate (Scheme 2).[14] The overall stereochemical outcome (retention versus inversion) will in this scenario be determined by the ratio of **9** and **10** at equilibrium, provided the rate of elimination is the same. In case of a shorter-lived carbanion, the internal 60° rotation of the carbanion followed by leaving group expulsion precedes the internal 120° rotation and makes the Ad$_N$-E reaction stereoretentive (Scheme 2).[7,15,16]

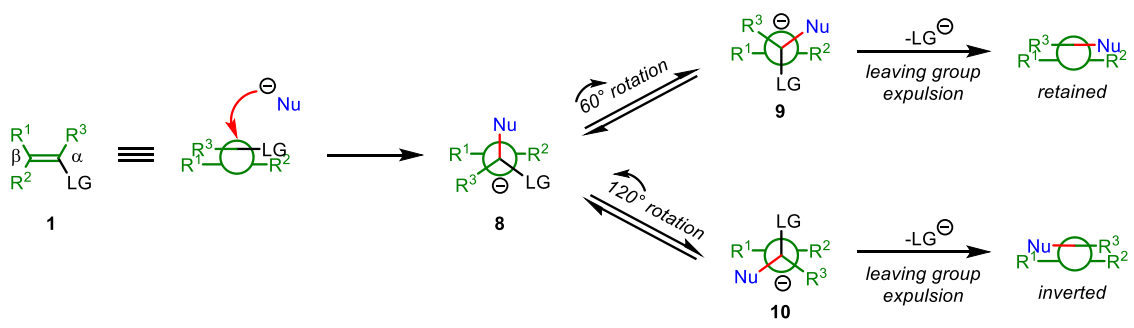

Scheme 2. Possible stereochemical outcome of the Ad$_N$-E reaction demonstrated by Newman projections.

For concerted nucleophilic vinylic substitutions it has been determined by computational studies that, for unactivated systems (CH_2=CHLG with LG as the leaving group), out-of-plane attack ($S_NV\pi$) is favoured over in-plane attack ($S_NV\sigma$) except in some cases where the leaving group is a chloride or a bromide.[9,17,18] With the unactivated system CH_2=CHCl, it was demonstrated that the $S_NV\pi$ route is energetically preferred over the $S_NV\sigma$ when strong nucleophiles such as OH^- or SH^- are used, but that the reverse is the case with weaker nucleophiles Br^- or Cl^-, with an energy difference of 7.4 and 4.8 kcal/mol, respectively, to the $S_NV\pi$ route.[19] Using the same model vinylic system (CH_2=CHCl) Lee and co-workers calculated that the transition states (TS) involved in the $S_NV\sigma$ pathway are relatively loose with a large extent of leaving group–carbon bond cleavage (55-65%) and a small degree of nucleophile–carbon bond formation (30-35%). In contrast, the TS for the $S_NV\pi$ route are quite tight with a large extent of nucleophile–carbon bond formation (55-60%) and a small extent of leaving group–carbon bond cleavage (25-40%) resulting in the partial breakage of the alkene π bond (Figure 1).[19,20] A large amount of deformation energy (ΔE_{def}), required to deform the unactivated system (CH_2=CHCl) to its TS geometry without having a significant nucleophile interaction, is associated with the loose TS involved in the $S_NV\sigma$ route and should result in a high activation barrier. However, due to the large extent of leaving group–carbon bond cleavage in the loose $S_NV\sigma$ TS the development of a considerable positive charge at the α-carbon is suggested and hypothesised to give strong electrostatic interactions with the nucleophilic anion, accordingly compensating for the high ΔE_{def}.[19]

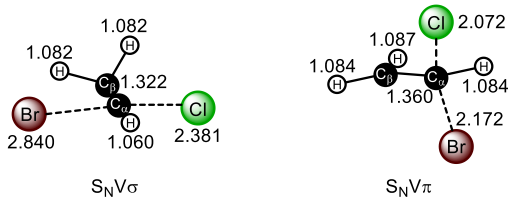

Figure 1. Transition states involved in the $S_NV\sigma$ and $S_NV\pi$ pathways for nucleophilic attack of Br^- at the unactivated vinylic system CH_2=CHCl. Bond lengths are depicted in angstroms (Å).

1.1.2 Intermolecular Substitutions

The intermolecular nucleophilic vinylic substitution is a powerful method utilised in the synthesis of various substituted vinyl ethers and aliphatic olefins, and its scope has been investigated with various nucleophiles and leaving groups. In this section, examples of the S_NV reaction that occur via an intermolecular nucleophilic attack are described and divided based on the origin of the leaving group.

1.1.2.1 With Iodanyl Leaving Groups

Intermolecular S_NV reactions of vinyl iodonium salts have been extensively studied because of the excellent functionality of an iodanyl group (i.e. $–I^+Ph$ or –IPhX) as a leaving group.[21,22] Depending on the reaction conditions and the structure of the vinyl iodonium salts, the stereochemistry of the S_NV products range from exclusive retention to complete inversion. In solution, the structure of the chloride salt of the vinyl iodonium **11** equilibrates with λ^3-chloroiodanes **12** and **13**, and at higher chloride concentrations with dichloroiodate **14**, with a decrease of reactivity going from free iodonium compound **11** to the associated iodonium compounds **12**, **13** and **14** (Scheme 3).[23]

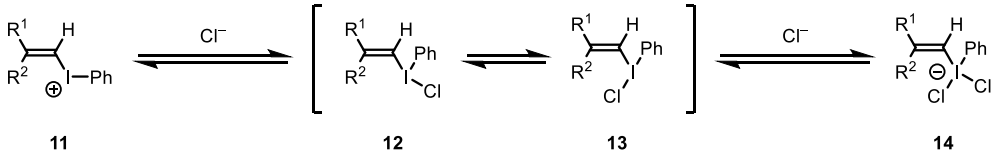

Scheme 3. The structure of the chloride salt of vinyl iodonium 11 equilibrates in solution with λ^3-chloroiodanes 12 and 13, and at higher chloride concentrations with dichloroiodate 14.

Ochiai *et al.* reported that complete inversion of configuration was observed in the case of the intermolecular substitution of (*E*)-1-alkenyl(phenyl)iodonium tetrafluoroborates (**(*E*)-15**) with tetrabutylammonium halides (**16**) via an in-plane $S_NV\sigma$ route (Scheme 4A).[23–26] However, when the halide was fluoride the reaction only yielded 1-alkyne **18**, which with deuterium labelling experiments was determined to be a result of α-elimination (Scheme 4B).[25] (*Z*)-1-Haloalkenes bearing various alkyl groups (**17**) were afforded in good yields and the amount of β-elimination side-product **18** reduced with a decrease in halide concentration and decreased according to $Cl^- > Br^- > I^-$.[23,25] An increase in the amount of β-elimination side-product **18** was observed with bulkier R substituents, following the order R = *i*-Pr > *n*-C_8H_{17} > Me (Scheme 4C). The S_NV reaction of (*Z*)-1-alkenyl(phenyl)iodonium tetrafluoroborates (**(*Z*)-15**) was unsuccessful and only afforded elimination product **18** due to the antiperiplanar arrangement of the β-proton and the iodobenzene leaving group leading to facile *anti*-β-elimination (Scheme 4D).[23] Interestingly, the S_NV reaction of (*Z*)-(β-benzoyloxyvinyl)phenyl-λ^3-iodanes **19** with tetrabutylammonium halides **16** effectively gave the stereoinverted (*E*)-haloalkenes **20**; no *anti*-β-elimination was observed (Scheme 4E).[27]

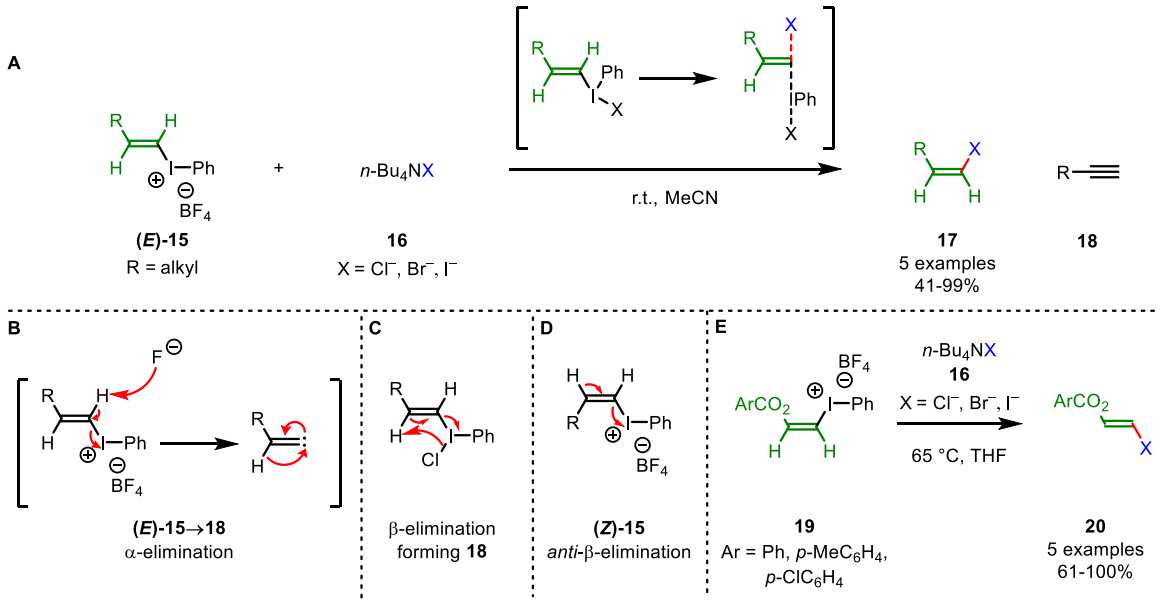

Scheme 4. Intermolecular nucleophilic vinylic substitution of (*E*)-1-alkenyl(phenyl)iodonium tetrafluoroborates (*E*)-15 and (*Z*)-(β-benzoyloxyvinyl)phenyl-λ^3-iodanes 19 with tetrabutylammonium halides 16 affording (*Z*)-1-haloalkenes 17 and (*E*)-1-haloalkenes 20 respectively with complete inversion of configuration (A & E) and their competing elimination reactions (B, C & D). Blue represents the nucleophile. Green represents the electrophile. Red represents the new bonds formed.

Besides tetrabutylammonium halides, Ochiai and co-workers demonstrated that **(*E*)-15** bearing various alkyl groups also react the same in S_NV reactions with formamides,[28] phosphoroselenoates,[29] dithiocarbamates,[30] and thioamides and thioureas.[31,32] Their attempt of reacting **(*E*)-15** with the conjugate anions of superacids e.g. TfOH, Tf_2NH, Tf_2CH_2, and Tf_3CH was unsuccessful; only ligand exchange was observed.[33] However, it was demonstrated that these superacids can be used as weak nucleophiles (**22**) in the intermolecular vinylic substitution of equivalent (*E*)-β-alkylvinyl(aryl)-λ^3-bromanes (**21**), presumably due to the greater leaving group ability of the bromanyl group in comparison to the iodanyl group (Scheme 5).[33]

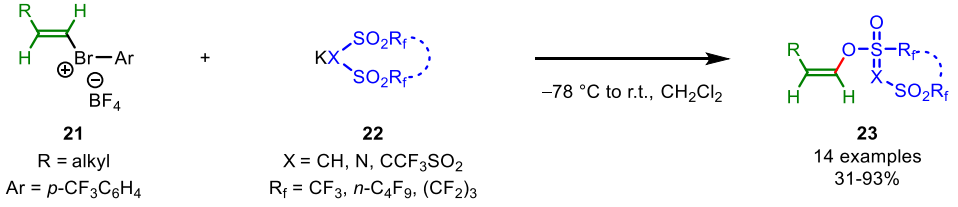

Scheme 5. Intermolecular nucleophilic vinylic substitution of (*E*)-β-alkylvinyl(aryl)-λ^3-bromanes 21 with the conjugate anions of superacids 22 affording (*Z*)-alkenes 23 with complete inversion of configuration. Blue represents the nucleophile. Green represents the electrophile. Red represents the new bonds formed.

In contrast to the stereoinverting S_NV reaction of **(*E*)-15** (Scheme 4A), exclusive retention of configuration was obtained in the S_NV reaction of (*Z*)-(β-phenylsulfonyl)alkenyl)iodanes (**24**) with tetrabutylammonium halides (**16**) and sodium benzenesulfinate (Scheme 6).[34,35] Alkenes **25** exhibiting *Z*-geometry were afforded in high yields. Mechanistically, it was proposed that the Ad_N-E mechanism was operative, in which the β-phenylsulfonyl group facilitates perpendicular attack (Michael-type addition) of the nucleophile to the carbon-carbon double-bond resulting in an α-sulfonyl-stabilised carbanion intermediate (**TS-24a**). Then, internal 60° rotation (**TS-24a**→ **TS-24b**) – which is favoured over internal 120° rotation due to the avoidance of unfavourable eclipsing interactions (between non-hydrogen substituents) – and elimination yield the substituted alkenes **25**.

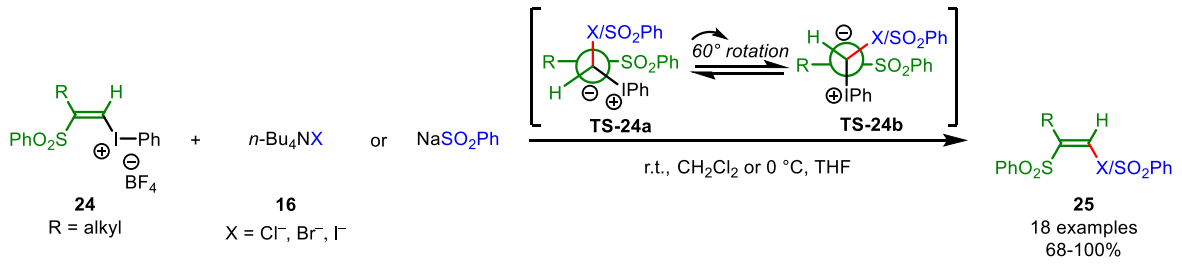

Scheme 6. Intermolecular nucleophilic vinylic substitution of (*Z*)-(β-phenylsulfonyl)alkenyl)iodanes 24 with tetrabutylammonium halides 16 or sodium benzenesulfinate to afford alkenes 25 with exclusive retention of configuration. Blue represents the nucleophile. Green represents the electrophile. Red represents the new bonds formed.

1.1.2.2 With Chloro and Chloranyl Leaving Groups

The intermolecular S_NV method was also effectively applied to chlorinated alkenes. For example, by reaction of various 3-chloro-benzofuran-2-carbonyl derivatives (**26**) with aryl thiols (**27**) in the presence of triethylamine, a range of 3-sulfenylated benzo[b]furans (**28**) could be easily synthesised in high yields (Scheme 7).[36]

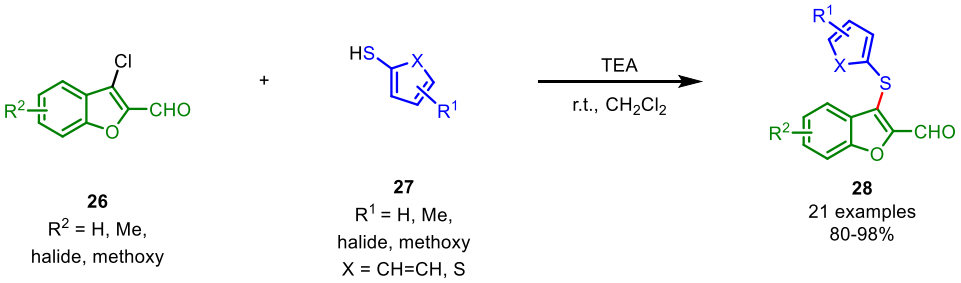

Scheme 7. Intermolecular nucleophilic vinylic substitution of various 3-chloro-benzofuran-2-carbonyl derivatives 26 with aryl thiols 27 to synthesise a range of 3-sulfenylated benzo[b]furans 28 in high yields. Blue represents the nucleophile. Green represents the electrophile. Red represents the new bonds formed.

More interestingly, enantioselective intermolecular S_NV reactions were reported for the functionalisation of 1,3-dicarbonyl compounds and 3-substituted oxindoles by reaction of β-chloroalkene ketones, thereby forming vinyl substituted quaternary carbon stereocentres.[37,38]

With the use of potassium fluoride and a chiral amino-acid derived quaternary ammonium salt (**31**) as a chiral phase-transfer catalyst (PTC), various (hetero)aromatic β-chloropropenones (**29**) were reacted with a range of 3-alkyl and 3-aryl substituted oxindoles (**30**) (Scheme 8A).[38] This successfully led to the formation of oxindole derivatives bearing a quaternary centre (**32**) in high yields with enantioselectivities of 59–91% *ee* and nearly complete stereospecificity with respect to the *Z*-geometry of the double-bond (Scheme 8A). When a PTC without a quaternary ammonium centre or with a blocked amide NH was used, a drop in enantioselectivity to 3% and 2% *ee* was observed, suggesting that the asymmetric induction relies on a quaternary ammonium centre and hydrogen-bonding interactions illustrated by transition state structure **33**, based on an X-ray crystal structure (Scheme 8B).

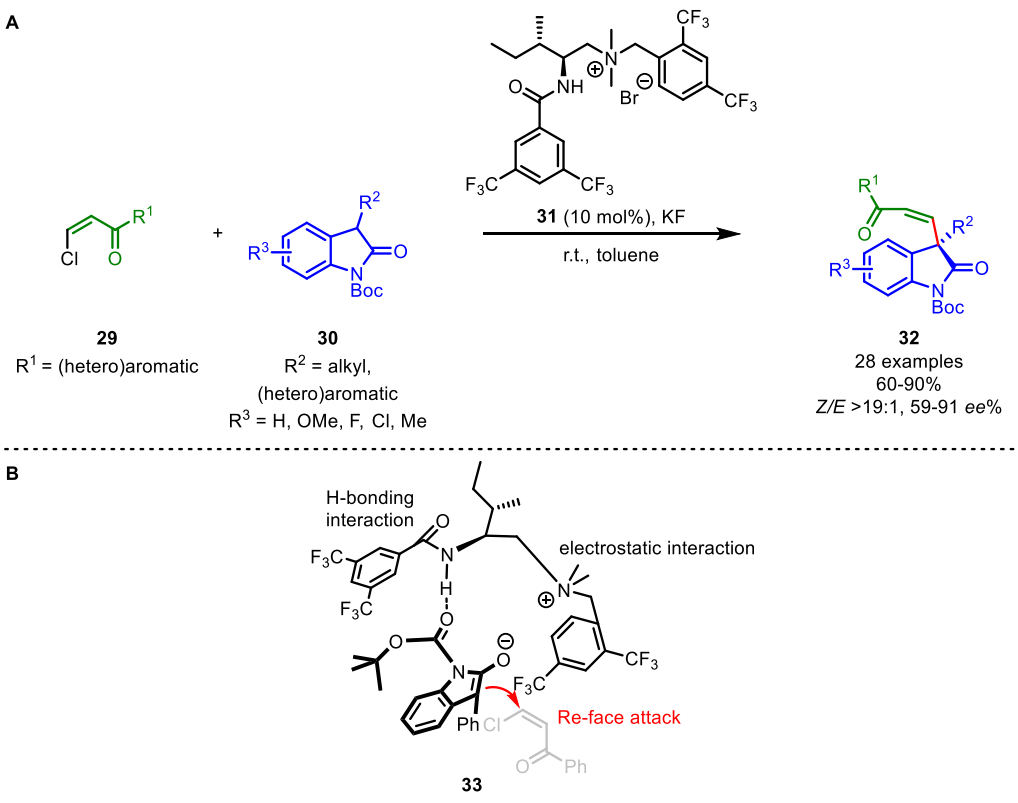

Scheme 8. Enantioselective intermolecular nucleophilic vinylic substitution of (hetero)aromatic β-chloropropenones 29 to synthesise various substituted oxindoles 32 (A) and the proposed transition state 33 responsible for the asymmetric induction (B). Blue represents the nucleophile. Green represents the electrophile. Red represents the new bonds formed.

Furthermore, with the use of potassium carbonate and a PTC derived from cinchonine (**35**), various aliphatic and (hetero)aromatic β-chloropropenones (**29**) were reacted with a range of cyclic β-ketoesters

(**34**), leading to the formation of substituted cyclic β-ketoesters (**36**) in good yields with enantioselectivities of ≥91% *ee* and nearly complete stereospecificity with respect to the *Z*-geometry of the double-bond (Scheme 9A).[37] The use of acyclic β-ketoesters resulted in lower enantioselectivities (<40% *ee*). The nearly complete retention of the *Z*-configured carbon-carbon double-bond was explained with the proposal that the reaction follows an Ad_N-E route. First, the chiral PTC-complexed enolate derived from the cyclic β-ketoester (**34**) undergoes (enantioselective) addition to **29**, the rate-determining step, giving the anionic intermediate as an inconsequential mixture of diastereomers (**37** and **38**). For the elimination of the chloride leaving group to occur, the C–Cl σ* orbital and the p orbital of the enolate are required to be aligned periplanar; this requirement is met by a 60° or 120° bond rotation of which the former is preferred due to the avoidance of destabilising eclipsing interactions (between non-hydrogen substituents), resulting in stereoretention (Scheme 9B). This explanation can also be used for the observed *Z*-selectivity in the formation of oxindoles **32** (Scheme 8).

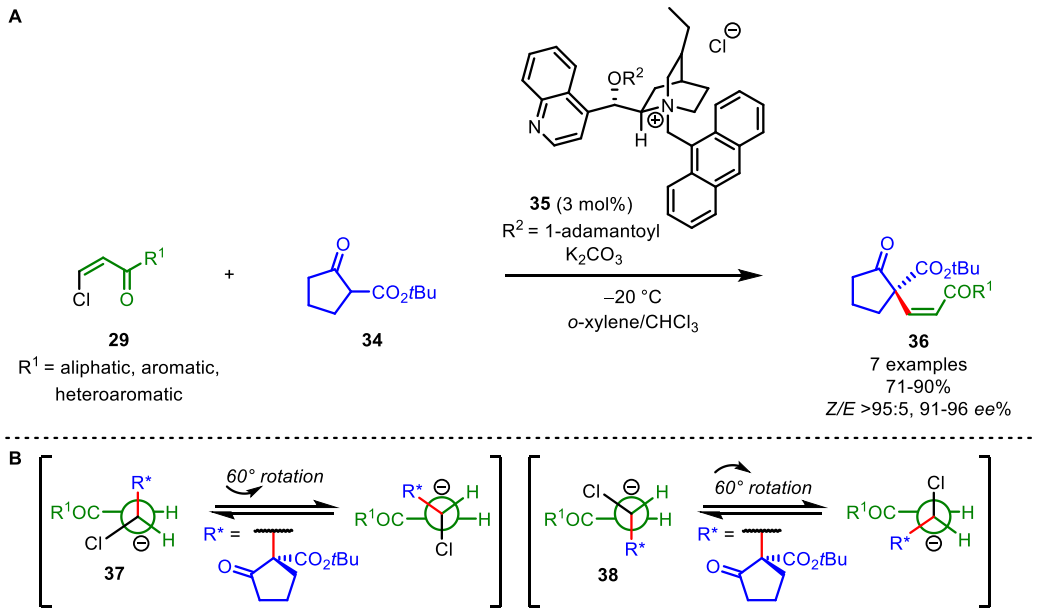

Scheme 9. Enantioselective intermolecular nucleophilic vinylic substitution of aliphatic and (hetero)aromatic β-chloropropenones 29 to synthesise various substituted cyclic β-ketoesters 36 (A) and the proposed preferred rotation of the reaction intermediate (B). Blue represents the nucleophile. Green represents the electrophile. Red represents the new bonds formed.

Similarly, β-chloroalkenones possessing electron-poor and electron-rich (hetero)aromatic groups (**29**) were substituted by α-substituted-α-cyanoacetates bearing alkyl and (hetero)aromatic groups (**39**), using a dimeric PTC derived from cinchonine (**40**) under phase-transfer conditions with cesium carbonate as base. Vinyl substituted quaternary carbon stereocentres (**41**) were formed in good yields with enantioselectivities of ≥84% ee and nearly complete stereospecificity with respect to the *Z*-geometry of the double-bond (Scheme 10).[39]

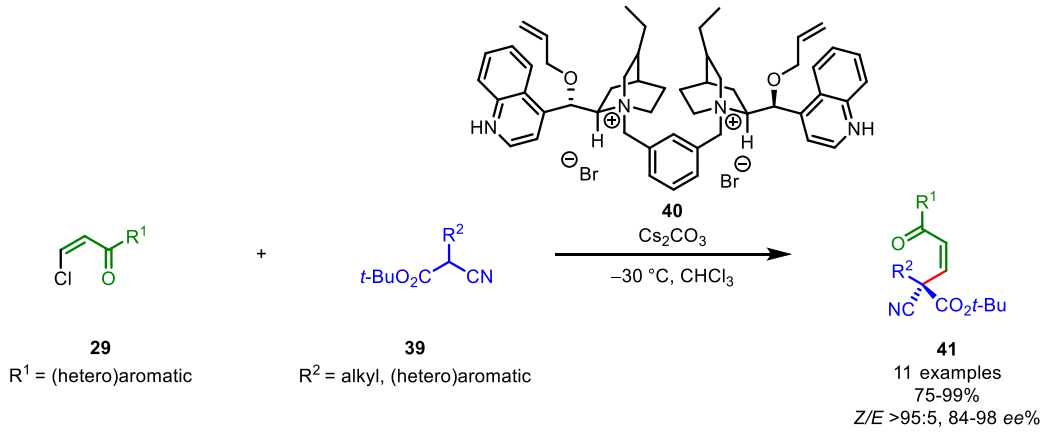

Scheme 10. Enantioselective intermolecular nucleophilic vinylic substitution of β-chloroalkenones 29 by α-substituted-α-cyanoacetates 39. Blue represents the nucleophile. Green represents the electrophile. Red represents the new bonds formed.

A chloranyl group has also been used as the leaving group in intermolecular S_NV reactions, like the iodanyl group described in section 1.1.2.1. (*E*)-Chlorovinyl-λ^3-chlorane **42** was reported to react under mild conditions with various sterically hindered and weak oxygen, sulfur and aromatic carbon nucleophiles, such as perfluoroalkanesulfonate and mesitylene, to afford products **43** in moderate to high yields with complete inversion of configuration (Scheme 11).[40] DFT calculations of the reaction of **42** with mesitylene as the nucleophile showed that a $S_NV\sigma$ route (Scheme 11, **44**→**45**) is followed with an activation energy of 19.6 kcal/mol. Then, a barrierless rearomatisation yields the inverted product **43**. In addition, the S_NV reaction was demonstrated to be high yielding when starting from the alternative isomer **(*Z*)-42** leading to the stereospecific formation of the inverted products **(*E*)-43** exhibiting *E*-geometry.

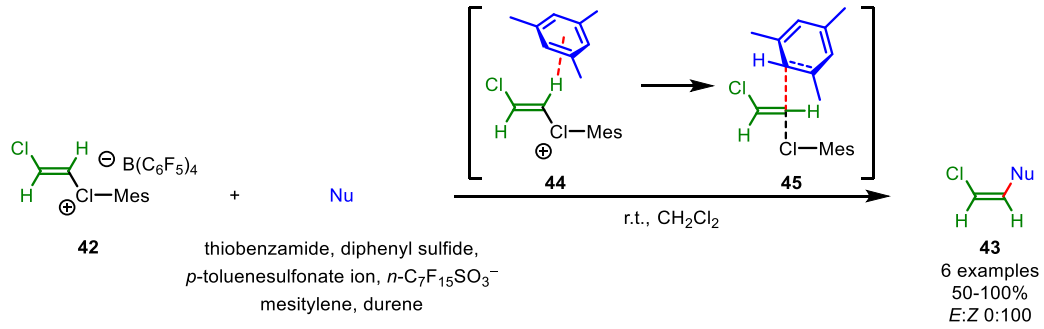

Scheme 11. Intermolecular nucleophilic vinylic substitution of (*E*)-chlorovinyl-λ^3-chlorane 42 with various sterically hindered and weak oxygen, sulfur, and carbon nucleophiles to afford products 43 in moderate to high yields with complete inversion of configuration. Blue represents the nucleophile. Green represents the electrophile. Red represents the new bonds formed.

1.1.2.3 With Nitro Leaving Groups

More recently, attention has been returned towards applying the intermolecular S_NV reaction to nitroolefins in which the nitro group acts as the leaving group. It was already proven in earlier days that the S_NV reaction can take place between activated α,β-dinitro olefins (**46**) and nucleophiles such as ammonia, azide, aniline, thiocyanate and thiols, but also 1,2-ethanedithiol and 2-mercaptoethanol (Scheme 12A).[41–43] Interestingly, in most cases complete *Z*-stereoselectivity was observed regardless of starting from *E*- or *Z*-starting materials. This can be explained with the conformational structures of the intermediates; after attack of the nucleophile on *Z*- and *E*- starting materials (**(*Z*)-46** and **(*E*)-46**), intermediates **48** and **50** are generated that by free rotation can transform to **49** and **51** (Scheme 12B). In case of attractive interactions, such as hydrogen bonding, between the nitro group and the nucleophile, conformational structure **49** is preferred and leads to the *Z*-alkene geometry (**47**). If those interactions are of more repulsive character, intermediate **51** is preferred and the equilibrium shifts towards the *E*-configuration (**(*E*)-47**).

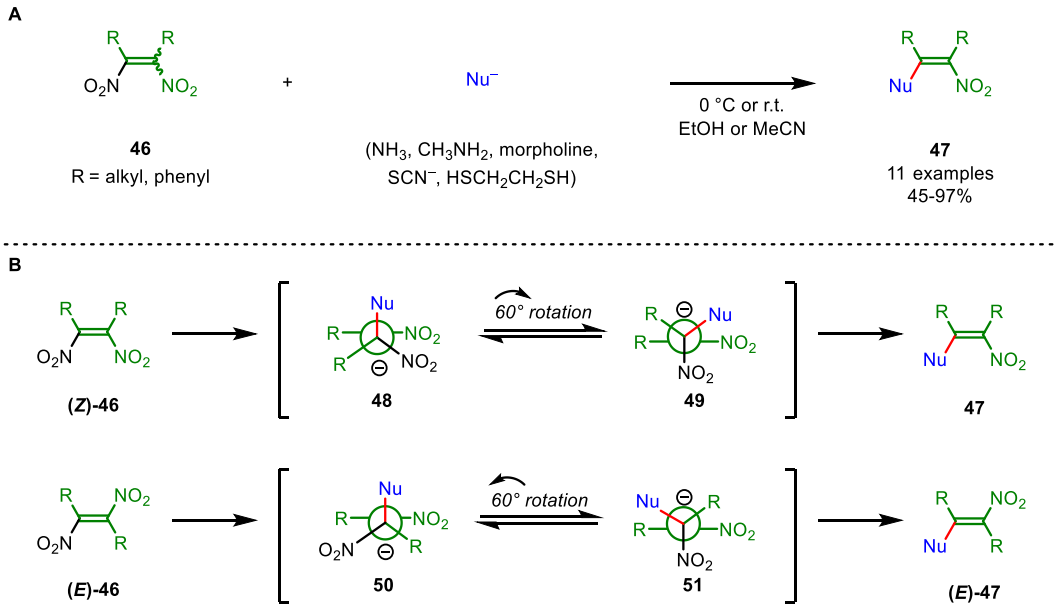

Scheme 12. Intermolecular nucleophilic vinylic substitution of activated α,β-dinitro olefins 46 with various nucleophiles to afford in most cases products with complete *Z*-stereoselectivity (A) and the proposed preference of reaction intermediates (B). Blue represents the nucleophile. Green represents the electrophile. Red represents the new bonds formed.

The nitro group is however strongly electron-withdrawing and can redirect the attack of the nucleophile at the β- instead of the α-vinylic carbon, resulting in a 1,4-addition of the nucleophile, possibly followed by a 1,2-*trans* elimination of an alternative leaving group at the β-position.[44] Tang and co-workers postulated that the desired S_NV reaction – substitution of the α-nitro leaving group by nucleophilic

attack at the α-vinylic carbon – would take place with the presence of an electron-withdrawing group at the β-vinylic carbon and presented a successful S_NV reaction of 3-alkenyl oxoindoles (**52**).[44] In the presence of diisopropylethylamine (DIPEA), (*E*)-3-alkenyl oxoindoles (**52**) were reacted with various nucleophiles (alcohols, amines and thiols), so generating the S_NV products **53** in good yields with *E*/*Z* ratios of 10:1 to >20:1 (Scheme 13). Less nucleophilic alcohols, amines and thiols gave lower yields and bulkier nucleophiles resulted in lower *E*/*Z* selectivities. The nucleophilic addition was accelerated due to the electron-withdrawing effects of the phenyl-, carbonyl- and nitro groups and gave conformational structure **54** that via a preferred 60° rotation can form **55**, from which NO_2-elimination yielded the products **53** mainly with retention of the carbon-carbon double-bond geometry (Scheme 13).

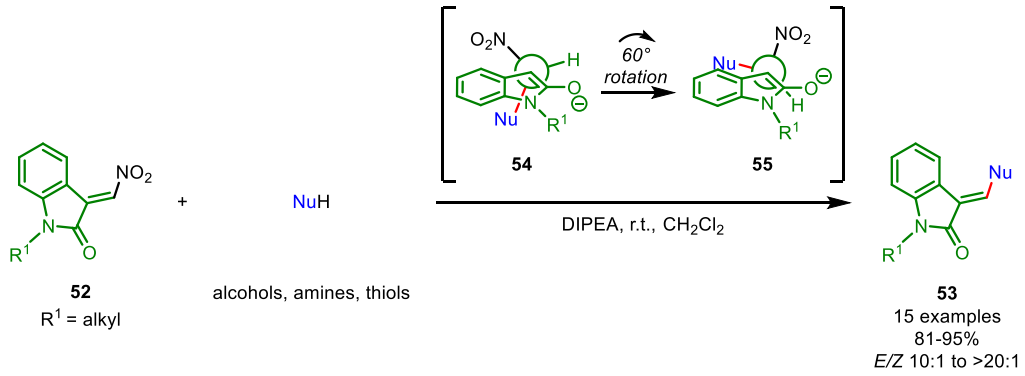

Scheme 13. Intermolecular nucleophilic vinylic substitution of (*E*)-3-alkenyl oxoindoles 52 with various nucleophiles to afford the products 53 with high *E*/*Z* selectivity. Blue represents the nucleophile. Green represents the electrophile. Red represents the new bonds formed.

Similarly, Pedro *et al.* reported the intermolecular nucleophilic vinylic substitution of 3-alkenyl oxoindoles (**52**) by pyrazol-3-ones (**56**).[45] In the presence of triethylamine, various *N*-substituted 3-alkenyl oxoindoles **52** and a range of pyrazol-3-ones **56** bearing alkyl and aromatic groups reacted to yield 3-pyrazolylidene-2-oxindole compounds **57** in moderate to good yields with excellent stereo- and regioselectivity (Scheme 14). The high stereoselectivity for the *Z*-isomer can be explained by the fact that upon regioselective nucleophilic addition to the α-carbon of the nitroalkene in **52** conformational structure **58** favours a 120° rotation instead of the normally preferred 60° rotation due to the depicted presence of coordination between the formed enol of the pyrazolone and the enolate of the oxindole moiety. Subsequently, NO_2-elimination from conformational structure **59** results in the synthesis of compounds **57** with high *Z*-stereoselectivity.

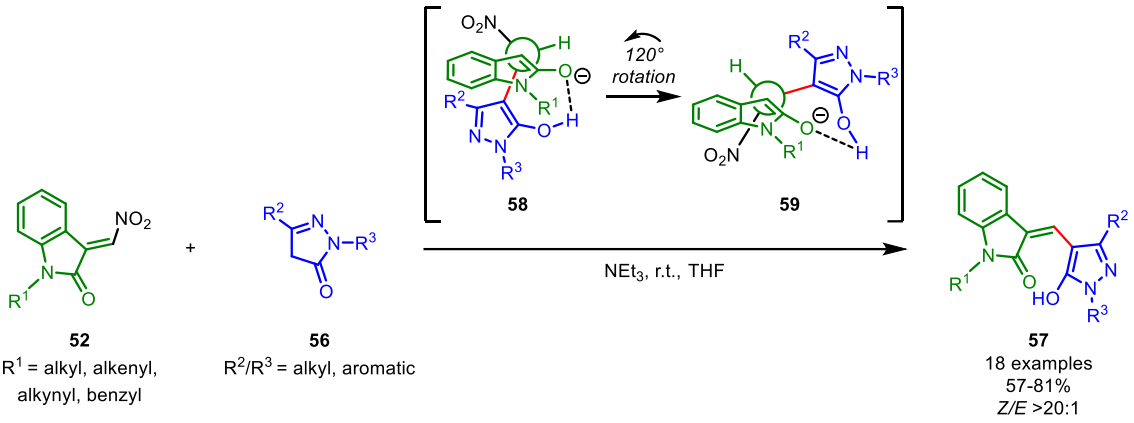

Scheme 14. Intermolecular nucleophilic vinylic substitution of 3-alkenyl oxoindoles 52 with various pyrazol-3-ones 56 to afford 3-pyrazolylidene-2-oxoindole compounds 57 with high stereoselectivity for the *Z*-isomer. Blue represents the nucleophile. Green represents the electrophile. Red represents the new bonds formed.

With the success Pedro and co-workers obtained in the S_NV reaction using pyrazol-3-ones **56**, they extended their methodology to the use of pyrazol-3-ones substituted at the 4-position,[45] focusing on a method to prepare the desired products, containing a fully substituted carbon stereocentre, in enantioenriched form.[46] In the presence of the chiral organocatalyst $(DHQ)_2Pyr$ (**61**), various *N*-substituted 3-alkenyl oxoindoles **52** were reacted with 4-substituted pyrazol-3-ones (**60**) to yield products **62** in high yields with excellent regioselectivity, moderate to good enantioselectivity and high stereocontrol over the olefin geometry (Scheme 15A). The enantioselectivity was proposed to originate from 2 key interactions: π-π stacking interaction between the 3-alkenyl oxoindole **52** and the catalyst **61**, and intramolecular hydrogen bonding between the enol form of the 4-substituted pyrazol-3-one **60** and the quinuclidine moiety of the catalyst **61** (Scheme 15B). Interestingly, high stereoselectivity is observed for the *E*-isomer, which is in contrast to the previously discussed reactions with 4-unsubstituted pyrazol-3-ones which afford the *Z*-isomer. This can be rationalised through conformational structure **63** which favours to undergo the preferred 60° rotation to form **64**, which upon NO_2 elimination gives compounds **62** with high *E*-stereoselectivity (Scheme 15C).

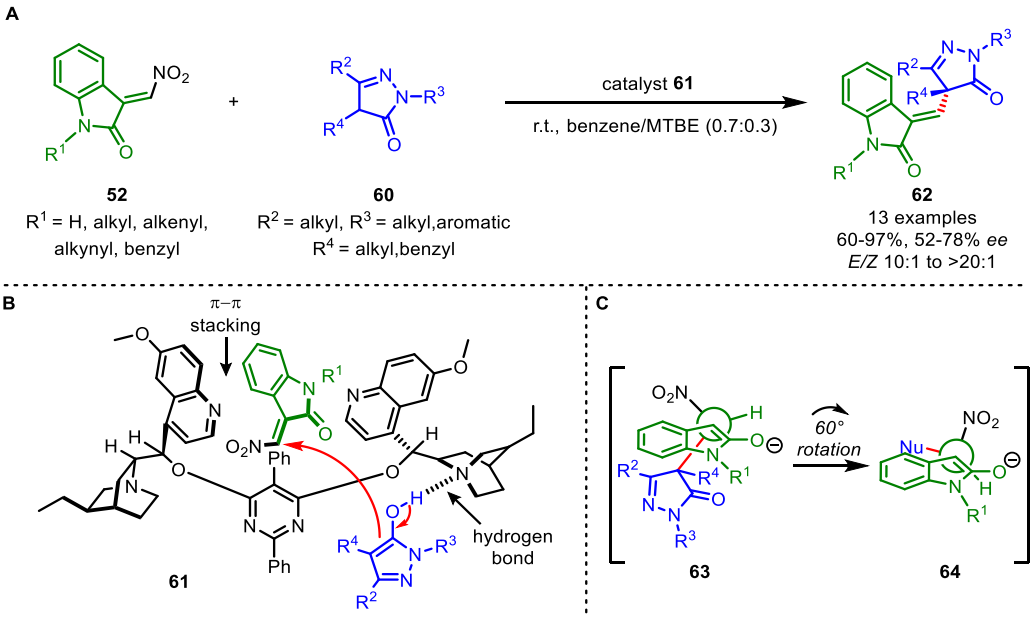

Scheme 15. Intermolecular nucleophilic vinylic substitution of *N*-substituted 3-alkenyl oxoindoles 52 with various pyrazol-3-ones 60 to afford 3-pyrazolylidene-2-oxoindole compounds 62 (A) with moderate enantioselectivity due to the use of the organocatalyst 61 (B) and high stereoselectivity for the *E*-isomer (C). Blue represents the nucleophile. Green represents the electrophile. Red represents the new bonds formed.

1.1.2.4 With Fluoro Leaving Groups

The intermolecular S_NV reaction was also demonstrated to be effective with *gem*-difluorinated alkenes due to its polarised and high electron-deficient nature.[47] For example, Cao and co-workers, shortly followed by others, developed high yielding S_NV reactions of mono-arylated *gem*-difluoroalkenes (**65**) with various nucleophiles such as pyrazole and imidazole derivatives (**65**→**66**),[48] terminal alkynes (**65**→**67**),[49] pyrazoline-5-ones (**65**→**68**),[50] benzylnitrile (**65**→**69**),[51] alleonates (**65**→**70**),[52] trimethylsilylcyanide and trimethyl(trifluoromethyl)silane (**65**→**71**),[53] dialkyl phosphites/diarylphosphine oxides (**65**→**72**),[54] and sodium sulfinates (**65**→**73**) (Scheme 16A).[55] The high stereoselectivity observed in the S_NV reaction using terminal alkynes, benzylnitrile and trimethylsilylcyanide as the nucleophile can be explained by an Ad_N-E mechanism, in which upon nucleophilic attack intermediate **74** with a short-lived carbanion is formed (Scheme 16B). Internal rotation of intermediate **74** can then form either conformational intermediate **75** or **76**; the latter is preferred as it mitigates the unfavourable electronic repulsion between the fluorine atom and the aryl group and so upon fluoride-elimination leads to the observed *E*-stereoselectivity. In case of the nucleophiles sodium sulfinate and trimethyl(trifluoromethyl)silane (**77**), conformational intermediate **78** is preferred over **79** as it mitigates the unfavourable steric repulsion between the aryl group and bulkier sulfonate and trifluoromethyl group, and so explains the observed *E*-stereoselectivity (Scheme

16C). Presumably, the low to moderate stereoselectivity in the other examples of the S_NV reaction is caused by the existence of a long-lived carbanion in the Ad_N-E pathway.

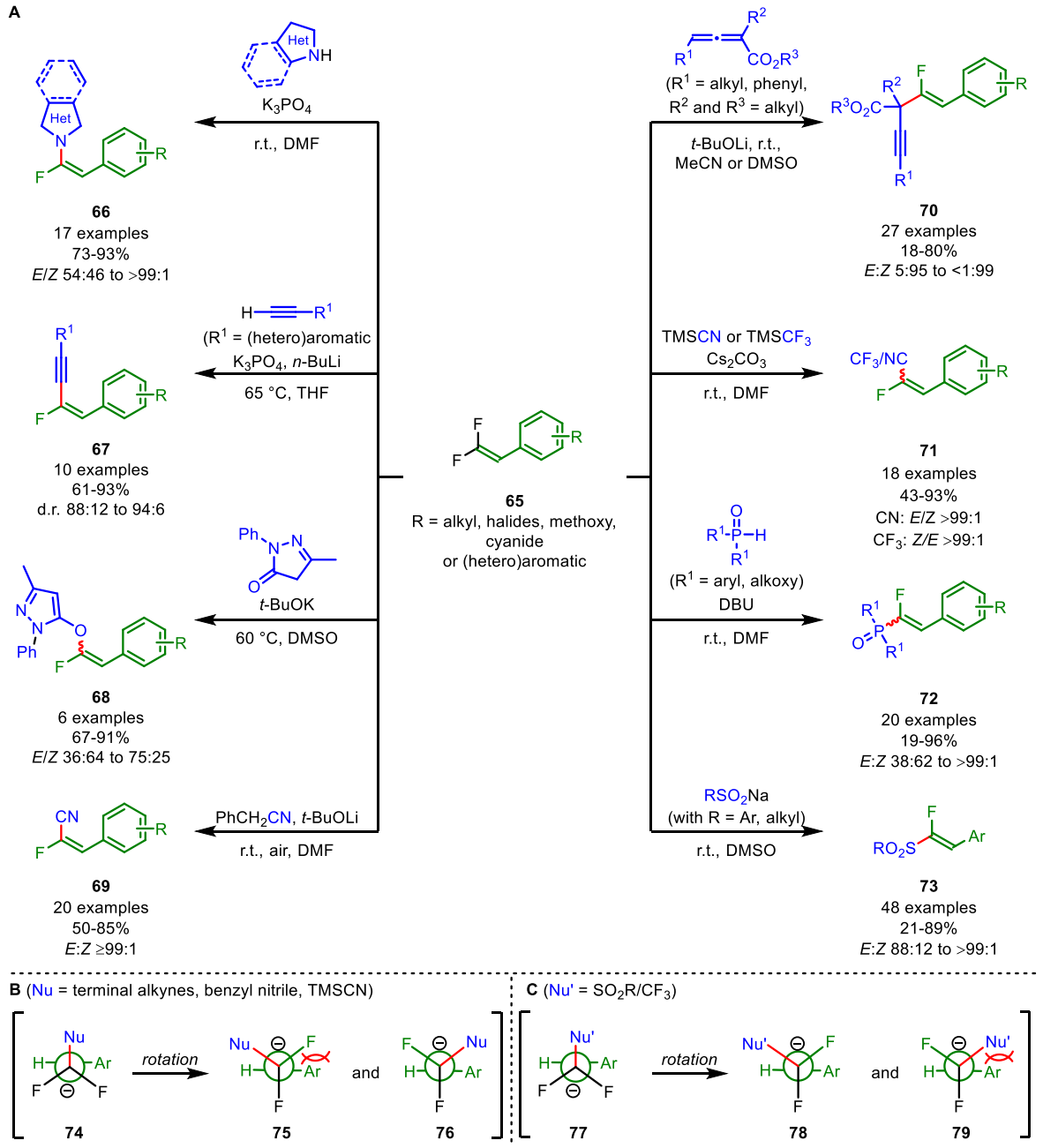

Scheme 16. Intermolecular nucleophilic vinylic substitution of mono-arylated *geminal* difluoroalkenes 65 with various nucleophiles (A) and the corresponding conformational structures of the intermediates to explain the observed stereoselectivity (B & C). Blue represents the nucleophile. Green represents the electrophile. Red represents the new bonds formed.

In addition, Cao and co-workers expanded the S_NV reaction to di-arylated *gem*-difluoroalkenes (**80**) and used various nucleophiles such as pyrazole and imidazole derivatives (**80**→**81**),[48] terminal alkynes (**80**→**82**),[49] arylboronic acids under air (**80**→**83**),[56] and 2-phenyl-1,3,4-oxadiazole (**80**→**84**),[57] benzoxazoles (**80**→**85**)[57] and benzothiazoles (**80**→**86**)[57] with similar success (Scheme 17).

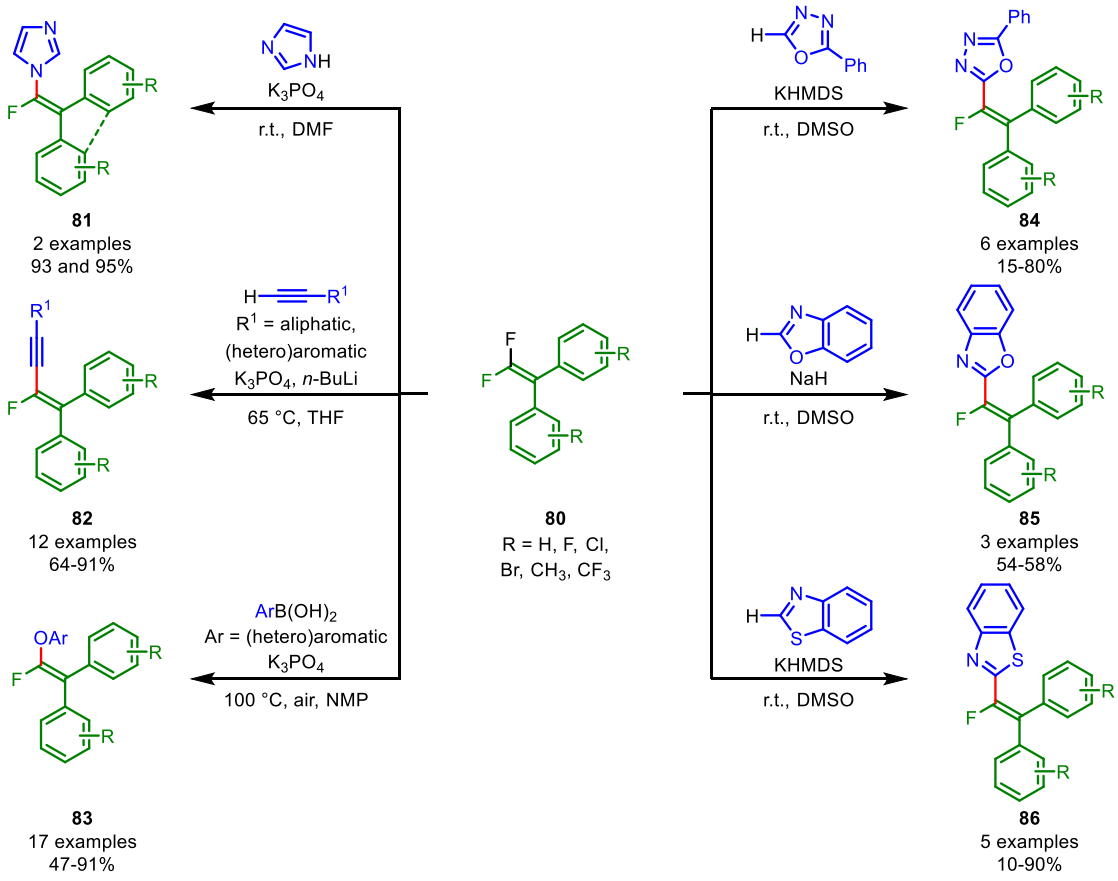

Scheme 17. Intermolecular nucleophilic vinylic substitution of di-arylated *geminal* difluoroalkenes 80 with various nucleophiles. Blue represents the nucleophile. Green represents the electrophile. Red represents the new bonds formed.

Besides arylated *gem*-difluoroalkenes, differently substituted and monofluorinated alkenes, generally less reactive than *gem*-difluoroalkenes, also proved to be useful for the intermolecular S_NV reaction. For example, Tsui and co-workers demonstrated that various (*E*)-β-monofluoroacrylates (**87**) can react with oxygen, sulfur and nitrogen nucleophiles (e.g. phenols, 2-naphthol, estrone, aliphatic alcohols, carboxylic acid, 2-naphthalenethiol and indole, imidazole and pyrazole derivatives) or Grignard reagents to generate trisubstituted alkenes (**88** and **89**) in good to high yields with excellent stereocontrol (Scheme 18).[58,59] This success can be explained by the installation of the α-ester group, which activates the double-bond and so increases the reactivity of monofluoroalkenes **87** for the desired S_NV reaction; control experiments showed that by replacing the α-ester group with a hydrogen, no reaction was observed.

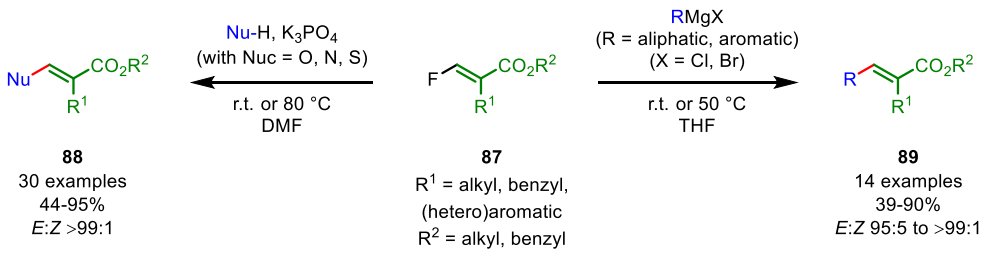

Scheme 18. Intermolecular nucleophilic vinylic substitution of substituted, monofluorinated alkenes 87 with various nucleophiles. Blue represents the nucleophile. Green represents the electrophile. Red represents the new bonds formed.

1.1.3 Intramolecular Substitutions

With interest in developing a powerful method for the synthesis of cyclic compounds, the intramolecular vinylic substitution reaction has received significant attention and its scope has been investigated with various nucleophiles and leaving groups. In this section, recent examples are described and divided based on the identity of the leaving group.

1.1.3.1 With Fluoro Leaving Groups

Besides intermolecular S_NV reactions (section 1.1.2.4), intramolecular S_NV reactions of *geminal* difluoroalkenes with various oxygen, nitrogen, sulfur and carbon nucleophiles for the synthesis of fluorinated carbo- and heterocycles have been extensively studied by Ichikawa and co-workers (Scheme 19).[60] By taking advantage of the two fluorines, which activate the carbon-carbon double-bond and act as a good leaving group, a wide range of 5-*endo*-*trig* cyclisations, generally disfavoured with first row nucleophiles according to Baldwin's rules,[61,62] have been realised.[60]

When difluorostyrenes bearing hydroxy and tosylamido groups at the ortho position (**90**) were reacted with sodium hydride or DBU, oxygen or nitrogen substitution of one of the fluorines via the S_NV reaction afforded 2-fluorobenzo[b]furans and indoles (**91**) in high yields (Scheme 19A).[63,64] In contrast, under the same conditions, both *E*- and *Z*-monofluorostyrenes (R = *n*-butyl) bearing an ortho hydroxyl group generated the benzo[b]furan in low yields of 17% and 19% respectively, and the analogous dibromostyrene (**90-Br$_2$**, R = *n*-butyl) generated 2-bromobenzo[b]furan **91-Br** in only a 15% yield, while the dichlorostyrene variant (**90-Cl$_2$**) gave no reaction. The authors proposed that a repulsive interaction between the π-electrons of the carbon-carbon double-bond and the fluorine lone pairs polarises the carbon-carbon double-bond and decreases electron density at the α-carbon, facilitating the S_NV reaction via the Ad_N-E route; this repulsive electronic interaction is less prevalent in the corresponding chloro- and bromo-systems.[60]

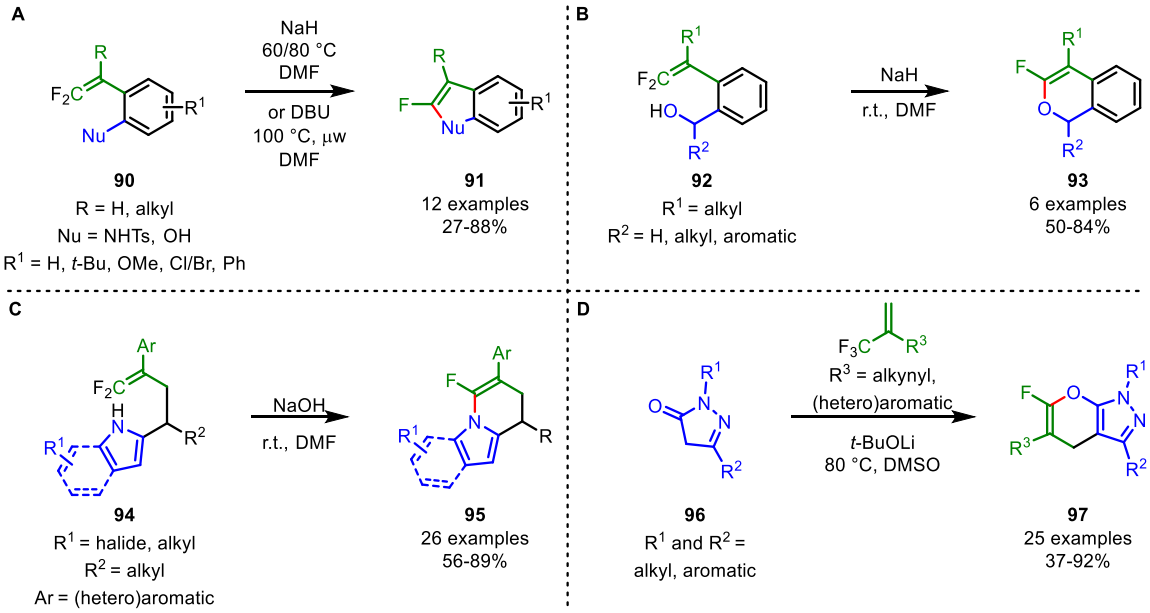

Scheme 19. Intramolecular S_NV reactions of geminal difluoroalkenes by oxygen and nitrogen nucleophiles to generate fluorinated heterocycles. Blue represents the nucleophile. Green represents the electrophile. Red represents the new bonds formed.

In addition to the effectiveness of the intramolecular S_NV reaction in the synthesis of 2-fluorinated indoles and benzofurans (**91**), the intramolecular substitution method has also been successfully applied to the generation of fluorinated 6-membered heterocycles. When difluorostyrenes **92**, possessing primary and secondary alkyl groups (R^1) and an ortho-tethered oxygen nucleophile, were reacted with sodium hydride, various fluorinated benzo[b]pyrans **93** were afforded in moderate to good yields (Scheme 19B).[65] By reaction of *gem*-difluoroalkenes **94** possessing a tethered nitrogen nucleophile with sodium hydroxide, a range of 5-fluoro-dihydroindolizines **95** was afforded in moderate to good yields (Scheme 19C).[66] Moreover, 6-fluoro-1,4-dihydropyrano[2,3-*c*]pyrazoles (**97**) were generated regio- and chemoselectively via a S_N2'/S_NV sequence by reaction of various pyrazolones (**96**) with (trifluoromethyl)alkenes and lithium *tert*-butoxide (Scheme 19D).[67]

To rule out the possibility of 2-fluorinated benzofurans and indoles (**91**) forming via a 6π-electrocyclisation instead of a S_NV reaction, and to expand the scope of this 5-*endo-trig* cyclisation, the benzene ring that acts as a linker between the difluoroalkene and the nucleophile was replaced by two sp^3 carbons. 1,1-Difluoro-1-butenes **100** bearing oxygen, nitrogen and sulfur nucleophiles were reacted with sodium hydride in DMF at 90 °C, generating various fluorinated dihydrofurans, pyrrolines and dihydrothiophenes (**101**) in good yields, confirming that a S_NV route, not a 6π-electrocyclisation, is followed (Scheme 20A).[68] Moreover, the S_NV reaction was demonstrated to be successful with sp^3-carbon nucleophiles: 1,1-difluoro-1-butenes possessing electronically diverse aromatic groups (R^1) and a tethered iodomethyl group (**102**) treated with *tert*-butyl lithium generated fluorinated cyclopentenes (**103**) in good yields (Scheme 20B).[69]

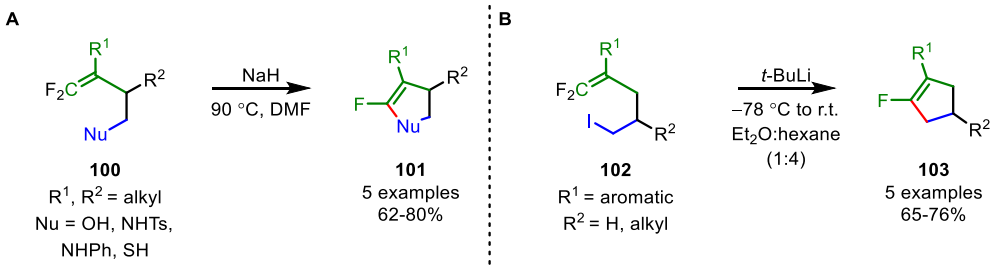

Scheme 20. Intramolecular S_NV reactions of geminal difluoroalkenes 100 and 102 by oxygen, nitrogen, sulfur, (A) and carbon nucleophiles (B) to generate fluorinated hetero- and carbocycles. Blue represents the nucleophile. Green represents the electrophile. Red represents the new bonds formed.

As the 5-*endo-trig* cyclisations described above are unusual, Ando and co-workers performed theoretical calculations to deduce a reaction mechanism and explain the high reactivity of the difluorostyrenes in comparison with the less reactive monofluoro-, dichloro- and dibromostyrenes.[70] DFT studies demonstrated that on treatment with sodium hydride in DMF, **104** bearing a methyl group at the β-carbon and a phenolate nucleophile adopts a first transition state structure (**104-TS**) in which for the difluoro compound the distances of the C-F bonds do not significantly change (Scheme 21). This is in contrast to the dibromo and dichloro compounds: in their first transition state structures (**104-TS**), the distance of one of the C–Br/Cl bonds increases by 0.17 Å and 0.15 Å respectively (Scheme 21). These data suggest that the S_NV reaction of the difluorostyrene follows an Ad_N-E mechanism and the dibromo- and dichlorostyrenes follow a concerted $S_NV\pi$ pathway, which is in line with the order of the leaving group ability (Br > Cl >> F) and electronegativity (F >> Cl > Br) of the halides. Compared to fluorine atoms, bromine and chlorine atoms are less effective in stabilising the negative charge upon nucleophilic attack to the alkene, and therefore exploit their leaving group ability, resulting in a concerted S_NV pathway. The poor reactivity of the dibromo- and dichlorostyrenes in this S_NV process agrees with the activation energies calculated to adopt the first transition state structures **104-TS**, which are relatively high – 26.7 and 27.0 kcal/mol in DMF for the dibromo- and dichlorostyrenes respectively – compared to the activation energy (21.3 kcal/mol in DMF) calculated for the difluorostyrene transition state structure (Scheme 21).

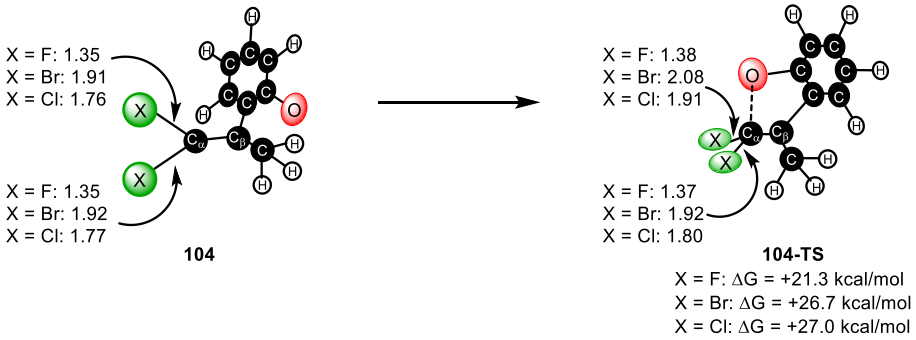

Scheme 21. Transition states and corresponding activation energies involved in the intramolecular nucleophilic vinylic substitution of hydroxystyrenes 104 bearing a fluoro, bromo or chloro leaving group. Bond lengths are depicted in angstroms (Å).

For the monofluoro hydroxystyrene, the activation energies to adopt the located TSs were calculated to be 25.8 kcal/mol in DMF for **(*E*)-105-TS** and 27.5 kcal/mol in DMF for **(*Z*)-105-TS** (Scheme 22), which are in agreement with the lower experimental yields for these substrates compared to the difluoro hydroxystyrene, which reacts through a lower energy TS (21.3 kcal/mol).[70] The theoretical calculations also showed that in **(*E*)-105** the oxyanion forms a hydrogen bond with the vinylic hydrogen and the C-F bond lengthens upon shortening of the C-O bond, hence suggesting that a concerted $S_NV\sigma$ route is followed for the nucleophilic attack, which is in line with the obtained inversion of configuration (Scheme 22A). In the case of **(*Z*)-105**, the fact that the oxyanion is not able to form a hydrogen bond with the vinylic hydrogen and the distance of the C-F bond does not increase upon approach of the oxyanion suggests that the S_NV follows a multistep Ad_N-E pathway (Scheme 22B).

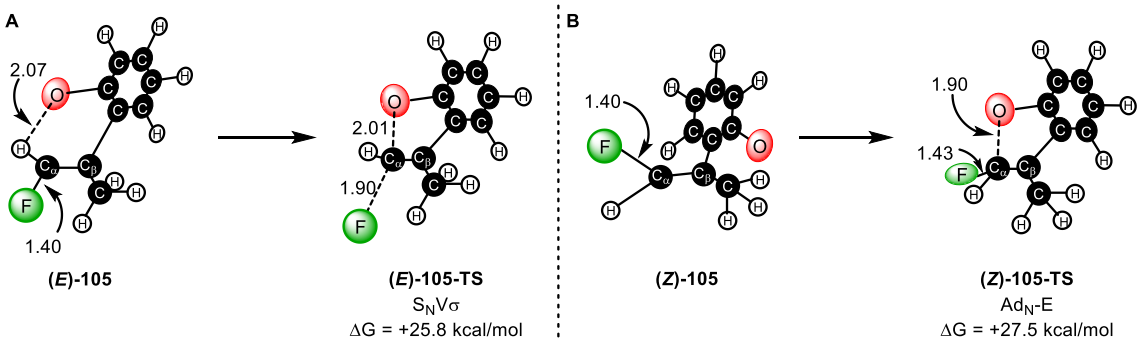

Scheme 22. Transition states and corresponding activation energies involved in the intramolecular nucleophilic vinylic substitution of monofluoro hydroxystyrenes (*E*)-105 (A) and (*Z*)-105 (B). Bond lengths are depicted in angstroms (Å).

1.1.3.2 With Chloro Leaving Groups

Intramolecular S_NV reactions of chloroalkenes with oxygen and nitrogen nucleophiles for the synthesis of various heterocycles have been studied by Narasaka and co-workers.[71] By reacting phenol or aniline substituted vinyl chlorides **106** at room temperature with sodium hydride, a benzofuran and an indole (**107**) were obtained in yields of 95% and 77%, respectively (Scheme 23A).[71] For vinyl chlorides with *Z*-geometry the reaction was unproductive, even after heating at elevated temperatures. When a mixture of *E*- and *Z*-deuterated vinyl chlorides **108** was reacted with sodium hydride, the generated benzofuran product **109** still contained the deuterium at the 2-position and the *Z*-isomer **(*Z*)-108** was recovered, thus excluding the possibility of the S_NV following an allylic isomerisation or vinyl carbene formation mechanism which could proceed with both isomers yet would not preserve the vinylic deuterium/hydrogen (Scheme 23B&C). In addition, dihydrofuran **111** was obtained effectively by reacting vinyl chloride **110** with sodium hydride, and thus the possibility of the previous substitution reactions with aromatic substrates **106** and **108** occurring via a 6π-electrocyclisation, instead of a S_NV-type process, was excluded (Scheme 23D).

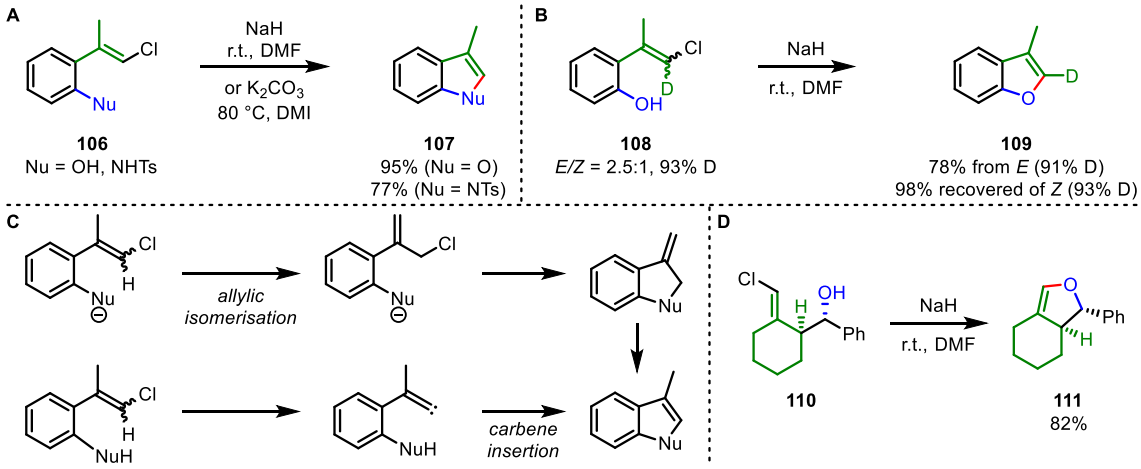

Scheme 23. Intramolecular nucleophilic vinylic substitution of vinyl chlorides 106 (A), 108 (B), which excludes the possibility of allylic isomerisation or carbene insertion (C), and 110 (D) by oxygen and nitrogen nucleophiles. Blue represents the nucleophile. Green represents the electrophile. Red represents the new bonds formed.

Calculations demonstrated that non-deuterated **(*E*)-108** adopted a transition state structure for the $S_NV\sigma$ route (**(*E*)-108-TS**), in which the carbon-carbon double-bond and the forming carbon-oxygen bond were shortened while the length of the breaking carbon-chloride bond increased, with an activation energy of 14.4 kcal/mol in DMF (Scheme 24A). An out-of-plane S_N2-type structure ($S_NV\pi$) was observed for the transition state of **(*Z*)-108** (**(*Z*)-108 -TS**) with an activation energy of 28.9 kcal/mol (Scheme 24B).[72] This relatively high activation energy is associated with steric repulsion between the

chloride and the oxyanion, and rationalises the unsuccessful results in the attempted cyclisation of the *Z*-vinyl chloride **(*Z*)-106**. Moreover, the steric clash depicted in Scheme 24B in combination with the smaller size of fluorine atoms compared to chlorine atoms is a probable explanation for the fact that higher activation energies, relative to difluorostyrenes, were obtained for the TSs of dichlorostyrene systems (Scheme 21).

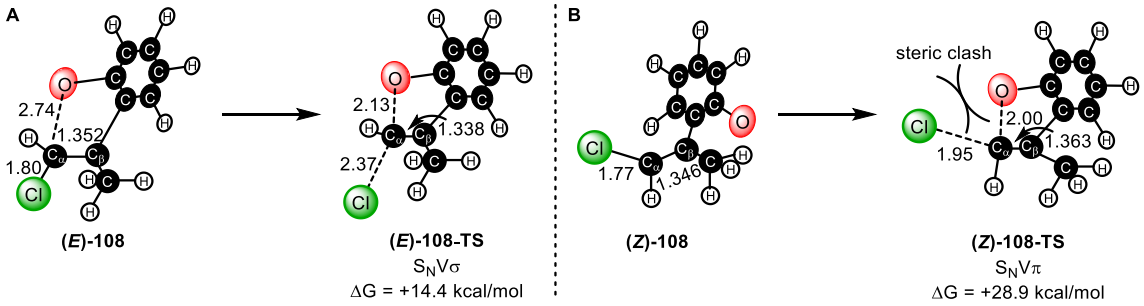

Scheme 24. Transition states involved in the intramolecular nucleophilic vinylic substitution of vinyl chlorides (*E*)-108 (A) and (*Z*)-108 (B). Bond lengths are depicted in angstroms (Å).

1.1.3.3 With Bromo Leaving Groups

Intramolecular S_NV reactions of bromooalkenes by nitrogen, sulfur, and carbon nucleophiles for the synthesis of various hetero- and carbocycles have been studied by Narasaka and co-workers.[73] When vinyl bromides bearing a tethered tosylamido group (**112**) were reacted with sodium hydride in DMI, substitution of the bromide via the S_NV reaction afforded various pyrrolines (**113**) in good yields (Scheme 25A).[71] The *Z*-isomer of the vinyl bromide (**(*Z*)-112**) gave pyrroline **113** in only 4% yield after an extended period of heating and 70% of the starting material **(*Z*)-112** was recovered. The low reactivity of **(*Z*)-112** was in agreement with theoretical calculations in which a transition structure corresponding to the $S_NV\pi$ route was located with a higher activation energy of 34.3 kcal/mol in DMF. For **112** DFT calculations demonstrated that the C–Br bond was approached by the nitrogen nucleophile from the backside in the plane of the carbon-carbon bond, and thus a $S_NV\sigma$ pathway was followed with an activation energy of 20.5 kcal/mol in DMF (Scheme 25B). It should be noted that since DMI and DMF have essentially the same dielectric constant ($\varepsilon = 37.60$ vs. 37.06 respectively), DMF was used as the reaction medium in the theoretical studies. The suggestion for the $S_NV\sigma$ was complemented by the structure of the TS (**112-TS**), in which upon decreasing of the C–N bond length (2.97 to 2.16 Å) the C–Br bond length increases (1.93 to 2.52 Å), but the length of the carbon-carbon double-bond shortens (1.334 to 1.322 Å), thus representing the change of the hybridisation state of the vinylic carbon (sp^2 to sp) upon interaction of the nucleophile with the σ* orbital of the C–Br bond (Scheme 25B).

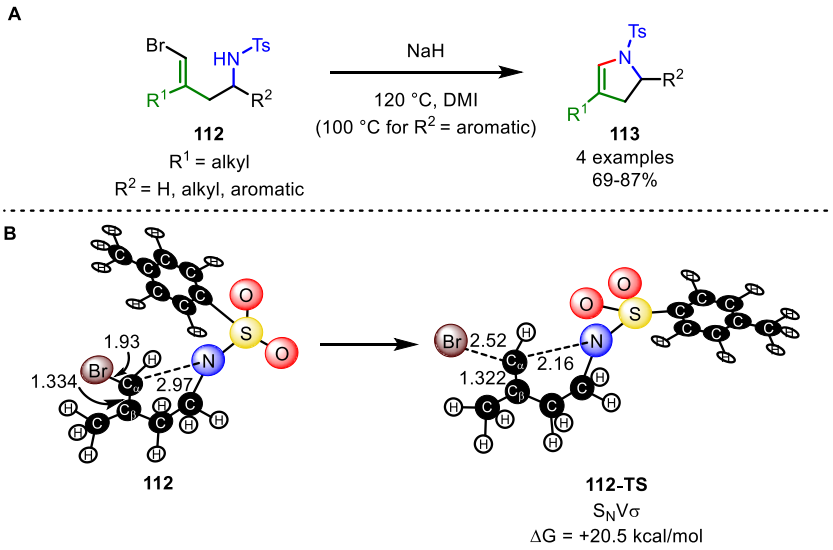

Scheme 25. Intramolecular nucleophilic vinylic substitution of vinyl bromides 112 by a nitrogen nucleophile (A) and the calculated structure of the corresponding transition state 112-TS (B). Bond lengths are depicted in angstroms (Å). Blue represents the nucleophile. Green represents the electrophile. Red represents the new bonds formed.

By reacting vinyl bromides bearing phenylsulfonyl and cyano groups (**114**) with sodium methoxide in DMI at 120 °C, cyclopentenes **115** were synthesised successfully (Scheme 26A).[71] Again, the *Z*-isomer of **114** (**(*Z*)-114**, R = $(CH_2)_2Ph$) was unreactive and gave no cyclisation product; this is in accordance with the $S_NV\pi$-type TS calculated for **(*Z*)-114** (**(*Z*)-114-TS**) with an activation energy of 29.9 kcal/mol in DMF (Scheme 26B), which is significantly higher than the activation energy (23.5 kcal/mol in DMF) calculated for the TS of **114** (**114-TS**) that displays a $S_NV\sigma$-type structure (Scheme 26C).

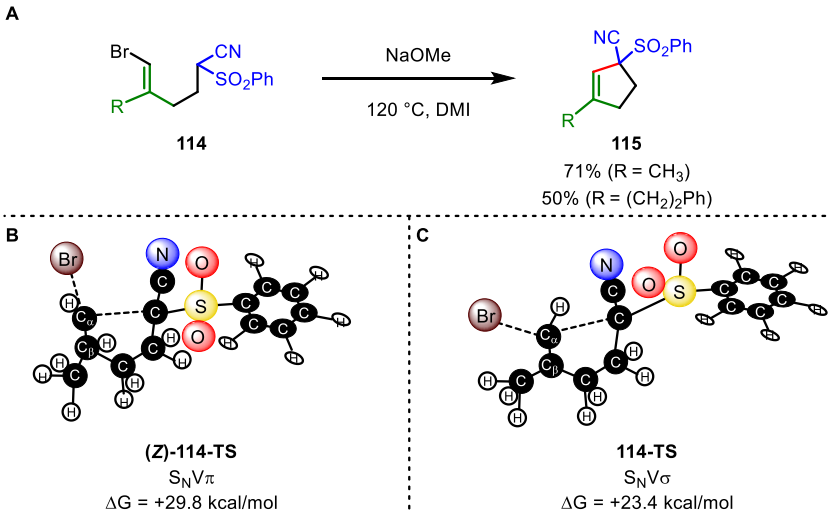

Scheme 26. Intramolecular nucleophilic vinylic substitution of vinyl bromides 114 by a carbon nucleophile (A) and the calculated structure of the corresponding transition states (B & C). Blue represents the nucleophile. Green represents the electrophile. Red represents the new bonds formed.

Like the vinyl bromides **112** and **114** bearing a nitrogen and carbon (pro)nucleophile, vinyl bromides **116** bearing a latent sulfur nucleophile also proved to be effective in the intramolecular S_NV reaction; both the *E*- and *Z*-isomers were transformed into dihydrothiophenes **117** with good yields (Scheme 27).[73,74] DFT calculations determined that for **(*E*)-116** a TS with the $S_NV\sigma$ type structure was on the reaction pathway with an activation energy of 12.5 kcal/mol in DMF and for **(*Z*)-116** a $S_NV\pi$ TS with an activation energy of 20.0 kcal/mol, the latter being significantly lower than the activation energies calculated for the $S_NV\pi$ TS of the *Z*-isomers of vinyl bromides **(*Z*)-112** (34.3 kcal/mol in DMF) and **(*Z*)-114** (29.9 kcal/mol in DMF), thus explaining the successful transformation of **(*Z*)-116** into **117** with the use of a sulfur nucleophile in this intramolecular S_NV reaction.

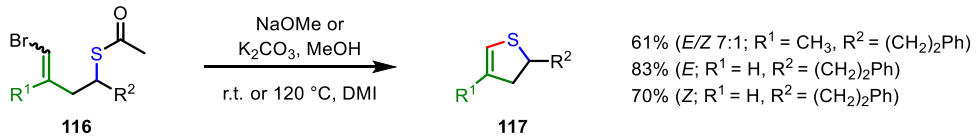

Scheme 27. Intramolecular nucleophilic vinylic substitution of vinyl bromides 116 in which thioacetates act as the nucleophile. Blue represents the nucleophile. Green represents the electrophile. Red represents the new bonds formed.

Thioamides and thioureas also proved to be successful in the S_NV reaction as various 2,5-disubstituted thiazoles (**119**), 6-alkylidene-5,6-dihydro-4*H*-1,3-thiazine derivatives (**121**) and 1,3,4-trisubstituted imidazole-2-thiones (**123**) were synthesised in good yields by reacting thioamides **118**, **120** and thioureas **122** with potassium carbonate or sodium hydroxide with TBAB (Scheme 28).[75,76] In the reaction of **118** and **122**, the initially formed exocyclic alkene undergoes internal isomerisation to give the products shown (**119** and **123**). Interestingly, with thioureas **122**, the nitrogen nucleophile outcompeted the sulfur nucleophile.

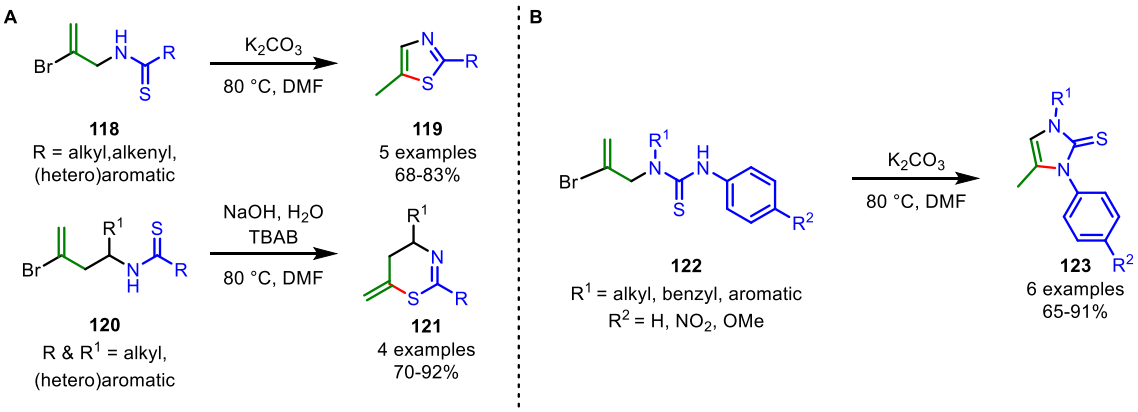

Scheme 28. Intramolecular nucleophilic vinylic substitution of vinyl bromides 118, 120 and 122 in which thioamides (A) and thioureas (B) act as the nucleophile. Blue represents the nucleophile. Green represents the electrophile. Red represents the new bonds formed.

Intramolecular sulfur substitution of bromide via the S_NV reaction was demonstrated to be high yielding for the synthesis of various thietanes (**125** and **127**) by reacting α-substituted and α-unsubstituted vinyl bromides **124** and **126** bearing a thioacetate group with potassium carbonate in DMI at 120 °C (Scheme 29A&B).[74,77] Only the $S_NV\pi$ TS (**124-TS**), with an activation energy of 20.0 kcal/mol in DMF, was identified for **124** (Scheme 29C); the $S_NV\sigma$ route becomes unfavourable due to steric clash between the isopropylidene group and the thiolate. Interestingly, theoretical calculations for the cyclisation of **126** identified both the $S_NV\pi$ (**126-TS1**) and $S_NV\sigma$ (**126-TS2**) TS structures with similar activation energies of 18.2 kcal/mol and 22.4 kcal/mol respectively in DMF (Scheme 29D).[71] However, the S_NV reaction of **(*Z*)-128** and **(*E*)-128** gave thietanes **(*Z*)-129** and **(*E*)-129**, respectively, with complete retention of configuration, which suggests that the reaction proceeds via the $S_NV\pi$ mechanism (Scheme 29E).[77]

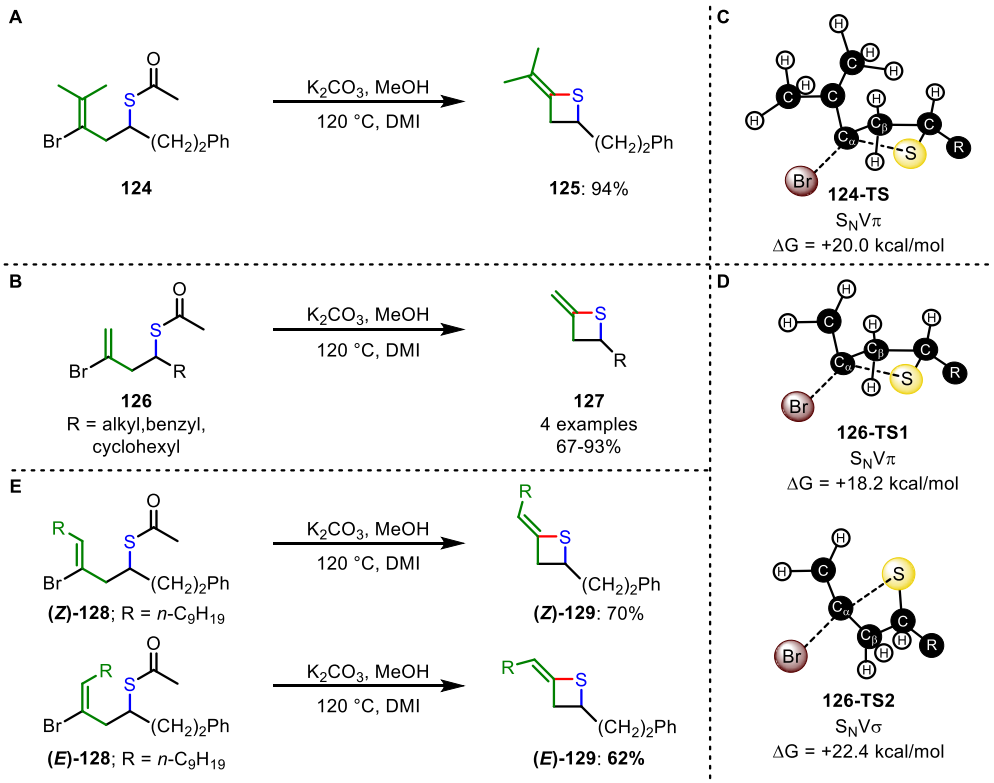

Scheme 29. Intramolecular nucleophilic vinylic substitution of vinyl bromides 124 (A) and 126 (B) by a sulfur nucleophile and the calculated structures of the corresponding transition states (C & D) with experimental proof for the $S_NV\pi$ mechanism (E). Blue represents the nucleophile. Green represents the electrophile. Red represents the new bonds formed.

Lithium alkylidene carbenoids bearing a bromo leaving group have been shown to undergo intramolecular S_NV reactions as well.[73] The treatment of geminal dibromopropenes **130** and dibromoalkenols **134** with *n*-BuLi gave indenes and dihydronapthalenes (**133**) and dihydrofurans (**135**) in good yields (Scheme 30A&B). It was envisioned that on reaction of **130** with *n*-BuLi a lithium-bromine exchange would take place resulting in the generation of an alkylidene carbenoid **131** – which is in equilibrium with the isomer in which the Br is *cis* to the tethered nucleophile as isomerisation occurs even at low temperatures – which then would be attacked intramolecularly to form alkenyllithium **132** that upon reaction with an electrophile would afford **133** (Scheme 30A). Theoretical calculations on the reaction with **134** (R = H) showed that the most stable alkoxy carbenoid structure **136** was formed and then, with a significantly low activation energy of 5.58 kcal/mol, transition state structure **136-TS** was adopted; the fact that the C–Br bond is almost broken upon a slight decrease in the distance between the incoming oxygen nucleophile and the α-carbon suggests a concerted $S_NV\sigma$ mechanism is followed (Scheme 30C).[78]

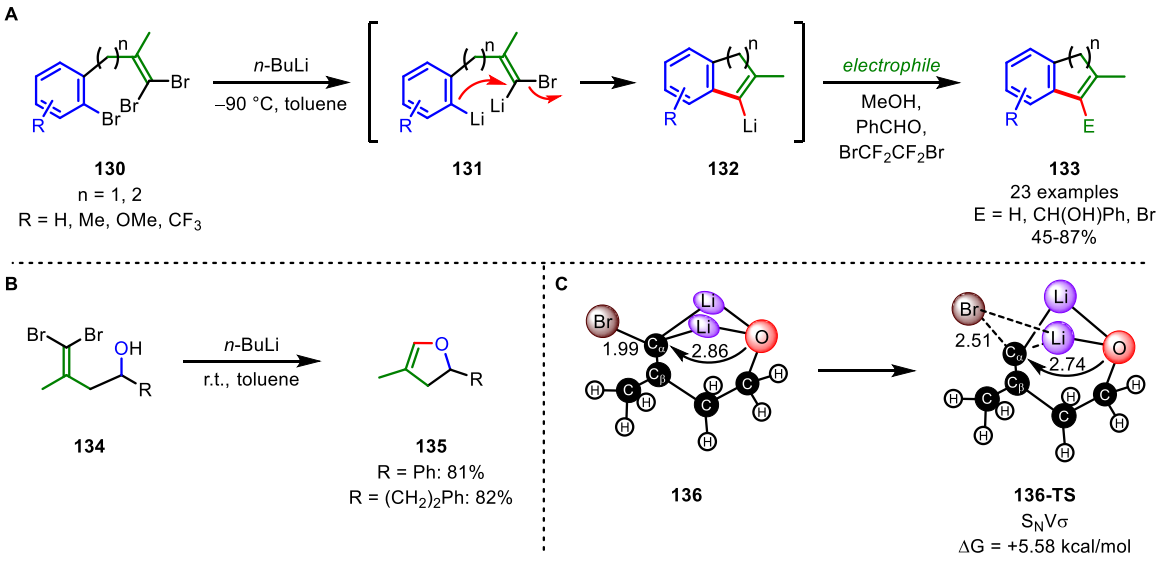

Scheme 30. Intramolecular nucleophilic vinylic substitution of lithium alkylidene carbenoids 130 and 134 bearing a bromo leaving group (A & B) and the calculated structure of the corresponding transition state for the rearrangement of 134 (C). Bond lengths are depicted in angstroms (Å). Blue represents the nucleophile. Green represents the electrophile. Red represents the new bonds formed.

1.2 The Use of Ureas in S_NV Reactions

As described in Section 1.1, nucleophilic vinylic substitution (S_NV) reactions have received considerable attention in recent years, and both inter- and intramolecular variants of the reaction have been demonstrated in the synthesis of various substituted aliphatic and (hetero)cyclic alkenes. Interestingly, examples of the S_NV reaction where a carbon nucleophile is used are rare, and all intramolecular S_NV reactions result in cyclisation products with expulsion of the leaving group. Formation of non-cyclised products in intramolecular S_NV reactions could, however, be established if the incoming nucleophile is tethered to the leaving group rather than having the leaving group and nucleophile on opposite sides of the alkene (Figure 2); this approach has been pioneered by Clayden and co-workers with the use of ureas (section 1.2.3).

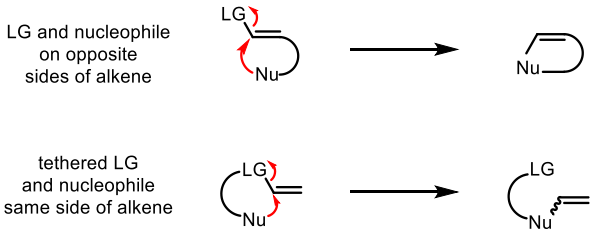

Figure 2. Formation of cyclised versus non-cyclised alkene products based on the position of the leaving group and the nucleophile on the starting alkene.

1.2.1 Ureas and their Conformations

Like S_NV reactions, ureas have not been well-recognised, rather they have been considered as unreactive and mainly ignored as a functional group since their synthesis was discovered in 1828 by Wöhler. However, more recently, ureas have emerged to the centre of synthetic chemistry and their utility has grown rapidly.[79] Urea derivatives now find use as scaffolds in supramolecular and medicinal chemistry, hydrogen-bonding organocatalysts, ion transporters, selective directors of lithiation, protecting groups and substrates for amination and novel rearrangements.[79,80]

The unique reactivity of ureas and their wide exploitation in medicinal and supramolecular chemistry originates, at least in part, from the predictable conformational properties of ureas. Because of the delocalisation of the non-bonded electrons on the nitrogens into the carbonyl, the urea moiety can be drawn in three possible resonance structures (**137**, **138** and **139**), in which an approximate trigonal planar geometry is adopted for the urea nitrogens and the substantial N–C double-bond character gives rise to the planar conformation of the urea (Figure 3).[81]

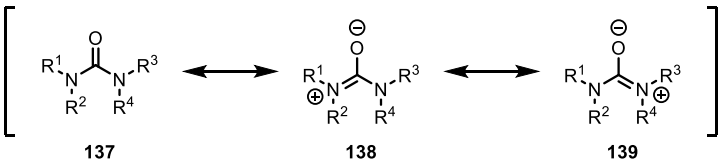

Figure 3. The resonance structures of ureas.

The four substituents on nitrogen are well organised due to the planarity of the urea backbone (N–C(=O)–N), but the N-substituents themselves can twist out of the urea plane to minimise unfavourable intramolecular non-bonding interactions, which can play a key role in the overall preference of the urea conformation. In the case of *N*,*N*'-diphenylurea **140**, a *Z*,*Z* conformation is preferred, mainly due to steric factors that prefer *N*-H > *N*-aryl > *N*-alkyl to be *anti* to the carbonyl, and delocalisation of π-electrons between the urea moiety and the coplanar aryl rings (Figure 4). However, in the case of mono-methylated derivative **141**, the *N*-aryl instead of the *N*-methyl prefers to be *anti* to the carbonyl in order to mitigate electronic repulsion between the π-electrons of the aromatic ring and the carbonyl oxygen lone pair (Figure 4). After double *N*-methylation, *N*,*N*'-diphenylurea **142** is formed with a favoured *E*,*E* conformation in which the aromatic rings are twisted out of the urea plane to minimise steric interactions of the ortho aromatic hydrogens with each other and the methyl groups, and allow additional stabilisation through π-π stacking interactions (Figure 4).[82,83]

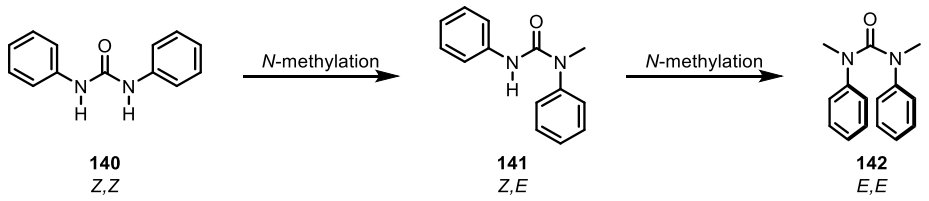

Figure 4. Conformational change of ureas depending on the four nitrogen substituents and their favoured interactions.

1.2.2 *N*-Aryl Migration in *N*-Benzyl and *N*-Allyl Ureas

New C–C bond formation methods have been developed by the Clayden group; by utilising the conformational restriction of the urea tether (section 1.2.1), intramolecular coupling partners are brought in close proximity enabling reactivity without the use of transition metals.

While investigating the lithiation sites of *N*-aryl ureas,[84,85] rearrangement of *N*-aryl-*N*'-benzyl urea **143** in which the *N*-aryl group migrates to the benzylic α-lithiated carbon forming urea **144** was observed (Scheme 31A).[86,87] Various benzylic ureas, containing sterically hindered, electron-deficient and/or electron-rich migrating aryl groups, were rearranged in high yields using *s*-BuLi. In addition, it was reported that enantiomerically pure *N*-aryl-*N*'-α-methylbenzyl ureas **145** rearranged to ureas **146** with a high degree of stereospecificity (Scheme 31B). As this rearrangement was much slower, DMPU was added, owing to its ability to increase the reactivity of the organolithiums formed upon lithiation.[88,89] It was proposed that the rearrangement is intramolecular as no cross-over products were found in the designated cross-over experiment; the initial deprotonation forms stereochemically retentive lithiation intermediate **147**, which then displays configurational stability at –78 °C over the reaction time (Scheme 31B).[90] For the nucleophilic attack on the migrating aryl group it was assumed, based on DFT calculations and modelling, that the lithium ion moves to the face of the phenyl group (**148**), pointing towards the migrating aryl group as in this way the lithium ion can stabilise the developing charge on the migrating aryl group.[91] The transition state **148** explains the stereochemically retentive outcome of the rearrangement of urea **145** to urea **146**, which is generated upon nucleophilic attack, breakage of the N–C bond and subsequent protonation (Scheme 31B).[86,92]

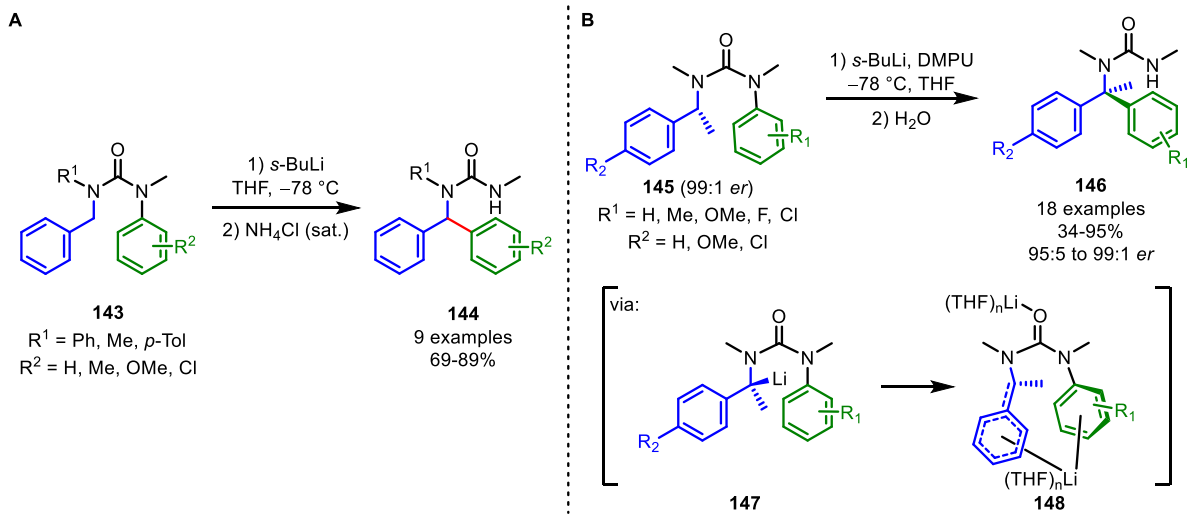

Scheme 31. *N*-Aryl migration to the benzylic α-lithiated carbon in *N*-aryl-*N*'-benzyl ureas 143 (A) and 145 (B). Blue represents the nucleophile. Green represents the electrophile. Red represents the new bonds formed.

With slightly adjusted conditions, this Clayden rearrangement method was expanded to *N*-α-methylbenzyl-*N*'-pyridylureas (**149→150**, Scheme 32A),[93] *N*-pyridinylmethyl-*N*'-arylureas (**151→152**, Scheme 32B),[94] more hindered benzyl ureas (**153→154**, Scheme 32C)[95] and *N*-benzyl-*N*'-benzofused ureas (**155→156**, Scheme 32D),[96] but also *S*-α-methylbenzyl-*N*'-aryl thiocarbamates (**157→158**, Scheme 32E)[97] and *O*-α-methylbenzyl-*N*'-aryl carbamates (**159→160**, Scheme 32F)[98]. Interestingly, the rearrangements generally took place with retention of stereochemistry, yet for the rearrangement of benzylic carbamate **159** inversion of stereochemistry was observed. An explanation for this is that the lithium ion is oxyphilic and thus will transfer, during the nucleophilic attack, to the oxygen adjacent to the carbonyl preferentially (**163→164**) instead of to the aryl group (**161→162**), but this is only possible when C–O bond rotation takes place to allow the Li–C bond to point away from the migrating aryl group (**161→163**) – resulting in inversion (Scheme 32G).[91]

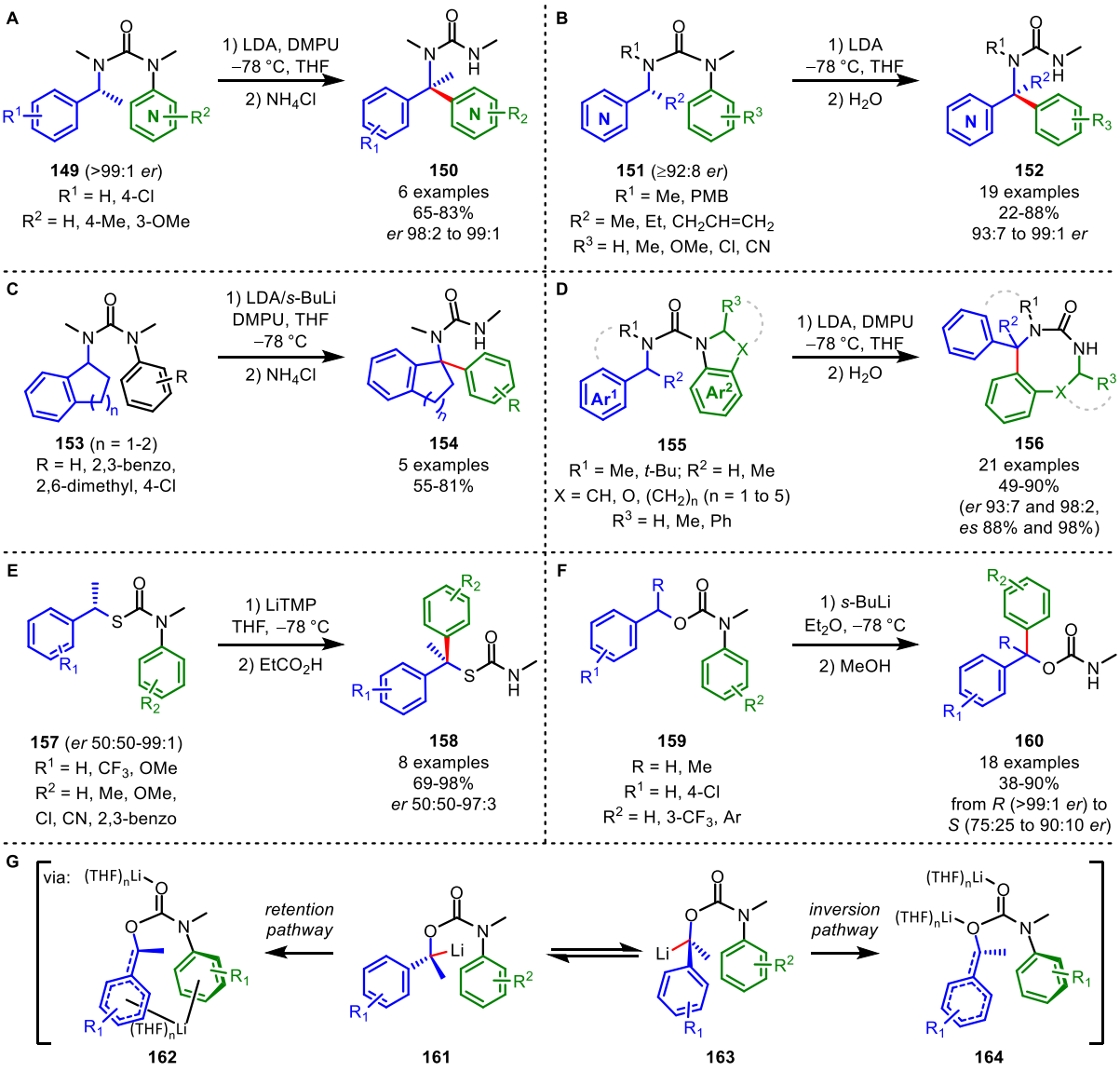

Scheme 32. *N*-Aryl migration to a broad scope of *N*-benzyl ureas (A–D), thiocarbamates (E) and carbamates (F) and the corresponding intermediates to explain observed stereochemistry (G). Blue represents the nucleophile. Green represents the electrophile. Red represents the new bonds formed.

Besides successfully extending the *N*-aryl migration to amino-acid and amino-nitrile derived ureas,[99–105], Clayden and co-workers also proved that the rearrangement method is effective with *N*-aryl-*N*'-allyl ureas. Upon treatment of *N*-aryl-*N*'-allyl ureas **165** with LDA and DMPU in the coordinating solvent THF, both electron-rich and electron-deficient aryl groups were successfully migrated yielding *N*-vinyl ureas **166** exhibiting *Z*-geometry (Scheme 33A).[106] It was proposed that first deprotonation takes place at the α-allylic carbon to form *N*-lithioallyl intermediate **167**, which then undergoes an intramolecular nucleophilic attack on the distal aryl group yielding lithiated urea **168**. A second lithiation (**169**) takes place whereupon **166** is formed in moderate to high yields. When a second aryl group (**170**) is installed, another *N*-aryl migration can take place enantioselectively with the use of a chiral lithium amide, *N*-isopropyl-α-methylbenzylamine as a lithium salt, to afford *N*-allyl ureas **171**

(Scheme 33B).[106] Based on the rearrangement of racemic *N*-allyl urea **172** with the same chiral lithium amide, it was determined that the formation of the allyllithium, and not the rearrangement itself, gives rise to the stereoselectivity, as **171** was obtained in racemic form (Scheme 33B).[106]

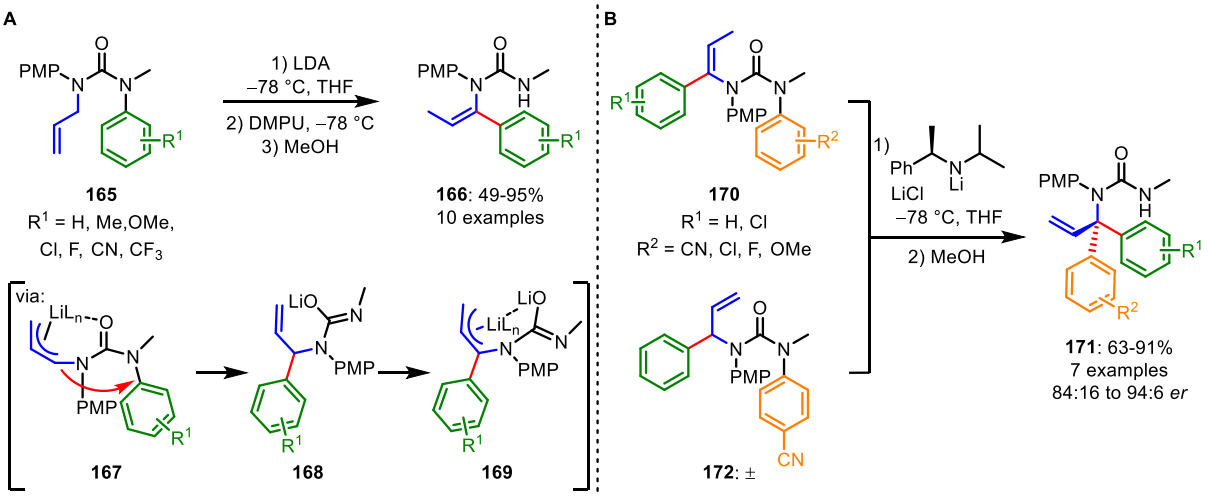

Scheme 33. *N*-Aryl migration to the allylic α-lithiated carbon in *N*-aryl-*N*'-allyl urea 165 (A) and *N*-aryl-*N*'-vinyl urea 170 (B). Blue represents the nucleophile. Green represents the electrophile. Red represents the new bonds formed. Orange represents the second electrophile.

1.2.3 *N*-Vinyl Migration in *N*-Benzyl Ureas and Amino-Nitrile and Amino-Acid Derived Ureas

Besides *N*-aryl ureas that undergo intramolecular rearrangements (section 1.2.2), *N*-vinyl ureas (or *N*-carbamoyl enamines) have emerged as a valuable compound class displaying remarkable reactivity toward strong bases, in particular organolithiums.[107,108] Enamines possess ambiphilic reactivity,[107] clearly exemplified by *N*-vinyl urea **173** that on electrophilic attack of bromine gives β-bromoenamine **174** (Scheme 34A), yet affords carbolithiation product **176** on nucleophilic attack of an organolithium at the same site (Scheme 34B).[108] The electrophilic character of *N*-vinyl ureas towards organolithiums can be attributed to the combination of the reactive π complex being bonded to the electron-deficient urea nitrogen and the electron-rich C=O group being able to coordinate to the lithium.[79] Interestingly, it was found that the initial carbolithiation was followed by an attack of the formed benzyllithium on the second electrophilic site – the *N*-aryl ring (green in **176**) – to yield rearrangement product **177** (Scheme 34B).[106,109–111]

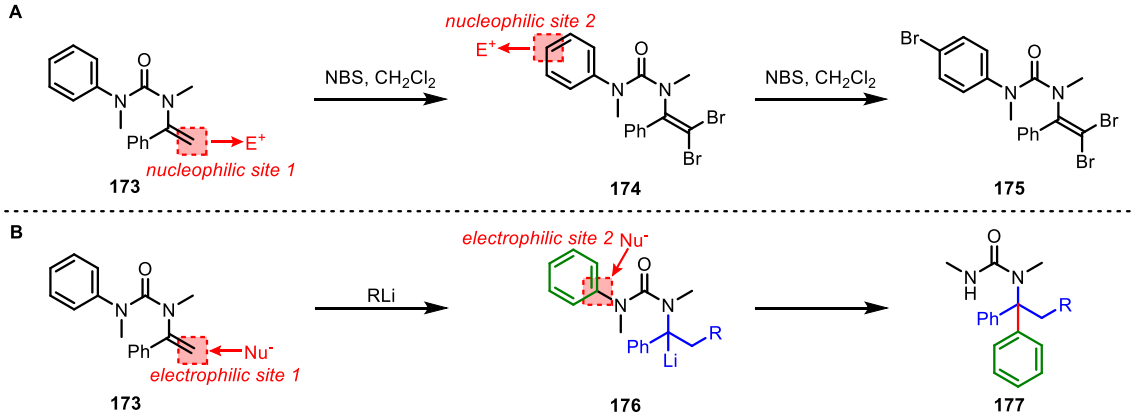

Scheme 34. *N*-Vinyl urea 173 possesses ambiphilic reactivity which is illustrated by the electrophilic attack of bromine (A) and nucleophilic attack of an organolithium (B). Blue represents the nucleophile. Green represents the electrophile. Red represents the new bonds formed.

Given that the intramolecular nucleophilic substitution at aryl groups, including electron-rich variants, of *N*-aryl ureas results in the migration of those aryl groups to the lithiated centre (Scheme 34B), the N→C migration of vinyl groups was examined to investigate the feasibility of an intramolecular S_NV reaction in the synthesis of non-cyclised products with ureas serving a dual role as both the leaving group and the linker to the tethered carbon nucleophile.

With success, various *N*-vinyl-*N*'-benzyl ureas (**178**) were rearranged using *s*-BuLi at –78 °C in THF generating non-cyclised N→C vinyl migration products **179** in good yields, as exclusive *Z*-isomers (Scheme 35A).[112] The addition of DMPU, a lithium-coordinating additive known to form solvent-separated ion pairs and facilitate the nucleophilic attack of organolithiums on alkenes/arenes, enabled the N→C vinyl migration of enantiopure ureas **180** and led to the completely enantiospecific formation of rearrangement products **181** in moderate to good yields (Scheme 35B).[112] Under similar conditions, *N*-vinyl ureidonitriles **182** rearranged by nucleophilic attack of the lithiated nitrile moiety on the *N*-vinyl group and generated, with high tolerance for steric bulk, N→C migration products **183** in good to excellent yields with retention of the carbon-carbon double-bond geometry (Scheme 35C).[113] Using KHDMS as the base, enantio- and diastereomerically pure *N*-vinylureido imidazolidinones **184** bearing a wide variety of alkyl or benzyl groups underwent diastereoselective N→C vinyl migration to generate products **185** in moderate to excellent yields with preservation of enantiopurity and retention of the carbon-carbon double-bond geometry (Scheme 35D).[114] The vinyl group migrates *anti* to the *tert*-butyl group in the case of the *E*- and *Z*-isomers as the top face of the derived enolate of ureas **184** is less hindered. However, the diastereoselectivity of the migration for the *E*-isomers is sensitive to competition between the olefins and the R^2 groups for the *anti*-position to the *tert*-butyl, and thus is dependent on the size of the R^2 group: the more hindered, the lower the diastereoselectivity obtained.[114]

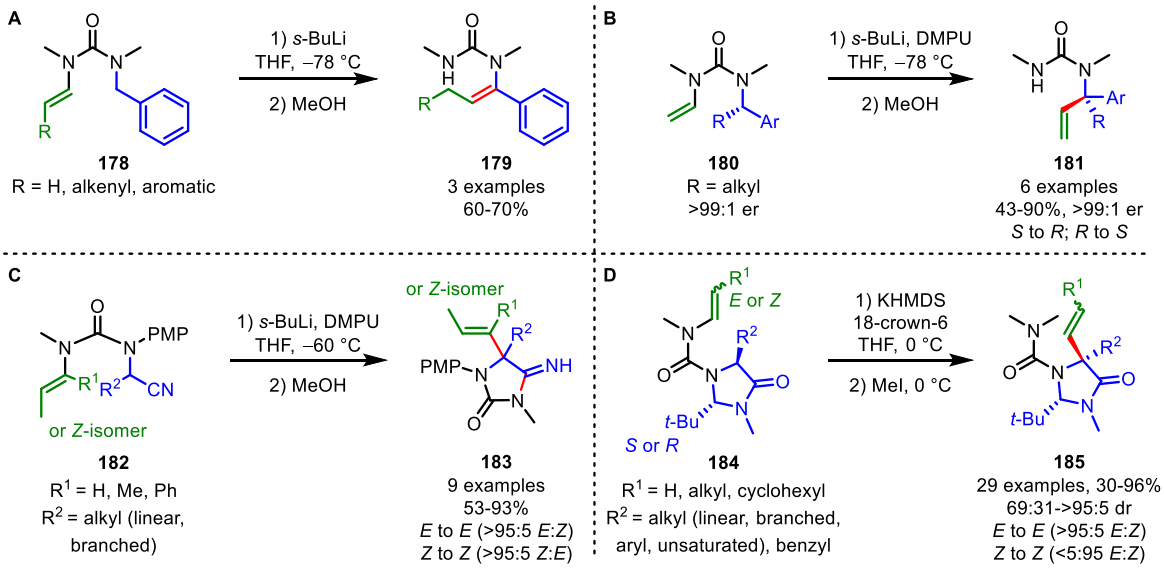

Scheme 35. Intramolecular S_NV reaction of *N*-vinyl-*N'*-benzyl ureas 178 (A) and 180 (B), *N*-vinylureidonitriles 182 (C) and *N*-vinylureido imidazolidinones 184 (D) by treatment with *s*-BuLi or KHMDS to generate various non-cyclised rearrangement products. Blue represents the nucleophile. Green represents the electrophile. Red represents the new bonds formed.

As described at the start of this section, *N*-carbamoyl enamines (*N*-vinyl ureas) are typically associated with having nucleophilic character and reacting with electrophiles such as bromines; hence, the success of the N→C vinyl migration using *N*-carbamoyl enamines **178**, **180**, **182** and **184** as internal electrophilic vinylating agents makes elucidating the reaction mechanism of significant interest. *In situ* IR spectroscopy experiments and DFT calculations were performed with ureas **180**, **182** and **184**, and the mechanisms proposed are depicted in Scheme 36.[112,113] The first step in all three of the proposed mechanisms is deprotonation followed by coordination of the counterions to form complexes **186**, **192** and **196**. The counterions organise in such a way that they can stabilise the developing negative charge upon intramolecular attack of the carbon nucleophile, which results in a *syn* addition to the carbon-carbon double-bond, retaining its geometry. Five-membered intermediates **188** and **193** are then formed; these are not detected but their existence is expected and supported by the rare cases where cyclised products (**190**→**191**) were obtained when, probably, **188** is more stable than **187** and **189**, yet the cyclisation may be reversible. With **193** bond rotation takes place and generates **194** that subsequently undergoes *anti*-elimination, likewise with intermediate **188**, to form compounds **189** and **195** (Scheme 36A&B). Steric interactions prevent the bond rotation of **198** and thus *syn*-elimination is thermodynamically favourable, resulting in compound **199** where the carbon-carbon double-bond geometry is retained (Scheme 36C). The proposed mechanisms of the N→C vinyl migration show a S_NV reaction that follows an addition-elimination route, yet the precise mechanisms are still not clear and require further investigation. Besides the proposed multistep Ad_N-E pathway, a concerted $S_NV\pi$ mechanism could be followed and account for the apparent stereoretention in these N→C vinyl migrations.

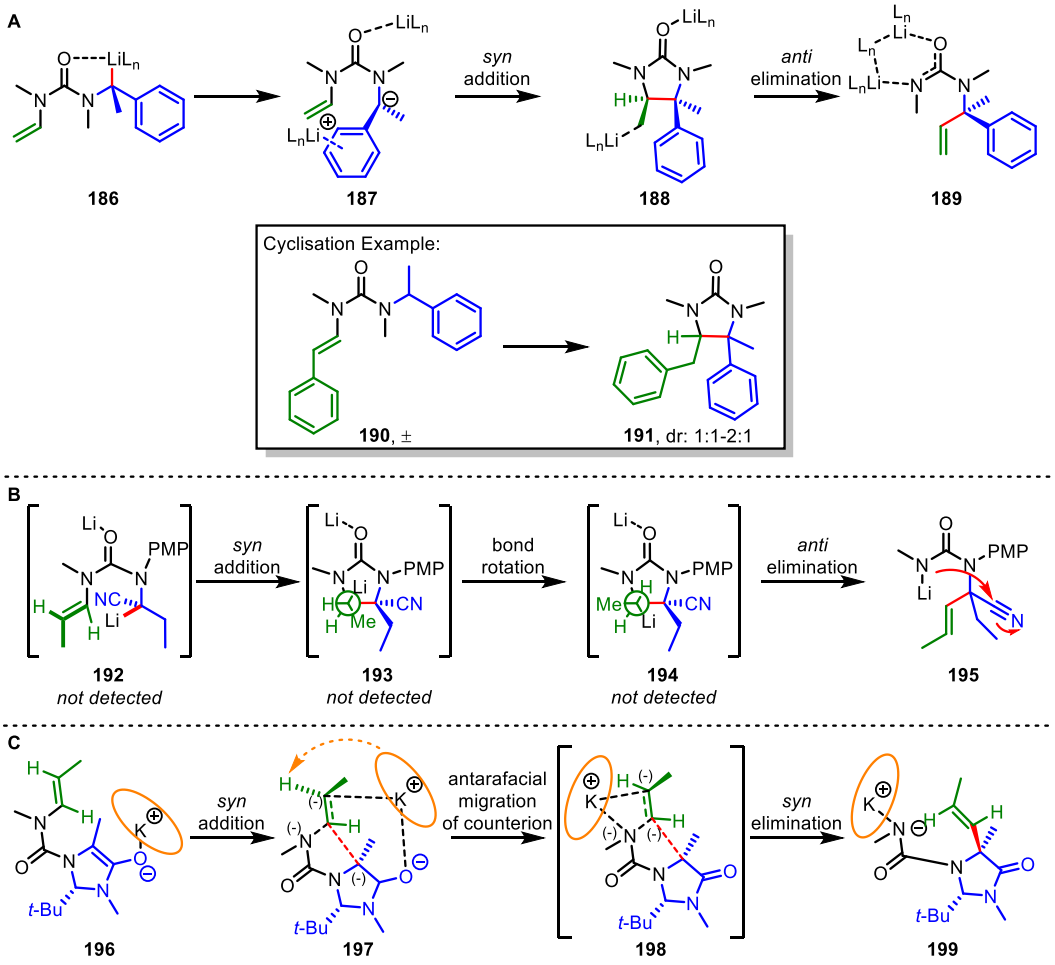

Scheme 36. Comparison of the proposed mechanisms and corresponding intermediates in the rearrangement of ureas 180 (A), 182 (B) and 184 (C).

1.3 Project Aim

As described in section 1.2.2, Clayden and co-workers have demonstrated that *N*-allyl groups in *N*-aryl-*N*'-allyl ureas are effective in the N→C migration of aryl groups by having the allyl group act as the carbon nucleophile. Similarly, they developed an intramolecular S_NV reaction of *N*-vinyl ureas by using carbon nucleophiles such as benzyl groups and imidazolidinones while having the urea serve a dual role as both the leaving group and the linker to the tethered carbon nucleophile, so giving access to a set of non-cyclised alkenes (section 1.2.3).

Taking inspiration, the aim of this project is to investigate the applicability of the N→C vinyl migration to symmetrical and unsymmetrical *N*,*N*'-diallyl ureas (**200**) for the development of a novel intramolecular S_NV reaction, unlocking access to a wider range of unusual non-cyclised alkenes (**201** and/or **202**) (Scheme 37). It was hypothesised that upon treatment of base, α-deprotonation of **200** would lead to isomerisation of an allyl group (**203**→**204**). Then, bond rotation after a second α-

deprotonation (**204**→**205**) could enable the intramolecular nucleophilic attack on the vinylic carbon in **205** to form **201** and upon an additional isomerisation **202** (Scheme 37).

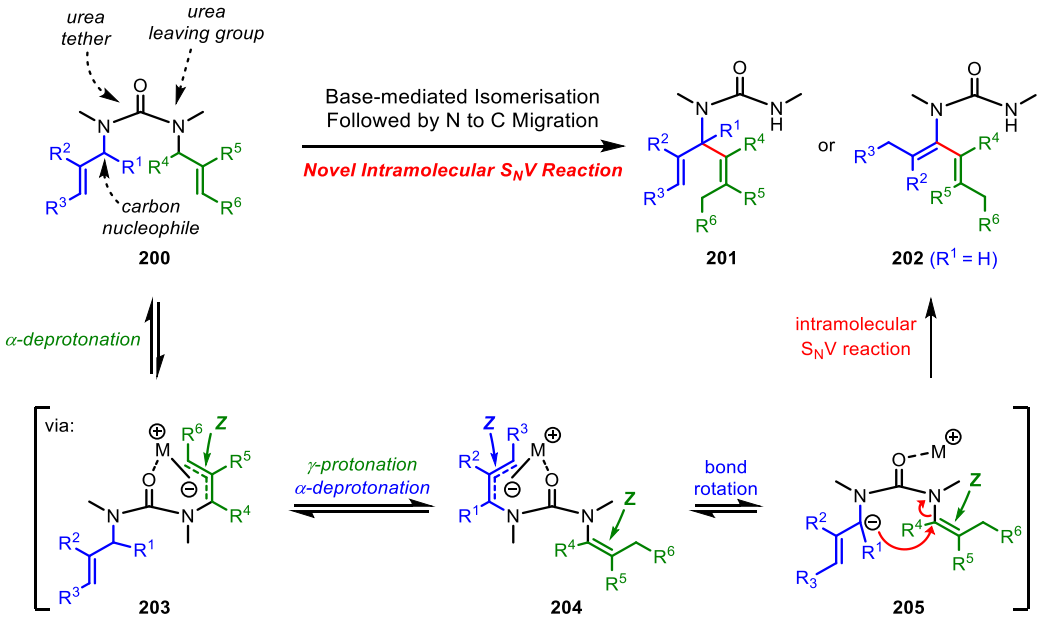

Scheme 37. Potential new intramolecular S_NV reaction exploiting the N→C vinyl migration in symmetrical and unsymmetrical *N*,*N*'-diallyl ureas and the hypothesised mechanism of action.

The first stage of this project would be initiated by examining the feasibility and limitation of the N→C vinyl migration using a simple symmetrical diallyl urea. In this way, optimal conditions could be developed, which could be utilised to first probe the affectability of this intramolecular S_NV reaction by installing a methyl group at the α-, β-, and γ-position of the *N*-allyl group respectively to then extend to more complex diallyl ureas containing more functionality. However, first, a simple, effective general method to prepare a variety of symmetrical and unsymmetrical *N*,*N*'-diallyl ureas should be developed.

Subsequently, the unusual reactivity at sp^2-hybridised carbons with its corresponding mechanism and the potential stereospecificity of the alkene geometry would be explored by various mechanistic studies. Moreover, the use of unsymmetrical *N*,*N*'-diallyl ureas would raise intriguing questions about the regioselectivity of this intramolecular S_NV reaction, because opposite directions of N→C vinyl migration would lead to structurally isomeric products.

Later stages would focus on exploiting the N→C vinyl migration products in for example cycloaddition chemistry,[115] with the anticipation to enable the synthesis of new valuable scaffolds and structural libraries for drug discovery and medicinal chemistry.

2.0 Synthesis of Symmetrical and Unsymmetrical Diallyl Ureas

The work presented in this chapter has been partially published in the first author publication:

B. C. Van Veen, S. M. Wales, J. Clayden, *J. Org. Chem.* **2021**, *86*, 8538–8543.[1]

2.1 Initial Results

Previous work in the Clayden group has shown that the reaction between amines and carbamoyl chlorides or isocyanates is an established and reliable method to access functionalised ureas.[93,104,106,108,116,117] For the purposes of generality, it was considered that with the use of carbamoyl chlorides a wider range of variously substituted symmetrical and unsymmetrical diallyl ureas could be synthesised more accessibly.

With the use of conditions slightly adjusted compared to those reported previously by Clayden *et al.*,[99,114] a high yielding method was developed, consisting of two steps: chloroformylation of secondary amines (e.g. *N*-methyl-*N*-allylamine) using triphosgene, followed by reaction of the generated carbamoyl chloride with the same or another amine to form the symmetrical or unsymmetrical diallyl ureas (Scheme 38A). Then if desired, their *E*-isomerised divinyl derivatives could be easily prepared by stereoselective olefin isomerisation using a ruthenium catalyst (Scheme 38B).[113]

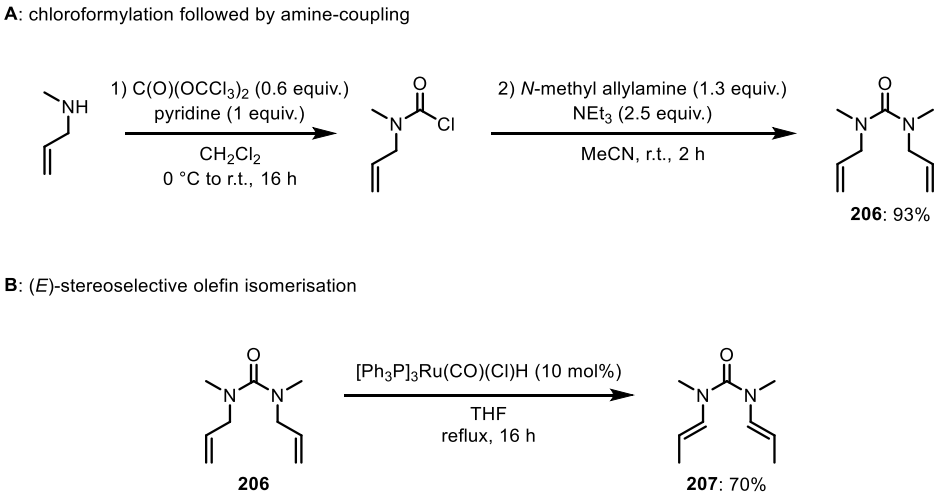

Scheme 38. General method for the synthesis of symmetrical and unsymmetrical diallyl and *E*-vinyl ureas.

This stereoselective alkene isomerisation can be mechanistically explained according to a metal hydride addition-elimination pathway, displayed in Scheme 39.[118–120] The first step is the coordination of alkene **208** to the ruthenium hydride species, whereupon species **209** is generated. Then, organoruthenium complexes **210** and **211** can be afforded by insertion into the metal hydride bond. The formation of primary alkyl **210** is more thermodynamically favoured, but kinetically reversible. β-Hydride elimination of **211** will generate organoruthenium complex **212** which forms product **213** and regenerates the catalyst. The fact that the β-hydride elimination is *E*-selective can be explained with a Newman projection. In comparison with the transition state towards *Z*-geometry, the transition state towards *E*-geometry experiences less steric clash of the methyl group with the urea moiety, of which the carbonyl could coordinate to the ruthenium catalyst as well, and thus is favoured.

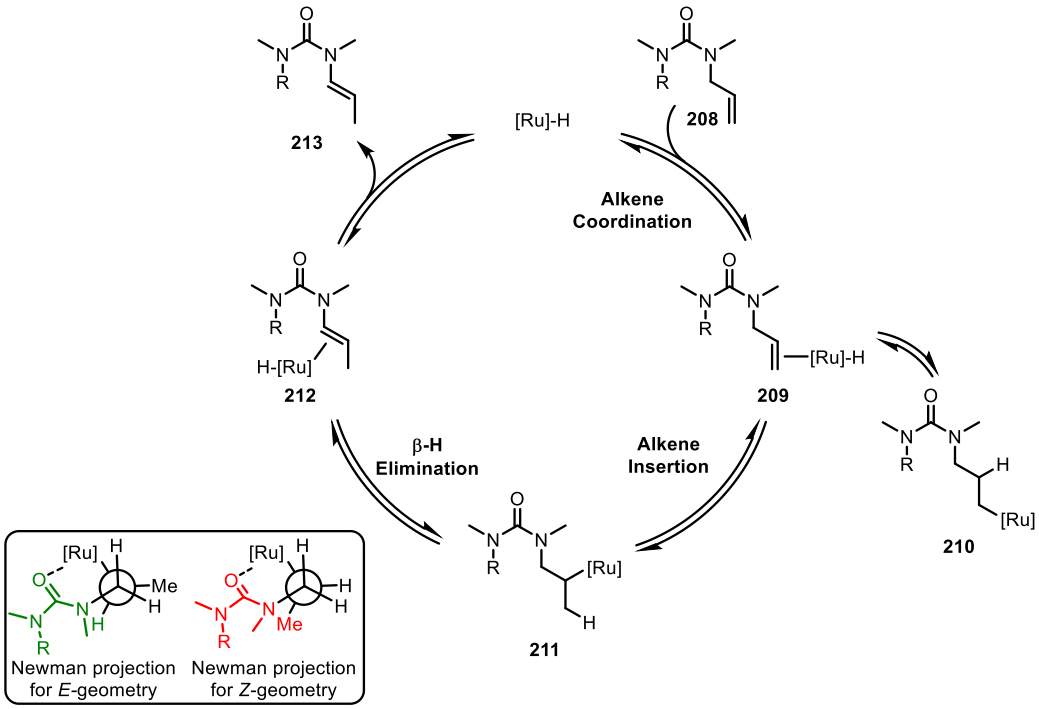

Scheme 39. Mechanistic explanation for the *E*-stereoselective olefin isomerisation using a ruthenium catalyst.

The high effectiveness of this starting urea synthesis method was demonstrated with the synthesis of the first set of (di)allyl ureas generated in good to excellent yields, with applicability to both *N*-methylated *N*-alkyl and *N*-allyl amines, even as endocyclic *N*-allyl amines (Scheme 40). Yet, when we wanted to synthesise a wider range of diallyl ureas in order to develop the key N→C vinyl migration method, it was found that the commercial availability of variously substituted *N*-methyl allylamines is very limited and thus presented a major drawback to the current synthesis method. Therefore, this chapter discusses the various attempts to generalise both the direct synthesis of symmetrical and unsymmetrical diallyl ureas, along with the synthesis of substituted *N*-methyl allylamines.

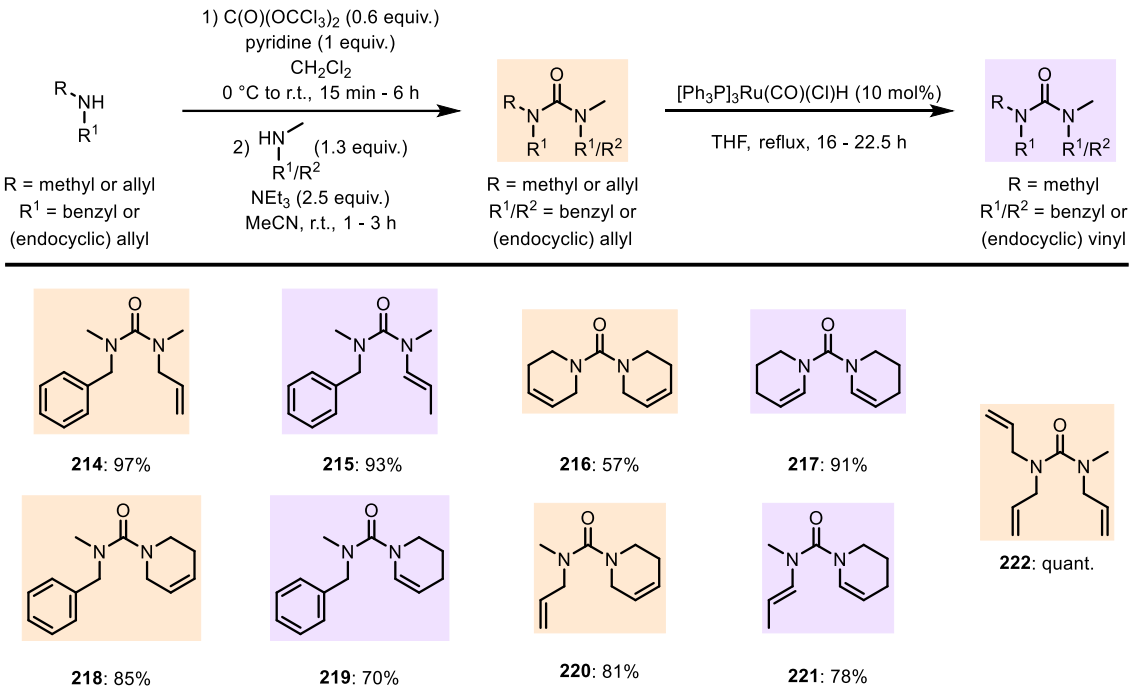

Scheme 40. Synthesis of (di)allyl and (*E*)-(di)vinyl ureas.

2.2 Results and Discussion

2.2.1 Direct Urea *N*-Allylation using Allyl Halides and Sulfonates

With the aim of finding a general method to synthesise variously substituted symmetrical and unsymmetrical diallyl ureas, we proposed that a more straightforward and efficient way would be to perform direct *N*-allylation of 1,3-dimethylurea **223** and 1-allyl-1,3-dimethylurea **224** with allyl halides or sulfonates.

Initially, when **223** was treated with 1.2 equivalents of allyl bromide and 1.0 equivalent of sodium hydride, mono-allylation product **224** was afforded in a modest yield of 40%, accompanied by the (readily separated by column chromatography) symmetrical diallyl urea **206** in 12% yield (Table 1, entry 1). Treating **223** with 2 equivalents of allyl bromide and 2.2 equivalents of sodium hydride afforded symmetrical diallyl urea **206** in a good yield of 75%, with mono-allylation product **224** in 13% yield (entry 2).

Table 1. Discovery of conditions for the direct *N*-allylation of 1,3-dimethylurea 223.

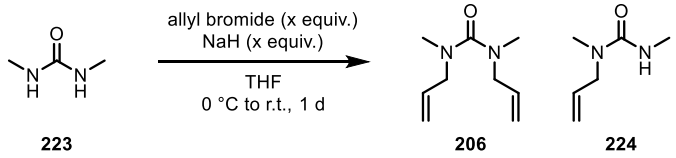

Entry	Allylbromide (equiv.)	NaH (equiv.)	206 (%)	224 (%)
1	1.2	1	12	40
2	2	2.2	75	13

With the success of the direct double *N*-allylation of **223** with a simple allyl bromide, the use of substituted allyl halides was attempted next for the syntheses of variously substituted *N*-allyl ureas (Scheme 41). However, when **223** was reacted with geranyl bromide and sodium hydride, symmetrical urea **226** was afforded in only a 40% yield yet accompanied by unsymmetrical urea **225** in a yield of 47%. The reaction of **223** with crotyl bromide afforded the desired urea **228** in only 20% yield; majorly unsymmetrical urea **227** was isolated in a yield of 57%. Similarly, the reaction of **223** with 3-bromo-2-methylpropene generated mono-allylation product **229** in 59% yield, yet only 9% yield of di-allylation product **230** was afforded. The reaction of **223** with commercially available α- and β-substituted allyl chlorides did not generate the desired symmetrical ureas **232**, **234** and **236**; only mono-allylated ureas **233** and **235** were afforded in low yields of 13% and 2%.

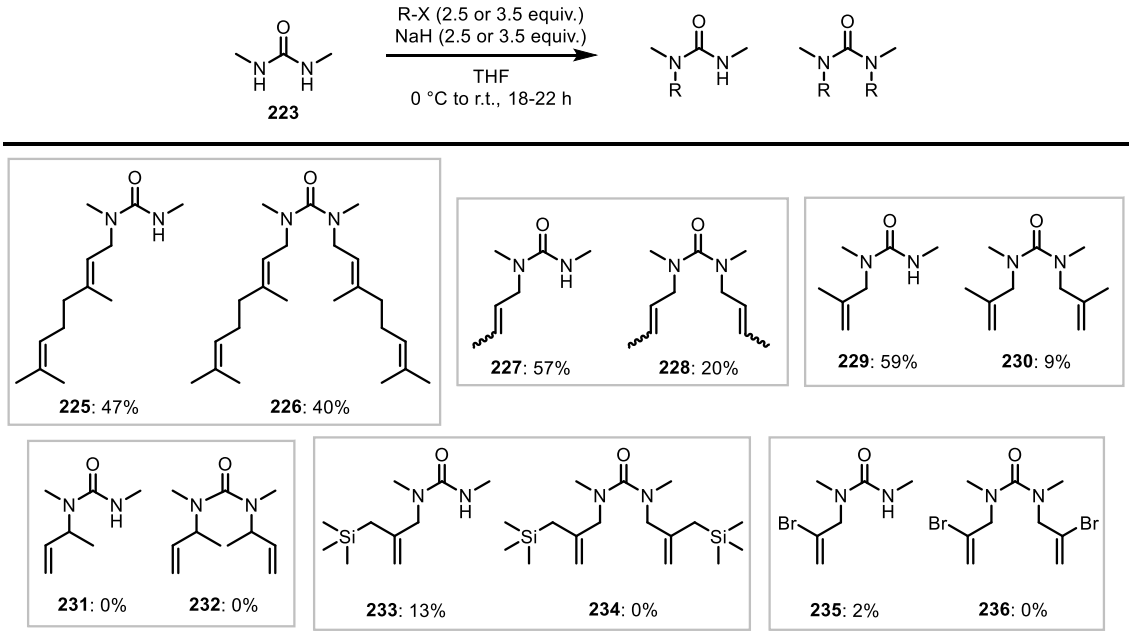

Scheme 41. Attempted direct double *N*-allylation of 1,3-dimethylurea 223 with various allyl halides.

Despite the unproductive double *N*-allylation of **223**, synthesis of unsymmetrical diallyl ureas was attempted through *N*-allylation of 1-allyl-1,3-dimethylurea **224** – prepared on a larger scale via chloroformylation of *N*-allylmethylamine and subsequent reaction with *N*-methylamine – under a variety of conditions (Scheme 42). However, the reaction of **224** with 3-chloro-1-butene, *trans*-2-chloromethylvinylboronic acid pinacol ester and prenyl bromide (in attempt to generate **237**, **238** and **239**) remained unsuccessful, even with elevated reaction temperatures, the use of TBAB as an additive to promote *in situ* conversion of the allyl chloride electrophile to the bromide, or with KHMDS as the base instead of NaH. Only when **224** was reacted with geranyl bromide, the formation of unsymmetrical urea **240** was observed in a low ratio of 0.2:1 with the unreacted starting urea (determined by NMR).

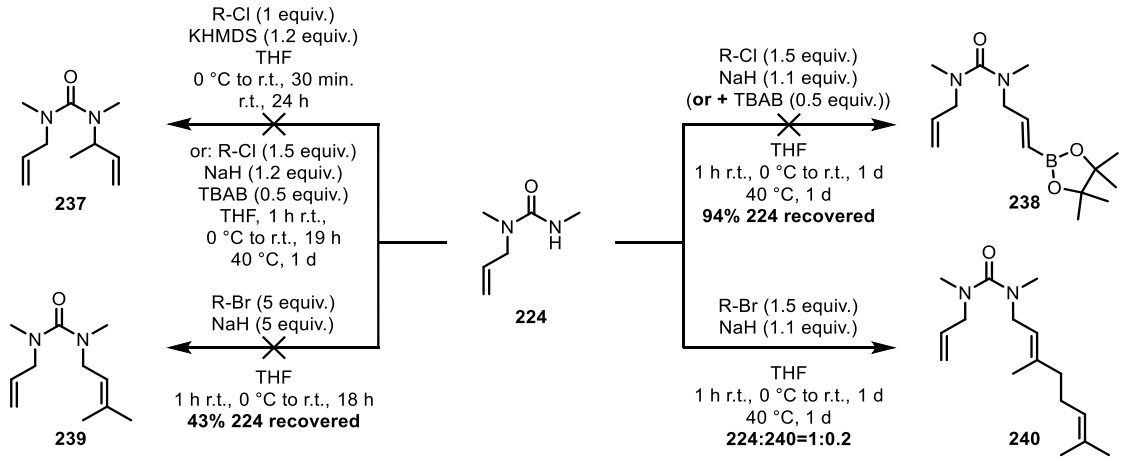

Scheme 42. Attempted direct *N*-allylation of 1-allyl-1,3-dimethylurea 224 with various allyl halides.

The direct *N*-allylation of γ-methyl-substituted derivative **227** proved more successful (with elevated temperatures and adding additional portions of the allylbromides and NaH during the reaction to increase the extent of conversion): unsymmetrical ureas **241** and **242** were afforded in yields of 35% (64% yield BRSM) and 46% (67% yield BRSM) (Scheme 43). Elevated temperatures were applied in the case of product **241** to try inducing a 3,3-sigmatropic rearrangement in case the allyl group had reacted at the oxygen instead of the nitrogen; no significant change was observed by TLC. The reaction of β-methyl-substituted derivative **229** with allyl bromide proved also successful and resulted in the formation of unsymmetrical urea **243** in a yield of 36% (61% yield BRSM) (Scheme 43). However, no reaction of **229** with 2-((trimethylsilyl)methyl)allyl chloride or 2-bromoallyl bromide took place.

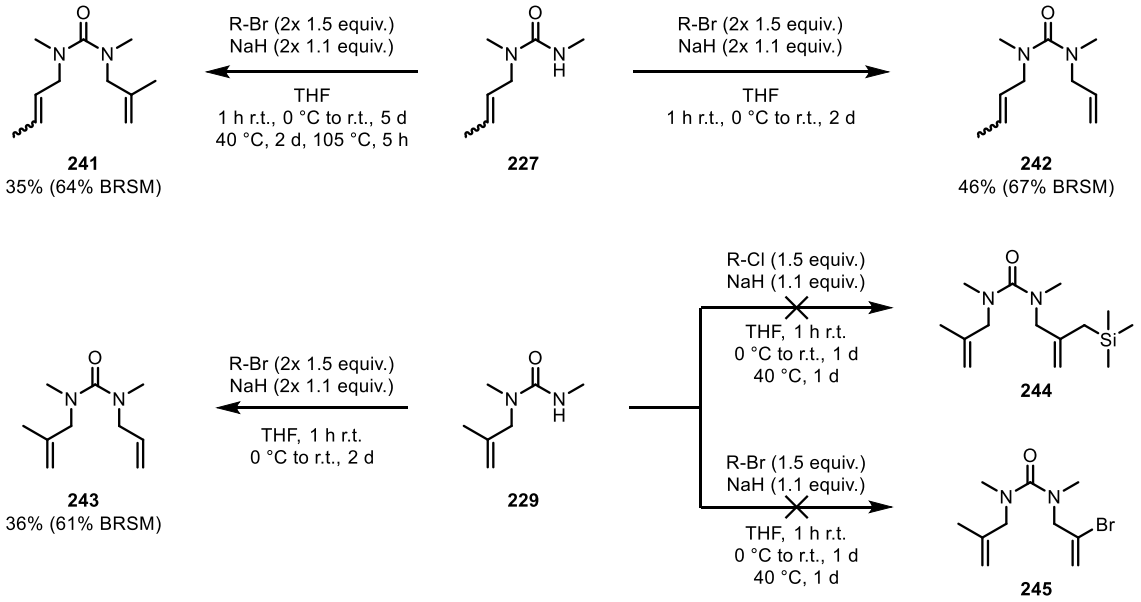

Scheme 43. Direct *N*-allylation of unsymmetrical ureas 227 and 229 with various allyl halides.

Overall, these results show that the base-promoted reaction of **223** with an α- or β-substituted allyl halide was mostly unsuccessful. In general, this method, starting from 1,3-dimethylurea **223** or a mono-allylated urea (e.g. **224**, **227** and **229**), is not consistently efficient and high yielding for the synthesis of symmetrical and unsymmetrical diallyl ureas. It was hypothesised that with a better leaving group such as a sulfonate in place of the halide this method could be more productive.

However, even though tosylation of 4,4,4-trifluorocrotyl alcohol and *trans*-3-(trimethylsilyl)allyl alcohol successfully provided the required electrophiles, which were used without further purification, the reaction of the tosylates with **224** and sodium hydride did not generate the desired ureas **246** and **247** (Scheme 44). Neither the addition of TBAB (to increase the nucleophilicity of the ureido anion by exchanging sodium for tetrabutylammonium) nor the application of moderate heat (40 °C) over an extended period of time promoted the desired reactions; only TBAB, the tosylates and starting material **224** were observed by crude NMR.

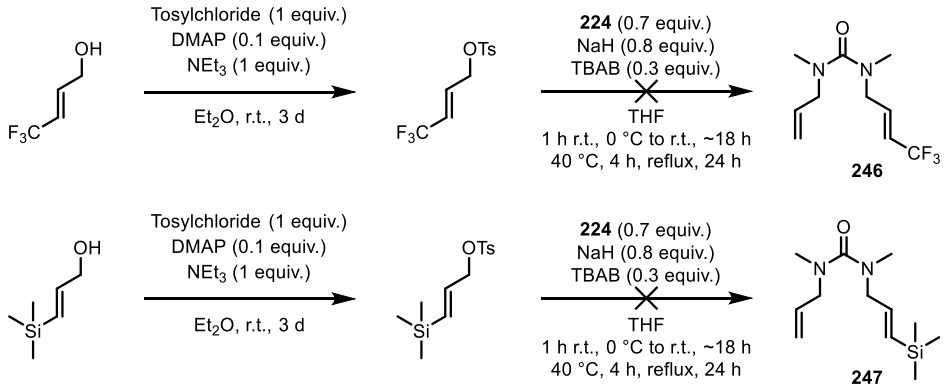

Scheme 44. Attempted direct *N*-allylation of 1-allyl-1,3-dimethylurea 224 with allyl sulfonates.

2.2.2 *N*-Allylation of Methylamine using Allyl Halides and Sulfonates

Despite the somewhat encouraging results in the synthesis of symmetrical and unsymmetrical diallyl ureas by reacting 1,3-dimethylurea and mono-allylated ureas with allyl halides, this method did not prove generally high yielding and consistent. Furthermore, the method was not applicable to the synthesis of α-substituted substrates. Therefore, mindful of the success with the original chloroformylation/amine-coupling method to assemble the desired ureas, we aimed to find a general and efficient way to access variously substituted *N*-methyl allylamines. This would then enable the easy formation of a range of symmetrical and unsymmetrical diallyl ureas by a simple 'mix-and-match' process using the chloroformylation/amine-coupling method.

Besides their application as starting materials for a range of synthetic transformations, allylic amines are widely used for the construction of natural products and pharmaceutical targets.[121,122] Therefore, it is unsurprising that various methods for the practical synthesis of allylic amines have been extensively developed. A few of the most well-known and widely applied approaches include Tsuji–Trost like reactions, which transforms allylic alcohols, acetates, halides, or carbonates via amination using a transition-metal catalyst;[123–127] the Gabriel synthesis, transforming allylic halides using potassium phthalimide as the amine nucleophile;[128–130] and the Overmann rearrangement that transforms allylic trichloroacetimidates thermally by [3,3]-sigmatropic rearrangement.[131–134]

Perhaps the operationally simplest method is the classical substitution of allyl halides or sulfonates with an *N*-alkylamine, and this was thus first attempted to gain wider access to *N*-methyl allylamine derivatives. To an excess of *N*-methylamine was slowly added an allyl bromide or chloride (to suppress double *N*-allylation), giving intermediates that were subjected (without purification) to chloroformylation and subsequent reaction with *N*-allylmethylamine, and afforded symmetrical and unsymmetrical ureas **248**, **249**, **240**, **250** and **251** in moderate to high yields (Scheme 45). Unfortunately,

this *N*-methylamine strategy proved ineffective in the synthesis of a *N*-methylated-α-methyl-substituted allylamine **237**.

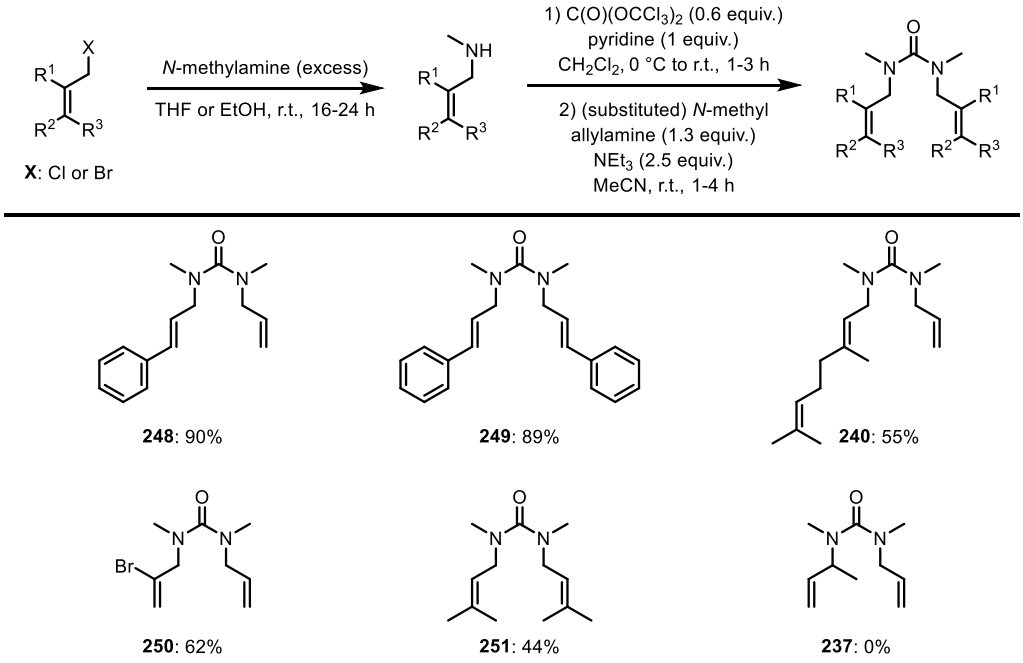

Scheme 45. *N*-allylation of *N*-methylamine and its subsequent use in the chloroformylation/amine-coupling method to synthesise symmetrical and unsymmetrical diallyl ureas.

Further attempts to prepare *N*-methyl allylamine derivatives by allylic substitution were directed towards increasing the reactivity of the electrophile using allyl sulfonates instead of allyl halides. With the use of conditions reported by Clayden *et al.*,[113] 4,4,4-trifluorocrotyl alcohol and *trans*-3-(trimethylsilyl)allyl alcohol were successfully converted to their mesylate esters, then treated with excess *N*-methylamine as described above and used without further purification. Subsequent chloroformylation and amine-coupling resulted in the synthesis of unsymmetrical ureas **246** and **247**, inaccessible via the direct urea *N*-allylation method (section 2.2.1), albeit in low yields of 13% and 4% (Scheme 46).

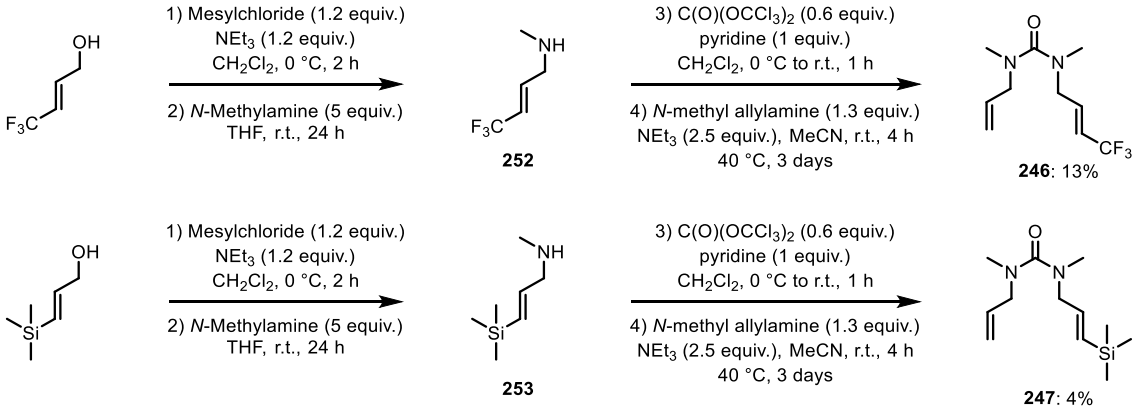

Scheme 46. Mesylation of allyl alcohols followed by substitution with *N*-methylamine to synthesise unsymmetric diallyl ureas via the chloroformylation/amine-coupling method.

The low yields for **246** and **247** afforded via the chloroformylation/amine-coupling method raised a concern as previous results with similar analogues were consistently high yielding (section 2.1). Additionally, the mesylation of allyl alcohols and their reaction with *N*-methylamine is reported to give good yields of substitution products for similar compounds.[135,136] This experimental and literature evidence seemingly contradicts the apparent poor results in transforming allyl halides or allyl sulfonates into their corresponding methylamine derivatives and subsequent urea derivatives; thus, another explanation – volatility – for the low yields was considered.

The boiling points of related amines, *N*-methyl *cis*-3-(trimethylsilyl)allyl amine ***cis*-253** and *N*,*N*'-dimethyl *trans*-3-(trimethylsilyl)allyl amine **254**, are 50 °C at 10 mmHg[137] and 76–80 °C at 12 mmHg[138] (Figure 5). From this it can be hypothesised that **252** and **253** have similar – or lower in case of **252** due to the presence of the fluorine atoms – boiling points and may have partially evaporated during concentration of the reaction mixtures *in vacuo* and their placement under high vacuum for 10 minutes. In addition, the boiling points of *N*-methyl α-methylallylamine **255** (76 °C at 760 mmHg),[139] *N*-methyl β-methylallylamine **256** (86–86.5 °C at 760 mmHg)[140] and *N*-methyl γ-methylallylamine **257** (78–86 °C at 760 mmHg)[141] are relatively low (Figure 5), which may also explain the failure to observe *N*-methyl α-methylallylamine **255** in substitution attempts described above for the synthesis of **237**.

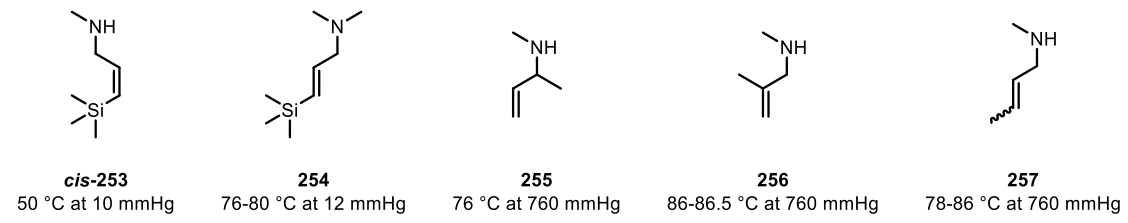

Figure 5. Literature boiling points of selected *N*-methyl allyl amine derivatives.

A potential solution to overcome the practical issue associated with the volatility of these *N*-methyl allylamine intermediates would be to convert them into their corresponding hydrochloride salts before concentration of the reaction mixtures; however, since an excess of *N*-methylamine is required in the substitution reactions to suppress double *N*-allylation, the remaining *N*-methylamine would also be converted to its hydrochloride salt, resulting in a mixture of ammonium salts, thus hindering a clean chloroformylation in the next step.

An alternative approach to avoid volatility issues would be to perform substitution of the allyl electrophile with *tert*-butyl carbamate; the isolated substitution product could then be subjected to sequential *N*-methylation and Boc deprotection (with TFA or HCl) to form the desired *N*-methyl allylamine as a pure HCl salt. Towards this end, α-, β- and γ-substituted allyl alcohols were tosylated using *n*-BuLi[142] to give allyl sulfonates **258**, **259**, **260** and **261** in good to high (crude) yields (Scheme 47). However, attempts to form **262** and **263** by substituting tosylates **259** and **260** with *tert*-butyl carbamate using cesium carbonate and sodium hydride resulted in intractable mixtures (Scheme 47).

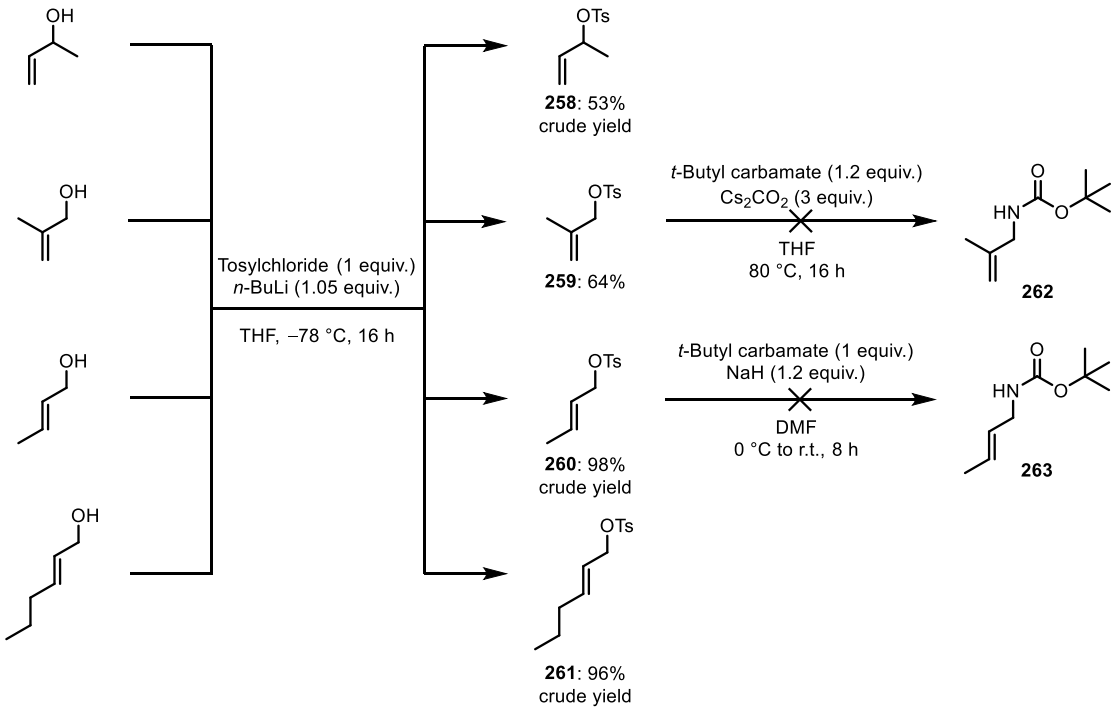

Scheme 47. Tosylation of α-, β-, and γ-substituted allyl alchols using *n*-BuLi and attempted substitution of tosylates with *tert*-butyl carbamate.

2.2.3 *N*-Methyl Allyl Amine Hydrochloride Salts via a Mitsunobu Strategy

Since there remained a practical issue associated with the volatility of the required *N*-methyl allylamine derivatives, and the substitution of allyl electrophiles with *tert*-butyl carbamate proved unsuccessful, a reliable, alternative way to prepare non-commercially available, structurally diverse *N*-methyl allylamine derivatives was still required. To avoid handling the volatile *N*-methyl allylamine freebases, and to be able to cleanly obtain them as hydrochloride salts, the aim remained to synthesise the corresponding *N*-Boc protected amine precursors.

Another operationally simple and highly effective method to synthesise allylic amines is to transform commercially or readily available allyl alcohols under Mitsunobu conditions.[121,143,144] Most commonly, phthalimide is used as the nitrogen nucleophile, yet its deprotection is associated with undesirable conditions which has led to extensive research into alternative Mitsunobu nitrogen nucleophiles.[128,145] Those nucleophiles include imidodicarbonates and acyl- and sulfonylcarbamates, which require deprotection conditions that are less vigorous in comparison to the ones used with deprotection of the phthaloyl group. Nevertheless, using these pronucleophiles under Mitsunobu conditions still yield, upon deprotection, (volatile) *N*-methyl allylamine freebases.

In 1998, a new Mitsunobu nitrogen nucleophile, *N*-Boc ethyl oxamate (**264**), that upon deprotection yields the product of formal substitution with *tert*-butyl carbamate (section 2.2.2), was reported by Berrée and co-workers.[146] Its use has been successfully demonstrated in the transformation of both primary and secondary alkyl alcohols under Mitsunobu conditions (Scheme 48).[144,147–150] This Mitsunobu reaction proceeds through initial attack of triphenylphosphine onto DEAD, generating phosphonium intermediate **266** that deprotonates **264**. Subsequently, the alkyl alcohol attacks the resulting phosphonium intermediate **267**, forming oxyphosphonium intermediate **268** expelling the DEAD-H_2 by-product. The deprotonated Mitsunobu nucleophile **264** then undergoes an S_N2 reaction with **268** to afford *N*-Boc alkyl carbamate **265** and triphenylphosphine oxide.[151] After C–N bond formation in the Mitsunobu reaction, the ethoxalyl group – required to lower the pK_a of the carbamate reagent (pK_a 8.8 in EtOH/H_2O)[146] – can be easily cleaved under mild hydrolysis conditions, giving the corresponding *N*-Boc protected amines.[152] Surprisingly, only two isolated examples of converting allylic alcohols with *N*-Boc ethyl oxamate **264** under Mitsunobu conditions were found in the literature.[146,153]

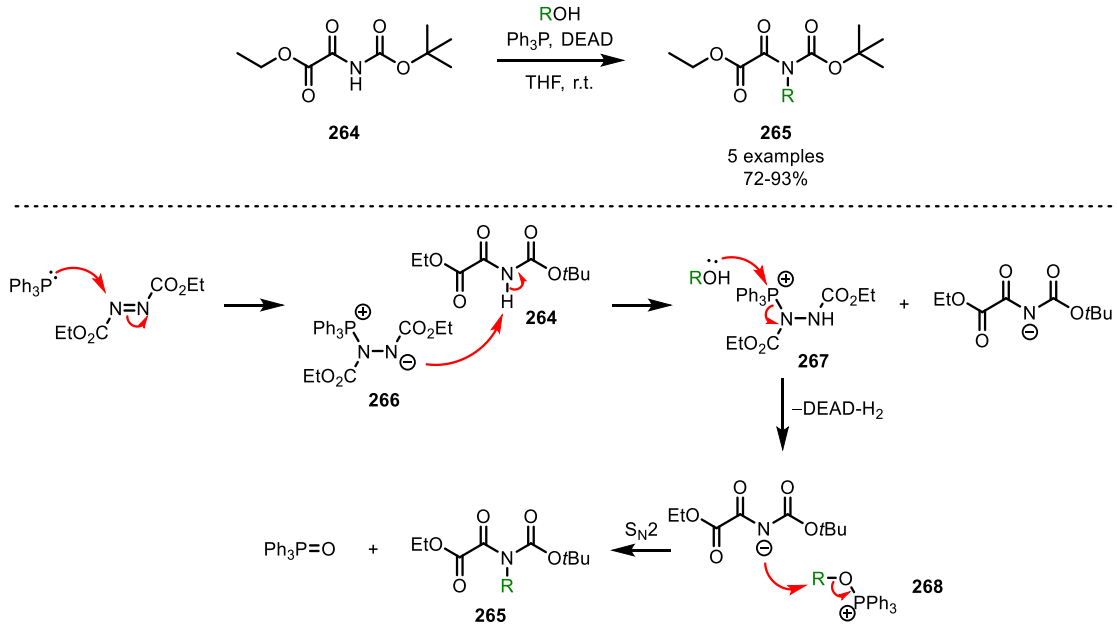

Scheme 48. The Berrée Mitsunobu reaction between *N*-Boc ethyloxamate 264 and alkyl alcohols with its mechanism.

Due to the appealing nature of using this simple method to access allylic amines in *N*-Boc protected form, its applicability to a range of commercially available or easily accessible allylic alcohols was investigated.[1] For this, following the literature procedure,[146,152] Mitsunobu nitrogen nucleophile **264** was easily prepared on decagram scale: ethyl oxamate (170 mmol) was first reacted with oxalyl chloride – both very cheap reagents – to give ethyloxalyl isocyanate, which was subsequently treated with *tert*-butanol, affording **264** in a yield of 70% (Scheme 49).

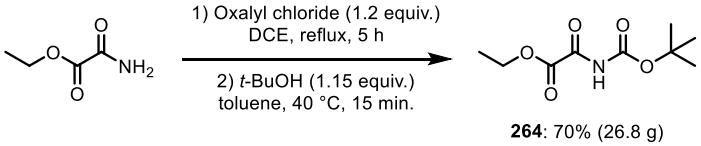

Scheme 49. Reaction of oxalyl chloride with ethyl oxamate generating ethyloxalyl isocyanate that upon treatment with *tert*-butanol yields *N*-Boc ethyl oxamate 264.

Initially, Mitsunobu substitution of 3-buten-2-ol or crotyl alcohol with *N*-Boc ethyl oxamate **264** was attempted with triphenylphosphine and DEAD. Upon hydrolysis with lithium hydroxide, *N*-Boc allylic carbamates **269** and **263** were afforded in low yields of 36% and 27%, respectively (Scheme 50).[1] Encouragingly, substitution of DEAD with DIAD resulted in significantly improved yields: 63% for **269** and 73% for **263**.

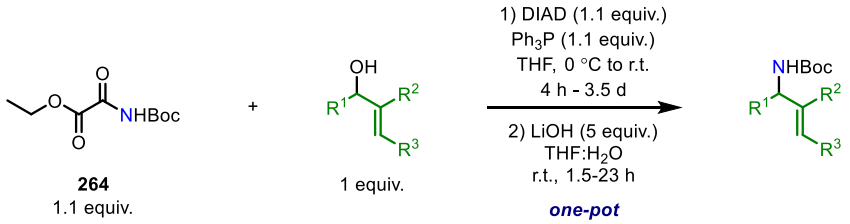

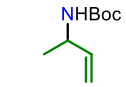

269
2.15 g, 12.6 mmol
63% (**36%**)[a]

262
3.21 g, 18.8 mmol
85%

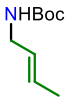

263
2.53 g, 14.8 mmol
73% (**27%**)[a,b]

270
3.46 g, 17.4 mmol
86%

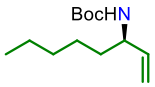

271
424 mg, 1.86 mmol
68%, e.r. ≥99:1
(±-**271**: 1.05 g,
4.62 mmol, **77%**)

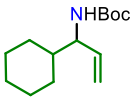

272
0.75 g, 3.14 mmol
28%

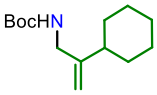

273
0.75 g, 3.13 mmol
86%

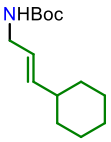

274
1.55 g, 6.49 mmol
93%

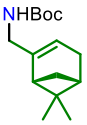

275
2.23 g, 8.86 mmol
88%

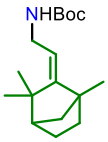

276
0.52 g, 1.85 mmol
72%

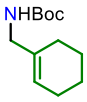

277
0.57 g, 2.67 mmol
75%

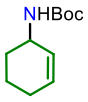

278
1.02 g, 5.15 mmol
58%

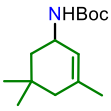

279
474 mg, 1.98 mmol
44%

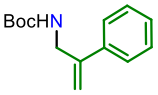

280
3.91 g, 16.8 mmol
77%

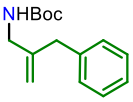

281
2.35 g, 9.49 mmol
79%

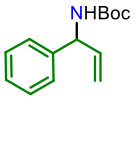

282
428 mg, 1.83 mmol
18%

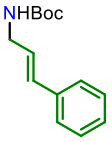

283
520 mg, 2.23 mmol
22%

284
0.62 g, 3.39 mmol
15%

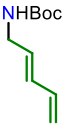

285
1.02 g, 5.59 mmol
25%

286
2.24 g, 11.4 mmol
76%

287
0.72 g, 3.91 mmol
39%

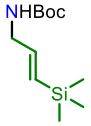

288
0.83 g, 3.62 mmol
94%

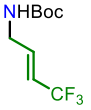

289
1.33 g, 5.89 mmol
91%

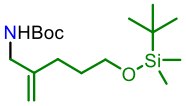

290
2.53 g, 7.68 mmol
86%

291
0.85 g, 4.71 mmol
80%

Scheme 50. Scope for the synthesis of *N*-Boc protected allylic amines under Mitsunobu conditions.[1] [a]Using DEAD instead of DIAD. [b]Contains the *cis* isomer as a minor impurity carried through from the starting material.

With these effective Mitsunobu conditions in hand, the method was expanded to a broader range of substituted primary and secondary allylic alcohols, successfully yielding *N*-Boc allylic carbamates in moderate to excellent yields, on multigram scale for most cases (Scheme 50).[1] Methyl-substitution at the α-, β-, or γ-position of the allylic system was tolerated (**269**, **262** and **263**), and the reactions were also successful with longer propyl and pentyl substituents (**270** and **271**). Using enantiopure starting material (*S*)-1-octen-3-ol (e.r. ≥ 99:1) confirmed the enantiospecificity of this Mitsunobu substitution, as *N*-Boc allylic carbamate **271** was formed without loss of enantiopurity (e.r. ≥ 99:1), presumably through stereochemical inversion.[1,153] Furthermore, the reaction tolerated bulkier alkyl-substituents at the α-, β-, or γ-positions of the allylic system (**272**, **273** and **274**), giving a single regioisomer for secondary allylic amine **272** (as observed with **269** and **271**), and was also successful with the bulkier terpenoid rings (**275** and **276**) and other similar cyclohexenes (**277**, **278** and **279**).

In addition to the effective reaction of cinnamyl alcohol with *N*-Boc ethyl oxamate demonstrated by Berrée and co-workers,[146] 2-phenyl-2-propen-1-ol and 2-benzylallyl alcohol were suitable substrates as well, enabling access to **280** and **281** in yields of 77% and 79%, respectively (Scheme 50). In contrast to the regioselective formation of **269**, **271** and **272** from branched allylic alcohols, a mixture of regioisomers **282** and **283** was afforded upon reaction of α-vinylbenzyl alcohol under the standard Mitsunobu conditions. Various conditions (DEAD, ADDP and elevated temperatures) were attempted to improve the yield and selectivity for **282**, yet those conditions produced the same product ratio, and similar or worse yields. The same regioselectivity issue was observed for the Mitsunobu reaction of 1,4-pentadien-3-ol, which gave **284** mixed with regioisomer **285**. This observed regioselectivity issue might be explained by a (partial) switch in mechanism from the normal S_N2 to an S_N1 due to the formation of highly stabilised carbocations. Hexa-2,4-dien-1-ol and 2-methylenebut-3-en-1-ol yielded dienes **286** and **287** with complete regiospecificity.

Moreover, the Mitsunobu reaction tolerated allylic alcohols bearing electron-donating or -withdrawing groups, giving **288** and **289** in excellent yield (Scheme 50). Transformation of 5-((*tert*-butyldimethylsilyl)oxy)-2methylenepentan-1-ol gave **290** in high yield. Easily accessible 4-(*tert*-butyldimethylsilyl)-2-methylenebut-3-yn-1-ol, consisting of a TMS-protected alkyne, was also successfully used under the Mitsunobu conditions, yet upon hydrolysis of the ethoxalyl group using lithium hydroxide the TMS group was removed, yielding amine **291**. Then, treatment of **291** with *n*-BuLi and *tert*-butyldimethylsilyl chloride gave access to **292** in moderate yield (Scheme 51).

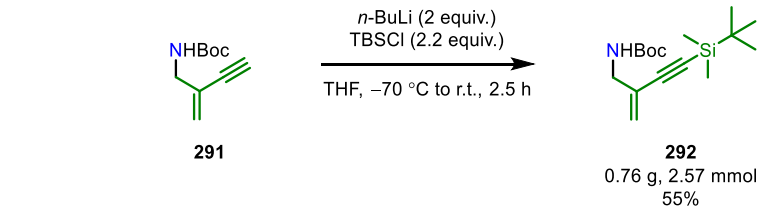

Scheme 51. Protection of *N*-Boc allyl carbamate 291 with *tert*-butyldimethylsilyl chloride yielding *N*-Boc allyl carbamate 292 in moderate yield.

Interestingly, *N*-Boc ethyl oxamate **264** could also be coupled with allylic halides using potassium *tert*-butoxide, as demonstrated with the synthesis of *N*-Boc allyl carbamate **293** in a yield of 59% (Scheme 52).[152] This broadens the applicability of **264** as a nitrogen nucleophile in the synthesis of allylic amines as not only allylic alcohols but also commercially or readily available allylic halides can be utilised as electrophiles.

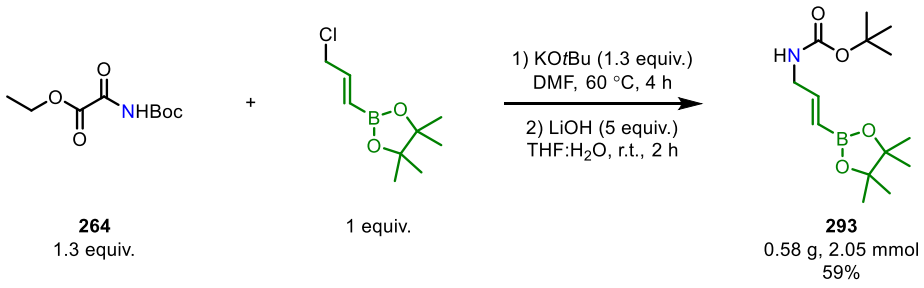

Scheme 52. Direct *N*-allylation of *N*-Boc ethyl oxamate 264 with an allylic halide using potassium *tert*-butoxide for the synthesis of *N*-Boc protected allylic amine 293.

To transform the *N*-Boc protected allylamines to the desired *N*-methyl hydrochloride salts, *N*-methylation was performed with the *N*-Boc allylic carbamates using sodium hydride and methyl iodide (Scheme 53). Then, deprotection of the Boc group using an excess of TFA followed by the addition of anhydrous HCl in MeOH or Et_2O (for anion exchange) gave the corresponding amine·HCl salts as generally easy-to-handle solids.[1] No chromatography is involved in these three steps, and thus a simple procedure that gives access to a broad range of *N*-methylated allylic amine hydrochloride salts in high yield was developed (Scheme 53). In case of the formation of **315** in 52% yield, hydrochloride salt **314** was initially generated due to the use of TFA for the Boc deprotection, which additionally removed the TBS protecting group (Scheme 53).

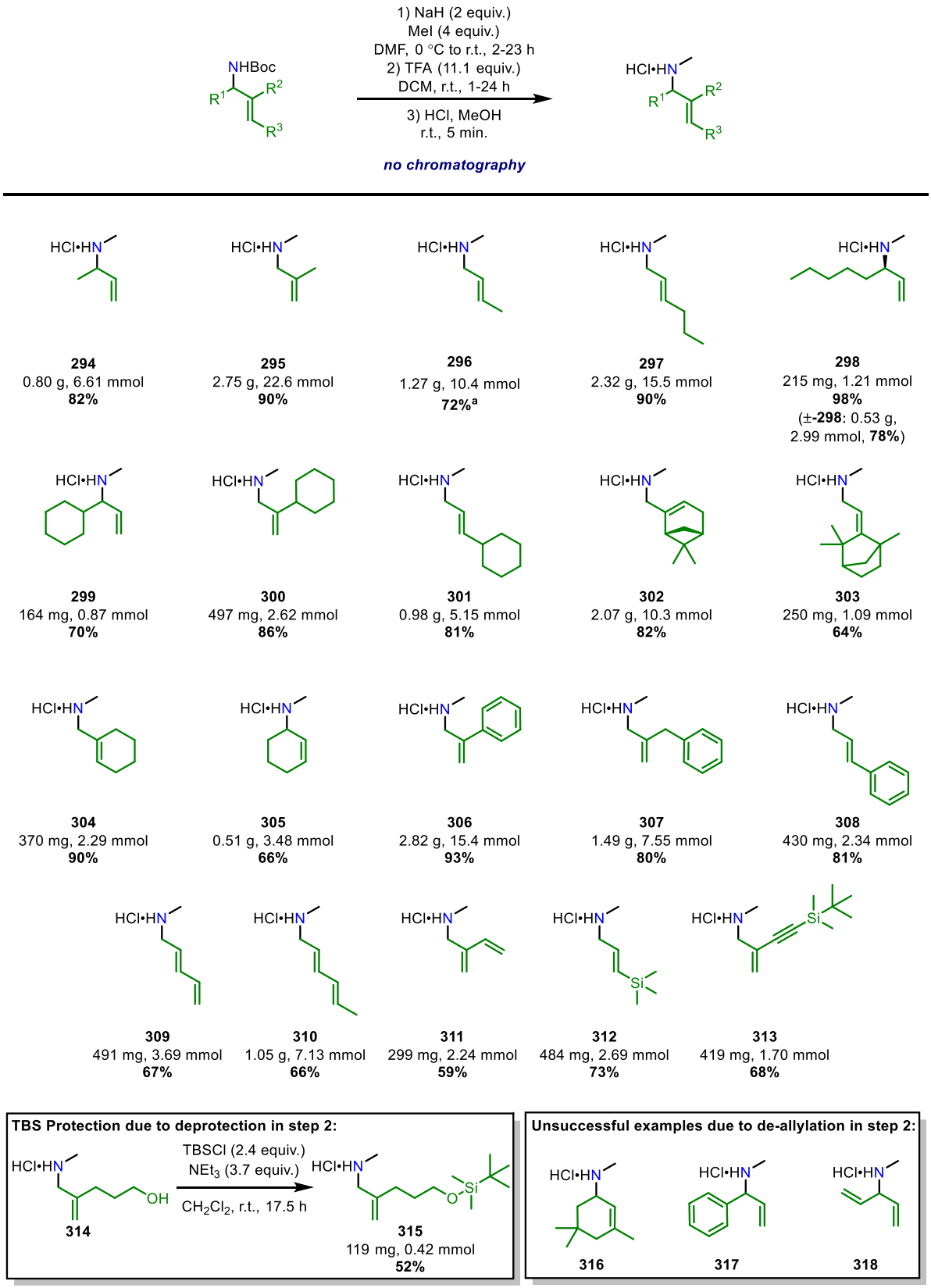

Scheme 53. Scope for the synthesis of *N*-methyl allylamine hydrochloride salts. [a]Contains the *cis* isomer as a minor impurity carried through from the starting material.

Unfortunately, the limitation to the deprotection with TFA was that in some cases (**279**, **282**, **284**), de-allylation first takes place, generating *N*-methylamine hydrochloride salt after subsequent Boc deprotection instead of *N*-methyl allylamine hydrochloride salts **316**, **317** and **318** (Scheme 53 and Scheme 54). This competitive de-allylation is enabled by the formation of a more stable allylic cation in comparison to the desired *tert*-butyl cation. Therefore, in these cases, Boc-deprotection was attempted without acid, using H_2O and heat (100 °C in μW), yet this approach was unsuccessful and gave intractable mixtures.

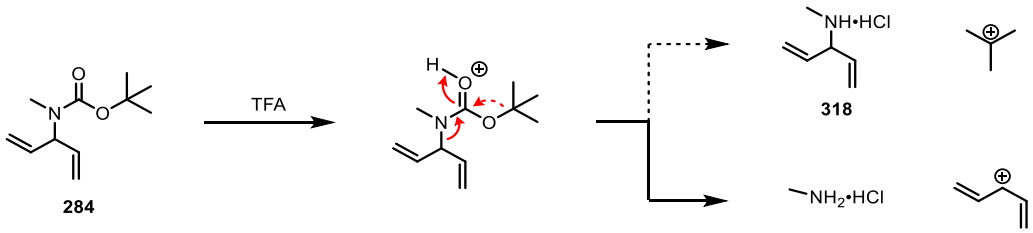

Scheme 54. Competitive de-allylation instead of the desired Boc deprotection due to the ability of the formation of a more stable allylic cation. Competitive de-allylation is represented by the plain arrows; desired Boc deprotection is represented by the dashed arrows.

Importantly, this method demonstrated that substitution at the α-, β-, and γ-position of the allylic system was tolerated and thus allowed for general applicability to structurally diverse substrates. Furthermore, the method has proven to be practical and scalable, and thus circumvents the problem of dealing with volatile *N*-methyl allylamines.[1]

Since this method (Scheme 50 and Scheme 53) requires several steps to arrive at the desired *N*-methyl allylamines, it was suggested to improve the overall step-economy towards the desired urea substrates by using a different nitrogen nucleophile in the Mitsunobu reaction. The Boc group was thus replaced by an *N*-allyl carbamoyl moiety (Scheme 55), such that one half of the target urea was already installed. For this, the ethyloxalyl isocyanate, formed again by reacting ethyl oxamate with oxalyl chloride, was treated with *N*-methyl allylamine instead of *tert*-butanol to afford *N*-methyl-*N*-allyl ethyl oxamate **319** in a yield of 70% (Scheme 55). **319** was then subjected to the standard Mitsunobu allylation using DIAD, triphenylphosphine and a secondary alcohol. After cleavage of the ethoxalyl group with lithium hydroxide, urea **320** was afforded, albeit in a low yield of 8%. Attempts with ADDP instead of DIAD (to improve the yield) and use of a primary alcohol (crotyl alcohol) were unsuccessful giving intractable mixtures. The reason for the low yield of **320** is likely caused by a less effective Mitsunobu reaction, probably due to the decreased acidity of **319** relative to **264** resulting from replacement of the Boc group with a carbamoyl unit. *N*-Boc ethyl oxamate **264** has a pK_a of 8.8,[146] which is sufficiently acidic to successfully undergo Mitsunobu reactions; the pK_a rule for a successful Mitsunobu states that the pK_a

of the pronucleophile must be 11 or below.[144] Therefore, this idea for the synthesis of the desired ureas was not further pursued.

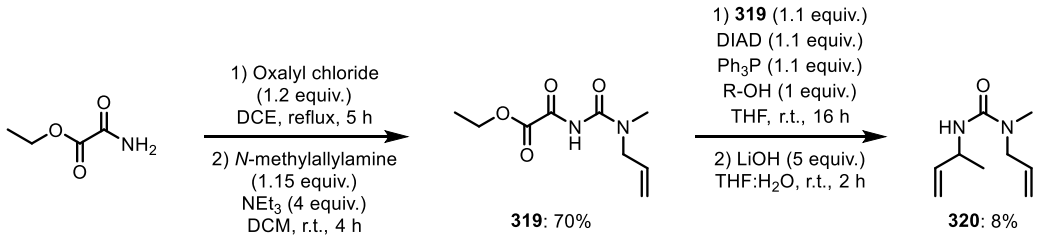

Scheme 55. Synthesis of *N*-methyl-*N*-allyl ethyl oxamate 319 and its subsequent *N*-allylation with a secondary alcohol under Mitsunobu conditions.

With the now accessible *N*-methyl allylamines, a broad range of symmetrical and unsymmetrical diallyl ureas were synthesised by a 'mix-and-match' process involving chloroformylation of one amine component and urea formation with the same or another amine. Various combinations were made, enabling the possibility to explore the key N→C vinyl migration method to investigate whether alternatively substituted allyl groups can still act as the nucleophilic anion-stabilising and the electrophilic migrating groups. For this purpose, a wide range of diallyl ureas was successfully synthesised in moderate to excellent yields (Scheme 56). The method proved even to be effective with rather bulky substituted *N*-methyl allylamine hydrochloride salts.

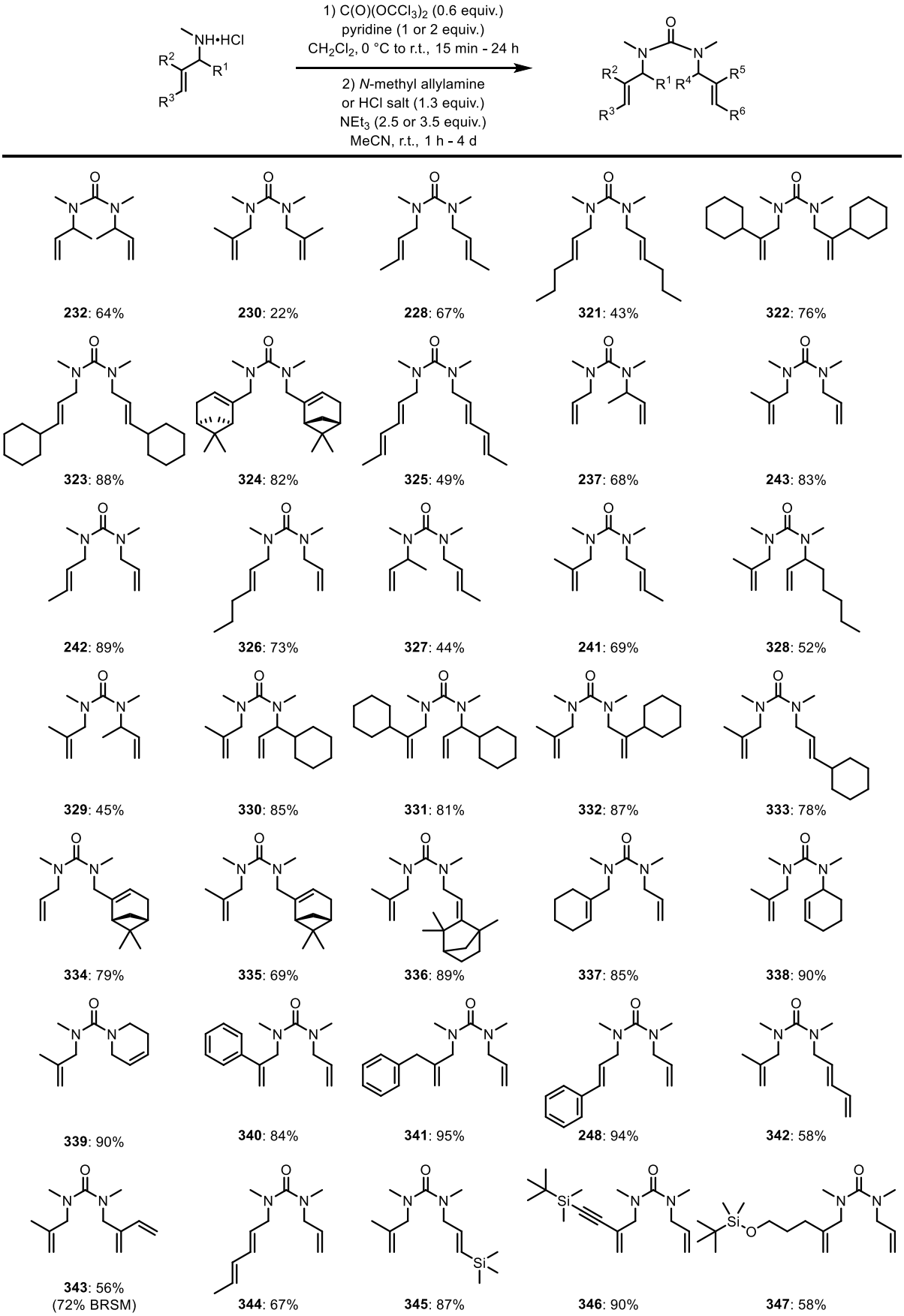

Scheme 56. Scope for the synthesis of symmetrical and unsymmetrical variously substituted diallyl ureas via the chloroformylation/amine-coupling method using *N*-methyl allyl amine hydrochloride salts.

2.4 Conclusions

As demonstrated in this chapter, the synthesis of *N*,*N*'-diallyl ureas via chloroformylation of *N*-methyl allylamine derivatives and subsequent amine-coupling (urea formation) is reliable and high yielding, but the limited commercial availability of *N*-methyl allylamines presented a drawback to this approach. Alternative strategies were thus investigated in order to develop a general method for the synthesis of diallyl ureas.

To summarise, the reaction of allylic halides or sulfonates with 1,3-dimethylurea **223** and 1-allyl-1,3-dimethylurea **224** in the presence of sodium hydride to achieve direct urea *N*-allylation was moderately productive for β- and γ-substituted allylic systems; the reactions were not consistent and not high yielding. Furthermore, this method failed to provide any desired product with α-substituted allyl halides/sulfonates.

Alternatively, generating *N*-methyl allylamines (to use for the chloroformylation/amine-coupling method) by treating allylic halides or sulfonates with *N*-methylamine was only effective in a small number of cases and the volatility of the products presented a significant practical limitation. Reaction of tosylated allylic alcohols with *tert*-butyl carbamate to avoid the volatility issues of the generated *N*-methyl allylamines was unproductive.

Fortunately, various α-, β- and γ-substituted *N*-methyl allylamines were synthesised as their pure hydrochloride salts by reacting *N*-Boc ethyl oxamate **264** under Mitsunobu conditions with various allylic alcohols (including secondary allylic alcohols) and subsequently deprotecting the *N*-methylated Mitsunobu products. A reliable, practical, and scalable method to prepare *N*-methyl allylamine derivatives has thus been identified and published as it is believed that this method is of significant practical value for organic chemists.[1] For this work, it has now enabled facile access to a wide range of *N*,*N*'-diallyl ureas via the established chloroformylation/amine-coupling approach.

3.0 N→C Vinyl Migration of Symmetrical and Unsymmetrical Diallyl Ureas

3.1 Preliminary Studies

It was intended to develop a novel intramolecular S_NV reaction where a vinyl group undergoes N→C migration in a *N*,*N*'-diallyl urea after *in situ* isomerisation (section 1.3). For this, the conformational restriction of the urea would be employed to serve as a tether between the unsaturated coupling partners. From previous work it is known that various vinyl groups are able to act as the electrophile in the successful N→C migration of *N*-benzyl-*N*'-vinyl ureas, *N*-vinylureidonitriles and *N*-vinylureido imidazolidinones.[112–114,154] On the other hand, previous work demonstrated that an unsubstituted allyl group is able to act as the nucleophile in the N→C migration of aryl groups in *N*-aryl-*N*'-allyl ureas.[106] The first stage of this work was initiated by studying the feasibility of using an allyl chain as the migrating group – the electrophile – aiming to expand the N→C vinyl migration reaction to *N*,*N*'-diallylureas, which has not yet been reported. All the starting diallyl ureas were synthesised using the chloroformylation/amine-coupling method discussed in Chapter 2.0.

Accordingly, to check the feasibility of N→C vinyl migration with a simple allyl group, which needs to be isomerised separately or *in situ* as part of the rearrangement cascade, it is important to test if it can migrate towards another group that has been shown to work efficiently in previous N→C migration reactions (Scheme 57). It was decided to use a benzyl group as the pronucleophile – the anion-stabilising group – due to its ability of migrating vinyl groups in lithiobenzylic ureas.[112]

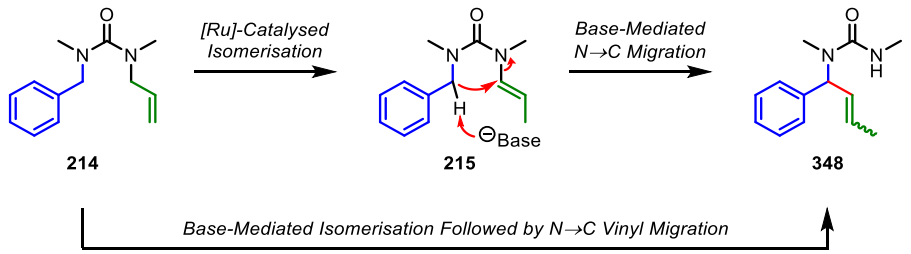

Scheme 57. Proposed rearrangement of unsymmetrical *N*-benzyl-*N*'-allyl urea 214 and *N*-benzyl-*N*'-vinyl urea 215. Blue represents the nucleophile. Green represents the electrophile. Red represents the new bonds formed.

For the *in situ* isomerisation followed by N→C vinyl migration, conditions similar to those reported by Clayden *et al.* were first attempted on *N*-benzyl-*N*'-allyl urea **214**.[112] The stoichiometry of the base was reduced to prevent the formation of a double anion by deprotonation of both *N*-substituents.

Unfortunately, upon treating **214** with 1.2 equivalents of LDA at −78 °C for 3 h, no migration product **348** was observed. Instead, cyclisation product **349** was obtained in a 52% yield with a *syn*:*anti* ratio of 1.4:1, assigned following NOE analysis (Scheme 58).

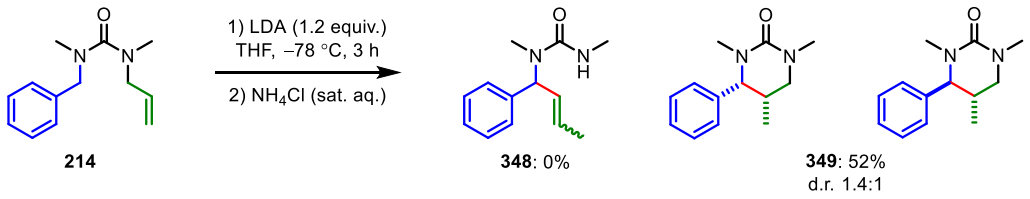

Scheme 58. Attempted N→C vinyl migration of *N*-benzyl-*N*'-allyl urea 214 resulted in the generation of undesired cyclisation product 349. Blue represents the nucleophile. Green represents the electrophile. Red represents the new bonds formed.

For the desired migration product **348** to form, it was proposed that a cascade of deprotonations and re-protonations was required in the correct order; the first deprotonation/re-protonation sequence sets up the *in situ* isomerisation of the allyl chain, facilitating the second deprotonation/re-protonation sequence to establish the actual N→C vinyl migration (Scheme 59). Presumably, cyclisation product **349** was formed through an initial α-deprotonation at the *N*-benzylic carbon instead, followed by a 6-*exo*-*trig* cyclisation. Deprotonation of the benzylic position is likely preferred over the less acidic allylic position, and thus the required isomerisation of the allyl chain is significantly slower or entirely outcompeted and therefore inhibiting the desired N→C vinyl migration.

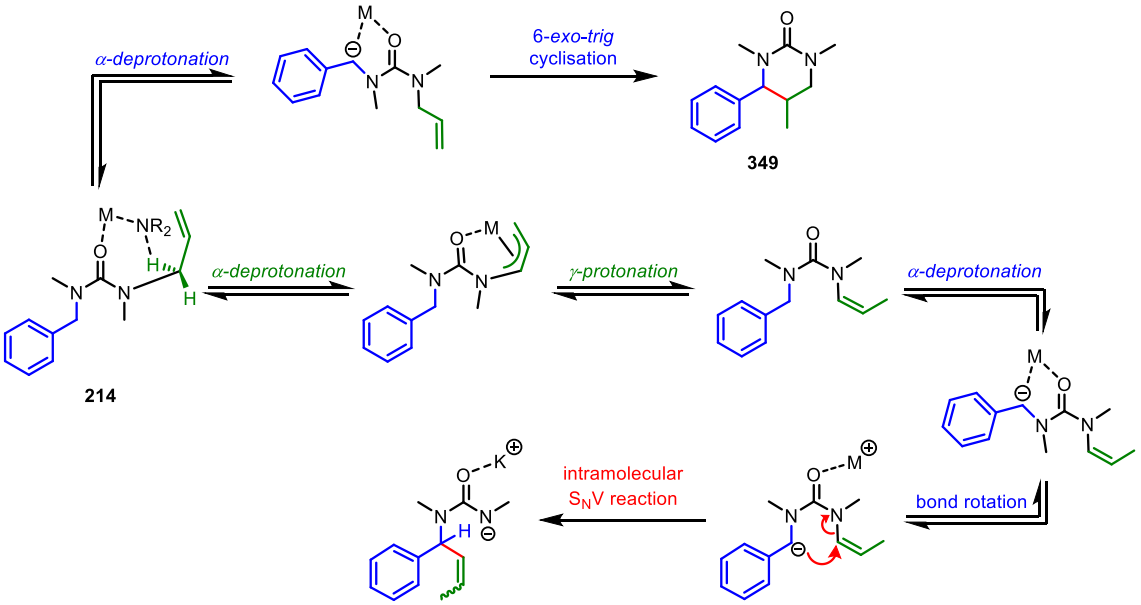

Scheme 59. Proposed mechanism for the N→C vinyl migration and competitive 6-*exo*-*trig*-cyclisation of *N*-benzyl-*N*'-allyl urea 214. Blue represents the nucleophile. Green represents the electrophile. Red represents the new bonds formed.

An explanation for the observed *syn*:*anti* ratio of **349** was proposed by considering the possible transition states. The transition state towards cyclisation of **214** contains five sp^2-hybridised atoms (1 carbonyl, 1 alkene, 2 ureido nitrogens and 1 carbanion) and therefore is assumed to adopt a pseudo-half-chair transition state by analogy with DMPU (Figure 6). From this there are two possible transition states: one with the double-bond in a pseudo-equatorial position (**350**), while the other possible transition state **351** consists of a pseudo-axial orientated double-bond. The latter transition state (**351**) is favoured as it mitigates steric interactions between the alkene and the phenyl ring. However, the difference in the *syn*:*anti* ratio is not significant and a reason for this could be that the difference in energy between the two transition states is not substantial.

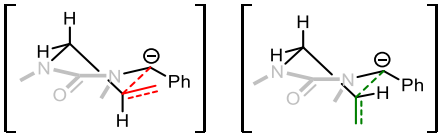

Figure 6. Possible pseudo-half-chair transition states 350 and 351 that urea 214 could adopt towards its cyclisation.

The hypothesis of a slow or completely absent alkene isomerisation was further supported by the successful N→C vinyl migration of *N*-benzyl-*N*'-(*E*)-vinyl urea **215** under the same conditions, where the original allyl group was first isomerised into an *E*-vinylic substituent by ruthenium-catalysis (section 2.1), yielding migration product **348** in a yield of 81% with complete retention of the alkene geometry (Scheme 60). Presumably, as no *in situ* isomerisation was required in this case, upon α-deprotonation of the *N*-benzylic carbon, nucleophilic attack at the sp^2-hybridised carbon of the *E*-vinyl group led to the desired N→C vinyl migration.

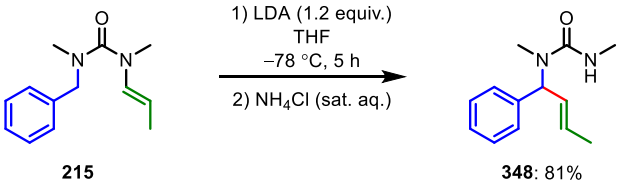

Scheme 60. Successful N→C vinyl migration of *N*-benzyl-*N*'-(*E*)-vinyl urea 215 yielding migration product 348. Blue represents the nucleophile. Green represents the electrophile. Red represents the new bonds formed.

3.2 Results and Discussion

3.2.1 Reaction Discovery and Optimisation

The preliminary results with unsymmetrical *N*-benzyl-*N*'-allyl urea **214** and *N*-benzyl-*N*'-(*E*)-vinyl urea **215** (section 3.1) indicate that with the use of LDA the N→C migration of the *E*-vinyl group is effective unlike the allyl group, presumably as it needs to undergo *in situ* isomerisation first. Therefore, attention was next turned to develop and optimise the N→C vinyl migration method with simple *N*,*N*'-(*E*)-divinylurea **207** – using another *E*-vinyl group instead of a benzyl group as the nucleophile (Scheme 61). For the N→C vinyl migration of **207** to be successful and form urea **352** it was hypothesised that first γ-deprotonation of one of the vinyl chains (blue) needed to take place to then allow the nucleophilic attack at the sp^2-hybridised carbon of the other vinyl chain (green).

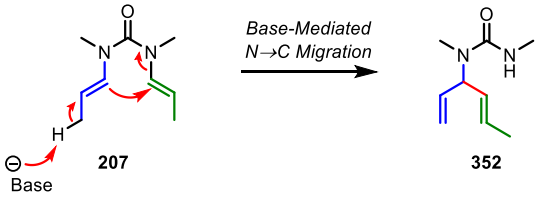

Scheme 61. Proposed N→C vinyl migration of *N*,*N*'-(*E*)-divinylurea 207. Blue represents the nucleophile. Green represents the electrophile. Red represents the new bonds formed.

Initial work began with the same conditions used for the successful N→C vinyl migration of *N*-benzyl-*N*'-(*E*)-vinyl urea **215**, yet by treating *N*,*N*'-(*E*)-divinylurea **207** with 1.2 equivalents of LDA at −78 °C no migration product **352** was observed (Table 2, entry 1). Then the addition of DMPU was attempted, as this additive is known to solvate lithium cations and thus increases the reactivity of organolithium reagents by dissociating them.[88,89,98,106] However, only starting urea **207** was observed by crude ^{1}H NMR (entry 2). Lithium chloride is another well-known additive that generally has beneficial effects on various organolithium reactions by deaggregating organolithium aggregates and thus solubilising the reaction.[155,156] Yet again, upon the addition of lithium chloride no migration product **352**, only starting material **207** was observed (entry 3). The same negative result was obtained with increasing the reaction temperature to −40 °C (entry 4). When LDA was added at 0 °C instead and the reaction mixture was stirred at room temperature, starting urea **207** was no longer observed, yet neither was the desired migration product **352** (entry 5).

Table 2. Screening of conditions using LDA for the N→C vinyl migration of symmetrical *N,N'*-(*E*)-divinylurea 207.[a]

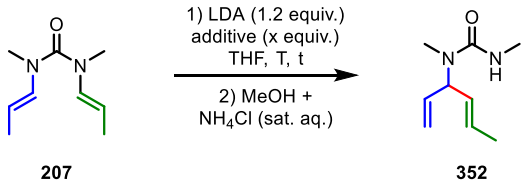

207 352

Entry	Base (1.2 equiv.)	Additive (equiv.)	T [°C]	Time [h]	Crude NMR observation
1[b]	LDA[c]	-	−78	3.5	starting urea **207**
2	LDA[d]	DMPU (5.0)	−78	2	starting urea **207**
3	LDA[e]	LiCl[f] (1.2)	−78	2h45	starting urea **207**
4	LDA	-	−40	3h40	starting urea **207**
5	LDA	-	0 to r.t.	2	**353**[g]

Blue represents the nucleophile. Green represents the electrophile. Red represents the new bonds formed. [a]Reactions were performed on a 0.60 mmol scale. [b]Reaction was performed on a 0.10 mmol scale. [c]Commerical LDA (2.0 M in THF) was used. [d]2.2 equivalents of LDA were used. [e]0.85 equivalents of base were used. [f]Oven dried. [g]**353** was isolated in 31% yield.

The ^{1}H, ^{13}C and 2D NMR spectra of the isolated side-product **353** in entry 5 (Table 2) suggested the presence of an aldehyde group and thus the chemical structure of compound **353** was proposed and confirmed by HRMS (Scheme 62). To get the proposed aldehyde moiety in **353**, LDA may have attacked the carbonyl of the urea. This could result in the expulsion of the 1-aza allyl anion (**354**), which can either attack via the nitrogen to give back starting urea **207** or via the lithiated carbon (**355**) to give intermediate **356** that upon hydrolysis can generate the aldehyde containing compound **353**.

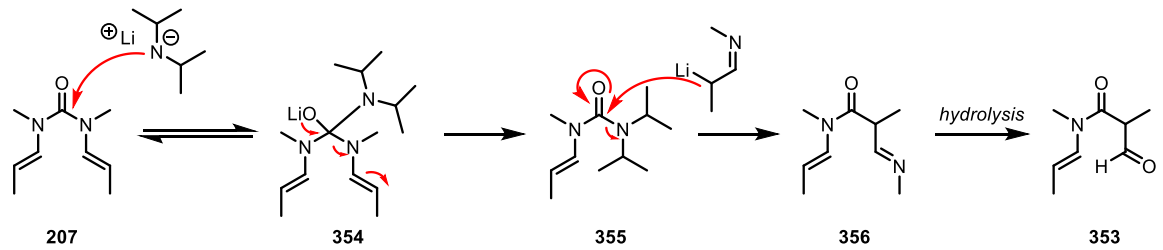

207 354 355 356 353

Scheme 62. Proposed formation of 353 containing the aldehyde moiety.

Moving forward, a range of other bases, either with or without additives, were screened under various reaction temperatures (Table 3). However, even with the stronger bases *s*-BuLi and *n*-BuLi and increasing the reaction temperature to −40 °C only starting urea **207** was observed by crude ^{1}H NMR

(entries 1 and 2). The same outcome was obtained when using DMPU while warming up from −78 °C to room temperature (entry 3). With the use of LiTMP a complex mixture was afforded at −78 °C (entry 4), but when the reaction was performed at −40 °C a compound different from starting urea **207** and desired migration product **352** was obtained (entry 5). Unfortunately, deduction of the structure of this unexpected compound remained unsuccessful. Even the use of an *in situ* generated 'superbase' (*n*-BuK) did not result in the desired rearrangement of **207** to **352** (entry 6), which was also the case when using KHMDS at −78 °C (entry 7). When **207** was reacted at 0 °C with KHMDS in the presence of 18-crown-6, an additive that has the ability to complex potassium cations thus makes the base more reactive,[157,158] compound **357** was afforded in a 55% yield and tentatively identified to contain a nitrile group (entry 8). Unfortunately, elucidation of the mechanism for the proposed formation of **357** remained unsuccessful.

Table 3. Screening of bases for the N→C vinyl migration of symmetrical *N*,*N*'-(*E*)-divinylurea 207.[a]

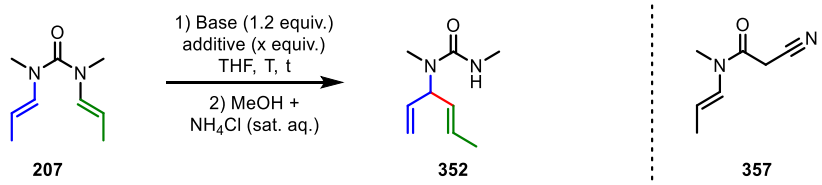

Entry	Base (1.2 equiv.)	Additive (equiv.)	T [°C]	Time [h]	Crude NMR observation
1	*s*-BuLi	-	−40	2.5	starting urea **207**
2	*n*-BuLi	-	−40	2h40	starting urea **207**
3[b]	*s*-BuLi	DMPU (10 vol%)	−78 to r.t.	5 to o/n	starting urea **207**
4[b]	LiTMP[c]	-	−78	4	complex mixture
5	LiTMP[c]	-	−40	3h40	unidentified compound
6	*n*-BuLi[d] + *t*-BuOK[d]	-	−78	22	complex mixture
7	KHMDS	-	−78	5	starting urea **207**
8[e]	KHMDS[d]	18-crown-6[f] (2.2)	0	4.5	**357**

Blue represents the nucleophile. Green represents the electrophile. Red represents the new bonds formed. [a]Reactions were performed on a 0.60 mmol scale. [b]Reaction was performed on a 0.10 mmol scale. [c]Freshly prepared by reacting TMP (1 equiv.) with *n*-BuLi (1 equiv.; 1.6 M in hexanes) in anhydrous THF (2.5 mL/mmol) for 1 h at 0 °C to r.t. [d]2 equivalents were used. [e]**357** was isolated in 55% yield. [f]Recrystallised from MeCN and used in a solution of 1.25 M in THF.

Despite the extensive attempts using various bases, additives and temperatures, the N→C vinyl migration of **207** remained unsuccessful (Table 2 and Table 3). These results suggest that the required

γ-deprotonation or desired isomerisation followed by the rearrangement does not take place. For the latter, it could be reasoned that the double-bond in **207** is more substituted, thus more stable, than the terminal alkene, which would be formed upon isomerisation of one of the vinyl chains. Even though urea carbonyls are well known to direct metalation of proximal C–H bonds through coordination to potassium or lithium bases,[79] it was hypothesised that the *E*-alkene geometry prevents this mode of activation because the carbonyl cannot direct the base intramolecularly to the γ-C–H bonds.

Even though the attempt to migrate the allyl group in *N*-benzyl-*N*'-allyl urea **214** resulted in the undesired cyclisation product **349** (section 3.1), attention was next turned to the N→C vinyl migration of symmetrical *N*,*N*'-diallyl urea **206** (Scheme 63). For the desired migration product **358** to form, it was proposed that first α-deprotonation and *in situ* isomerisation needed to take place on one allyl group to form a vinyl chain (green), presumably in *Z*-geometry, that upon α-deprotonation of the other allyl group (blue) can undergo the N→C migration.

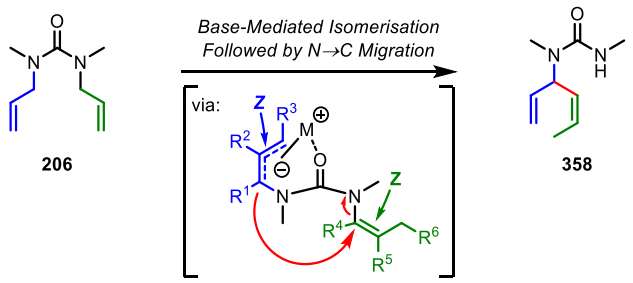

Scheme 63. Proposed N→C vinyl migration of symmetrical *N*,*N*'-diallyl urea 206. Blue represents the nucleophile. Green represents the electrophile. Red represents the new bonds formed.

Encouragingly, a first attempt to rearrange **206** with only a slight excess of LDA, again to avoid the formation of an unproductive dianion, at −78 °C for 3.5 h gave the desired migration product **358**, exhibiting *Z*-alkene geometry, in a yield of 2% (Scheme 64). In addition, isomerised migration product **359**, also exhibiting *Z*-alkene geometry, was isolated in a 5% yield. This initial hit, albeit significantly low yielding, demonstrated that the required isomerisation of an allyl group followed by the N→C vinyl migration was feasible with a simple diallyl urea. However, mostly cyclisation products **360** and **361** were obtained, which must arise upon α-deprotonation at one of the allylic positions followed by a 6-*exo*-*trig* cyclisation onto the other allyl group. From this it was evident that, under the current conditions, the required *in situ* allyl-to-vinyl isomerisation is too slow to compete with the undesired 6-*exo*-*trig* cyclisation.

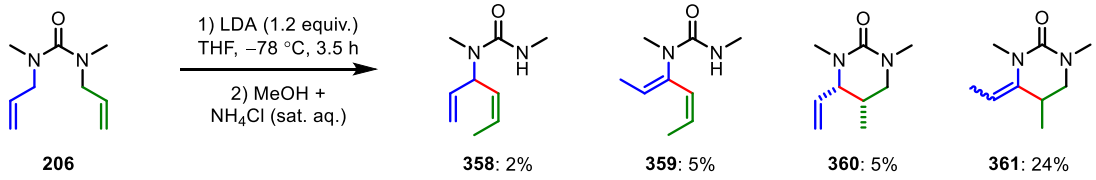

Scheme 64. Initial hit when exposing diallyl urea 206 to a slight excess of LDA. Blue represents the nucleophile. Green represents the electrophile. Red represents the new bonds formed.

Having elucidated the different possible outcomes when exposing diallyl urea **206** to LDA, optimisation studies were started. It should be mentioned that there is poor mass balance in most reactions, which is possibly due to decomposition before or after work-up and/or difficult purification of unidentified, complex reaction mixtures.

At first the effect of different reaction temperatures using 1.2 equivalents of LDA was investigated (Table 4). The reaction at −78 °C was repeated, yet a longer reaction time was applied; slightly higher yields of cyclisation product **360** and migration product **358** were obtained, but in similar ratios (entry 1). Increasing the temperature to −40 °C still gave mostly isomerised cyclisation product **361** in a yield of 30%, and this time only a total yield of 2% was obtained for conjugated migration products **359** and **362** (entry 2). This result indicates that with increasing temperature, under these conditions, unconjugated migration product **358** isomerises immediately, or via **359**, into the most thermodynamically favoured conjugated migration product **362**. In addition, it was found that when performing the reaction at −20 °C more of migration product **362**, and less of cyclisation products **360** and **361**, were formed (entry 3). At 0 °C to room temperature the reaction of **206** with LDA gave very low yields of both cyclisation product **360** and migration products **359** and **362** (entry 5). Overall, these results suggest that the total yields are significantly low under warmer reaction conditions, and at cooler temperatures (−78 °C and −40 °C) the alkene isomerisation – the proposed first reaction sequence of the N→C vinyl migration cascade – is slower to compete with the undesired 6-*exo*-*trig* cyclisation.

Table 4. Reaction temperature screen when using LDA for the N→C vinyl migration of diallyl urea 206.[a]

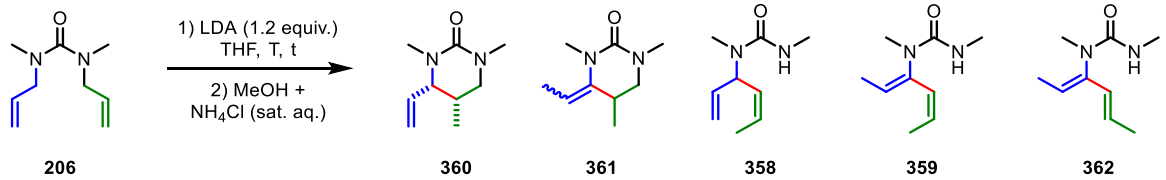

206 360 361 358 359 362

Entry	LDA (equiv.)	T [°C]	Time [h]	Isolated Yield [%]				
				360	**361**	**358**	**359**	**362**
1	1.2	−78	24	16	22	14	-	-
2	1.2	−40	3.5	-	30	-	1	1
3	1.2	−20	3.5	5	7	-	-	20
4	1.2	0 to r.t.	2	4	-	-	2	9

Blue represents the nucleophile. Green represents the electrophile. Red represents the new bonds formed. [a]Reactions were performed on a 0.40 – 0.61 mmol scale.

The stoichiometry of LDA was next explored with a reaction temperature of −78 °C (Table 5). When using 0.1 equivalents of LDA, no conversion of starting urea **206** was observed by crude ^{1}H NMR (entry 1). However, with the use of 0.5 equivalents of LDA, cyclisation products **360** and **361** were obtained in a total yield of 41% and migration product **358** in a 6% yield (entry 2); these are similar to the amounts obtained when 1.2 equivalents of LDA were used (Scheme 64 and Table 4, entry 1). Besides the known reaction products, partially *Z*-isomerised urea **363** and fully *Z*-isomerised urea **364** – assumed to be reaction intermediates – were isolated in yields of 9% and 1% (entry 2). Increasing the amount of LDA to 2 equivalents gave less of cyclised products **360** and **361**, and the highest total yield (30% yield) thus far was obtained for migration products **358** and **359** (entry 3). Unfortunately, increasing the reaction time did not improve the yields further (entry 4). The ratio between **358** and **359** did change towards **359**, which suggests that with warmer temperatures, and over time, migration product **358** also isomerises into **359**. Warmer reaction temperatures (−40 °C, −20 °C and −78 °C to 0 °C) with the use of 2 equivalents of LDA were also attempted however gave highly complex mixtures; only small amounts of cyclisation products **360** and **361** were observed, but no accurate yields could be determined. Finally, reverse addition – addition of starting urea **206** to LDA – was attempted; no significant effect was observed on the yields and ratio of the cyclisation and migration products (entry 5). Only this time, presumed reaction intermediates **363** and **364** were also afforded, adding up to a better mass balance of the reaction.

Table 5. LDA stoichiometry screen for the N→C vinyl migration of diallyl urea 206.[a]

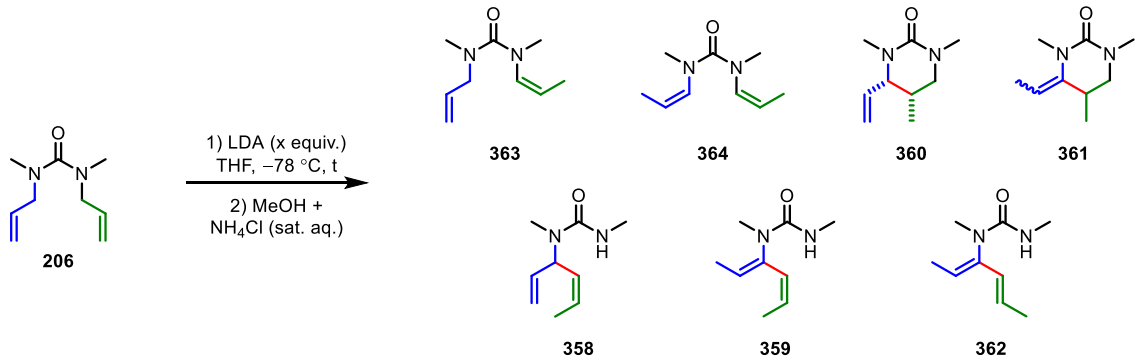

Entry	LDA (equiv.)	T [°C]	Time [h]	Isolated Yield [%]						
				363	**364**	**360**	**361**	**358**	**359**	**362**
1	0.1	−78	3.5	-	-	-	-	-	-	-
2[b]	0.5	−78	3.5	9	1	19	22	6	-	-
3[c]	2	−78	4	-	-	6	9	24	6	-
4	2	−78	24	-	-	10	6	11	13	-
5[d,e]	2	−78	3.5	8	20	6	5	33	-	-

Blue represents the nucleophile. Green represents the electrophile. Red represents the new bonds formed. [a]Reactions were performed on a 0.40 – 0.59 mmol scale. [b]Starting urea **206** was recovered in 11% yield. [c]Yields are determined by ^{1}H NMR using 1,2,4-trimethoxybenzene as an internal standard. [d]Reverse addition: **206** was added to the base. [e]Starting urea **206** was recovered in 1% yield.

As the choice of solvent is known to have an effect on the reactivity of organolithiums, Et_2O and toluene were trialled.[159] Yet, in both cases no cyclisation and no migration products were observed (Table 6). A complex mixture was obtained with Et_2O (entry 1), while partially and fully *Z*-isomerised ureas **363** and **364**, assumed to be reaction intermediates, were generated with toluene (entry 2). Besides recovery of starting urea **206** in 5% NMR yield, mono-allylated urea **224** – presumably formed due to hydrolysis of the *Z*-vinyl chain in **363** – was observed (entry 2).

Table 6. Solvent screen for the N→C vinyl migration of diallyl urea 206.[a]

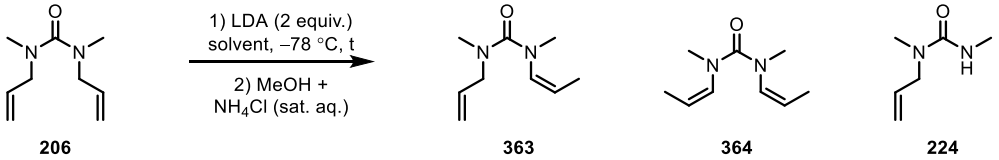

206 363 364 224

Entry	Solvent	Time [h]	NMR Yield [%]		
			224	363	364
1	Et_2O	24.5	-	-	-
2[b]	toluene	4	3	21	20

[a]Reactions were performed on a 0.59 and 0.60 mmol scale. Reverse addition was applied: **206** was added to the base. The yields are determined by ^{1}H NMR using 1,2,4-trimethoxybenzene as an internal standard. [b]Starting urea **206** was recovered in 5% yield.

Based on the reaction temperature, LDA stoichiometry, and solvent screens (Table 4, Table 5 and Table 6), it was concluded that the highest yields (max. 33% yield) for the desired migration products were obtained when 2 equivalents of LDA were used in THF at −78 °C. A final screen when using LDA for the N→C migration of diallyl urea **206** involved the addition of DMPU as a co-solvent to make a more reactive base (Table 7). Interestingly, it was found that with the use of DMPU the reaction can be made (completely) selective towards the synthesis of cyclisation products **360** and **361**. This may be explained by the coordination of DMPU to the lithium cation, whereupon the coordination of the lithium cation to the carbonyl and the carbanion is reduced. In this way, the carbanion would be more reactive and favour cyclisation over the slower isomerisation step (section 3.2.2).

Table 7. Screening the effect of addition of DMPU when using LDA for the N→C vinyl migration of diallyl urea 206.[a]

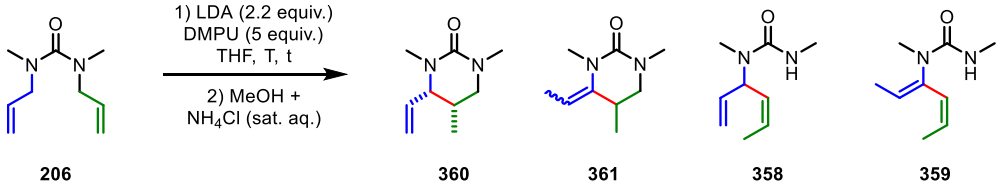

206 360 361 358 359

Entry	LDA Addition	T [°C]	Time [h]	NMR Yield [%]			
				360	361	358	359
1	Normal	−78	24	10	31	3	-
2	Normal	−78 to 0	24	-	49	-	-
3[b]	Reverse	−78	4.5	7	53	-	1

Blue represents the nucleophile. Green represents the electrophile. Red represents the new bonds formed. [a]Reactions were performed on a 0.40 and a 0.58 mmol scale. Normal LDA addition: base added to **206**. Reverse LDA addition: **206** added to base. The yields are determined by ^{1}H NMR using 1,2,4-trimethoxybenzene as an internal standard. [b]Isolated yields.

With the yields for the migration products plateauing around 30%, the use of other bases was next considered (Table 8). The previous results suggest that the isomerisation, essential for the desired N→C vinyl migration, is significantly slower than the competing cyclisation reaction. Thus, for the isomerisation to outcompete the cyclisation a more rapid re-protonation of the allylic anion needs to take place, it was hypothesised that the use of a base with a conjugate acid of a lower pK_a would be beneficial. As such, the use of LiTMP and *s*-BuLi, bases with conjugate acids of a higher pK_a in comparison to LDA, and the use of KHMDS, a base with a conjugate acid of a lower pK_a, were investigated.[160–162] When **206** was reacted with LiTMP at −78 °C only a complex mixture was afforded (entry 1). In case of *s*-BuLi, mostly cyclisation products **360** and **361** were afforded when the reaction was performed at −78 °C (entries 2 and 3), in contrast to the fact that only migration product **362** was afforded when the reaction mixture was warmed up from −78 °C to 0 °C (entry 4). In general, a poor mass balance of the reaction was afforded with the use of *s*-BuLi as the base. However, as suspected, with the use of KHMDS at 0 °C a significantly cleaner conversion of **206** to migration product **362**, without any cyclisation competition, was obtained with a yield of 25% (entry 5). The presence of significant amounts of starting urea **206** and fully *Z*-isomerised urea **364** proved promising as **364** was assumed to be the reaction intermediate towards migration product **362**. Therefore, it was anticipated that with slight adjustments to the conditions when using KHMDS the yield of the N→C vinyl migration of **206** could be significantly improved.

Table 8. Screening of bases for the N→C vinyl migration of diallyl urea 206.[a]

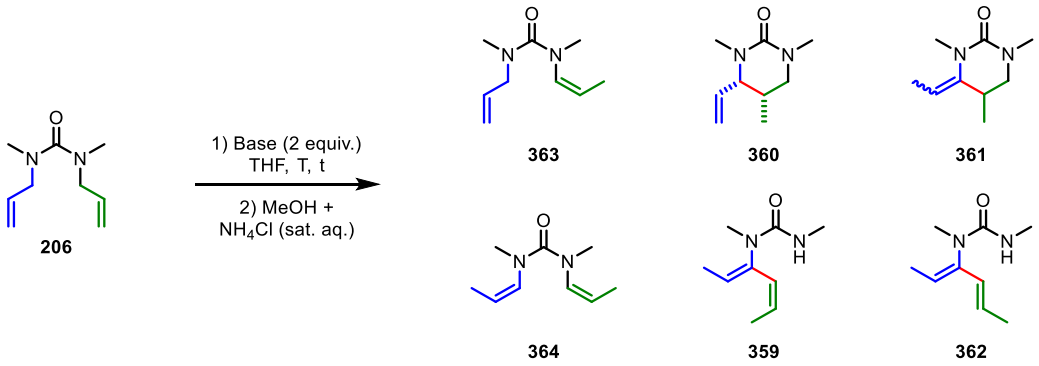

Entry	Base (2 equiv.)	T [°C]	Time [h]	NMR Yield [%]					
				363	364	360	361	359	362
1[b]	LiTMP	−78	4	-	-	-	-	-	-
2[b,c]	*s*-BuLi	−78	25	12	3	19	7	7	-
3	*s*-BuLi	−78	24	-	-	5	14	-	13
4	*s*-BuLi	−78 to 0	24	-	-	-	-	-	12
5[d]	KHMDS	0	4.5	-	48	-	-	25[e]	

Blue represents the nucleophile. Green represents the electrophile. Red represents the new bonds formed. [a]Reactions were performed on 0.40 – 0.60 mmol scale. The yields are determined by ^{1}H NMR using 1,2,4-trimethoxybenzene as an internal standard. [b]Reverse addition: **206** added to base. [c]**206** was observed in 8% NMR yield. [d]**206** was observed in 19% NMR yield. [e]The ratio between **359** and **362** was unidentifiable.

Having achieved the desired chemoselectivity for the generation of migration product **362**, the effect of using 18-crown-6 as an additive with various reaction temperatures and the effect of the base counterion were subsequently investigated in an attempt to increase the yield of the reaction (Table 9). By taking the conditions of entry 5 in Table 8 and adding 2.2 equivalents of 18-crown-6, fully *Z*-isomerised urea **364** and migration product **362** were obtained in similar yields (Table 9, entry 1). However, when the reaction was left for longer, migration product **362** was solely afforded in a moderate yield of 42% (entry 2). Delightfully, by adding KHMDS and 18-crown-6 at −78 °C and slowly warming the reaction mixture to 0 °C the yield of the desired migration product **362** was finally improved to 86% (entry 3).

Under otherwise identical reaction conditions, the N→C vinyl migration of **206** was performed by substituting KHMDS with LiHMDS and NaHMDS; essentially, comparing the effect of complexed potassium versus non-complexed sodium and lithium (entries 3 to 5). The results confirmed that the use of KHMDS in combination with 18-crown-6 are the optimal conditions to generate migration product **362** in a high yield (entry 3).

The use of LiHMDS in the N→C vinyl migration of **206** was shown to be ineffective as migration product **359** was observed in only 7% NMR yield, and 25% of the starting urea **206** was returned (entry 4). The formation of propionaldehyde **365** in a yield of 29% and urea **224** in a similar yield of 30% was unexpected. It was hypothesised that hydrolysis of a vinyl group had taken place on an undetected compound where only one allyl group was isomerised, like **363**. This can be rationalised by either a too acidic work-up or the presence of water and acid in the deuterated chloroform used for the NMR analysis.

When NaHMDS was used instead, the N→C vinyl migration was also less effective as **362** was only generated in a 30% yield (entry 5). Fully *Z*-isomerised urea **364** was afforded in a yield of 24%. In addition, propionaldehyde **365** was generated in a yield of 22% and urea **366** in a yield of 19%. In both the reactions in entry 4 and 5 a small amount of fully *E*-isomerised urea **207** was afforded.

Table 9. Addition of 18-crown-6 screen and counterion study for the N→C vinyl migration of diallyl urea 206.[a]

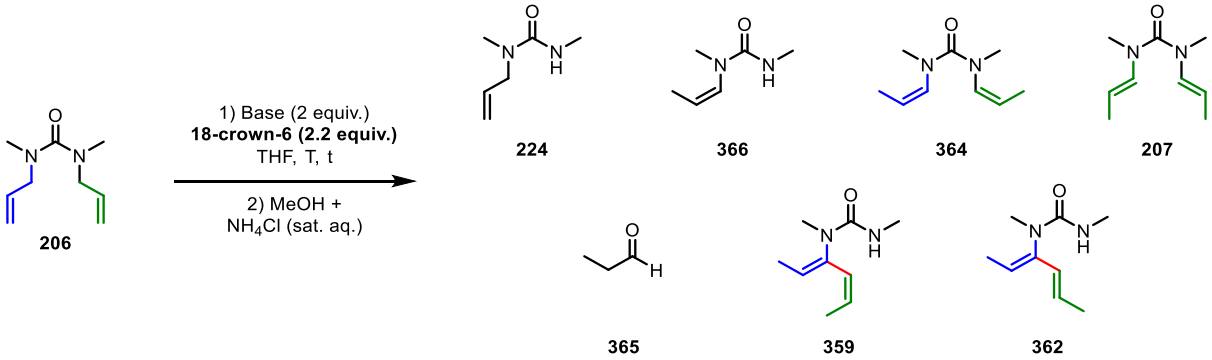

Entry	Base (2 equiv.)	T [°C]	Time [h]	NMR Yield [%]						
				365	**224**	**366**	**364**	**207**	**359**	**362**
1	KHMDS	0	4.5	-	-	-	26	-	-	33
2	KHMDS	0	23	-	-	-	-	-	-	42
3	KHMDS	−78 to 0	24	-	-	-	-	-	-	86[b]
4[c]	LiHMDS	−78 to 0	24	29	30	-	2	8	7	-
5	NaHMDS	−78 to 0	24	20	-	19	24	3	28	-

Blue represents the nucleophile. Green represents the electrophile. Red represents the new bonds formed. [a]Reactions were performed on 0.59 – 0.66 mmol scale. The yields are determined by ^{1}H NMR using 1,2,4-trimethoxybenzene as an internal standard. [b]Isolated yield. [c]**206** was observed in 25% NMR yield.

From these extensive optimisation studies, it was observed that, under certain conditions, symmetrical *N*,*N*'-(*Z*)-divinyl urea **364** was generated. Presumably, **364** is a reaction intermediate along the course

of the demanding N→C vinyl migration cascade, which is in contrast to the so far unsuccessful participation of symmetrical *N*,*N*'-(*E*)-divinyl urea **207** in the N→C vinyl migration. Therefore, it was of interest to attempt the optimised conditions (Table 9, entry 3) for the N→C vinyl migration of symmetrical *N*,*N*'-(*E*)-divinyl urea **207**. Compound **207** was subjected to 2 equivalents of KHMDS and 2.2 equivalents of 18-crown-6 at −78 °C and then the reaction mixture was gradually warmed up to 0 °C; still only starting urea **207** was observed in a 98% NMR yield (Scheme 65).

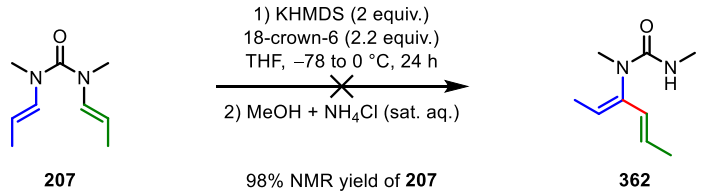

Scheme 65. Attempted N→C vinyl migration of symmetrical *N*,*N*'-(*E*)-divinyl urea 207 using the optimised reaction conditions. Blue represents the nucleophile. Green represents the electrophile. Red represents the new bonds formed. The yield is determined by ^{1}H NMR using 1,2,4-trimethoxybenzene as an internal standard.

During the optimisation process of the N→C vinyl migration of symmetrical diallyl urea **206** it was discovered that the reaction outcome was highly dependent on the base used and the presence of metal-coordinating additives. In summary, using LDA at −78 °C gives mostly migration product **358** however in low yields and in presence of the undesired cyclisation products **360** and **361**. Then, by adding DMPU the reaction outcome is chemoselectively steered towards cyclisation product **361** in good yields, while with KHMDS and 18-crown-6 at −78 °C to 0 °C migration product **362** is afforded cleanly in high yield. It was of interest to see whether this chemoselectivity obtained with KHMDS/18-crown-6 also applied to the N→C vinyl migration of *N*-benzyl-*N*'-allyl urea **214**, which with use of LDA underwent the competitive 6-*exo*-*trig* cyclisation.

Therefore, urea **214** was subjected to 2 equivalents of KHDMS and 2.2 equivalents of 18-crown-6 at −78 °C and then the reaction mixture was allowed to gradually warm up to 0 °C. This pleasingly resulted in the formation of N→C vinyl migration product **367** in a high yield of 80% (Scheme 66). Under the same optimised condition, migration product **367** was also obtained in a 42% NMR yield when starting from *N*-benzyl-*N*'-(*E*)-vinyl urea **215** (Scheme 66). An explanation for the lower yield could be that the migration of an *E*-vinyl chain is more challenging than migrating a *Z*-vinyl chain. The divergent results obtained with *N*-benzyl-*N*'-allyl urea **214** complement the hypothesis of the N→C vinyl migration reaction outcome to be highly dependent on the choice of base. Presumably, when using LDA, the undesired cyclisation reaction (to **349**) occurs due to an initial α-deprotonation of the benzylic carbon in **214** before isomerisation of the *N*-allyl chain. Previous studies in our group have shown that, in ureas with both benzylic and allylic protons, deprotonation can occur at either of these methylene sites, and

complete regioselectivity may be obtained as a result of kinetic control.[117] In those cases, the resultant metalated species did not equilibrate to other regioisomers prior to the desired rearrangements. Based on these observations, it is plausible that in **214**, KHMDS selects the allylic protons while LDA targets the benzylic protons; this proposal may be supported by the greater steric hindrance of KHMDS versus LDA if kinetic factors are governing the regioselectivity.

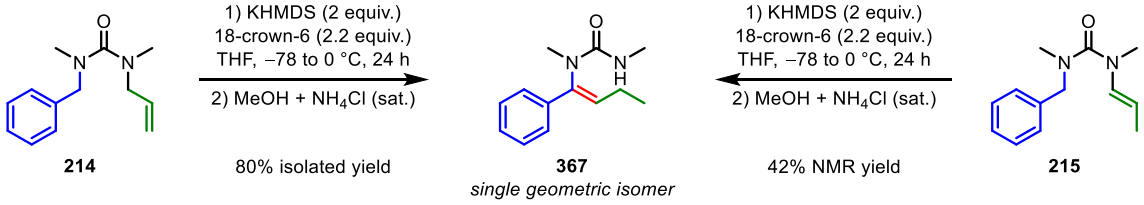

Scheme 66. N→C Vinyl migration of *N*-benzyl ureas 214 and 215 using the optimised rearrangement conditions.

Taken together, the results obtained in the optimisation study imply that for a successful N→C vinyl migration starting from symmetrical and unsymmetrical diallyl or divinyl ureas, an allyl or a *Z*-vinyl chain on at least one side of the urea is needed to act as the nucleophile. With the optimised migration conditions in hand, the optimisation for this N→C vinyl migration of symmetrical diallyl urea **206** was concluded, and focus was turned to extending the developed method to more complex diallyl ureas containing more functionality.

3.2.2 Proposed Mechanism

Having performed the extensive optimisation study and afforded the divergent reaction outcomes, a mechanism for the N→C vinyl migration of symmetrical diallyl urea **206** towards migration products **358** and **362**, but also cyclisation products **360** and **361**, was suggested. The fact that fully isomerised *N*,*N*'-(*Z*)-divinyl urea **364** was observed multiple times and the inability of fully isomerised *N*,*N*'-(*E*)-divinyl urea **207** to undergo the N→C vinyl migration led to the proposal of a one-pot, cascade olefin isomerisation/N→C vinyl migration reaction (Scheme 67). In-depth mechanistic studies were planned for confirmation of this proposed mechanism (section 3.2.5).

The first step in the proposed cascade is deprotonation α to the urea nitrogen of **206** by the base KHMDS to form allyl potassium species **368** adopting a *Z*-geometry in agreement with Beak and co-workers[163] who showed that removal of the allyl α-proton is facilitated by bridging of the carbon-carbon double-bond and the carbonyl by the potassium aggregate (Scheme 67A).[108] From **368** it is now possible to either undergo the competitive 6-*exo*-*trig* cyclisation forming **360** and **361** or the desired γ-re-

protonation to give **363**. The driving force for the formation of **361** from **360** could be that a more substituted, thus more stable, double-bond is formed.

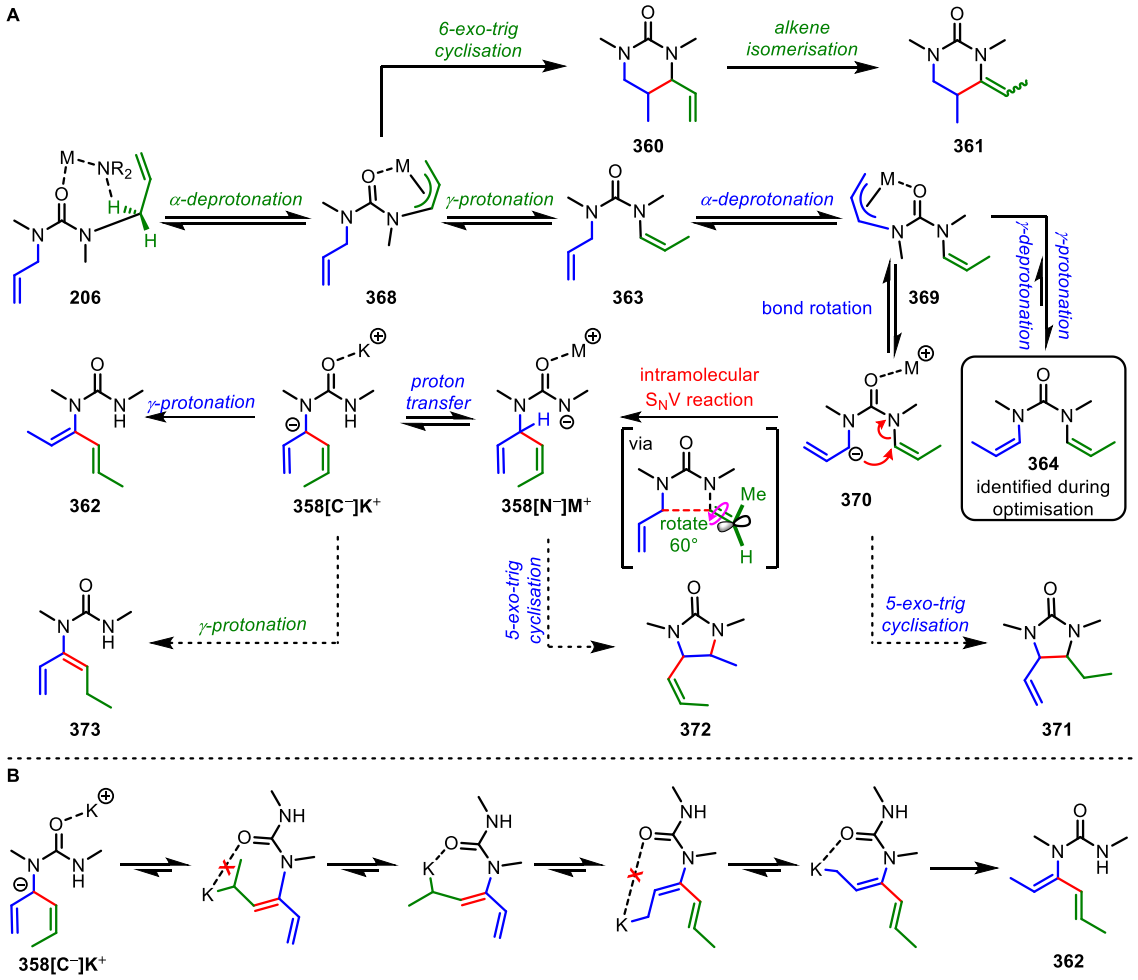

Scheme 67. Proposed heavily demanding, one-pot N→C vinyl migration cascade reaction pathway of symmetrical diallyl urea 206 (A) and the alkene isomerisation of migration product 358 to migration product 362 (B). Blue represents the anion-stabilising group (the nucleophile). Green represents the migrating group (the electrophile).

From intermediate **363** another α-deprotonation followed by protonation at the γ-position explains the formation of urea **364**. Bond rotation of **369** gives **370**, which may undergo an intramolecular S_NV reaction via a multistep Ad_N-E with preferred internal 60° rotation of the carbanion (as shown in Scheme 67A) or a concerted $S_NV\pi$ route, as the alkene geometry seems to be retained in **358** and **359** before *in situ* isomerisation to **362** (mechanistic studies were planned for confirmation: section 3.2.5.3). Migration product **358** is the end product in case of LDA, yet with the use of KHMDS, a proton transfer in product **358[N⁻]M⁺** takes place followed by γ-protonation to form conjugated migration product **362**, of which the *Z*,*E*-geometry was determined by NOE analysis. The *Z*,*E*-geometry can be explained by the preferred orientations in which the potassium can coordinate to both the urea carbonyl and the

carbanion, and less allylic strain is experienced (Scheme 67B). The fact that the urea **207** exhibiting *E*,*E*-alkene geometry turned out to be unsuccessful in the N→C vinyl migration can be explained by its alkene-geometry and that the carbonyl group is no longer able to direct the potassium base to abstract the remote γ-proton.

When looking at this proposed mechanism, it is evident that at multiple points, besides the observed 6-*exo-trig* cyclisation, various other side-reactions could take place (represented with dashed arrows in Scheme 67A). These would give other products like cyclised ureas **371** and **372**, caused by 5-*exo-trig* cyclisation before or after the N→C vinyl migration, or migrated urea **373**, by γ-protonation of the alkene group in green. It is therefore very pleasing that in this heavily demanding reaction cascade a clean, high yielding conversion of starting urea **206** to desired migration product **362** was achieved with the use of KHMDS in combination with 18-crown-6.

3.2.3 Substrate Scope

Having determined the most optimal migration conditions (section 3.2.1), the scope of the N→C vinyl migration reaction was next explored, aiming to expand the method to more highly substituted and functionalised symmetrical and unsymmetrical diallyl ureas. Mindful of the proposed heavily demanding reaction cascade based on the N→C vinyl migration of diallyl urea **206** (section 3.2.2, Scheme 67), it would be of interest to see whether the method would still be selective for a similar *in situ* allyl-to-vinyl isomerisation followed by a S_NV sequence, forming the desired migration products.

3.2.3.1 Rearrangement of Alkyl Substituted Diallyl Ureas

One structural feature of initial interest was to place a methyl substituent at different positions on the *N*-allyl chain to determine whether substituents α, β and/or γ to the nitrogen affect the ability of the *N*-allyl group to act as both the nucleophilic anion-stabilising and the electrophilic migrating group.

Therefore, symmetrical β-methyl substituted diallyl urea **230** was firstly submitted to the optimised reaction conditions, which resulted in the successful synthesis of migration product **374** in a high yield of 82% (Scheme 68). The reaction of symmetrical α- and γ-methyl substituted diallyl ureas **232** and **228** proceeded slightly less effective due to competing reactivities, yet still revealed that the key N→C vinyl migration was feasible (Scheme 68). From urea **232** cyclisation products **375**, **376** and **377** were afforded as a mixture in a total yield of 49%. In addition, urea **378** was afforded in 19% yield as a side-product and explains the lower rearrangement yield; presumably, deprotonation of the α-methyl led to

de-allylation with elimination of the urea anion and formation of 1,3-butadiene (Scheme 69A). Starting urea **228** did give the desired migration product **379** accompanied by its isomer **380** (ratio 0.5:1), although in a lower total yield of 29% and revealed the same competitive side-reaction by the yielding of urea **381** in 26% yield (Scheme 68 and Scheme 70A). However, this competitive elimination seemed significantly more problematic with γ-methyl substituents; a good total yield of migration product **382** and its isomer **383** (ratio 1:1) was obtained from the N→C vinyl migration of symmetrical γ-propyl substituted diallyl urea **321** (Scheme 68).

Having established that significantly small alkyl substituents at the α-, β-, or γ-position do not affect the anion-stabilising and migrating ability of the respective allyl group, it was attempted to expand the scope with bulkier alkyl groups. The N→C vinyl migration of symmetrical β-cyclohexyl substituted diallyl urea **322** was highly successful, giving relatively sterically demanding migration products **384** and **385** in a good total yield of 64% (Scheme 68). In addition, urea **386** – assumed to be the reaction intermediate – was afforded in 4% yield, accompanied by its hydrolysis side-products **387** (3% yield) and **388** (4% yield). Instead of four peaks, six peaks for each cyclohexyl group were observed in the ^{13}C NMR spectrum of both **384** and **385**, suggesting that they consist as a mixture of two enantiomeric rotamers due to restricted/slow bond rotation of the N–C (in blue) or C–C (in red) bond, which renders the pairs of carbons on the cyclohexyl ring diastereotopic. The energy barrier to the rotation of these rotamers appeared low as coalescence of the cyclohexyl peaks was observed at 55 °C. A moderate total yield (43%) of migration products **389** and **390** was obtained by the reaction of symmetrical diallyl urea **324** containing a set of bulky terpenoid rings (Scheme 68). The ^{1}H and ^{13}C NMR spectra of **389** and **390** showed doubling of all peaks, which could be due to a mixture of *E*/*Z* isomers of the double bond in blue or due to restricted/slow bond rotation of the N–C (in blue) or C–C (in red) bond, rendering diastereomers due to the presence of the stereocentres. The latter is more likely because of the crystal structure of **389** and the coalescence of the proton and carbon peaks in **389** and **390** at elevated temperatures (52 °C and 95 °C).

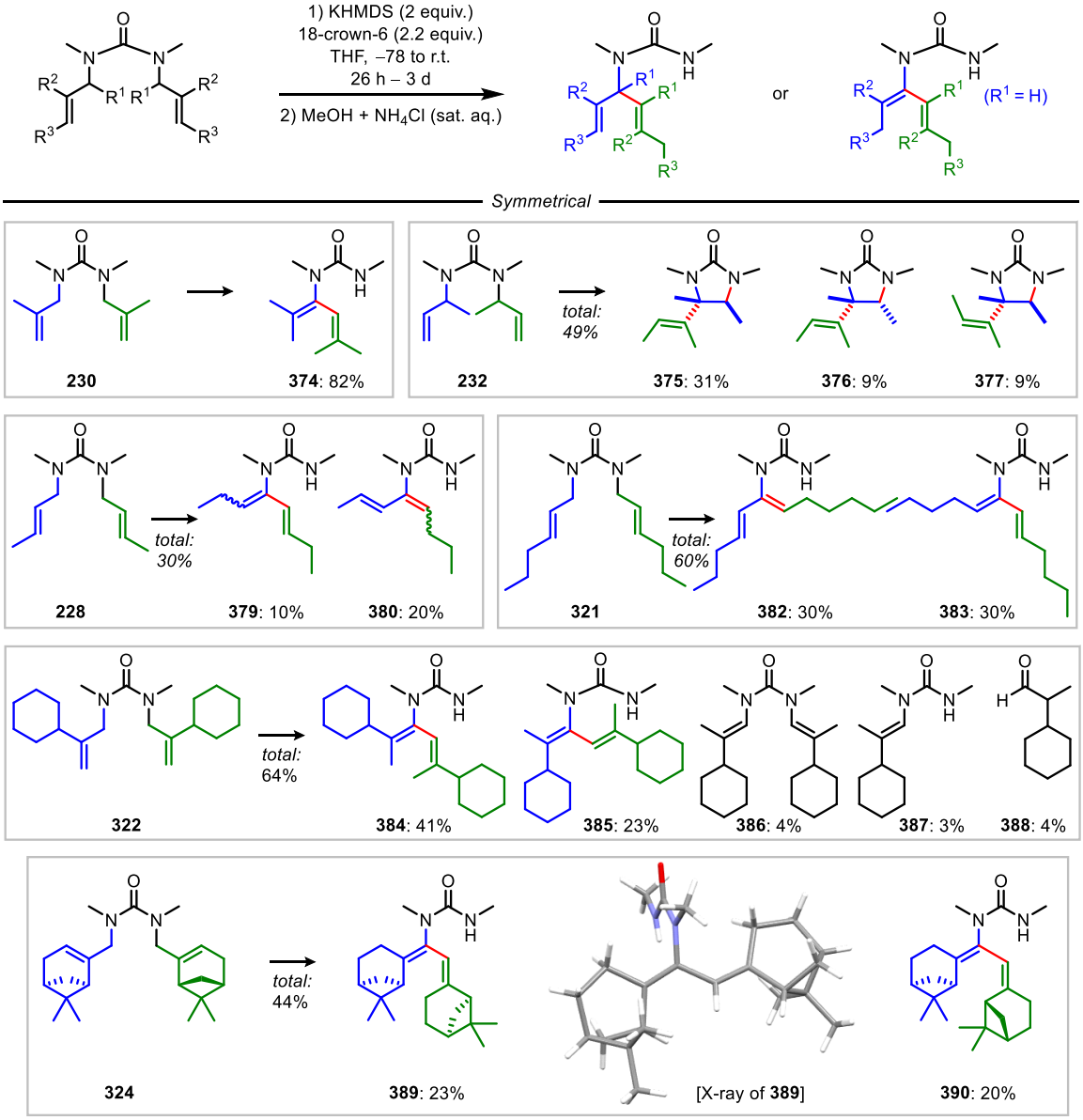

Scheme 68. Scope for the N→C vinyl migration of symmetrical α-, β-, and γ-alkyl substituted diallyl ureas. Blue represents the nucleophile. Green represents the electrophile. Red represents the new bonds formed. The squiggly bond in **379** and **380** means that the compound is a single isomer yet of unknown configuration.

Based on the atom connectivity, imidazolidinones **375**, **376** and **377** could only have resulted from the actual N→C migration taking place on urea **232**, which then is followed by an *in situ* basic hydroamination of the less substituted terminal alkene in the initial migration product (assumed to be **392**, Scheme 69B). This undesired cyclisation reaction may be explained by the fact that the normally observed isomerisation of the two alkenes into conjugation cannot occur due to the presence of the fully substituted α-carbon atom in the initial migration product. The *anti*:*syn* ratio was proposed to stem from the possible transition states assumed to be in envelope conformation (Scheme 69C). There are two possible transition states: one with the double-bond in a pseudo-equatorial position (**393** and **394**), while the other transition state **395**/**396** consists of a pseudo-axial orientated double-bond. The latter transition

state (**395**/**396**) is more disfavoured as it experiences steric interactions between the terminal alkene and the more substituted alkene in pseudo-equatorial position. The isomerisation of the more substituted alkene may be explained by the fact that a more thermodynamically stable *E*-geometry is adopted (**393** versus **394** and **395** versus **396**), in which also steric interactions between the terminal methyl group (represented in green and red) and the imidazolidinone moiety are mitigated.

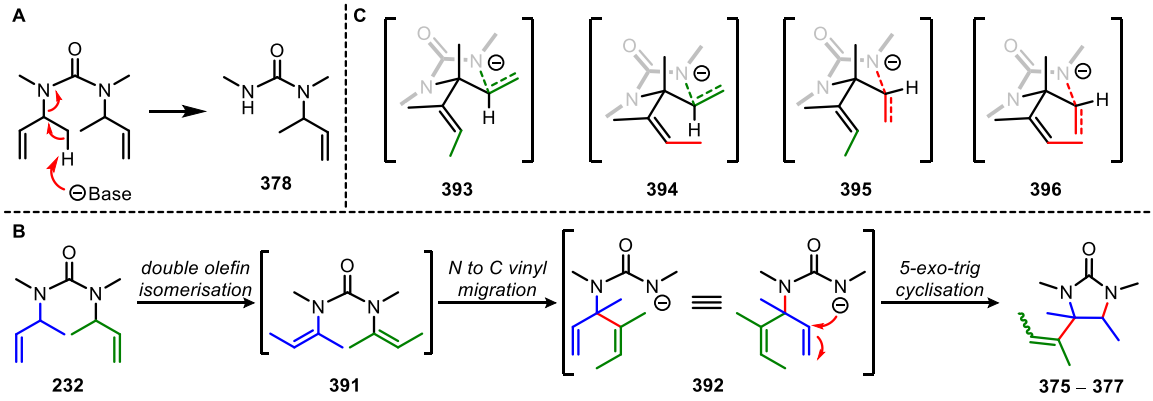

Scheme 69. Schematic explanation for the observed de-allylation (A) and 5-*exo-trig* cyclisation with corresponding transition state structures (B and C) in the N→C vinyl migration of symmetrical α-methyl substituted diallyl urea 232. Blue represents the nucleophile. Green represents the electrophile. Red represents the new bonds formed.

As explained above, the de-allylation observed with starting urea **228** was a result of δ-deprotonation, possible due to the presence of the γ-methyl substituent, which led to elimination of the ureido anion and thus upon protonation the formation of urea **381** (Scheme 70A). The same δ-deprotonation was observed with the attempted N→C vinyl migration of symmetrical *N*,*N*'-diprenyl urea **251**, giving exclusively mono-de-allylated urea **397** (Scheme 70B). An explanation for the fact that the competitive elimination was not or less problematic with γ-propyl substituents may be that the δ-C–H in urea **228** is more acidic than in urea **321** where the anion is destabilised by a slight inductive effect of the neighbouring carbon atoms in the propyl chain (Scheme 70C).

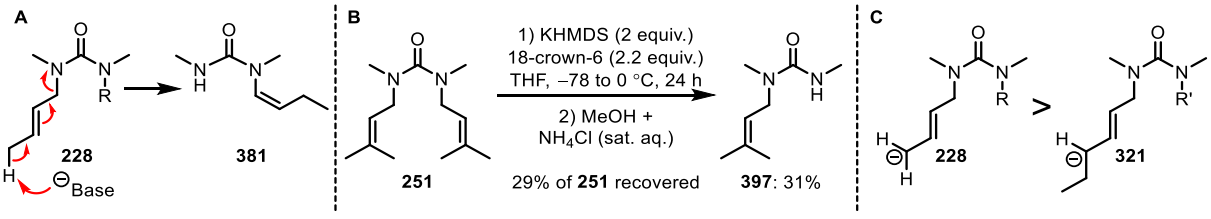

Scheme 70. Schematic explanation for the competitive de-allylation by deprotonation of the γ-methyl substituent in 228 forming 381 (A), the thus unsuccessful N→C vinyl migration of symmetrical diprenyl urea 251 (B) and the anion stability in comparison to a γ-propyl substituent (C).

In contrast to the successful outcome of the N→C vinyl migration of symmetrical β-cyclohexyl substituted diallyl urea **322** (Scheme 68), when starting from symmetrical γ-cyclohexyl substituted diallyl urea **323**, even with elevated temperatures, only proposed 6-*exo-trig* cyclised product **398** was observed in 7% NMR yield (Scheme 71). Presumably, the *in situ* isomerisation of the γ-cyclohexyl substituted allyl chain was slow or not occurring and thus upon α-deprotonation of one allyl chain a 6-*exo-trig* cyclisation took place onto the other allyl chain in **399**, generating **400** that upon *in situ* isomerisation formed the observed product **398**.

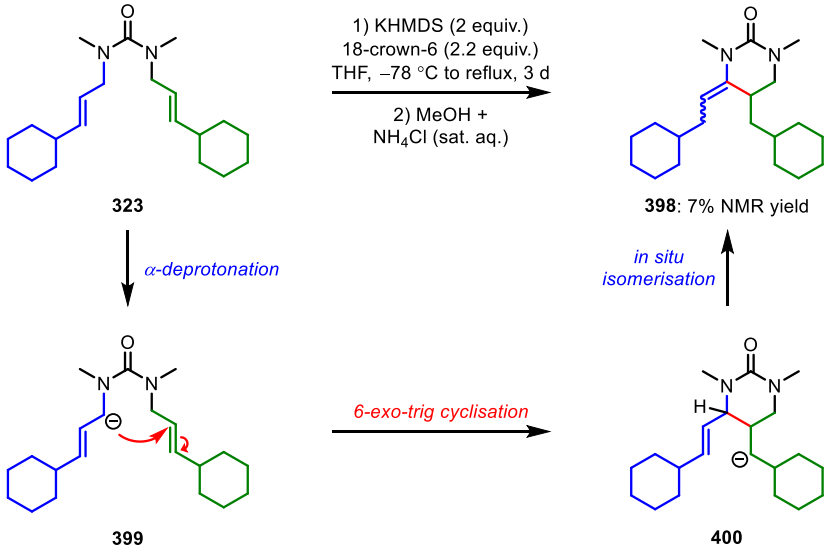

Scheme 71. Attempted N→C vinyl migration of symmetrical γ-cyclohexyl substituted diallyl urea 323, resulting in the undesired 6-*exo-trig* cyclisation product 398 in low yield. Blue represents the nucleophile. Green represents the electrophile. Red represents the new bonds formed. The yield is determined by ^{1}H NMR using 1,2,4-trimethoxybenzene as an internal standard.

As the general tolerance of this N→C vinyl migration towards symmetrical α-, β- and γ-substituted diallyl ureas was established, the method was next explored with unsymmetrical structurally varied diallyl ureas (Scheme 72). Greater complexity was expected with the unsymmetrical diallyl ureas since either *N*-allyl group could act as the nucleophilic anion-stabilising or the electrophilic migrating group. As anticipated, the N→C vinyl migration of unsymmetrical α-methyl-substituted allyl urea **237** gave both migration product **401** (from an α-methyl-substituted electrophile) and cyclisation products **402** and **403** (from an α-methyl-substituted nucleophile) with a moderate total yield of 66% (Scheme 72). The diastereomeric ratio (0.65:0.35) can be explained with the same transition states (**393** and **395**) used for cyclisation products **375**, **376** and **377** in Scheme 69; transition state **395** leading to **403** is more disfavoured as it experiences steric interactions between the terminal alkene and the *E*-alkene in pseudo-equatorial position.

The same unselective, yet successful, N→C vinyl migration was achieved with unsymmetrical ureas **242** and **326** in which an unsubstituted allyl group was paired with a γ-methyl and a γ-propyl substituted allyl group, respectively (Scheme 72). In both cases, each side of the diallyl urea was able to act as the anion-stabilising and the migrating group, giving both regioisomers **404** and **405**, and **406** and **407** together with its isomer **408**. The moderate total yields achieved may be explained by the competitive δ-deprotonation taking place, resulting in the undesired de-allylation proved with the presence of partially de-allylated urea **366** in 14% yield.

Combination of an α-methyl- with a γ-methyl substituted allyl group (**327**) resulted in a low yielding rearrangement; this could have been expected due to the possibility of de-allylation occurring on both allyl groups (Scheme 72). Yet, cyclisation product **409**, which has formed after N→C vinyl migration with the α-methyl substituted allyl group acting as the nucleophile, was isolated in a yield of 13%.

However, intriguingly, complete regioselective N→C vinyl migration was achieved with unsymmetrical ureas **337** and **243** that consist of an unsubstituted allyl group and a 1-cyclohexenylmethyl group and a β-methyl substituted allyl group, respectively (Scheme 72). The N→C vinyl migration of urea **337** effectively generated migration product **410** in 66% yield; the 1-cyclohexenylmethyl group has acted solely as the nucleophile. Similarly, migration product **411**, for which the β-methyl substituted allyl chain in **243** acted as the nucleophile, was exclusively generated in a high yield of 70%.

This observed regioselectivity was subsequently explored by pairing the β-methyl substituted allyl group with an α-methyl (**329**) and a γ-methyl substituted allyl partner (**241**) (Scheme 72). From urea **329,** the N→C vinyl migration resulted in the regioselective formation of migration products **412** and **413** in high yield, with the β-methyl substituted allyl group exclusively acting as the nucleophile. By contrast, urea **241** gave a mixture of **414** (from a β-methyl substituted nucleophile) and regioisomers **415** and **416** (from a γ-methyl substituted nucleophile). Competitive de-allylation, resulting in the formation of partially de-allylated urea **417** in 27% yield, is the cause of the moderate total reaction yield.

Based on these divergent results concerning the regioselectivity, it was hypothesised that the β-methyl substituted allyl chain undergoes a significantly slower *in situ* allyl-to-vinyl isomerisation than the α-methyl substituted and unsubstituted allyl groups; as soon as the α-methyl substituted/unsubstituted allyl chain is turned into a vinyl group, α-deprotonation of the β-methyl substituted allyl chain results in the N→C vinyl migration.

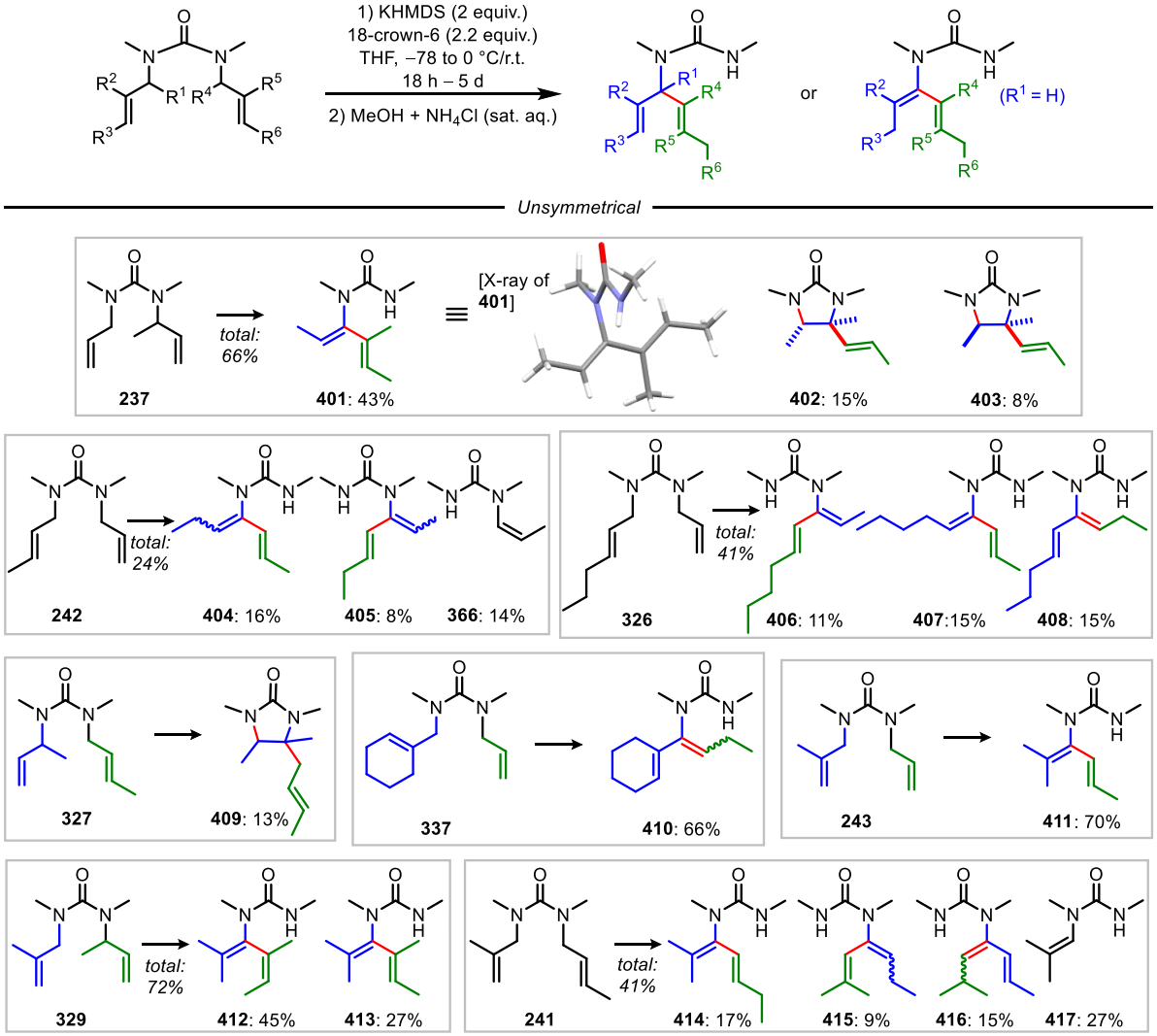

Scheme 72. Scope for the N→C vinyl migration of unsymmetrical α-, β-, and γ-alkyl substituted diallyl ureas. Blue represents the nucleophile. Green represents the electrophile. Red represents the new bonds formed. The squiggly bond means that the compound is a single isomer yet of unknown configuration.

The N→C vinyl migration of unsymmetrical geranyl-substituted diallyl urea **240** was unsuccessful and resulted, besides partial isomerisation into **418**, in the undesired γ-methyl deprotonation yielding deallylated, *Z*-vinyl urea **366** in 58% yield (Scheme 73).

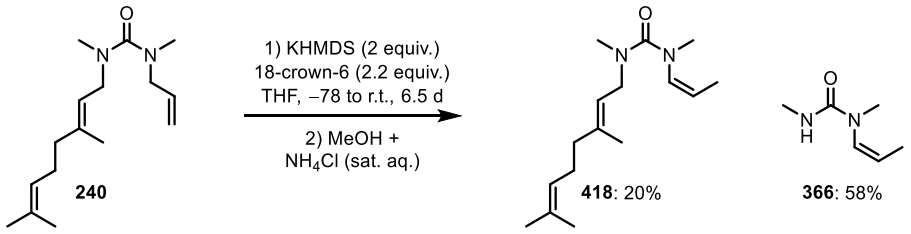

Scheme 73. Attempted N→C vinyl migration of unsymmetrical geranyl substituted diallyl urea 240, resulting in partial *in situ* isomerisation and de-allylation.

Building on the observed regioselectivity when combining a β-methyl substituted allyl group with an α-methyl substituted allyl group, unsymmetrical ureas **328**, **330**, **331**, **332** and **335** were submitted to the reaction conditions with the aim to expand the scope of the N→C vinyl migration and to introduce complexity (Scheme 74). As anticipated, in the case of ureas **328** and **330** the β-methyl substituted allyl group acted exclusively as the nucleophile, yet even more importantly: the significant bulkiness of the α-pentyl and α-cyclohexyl group did not affect their migration ability, affording migration products **419** and **420**, and **421** in excellent yield (Scheme 74).

The same successful regioselective N→C vinyl migration was achieved when using a β-cyclohexyl substituted allyl group as the nucleophile instead (**331**), giving remarkably hindered migration products **422** and **423**, albeit in low yield, along with urea **424**, which was assumed to be the reaction intermediate, in 55% yield (Scheme 74). Only when pairing a β-methyl substituted allyl group with a β-cyclohexyl substituted allyl partner (**332**) the regioselectivity was practically lost. Migration product **425** and regioisomers **426** and **427** were afforded in a 1.3:1 regioisomeric ratio with a slight favour of the smaller β-methyl substituted allyl group acting as the nucleophile (Scheme 74). Instead of four peaks, six peaks for the cyclohexyl group were observed in the ^{13}C NMR spectrum of **425**, **426** and **427**, suggesting that they consist as a mixture of two enantiomeric rotamers due to restricted/slow bond rotation of the N–C (in blue) or C–C (in red) bond. The energy barrier to the rotation of these rotamers appeared low as coalescence of the cyclohexyl peaks was observed at 55 °C. In addition, urea **428** – assumed to be the reaction intermediate – was afforded in 15% yield. Similar results were found with urea **335** in which the β-methyl substituted allyl group was combined with a 1-cyclohexenylmethyl derivative; migration products **429** and **430**, and regioisomer **431** were afforded in a 1.9:1 regioisomeric ratio with a more significant favour for the 1-cyclohexenylmethyl derivative acting as the electrophile (Scheme 74). The ^{1}H and ^{13}C NMR spectra of **429** and **430**, and **431** showed doubling of all peaks, which was presumably caused by restricted/slow bond rotation of the N–C (in blue) or C–C (in red) bond, rendering diastereomers due to the presence of the stereocentres.

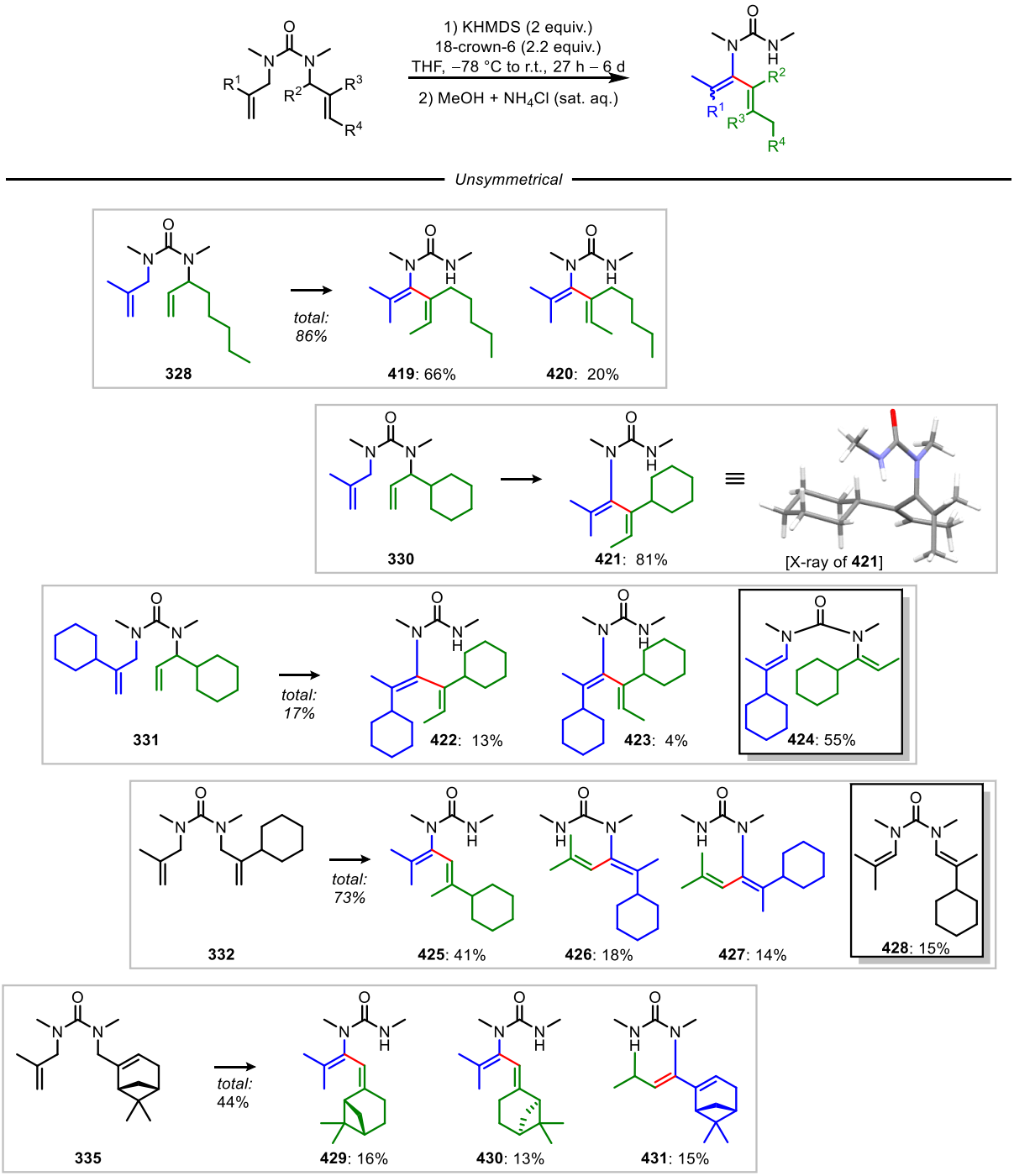

Scheme 74. Scope for the regioselective N→C vinyl migration of unsymmetrical β-alkyl substituted diallyl ureas. Blue represents the nucleophile. Green represents the electrophile. Red represents the new bonds formed.

Unfortunately, the attempted N→C vinyl migration of unsymmetrical urea **333** consisting of a β-methyl- and a γ-cyclohexyl substituted allyl group was unsuccessful; only partially *in situ* isomerised urea **432** was generated in 91% yield (Scheme 75). The isolation of **432** was an interesting result revealing that the *in situ* isomerisation of the γ-cyclohexyl allyl chain is significantly slower compared to the β-methyl allyl group, which itself isomerises considerably slow or even not at all. This raised the

following question: why did α-deprotonation of the γ-cyclohexyl substituted allyl chain not result into the desired N→C vinyl migration as soon as the β-methyl substituted allyl chain had isomerised? To explore this intriguing result, the partially isomerised intermediate **432** was resubmitted to the N→C vinyl migration conditions, aiming to establish α-deprotonation of the γ-cyclohexyl substituted allyl group followed by nucleophilic attack on the (already in place) vinyl group (Scheme 75). However, starting urea **432** only was observed in the crude ^{1}H NMR in a 60% yield. When repeating the same reaction with more forcing conditions using elevated temperatures of 40 °C followed by reflux, which eventually resulted into decomposition of 18-crown-6, small amounts of migration products **433** and **434** were observed; yet, mostly starting urea **432** was observed (Scheme 75). Due to the small scale of this reaction, purification of the crude mixture gave a mixture of the two migration products, ^{1}H NMR was used to tentatively assign them as **433** and **434**.

These results agree with the unsuccessful N→C vinyl migration of symmetrical γ-cyclohexyl substituted diallyl urea **323** and suggest that under the current reaction conditions the γ-cyclohexyl substituted allyl group is not effectively forming the allylic anion species. This limits its ability to act as the nucleophile and also as the electrophile as the γ-cyclohexyl substituted allyl group cannot subsequently undergo the *in situ* olefin isomerisation to the *Z*-vinyl geometry. An explanation for this may be that the γ-cyclohexyl substituent prevents coordination of the allyl-anion generated after α-deprotonation to the urea, which is required for *Z*-isomerisation.

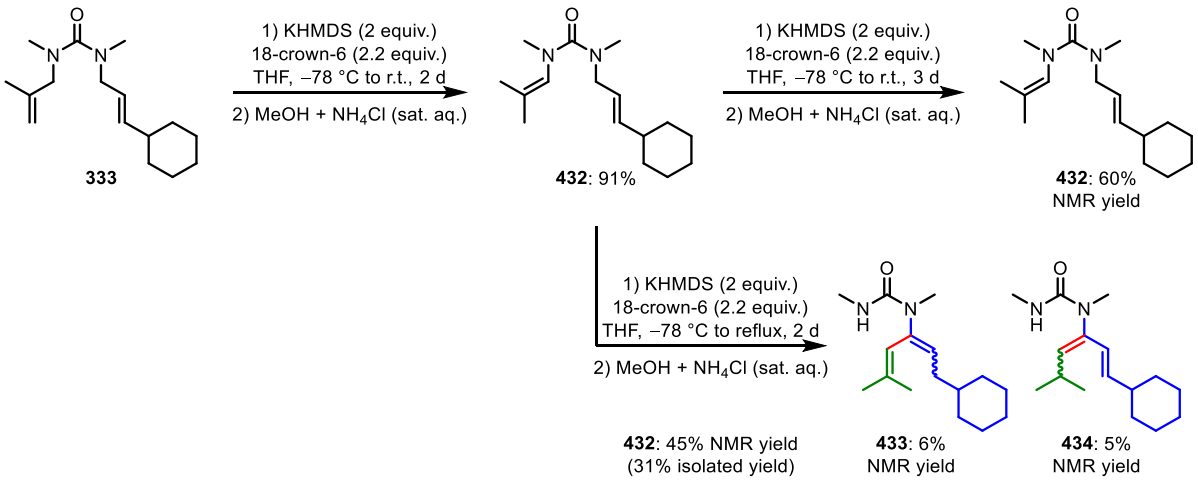

Scheme 75. Attempted N→C vinyl migration of unsymmetrical β-methyl- and γ-cyclohexyl substituted diallyl urea 333 and partially isomerised derivative 432. Blue represents the nucleophile. Green represents the electrophile. Red represents the new bonds formed. The squiggly bond means that the compound is a single isomer yet of unknown configuration.

Similar ineffective results were obtained for the N→C vinyl migration of unsymmetrical ureas **338** and **336**, consisting of a β-methyl-substituted allyl group and a *N*-cyclohexene group and *N*-1,3,3-trimethylbicyclo[2.2.1]heptan-2-ylideneethyl group, respectively (Scheme 76). When urea **338** was

treated with the optimal N→C vinyl migration conditions only partially isomerised urea **435** was observed in the crude ^{1}H NMR, yet upon purification by column chromatography hydrolysis of the vinyl group resulted in a mixture of **435**, de-vinylated urea and isobutyraldehyde. Therefore, the reaction was repeated, and the crude reaction mixture was this time purified by column chromatography with the use of neutralised silica; **435** was afforded in 95% yield (Scheme 76A). Urea **435** was resubmitted to the N→C vinyl migration conditions, yet even with elevated temperatures only de-allylated urea **417** was observed in 49% NMR yield (Scheme 76A). Note, no conversion of **435** was observed at room temperature.

Reaction of urea **336** under the optimal N→C vinyl migration conditions resulted in the formation of partially isomerised urea **436** in an NMR yield of 65% (Scheme 76B). Repeating the reaction with longer reaction time, the addition of more equivalents of KHMDS and 18-crown-6, and elevated reaction temperature resulted, besides partially isomerised urea **436** in 30% yield, in the formation of cyclisation product **437**, albeit in a low yield of 16% (Scheme 76B). Based on the atom connectivity, N→C vinyl migration of **336** had taken place first with the β-methyl substituted allyl group acting as the electrophile and was followed by a 6-*endo*-*trig* cyclisation (**438**→**437**).

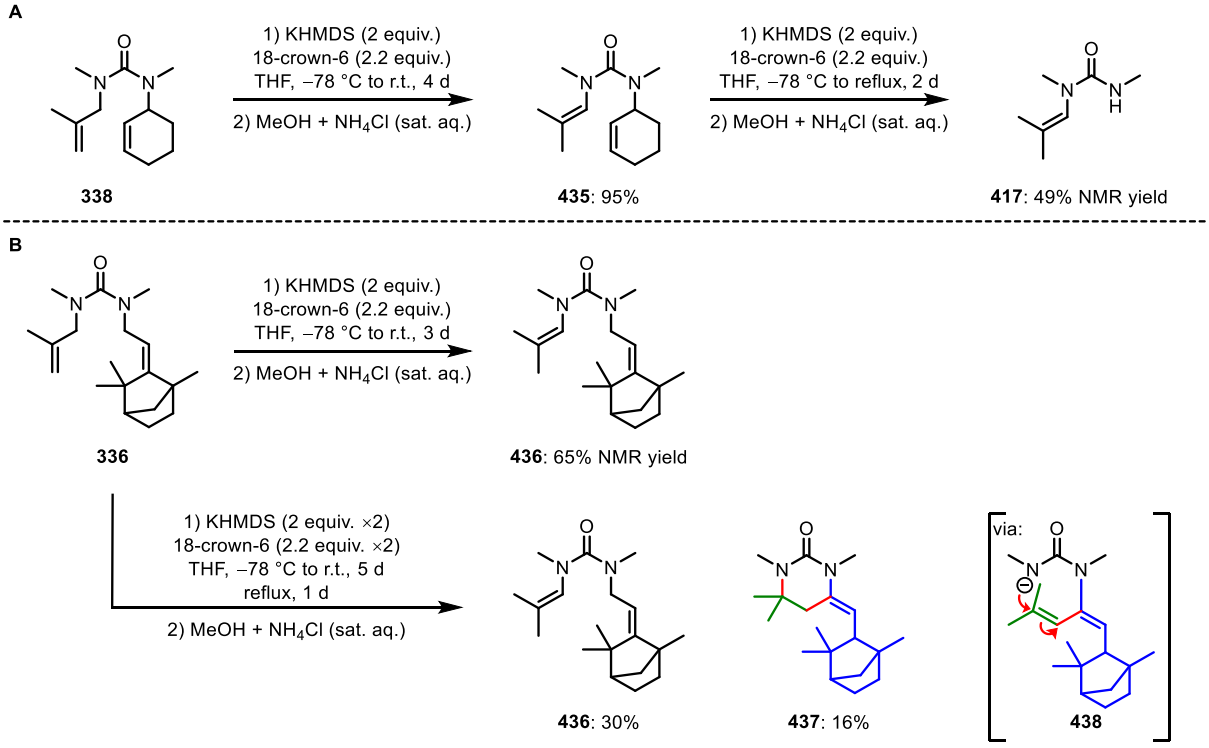

Scheme 76. Attempted N→C vinyl migration of unsymmetrical urea 338 and partially isomerised derivative 435 (A) and unsymmetrical urea 336 (B). Blue represents the nucleophile. Green represents the electrophile. Red represents the new bonds formed. The NMR yields are determined by ^{1}H NMR using 1,2,4-trimethoxybenzene as an internal standard.

It was concluded that both the *N*-cyclohexene group (from **338**) and the *N*-1,3,3-trimethylbicyclo[2.2.1]heptan-2-ylideneethyl group (from **336**) were not capable to act as the electrophilic migrating group under these reaction conditions. In contrast to the *N*-cyclohexene group, the *N*-1,3,3-trimethylbicyclo[2.2.1]heptan-2-ylideneethyl group is capable to act as the nucleophilic anion-stabilising group yet with very low efficacy. Presumably, for the *N*-cyclohexene it is not possible to have the allylic-anion generated after α-deprotonation to coordinate to the carbonyl, while for the *N*-1,3,3-trimethylbicyclo[2.2.1]heptan-2-ylideneethyl group it is possible yet challenging due to its sterically demanding structure.

3.2.3.2 Rearrangement of Phenyl-, Benzyl- and Vinyl-Substituted Diallyl Ureas

Having explored a range of diallyl ureas containing alkyl substituents at the α-, β-, and γ-position, attention was next turned to investigate the use of other substituents; to further expand the scope of this N→C vinyl migration method, a range of phenyl-, benzyl- and vinyl-substituted diallyl ureas were subjected to the optimised reaction conditions.

The investigation began with symmetrical dicinnamyl urea **249** to determine, without the added complexity of possible regioisomers, whether the *N*-cinnamyl group can act as the nucleophilic anion-stabilising group and the electrophilic migrating group. Unfortunately, no conversion of starting urea **249** to desired migration product **439** was achieved; only cyclisation product **440** was afforded in 42% yield (Scheme 77A). This result suggests that the required, initial *in situ* olefin isomerisation is very slow or non-existent under the current reaction conditions. Like observed with symmetrical γ-cyclohexyl substituted diallyl urea **323** (Scheme 71), α-deprotonation at one of the allylic positions resulted in a 6-*exo*-*trig* cyclisation onto the other *N*-cinnamyl group, forming **442**, from **441**, that upon *in situ* isomerisation gave the observed product **440**.

Even though the N→C vinyl migration of *N*,*N*'-(*E*)-divinyl urea **207** was ineffective, it was of interest to see whether pre-isomerisation of **249** to **443** would enable the N→C vinyl migration. Therefore, urea **249** was pre-isomerised with the use of a ruthenium catalyst (section 2.1),[113] forming urea **443** with *E*-geometry for both vinyl chains in high yield (section 5.3.2). Submission of starting urea **443** to the N→C vinyl migration conditions resulted in the formation of cyclisation product **445**, observed by crude ^{1}H NMR; again, none of the desired migration product **444** (or **447**) was detected (Scheme 77B). Intriguingly, unlike with *N*,*N*'-(*E*)-divinyl urea **207**, γ-deprotonation did take place and resulted in desired olefin isomerisation/N→C vinyl migration sequence which was then followed by a 5-*exo*-*trig* cyclisation. A reason for the successful γ-deprotonation could be that, in comparison to **207**, a more stable anion gets formed due to the conjugation with the phenyl group (**446**). The presence of the phenyl

group may also explain the observed cyclisation; attack of the *in situ* generated ureido anion after N→C vinyl migration (**446**→**447**) onto the phenyl-substituted alkene (blue in **447**) could be envisioned, with the phenyl ring acting as a stabilising anion trap (**447**→**448**). Then *in situ* olefin isomerisation of **448** gave the observed cyclisation product **445**.

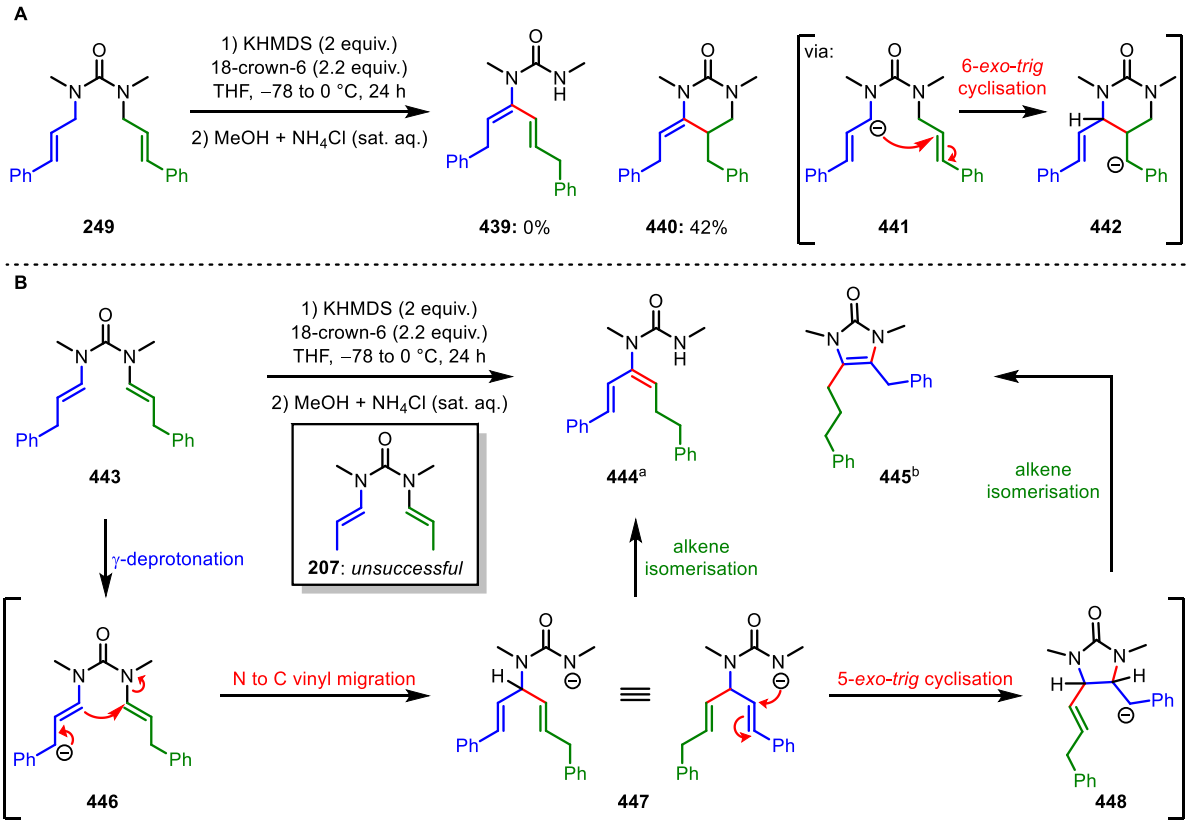

Scheme 77. Rearrangement of symmetrical phenyl-substituted diallyl urea 249 (A) and its pre-isomerised equivalent 443 (B). Blue represents the nucleophile. Green represents the electrophile. Red represents the new bonds formed. [a]Not observed by crude ^{1}H NMR. [b]Observed by crude ^{1}H NMR with complete conversion of the starting urea.

The same results were obtained for the reaction of unsymmetrical ureas **248**, **451** and **452**, forming cyclisation product **450** exclusively in all cases (Scheme 78). It can be assumed that the N→C vinyl migration of **248** was regioselective with the *N*-cinnamyl group acting as the nucleophile and the *N*-allyl group as the electrophile. A reason for this may be that the olefin isomerisation of the *N*-allyl group is significantly more rapid due to the formation of a more substituted, thus more stable alkene; the energy difference between the *N*-cinnamyl group and its isomerised derivative is supposedly not substantial. Upon isomerisation of the *N*-allyl chain (**248**→**459**), α-deprotonation of the *N*-cinnamyl group enabled nucleophilic attack onto the *N*-vinyl group (**460**), resulting in the regioselective N→C vinyl migration (**462**) followed by 5-*exo*-*trig* cyclisation with the phenyl ring (blue in **462**→**463**) acting as a stabilising anion trap (Scheme 79A). For **451** and **452** it was hypothesised that the *E*-geometry of

the vinyl group was the origin of the regioselectivity, with the *N*-cinnamyl group being the only possible nucleophile that upon α- or γ-deprotonation, respectively, followed the same mechanism as **460** in Scheme 79A.

Aiming to prevent the undesired cyclisation after the N→C vinyl migration, unsymmetrical ureas **340** and **341**, possessing a β-phenyl- and a β-benzyl substituted allyl group, respectively, were subjected to the reaction conditions (Scheme 78). It was envisioned that, due to its position, the phenyl ring would now be unable to act as a cyclisation trap after the N→C vinyl migration. Unfortunately, migration product **453** from starting urea **340** was only produced in 12% yield; mostly, cyclisation product **454** was generated in 72% yield. From starting urea **341** cyclisation product **457**, instead of expected migration product **456**, was afforded in a good yield of 65%.

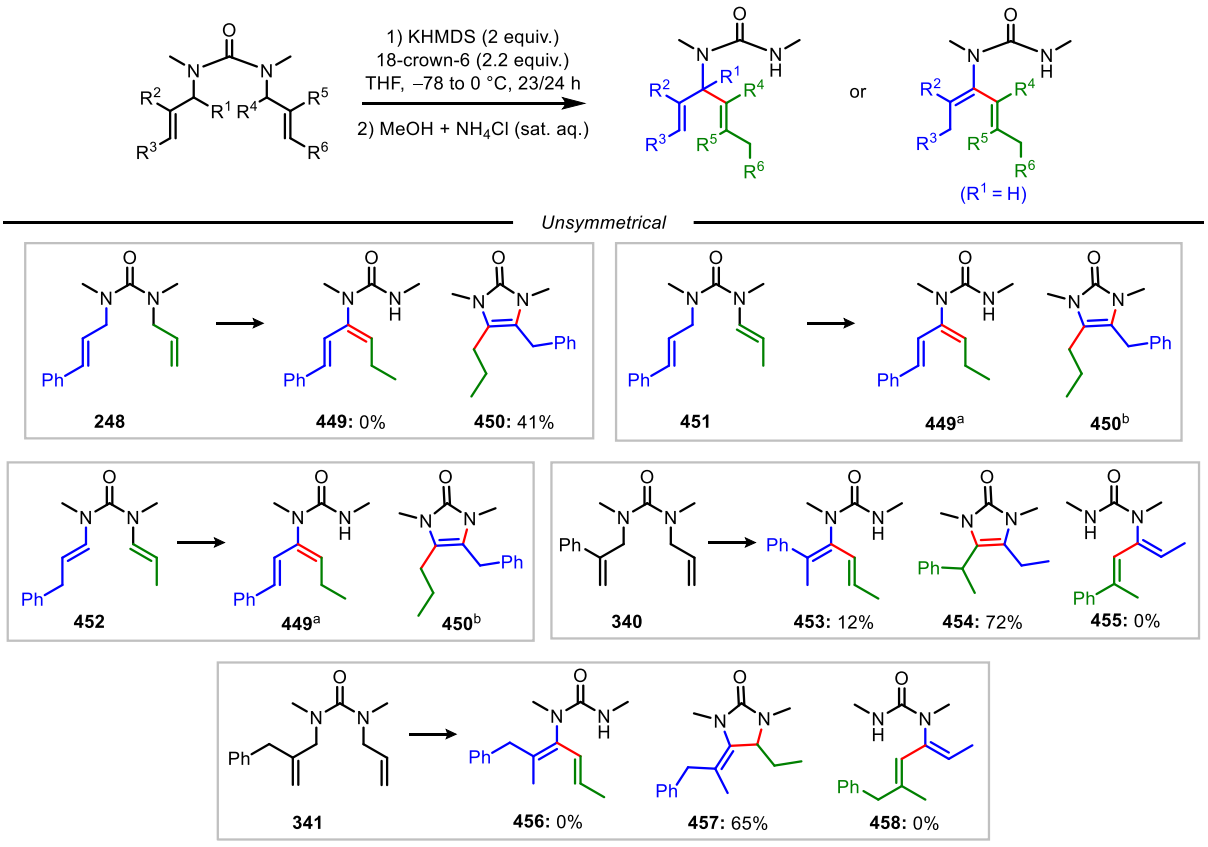

Scheme 78. Rearrangement of unsymmetrical phenyl- and benzyl-substituted diallyl ureas. Blue represents the nucleophile. Green represents the electrophile. Red represents the new bonds formed. [a]Not observed by crude ^{1}H NMR. [b]Observed by crude ^{1}H NMR with complete conversion of the starting urea.

From the atom connectivity in both cyclisation products **454** and **457**, it is not possible to tell whether the 5-*exo*-*trig* cyclisation has taken place before or after the N→C vinyl migration. However, based on the N→C vinyl migration results so far, it was believed that for urea **341**, due to the basic conditions and the benzylic position, *in situ* isomerisation gave fully isomerised urea **464** where the double bond

in blue resides in conjugation with the phenyl substituent (Scheme 79B). Upon α-deprotonation (**465**), the N→C vinyl migration would give hypothesised migration product **466** that would isomerise into **467**, to form a stable conjugated diene system. In this case, it is easy to envision that the positioning of the double-bonds conjugated with the phenyl ring in migration product **467** is now set up as a cyclisation trap for the ureido anion, resulting in the formation of **468** and upon protonation **457**. For starting urea **340** the most likely explanation was assumed to be that the β-phenyl substituted alkene (green in **472**) – styrene – is a significantly better electrophile than the *Z*-vinyl group (green in **470**) (Scheme 79C). Therefore, the unsubstituted allyl will be favoured to act as the nucleophile, forming migration product **473** initially, which also provides a cyclisation trap resulting in the formation of **474** that upon alkene isomerisation gave **454**, instead of the formation of migration product **455** upon protonation of **473**.

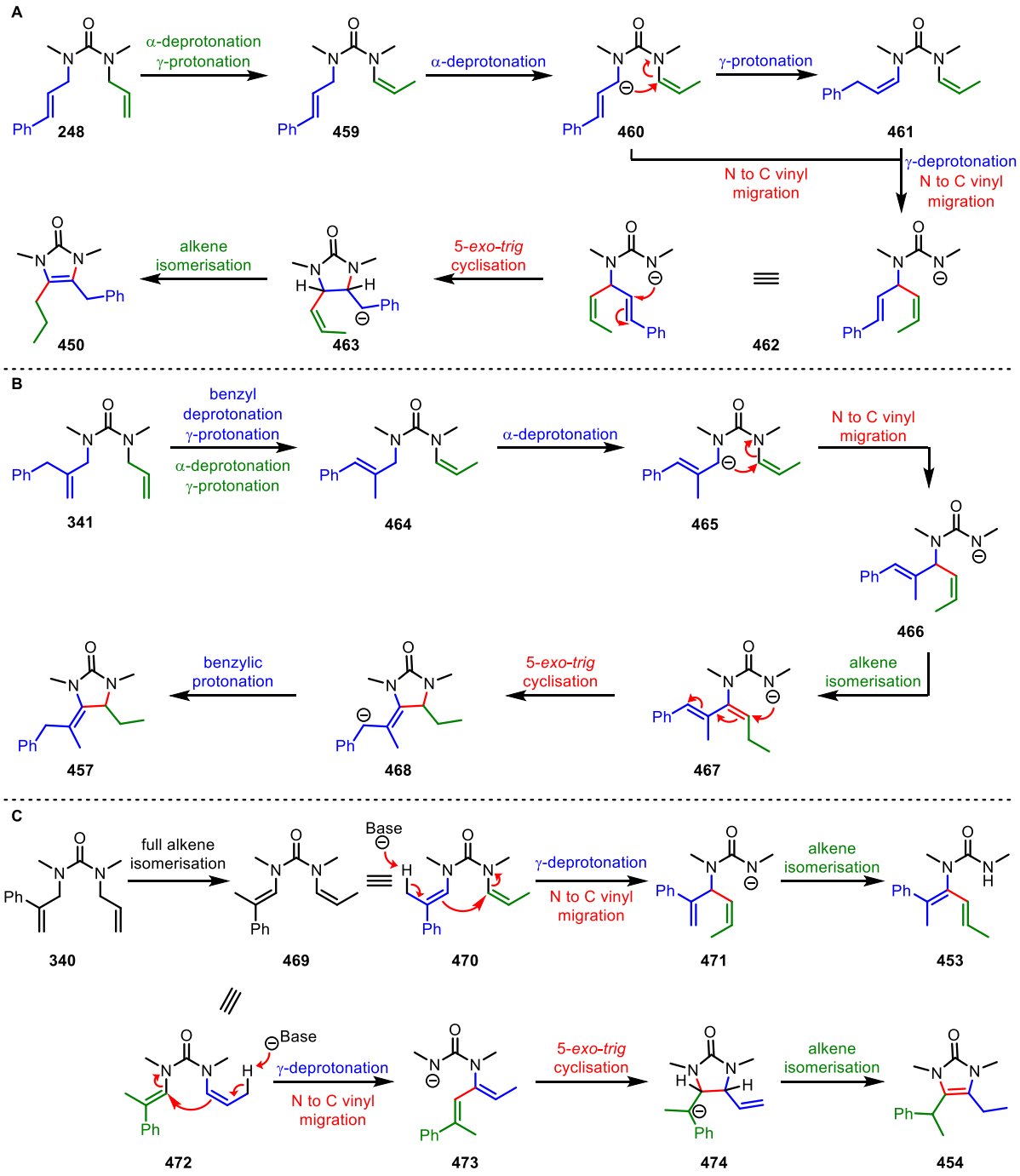

Scheme 79. Proposed mechanistic pathways for the N→C vinyl migration followed by 5-*exo-trig* cyclisation for ureas 248, 451 and 452 (A), 341 (B) and 340 (C). Blue represents the nucleophile. Green represents the electrophile. Red represents the new bonds formed.

Moving forward, it was of interest to determine whether the N→C vinyl migration method would be effective for compounds containing dienes and thus vinyl-substituted diallyl ureas were also subjected to the reaction conditions. The investigation started off with the N→C vinyl migration of symmetrical γ-1-propenyl substituted diallyl urea **325** yet resulted in a messy mixture and migration product **475** was not observed; upon purification, the only identifiable compound was urea **476** (Scheme 80). The

formation of **476** and the low reaction yield of 16% can be explained by the possibility of de-allylation taking place by ζ-deprotonation, resulting in elimination of the ureido anion (**477**) that can then perform a 5-*exo-trig* cyclisation onto the other allyl chain, if still intact, to form **478** and thus upon protonation **476** (Scheme 80).

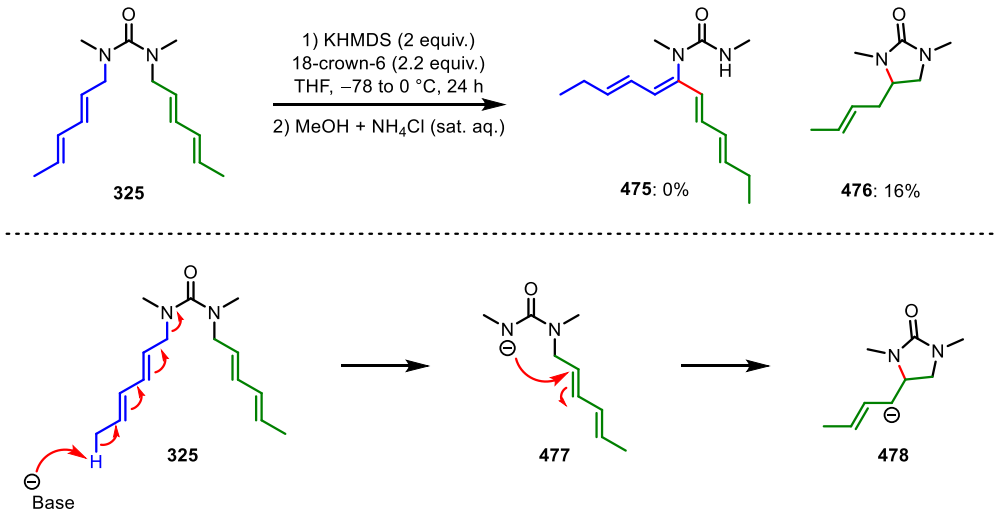

Scheme 80. Attempted N→C vinyl migration with γ-1-propenyl substituted diallyl urea 325, resulting in de-allylation followed by 5-*exo*-*trig*-cyclisation. Blue represents the nucleophile. Green represents the electrophile. Red represents the new bonds formed.

The N→C vinyl migration of the unsymmetrical γ-1-propenyl substituted diallyl urea **344** resulted in the formation of cyclisation product **481**, although in rather low yield of 8% due to the possibility of de-allylation because of the γ-1-propenyl substituent – proven by the presence of partially de-allylated urea **366** in 28% yield (Scheme 81). Starting ureas **342** and **343** consisting of a β-methyl- and a β- and a γ-vinyl substituted allyl group, respectively – where no ζ-deprotonation is possible – were also subjected to the N→C vinyl migration conditions but resulted in the formation of cyclisation products **484** and **485** (7% and 27% yield), and **489** (86% yield), respectively (Scheme 81). The presence of nitrile containing compound **486** in 22% yield was unexpected, and its formation mechanism has not been elucidated. The *anti*-conformation assigned by NOE analysis for urea **489** could be explained by the possible transition state **490**, assumed to be in an envelope conformation; both *N*-group reside in a pseudo-equatorial position to mitigate steric interactions.

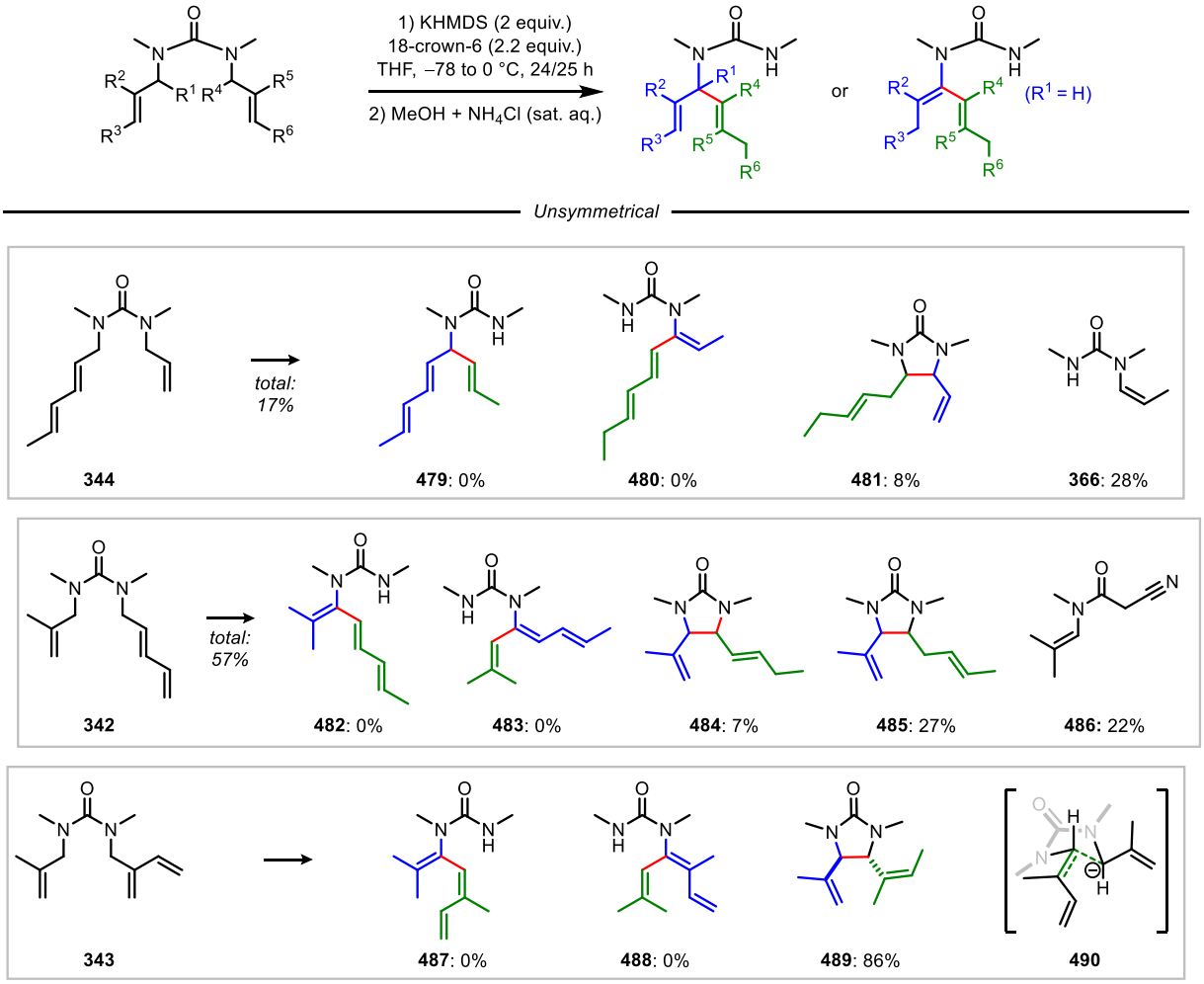

Scheme 81. Scope for the N→C vinyl migration of unsymmetrical β- and γ-vinyl substituted diallyl ureas. Blue represents the nucleophile. Green represents the electrophile. Red represents the new bonds formed.

To explain the formation of cyclisation product **481**, it was hypothesised that the olefin isomerisation of the γ-1-propenyl substituted allyl chain is relatively rapid as a more stable diene in conjugation with the urea moiety (**344**→**491**→**492**) would be formed (Scheme 82). Then, α-deprotonation of the unsubstituted allyl group (blue in **493**) would result in the nucleophilic attack at the vinylic carbon, forming migration product **494** which consist of a diene that then could act as an anion trap, enabling the observed 5-*exo*-*trig* cyclisation to **495**, which upon *in situ* alkene isomerisation would give **481**. Alternatively, it could be that the desired elimination of the ureido anion to form **480** did not occur; stabilisation of a carbanion by the alkene system (**493**→**495**) could be envisioned and would explain the formation of cyclisation product **481** upon another alkene isomerisation (Scheme 82).

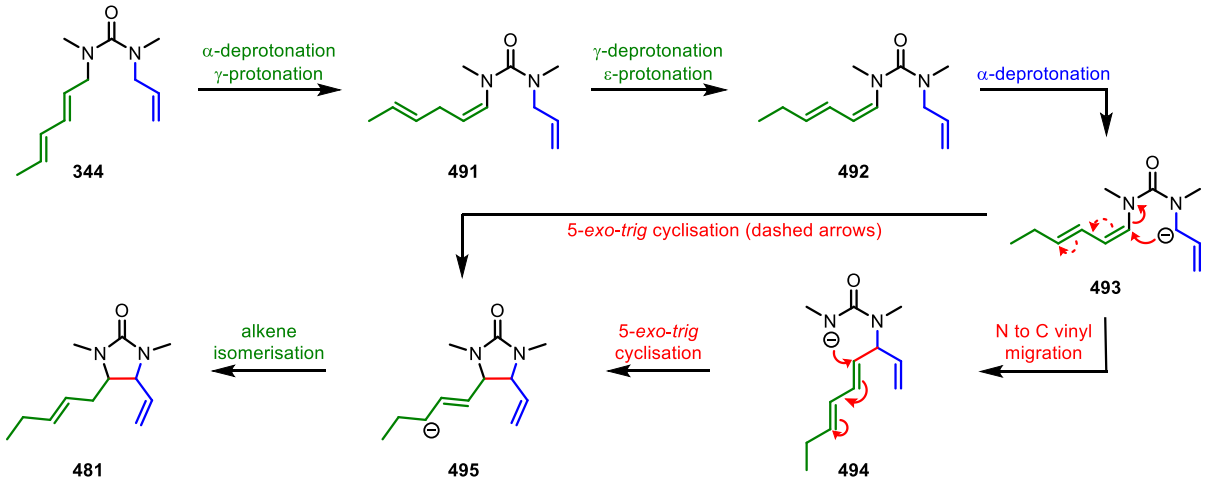

Scheme 82. Proposed mechanistic pathway for the N→C vinyl migration followed by 5-*exo*-*trig* cyclisation for urea 344 forming 481. Blue represents the nucleophile. Green represents the electrophile. Red represents the new bonds formed.

The formation of cyclisation products **484** and **485**, and **489** can be explained by the occurrence of the N→C vinyl migration in which the β-methyl substituted allyl group acted as the nucleophile (Scheme 83). This was not surprising as the β-methyl substituted allyl group which has shown to excel as the nucleophile was combined with the vinyl-substituted allyl groups which were assumed to undergo olefin isomerisation quickly to form more stable dienes that are in conjugation with the urea moiety. As described in the paragraph above, it was hypothesised that olefin isomerisation of the vinyl-substituted allyl chains is relatively rapid as a more stable diene in conjugation with the urea moiety would be formed (**497** and **501** – not observed). Then, α-deprotonation of the β-methyl substituted allyl group could result in the desired nucleophilic attack, forming migration products **499** and **503**. However, by acting as an anion trap, the diene in **499** and **503** could enable the observed 5-*exo*-*trig* cyclisation to **500** and **504**, which upon *in situ* alkene isomerisation would give **485** and **489**. The other possibility is that, after α-deprotonation of the β-methyl substituted allyl group, the desired nucleophilic attack was followed by the undesired stabilisation of the carbanion by the alkene system (dashed arrows in **498** and **502**), directly forming cyclisation products **484** and **485**, and **489**.

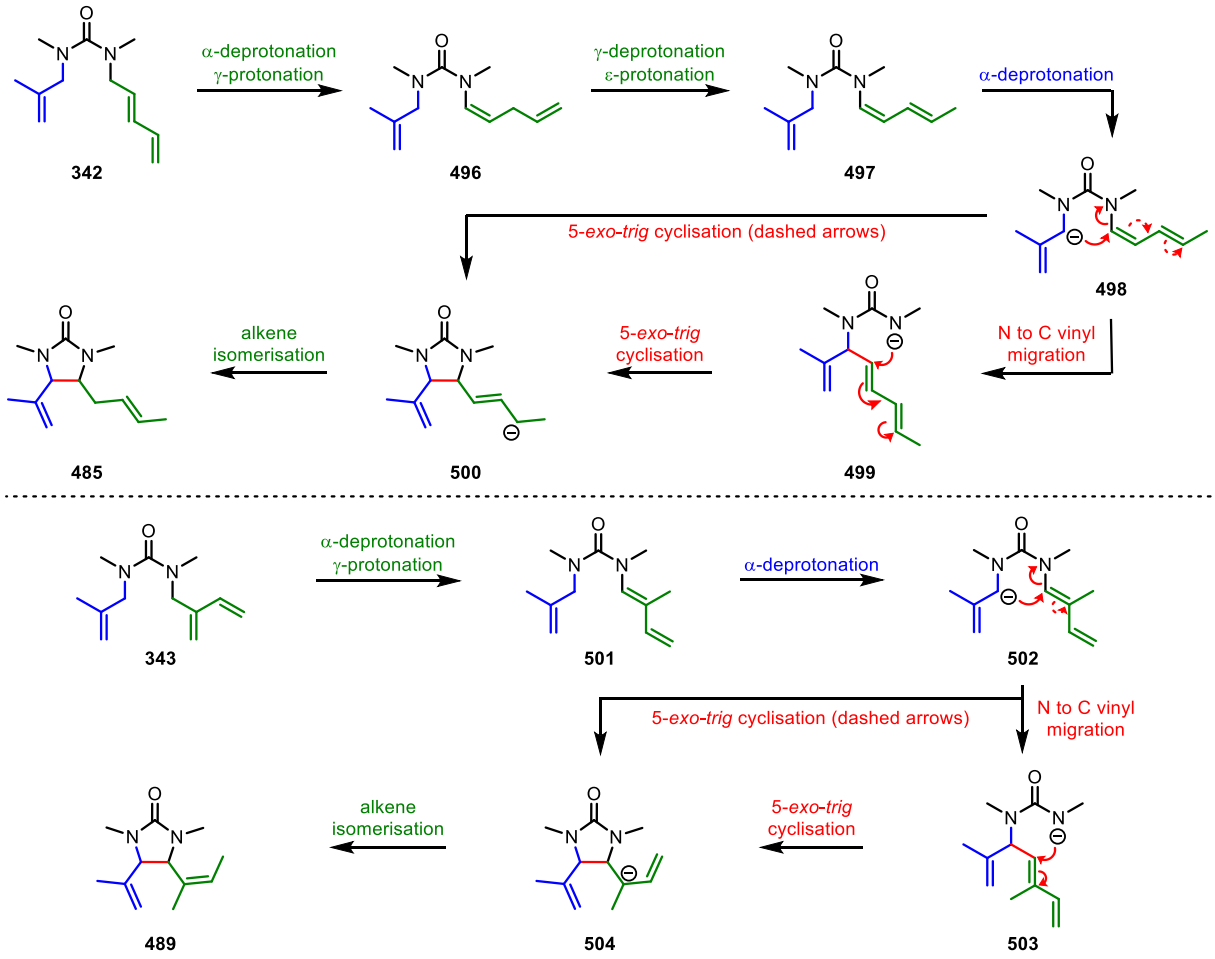

Scheme 83. Proposed mechanistic pathways for the N→C vinyl migration followed by 5-*exo*-*trig* cyclisation for ureas 342 and 343. Blue represents the nucleophile. Green represents the electrophile. Red represents the new bonds formed.

Furthermore, we wanted to probe the importance or necessity of the presence of a methyl group on both urea nitrogens, to determine whether other groups such as an N–H or an additional allyl chain, on one of the urea nitrogens would be tolerated in the N→C vinyl migration of *N*-allyl ureas. Attention was turned to attempting this methodology with unsymmetrical *N*,*N*'-triallyl urea **222**; it was of interest to examine whether the additional allyl group on one of the urea nitrogens would act as an anion-stabilising or migrating group and how it would affect the outcome of the N→C vinyl migration. The intriguing possibility of a double N→C vinyl migration was also raised, enabling access to complex, sterically hindered tertiary amines. However, unfortunately submitting **222** to the optimised KHMDS/18-crown-6 conditions only resulted in partial isomerisation, forming **506**, **507** and **508** (Scheme 84).

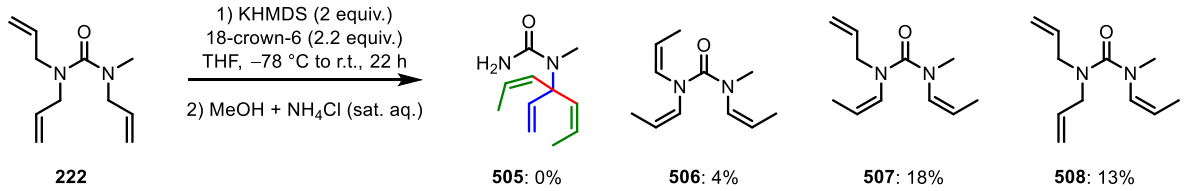

Scheme 84. Attempted N→C vinyl migration of *N*,*N*'-triallyl urea 222 to determine whether having an allyl chain instead of a methyl group on one of the urea nitrogens would affect the rearranging ability of *N*-allyl ureas.

3.2.3.3 Rearrangement of Functionalised Diallyl Ureas

Besides the hydrocarbon substituted allyl chains, the tolerance of functional groups such as protected alcohols and alkynes, silyl groups and bromide substituents in the N→C vinyl migration was investigated. Unfortunately, the attempted N→C vinyl migration of unsymmetrical β-alkyne substituted diallyl urea **346** resulted in a complex mixture from which, even upon purification, no compound structures could be elucidated (Scheme 85).

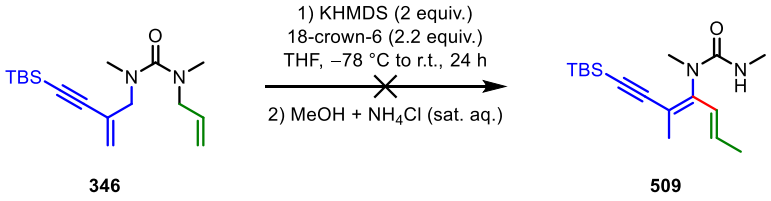

Scheme 85. Attempted N→C vinyl migration of unsymmetrical β-alkyne substituted diallyl urea 346 resulted in a complex, unidentifiable mixture. Blue represents the nucleophile. Green represents the electrophile. Red represents the new bonds formed.

When urea **347** substituted with a TBS-protected alcohol was submitted to the optimised reaction conditions, instead of migration product **510**, cyclisation products **511** and **512** that have lost the −OTBS functional group were afforded in a total yield of 52% (Scheme 86). Based on the atom connectivity, it could be established that the β-substituted allyl group had acted as the nucleophile in the N→C vinyl migration, but 5-*exo-trig* cyclisation had occurred subsequently due to the presence of a diene moiety formed upon loss of the protected alcohol. This elimination could have happened before or after the N→C vinyl migration, but in either case results from a δ-deprotonation due to the increased acidity of the δ-C–H now adjacent to the alkene. The required alkene isomerisation could yield ureas **513** or **516**; with isomerised urea **513** the δ-C–H deprotonation could be envisioned prior to the N→C vinyl migration, forming isomerised urea **514**. However, with isomerised urea **516** it was anticipated that the δ-C–H deprotonation would occur after the N→C vinyl migration of urea **517**. From either urea **514** or

urea **517** migration product **515** would be produced, and then the ureido anion in **515** could be trapped by the diene moiety forming an allylic-anion species that upon protonation gave the observed cyclisation products **511** and **512**.

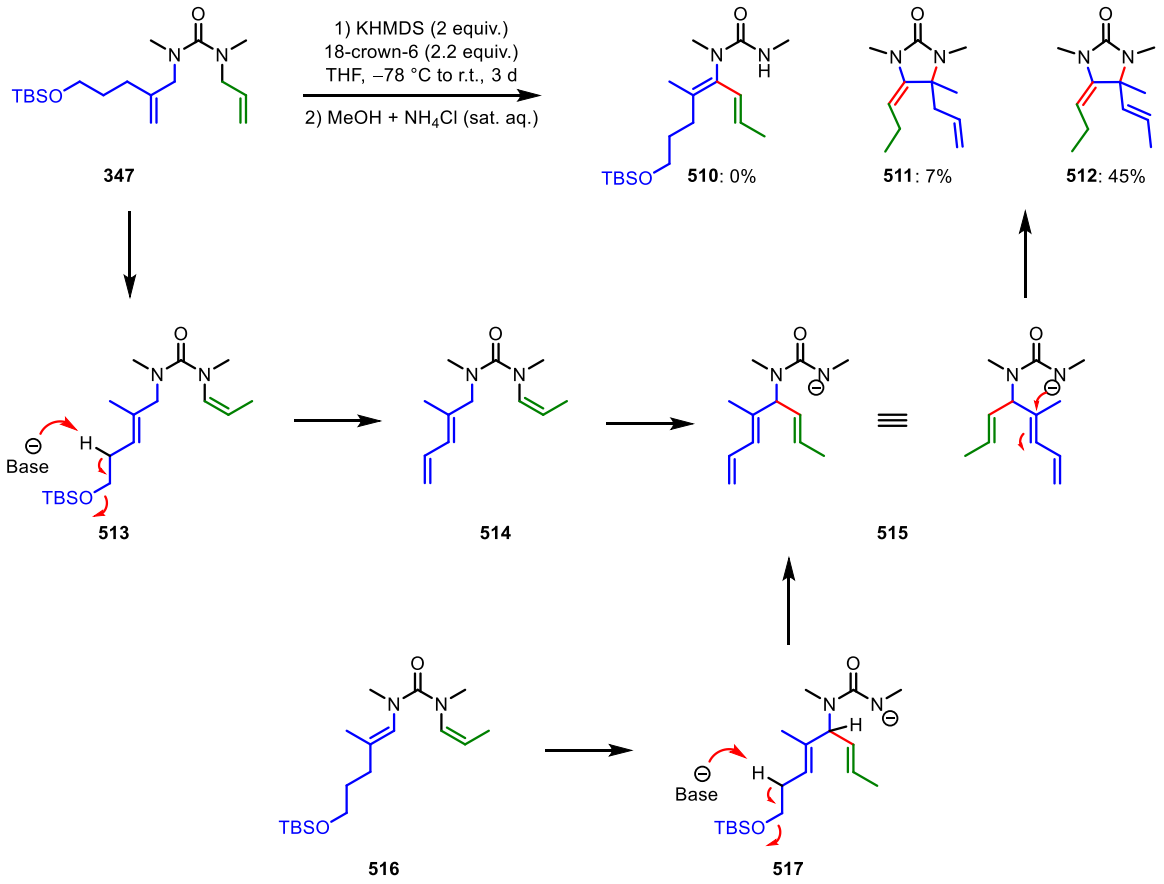

Scheme 86. N→C vinyl migration of unsymmetrical urea 347, containing a TBS-protected alcohol, followed by the undesired 5-*exo*-*trig* cyclisation formed cyclisation products 511 and 512. Blue represents the nucleophile. Green represents the electrophile. Red represents the new bonds formed.

Surprisingly, the N→C vinyl migration of unsymmetrical β-methyl- and γ-trimethylsilyl substituted diallyl urea **345** resulted in the generation of migration product **411**, the formal migration product of starting urea **243** (Scheme 87). It was hypothesised that under the reaction conditions KHMDS attacked the silyl group (**518**), which led to desilylation, giving urea **243** or **519** that consists of a β-methyl substituted and an unsubstituted allyl group, or its *Z*-vinyl equivalent, that then successfully underwent the N→C vinyl migration.

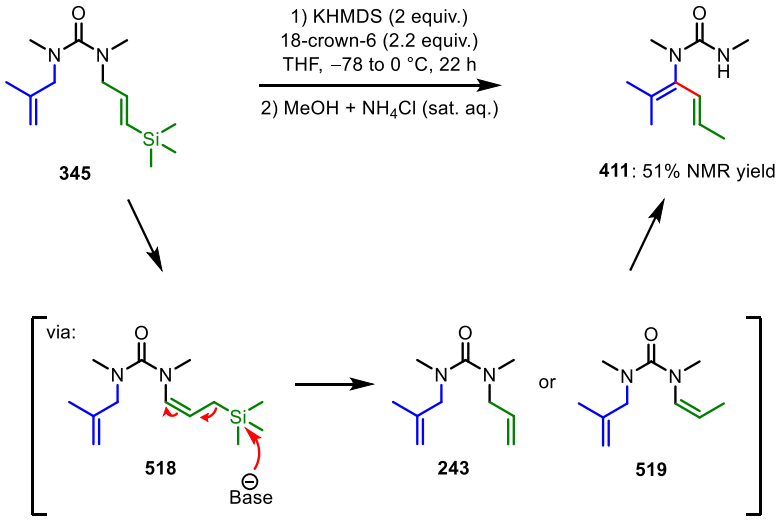

Scheme 87. N→C vinyl migration of unsymmetrical β-methyl and γ-trimethylsilyl substituted diallyl urea 345, resulted in migration product 411 with loss of the TMS group. The yield is calculated based on ^{1}H NMR analysis with the internal standard 1,2,4-trimethoxybenzene. Blue represents the nucleophile. Green represents the electrophile. Red represents the new bonds formed.

By reacting unsymmetrical β-bromide substituted diallyl urea **250** with 2 equivalents of KHMDS and 2.2 equivalents of 18-crown-6 at 0 °C, desired migration product **520** was not formed; instead debrominated, cyclisation products **521** and **522** were observed in NMR yields of 58% and 18%, respectively (Scheme 88). When the reaction was repeated with the optimised N→C vinyl migration conditions (2 equivalents of KHMDS and 2.2 equivalents of 18-crown-6 with a reaction temperature of −78 °C slowly warming up to room temperature), only cyclisation product **521** was observed by crude ^{1}H NMR.

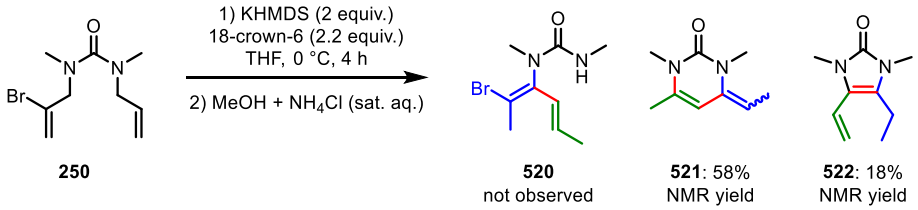

Scheme 88. Rearrangement of unsymmetrical β-bromide substituted diallyl urea 250 resulted in the formation of dibrominated, cyclisation products 521 and 522. The yield is calculated based on ^{1}H NMR analysis with the internal standard 1,2,4-trimethoxybenzene. Blue represents the nucleophile. Green represents the electrophile. Red represents the new bonds formed. The squiggly bond means that the compound is a single isomer yet of unknown configuration.

The atom connectivity of cyclised product **521** suggested that it could have resulted from the formation of the migration product **524** at first, which was then followed by a 6-*endo-trig* cyclisation with the bromide substituent acting as the leaving group (Scheme 89A). Some support for this mechanistic hypothesis comes from a report by Narasaka and co-workers in which bromoalkenes undergo similar

intramolecular vinylic substitution reactions with nitrogen nucleophiles, namely tosylamides.[71] The cyclisation of these bromoallyl sulfonamides was only found to be successful with the *E*-isomer; in the reaction of **250**, the olefin isomerisation would have generated reaction intermediate **523** in which the bromo group is in *E*-geometry with respect to the tethered urea from which stereoretentive N→C vinyl migration would have generated **524**. Finally, the acidic proton α to the nitrogen in urea **525** may be deprotonated to form the more stable, conjugated diene **521**. However, this step could also have taken place before the 6-*endo-trig* cyclisation.

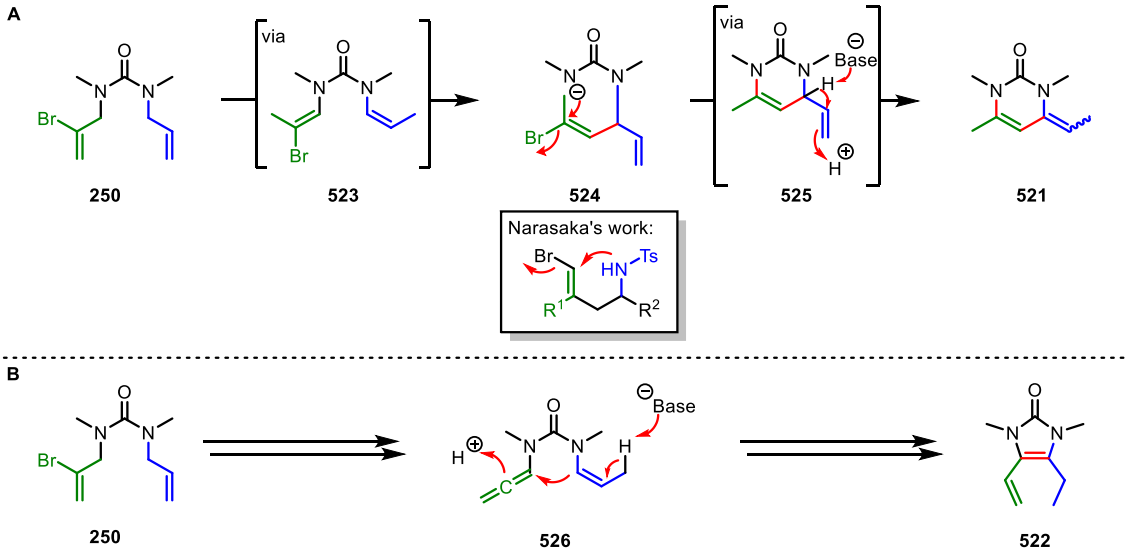

Scheme 89. Proposed mechanism for the formation of dibrominated, cyclisation products 521 (A) and 522 (B). Blue represents the nucleophile. Green represents the electrophile. Red represents the new bonds formed.

The atom connectivity of **522** suggests initial formation of allene **526** by a base-promoted elimination process (Scheme 89B). Then, **522** is formed via a 5-*exo-trig* cyclisation of **526** followed by double-bond isomerisation, as similarly observed by Clayden and co-workers.[112] In the presence of base, it has been demonstrated that dehydrobromination of an *N*-allyl group that has a bromide in the β-position can take place to form an allene.[164] The alternative formation of an alkyne is calculated to be both thermodynamically and kinetically less preferential, because in the case of the allene the formed carbanion is in conjugation with the urea and thus will have a higher stability and be formed more easily.[164]

3.2.3.4 Rearrangement of Endocyclic Diallyl Ureas

With the success of the N→C vinyl migration of variously substituted symmetrical and unsymmetrical linear diallyl ureas, the focus was turned to performing this rearrangement with endocyclic diallyl ureas. In this way, it was hypothesised that the N→C migration of the endocyclic vinyl group – either conventionally prepared or generated *in situ* by base-mediated isomerisation of the endocyclic allyl group – would lead to a migratory ring expansion and thus a new method to generate medium rings (Scheme 90).

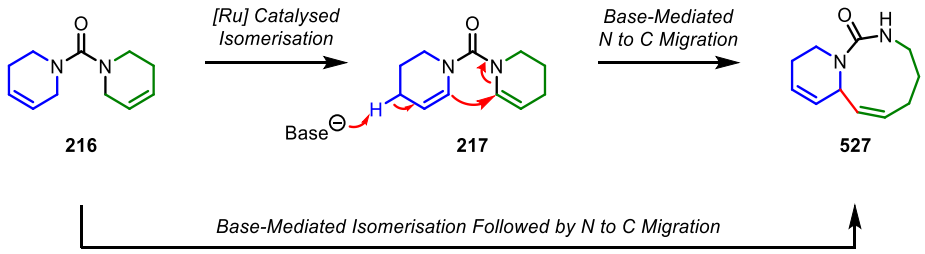

Scheme 90. Proposed migratory ring expansion of symmetrical endocyclic diallyl ureas. Blue represents the nucleophile. Green represents the electrophile. Red represents the new bonds formed.

Unfortunately, upon submission of either symmetrical endocyclic diallyl urea **216** or divinyl urea **217** to the optimal N→C vinyl migration conditions, no conversion to migration product **527** was observed; crude ^{1}H NMR showed that only allyl-to-vinyl isomerisation of **216** to **217** was achieved (Scheme 91). An explanation for these results may be that in divinyl urea **217** the γ-deprotonation can no longer be directed by coordination of the potassium to the carbonyl due to conformation constraints imposed by the cyclic structure; thus, the endocyclic vinyl group is unable to act as the nucleophile in the N→C vinyl migration.

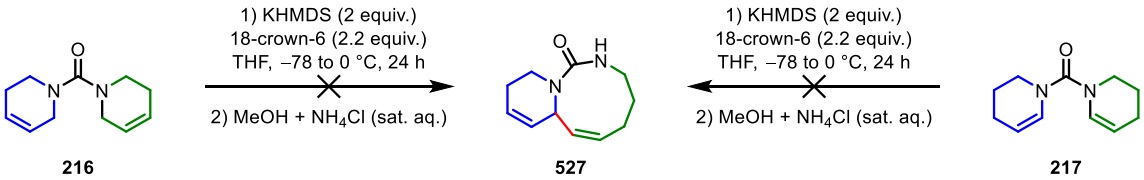

Scheme 91. Attempted N→C vinyl migration of symmetrical endocyclic diallyl urea 216 and divinyl urea 217 aiming to form ring-expanded migration product 527. Blue represents the nucleophile. Green represents the electrophile. Red represents the new bonds formed.

To discover whether the *in situ* generated endocyclic vinyl group can however act as the electrophilic migrating group, the N→C migration was attempted with unsymmetrical *N*-benzyl and *N*-allyl ureas **218** and **220** that contain anion-stabilising groups capable of nucleophilic substitution at an adjacent vinyl α-C(sp^2) centre. Unfortunately, in both cases none of the desired ring-expanded migration products were afforded (Scheme 92). Starting urea **218** was essentially unaffected under the reaction conditions, observed in 97% NMR yield (Scheme 92A). Yet from **220** a small amount of migration product **529** was obtained instead. Prior to its alkene isomerisation, α-deprotonation of the endocyclic *N*-allyl group resulted in the N→C migration of the acyclic (*in situ* isomerised) vinyl group (Scheme 92B). In addition, fully isomerised urea **530** was observed in 40% NMR yield and served to inhibit the N→C vinyl migration as the endocyclic vinyl group can now no longer act as the nucleophilic anion-stabilising group.

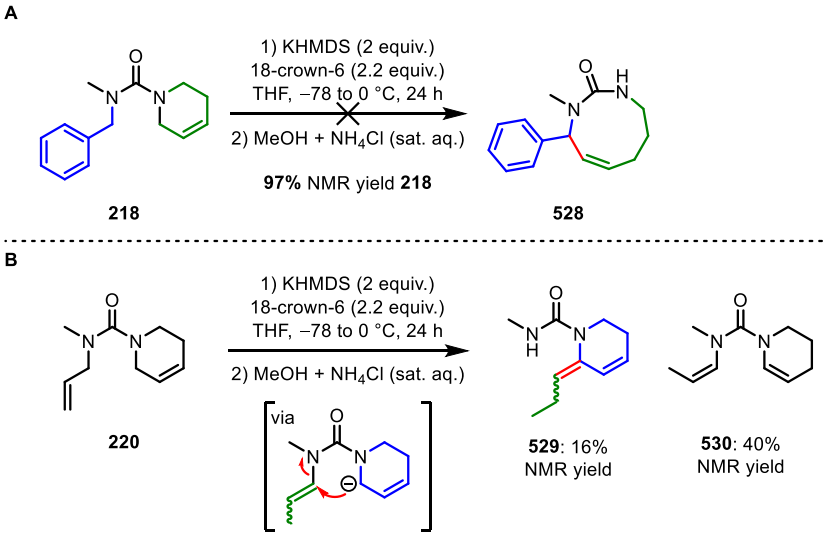

Scheme 92. Attempted N→C vinyl migration of unsymmetrical *N*-benzyl and *N*-allyl ureas 218 and 220. Blue represents the nucleophile. Green represents the electrophile. Red represents the new bonds formed. The squiggly bond means that the compound is a single isomer yet of unknown configuration. The NMR yields are determined by ^{1}H NMR using 1,2,4-trimethoxybenzene as an internal standard.

Collectively, the results from the attempted N→C vinyl migration of **216**, **217**, **218** and **220** suggest that while the endocyclic *N*-allyl group is able to be α-deprotonated to subsequently act as a nucleophile, it does not exhibit umpolung reactivity as the electrophilic migrating group. This limits the possibility of the envisioned N→C vinyl migratory ring expansion method under these conditions.

3.2.4 Product Transformations

With the substrate scope of the N→C vinyl migration of symmetrical and unsymmetrical diallyl ureas explored, attention was next directed at investigating possible transformations with the migration products. It should be mentioned that these transformations are unoptimised, leaving potential for improvement in yields and selectivity.

As the N→C vinyl migration products consist of conjugated dienes, it was reasonable to explore their use in a Diels-Alder reaction (Scheme 93).[165,166] Therefore, the reaction of migration product **362** was first attempted with a slight excess of dimethyl acetylenedicarboxylate at elevated temperatures; Diels-Alder products **531** and **532** were successfully afforded in a moderate total yield of 42%. Interestingly, under these reaction conditions the more substituted, thus more stable, double-bond has formed in **532** from **531**, through isomerisation of one of the double-bonds. In addition, the Diels-Alder reaction of migration product **362** could also be carried out with maleic anhydride as the dienophile, giving isomerised Diels-Alder cyclisation product **533**. The difference between the NMR yield and the isolated yield is due to decomposition of **533** on silica gel during column chromatography purification. The major product **533** was identified as the *exo*-product by comparison of the NMR *J*-coupling values of a related *exo*-cycloadduct (**534**).[167]

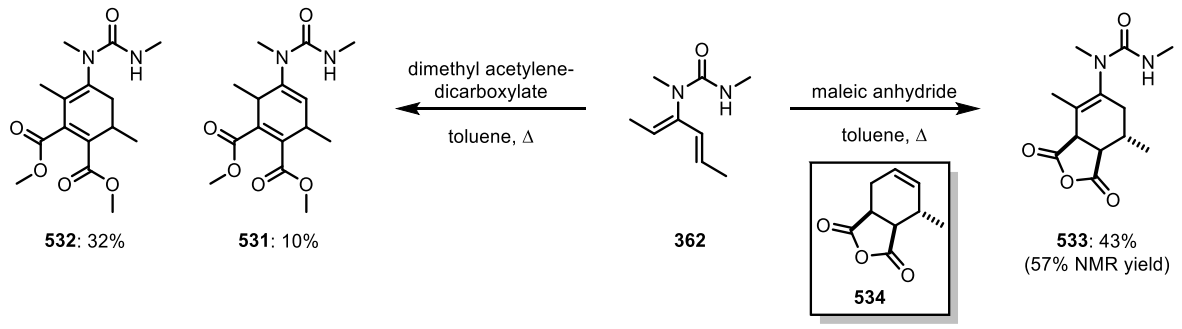

Scheme 93. The use of migration product 362 as the diene in the Diels-Alder reaction with dienophiles dimethyl acetylenedicarboxylate and maleic anhydride.

The fact that the major product of this Diels-Alder reaction was identified as the *exo*-product disagrees with the empirical '*endo* rule' formulated by Alder and Stein.[168,169] There are various arguments that explain the preference for the *endo*-product formation, with the possibility of secondary orbital interactions generally seen as one of the most important factors (Scheme 94).[170,171] Yet, more recently, it is understood that the contribution of these interactions are relatively small, and other factors such as activation strain and energy decomposition are more controlling for *endo*/*exo* selectivity.[172,173] For example, the high *endo* selectivity in the familiar Diels-Alder reaction between maleic anhydride and

cyclopentadiene is attributed to stronger electrostatic attractions, introduced by the highly polarised carbonyls, between the carbon frame of maleic anhydride and the diene framework.[173–175] Contrarily, it was assumed, by comparison of the Diels-Alder reaction between migration product **362** and maleic anhydride with the reaction of cyclopentadiene, that the selectivity towards the *exo*-product is due to repulsive electrostatic interactions between the urea moiety and the highly polarised carbonyls in **TS-*endo*** (Scheme 94).[174]

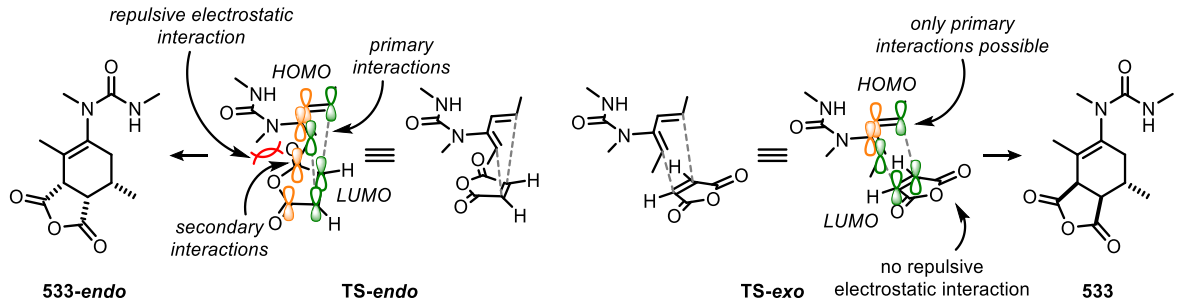

Scheme 94. Schematic explanation for the observed preference for the *exo*-Diels-Alder product 533.

Furthermore, it was imagined that the N→C vinyl migration products could be easily transformed to *N*-methyl alkyl amines. Applying this to the more complex migration products would give access to *N*-methyl alkyl amines that are otherwise not readily available; a whole range of new, complex *N*-methyl alkyl amines could be accessed and utilised as building blocks. For this, the transformation of the migration product **362** was attempted. Hydrogenation with use of palladium on carbon successfully resulted in the formation of saturated migration product **535** in a good yield of 67% (Scheme 95). Then, the urea hydrolysis was effectively performed with an excess of an aqueous solution of sodium hydroxide and microwave heating; subsequent treatment with an excess of hydrogen chloride – methanol solution, to avoid volatility issues, afforded *N*-methyl alkyl amine **536** in an excellent yield of 96% (Scheme 95).

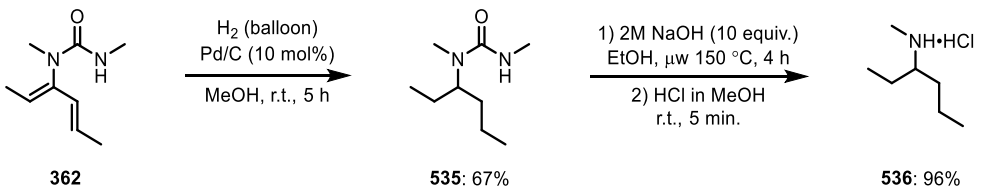

Scheme 95. Alkylamine hydrochloride salt formation via hydrogenation and urea hydrolysis starting from migration product 362.

Enone formation was considered as another possible transformation of migration product **362**. Suprisingly, migration product **362** appeared to be stable under similar conditions used to cleave the urea moiety of saturated product **535**; no conversion to conjugated enone **537** was observed (Scheme 96). The urea hydrolysis of **362** was also tried with acidic conditions, which resulted in a complex mixture; the only identifiable products were the desired enone **537**, along with 5-methoxy-3-hexanone **538**, afforded as a mixture (Scheme 96). Caution was taken during purification and concentration *in vacuo* of these volatile compounds, however low yields were still attained. Repeating the reaction in acetonitrile in an attempt to exclusively form enone **537** resulted in an even more complex mixture, and enone **537** was not present.

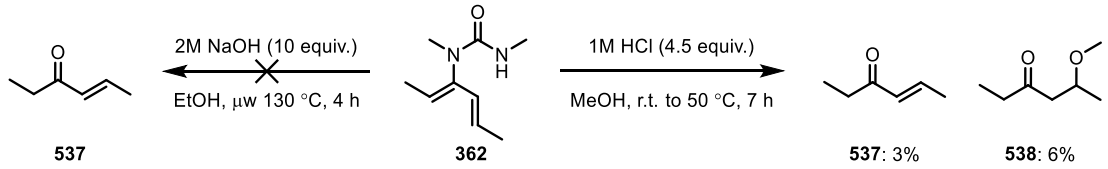

Scheme 96. Attempted enone formation by transformation of migration product 362.

Finally, we wondered whether upon *N*-allylation of the migration products, another N→C vinyl migration could be performed (Scheme 97). As a vinyl group – the original alkene framework of migration product **362** – was already in place, it was hypothesised that α-deprotonation of the unsubstituted allyl group in urea **539** would result into a regioselective N→C vinyl migration forming **540**. Another allylation would give **541** that could undergo another regioselective N→C vinyl migration yielding migration product **542**. From this, allylation and N→C vinyl migration could be conducted 'infinitely' and would enable access to complex polyalkenes. This idea would only be successful if the unsubstituted allyl group always exclusively acts as the nucleophile. If the unsubstituted allyl group acts as the electrophile, a migration product containing a quaternary centre at the crucial α-carbon (**545**, Scheme 98) would be formed and prevent the possibility of 'infinite' N→C vinyl migrations.

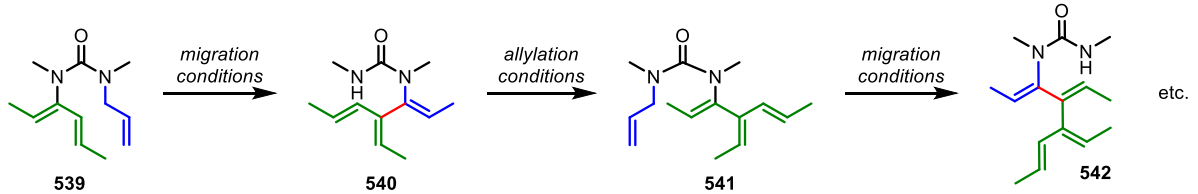

Scheme 97. Proposed 'infinite' N→C vinyl migration by allylation of the migration products. Blue represents the nucleophile. Green represents the electrophile. Red represents the new bonds formed.

To explore this idea, migration product **362** was reacted with sodium hydride and allylbromide and successfully generated urea **539** in a good yield of 66% (Scheme 98). Unfortunately, upon treating urea **539** with the optimised N→C vinyl migration conditions cyclisation products **543** and **544** were afforded in a moderate total yield of 44% (Scheme 98). The atom connectivity of **544** revealed that the N→C vinyl migration of **539** had unfortunately occurred with the unsubstituted allyl group acting as the electrophile, forming initially migration product **545**, which then underwent 5-*exo*-*trig* cyclisation onto the terminal alkene. Cyclisation product **543** could be formed upon 5-*exo*-*trig* cyclisation before or after the desired N→C vinyl migration (forming **540**) with the unsubstituted allyl group acting as the nucleophile.

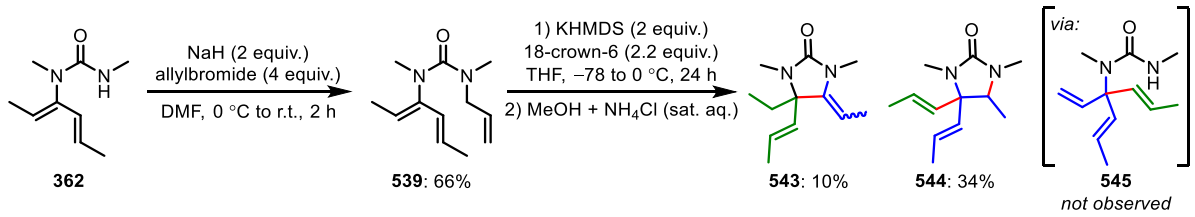

Scheme 98. Attempted 'infinite' N→C vinyl migration of unsymmetrical urea 539, formed upon allylation of migration product 362. Blue represents the nucleophile. Green represents the electrophile. Red represents the new bonds formed. The squiggly bond means that the compound is a single isomer yet of unknown configuration.

3.2.5 Mechanistic Studies

3.2.5.1 NMR Studies

In order to substantiate the proposed mechanism of the *in situ* isomerisation/N→C vinyl migration cascade reaction, NMR studies were conducted to follow the reaction course and identify any intermediates.

During the optimisation studies it was found that under certain conditions (section 3.2.1) isomerised symmetrical divinyl urea **364** exhibiting *Z*-geometry on both alkene chains was generated. From this, it was hypothesised that **364** is an intermediate in the desired N→C vinyl migration reaction. To confirm this hypothesis and to explore whether other reaction intermediates were at play during the course of the reaction, two NMR studies were conducted. The proposed, rather complex, tandem sequence of isomerisations and nucleophilic substitution (section 3.2.2) that generates the migration products was monitored by NMR spectroscopy at certain time and temperature intervals in two different ways; experiment one involved taking NMR spectra of reaction aliquots and experiment two involved reaction monitoring *in situ*.

For experiment one, the reaction was set up as standard following General Procedure **3C** (section 5.3.1). After stirring the reaction mixture containing **206**, KHMDS and 18-crown-6 in THF for 22 hours at −78 °C, an aliquot was quenched with MeOH at −78 °C and then analysed immediately by ^{1}H NMR. Complete conversion of **206** to **364** was observed (Figure 7). The reaction mixture was then warmed up to –40 °C and stirred for 22 hours, after which another aliquot was examined by ^{1}H NMR spectroscopy, showing that **364** was still solely present. A further aliquot was taken after 25 hours at –20 °C and this time the ^{1}H NMR spectrum showed almost complete conversion of **364** to migration product **362** (ratio **364**:**362** is 0.3:1). Complete conversion of *in situ* isomerised urea **364** to **362** was achieved by warming to 0 °C for 7 hours. To probe the stability of **362**, the reaction mixture was stirred for 3 days at room temperature; the ^{1}H NMR spectrum showed that migration product **362** was still present, but decomposition was taking place, shown by the unidentifiable peaks appearing between 3.5 – 0.5 ppm (Figure 7).

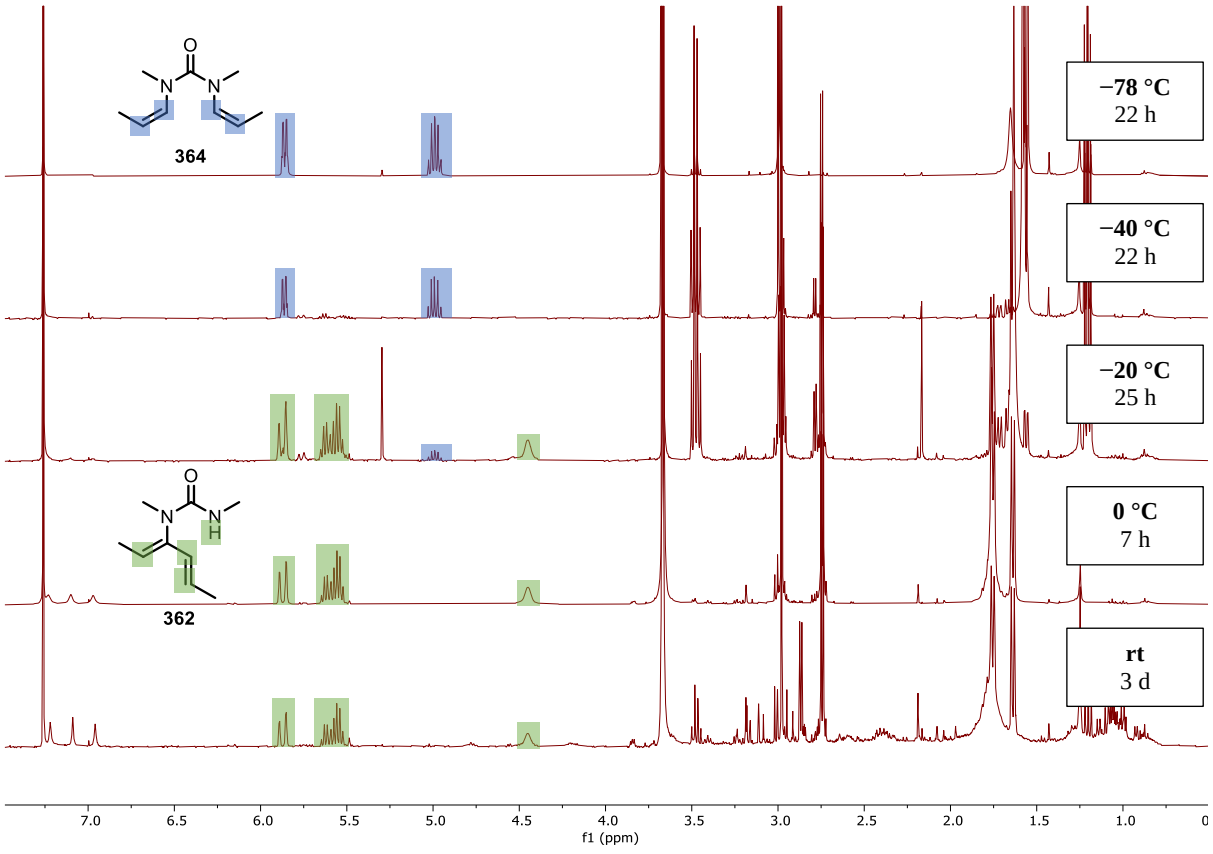

Figure 7. NMR experiment one: an overlay of ^{1}H NMR spectra of the proposed allylic isomerisation, N→C vinyl migration cascade of diallyl urea 206. Blue represents *in situ* isomerised urea **364**. Green represents migration product **362**.

For experiment two, the reaction was also set up following General Procedure **3C** (section 5.3.1). Then a portion of the reaction mixture was transferred into an NMR tube. To ensure the entire set-up was as

anhydrous as possible, a flame-dried flask connected to an oven-dried NMR tube via an oven-dried cannula was placed under vacuum and nitrogen as one system. Upon addition of KHMDS, the nitrogen flow into the NMR tube was exchanged with a nitrogen flushed balloon and then, with the use of a cannula, the NMR tube was filled at −78 °C (Figure 8). The NMR tube was loaded into the NMR machine with the NMR probe cooled down to −78 °C; the NMR spectra were then recorded at each time and temperature while slowly warming the NMR probe.

Figure 8. Reaction set-up and subsequent transfer of the reaction mixture into an NMR tube via a cannula at −78 °C.

The ^{1}H NMR spectra were thus recorded in non-deuterated THF and showed that at –78 °C **206** was instantly isomerised into **364** (Figure 9). The very small amount of migration product **362** visible might be caused by the exposure to room temperature while transferring the NMR tube as quick as possible from the –78 °C dewar into the NMR machine, which was already cooled to –78 °C. Between –60 °C and –40 °C no significant conversion of **364** was detected, yet after 1 h at –20 °C slight conversion of **364** to migration product **362** was observed. Then, the ^{1}H NMR taken after 40 min at 0 °C showed that **364** was converted significantly into **362** and after 3 h at 0 °C, *in situ* isomerised urea **364** was fully converted to migration product **362**. According to the ^{1}H NMR spectrum recorded after stirring the reaction mixture for 16 h at 0 °C, migration product **362** was still exclusively present (Figure 9).

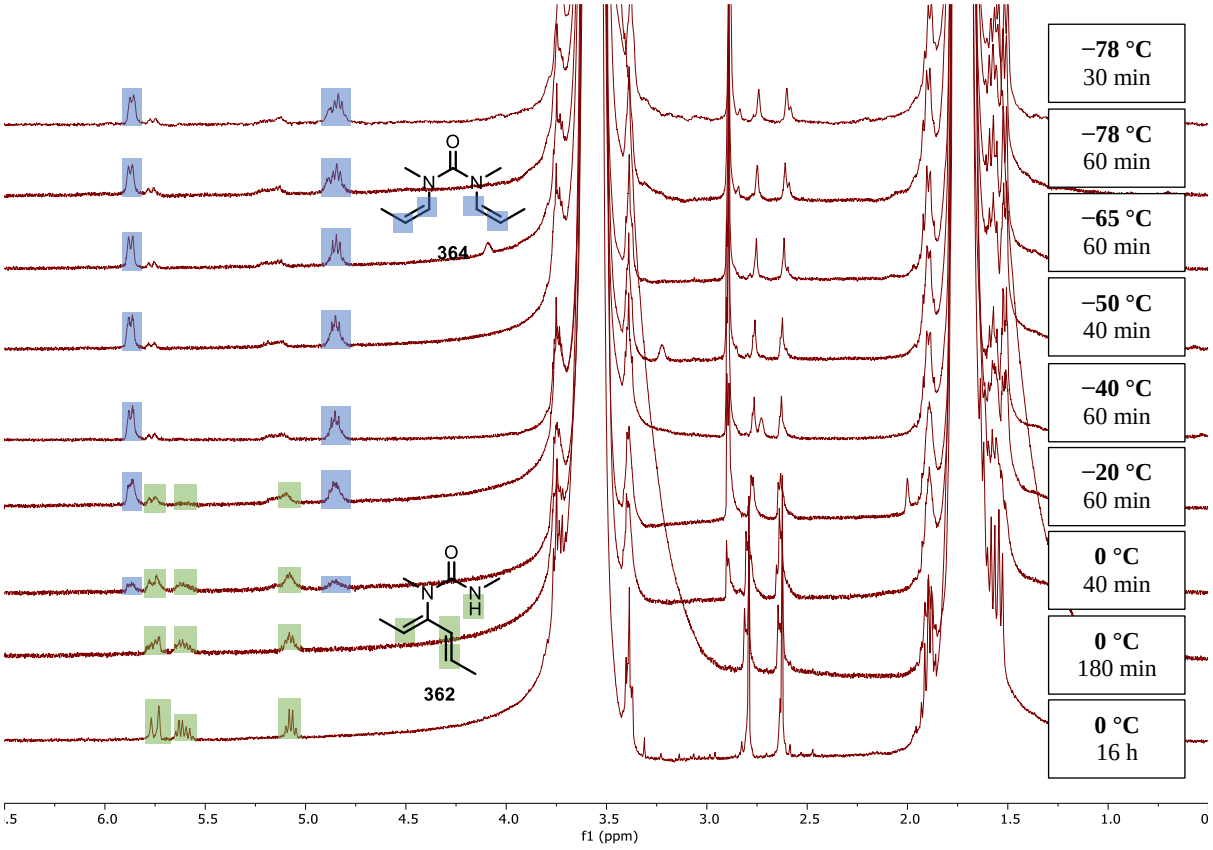

Figure 9. NMR experiment two: an overlay of ^{1}H NMR spectra in non-deuterated THF on the proposed allylic isomerisation, N→C vinyl migration cascade of 206. Blue represents *in situ* isomerised urea **364**. Green represents migration product **362**.

Overall, both NMR experiments demonstrate that upon addition of KHMDS at −78 °C starting urea **206** gets rapidly converted to *N*,*N*'-(*Z*)-divinyl urea **364**, and at temperatures between –20 °C and 0 °C **364** undergoes clean conversion to migration product **362** (Scheme 99). These results confirm that *in situ* isomerised urea **364**, exhibiting *Z*-geometry on both alkene chains, is a key intermediate in the reaction and the only substantial reaction intermediate detectable by ^{1}H NMR.

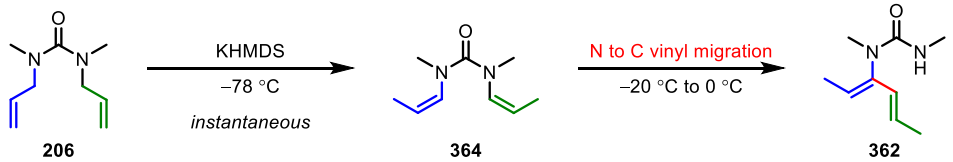

Scheme 99. Overview for the conversion of starting urea 206 to *in situ* isomerised urea 364 at –78 °C, which converted to migration product 362 at temperatures between –20 °C and 0 °C. Blue represents the nucleophile. Green represents the electrophile. Red represents the new bonds formed.

3.2.5.2 KHMDS and 18-crown-6 Stoichiometry Studies

In order to gain more insight into the heavily demanding reaction cascade (specifically olefin isomerisation and vinyl migration with subsequent isomerisation, Scheme 100), KHMDS and 18-crown-6 stoichiometry studies were performed with the use of unsymmetrical *N*-benzyl-*N*'-allyl urea **214**, and symmetrical *N*,*N*'-diallyl urea **206** and *N*,*N*'-(*Z*)-divinyl urea **364**. In particular, we wanted to probe the importance of the stoichiometry of the base and crown ether, and how it may affect each stage of the mechanism.

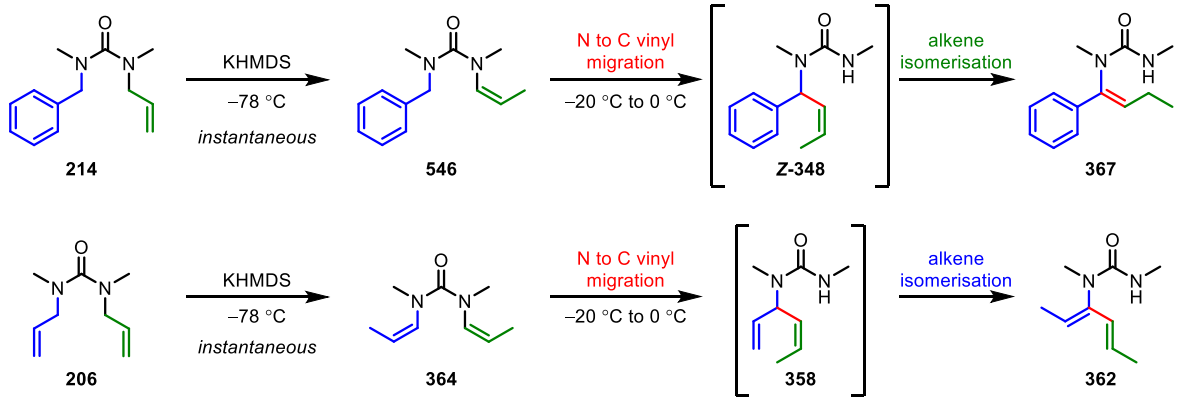

Scheme 100. Overview for the proposed conversion of starting ureas 214 and 206 to *in situ* isomerised ureas 546 and 364 at –78 °C, which converted to migration products 367 and 362, via migration products *Z*-348 and 358, at temperatures between –20 °C and 0 °C. Blue represents the nucleophile. Green represents the electrophile. Red represents the new bonds formed.

As was shown in the preliminary and optimisation studies (section 3.1 and 3.2.1), for the N→C vinyl migration of **214** and **206** to be successful the allyl-to-vinyl isomerisation by an α-deprotonation/γ-protonation sequence (green) must occur before the additional α-deprotonation of the other benzylic/allylic position (blue in **214** and **206**, Scheme 100). However, the precise mechanism of this alkene isomerisation is not yet clear, and there are multiple possible pathways; intermolecular equilibration of neutral and anionic allyl species (Scheme 101A), γ-protonation via proton transfer from the benzylic position (Scheme 101B), or reaction of the allyl-anion with the conjugate acid of the base resulting in the required γ-protonation (Scheme 101C). The latter is more likely when using a base that has a conjugate acid of lower pK_a than, for example, the allyl-anion. This may explain why KHMDS (pK_a of 26) promotes the desired isomerisation/N→C vinyl migration sequence significantly more than LDA (pK_a of 36).[162]

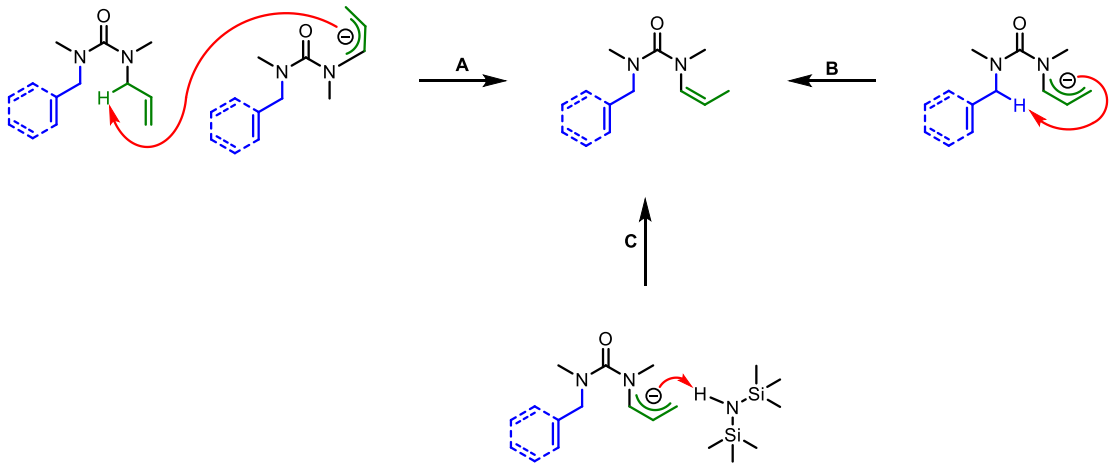

Scheme 101. Possible pathways for the allyl-to-vinyl isomerisation of urea 214 and 206. Blue represents the nucleophile. Green represents the electrophile. Red represents the new bonds formed.

The base-dependency is also evident on the reaction course after the desired N→C vinyl migration. In the KHMDS/18-crown-6 promoted rearrangement of both **215** and **214**, urea **367** is the end-product while with LDA, **348** is produced from **215** without further alkene isomerisation (Scheme 102). The same applies for the rearrangement of **206** that gives mostly migration product **358** with the use of LDA, while conjugated migration product **362** is exclusively formed with KHMDS/18-crown-6 (Scheme 102).

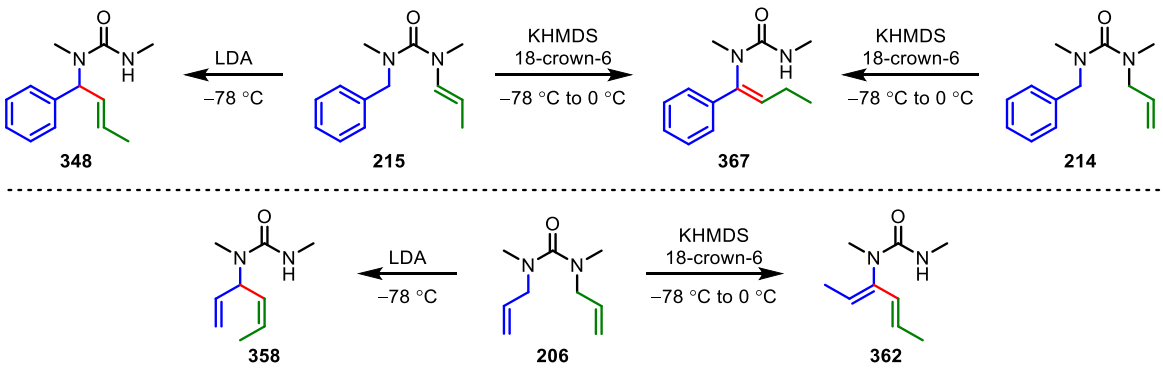

Scheme 102. Overview of the base-dependent outcomes of the N→C vinyl migration of ureas 215, 214 and 206. Blue represents the nucleophile. Green represents the electrophile. Red represents the new bonds formed.

It appears that the KHMDS/18-crown-6 combination may enable formation of **547** via another deprotonation at the benzylic/allylic position, which is relatively acidic due to conjugation with not only the benzyl ring/terminal alkene (blue) and the urea, but also the vinyl group (green) (Scheme 103A). Even though LDA is more basic than KHMDS, the reactivity of the anion in KHMDS is increased in the presence of 18-crown-6 due to its complexing activity with the potassium ion, perhaps resulting in the additional deprotonation that leads to the formation of migration products **367** and **362**. Moreover,

previous reported N→C vinyl migrations in *N*-benzyl ureas with *s*-BuLi afforded isomerised migration products like **367**, suggesting that LDA is not strong enough for the additional deprotonation.[112] Alternatively, the additional deprotonation may take place intermolecularly by catalytic alkene isomerisation of **549** (Scheme 103B) or intramolecularly by a 1,4-transfer to the negatively charged urea nitrogen in **548**, which is more reactive with an 18-crown-6-complexed potassium counterion (**550**) than an oxyphilic lithium counterion (**551**) (Scheme 103C).

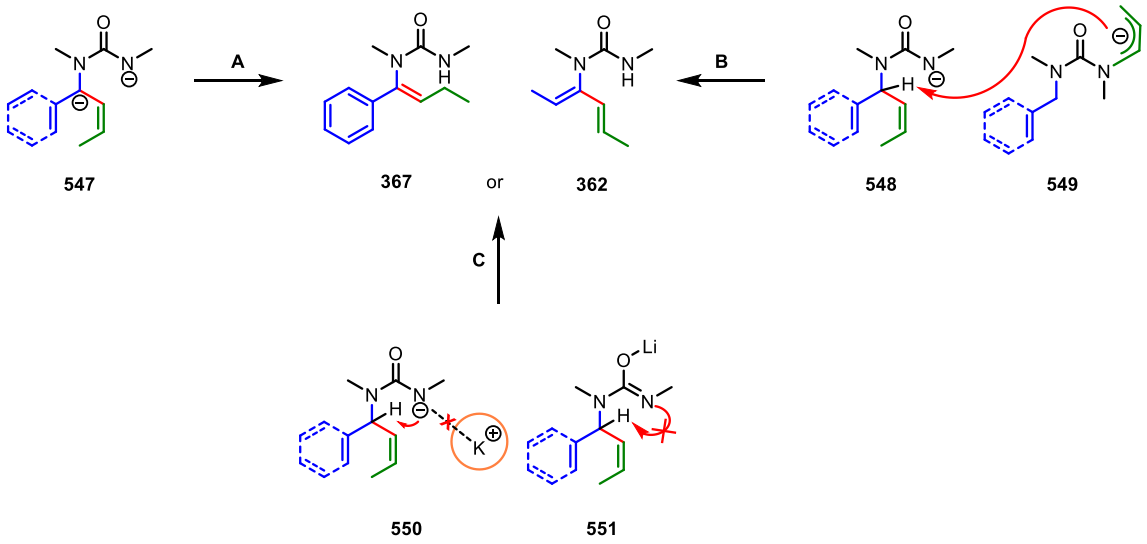

Scheme 103. Possible pathways for the additional deprotonation forming migration product 367 and 362. 18-Crown-6 is depicted by the orange circle.

Considering the similar pK_a values of alkyl ureas and bis(trimethylsilyl)amine (HMDS), the by-product of deprotonation with KHMDS, it seemed reasonable to investigate whether the rearrangement of **214** to **367** and **206** to **362** could be accomplished in a catalytic manner. Therefore, the effect of reducing the equivalents of KHMDS was studied for the N→C vinyl migration of **214** and **206**.

The reaction of urea **214** with 2 equivalents of KHMDS in the presence of 2.2 equivalents of 18-crown-6 gave migration product **367** in an 80% yield (Table 10, entry 1). Reducing the amount of KHMDS to 1 equivalent had little effect: **367** was obtained in a similarly good yield of 72% (entry 2). In addition, isomerised *N*-benzyl-*N*'-(*Z*)-vinyl urea **546**, which is hypothesised to be an intermediate in the rearrangement, was afforded in 8% yield. The efficiency of this reaction (entry 2) and absence of unconjugated migration product **348** in the crude mixture is telling because it rules out the stoichiometric accumulation of dianion **547** being the source of conjugated migration product **367** (Scheme 103). Therefore, **367** likely arises by catalytic alkene isomerisation of **549** to **548** through a transient dianion **547** or through converting **548** to **548(C−)** by intramolecular proton transfer (Scheme 103B and C). With 0.5 equivalents of KHMDS, migration product **367** was only generated in 3% yield

but was accompanied by urea **546** in 50% yield (entry 3). The use of just 0.2 equivalents of KHMDS resulted mostly in urea **546**, which was afforded in a yield of 49% (entry 4). In addition, migration product **367** was obtained in a 7% yield and 25% of starting urea **214** was recovered. This result provides convincing evidence that the alkene isomerisation is a catalytic process, although of modest efficiency under the current conditions.

Table 10. KHMDS and 18-crown-6 stoichiometry screen for the N→C vinyl migration of 214.[a]

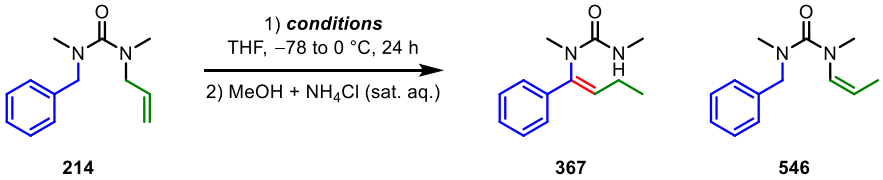

Entry	Conditions		NMR Yield [%]		
	KHMDS (equiv.)	18-crown-6 (equiv.)	214	546	367
1	2	2.2	-	-	80[b]
2	1	1.1	-	8	72
3	0.5	0.55	-	50	3
4	0.2	0.22	25	49	7

[a]Reactions were performed on a 0.36 mmol scale. The yields are determined based on ^{1}H NMR analysis using 1,2,4-trimethoxybenzene as an internal standard. [b]Isolated yield.

With the understanding that the alkene isomerisation process is catalytic for *N*-benzyl-*N*'-allyl urea **214**, we wondered how the stoichiometry of KHMDS and 18-crown-6 affects the total isomerisation/N→C vinyl migration cascade reaction of **206** to **362**, the alkene isomerisation of **206** to **364** and the N→C vinyl migration of **364** to **362**. Moreover, with diallyl urea **206** and (*Z*)-divinyl urea **364**, the requirement of 18-crown-6 in both the alkene isomerisation and the N→C vinyl migration was investigated.

In agreement with the observations in the NMR studies for the allyl-to-vinyl isomerisation at −78 °C being the first step of the reaction cascade (section 3.2.4.1), treating symmetrical diallyl urea **206** with 2 equivalents of KHMDS in the presence of 18-crown-6 at −78 °C successfully gave (*Z*)-isomerised urea **364** in an NMR yield of 79% (Table 11, entry 1). However, the conversion of **206** to **364** was completely suppressed when the reaction was performed without 18-crown-6; just a small amount of **363**, where only one allyl group of the urea had isomerised, was observed (Table 11, entry 2). In contrast, reducing the amount of KHMDS to 1 equivalent had little effect: *N*,*N*'-(*Z*)-divinyl urea **364** was obtained in a similar yield of 72% by NMR (Table 11, entry 3). In addition, partially isomerised urea

363 was observed in a 16% NMR yield, suggesting that lowering the equivalents of base slows down the conversion of **206** to **363**, and then to **364** (Table 11, entry 3). This suggestion was confirmed with the use of 0.5 equivalents of KHMDS, where fully isomerised urea **364** was afforded in an equimolar ratio with partially isomerised urea **363** (Table 11, entry 4). No conversion of **206** to **364** (or **363**) was observed when just 0.2 equivalents of KHMDS was used, yet it was hypothesised that with a significantly longer reaction time conversion of **206** to **363** or **364** may have been observed (Table 11, entry 5).

Table 11. KHMDS and 18-crown-6 stoichiometry screen for the allyl-to-vinyl isomerisation of 206 to 364.[a]

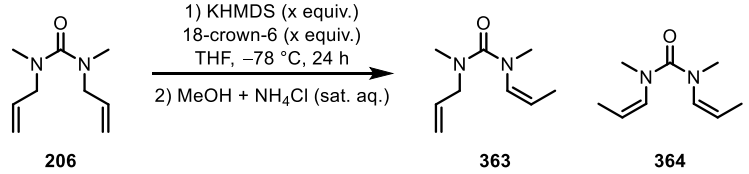

Entry	KHMDS (equiv.)	18-crown-6 (equiv.)	NMR Yield [%]		
			206	**363**	**364**
1	2	2.2	-	-	79
2	2	0	90	2	-
3	1	1.1	-	16	72
4	0.5	0.55	-	44	44
5	0.2	0.22	89	-	-

[a]Reactions were performed on a 0.40 mmol scale. The yields are determined based on ^{1}H NMR analysis using 1,2,4-trimethoxybenzene as an internal standard.

The second part of the demanding rearrangement cascade is the N→C vinyl migration – the nucleophilic vinylic substitution – followed by an additional alkene isomerisation and was examined with an KHMDS/18-crown-6 stoichiometry study on the conversion of **364** to **362** (Table 12). Urea **364** was prepared on a larger scale using the N→C vinyl migration conditions, yet the reaction was quenched at −20 °C (Scheme 104). In this way, **364** can be easily isolated from the small amount of **362** that was formed, which contrasted the inseparable mixture of **364** and **363** that was formed upon quenching the reaction at −78 °C.

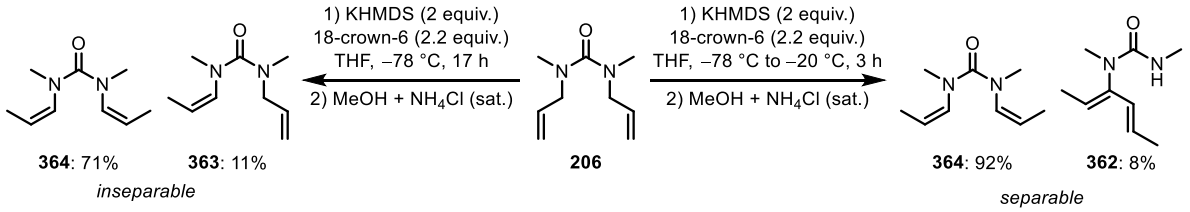

Scheme 104. Large scale preparation of *N,N*'-divinyl urea 364 using adjusted N→C vinyl migration conditions on starting urea 206.

As expected, the reaction of *N,N*'-(*Z*)-divinyl urea **364** with 2 equivalents of KHMDS in the presence of 2.2 equivalents of 18-crown-6 gave migration product **362** in a good 68% NMR yield (Table 12, entry 1). More interestingly, when performing the same reaction without 18-crown-6 the conversion of **364** to **362** was practically completely suppressed; this suggested that 18-crown-6 significantly stimulates the required γ-deprotonation of the *Z*-vinyl chains for the S_NV (Table 12, entry 2). In contrast to the unchanged formation of **364** from **206** when using, instead of 2 equivalents, 1 equivalent of KHMDS (Table 11, entry 3), the formation of **362** from **364** was negatively affected by the reduction of equivalents of base (Table 12, entry 3). With 0.5 equivalents of KHMDS, migration product **362** was only observed in an 8% NMR yield and the use of just 0.2 equivalents gave no conversion to **362** (Table 12, entry 4 and 5).

Table 12. KHMDS and 18-crown-6 stoichiometry screen for the N→C vinyl migration of 364 to 362.[a]

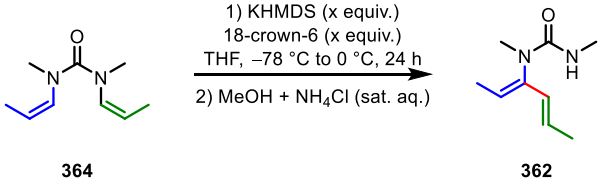

Entry	KHMDS (equiv.)	18-crown-6 (equiv.)	NMR Yield [%]	
			364	362
1	2	2.2	-	68
2	2	0	71	3
3	1	1.1	25	48
4	0.5	0.55	75	8
5	0.2	0.22	88	-

[a]Reactions were performed on a 0.40 mmol scale. The yields are determined based on ^{1}H NMR analysis using 1,2,4-trimethoxybenzene as an internal standard.

To complete the stoichiometry studies and enable comparisons, a final KHMDS/18-crown-6 stoichiometry study was performed with symmetrical diallyl urea **206** to examine the effect on the entire alkene isomerisation/N→C vinyl migration cascade. As observed in the optimisation studies (section 3.2.1), the N→C vinyl migration of **206** with 2 equivalents of KHMDS and 2.2 equivalents of 18-crown-6 generated migration product **362** in good yield (Table 13, entry 1). Interestingly, without 18-crown-6 but with slowly warming the reaction mixture up from −78 °C to 0 °C, conversion of **206** to **364** was achieved (Table 13, entry 2) and contrasts the suppressed formation of **364** without 18-crown-6 when the reaction was kept at −78 °C (Table 11, entry 2). In addition, besides the formation of **363** in 5% NMR yield, **362** was observed in a 28% NMR yield (Table 13, entry 2) which is significantly higher than the 3% NMR yield of **362** observed in the conversion of **364** under the same conditions (Table 12, entry 2). These results suggest that without 18-crown-6 the conversion of **206** to **364** requires elevated temperatures, and the formation of **362** takes place immediately from **363** instead of **364** in this case. Once **206** has completely isomerised to **364**, the N→C vinyl migration is very sluggish without the presence of 18-crown-6. Note that the alkene isomerisation to form the most stable conjugated diene (*Z*,*E*) was also affected when there was no 18-crown-6 present in the reaction as conjugated diene **359** with a *Z*,*Z*-geometry was present as well (Table 13, entry 2).

Again, reducing the amount of KHMDS to 1 equivalent had little effect: migration product **362** was observed in a 75% NMR yield (Table 13, entry 3). With 0.5 equivalents of KHMDS, migration product **362** was only observed in an 8% NMR yield, and fully isomerised urea **364** and partially isomerised urea **363** were observed in a 60% and 21% NMR yield respectively (Table 13, entry 4). As it was of interest to determine whether the whole reaction cascade is catalytic but just significantly slower with substoichiometric amounts of KHDMS and 18-crown-6, the reaction with just 0.5 equivalents of KHMDS was left to stir for a longer period of time. However, similar amounts of **364** and **362** were observed without the presence of any **363** (Table 13, entry 5). To see whether **362** was decomposing over time under these conditions, a shorter amount of time for the reaction with 0.5 equivalents of KHMDS was attempted, providing a slightly improved yield of migration product **362** (Table 13, entry 6). This might suggest that **362** decomposes under these conditions, but when **362** was resubmitted to the optimal reaction conditions (2 equivalents of KHMDS and 2.2 equivalents of 18-crown-6) no decomposition or reaction was observed. The use of just 0.2 equivalents gave no conversion of **206** to **362** and only a small amount of partially isomerised urea **363** was observed (Table 13, entry 7).

Table 13. KHMDS and 18-crown-6 stoichiometry screen for the N→C vinyl migration of 206 to 362.[a]

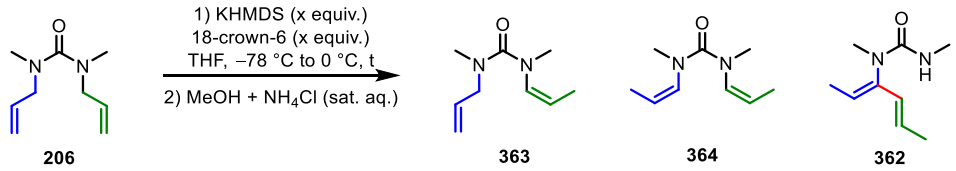

Entry	Time (h)	KHMDS (equiv.)	18-crown-6 (equiv.)	NMR Yield [%]			
				206	363	364	362
1	24	2	2.2	-	-	-	77
2	24	2	0	-	5	54	28[b]
3	24	1	1.1	-	-	8	75
4	24	0.5	0.55	-	21	60	8
5	69	0.5	0.55	-	-	60	5
6	16	0.5	0.55	-	-	69	24
7	24	0.2	0.22	88	5	-	-

[a]Reactions were performed on a 0.40 mmol scale. The yields are determined based on ^{1}H NMR analysis using 1,2,4-trimethoxybenzene as an internal standard. [b]1:1 ratio of *Z*,*Z*- and *Z*,*E*-alkene geometry in the migration product.

In summary, the results obtained in these KHMDS/18-crown-6 stoichiometry studies appear to indicate that a persistent anionic species is formed after N→C vinyl migration, likely an ureido anion, which is insufficiently basic to deprotonate bis(trimethylsilyl)amine or other reaction intermediates present, precluding the possibility of an efficient catalytic process. Nonetheless, the formation of migration products **367** and **362** with the use of 0.2 and 0.5 equivalents of KHMDS, even as minor products, suggest the rate of product formation and/or base turnover may be prohibitively slow with substoichiometric quantities of KHMDS. Interestingly, it was demonstrated that 18-crown-6 is a requirement in both the allyl-to-vinyl isomerisation sequence and the N→C vinyl migration sequence, presumably by stimulating the required α- and γ-deprotonations.

3.2.5.3 Stereospecificity Studies

During the optimisation of the N→C vinyl migration of symmetrical diallyl urea **206** (section 3.2.1), it was discovered that upon use of LDA unconjugated migration product **358** exhibiting *Z*-alkene geometry was formed as the major product, while employing the optimised KHMDS conditions yielded exclusively conjugated migration product **362** exhibiting *Z*,*E*-alkene geometry (Scheme 105). However,

under certain conditions conjugated migration product **359** exhibiting *Z*,*Z*-alkene geometry was also formed (Scheme 105). Based on this possibility of forming all three migration products from the same starting urea and mindful of fully *Z*-isomerised urea **364** being the reaction intermediate, it was suspected that the N→C vinyl migration may be stereospecific. Then, upon the additional deprotonation, which was more apparent with KHMDS/18-crown-6 than with LDA, isomerisation takes place to form the more thermodynamically stable *Z*,*E*-alkene geometry in **362**.

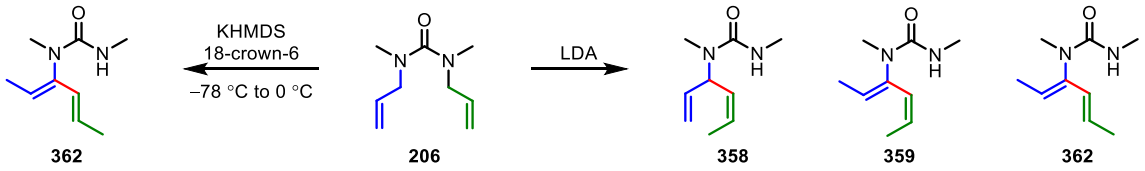

Scheme 105. Overview of the different N→C vinyl migration products when treating starting urea 206 with KHMDS/18-crown-6 or LDA. Blue represents the nucleophile. Green represents the electrophile. Red represents the new bonds formed.

To confirm our suspicions that the N→C vinyl migration was stereospecific, it was attempted to synthesise unsymmetrical, partially pre-isomerised, urea **554** that consists of a *N*-allyl group and a *N*-(*E*)-vinyl group. The preparation was firstly trialled by ruthenium-catalysed isomerisation of *N*-allyl carbamoyl chloride **552**,[113] which was made under the chloroformylation conditions described in section 2.1. However, **552** proved unstable under the isomerisation conditions and the desired isomerised carbamoyl chloride **553** was not obtained (Scheme 106).

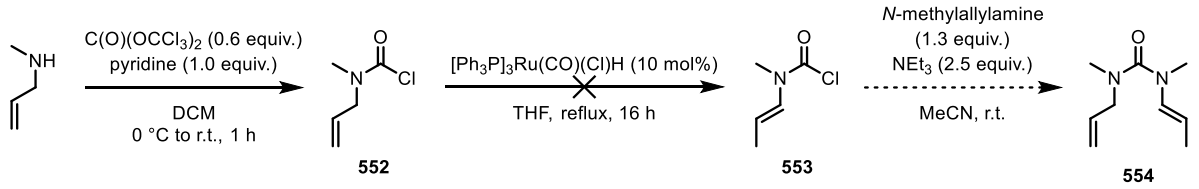

Scheme 106. Chloroformylation with *N*-methyl allylamine followed by the attempted ruthenium-catalysed isomerisation of *N*-allyl carbamoyl chloride 552 to form *N*-(*E*)-vinyl carbamoyl chloride 553.

Subsequently, *N*-(*E*)-vinyl-*N*'-hydroxysuccinimidoyl carbamate **555** was generated in a high yield of 85% by reaction of *N*-methyl allylamine with disuccinimidyl carbonate and then successful ruthenium-catalysed isomerisation (Scheme 107). Unfortunately, when **555** was reacted with *N*-methyl allylamine and triethylamine at room temperature, the desired urea **554** was only formed in a 17% yield. Besides recovery of the starting material **555** in 19% yield, the major product was found to be **556** in which the *N*-hydroxysuccinimide group was ring-opened by *N*-methyl allylamine. The use of phenyl

chloroformate to generate a better leaving group for the amine-coupling step was also trialled (Scheme 107). *N*-Allyl phenyl carbamate was generated by a one-step reaction of *N*-methyl allylamine with phenylchloroformate and then quantitatively isomerised into *N*-(*E*)-vinyl phenyl carbamate **557**. However, once again, the amine-coupling using *N*-methylallyl amine and triethylamine in acetonitrile was not successful at room temperature, nor with thermal or microwave heating over an extended period.

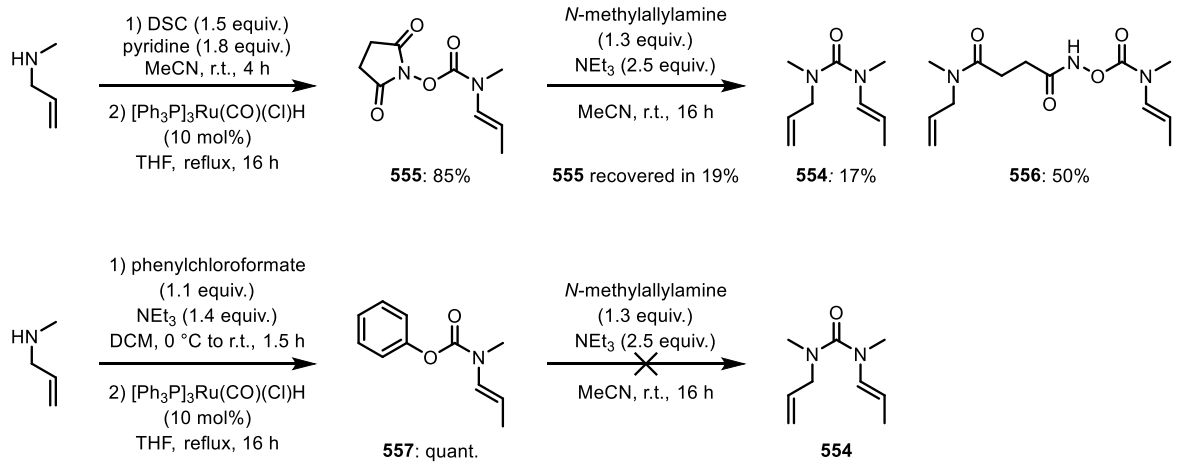

Scheme 107. Formation of *N*-(*E*)-vinyl-*N*'-hydroxysuccinimidoyl carbamate 555 and *N*-(*E*)-vinyl phenyl carbamate 557 and their attempted amine-coupling.

Analogous to *N*-(*E*)-vinyl phenyl carbamate **557**, *N*-(*E*)-vinyl 4-nitrophenyl carbamate **559** was synthesised in two steps via *N*-allyl 4-nitrophenyl carbamate **558** to attempt the amine-coupling with the assumption that a better leaving group could prove advantageous (Scheme 108). When reacting **559** with *N*-methylallylamine and triethylamine in acetonitrile at room temperature, no formation of desired unsymmetrical *N*-allyl-*N*'-(*E*)-vinyl urea **554** was observed. Upon heating **559** in the presence of *N*-methylallylamine and triethylamine in acetonitrile, for 4 h at 100 °C (μW) followed by 2 h at 150 °C (μW), complete conversion of starting material **559** was observed by TLC; yet only 1-allyl-1,3-dimethylurea **224** was afforded in a moderate yield of 39%. It was hypothesised that upon column chromatography on silica the unstable *N*-(*E*)-vinyl chain underwent hydrolysis, as previously observed (section 3.2.1, Table 6 and Table 9). Eventually, it was found that reaction of **559** with *N*-methyl allylamine and potassium carbonate in DMF at 130 °C, followed by chromatographic purification on neutralised silica (section 5.1) successfully afforded urea **554** in an excellent yield of 93% (Scheme 108). Then, if desired, isomerisation of urea **554** with adjusted N→C vinyl migration conditions (based on the stoichiometry studies, not warming to 0 °C), afforded urea **560** containing both an *E*- and a *Z*-vinyl chain in a high yield of 88% (Scheme 108).

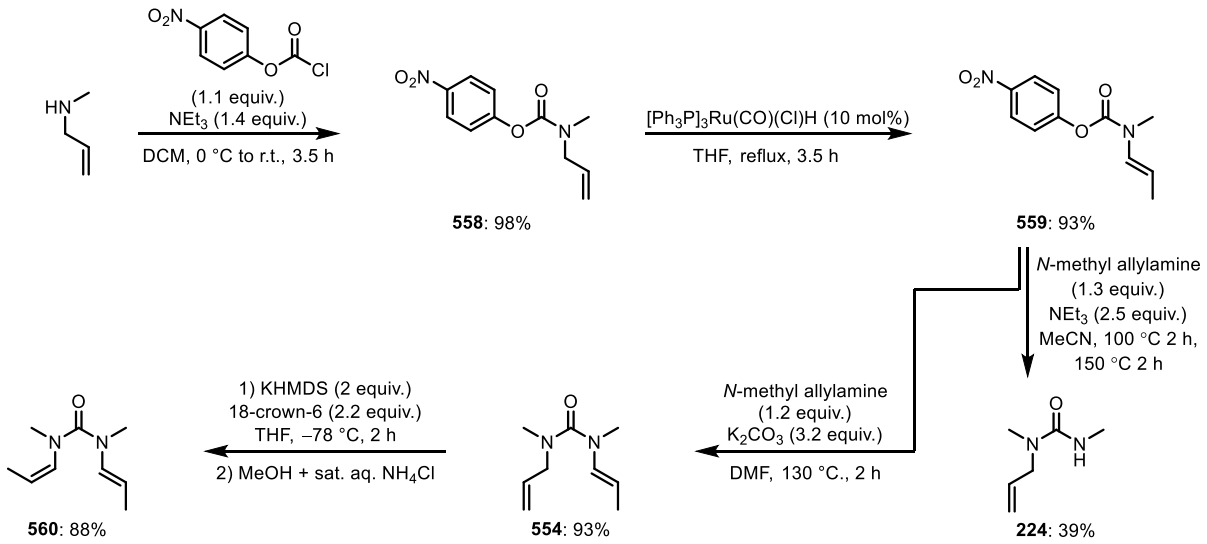

Scheme 108. Synthetic route for unsymmetrical *N*-allyl-*N*'-(*E*)-vinyl urea 554 and *N*-(*Z*)-vinyl-*N*'-(*E*)-vinyl urea 560.

By submitting unsymmetrical *N*-allyl-*N*'-(*E*)-vinyl urea **554** and *N*-(*Z*)-vinyl-*N*'-(*E*)-vinyl urea **560** to the LDA and KHMDS/18-crown-6 N→C vinyl migration conditions, and by exploiting the proposed inability of the *E*-vinyl group to act as the nucleophile, it could now be established whether the *E*-alkene geometry is retained in the unconjugated migration product. It was found that with the use **554** under the LDA rearrangement conditions, besides conjugated migration product **362** in 19% isolated yield, unconjugated migration product **352** exhibiting *E*-alkene geometry was generated in 43% yield; the alkene geometry of **352** served to show that the initial N→C vinyl migration was stereospecific (Scheme 109). Interestingly, the rearrangement of **554**, under the LDA conditions, turned out to be significantly cleaner and higher yielding (total of 61% yield) than when starting the N→C vinyl migration with diallyl urea **206** (33% yield; section 3.2.1, Table 5, entry 5). In contrast to **206**, the N→C vinyl migration of **554** under the optimal KHMDS/18-crown-6 conditions was significantly lower yielding (Scheme 109); migration product **362** was observed in a moderate NMR yield of 44%, instead of the high 87% yield achieved with starting urea **206** (section 3.2.1, Table 9, entry 3). Fully isomerised *N*-(*Z*)-vinyl-*N*'-(*E*)-vinyl urea **560** and *N*,*N*'-(*E*)-divinyl urea **207** were obtained in NMR yields of 28% and 15% respectively (Scheme 109). The formation of **207** might be explained by the observed lower migration ability of the *E*-vinyl chain when using the KHMDS/18-crown-6 conditions, whereupon the *Z*-vinyl chain upon γ-deprotonation isomerises into the more thermodynamically stable *E*-alkene geometry instead of executing the desired nucleophilic vinylic attack.

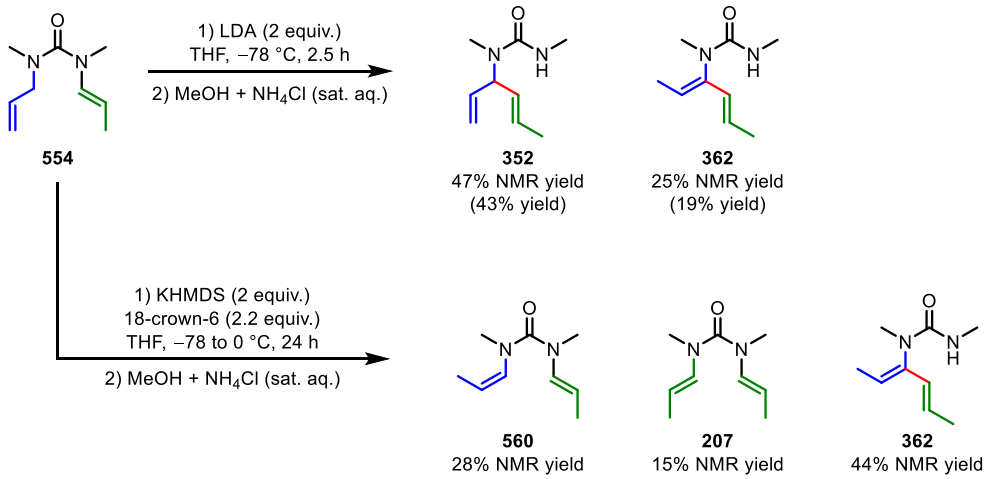

Scheme 109. Probing the stereospecificity of the initial N→C vinyl migration step with *N*-allyl-*N*'-(*E*)-vinyl urea 554. Blue represents the nucleophile. Green represents the electrophile. Red represents the new bonds formed. The NMR yields are determined based on ^{1}H NMR analysis using 1,2,4-trimethoxybenzene as an internal standard.

Pleasingly, the same stereospecificity was observed when subjecting *N*-(*Z*)-vinyl-*N*'-(*E*)-vinyl urea **560**, in which the *E*-vinyl group can only act as the electrophilic migration group, to the LDA rearrangement conditions, forming unconjugated migration product **352** exhibiting *E*-alkene geometry (Scheme 110). However, this time the N→C vinyl migration did not involve a clean conversion of **560** to **352** and **362** and was significantly low yielding. Hydrolysis side-products **365**, **366** and **561**, and additional *in situ* isomerised urea **207** were observed, as well as the undesired 5-*exo*-*trig* cyclisation product **562** (presumably formed before the N→C vinyl migration); a reason for these undesired reactions may be the lower migration ability of the *E*-vinyl chain, but more so that the γ-deprotonation of the *Z*-vinyl group appears challenging with LDA. The low efficacy of the N→C vinyl migration of **560** when using the KHMDS/18-crown-6 conditions complemented the suggestion that the alkene geometry of the *N*-vinyl chain of the electrophile is crucial for its migrating capability; the *Z*-vinyl chain is a significantly better migrating group than a *E*-vinyl chain (Scheme 110).

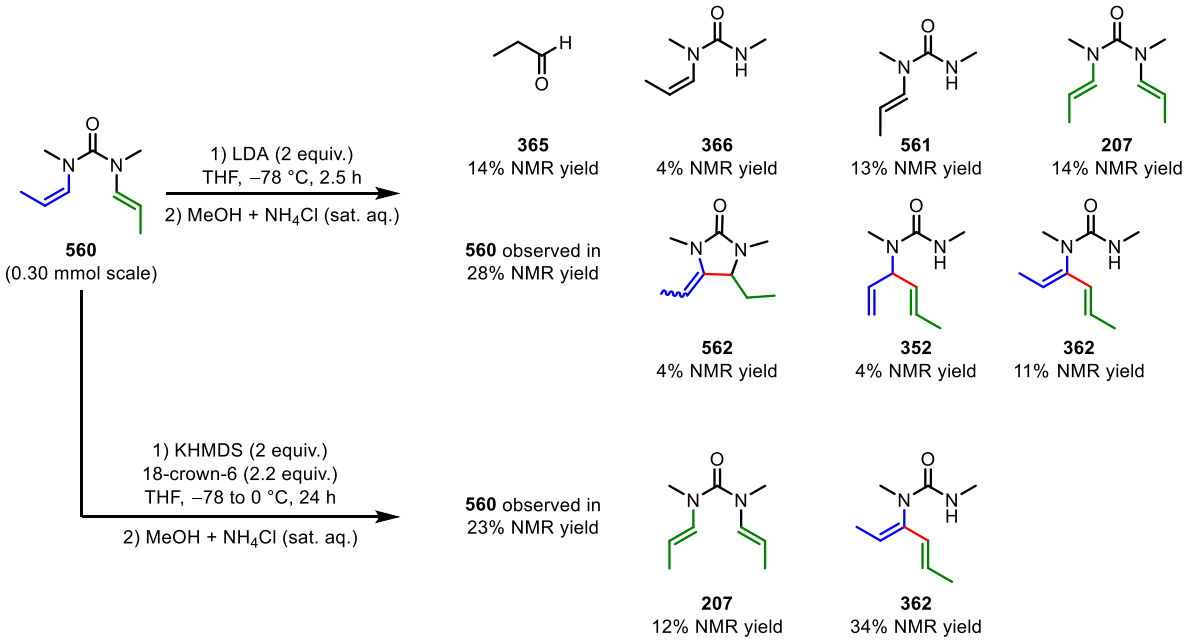

Scheme 110. Probing the stereospecificity of the initial N→C vinyl migration step with *N*-(*Z*)-vinyl-*N*'-(*E*)-vinyl urea 560. Blue represents the nucleophile. Green represents the electrophile. Red represents the new bonds formed. The NMR yields are determined based on ^{1}H NMR analysis using 1,2,4-trimethoxybenzene as an internal standard.

Finally, the stereospecificity of the initial N→C vinyl migration was probed with *N*,*N*'-(*Z*)-divinyl urea **364**, expecting to form unconjugated migration product **358** with *Z*-alkene geometry. Even though a low NMR yield of 5% was observed for the unconjugated migration product, it was established that **358** exhibited the *Z*-alkene geometry as anticipated (Scheme 111).

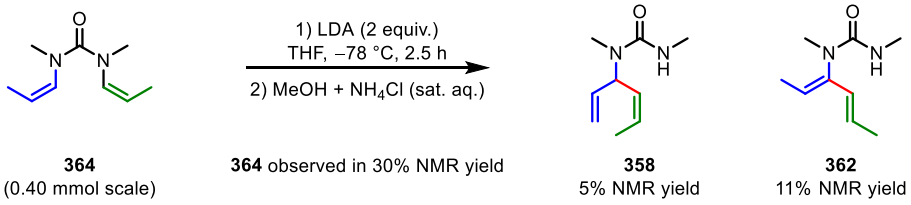

Scheme 111. Probing the stereospecificity of the N→C vinyl migration step with *N*,*N*'-(*Z*)-divinyl urea 364. Blue represents the nucleophile. Green represents the electrophile. Red represents the new bonds formed. The yields are determined by ^{1}H NMR using 1,2,4-trimethoxybenzene as an internal standard.

These stereospecificity studies demonstrated that in the N→C vinyl migration the alkene geometry of the starting urea is retained in the unconjugated migration product. From this it can be concluded that a $S_NV\sigma$ reaction mechanism is not operative, as this would give inversion of the alkene geometry. Instead, it is assumed that a $S_NV\pi$ or an Ad_N-E with a shorter-lived carbanion pathway is operative, although further mechanistic studies are required to distinguish between these two possible pathways.

3.2.5.4 Regioselectivity Studies

3.2.5.4.1 Regioselectivity Studies with a Deuterium Labelled *E*-Vinyl Chain

During the optimisation studies (section 3.2.1) it was found that the N→C vinyl migration of *N*,*N*'-(*E*)-divinyl urea **207** proved ineffective. In contrast, during the NMR studies (section 3.2.5.1), *N*,*N*'-(*Z*)-vinyl urea **364** was revealed as the reaction intermediate. From these combined results, it was hypothesised that, unlike the *Z*-vinyl group, the *E*-vinyl group cannot act as the nucleophile, but presumably could act as the electrophile and so provide regioselectivity to the N→C vinyl migration.

To confirm that the *E*-vinyl group can only act as the electrophile, the synthesis of deuterium-labelled ureas **554-D** and **560-D** was planned (Scheme 112). The same synthetic route was used as developed for the synthesis of ureas **554** and **560** (section 3.2.5.3, Scheme 108), with the only difference being the use of D_2O in anhydrous dioxane for the ruthenium-catalysed isomerisation to obtain deuterium-labelled *N*-vinyl 4-nitrophenyl carbamate **559-D**.[176] Then, upon amine-coupling and additional olefin isomerisation deuterium-labelled ureas **554-D** and **560-D** were obtained in high yields of 88% and 87%, respectively, with significant deuterium incorporation at the α-, β-, and γ-position of the *E*-vinyl chain.

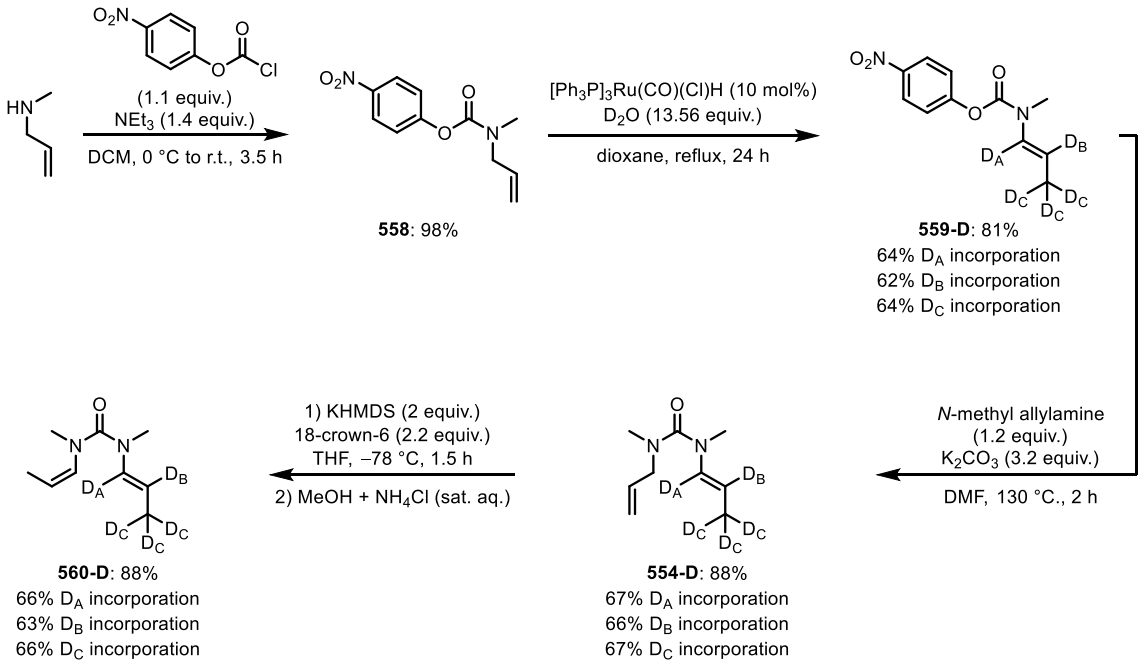

Scheme 112. Synthetic route for unsymmetrical deuterium-labelled *N*-allyl-*N*'-(*E*)-vinyl urea 554-D and *N*-(*Z*)-vinyl-*N*'-(*E*)-vinyl urea 560-D.

It was found that when deuterium-labelled urea **554-D** was subjected to the LDA and KHMDS/18-crown-6 conditions, the N→C vinyl migration had occurred regioselectively in both cases with the deuterium-labelled *E*-vinyl group exclusively acting as the electrophile (Scheme 113). Similar product yields were obtained as with urea **554** (section 3.2.5.3, Scheme 109) and thus confirms that the N→C vinyl migration of an *E*-vinyl group is significantly slower than a *Z*-vinyl group. For the reaction under the KHMDS/18-crown-6 conditions, slight changes in deuterium incorporation were observed in the reaction intermediates **560-D** and **207-D**, this could be due to possible hydrogen-deuterium scrambling during work-up and column purification, and/or due to the use of (slightly acidic) $CDCl_3$ in the NMR tube. As described in section 3.2.5.3, the formation of urea **207-D** may be explained by the fact that upon γ-deprotonation isomerisation of the *Z*-vinyl chain into the more thermodynamically stable *E*-alkene geometry takes place instead of the desired N→C vinyl migration due to the poor migration ability of the *E*-vinyl group (here the deuterated *E*-vinyl group of **560-D**).

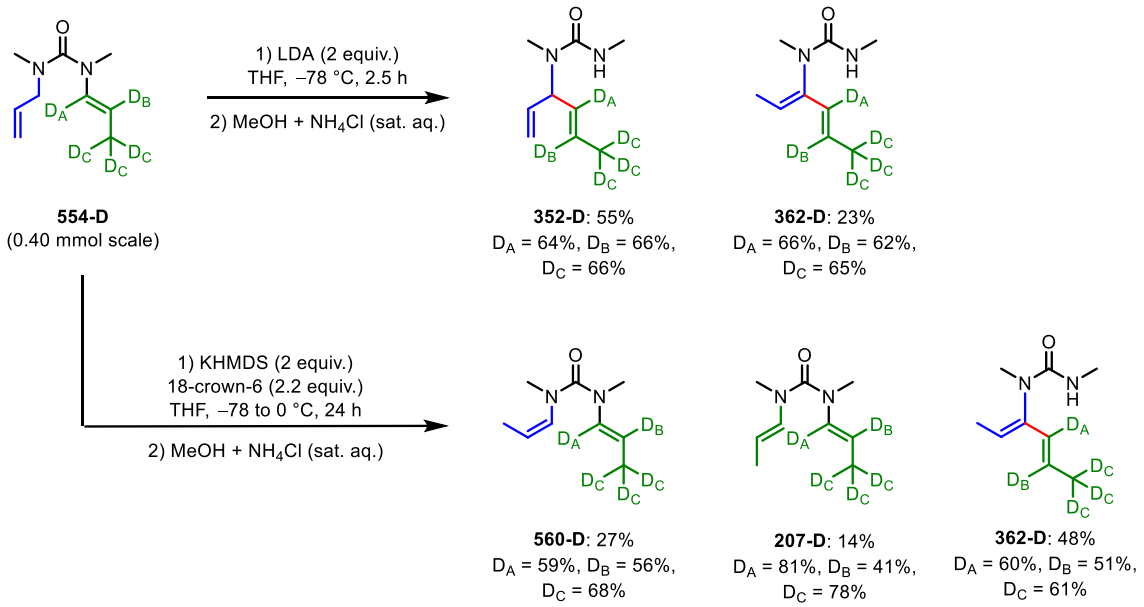

Scheme 113. Probing the regioselectivity of the N→C vinyl migration with deuterium-labelled *N*-allyl-*N*'-(*E*)-vinyl urea 554-D. Blue represents the nucleophile. Green represents the electrophile. Red represents the new bonds formed. The yields are determined by ^{1}H NMR using 1,2,4-trimethoxybenzene as an internal standard.

As expected, the same regioselectivity was observed when subjecting deuterium-labelled *N*-(*Z*)-vinyl-*N*'-(*E*)-vinyl urea **560-D** to the LDA and KHMDS/18-crown-6 N→C vinyl migration conditions, forming migration product **362-D** for which the deuterium-labelled *E*-vinyl chain has exclusively acted as the electrophile (Scheme 114). The low conversion of starting urea **560-D** confirmed the hypothesis that γ-deprotonation of the *Z*-vinyl group is challenging with LDA, and the *E*-vinyl chain is a poor migrating group for both cases.

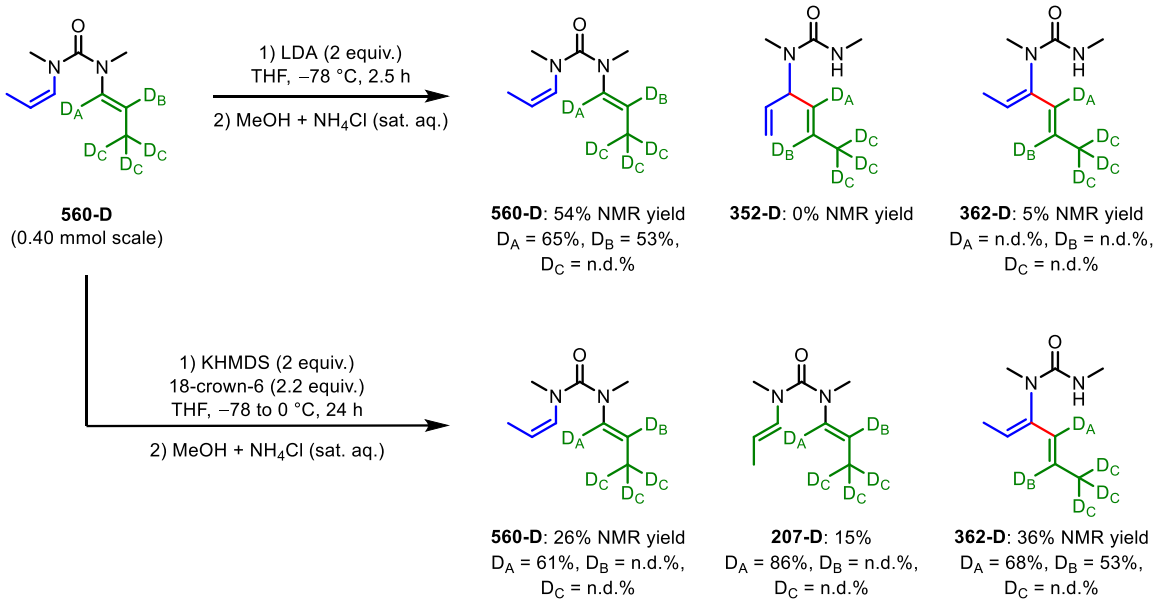

Scheme 114. Probing the regioselectivity of the N→C vinyl migration with deuterium-labelled *N*-(*Z*)-vinyl-*N*'-(*E*)-vinyl urea 560-D. Blue represents the nucleophile. Green represents the electrophile. Red represents the new bonds formed. The yields are determined by ^{1}H NMR using 1,2,4-trimethoxybenzene as an internal standard. n.d. = not determined, due to overlapping signals in ^{1}H NMR spectrum.

3.2.5.4.2 Regioselectivity Studies with a β-Methyl Substituted Allyl Chain

During the exploration of the substrate scope (section 3.2.3.1) it was found that the N→C vinyl migration of unsymmetrical ureas containing a β-substituted allyl group and an unsubstituted- or α-substituted allyl group is regioselective; the β-substituted allyl group exclusively acts as the nucleophile. For example, when unsymmetrical urea **243**, that consists of an unsubstituted allyl group and a β-methyl substituted allyl group, was submitted to the N→C vinyl migration conditions, migration product **411** was isolated in a good yield of 70% (Scheme 115). Regioisomer **563** was tentatively observed in less than 7% yield in the crude ^{1}H NMR, although was not isolated after purification.

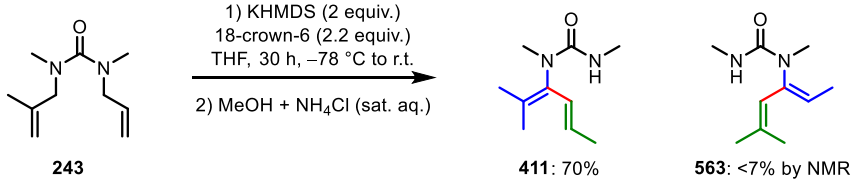

Scheme 115. Regioselective N→C migration of unsymmetrical diallyl urea 243, consisting of a β-methyl substituted and an unsubstituted allyl group. Blue represents the nucleophile. Green represents the electrophile. Red represents the new bonds formed.

This observed regioselectivity raised the interest in discovering its origin, which could then also provide more insight into the heavily demanding reaction cascade pathway involved in the N→C vinyl migration of symmetrical and unsymmetrical diallyl ureas. It was hypothesised that a potential difference in the rate of the crucial *in situ* allyl-to-vinyl isomerisation may be the cause of the regioselectivity. If the unsubstituted allyl group isomerises significantly more rapidly, then α-deprotonation of the β-methyl substituted allyl group could immediately result in the formation of migration product **411**. This hypothesis was confirmed by the result obtained when the N→C vinyl migration of **243** was performed from −78 °C to 0 °C, instead of room temperature in order to observe the reaction intermediates; partially isomerised urea **564** was observed alongside fully isomerised urea **565** and migration product **411** (Scheme 116).

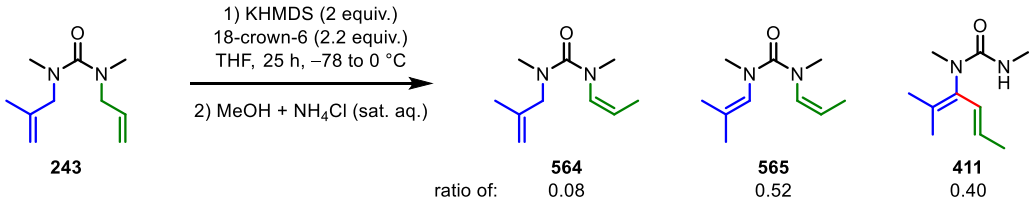

Scheme 116. Performing the regioselective N→C vinyl migration of unsymmetrical urea 243 at colder temperatures revealed the presence of partially isomerised urea 564. Blue represents the nucleophile. Green represents the electrophile. Red represents the new bonds formed.

It was suggested that by submitting fully isomerised urea **565** to the N→C vinyl migration conditions, it could be established whether the difference in rate of isomerisation was the actual origin of the observed regioselectivity – if so, both regioisomers **411** and **563** should be formed. Therefore, urea **565** was prepared on a larger scale using the N→C vinyl migration conditions; the reaction was quenched at −20 °C, instead of colder temperatures, to ensure there was no partially isomerised urea **564** present anymore in the reaction mixture (Scheme 117). Urea **565** was easily isolated in a yield of 60% from small amounts of migration products **566** (4% yield) and **(*Z*)-411** (15% yield).

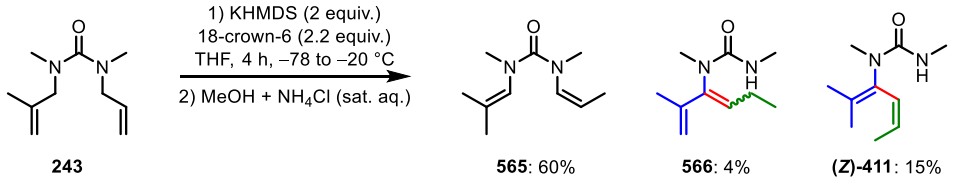

Scheme 117. Larger scale preparation of fully isomerised urea 565 using adjusted N→C vinyl migration conditions on starting urea 243. Blue represents the nucleophile. Green represents the electrophile. Red represents the new bonds formed.

Against expectations, regioisomer **411** was still the major product, formed in a yield of 65% (Scheme 118A). Besides the presence of unconjugated migration product **567**, a product tentatively assigned as regioisomer **563** was isolated in <3% yield; due to the small quantity of material and the presence of impurities its structure could not be definitely elucidated as **563**.

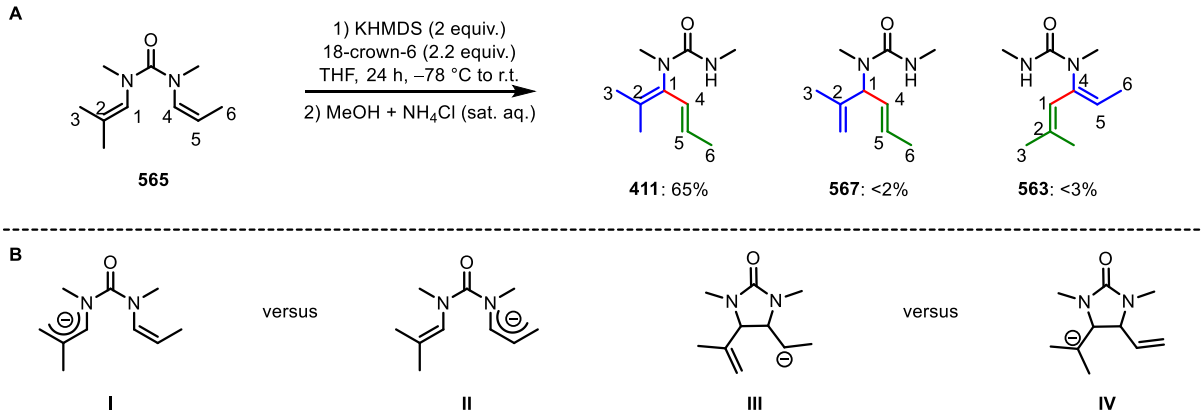

Scheme 118. N→C vinyl migration of fully isomerised urea 565 to determine the regioselectivity origin (A) and demonstration of the possible anions involved (B). Blue represents the nucleophile. Green represents the electrophile. Red represents the new bonds formed.

However, due to the regioselective formation of migration product **411** from starting urea **565**, it can be assumed that the difference in rate of isomerisation was not the origin of the regioselectivity. The rate, or possibility, of γ-deprotonation cannot be used to explain the regioselective N→C vinyl migration as both vinyl chains in urea **565** involve the deprotonation of a methyl group. Instead, when the possible reaction intermediates were considered, two theories were proposed that, individually or combined, could explain the origin of the regioselectivity (Scheme 118B). The first theory involved the allylic species formed upon γ-deprotonation: the presence of the β-substituent may have made its allylic species **I** significantly more reactive than the unsubstituted allylic species **II**. The second proposal considered the energy barrier that has to be overcome to partially or fully – depending on whether the mechanism follows a concerted or an addition-elimination pathway – form an anion in the nucleophilic vinylic substitution step. To generate regioisomer **563** an anion must form at a tertiary carbon **IV** compared to the case of regioisomer **411** where the anion would be formed at a secondary carbon **III**, and thus would have a lower activation energy barrier.

3.2.5.5 Kinetic Isotope Effect Studies

Based on the stereospecificity studies and the observed retention of the alkene geometry (section 3.2.5.3), it was concluded that the N→C vinyl migration of *N*,*N*'-diallylureas does not operate via the concerted $S_NV\sigma$ pathway. To gain insight into whether, instead, a concerted $S_NV\pi$ or a stepwise Ad_N-E with a shorter-lived carbanion pathway is in operation, deuterium and natural abundance ^{13}C kinetic isotope effect studies were performed.

Determination of kinetic isotope effects (KIEs) has been recognised as a valuable tool to investigate reaction mechanisms and corresponding transition states.[177] This is mainly because of differences in zero-point energy (ZPE) and thus in reaction rate, enabling useful information concerning the rate-determining step of the reaction to be obtained. ZPE corresponds to the vibrational energy (E_n) of a molecule in its ground-state and is, according to Hooke's law (Equation 1), dependent on the stretching frequency (ν) of the covalent bond of interest (Equation 2), which is in turn determined by the reduced mass (μ) of the two involved atoms (Equation 3). As a result, the lighter isotope, for example hydrogen, will have a greater bond vibration frequency and thus a higher ZPE in comparison to its heavier isotope equivalent – deuterium; this means that less energy is required to dissociate the bond connecting the lighter isotope (C–H), resulting in an increased rate of the reaction (Figure 10).[177,178]

(1) $E_n = \left(n + \frac{1}{2}\right) h\nu$ (with n = principal quantum number and h = Planck's constant)

(2) $\nu = \frac{1}{2\pi c}\sqrt{\frac{k}{\mu}}$ (with c = speed of light and k = force constant)

(3) $\mu = \frac{m_1 m_2}{m_1 + m_2}$ (with m = mass)

(4) $KIE = \frac{k_L}{k_H}$ (with k = rate constant)

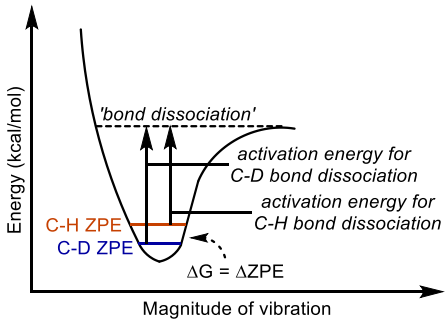

Figure 10. Morse potential curve for C–D and C–H bonds.

The reaction rate constants (k) for the lighter (k_L) and heavier (k_H) isotope can then be used to calculate the KIE (Equation 4) and based on the magnitude of the KIE, the nature of the rate-determining step of the reaction could be obtained. When the k_L/k_H is equal to one, there is no KIE, which means that the isotopic bond of interest does not participate in the rate-determining step of the reaction. However, if a k_L/k_H of greater than one is measured, this corresponds to a normal isotope effect, while in the case of an inverse isotope effect, where the heavier isotope reacts faster, a k_L/k_H of less than one would be measured. A normal KIE is classified as primary KIE if the rate-determining step involves the formation or dissociation of the studied bond. The simplest way to treat a primary KIE would be to consider the studied bond as fully dissociated at the transition state, so that it could be assumed that only the ZPE differences of the ground state controls the KIE (Figure 10). Yet, a more realistic view would be to include the ZPE difference of the transition state for the determination of the primary KIE as most times the bond being studied is not fully dissociated at the transition state (Figure 11). This means that the thermodynamics of the reaction (early or late TS) but also the (non-)linearity of the transition state now play a role in determining the magnitude of the primary KIE.[179]

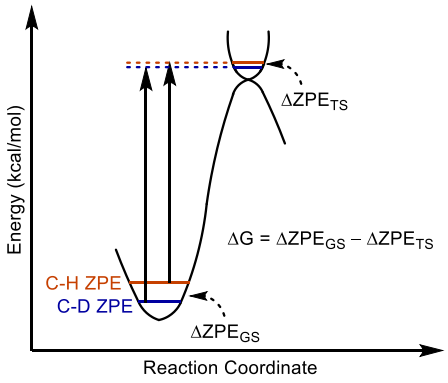

Figure 11. Morse potential curve for C–D and C–H bonds, considering the ZPE difference of the transition state.

Concerning secondary KIEs, generally smaller than primary KIEs, the studied bond is not formed or dissociated in the rate-determining step; factors such as hyperconjugation, steric effects and hybridisation state changes of the isotopic bond affect the ZPE.[179] The out-of-plane bend of a sp^2-hybridised carbon (800 cm^{-1}) is looser than for a sp^3-hybridised carbon (1350 cm^{-1}). Thus, by changing from sp^2 to sp^3 hybridisation, in other words from a loose to a stiffer bond, the transition state has a larger difference in the ZPE than the ground-state, resulting in $k_L/k_H < 1$, which means that a faster reaction is observed with the heavier isotope (Figure 12A). This process is classified as the inverse secondary KIE; a normal secondary KIE involves the change in hybridisation state of the isotopic bond from sp^3 to sp^2 and has $k_L/k_H > 1$ (Figure 12B).[180]

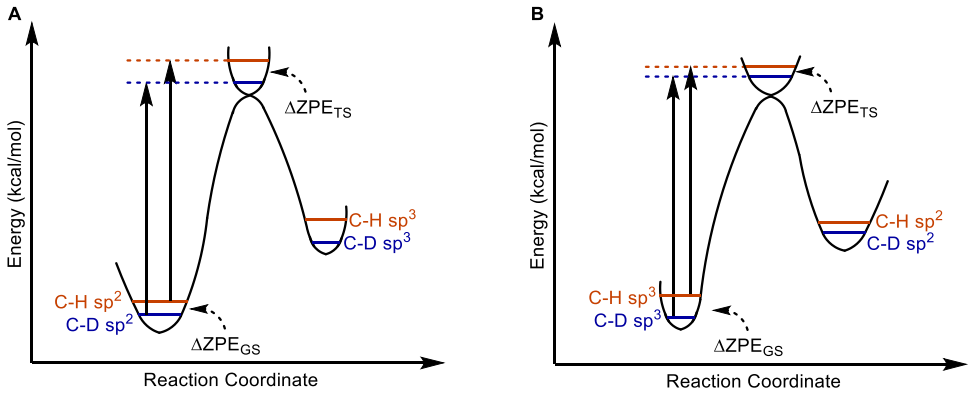

Figure 12. Morse potential curve for C–D and C–H bonds experiencing a hybridisation change from sp^2 to sp^3 (A) and sp^3 to sp^2 (B).

3.2.5.5.1 Deuterium Kinetic Isotope Effect Studies

It was believed that by performing the N→C vinyl migration with a urea containing a deuterium-labelled *E*-vinyl group (the migrating group) more insight could be obtained on whether or not a full anion is formed at the β-carbon of the vinyl chain in **570-D**, and thus whether an Ad_N-E pathway is followed (Scheme 119). In this case, both the α- and β-carbon atoms would change their hybridisation state from sp^2 to sp^3, and thus an inverse secondary KIE should be measurable. It would then be expected that the deuterated molecules react faster than the non-deuterated molecules, resulting in lower deuterium incorporation at the α- and β-position of the deuterium-labelled *E*-vinyl chain in the reaction intermediate (**569-D**) during the course of the N→C vinyl migration.

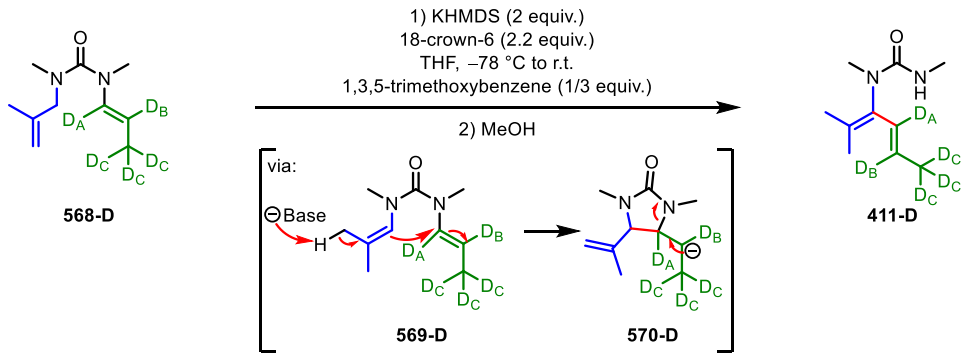

Scheme 119. N→C Vinyl migration of urea 568-D containing a deuterium-labelled migrating group to determine whether an Ad_N-E pathway is followed. Blue represents the nucleophile. Green represents the electrophile. Red represents the new bonds formed.

To test this hypothesis, deuterium-labelled urea **568-D** was prepared, following the synthetic route developed to afford partially deuterated and isomerised ureas (section 3.2.5.4.1), in good yield with a good level of deuterium incorporation at the α-, β-, and γ-position of the *E*-vinyl chain (Scheme 120).

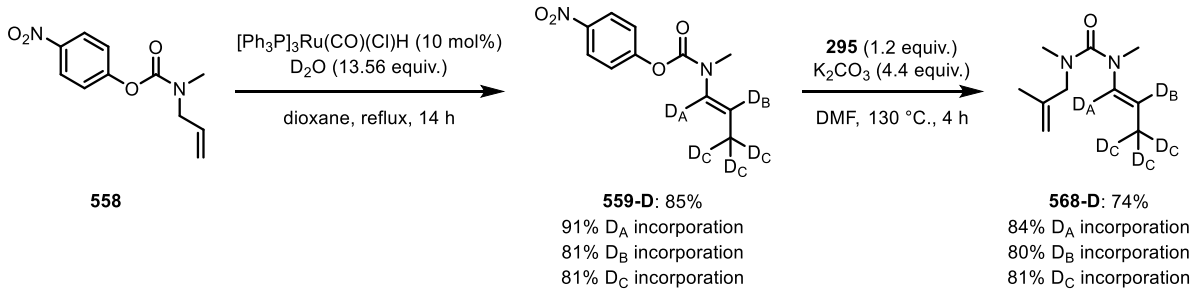

Scheme 120. Synthetic route for unsymmetrical deuterium-labelled urea 568-D.

To allow determination of both the conversion and the deuterium incorporation of reaction intermediate **569-D** in the course of the N→C vinyl migration, the reaction was set up as normal with a known amount of internal standard, 1,3,5-trimethoxybenzene (Scheme 119). Since the NMR studies revealed that the N→C vinyl migration only occurs at temperatures between −20 °C and room temperature, after gradually warming up from −78 °C to 0 °C the reaction flask was placed at room temperature and the first aliquot was taken directly. The aliquot was quenched with MeOH, then a crude ^{1}H NMR was taken immediately without work-up, using deuterated toluene as the NMR solvent to eliminate potential hydrogen-deuterium exchange in the NMR sample. Over a time period of almost 6 hours, 22 aliquots were taken at room temperature and analysed by crude ^{1}H NMR. The analysis of all crude ^{1}H NMR spectra showed that as the amount of reaction intermediate **569-D** decreased, the yield of migration product **411-D** increased; the final NMR yield of migration product **411-D** was as expected (Scheme 121 and Figure 13).

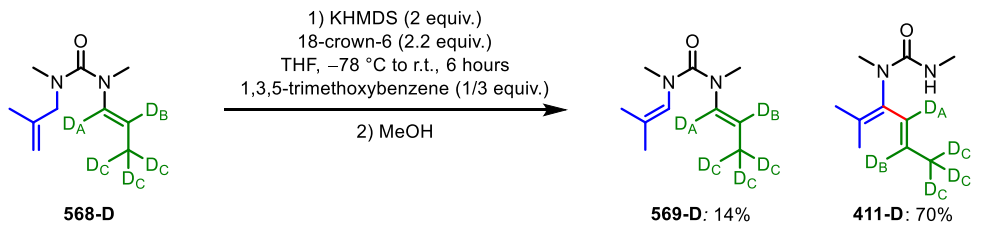

Scheme 121. N→C vinyl migration of 568-D analysed by ^{1}H NMR, forming migration product 411-D and reaction intermediate 569-D. Blue represents the nucleophile. Green represents the electrophile. Red represents the new bonds formed. The yields are determined by ^{1}H NMR using 1,3,5-trimethoxybenzene as an internal standard.

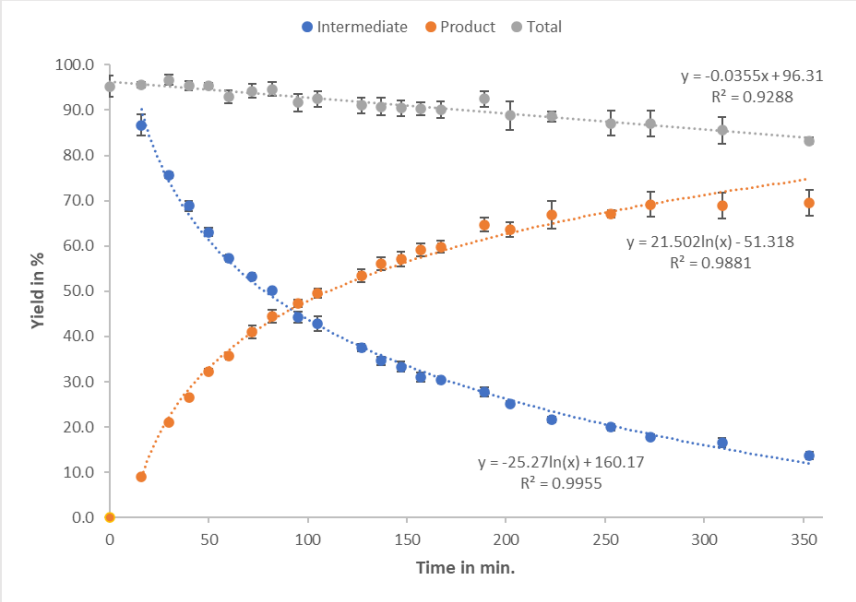

Figure 13. Reaction profile of the N→C vinyl migration started from urea 568-D, following the conversion of reaction intermediate 569-D to migration product 411-D at room temperature.

Moreover, the analysis of all crude ^{1}H NMR spectra showed that the deuterium incorporation at the α-position of the migrating group in reaction intermediate **569-D** had not significantly changed; a fluctuating deuterium-incorporation of between 84.0% and 85.3% was measured over time, having started with deuterium-incorporation of 84.0% (Figure 14). Similarly, when looking at the deuterium incorporation at the β-carbon of reaction intermediate **569-D**, only a slight increase of about 5% was observed which either suggests that the non-deuterated molecules have reacted slightly faster than the deuterated molecules, or this value is not significant, given the size of inevitable errors in integration of the crude ^{1}H NMR spectra (Figure 14). However, the results of this preliminary study suggested that the N→C vinyl migration does not involve the formation of a full anion at the β-position of the vinyl chain. This would mean that the Ad_N-E pathway is also not operative, leaving the options of the N→C vinyl migration following a $S_NV\pi$ mechanism or a mechanism that is on the continuum of the Ad_N-E and $S_NV\pi$ pathways.

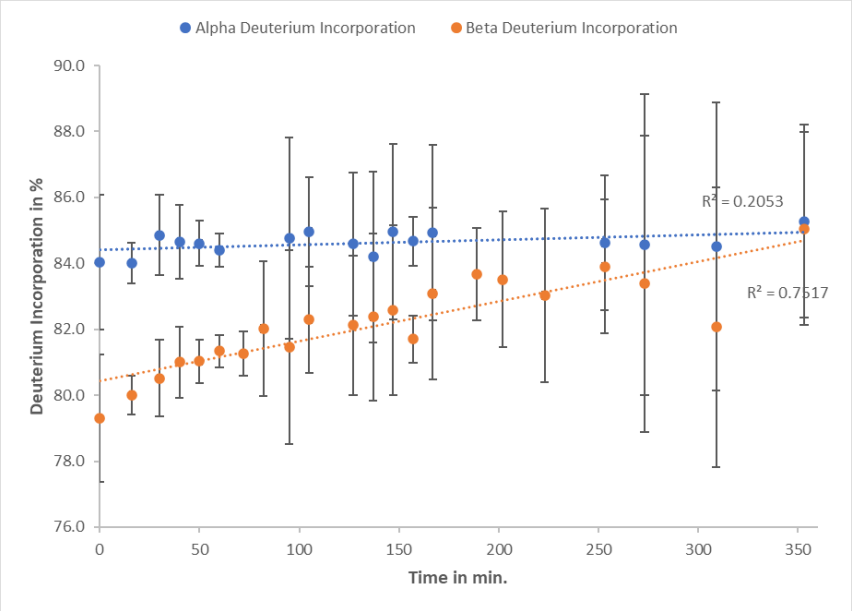

Figure 14. Deuterium incorporation at the α- and β-position of the migrating group in reaction intermediate 569-D over the course of the N→C vinyl migration of starting urea 568-D.

When looking at the migrated group in product **411-D** over the course of the N→C vinyl migration of **568-D**, the deuterium incorporation at the α-position fluctuated between 71.4% and 85.3% (Figure 15). Yet at the β-carbon a significant reduction from around 74% to 55% in deuterium incorporation was observed. However, this reduction may be explained by the alkene isomerisation that takes place after the N→C vinyl migration, resulting in hydrogen-deuterium scrambling. Thus, no accurate representation of the actual deuterium incorporation of N→C vinyl migration product **411-D** could be obtained.

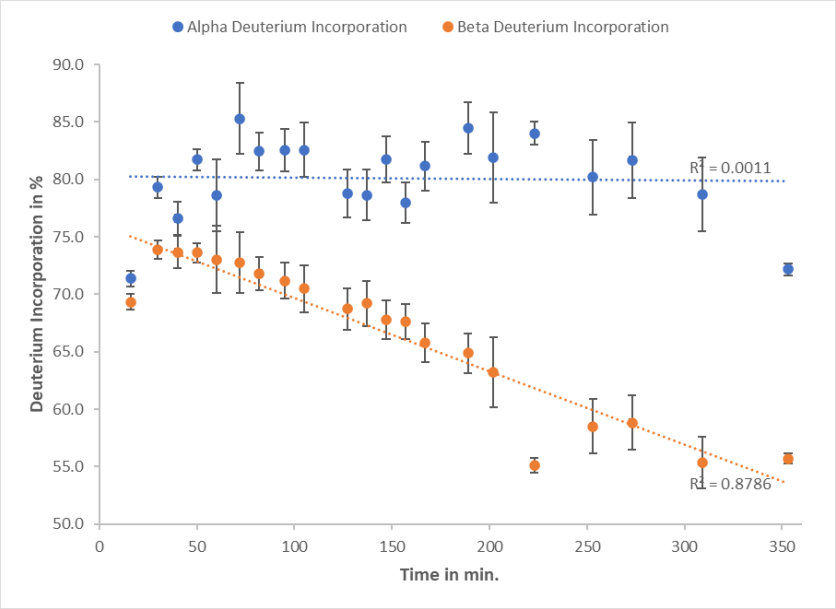

Figure 15. Deuterium incorporation at the α- and β-position of the migrated group in migration product 411-D over the course of the N→C vinyl migration of starting urea 568-D.

3.2.5.5.2 Natural Abundance ^{13}C Kinetic Isotope Effect Determination

Another way to determine the KIE for a reaction is to utilise the isotopic composition of molecules at natural abundance.[181] If the lighter isotopes react faster than their heavier equivalents, the unreacted starting material will show enrichment of the heavier isotope during the course of the reaction, and a KIE will be measurable. This change in proportion of the heavier isotope in the unreacted starting material (R) and the original starting material (R_0) is expressed by R/R_0 and is determined by the relative reaction rate of the lighter and heavier isotopes (KIE) and the conversion of starting material (F) (Equation 5). The KIE becomes significantly measurable when the starting material nears complete conversion ($F \rightarrow 1$) and R/R_0 approaches infinity; e.g. when the starting material has almost reacted completely (99%) in a reaction with a KIE of 1.05, the heavier isotope will be enriched in about ~25% in the unreacted starting material.[181] However, the uncertainty in the starting material conversion (ΔF), the KIE magnitude and the analysis precision ($\Delta R/R_0$) all affect the accuracy of the KIE measurement (Equations 6). The uncertainty of this measured KIE can be calculated with Equations 7 and 8, where ΔKIE_F is related to ΔF and ΔKIE_R is related to $\Delta R/R_0$.

(5) $$R/R_0 = (1-F)^{\frac{1}{KIE}-1}$$

(6) $$KIE_{calcd} = \frac{\ln(1-F)}{\ln(1-F)R/R_0}$$

(7) $$\Delta KIE_F = \frac{-\ln(R/R_0)}{(1-F)ln^2[(1-F)R/R_0]}\Delta F$$

(8) $$\Delta KIE_R = \frac{-\ln(1-F)}{(R/R_0)ln^2[(1-F)R/R_0]}\Delta(R/R_0)$$

Based on these equations, when the analysis of $\Delta R/R_0$ is highly accurate the uncertainty of the measured KIE (ΔKIE) is controlled by ΔKIE_F and thus the amount of conversion is inconsequential. However, generally, integration of NMR spectra is not highly accurate; in this case, ΔKIE_R dominates ΔKIE while ΔKIE_F can be neglected and thus it is beneficial to run the reaction to a higher conversion to achieve a more accurate KIE measurement.[181]

A general high precision method to utilise the isotopic ratio of molecules at natural abundance for the measurement of KIEs with ^{13}C NMR analysis was developed by Singleton and Thomas.[181] After stopping the studied reaction at around 72-99% conversion and recovering the starting material, ^{13}C NMR analysis can be performed. Then, the averaged integrations of carbon atoms that do not participate in the reaction mechanism (KIE = 1 is assumed), or of an internal standard, can be compared to the integrations of the carbon atoms of interest that participate in the reaction mechanism (R/R_0). Based on this data, equations 5 to 8 can be used to determine the KIE of a reaction and its uncertainty. Limitations of this method include the larger scale at which the reactions have to be performed in order to be able to recover enough starting material, and the studied reaction must be irreversible and not change mechanism over the course of the reaction. Nevertheless, the Singleton method has been successfully applied in determining KIEs of various reactions,[182–187] including at the University of Bristol by the Bower group.[188,189]

A similar natural abundance ^{13}C KIE experiment was performed as a preliminary study for the N→C vinyl migration of urea **568**, prepared in high yield (Scheme 122), to determine whether or not a full anion is formed at the β-carbon of the vinyl chain in the reaction intermediate (green in **570**, Scheme 123).

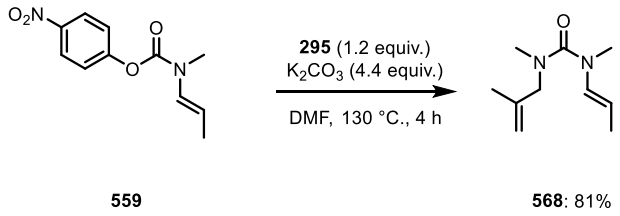

559 **568**: 81%

Scheme 122. Synthesis of unsymmetrical, partially isomerised urea 568 in high yield.

For this experiment, we aimed for 50% conversion of the starting material **568**, so we could see substantial signals in the ^{13}C NMR spectra of the reaction intermediate. The first and second run of the reaction were both quenched after 4.75 hours, giving conversions of around 51% and 35% respectively, and analysed by quantitative ^{13}C NMR without work-up or column chromatography (section 5.3.4). This meant that the analysed data cannot provide an accurate KIE value yet could show whether there is a measurable effect at the studied reaction centres.

The integration of the carbon atoms in intermediate **569** that are involved in the reaction mechanism (*R*) was compared to the averaged integration of the other carbon atoms in **569** that are not at the reaction centre (R_0) (section 5.3.4). The latter was also used to calculate the conversion of the reaction (*F*) by comparison to the averaged integration of the internal standard 1,3,5-trimethoxybenzene (section 5.3.4). In the N→C vinyl migration of **568** to **411** via **569**, KIEs were measurable at the α- and β-position of the *E*-vinyl group in reaction intermediate **569** (Scheme 123). The KIE at the γ-position of the *E*-vinyl group in **569** seemed to be equal to 1 within the size of the calculated error (Scheme 123). Thus, this preliminary data suggested that there is no effect at the γ-position, alternatively the KIE is too small to be measured under these conditions. Further work is required for the collection of accurate experimental data, but also theoretical KIE values ought to be calculated to develop more insight into the mechanism of the N→C vinyl migration reaction (section 4.0).

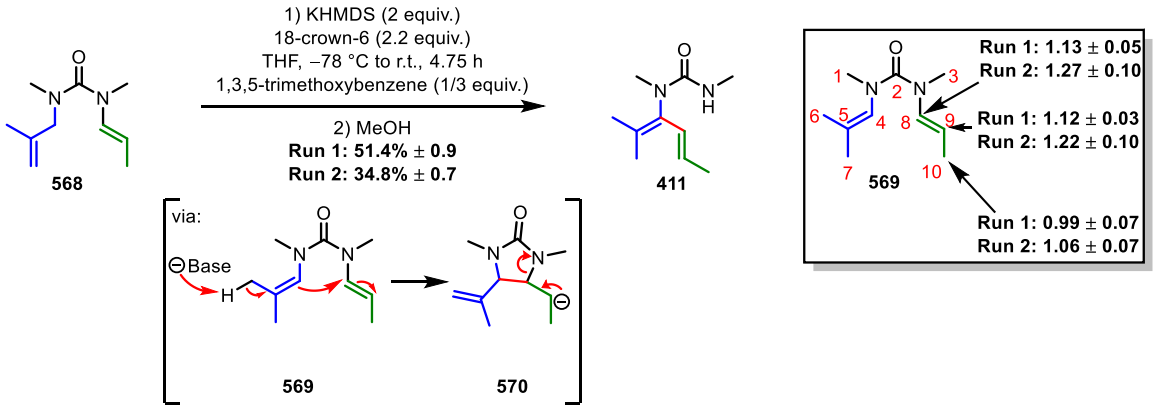

Scheme 123. Measurable ^{13}C natural abundance KIEs for the N→C vinyl migration of 568 to 411 via reaction intermediate 569. Blue represents the nucleophile. Green represents the electrophile. Red represents the new bonds formed.

3.3 Conclusions

To conclude, a novel intramolecular nucleophilic vinylic substitution reaction has been developed which makes use of carbon nucleophiles – *N*,*N*'-diallyl ureas – and gives access to complex non-cyclised alkenes. The N→C vinyl migration was successfully optimised with simple symmetrical *N*,*N*'-diallyl urea (**206**), while the rearrangement of symmetrical *N*,*N*'-(*E*)-divinylurea (**207**) remained unproductive. Having elucidated the different possible outcomes, a rather complex, tandem sequence of isomerisations and nucleophilic substitution was proposed for the N→C vinyl migration reaction with symmetrical *N*,*N*'-(*Z*)-divinyl urea **364** as the crucial reaction intermediate.

Pleasingly, the method was effectively applied to symmetrical substituted diallyl ureas, including bulky substituents. Greater complexity was observed with unsymmetrical diallyl ureas as both *N*-allyl groups can act as the nucleophilic anion-stabilising or the electrophilic migrating group. Interestingly, complete regioselectivity in the N→C vinyl migration was obtained by incorporation of a β-substituent on one of the allyl chains or by introduction of an *E*-vinyl chain on one side of the urea.

Unfortunately, it was found that the N→C vinyl migration of diallyl ureas has some principal limitations. In cases where the initial allyl-to-vinyl isomerisation was sufficiently slow, 6-*exo*-*trig* cyclisation could outcompete the desired nucleophilic vinylic substitution. Similarly, 5-*exo*-*trig* cyclisation could arise before or after the N→C vinyl migration when the urea contains an anion-stabilising 'trap' like a phenyl ring or a diene. De-allylation of the starting urea was observed in the presence of α- and γ-methyl substituents due their deprotonation resulting in elimination of the urea anion, and thus limiting the yields of the rearrangement products. In summary, the general reactivity of the N→C vinyl migration of alkyl-substituted diallyl ureas is displayed in Table 14.

Table 14. General reactivity summary of the N→C vinyl migration of alkyl-substituted diallyl ureas.[a]

Substituent Combinations	unsubstituted	α	β	γ
unsubstituted	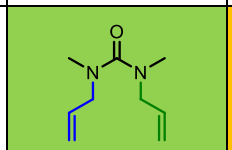	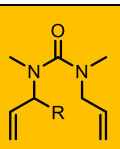	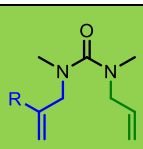	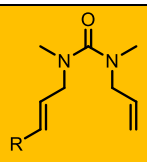
α			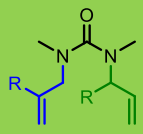	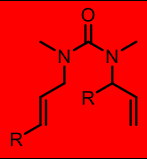
β			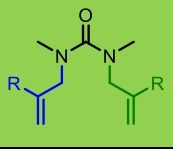	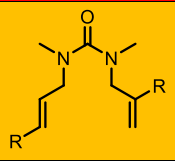
γ				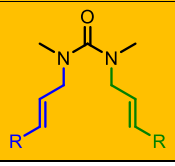

[a]Blue allyl group represents the nucleophile – anion-stabilising group. Green allyl group represents the electrophile – the migrating group. Black allyl group represents both nucleophile and electrophile. **Green box** represents high yielding N→C vinyl migrations. **Orange box** represents moderately effective N→C vinyl migrations that are followed by 5-*exo-trig* cyclisation reactions or compete with de-allylation. **Red box** represents non-effective N→C vinyl migrations due to high amounts of the competing de-allylation.

More insight into the heavily demanding reaction cascade was obtained by various mechanistic studies. Most interestingly it was concluded that the N→C vinyl migration is stereospecific, which excludes the possibility of the rearrangement following a $S_NV\sigma$ pathway that would give inversion of the alkene geometry. Based on the preliminary results of the deuterium kinetic isotope effect study, it was suggested that the N→C vinyl migration does not involve the formation of a full anion at the β-position of the vinyl chain, leaving the options of the N→C vinyl migration following a $S_NV\pi$ mechanism or a mechanism that lies somewhere on the continuum between the extremes of Ad_N-E and $S_NV\pi$. Preliminary natural abundance ^{13}C kinetic isotope effect studies confirmed there is an effect measurable at the reaction centres of interest, which in the future could be used in combination with theoretically calculated values to establish if a concerted $S_NV\pi$ or stepwise Ad_N-E is operative.

4.0 Overall Summary and Future Work

Inter- and intramolecular nucleophilic vinylic substitution (S_NV) reactions, in which nucleophiles displace leaving groups at an sp^2-hybridised vinylic carbon, have been the subject of some study and successfully applied in the synthesis of various vinyl ethers, endocyclic alkenes and unsaturated carbon frameworks. Remarkably, the use of carbon nucleophiles remains rare and all intramolecular S_NV reactions give cyclised products. Formation of non-cyclised products could however be established if the incoming nucleophile is tethered to the leaving group; this approach has been pioneered by Clayden and co-workers.

It was found that the N→C vinyl migration in *N*-benzyl ureas, and amino-acid and amino-nitrile derived ureas is an excellent intramolecular S_NV reaction to yield non-cyclised alkenes, with the ureas serving a dual role as both the leaving group and the linker to the tethered carbon nucleophile. Herein, a novel intramolecular S_NV reaction has been developed, where a vinyl group undergoes N→C migration on treatment of *N*,*N*'-diallyl ureas – the carbon nucleophiles – with base, enabling access to a wider range of non-cyclised alkenes.

Firstly, a practical method was developed to prepare *N*-methyl allylamines, which are generally volatile and have limited commercial availability, as their hydrochloride salts.[1] Various allylic alcohols were treated with *N*-Boc ethyl oxamate under Mitsunobu conditions followed by deprotection of the *N*-methylated Mitsunobu products to yield the *N*-methyl allylamine hydrochloride salts. By mix-and-matching these salts, facile access to a broad scope of diallyl ureas via the effective chloroformylation/amine-coupling method was now enabled. Alternative strategies to access the *N*-methyl allylamine derivatives or ureas more directly were investigated yet proved ineffective and inconsistent.

While the rearrangement of an unsubstituted symmetrical *N*,*N*'-(*E*)-divinylurea remained unproductive, the N→C vinyl migration was successfully optimised with an unsubstituted symmetrical diallyl urea. Having elucidated the different possible outcomes, a rather complex, tandem sequence of isomerisations and nucleophilic substitution was proposed for the N→C vinyl migration reaction with a symmetrical *N*,*N*'-(*Z*)-divinyl urea as the crucial reaction intermediate confirmed by (*in situ*) NMR experiments.

The rearrangement outcome of both the unsubstituted *N*,*N*'-diallyl urea and *N*-benzyl-*N*'-allyl urea were demonstrated to be strongly base-dependent; contrasting with LDA, KHMDS – a base with a lower pK_a of its conjugate acid – promotes the desired isomerisation/N→C vinyl migration sequence over the undesired cyclisation reaction before isomerisation. Based on KHMDS and 18-crown-6 stoichiometry studies, it was concluded that 18-crown-6 plays an important role in the allyl-to-vinyl isomerisation and

the N→C vinyl migration, which are both prohibitively slow with substoichiometric quantities of KHMDS.

The method was effectively extended to symmetrical diallyl ureas containing alkyl substituents, including rather bulky groups. Despite the complex reaction cascade, the starting ureas are, in most cases, cleanly converted to the desired rearranged products in good yields. Greater complexity was observed with unsymmetrical diallyl ureas as both *N*-allyl groups can act as the nucleophilic anion-stabilising or the electrophilic migrating group.

Interestingly, complete regioselectivity in the N→C vinyl migration of unsymmetrical diallyl ureas was obtained by incorporation of a β-substituent on one of the allyl chains or by introduction of an *E*-vinyl chain on one side of the urea, demonstrated by mechanistic studies with deuterium labelling. Mechanistic studies with unsymmetrical *N*-allyl-*N*'-(*Z*)-vinyl urea and *N*-allyl-*N*'-(*E*)-vinyl urea also proved that the actual N→C vinyl migration is stereospecific, which excludes the possibility of the rearrangement following a $S_NV\sigma$ pathway as inversion of alkene geometry would then result. With a preliminary deuterium kinetic isotope effect study on the rearrangement of *N*-β-methylallyl-*N*'-(*E*)-deuterated-vinyl urea, no significant change in deuterium incorporation at the *E*-vinyl chain in the reaction intermediate was observed, suggesting the stepwise Ad_N-E pathway, which should show a reduction in deuterium incorporation, is also not likely operative for the N→C vinyl migration.

The preliminary natural abundance ^{13}C kinetic isotope effect studies confirmed there is an effect measurable at the reaction centres of interest, which could be used in combination with theoretically calculated maximum values to confirm if the reaction proceeds via a concerted $S_NV\pi$ mechanism, and not a stepwise Ad_N-E mechanism. In the future, this natural abundance ^{13}C kinetic isotope effect study should be repeated by performing the N→C vinyl migration from the reaction intermediate (*N*-β-methylvinyl-*N*'-(*E*)-vinyl; **569** in Scheme 123). The reaction should be run to above 75% conversion and the unreacted starting material should be purified before DEPT ^{13}C NMR analysis with a high signal-to-noise ratio to achieve the highest possible accuracy in integration. The same NMR analysis should be performed with the starting material, and would be used as the R_0 in the KIE calculations. To improve this NMR experiment and obtain theoretical calculations for this study on the N→C vinyl migration, a collaboration with Dr. Eugene Kwan (Merk Research Laboratories) – an expert in KIE mechanistic studies – should be conducted.

Limitations of this intramolecular S_NV method were found to be competitive cyclisation with *N*-α-methyl, *N*-phenyl, *N*-benzyl, and *N*-vinyl substituted ureas and de-allylation with α-/γ-methyl substituted diallyl ureas. The latter was found to be less prevalent with propyl substituents. Before or after the N→C vinyl migration, 5- or 6-*exo-trig* cyclisation reactions occur due to significantly slow initial allyl-to-vinyl isomerisations or due to the presence of anion-stabilising 'traps' like dienes and styrenes.

Moreover, it was found that the tolerance of functional groups (e.g. silyl group, bromide, and protected alcohol) in this N→C vinyl migration of diallyl ureas is significantly limited by their position with regards to the alkene (before and after isomerisation). For example, in case of the TBS-protected-alcohol β-substituted diallyl urea, olefin isomerisation increased acidity of the δ-C–H now adjacent to the alkene. δ-Deprotonation led to the elimination of the –OTBS functional group (**513** or **517** in Scheme 124), generating a diene that can now act as anion-stabilising trap for the ureido anion formed upon the successful, regioselective N→C vinyl migration (**515** in Scheme 124). Going forward, by having the TBS-protected alcohol, for example, one carbon further away from the alkene in the starting urea (**571**) a successful N→C vinyl migration, forming urea **572**, is expected to be achievable (Scheme 124). This design process – keeping in mind the possible side-reactions – could be applied to other functional group-containing diallyl ureas to expand the substrate scope of this intramolecular S_NV reaction.

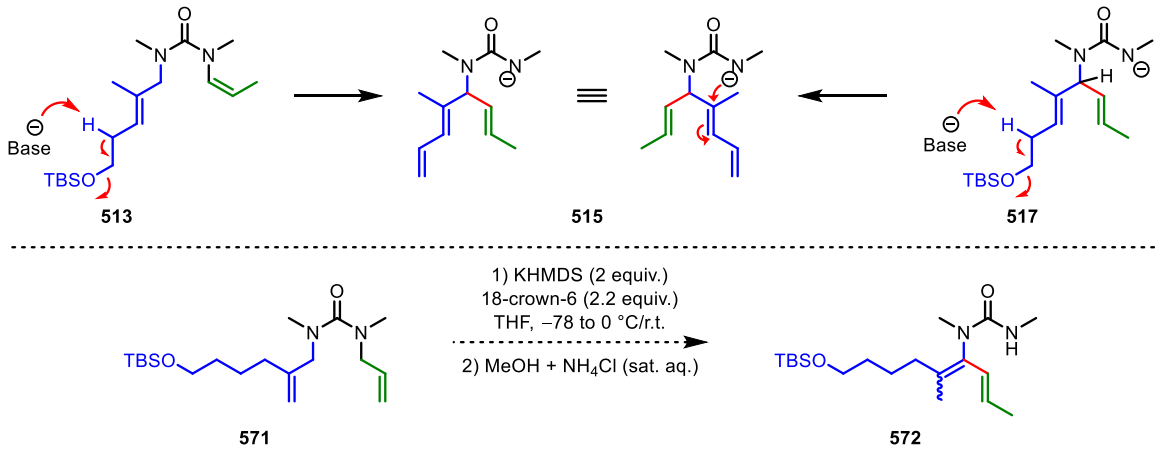

Scheme 124. Future work: regioselective N→C vinyl migration of unsymmetrical TBS-protected-alcohol β-substituted diallyl urea 571.

The unsuccessful rearrangement of symmetrical and unsymmetrical six-membered endocyclic *N*-allyl ureas suggested that the six-membered endocyclic *N*-allyl group, once isomerised, is not able to act as the nucleophile, thus limiting the possibility of the N→C vinyl migration followed by ring-expansion under these conditions. A reasonable explanation for this is that with the endocyclic *N*-vinyl group the required γ-deprotonation can no longer be directed by coordination of the potassium ion to the carbonyl due to conformational constraints imposed by the endocyclic structure. However, in the future, besides exploring reaction conditions using LDA (with DMPU), it would be interesting to see whether the ring-expanding N→C vinyl migration can take place when the endocyclic *N*-allyl group is pre-isomerised (**573**) and presumably can act as the electrophile (Scheme 125A). Moreover, using an exocyclic *N*-allyl group (**575**, **577** and **579**) instead might facilitate the N→C vinyl migration followed by ring-expansion,

generating medium-sized rings **576**, **578** and **580**, as now the allylmetal species can be stabilised by the carbonyl of the urea as observed with the successful diallyl rearrangements (Scheme 125B).

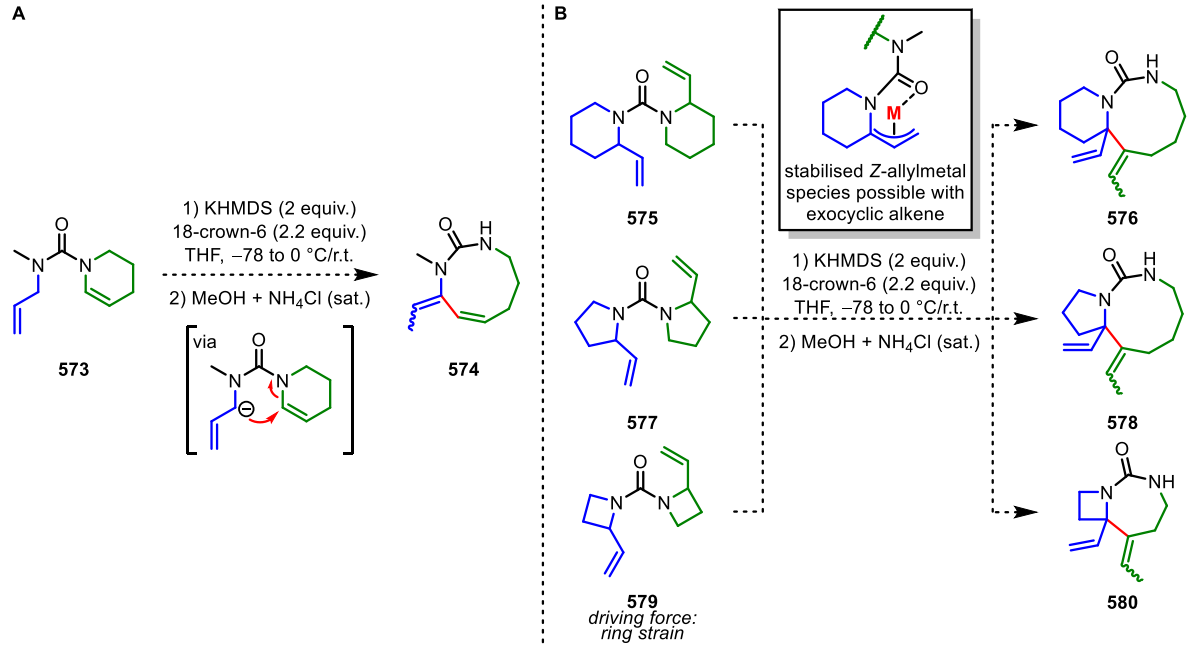

Scheme 125. Future work: N→C vinyl migration of unsymmetrical ureas 573 (A) and 575, 577 and 579 (B) may be possible due to pre-isomerisation (in A) and a stabilised *Z*-allylmetal species (in B), followed by ring-expansion, generating medium-rings 574 and 576, 578 and 580.

Finally, the synthetic applicability of the N→C vinyl migration product of the unsubstituted symmetrical *N*,*N*'-diallyl urea was demonstrated with Diels-Alder cycloaddition reactions and with its transformation to its *N*-methyl alkylamine equivalent by hydrogenation and urea hydrolysis. For future work, it would be interesting to see whether substitution of the *N*-methyl group with a *N*-alkyl group tethered to a dienophile (**581**) would enable the possibility of an intramolecular Diels-Alder reaction after the intramolecular S_NV reaction (Scheme 126). This would enable facile access to complex bicyclic compounds (**583**), with various sites present for further functionality.

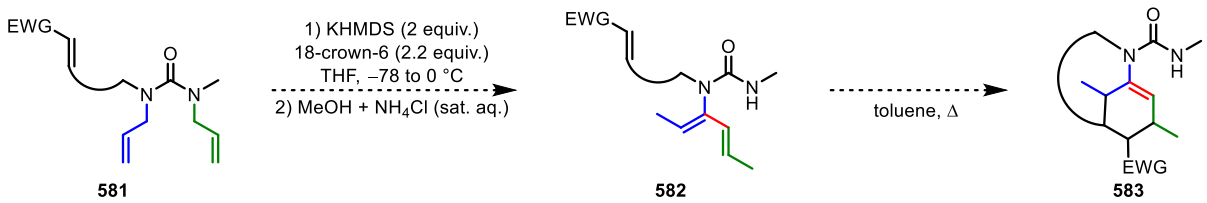

Scheme 126. Future work: N→C vinyl migration of unsymmetrical urea 581 followed by an intramolecular Diels-Alder reaction.

The hypothesised ‘infinite’ N→C vinyl migration (allylation of rearranged product → α-deprotonation of unsubstituted allyl group → regioselective migration of already in place vinyl group → repeat) was unfortunately prevented as, under the KHMDS/18-crown-6 conditions, the vinyl group – the original alkene framework of the migration product – had acted as the nucleophile instead of the electrophile, resulting in an undesired cyclisation after rearrangement. Future work should focus on investigating whether the ‘infinite’ N→C vinyl migration could be achieved by using LDA as during the mechanistic studies it was evident that γ-deprotonation of a *N*-(*Z*)-vinyl group with LDA is challenging yet α-deprotonation of an unsubstituted allyl group is feasible (Scheme 127).

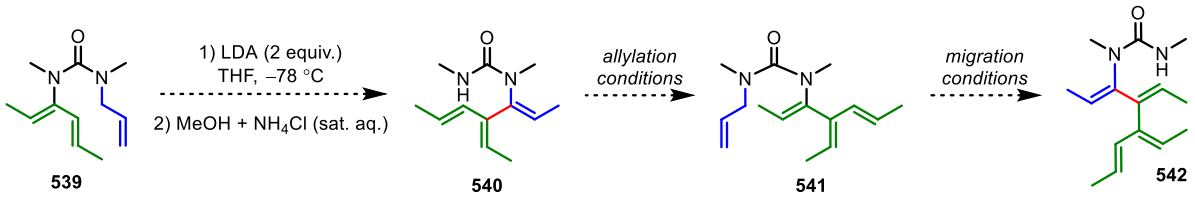

Scheme 127. Future work: ‘infinite’ N→C vinyl migration by using LDA and allylation of the migration products.

5.0 Supplementary Materials

5.1 General Information

All starting materials and reagents were obtained from commercial suppliers and used as received unless otherwise stated. All reactions were carried out under an atmosphere of anhydrous N_2, unless otherwise stated, and all glassware were oven- or flame-dried with a Bunsen burner. Anhydrous solvents were dried using an Anhydrous Engineering Grubbs-type system (alumina columns). Water is deionised and brine refers to a saturated aqueous solution of NaCl. DMPU and DIPA were distilled from CaH_2 and stored under nitrogen in a Young's tube.

Low temperature reactions performed over an extended period of time were carried out using a Thermo Scientific EK90 cryostat.

Reactions were tracked by TLC using aluminium-backed silica plates (0.25 mm, Merck, silica gel 60 F_{254}). Compounds were visualised by UV light and staining with an aqueous basic potassium permanganate ($KMnO_4$), followed by heating.

Normal phase flash column chromatography was carried out manually using silica gel (Aldrich, silica gel 60, 40-63 μm) or automatically using a Biotage Isolera flash purification system. Neutralised silica refers to silica gel (Aldrich, silica gel 60, 40-63 μm) that has been stirred in a mixture of triethylamine and pentane mixture (5:95) for 1 h, filtered, and dried to the air.

NMR spectra were recorded on a Bruker 400 MHz spectrometer, a Varian 500 MHz spectrometer, and a Bruker 500 MHz spectrometer with Cryo probe. Chemical shifts (δ) are reported in parts per million (ppm) and coupling constants (*J*) are reported in Hertz (Hz). Full characterisation was confirmed by 2D NMR experiments: COSY, HSQC and HMBC. Multiplicities are defined as follows: s singlet, d doublet, t triplet, q quartet, p pentet, m multiplet, b broad.

Melting points were recorded using a Stuart Scientific apparatus and are reported uncorrected in degrees Celsius (°C).

Infrared (IR) spectra were recorded on a Perkin-Elmer Spectrum Two FTIR spectrometer with an attenuated total reflectance (ATR) attachment; selected absorbances (ν_{max}) are reported in cm^{-1}.

High-resolution mass spectra (HRMS) were recorded on a Bruker microOTOF II instrument using electrospray ionisation (ESI), a Thermo Scientific Orbitrap Elite using atmospheric pressure chemical ionisation (APCI) and on a Synapt G2S using nanospray ionisation.

Compound names follow the IUPAC nomenclature and are generated by ChemDraw (PerkinElmer). The numbering used in these compound names do not represent the compound numbering (in red) used to assign the NMR spectra.

5.2 Synthesis of Symmetrical and Unsymmetrical Diallyl Ureas

The work presented in this chapter has been partially published in the first author publication:

B. C. Van Veen, S. M. Wales, J. Clayden, *J. Org. Chem.* **2021**, *86*, 8538–8543.[1]

5.2.1 General Procedures

General Procedure 2A (chloroformylation followed by amine-coupling):

An oven- or flame-dried round-bottom flask containing a magnetic stir bar was sealed with a suba seal and placed under anhydrous N_2. The flask was charged with triphosgene (0.6 equiv.) and anhydrous CH_2Cl_2 (16.7 mL/mmol), and then cooled down to 0 °C. Anhydrous pyridine (1 equiv. or 2 equiv. when the desired amine is in HCl salt form) was added and the reaction mixture was stirred for 5 min. The desired amine (1 equiv.) dissolved in anhydrous CH_2Cl_2 (10.0 mL/mmol) was then added. The reaction mixture was warmed to room temperature and stirred for between 15 min and 16 h. Then the reaction mixture was concentrated *in vacuo*, and the residue was re-dissolved in anhydrous MeCN (14.3 mL/mmol). The desired amine (1.3 equiv.) and triethylamine (2.5 equiv. or 3.5 equiv. when the desired amine is in HCl salt form) were then added. The reaction mixture was stirred for between 1 h and 4 d at room temperature, or a temperature otherwise stated. A saturated aqueous solution of $NaHCO_3$ (14 mL/mmol) and CH_2Cl_2 (14 mL/mmol) were added, and the organic phase was extracted. The aqueous phase was washed with CH_2Cl_2 (3×; 12 mL/mmol), and the organic phases were combined, dried over $MgSO_4$, filtered, and concentrated *in vacuo*. The crude product was then purified by normal-phase flash column chromatography.

General Procedure 2B (*E*-selective ruthenium-catalysed isomerisation):

An oven- or flame-dried round-bottom flask containing a magnetic stir bar was sealed with a suba seal and placed under anhydrous N_2. The flask was charged with the desired urea (1 equiv.), anhydrous THF (10.0 mL/mmol), and $[Ph_3P]_3Ru(CO)(Cl)H$ (10 mol%). The reaction mixture was stirred at reflux for between 16 and 22.5 h and then concentrated *in vacuo*. The crude product was purified by normal-phase flash column chromatography.

General Procedure 2C (direct urea *N*-allylation):

An oven- or flame-dried round-bottom flask containing a magnetic stir bar was sealed with a suba seal and placed under anhydrous N_2. The flask was charged with NaH (2.5 equiv. or 3.5 equiv.; 60% dispersion in mineral oil) and anhydrous THF (3.33 mL/mmol). 1,3-Dimethylurea (1 equiv.) in anhydrous THF (0.50 mL/mmol) was added. The reaction mixture was stirred for 1 h at room temperature and then cooled to 0 °C. The desired allyl bromide (2.5 equiv. or 3.5 equiv.) was added dropwise at 0 °C and the reaction mixture was stirred at room temperature for between 18 and 22 h. H_2O (5.00 mL/mmol) and Et_2O (2.00 mL/mmol) were added. The organic phase was extracted, and the aqueous phase was washed with Et_2O (3×; 2.00 mL/mmol). To retrieve all the mono-allylated product, the aqueous phase was washed twice with a mixture of $CHCl_3$:*i*-PrOH (3:1; 2.00 mL/mmol). The organic phases were combined, dried over $MgSO_4$, filtered, and concentrated *in vacuo*. The crude product was then purified by normal-phase flash column chromatography.

General Procedure 2D (Mitsunobu reaction followed by LiOH cleavage):[1]

Our reported procedure was followed.[1] An oven- or flame-dried round-bottom flask containing a magnetic stir bar was sealed with a suba seal and placed under anhydrous N_2. The flask was charged with *N*-Boc ethyl oxamate **264** (1.1 equiv.), triphenylphosphine (1.1 equiv.), the desired allyl alcohol (1 equiv.) and anhydrous THF (7.7 mL/mmol), and then cooled to 0 °C. DIAD (1.1 equiv.) was added dropwise at 0 °C. The reaction mixture was stirred at room temperature for between 4 h and 3.5 d, concentrated *in vacuo*, and redissolved in THF (3.2 mL/mmol) and H_2O (1.25 mL/mmol). LiOH (5 equiv.) was added, and the mixture was stirred at room temperature for between 1.5 and 23 h. After addition of H_2O (12 mL/mmol) and EtOAc (12 mL/mmol), the organic phase was extracted. The aqueous phase was washed with EtOAc (3×; 6 mL/mmol) and then the organic phases were combined, dried over $MgSO_4$, filtered, and concentrated *in vacuo*. The crude product was then purified by normal-phase flash column chromatography.

General Procedure 2E (*N*-methyl-*N*-allyl amine hydrochloride salt synthesis):[1]

Our reported procedure was followed.[1] An oven- or flame-dried round-bottom flask containing a magnetic stir bar was sealed with a suba seal and placed under anhydrous N_2. The flask was charged with the desired *N*-Boc allylcarbamate (1 equiv.) and anhydrous DMF or THF (1.7 mL/mmol), and was cooled to 0 °C. NaH (2 equiv.) was added slowly under a positive pressure of N_2 followed by the dropwise addition of iodomethane (4 equiv.) at 0 °C. The reaction mixture was stirred at room temperature for between 2 and 21.5 h and then quenched at 0 °C by the slow addition of a saturated aqueous solution of NH_4Cl (4 mL/mmol). Et_2O (12 mL/mmol) was added, and the aqueous phase was

washed with Et_2O (3×; 12 mL/mmol). The combined organic phases were concentrated *in vacuo* and the residue was redissolved in CH_2Cl_2 (5.3 mL/mmol). TFA (11.1 equiv.) was added, and the mixture was stirred at room temperature under air for between 1 h and 2.5 d. The reaction mixture was concentrated *in vacuo* and redissolved in MeOH (3 mL/mmol). While vigorously stirring, HCl (1.25 M in MeOH; 3.35 equiv.) was added rapidly and after 5 min. The reaction mixture was concentrated *in vacuo*, and then trituration with Et_2O gave the corresponding *N*-methyl-*N*-allyl amine hydrochloride salts.

5.2.2 Product Characterisation

1,3-Diallyl-1,3-dimethylurea (206)

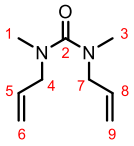

Reaction performed on 15.0 mmol scale following general procedure **2A** using *N*-allylmethylamine (1.44 mL, 15.0 mmol, 1.00 equiv.), triphosgene (2.67 g, 9.00 mmol, 0.600 equiv.) in anhydrous CH_2Cl_2 (250 mL), anhydrous pyridine (1.21 mL, 15.0 mmol, 1.00 equiv.), which was stirred for 16 h at 0 °C to room temperature. Reaction intermediate was redissolved in anhydrous MeCN (214 mL) and stirred with *N*-allylmethylamine (1.87 mL, 19.5 mmol, 1.30 equiv.) and triethylamine (5.23 mL, 37.5 mmol, 2.50 equiv.) for 2 h at room temperature. Flash column chromatography (5−15% acetone/petroleum ether) gave **206** as a pale-yellow liquid (2.34 g, 13.9 mmol, 93% yield). **IR** (film) ν_{max} 2916, 1637, 1485, 1381, 918, 778 cm^{-1}. **^{1}H NMR** (400 MHz, $CDCl_3$) δ 5.81 (ddt, *J* = 17.1, 10.2, 5.6 Hz, 2H, H^5 + H^8), 5.22 – 5.15 (m, 4H, H^6 + H^9), 3.72 (dt, *J* = 5.6, 1.6 Hz, 4H, H^4 + H^7), 2.74 (s, 6H, H^1 + H^3). **^{13}C NMR** (101 MHz, $CDCl_3$) δ 165.3 (C^2), 134.2 (C^5 + C^8), 117.0 (C^6 + C^9), 53.6 (C^4 + C^7), 36.2 (C^1 + C^3). **HRMS** (ESI-TOF) m/z: $[M + Na]^+$ Calcd for $C_9H_{16}N_2ONa$ 191.1155; Found 191.1150. Analytical data are in agreement with the literature.[190]

1,3-Dimethyl-1,3-di((*E*)-prop-1-en-1-yl)urea (207)

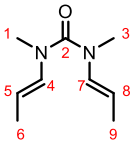

Reaction performed on 15.2 mmol scale following general procedure **2B** using **206** (2.56 g, 15.2 mmol, 1.00 equiv.) and $[Ph_3P]_3Ru(CO)(Cl)H$ (1.45 g, 1.52 mmol, 10 mol%) in anhydrous THF (152 mL), which was stirred for 16 h at reflux. Flash column chromatography (2−20% EtOAc/petroleum ether) gave **207** as a pale-yellow oil (1.79 g, 10.6 mmol, 70% yield). **IR** (film) ν_{max} 2922, 1651, 1366, 1116, 772 cm^{-1}. **^{1}H NMR** (400 MHz, $CDCl_3$) δ 6.48 (dq, *J* = 14.1, 1.6 Hz, 2H, H^4 + H^7), 4.80 (dq, *J* = 14.1, 6.6 Hz, 2H, H^5 + H^8), 2.97 (s, 6H, H^1 + H^3), 1.68 (dd, *J* = 6.6, 1.6 Hz, 6H, H^6 + H^9). **^{13}C NMR** (101 MHz, $CDCl_3$) δ 159.5 (C^2), 131.7 (C^4 + C^7), 103.0 (C^5 + C^8), 33.9 (C^1 + C^3), 15.4 (C^6 + C^9). **HRMS** (ESI-TOF) m/z: $[M + H]^+$ Calcd for $C_9H_{17}N_2O$ 169.1335; Found 169.1333.

1-Allyl-3-benzyl-1,3-dimethylurea (214)

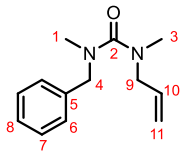

Reaction performed on 5.0 mmol scale following general procedure **2A** using *N*-benzylmethylamine (0.65 mL, 5.0 mmol, 1.0 equiv.) in anhydrous CH_2Cl_2 (50 mL), triphosgene (890 mg, 3.00 mmol, 0.600 equiv.) in anhydrous CH_2Cl_2 (50 mL), and pyridine (0.40 mL, 5.0 mmol, 1.0 equiv.), which was stirred for 1 h at 0 °C to room temperature. Reaction intermediate was redissolved in anhydrous MeCN (71 mL), and stirred with *N*-allylmethylamine (0.62 mL, 6.5 mmol, 1.3 equiv.) and triethylamine (1.74 mL, 12.5 mmol, 2.50 equiv.) for 3 h at room temperature. Flash column chromatography (7–60% EtOAc/petroleum ether) gave **214** as a pale-yellow liquid (1.06 g, 4.86 mmol, 97% yield). **IR** (film) ν_{max} 3503, 2910, 1635m 1382, 773, 698 cm^{-1}. **^{1}H NMR** (400 MHz, $CDCl_3$) δ 7.36 – 7.30 (m, 2H, H, H^7), 7.28 – 7.23 (m, 3H, H^6 + H^8), 5.82 (ddt, *J* = 17.2, 10.3, 5.7 Hz, 1H, H^{10}), 5.23 – 5.16 (m, 2H, H^{11}), 4.38 (s, 2H, H^4), 3.77 (dt, *J* = 5.7, 1.6 Hz, 2H, H^9), 2.79 (s, 3H, H^3), 2.74 (s, 3H, H^1). **^{13}C NMR** (101 MHz, $CDCl_3$) δ 165.5 (C^2), 138.1 (C^5), 134.2 (C^{10}), 128.7 (C^7), 127.7 (C^6), 127.2 (C^8), 117.2 (C^{11}), 54.4 (C^4), 53.7 (C^9), 36.7 (C^1), 36.2 (C^3). **HRMS** (ESI-TOF) m/z: $[M + H]^+$ Calcd for $C_{13}H_{19}N_2O$ 219.1492; Found 219.1495.

(*E*)-1-Benzyl-1,3-dimethyl-3-(prop-1-en-1-yl)urea (215)

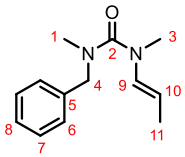

Reaction performed on 1.00 mmol scale following general procedure **2B** using **214** (218 mg, 1.00 mmol, 1.00 equiv.) and $[Ph_3P]_3Ru(CO)(Cl)H$ (95 mg, 0.10 mmol, 10 mol%) in anhydrous THF (10 mL), which was stirred for 22.5 h at reflux. Flash column chromatography (5−40% EtOAc/petroleum ether) gave **215** as a brown oil (202 mg, 0.925 mmol, 93% yield). **IR** (film) ν_{max} 2920, 1642, 1373, 1111, 772 cm^{-1}. **^{1}H NMR** (400 MHz, $CDCl_3$) δ 7.37 – 7.32 (m, 2H, H^7), 7.30 – 7.24 (m, 3H, H, H^6 + H^8), 6.52 (dq, *J* = 14.0, 1.5 Hz, 1H, H^9), 4.78 (dq, *J* = 14.0, 6.6 Hz, 1H, H^{10}), 4.41 (s, 2H, H^4), 3.00 (s, 3H, H^3), 2.75 (s, 3H, H^1), 1.65 (dd, *J* = 6.6, 1.5 Hz, 3H, H^{11}). **^{13}C NMR** (101 MHz, $CDCl_3$) δ 162.5 (C^2), 137.7 (C^5), 132.1 (C^9), 128.7 (C^7), 127.9 (C^6), 127.4 (C^8), 102.3 (C^{10}), 54.5 (C^4), 36.8 (C^1), 33.8 (C^3), 15.4 (C^{11}). **HRMS** (ESI-TOF) m/z: $[M + H]^+$ Calcd for $C_{13}H_{19}N_2O$ 219.1492; Found 219.1498.

Bis(3,6-dihydropyridin-1(2*H*)-yl)methanone (216)

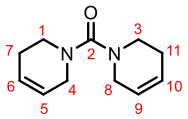

Reaction performed on 2.00 mmol scale following general procedure **2A** using 1,2,3,6-tetrahydropyridine hydrochloride (240 mg, 2.00 mmol, 1.00 equiv.) in anhydrous CH_2Cl_2 (20 mL), triphosgene (356 mg, 1.20 mmol, 0.600 equiv.) in anhydrous CH_2Cl_2 (20 mL), and pyridine (0.16 mL, 2.0 mmol, 1.0 equiv.), which was stirred for 2 h at 0 °C to room temperature. Reaction intermediate was redissolved in anhydrous MeCN (29 mL), and stirred with 1,2,3,6-tetrahydropyridine hydrochloride (311 mg, 2.60 mmol, 1.30 equiv.) and triethylamine (0.98 mL, 7.0 mmol, 3.5 equiv.) for 2 h at room temperature. Flash column chromatography (10–80% acetone/petroleum ether) gave **216** as a yellow oil (221 mg, 1.15 mmol, 57% yield). **IR** (film) ν_{max} 3032, 2912, 2836, 1633, 1416, 772, 652 cm^{-1}. **^{1}H NMR** (400 MHz, $CDCl_3$) δ 5.82 (dtt, *J* = 10.1, 3.9, 2.2 Hz, 2H, H^6 + H^{10}), 5.66 (dtt, *J* = 10.1, 3.2, 1.9 Hz, 2H, H^5 + H^9), 3.74 (p, *J* = 2.8 Hz, 4H, H^4 + H^8), 3.32 (t, *J* = 5.7 Hz, 4H, H^1 + H^3), 2.23 – 2.15 (m, 4H, H^7 + H^{11}). **^{13}C NMR** (101 MHz, $CDCl_3$) δ 164.3 (C^2), 125.7 (C^6 + C^{10}), 125.1 (C^5 + C^9), 46.4 (C^4 + C^8), 43.9 (C^1 + C^3), 25.4 (C^7 + C^{11}). **HRMS** (ESI-TOF) m/z: $[M + H]^+$ Calcd for $C_{11}H_{17}N_2O$ 193.1335; Found 193.1336.

Bis(3,4-dihydropyridin-1(2*H*)-yl)methanone (217)

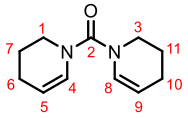

Reaction performed on 0.577 mmol scale following general procedure **2B** using **216** (111 mg, 0.577 mmol, 1.00 equiv.) and $[Ph_3P]_3Ru(CO)(Cl)H$ (55 mg, 0.058 mmol, 10 mol%) in anhydrous THF (5.8 mL), which was stirred for 16 h at reflux. Flash column chromatography (7−60% acetone/petroleum ether) gave **217** as a brownish oil (101 mg, 0.525 mmol, 91% yield). **IR** (film) ν_{max} 2927, 1637, 1388, 1224, 994, 772 cm^{-1}. **^{1}H NMR** (400 MHz, $CDCl_3$) δ 6.41 (dt, *J* = 8.3, 2.0 Hz, 2H, H^4 + H^8), 4.82 (dt, *J* = 8.3, 3.7 Hz, 2H, H^5 + H^9), 3.52 – 3.46 (m, 4H, H^1 + H^3), 2.06 (tdd, *J* = 6.2, 3.7, 2.0 Hz, 4H, H^6 + H^{10}), 1.89 – 1.82 (m, 4H, H^7 + H^{11}). **^{13}C NMR** (101 MHz, $CDCl_3$) δ 157.5 (C^2), 128.5 (C^4 + C^8), 105.0 (C^5 + C^9), 44.1 (C^1 + C^3), 22.5 (C^7 + C^{11}), 21.9 (C^6 + C^{10}). **HRMS** (ESI-TOF) m/z: $[M + H]^+$ Calcd for $C_{11}H_{17}N_2O$ 193.1335; Found 193.1336.

***N*-Benzyl-*N*-methyl-3,6-dihydropyridine-1(2*H*)-carboxamide (218)**

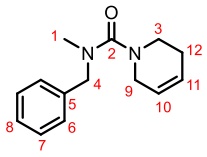

Reaction performed on 2.08 mmol scale following general procedure **2A** using 1,2,3,6-tetrahydropyridine hydrochloride (249 mg, 2.08 mmol, 1.00 equiv.), triphosgene (367 mg, 1.24 mmol, 0.596 equiv.) in anhydrous CH_2Cl_2 (42 mL), and pyridine (0.34 mL, 4.2 mmol, 2.0 equiv.), which was stirred at room temperature for 2 h. Reaction intermediate was redissolved in anhydrous MeCN (30 mL), and stirred with *N*-benzylmethylamine (0.35 mL, 2.7 mmol, 1.3 equiv.) and triethylamine (0.73 mL, 5.2 mmol, 2.5 equiv.) for 3 h at room temperature. Flash column chromatography (5–40% acetone/petroleum ether) gave **218** as a yellow oil (408 mg, 1.77 mmol, 85% yield). **IR** (film) ν_{max} 3031, 2915, 2837, 1634, 1398, 1074, 699 cm^{-1}. **^{1}H NMR** (400 MHz, $CDCl_3$) δ 7.36 – 7.30 (m, 2H, H^7), 7.29 – 7.23 (m, 3H, H^6 + H^8), 5.86 – 5.80 (m, 1H, H^{10}), 5.71 – 5.65 (m, 1H, H^{11}), 4.39 (s, 2H, H^4), 3.78 (p, *J* = 2.8 Hz, 2H, H^9), 3.36 (t, *J* = 5.6 Hz, 2H, H^3), 2.75 (s, 3H, H^1), 2.23 – 2.17 (m, 2H, H^{12}). **^{13}C NMR** (101 MHz, $CDCl_3$) δ 165.0 (C^2), 138.0 (C^5), 128.7 (C^7), 127.8 (C^6), 127.3 (C^8), 125.7 (C^{10}), 125.1 (C^{11}), 54.2 (C^4), 46.5 (C^9), 44.1 (C^3), 36.5 (C^1), 25.4 (C^{12}). **HRMS** (ESI-TOF) m/z: $[M + Na]^+$ Calcd for $C_{14}H_{18}N_2ONa$ 253.1311; Found 253.1310.

***N*-Benzyl-*N*-methyl-3,4-dihydropyridine-1(2*H*)-carboxamide (219)**

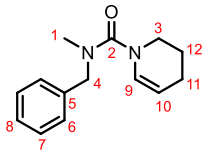

Reaction performed on 0.439 mmol scale following general procedure **2B** using **218** (101 mg, 0.439 mmol, 1.00 equiv.) and $[Ph_3P]_3Ru(CO)(Cl)H$ (42 mg, 0.044 mmol, 10 mol%) in anhydrous THF (4.4 mL), which was stirred for 17 h at reflux. Flash column chromatography (2−20% acetone/petroleum ether) gave **219** as a yellow oil (71 mg, 0.31 mmol, 70% yield; contains minor catalyst impurities). **^{1}H NMR** (400 MHz, $CDCl_3$) δ 7.36 – 7.30 (m, 2H, H^7), 7.29 – 7.23 (m, 3H, H^6 + H^8), 6.40 (dt, *J* = 8.3, 2.0 Hz, 1H, H^9), 4.78 (dt, *J* = 8.3, 3.7 Hz, 1H, H^{10}), 4.42 (s, 2H, H^4), 3.54 – 3.47 (m, 2H, H^3), 2.76 (s, 3H, H^1), 2.06 (tdd, *J* = 6.1, 3.7, 2.0 Hz, 2H, H^{11}), 1.86 (p, *J* = 6.1 Hz, 2H, H^{12}). **^{13}C NMR** (101 MHz, $CDCl_3$) δ 161.5 (C^2), 137.8 (C^5), 128.7 (C^7), 128.4 (C^9), 127.8 (C^6), 127.4 (C^8), 104.6 (C^{10}), 54.4 (C^4), 44.0 (C^3), 36.9 (C^1), 22.6 (C^{12}), 22.0 (C^{11}). Upon additional column purification the compound had decomposed, thus no full characterisation was obtained.

***N*-Allyl-*N*-methyl-3,6-dihydropyridine-1(2*H*)-carboxamide (220)**

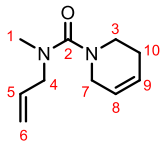

Reaction performed on 2.07 mmol scale following general procedure **2A** using 1,2,3,6-tetrahydropyridine hydrochloride (247 mg, 2.07 mmol, 1.00 equiv.), triphosgene (369 mg, 1.24 mmol, 0.599 equiv.) in anhydrous CH_2Cl_2 (42 mL), anhydrous pyridine (0.34 mL, 4.2 mmol, 2.0 equiv.), which was stirred for 6 h at 0 °C to room temperature. Reaction intermediate was redissolved in anhydrous MeCN (30 mL) and stirred with *N*-allylmethylamine (0.26 mL, 2.7 mmol, 1.3 equiv.) and triethylamine (0.73 mL, 5.2 mmol, 2.5 equiv.) for 3 h at room temperature. Flash column chromatography (5−40% acetone/petroleum ether) gave **220** as a yellow oil (304 mg, 1.69 mmol, 81% yield). **IR** (film) ν_{max} 2918, 2840, 1634, 1397, 1236, 922, 772, 653 cm^{-1}. **^{1}H NMR** (400 MHz, $CDCl_3$) δ 5.88 – 5.77 (m, 2H, H^5 + H^9), 5.69 – 5.63 (m, 1H, H^8), 5.23 – 5.15 (m, 2H, H^6), 3.77 – 3.69 (m, 4H, H^4 + H^7), 3.32 (t, *J* = 5.6 Hz, 2H, H^3), 2.76 (s, 3H, H^1), 2.22 – 2.13 (m, 2H, H^{10}). **^{13}C NMR** (101 MHz, $CDCl_3$) δ 164.8 (C^2), 134.3 (C^5), 125.7 (C^9), 125.1 (C^8), 117.1 (C^6), 53.5 (C^4), 46.5 (C^7), 44.0 (C^3), 35.9 (C^1), 25.4 (C^{10}). **HRMS** (ESI-TOF) m/z: $[M + Na]^+$ Calcd for $C_{10}H_{16}N_2ONa$ 203.1155; Found 203.1162.

(*E*)-*N*-methyl-*N*-(prop-1-en-1-yl)-3,4-dihydropyridine-1(2*H*)-carboxamide (221)

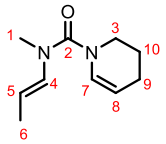

Reaction performed on 0.594 mmol scale following general procedure **2B** using **220** (107 mg, 0.594 mmol, 1.00 equiv.) and $[Ph_3P]_3Ru(CO)(Cl)H$ (57 mg, 0.060 mmol, 10 mol%) in anhydrous THF (5.9 mL), which was stirred for 18 h at reflux. Flash column chromatography (0−10% acetone/petroleum ether) gave **221** as a pale-yellow oil (83 mg, 0.46 mmol, 78% yield; contains minor catalyst impurities). **^{1}H NMR** (400 MHz, $CDCl_3$) δ 6.52 (dq, *J* = 14.1, 1.5 Hz, 1H, H^4), 6.36 (dt, *J* = 8.2, 2.0 Hz, 1H, H^7), 4.86 – 4.73 (m, 2H, H^5 + H^8), 3.50 – 3.45 (m, 2H, H^3), 2.98 (s, 3H, H^1), 2.07 (tdd, *J* = 6.2, 3.7, 2.0 Hz, 2H, H^9), 1.90 – 1.82 (p, *J* = 6.2 Hz, 2H, H^{10}), 1.68 (dd, *J* = 6.6, 1.5 Hz, 3H, H^6). **^{13}C NMR** (101 MHz, $CDCl_3$) δ 158.5 (C^2), 131.8 (C^4), 128.4 (C^7), 105.3 (C^8), 102.7 (C^5), 44.3 (C^3), 33.8 (C^1), 22.4 (C^{10}), 21.9 (C^9), 15.4 (C^6). Upon additional column purification the compound had decomposed, thus no full characterisation was obtained.

1,1,3-Triallyl-3-methylurea (222)

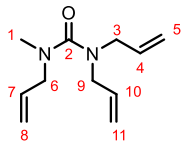

Reaction performed on 2.0 mmol scale following general procedure **2A** using diallylamine (0.25 mL, 2.0 mmol, 1.0 equiv.), triphosgene (356 mg, 1.20 mmol, 0.600 equiv.) in anhydrous CH_2Cl_2 (40 mL), and pyridine (0.16 mL, 2.0 mmol, 1.0 equiv.), which was stirred for 15 min at room temperature. Reaction intermediate was redissolved in anhydrous MeCN (28.6 mL), and stirred with *N*-methylallylamine (0.25 mL, 2.6 mmol, 1.3 equiv.) and triethylamine (0.70 mL, 5.0 mmol, 2.5 equiv.) for 1 h at room temperature. Flash column chromatography (5−40% acetone/pentane) gave **222** as a pale-yellow liquid (quantitative). **IR** (film) ν_{max} 3080, 2923, 1637, 1391, 1230, 918, 774 cm^{-1}. **^{1}H NMR** (400 MHz, $CDCl_3$) δ 5.87 – 5.75 (m, 3H, H^4 + H^7 + H^{10}), 5.22 – 5.13 (m, 6H, H^5 + H^8 + H^{11}), 3.76 – 3.70 (m, 6H, H^3 + H^6 + H^9), 2.76 (s, 3H, H^1). **^{13}C NMR** (101 MHz, $CDCl_3$) δ 164.9 (C^2), 134.3 (C^4 + C^{10}), 134.2 (C^7), 117.2 (C^5 + C^{11}), 117.0 (C^8), 53.6 (C^6), 50.4 (C^3 + C^9), 36.2 (C^1). **HRMS** (ESI-TOF) m/z: $[M + Na]^+$ Calcd for $C_{11}H_{18}N_2ONa$ 217.1311; Found 217.1315.

1-Allyl-1,3-dimethylurea (224)

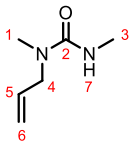

Reaction performed on 10 mmol scale following general procedure **2A** using *N*-allylmethylamine (0.96 mL, 10 mmol, 1.0 equiv.), triphosgene (1.78 g, 6.00 mmol, 0.600 equiv.) in anhydrous CH_2Cl_2 (200 mL), and anhydrous pyridine (0.81 mL, 10 mmol, 1.0 equiv.), which was stirred for 30 min at 0 °C to room temperature. Reaction intermediate was redissolved in anhydrous MeCN (143 mL) and stirred with *N*-methylamine (33 wt% in EtOH; 1.62 mL, 13.0 mmol, 1.30 equiv.) and triethylamine (3.48 mL, 25.0 mmol, 2.50 equiv.), which was stirred for 3.5 h at room temperature. Flash column chromatography (10−80% acetone/pentane) gave **224** as a pale-yellow oil (1.18 g, 9.21 mmol, 92% yield). **IR** (film) ν_{max} 3344, 2923, 1626, 1537, 772 cm^{-1}. **^{1}H NMR** (400 MHz, $CDCl_3$) δ 5.78 (ddt, *J* = 17.5, 9.8, 5.3 Hz, 1H, H^5), 5.19 – 5.11 (m, 2H, H^6), 4.35 (bs, 1H, H^7), 3.86 (dt, *J* = 5.3, 1.7 Hz, 2H, H^4), 2.86 (s, 3H, H^1), 2.80 (d, *J* = 4.7 Hz, 3H, H^3). **^{13}C NMR** (101 MHz, $CDCl_3$) δ 159.1 (C^2), 134.0 (C^5), 116.5 (C^6), 51.4 (C^4), 34.3 (C^1), 27.8 (C^3). **HRMS** (ESI-TOF) m/z: $[M + H]^+$ Calcd for $C_6H_{13}N_2O$ 129.1022; Found 129.1019. ^{1}H NMR spectrum is in agreement with the literature.[191]

(*E*)-1-(3,7-dimethylocta-2,6-dien-1-yl)-1,3-dimethylurea (225)

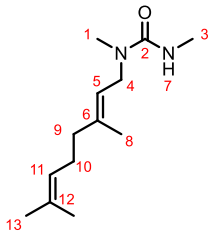

Reaction performed on 2.01 mmol scale following general procedure **2C** using NaH (200 mg, 5.00 mmol, 2.49 equiv.) in anhydrous THF (16.7 mL), 1,3-dimethylurea (177 mg, 2.01 mmol, 1.00 equiv.) in anhydrous THF (1 mL) and geranyl bromide (0.99 mL, 5.0 mmol, 2.5 equiv.), which was stirred for 18 h at 0 °C to room temperature. Flash column chromatography (0−40% acetone/petroleum ether) gave **225** as a dark brown/orange oil (214 mg, 0.954 mmol, 47% yield). **IR** (film) ν_{max} 3333, 2917, 1626, 1538, 1376, 1272, 1238, 750 cm^{-1}. **^{1}H NMR** (400 MHz, $CDCl_3$) δ 5.03 (t, *J* = 6.6 Hz, 1H, H^5), 4.95 (tt, *J* = 6.8, 1.5 Hz, 1H, H^{11}), 4.85 – 4.61 (m, 1H, H^7), 3.76 (d, *J* = 6.6 Hz, 2H, H^4), 2.72 (s, 3H, H^1), 2.68 (s, 3H, H^3), 2.06 – 1.82 (m, 4H, H^9 + H^{10}), 1.56 (s, 6H, H^{13}), 1.49 (s, 3H, H^8). **^{13}C NMR** (101 MHz, $CDCl_3$) δ 159.1 (C^2), 138.8 (C^6), 131.5 (C^{12}), 123.7 (C^{11}), 120.4 (C^5), 46.0 (C^4), 39.4 (C^9), 33.6 (C^1), 27.5 (C^3), 26.2 (C^{10}), 25.5 (C^{13}), 17.5 (C^8), 15.9 (C^{13}). **HRMS** (ESI-TOF) m/z: $[M + Na]^+$ Calcd for $C_{13}H_{24}N_2ONa$ 247.1781; Found 247.1777.

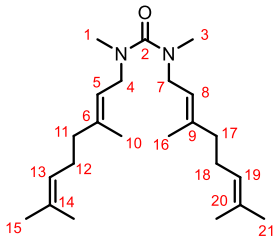

In addition, 1,3-bis((*E*)-3,7-dimethylocta-2,6-dien-1-yl)-1,3-dimethylurea **226** was afforded as a dark brown/orange oil (287 mg, 0.796 mmol, 40% yield). **^{1}H NMR** (400 MHz, $CDCl_3$) δ 5.27 – 5.17 (m, 2H, H^5 + H^8), 5.11 – 5.03 (m, 2H, H^{13} + H^{19}), 3.74 (d, *J* = 6.0 Hz, 4H, H^4 + H^7), 2.74 – 2.71 (m, 6H, H^1 + H^3), 2.13 – 1.96 (m, 8H, H^{11} + H^{12} + H^{17} + H^{18}), 1.66 (d, *J* = 7.2 Hz, 6H, H^{15} + H^{21}), 1.65 (s, 6H, H^{15} + H^{21}), 1.60 (s, 6H, H^{10} + H^{16}). Upon additional column purification the compound had decomposed, thus no full characterisation was obtained.

1-(But-2-en-1-yl)-1,3-dimethylurea (227)

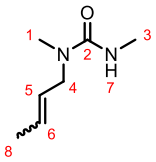

Reaction performed on 10.0 mmol scale following general procedure **2C** using NaH (1.40 g, 35.0 mmol, 3.50 equiv.) in anhydrous THF (117 mL), 1,3-dimethylurea (881 mg, 10.0 mmol, 1.00 equiv.) in anhydrous THF (5 mL) and crotyl bromide (3.60 mL, 35.0 mmol, 3.50 equiv.), which was stirred for 22 h at 0 °C to room temperature. Flash column chromatography (20−80% acetone/petroleum ether) gave **227** as a yellow oil (817 mg, 5.75 mmol, 57% yield). **IR** (film) ν_{max} 3344, 2918, 1627, 1536, 1238, 967, 564 cm^{-1}. **^{1}H NMR** (400 MHz, $CDCl_3$) (suspected mixture of *E*:*Z* in a 0.7:0.3 ratio) δ 5.68 – 5.52 (m, 1H, H^6), 5.44 – 5.33 (m, 1H, H^5), 4.40 (bs, 1H, H^7), 3.91 – 3.88 (m, 0.6H, *Z*-H^4), 3.78 – 3.74 (m, 1.4H, *E*-H^4), 2.82 (s, 0.9H, *Z*-H^1), 2.82 (s, 2.1H, *E*-H^1), 2.78 (s, 0.9H, *Z*-H^3), 2.77 (s, 2.1H, *E*-H^3), 1.69 – 1.65 (m, 3H, H^8). **^{13}C NMR** (101 MHz, $CDCl_3$) δ 159.1 (C^2), 127.9 (*E*-C^6), 127.4 (*Z*-C^6), 126.7 (*E*-C^5), 126.5 (*Z*-C^5), 50.7 (*E*-C^4), 45.2 (*Z*-C^4), 34.1 (*E*-C^1), 34.0 (*Z*-C^1), 27.8 (*Z*-C^3), 27.7 (*E*-C^3), 17.7 (*E*-C^8), 12.9 (*Z*-C^8). **HRMS** (ESI-TOF) m/z: $[M + Na]^+$ Calcd for $C_7H_{14}N_2ONa$ 165.0998; Found 165.1004.

In addition, 1,3-di((*E*)-but-2-en-1-yl)-1,3-dimethylurea **228** was afforded as a pale-yellow liquid (385 mg, 1.96 mmol, 20% yield).

1,3-Dimethyl-1-(2-methylallyl)urea (229)

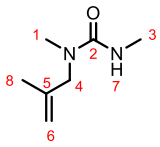

Reaction performed on 10.0 mmol scale following general procedure **2C** using NaH (1.40 g, 35.0 mmol, 3.50 equiv.) in anhydrous THF (117 mL), 1,3-dimethylurea (881 mg, 10.0 mmol, 1.00 equiv.) in anhydrous THF (5 mL) and 3-bromo-2-methylpropene (3.53 mL, 35.0 mmol, 3.50 equiv.), which was stirred for 22 h at 0 °C to room temperature. Flash column chromatography (20% acetone/petroleum ether) gave **229** as a yellow oil (846 mg, 5.95 mmol, 59% yield). **IR** (film) ν_{max} 3344, 2916, 1628, 1536, 1374, 1239, 892, 575 cm^{-1}. **^{1}H NMR** (400 MHz, $CDCl_3$) δ 4.88 – 4.85 (m, 1H, H^6), 4.81 – 4.78 (m, 1H, H^6), 4.41 (bs, 1H, H^7), 3.76 (s, 2H, H^4), 2.85 (s, 3H, H^1), 2.78 (s, 3H, H^3), 1.68 (s, 3H, H^8). **^{13}C NMR** (101 MHz, $CDCl_3$) δ 159.3 (C^2), 141.7 (C^5), 111.5 (C^6), 54.8 (C^4), 34.6 (C^1), 27.8 (C^3), 19.9 (C^8). **HRMS** (ESI-TOF) m/z: $[M + Na]^+$ Calcd for $C_7H_{14}N_2ONa$ 165.0998; Found 165.1004.

In addition, 1,3-dimethyl-1,3-bis(2-methylallyl)urea **230** was afforded as a pale-yellow liquid (182 mg, 0.927 mmol, 9% yield).

1,3-Dimethyl-1-(2-((trimethylsilyl)methyl)allyl)urea (233)

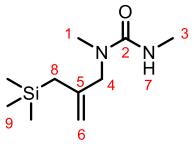

Reaction performed on 1.86 mmol scale following general procedure **2C** using NaH (184 mg, 4.61 mmol, 2.50 equiv.) in anhydrous THF (15.4 mL), 1,3-dimethylurea (164 mg, 1.86 mmol, 1.00 equiv.) in anhydrous THF (0.92 mL) and 2-(trimethylsilylmethyl)allyl chloride (0.83 mL, 4.6 mmol, 2.5 equiv.), which was stirred for 21 h at 0 °C to room temperature. Flash column chromatography (10−80% acetone/pentane) gave **233** as a pale-yellow oil (52 mg, 0.24 mmol, 13% yield). **IR** (film) ν_{max} 3344, 2953, 1632, 1538, 1246, 837 cm^{-1}. **^{1}H NMR** (400 MHz, $CDCl_3$) δ 4.66 – 4.61 (m, 2H, H^6), 4.46 (bs, 1H, H^7), 3.66 (s, 2H, H^4), 2.82 (s, 3H, H^1), 2.73 (d, *J* = 4.7 Hz, 3H, H^3), 1.41 (s, 2H, H^8), 0.00 (s, 9H, H^9). **^{13}C NMR** (101 MHz, $CDCl_3$) δ 159.3 (C^2), 142.9 (C^5), 107.8 (C^6), 55.2 (C^4), 34.7 (C^1), 27.7 (C^3), 23.6 (C^8), -1.3 (C^9). **HRMS** (ESI-TOF) m/z: $[M + Na]^+$ Calcd for $C_{10}H_{22}N_2OSiNa$ 237.1394; Found 237.1405.

1-(2-Bromoallyl)-1,3-dimethylurea (235)

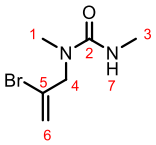

Reaction performed on 4.03 mmol scale following general procedure **2C** using NaH (1.99 g, 10.0 mmol, 2.48 equiv.) in anhydrous THF (33.3 mL), 1,3-dimethylurea (355 mg, 4.03 mmol, 1.00 equiv.) in anhydrous THF (2 mL) and 2,3-dibromopropene (0.98 mL, 10 mmol, 2.5 equiv.), which was stirred for 19.5 h at 0 °C to room temperature. Flash column chromatography (30–50% acetone/pentane) gave **235** as a yellow oil (16 mg, 0.077 mmol, 2% yield). **IR** (film) ν_{max} 3341, 2926, 1629, 1537, 1412, 1371, 1242, 1086, 771, 549 cm^{-1}. **^{1}H NMR** (400 MHz, $CDCl_3$) δ 5.72 (q, *J* = 1.7 Hz, 1H, H^6), 5.56 (dt, *J* = 2.2, 1.2 Hz, 1H, H^6), 4.55 (bs, 1H, H^7), 4.11 (t, *J* = 1.4 Hz, 2H, H^4), 2.89 (s, 3H, H^1), 2.80 (d, *J* = 4.6 Hz, 3H, H^3). **^{13}C NMR** (101 MHz, $CDCl_3$) δ 158.6 (C^2), 129.7 (C^5), 117.3 (C^6), 56.6 (C^4), 34.4 (C^1), 27.8 (C^3). **HRMS** (ESI-TOF) m/z: $[M + H]^+$ Calcd for $C_6H_{12}BrN_2O$ 207.0128; Found 207.0126.

1,3-Dicinnamyl-1,3-dimethylurea (249)

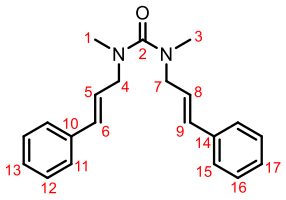

The starting reagent (*E*)-*N*-methyl-3-phenylprop-2-en-1-amine was synthesised as followed: an oven-dried flask containing a magnetic stir bar was sealed with a suba seal, placed under anhydrous N_2, and charged with *N*-methylamine (33 wt% in EtOH; 25.0 mL, 200 mmol, 20.0 equiv.). Cinnamyl chloride (1.39 mL, 9.98 mmol, 1.00 equiv.) was then added dropwise, and the reaction mixture was stirred at room temperature for 19 h. After concentrating *in vacuo*, $NaHCO_3$ (sat. aq. solution) and Et_2O were added, and the organic phase was extracted. The aqueous phase was washed with Et_2O (2×) and then the organic phases were combined, dried over $MgSO_4$, filtered, and concentrated *in vacuo*. Flash column chromatography (7−60% acetone/petroleum ether) gave (*E*)-*N*-methyl-3-phenylprop-2-en-1-amine as a yellow oil (963 mg, 6.54 mmol, 66% yield). **IR** (film) ν_{max} 3025, 2789, 1448, 966, 740, 691 cm^{-1}. **^{1}H NMR** (400 MHz, $CDCl_3$) δ 7.40 – 7.35 (m, 2H), 7.34 – 7.27 (m, 2H), 7.25 – 7.30 (m, 1H), 6.55 (dt, *J* = 15.9, 1.5 Hz, 1H), 6.30 (dt, *J* = 15.9, 6.4 Hz, 1H), 3.41 (dd, *J* = 6.4, 1.5 Hz, 2H), 2.49 (s, 3H), 2.40 (bs, 1H). **^{13}C NMR** (101 MHz, $CDCl_3$) δ 137.1, 132.3, 128.7, 127.6, 127.3, 126.5, 53.6, 35.6. **HRMS** (ESI-TOF) m/z: $[M + H]^+$ Calcd for $C_{10}H_{14}N$ 148.1121; Found 148.1125. Analytical data agrees with the literature.[192]

Reaction performed on 1.50 mmol scale following general procedure **2A** using (*E*)-*N*-methyl-3-phenylprop-2-en-1-amine (221 mg, 1.50 mmol, 1.00 equiv.) in anhydrous CH_2Cl_2 (15 mL), triphosgene (267 mg, 0.900 mmol, 0.600 equiv.) in anhydrous CH_2Cl_2 (15 mL), anhydrous pyridine (0.12 mL, 1.5 mmol, 1.0 equiv.), which was stirred for 1 h at 0 °C to room temperature. Reaction intermediate was redissolved in anhydrous MeCN (21.4 mL) and stirred with (*E*)-*N*-methyl-3-phenylprop-2-en-1-amine (287 mg, 1.95 mmol, 1.30 equiv.) and triethylamine (0.52 mL, 3.7 mmol, 2.5 equiv.) for 1 h at room temperature. Flash column chromatography (7−60% acetone/petroleum ether) gave **249** as a pale-yellow solid (427 mg, 1.33 mmol, 89% yield). **MP** 76−77 °C. **IR** (film) ν_{max} 3025, 2918, 1636, 1488, 1385, 1107, 966, 773, 735, 692 cm^{-1}. **^{1}H NMR** (400 MHz, $CDCl_3$) δ 7.41 – 7.37 (m, 4H, H^{11} + H^{15}), 7.35 – 7.29 (m, 4H, H^{12} + H^{16}), 7.27 – 7.22 (m, 2H, H^{13} + H^{17}), 6.54 (dt, *J* = 15.9, 1.6 Hz, 2H, H^6 + H^9), 6.24 (dt, *J* = 15.9, 6.1 Hz, 2H, H^5 + H^8), 3.94 (dd, *J* = 6.1, 1.6 Hz, 4H, H^4 + H^7), 2.85 (s, 6H, H^1 + H^3). **^{13}C NMR** (101 MHz, $CDCl_3$) δ 165.2 (C^2), 136.8 (C^{10} + C^{14}), 132.5 (C^6 + C^9), 128.7 (C^{12} + C^{16}), 127.7 (C^{13} + C^{17}), 126.5 (C^{11} + C^{15}), 125.8 (C^5 + C^8), 53.1 (C^4 + C^7), 36.4 (C^1 + C^3). **HRMS** (ESI-TOF) m/z: $[M + H]^+$ Calcd for $C_{21}H_{25}N_2O$ 321.1961; Found 321.1962.

(*E*)-1-Allyl-3-(3,7-dimethylocta-2,6-dien-1-yl)-1,3-dimethylurea (240)

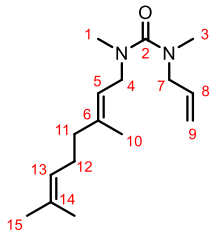

The starting reagent *N*-((*E*)-3,7-dimethyl-2,6-octadienyl)-*N*-methylamine was synthesised as followed: an oven-dried flask containing a magnetic stir bar was sealed with a suba seal and placed under anhydrous N_2. *N*-Methylamine (2 M in THF; 5.0 mL, 10 mmol, 5.0 equiv.) was added and then geranyl bromide (0.31 mL, 2.0 mmol, 1.0 equiv.) was added dropwise. The reaction mixture was stirred at room temperature overnight and then partitioned between CH_2Cl_2 and an aqueous solution of NaOH (1 M). After extracting the organic phase, the aqueous phase was washed with CH_2Cl_2 (2×). The combined organic phases were washed twice with an aqueous solution of HCl (1 M). The combined aqueous phase was basified with an aqueous solution of NaOH (1 M) to pH = 14 and washed with CH_2Cl_2 (2×). The organic phases were collected, dried over Na_2SO_4, filtered, and cautiously concentrated *in vacuo*, generating *N*-((*E*)-3,7-dimethyl-2,6-octadienyl)-*N*-methylamine that was used crude in the next step.

Reaction performed on 2.0 mmol scale following general procedure **2A** using *N*-((*E*)-3,7-dimethyl-2,6-octadienyl)-*N*-methylamine (2.0 mmol, 1.0 equiv.) in anhydrous CH_2Cl_2 (20 mL), triphosgene (356 mg, 1.20 mmol, 0.600 equiv.) in anhydrous CH_2Cl_2 (20 mL), anhydrous pyridine (0.16 mL, 2.0 mmol, 1.0 equiv.), which was stirred for 2 h at 0 °C to room temperature. Reaction intermediate was redissolved in anhydrous MeCN (28.6 mL) and stirred with *N*-allylmethylamine (0.25 mL, 2.6 mmol, 1.3 equiv.) and triethylamine (0.70 mL, 5.0 mmol, 2.5 equiv.) for 4 h at room temperature. Flash column chromatography (10−40% acetone/pentane) gave **240** as a yellow oil (293 mg, 1.11 mmol, 55% yield). **IR** (film) ν_{max} 2917, 1645, 1486, 1455, 1382, 774 cm^{-1}. **^{1}H NMR** (400 MHz, $CDCl_3$) δ 5.82 (ddt, *J* = 17.2, 10.3, 5.7 Hz, 1H, H^8), 5.23 – 5.14 (m, 3H, H^5 + H^9), 5.10 – 5.04 (m, 1H, H^{13}), 3.75 – 3.70 (m, 4H, H^4 + H^7), 2.74 (s, 3H, H^1/H^3), 2.71 (s, 3H, H^1/H^3), 2.14 – 1.97 (m, 4H, H^{11} + H^{12}), 1.67 (s, 3H, H^{15}), 1.64 (s, 3H, H^{10}), 1.59 (s, 3H, H^{15}). **^{13}C NMR** (101 MHz, $CDCl_3$) δ 165.4 (C^2), 139.2 (C^6), 134.5 (C^8), 131.7 (C^{14}), 124.1 (C^{13}), 120.8 (C^5), 117.0 (C^9), 53.7 (C^4/C^7), 48.5 (C^4/C^7), 39.8 (C^{11}), 36.2 (C^1/C^3), 35.8 (C^1/C^3), 26.6 (C^{12}), 25.8 (C^{15}), 17.8 (C^{15}), 16.3 (C^{10}). **HRMS** (ESI-TOF) m/z: $[M + H]^+$ Calcd for $C_{16}H_{29}N_2O$ 265.2274; Found 265.2282.

1-Allyl-3-(2-bromoallyl)-1,3-dimethylurea (250)

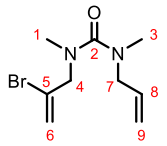

The starting reagent 2-bromo-*N*-methylprop-2-en-1-amine was synthesised as followed: an oven-dried flask containing a magnetic stir bar was sealed with a suba seal, placed under anhydrous N_2, and charged with *N*-methylamine (2 M in THF; 5.0 mL, 10 mmol, 5.0 equiv.). 2,3-Dibromopropene (0.20 mL, 2.0 mmol, 1.0 equiv.) was then added dropwise, and the reaction mixture was stirred at room temperature for 24 h. Then an aqueous solution of NaOH (1 M) and CH_2Cl_2 were added, and the organic phase was extracted. The aqueous phase was washed with CH_2Cl_2 (2×) and then the combined organic phase was washed twice with an aqueous solution of HCl (1 M). The combined aqueous phase was basified with an aqueous solution of NaOH (1 M) to pH = 14 and washed with CH_2Cl_2 (2x). The organic phases were collected, dried over Na_2SO_4, filtered, and cautiously concentrated *in vacuo*, generating 2-bromo-*N*-methylprop-2-en-1-amine that was used crude in the next step.

Reaction performed on 2.0 mmol scale following general procedure **2A** using 2-bromo-*N*-methylprop-2-en-1-amine (2.0 mmol, 1.0 equiv.) in anhydrous CH_2Cl_2 (20 mL), triphosgene (361 mg, 1.20 mmol, 0.600 equiv.) in anhydrous CH_2Cl_2 (20 mL), anhydrous pyridine (0.16 mL, 2.0 mmol, 1.0 equiv.), which was stirred for 2h20 at 0 °C to room temperature. Reaction intermediate was redissolved in anhydrous MeCN (28.6 mL) and stirred with *N*-allylmethylamine (0.25 mL, 2.6 mmol, 1.3 equiv.) and triethylamine (0.70 mL, 5.0 mmol, 2.5 equiv.) for 4 h at room temperature. Flash column chromatography (10% acetone/pentane) gave **250** as a yellow oil (308 mg, 1.25 mmol, 62% yield). **IR** (film) ν_{max} 2920, 1637, 1487, 1382, 1234, 1108, 922, 774 cm^{-1}. **^{1}H NMR** (400 MHz, $CDCl_3$) δ 5.88 – 5.78 (m, 2H, H^6 + H^8), 5.63 – 5.57 (m, 1H, H^6), 5.25 – 5.17 (m, 2H, H^9), 4.00 (s, 2H, H^4), 3.76 (dt, *J* = 5.7, 1.6 Hz, 2H, H^7), 2.81 (s, 3H, H^1), 2.78 (s, 3H, H^3). **^{13}C NMR** (101 MHz, $CDCl_3$) δ 164.7 (C^2), 134.0 (C^8), 130.3 (C^5), 118.0 (C^6), 117.3 (C^9), 58.6 (C^4), 53.5 (C^7), 36.9 (C^1), 36.1 (C^3). **HRMS** (ESI-TOF) m/z: $[M + H]^+$ Calcd for $C_9H_{16}BrN_2O$ 247.0441; Found 247.0449.

1,3-Dimethyl-1,3-bis(3-methylbut-2-en-1-yl)urea (251)

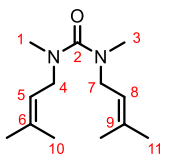

The starting reagent *N*-methyl-*N*-(3-methyl-2-buten-1-yl)amine was synthesised as followed: an oven-dried flask containing a magnetic stir bar was sealed with a suba seal, placed under anhydrous N_2, and

charged with *N*-methylamine (33 wt% in EtOH; 25.0 mL, 200 mmol, 20.0 equiv.). Prenyl bromide (1.16 mL, 10.0 mmol, 1.00 equiv.) was added dropwise, and the reaction mixture was stirred at room temperature for 16 h. Then $NaHCO_3$ (sat. aq. solution) and Et_2O were added, and the organic phase was extracted. The aqueous phase was washed with Et_2O (2×) and then to the combined organic phases HCl (2.0 M in Et_2O; 10 mL, 10 mmol, 1.0 equiv.) was added. To the extracted organic phase, NaOH (1 M solution) was added, after which the combined organic phases was cautiously concentrated *in vacuo*. Then, distillation gave *N*-methyl-*N*-(3-methyl-2-buten-1-yl)amine as a colourless liquid (211 mg, 2.13 mmol, 21% yield). **^{1}H NMR** (400 MHz, $CDCl_3$) δ 5.22 (t, *J* = 6.9 Hz, 1H), 3.15 (d, *J* = 6.9 Hz, 2H), 2.39 (s, 3H), 1.71 (s, 3H), 1.64 (s, 3H). **HRMS** (ESI-TOF) m/z: $[M + H]^+$ Calcd for $C_6H_{14}N$ 100.1121; Found 100.1117. The ^{1}H spectrum is in agreement with literature.[193]

Reaction performed on 0.90 mmol scale following general procedure **2A** using *N*-methyl-*N*-(3-methyl-2-buten-1-yl)amine (89 mg, 0.90 mmol, 1.0 equiv.) in anhydrous CH_2Cl_2 (9 mL), triphosgene (160 mg, 0.539 mmol, 0.599 equiv.) in anhydrous CH_2Cl_2 (9 mL), anhydrous pyridine (0.07 mL, 0.9 mmol, 1 equiv.), which was stirred for 1 h at 0 °C to room temperature. Reaction intermediate was redissolved in anhydrous MeCN (13 mL) and stirred with *N*-methyl-*N*-(3-methyl-2-buten-1-yl)amine (116 mg, 1.17 mmol, 1.30 equiv.) and triethylamine (0.31 mL, 2.2 mmol, 2.4 equiv.) for 2 h at room temperature. Flash column chromatography (10−80% acetone/petroleum ether) gave **251** as a yellow oil (90 mg, 0.40 mmol, 44% yield). **IR** (film) ν_{max} 2968, 2915, 1644, 1486, 1447, 1379, 1219, 1093, 772 cm^{-1}. **^{1}H NMR** (400 MHz, $CDCl_3$) δ 5.20 (tp, *J* = 6.8, 1.3 Hz, 2H, $H^5 + H^8$), 3.70 (d, *J* = 6.8 Hz, 4H, $H^4 + H^7$), 2.70 (s, 6H, $H^1 + H^3$), 1.73 (q, *J* = 1.3 Hz, 6H, $H^{10} + H^{11}$), 1.65 (s, 6H, $H^{10} + H^{11}$). **^{13}C NMR** (101 MHz, $CDCl_3$) δ 165.6 (C^2), 135.5 ($C^6 + C^9$), 121.0 ($C^5 + C^8$), 48.6 ($C^4 + C^7$), 35.9 ($C^1 + C^3$), 25.9 ($C^{10} + C^{11}$), 18.0 ($C^{10} + C^{11}$). **HRMS** (ESI-TOF) m/z: $[M + H]^+$ Calcd for $C_{13}H_{25}N_2O$ 225.1961; Found 225.1966.

1-Allyl-1,3-dimethyl-3-((*E*)-4,4,4-trifluorobut-2-en-1-yl)urea (246)

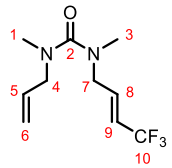

The starting reagent 4,4,4-trifluorocrotyl methylamine was synthesised as followed: an oven-dried flask containing a magnetic stir bar was sealed with a suba seal and placed under anhydrous N_2. 4,4,4-Trifluorocrotyl alcohol (129 mg, 1.02 mmol, 1.00 equiv.) and triethylamine (0.17 mL, 1.2 mmol, 1.2 equiv.) were added and dissolved in anhydrous CH_2Cl_2 (2.5 mL, 2.5 mL/mmol). The reaction mixture was cooled down to 0 °C and mesyl chloride (90 μL, 1.2 mmol, 1.2 equiv.) was then added dropwise. The reaction mixture was stirred at room temperature for 2 h. The reaction mixture was partitioned between CH_2Cl_2 and a saturated aqueous solution of Na_2CO_3. The organic phase was collected and

washed with brine, dried over $MgSO_4$, filtered, and concentrated *in vacuo*. The intermediate product was redissolved in anhydrous THF (0.36 mL, 0.36 mL/mmol) and methylamine (2 M in THF; 2.5 mL, 5.0 mmol, 4.9 equiv.) was added. The reaction mixture was stirred at room temperature for 24 h and then partitioned between CH_2Cl_2 and an aqueous solution of NaOH (1 M). After extracting the organic phase, the aqueous phase was washed with CH_2Cl_2 (2×). The combined organic phase was washed twice with an aqueous solution of HCl (1 M). The combined aqueous phase was basified with an aqueous solution of NaOH (1 M) to pH = 14 and washed with CH_2Cl_2 (2×). The organic phases were collected, dried over Na_2SO_4, filtered, and concentrated *in vacuo*, generating 4,4,4-trifluorocrotyl methylamine that was used crude in the next step.

Reaction performed on 1.02 mmol scale following general procedure **2A** using 4,4,4-trifluorocrotyl methylamine (1.02 mmol, 1.00 equiv.) in anhydrous CH_2Cl_2 (10 mL), triphosgene (185 mg, 0.623 mmol, 0.611 equiv.) in anhydrous CH_2Cl_2 (10 mL), and anhydrous pyridine (80 µL, 1.0 mmol, 1.0 equiv.), which was stirred for 1 h at 0 °C to room temperature. Reaction intermediate was redissolved in anhydrous MeCN (14.3 mL) and stirred with *N*-allylmethylamine (0.12 mL, 1.3 mmol, 1.3 equiv.) and triethylamine (0.35 mL, 2.5 mmol, 2.5 equiv.), which was stirred for 6 h at room temperature, followed by 3 days at 40 °C. Flash column chromatography (0−40% acetone/pentane) gave **246** as a yellow oil (31 mg, 0.13 mmol, 13% yield). **IR** (film) ν_{max} 2926, 1639, 1300, 1116, 924, 776 cm^{-1}. **^{1}H NMR** (400 MHz, $CDCl_3$) δ 6.45 – 6.32 (m, 1H, H^8), 5.87 – 5.70 (m, 2H, H^5 + H^9), 5.23 – 5.17 (m, 2H, H^6), 3.89 – 3.83 (m, 2H, H^7), 3.74 (dt, J = 5.6, 1.6 Hz, 2H, H^4), 2.78 (s, 3H, H^3), 2.77 (s, 3H, H^1). **^{13}C NMR** (101 MHz, $CDCl_3$) δ 165.0 (C^2), 136.7 (q, J_F = 6.2 Hz, C^8), 133.8 (C^5), 122.9 (q, J_F = 269.2 Hz, C^{10}), 120.2 (q, J_F = 34.0 Hz, C^9), 117.3 (C^6), 53.5 (C^4), 51.1 (C^7), 37.0 (C^3), 36.1 (C^1). **HRMS** (ESI-TOF) m/z: $[M + Na]^+$ Calcd for $C_{10}H_{15}F_3N_2ONa$ 259.1029; Found 259.1035.

(*E*)-1-Allyl-1,3-dimethyl-3-(3-(trimethylsilyl)allyl)urea (247)

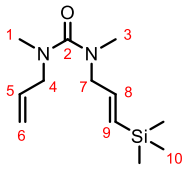

The starting reagent *trans*-3-(trimethylsilyl)allyl methylamine was synthesised as followed: an oven-dried flask containing a magnetic stir bar was sealed with a suba seal and placed under anhydrous N_2. *Trans*-3-(trimethylsilyl)allyl alcohol (0.15 mL, 1.0 mmol, 1.0 equiv.) and triethylamine (0.17 mL, 1.2 mmol, 1.2 equiv.) were added and dissolved in anhydrous CH_2Cl_2 (2.5 mL, 2.5 mL/mmol). The reaction mixture was cooled down to 0 °C and mesyl chloride (90 µL, 1.2 mmol, 1.2 equiv.) was then added dropwise. The reaction mixture was stirred at room temperature for 2 h. The reaction mixture was partitioned between CH_2Cl_2 and a saturated aqueous solution of Na_2CO_3. The organic phase was

collected and washed with brine, dried over $MgSO_4$, filtered, and concentrated *in vacuo*. The intermediate product was redissolved in anhydrous THF (0.36 mL, 0.36 mL/mmol) and methylamine (2.0 M in THF; 2.5 mL, 5.0 mmol, 5.0 equiv.) was added. The reaction mixture was stirred at room temperature for 24 h and then partitioned between CH_2Cl_2 and an aqueous solution of NaOH (1 M). After extracting the organic phase, the aqueous phase was washed with CH_2Cl_2 (2×). The combined organic phase was washed twice with an aqueous solution of HCl (1 M). The combined aqueous phase was basified with an aqueous solution of NaOH (1 M) to pH = 14 and washed with CH_2Cl_2 (2×). The organic phases were collected, dried over Na_2SO_4, filtered, and cautiously concentrated *in vacuo*, generating *trans*-3-(trimethylsilyl)allyl methylamine that was used crude in the next step.

Reaction performed on 1.0 mmol scale following general procedure **2A** using *N*-((*E*)-3,7-dimethyl-2,6-octadienyl)-*N*-methylamine (1.0 mmol, 1.0 equiv.) in anhydrous CH_2Cl_2 (10 mL), triphosgene (179 mg, 0.603 mmol, 0.603 equiv.) in anhydrous CH_2Cl_2 (10 mL), and anhydrous pyridine (80 µL, 1.0 mmol, 1.0 equiv.), which was stirred for 1 h at 0 °C to room temperature. Reaction intermediate was redissolved in anhydrous MeCN (14.3 mL) and stirred with *N*-allylmethylamine (0.12 mL, 1.3 mmol, 1.3 equiv.) and triethylamine (0.35 mL, 2.5 mmol, 2.5 equiv.), which was stirred for 6 h at room temperature, followed by 4 days at 40 °C. Flash column chromatography (25% acetone/petroleum ether) gave **247** as an orange oil (10 mg, 0.042 mmol, 4% yield). **IR** (film) ν_{max} 2955, 1647, 1384, 1248, 864, 838, 772 cm^{-1}. **^{1}H NMR** (400 MHz, $CDCl_3$) δ 5.97 (dt, *J* = 18.7, 4.9 Hz, 1H, H^8), 5.88 – 5.74 (m, 2H, H^5 + H^9), 5.24 – 5.13 (m, 2H, H^6), 3.77 (dd, *J* = 4.9, 1.5 Hz, 2H, H^7), 3.72 (dt, *J* = 5.7, 1.6 Hz, 2H, H^4), 2.75 (s, 3H, H^1/H^3), 2.73 (s, 3H, H^1/H^3), 0.06 (s, 9H, H^{10}). **^{13}C NMR** (101 MHz, $CDCl_3$) δ 165.4 (C^2), 141.7 (C^8), 134.3 (C^5), 132.5 (C^9), 117.0 (C^6), 55.9 (C^7), 53.6 (C^4), 36.2 (C^1/C^3), 36.2 (C^1/C^3), -1.1 (C^{10}). **HRMS** (ESI-TOF) m/z: $[M + H]^+$ Calcd for $C_{12}H_{25}N_2OSi$ 241.1731; Found 241.1740.

2-Methylallyl-4-methylbenzenesulfonate (259)

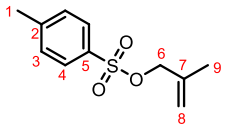

An oven-dried flask containing a magnetic stir bar was sealed with a suba seal and placed under anhydrous N_2. 2-Methyl-2-propen-1-ol (0.35 mL, 4.2 mmol, 1.0 equiv.) dissolved in anhydrous THF (14.5 mL, 3.45 mL/mmol) was cooled down to –78 °C and *n*-BuLi (2.50 M in hexanes; 1.76 mL, 4.40 mmol, 1.05 equiv.) was added dropwise. *p*-Toluenesulfonyl chloride (801 mg, 4.20 mmol, 1.00 equiv.) was then added dropwise and the reaction mixture was stirred at –78 °C for 24 h. The reaction mixture was diluted at –78 °C with cold petroleum ether (17 mL, 0.25 M), washed with a saturated aqueous solution of $NaHCO_3$ (17 mL, 4 mL/mmol; 2×) and the aqueous phases were combined and extracted with petroleum ether (21 mL, 5 mL/mmol; 3×). The organic phases were combined, dried over K_2CO_3

at 0 °C, filtered, and concentrated *in vacuo*. Flash column chromatography (5−40% acetone/petroleum ether) gave **259** as a pale-yellow oil (608 mg, 2.69 mmol, 64% yield). **IR** (film) ν_{max} 3393, 2924, 1356, 1173, 813, 664, 554 cm^{-1}. **^{1}H NMR** (400 MHz, $CDCl_3$) δ 7.84 – 7.76 (m, 2H, H^4), 7.38 – 7.30 (m, 2H, H^3), 5.01 – 4.91 (m, 2H, H^8), 4.43 (s, 2H, H^6), 2.45 (s, 3H, H^1), 1.69 (t, *J* = 1.2 Hz, 3H, H^9). **^{13}C NMR** (101 MHz, $CDCl_3$) δ 144.9 (C^2), 138.1 (C^7), 133.4 (C^5), 129.9 (C^3), 128.1 (C^4), 115.8 (C^8), 73.9 (C^6), 21.8 (C^1), 19.2 (C^9). **HRMS** (ESI-TOF) m/z: $[M + Na]^+$ Calcd for $C_{11}H_{14}O_3SNa$ 249.0556; Found 249.0566. The ^{1}H NMR spectrum is in agreement with the literature.[194]

_N_-Boc ethyl oxamate (264)

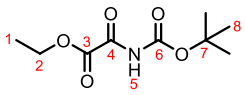

Reaction performed on 176 mmol scale following a literature procedure[152] using ethyl oxamate (20.6 g, 176 mmol, 1.00 equiv.), anhydrous DCE (52 mL, 0.28 mL/mmol), oxalyl chloride (17.9 mL, 211 mmol, 1.20 equiv.), anhydrous toluene (172 mL, 0.980 mL/mmol) and *tert*-butyl alcohol (19.4 mL, 202 mmol, 1.15 equiv.). Flash column chromatography (20% acetone/petroleum ether) gave the product **264** as a pale-yellow oil (26.8 g, 123 mmol, 70% yield). **IR** (film) ν_{max} 3271, 2983, 2923, 1738, 1708, 1496, 1371, 1307, 1242, 1132, 1018 cm^{-1}. **^{1}H NMR** (400 MHz, $CDCl_3$) δ 8.64 (bs, 1H, H^5), 4.38 (q, *J* = 7.1 Hz, 2H, H^2), 1.51 (s, 9H, H^8), 1.39 (t, *J* = 7.1 Hz, 3H, H^1). **^{13}C NMR** (101 MHz, $CDCl_3$) δ 159.7 (C^3 + C^4), 148.6 (C^6), 84.0 (C^7), 64.0 (C^2), 28.0 (C^8), 14.0 (C^1). **HRMS** (ESI-TOF) m/z: $[M + Na]^+$ Calcd for $C_9H_{15}NO_5Na$ 240.0842; Found 240.0840. Analytical data are in agreement with the literature.[1,152]

***tert*-Butyl but-3-en-2-ylcarbamate (269)**[1]

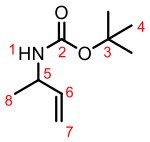

Reaction performed on 20.0 mmol scale following general procedure **2D** using 3-buten-2-ol (1.73 mL, 20.0 mmol, 1.00 equiv.), **264** (4.77 g, 22.0 mmol, 1.10 equiv.), triphenylphosphine (5.77 g, 22.0 mmol, 1.10 equiv.) and DIAD (4.33 mL, 22.0 mmol, 1.10 equiv.) in anhydrous THF (154 mL), which was stirred for 23.5 h at 0 °C to room temperature. The reaction intermediate was redissolved in THF (65 mL) and H_2O (25 mL), and stirred with LiOH (2.39 g, 99.8 mmol, 4.99 equiv.) for 21 h at room temperature. Flash column chromatography (2−20% acetone/petroleum ether) gave **269** as a pale-yellow solid (2.15 g, 12.6 mmol, 63% yield). **MP** 34–35 °C. **IR** (film) ν_{max} 3339, 2977, 2928, 1689,

1514, 1366, 1168, 917 cm^{-1}. **^{1}H NMR** (400 MHz, $CDCl_3$) δ 5.81 (ddd, *J* = 17.2, 10.4, 5.1 Hz, 1H, H^6), 5.14 (dt, *J* = 17.2, 1.4 Hz, 1H, H^7), 5.05 (dt, *J* = 10.4, 1.4 Hz, 1H, H^7), 4.43 (bs, 1H, H^1), 4.21 (bs, 1H, H^5), 1.44 (s, 9H, H^4), 1.20 (d, *J* = 6.8 Hz, 3H, H^8). **^{13}C NMR** (101 MHz, $CDCl_3$) δ 155.0 (C^2), 140.1 (C^6), 113.3 (C^7), 78.8 (C^3), 47.9 (C^5), 28.2 (C^4), 20.4 (C^8). **HRMS** (ESI-TOF) m/z: $[M + Na]^+$ Calcd for $C_9H_{17}NO_2Na$ 194.1151; Found 194.1154. Analytical data are in agreement with the literature.[195]

***tert*-Butyl (2-methylallyl)carbamate (262)**[1]

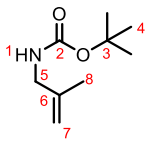

Reaction performed on 22.0 mmol scale following general procedure **2D** using 2-methyl-2-propen-1-ol (1.85 mL, 22.0 mmol, 1.00 equiv.), **264** (5.26 g, 24.2 mmol, 1.10 equiv.), triphenylphosphine (6.34 g, 24.2 mmol, 1.10 equiv.) and DIAD (4.76 mL, 24.2 mmol, 1.10 equiv.) in anhydrous THF (169 mL), which was stirred for 19 h at 0 °C to room temperature. The reaction intermediate was redissolved in THF (71 mL) and H_2O (28 mL), and stirred with LiOH (2.63 g, 110 mmol, 5.00 equiv.) for 2 h at room temperature. Flash column chromatography (5−40% acetone/petroleum ether) gave **262** as a yellow liquid (3.21 g, 18.7 mmol, 85% yield). **IR** (film) ν_{max} 3353, 2979, 1696, 1165, 751 cm^{-1}. **^{1}H NMR** (400 MHz, $CDCl_3$) δ 4.84 – 4.79 (m, 2H, H^7), 4.65 (bs, 1H, H^1), 3.65 (d, *J* = 6.2 Hz, 2H, H^5), 1.73 – 1.71 (m, 3H, H^8), 1.44 (s, 9H, H^4). **^{13}C NMR** (101 MHz, $CDCl_3$) δ 156.1 (C^2), 142.8 (C^6), 110.4 (C^7), 79.4 (C^3), 46.4 (C^5), 28.5 (C^4), 20.3 (C^8). **HRMS** (ESI-TOF) m/z: $[M + Na]^+$ Calcd for $C_9H_{17}NO_2Na$ 194.1151; Found 194.1159. Analytical data are in agreement with the literature.[196]

***tert*-Butyl but-2-en-1-ylcarbamate (263)**[1]

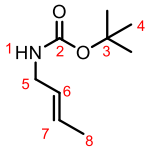

Reaction performed on 20.2 mmol scale following general procedure **2D** using 2-buten-1-ol (1.72 mL, 20.2 mmol, 1.00 equiv.), **264** (4.82 g, 22.2 mmol, 1.10 equiv.), triphenylphosphine (5.82 g, 22.2 mmol, 1.10 equiv.) and DIAD (4.37 mL, 22.2 mmol, 1.10 equiv.) in anhydrous THF (155 mL), which was stirred for 16.5 h at 0 °C to room temperature. The reaction intermediate was redissolved in THF (65 mL) and H_2O (25 mL), and stirred with LiOH (2.42 g, 101 mmol, 5.00 equiv.) for 1.5 h at room temperature. Flash column chromatography (5−40% acetone/petroleum ether) gave **263** as a pale-yellow liquid (2.53 g, 14.8 mmol, 73% yield). **IR** (film) ν_{max} 3348, 2977, 2932, 1692, 1513, 1248, 1168,

965 cm^{-1}. **^{1}H NMR** (400 MHz, $CDCl_3$) (suspected mixture of *E*:*Z* in a 0.9:0.1 ratio) δ 5.62 – 5.51 (m, 1H, H^6/H^7), 5.48 – 5.37 (m, 1H, H^6/H^7), 4.57 (bs, 1H, H^1), 3.73 (bs, 0.2H, *Z*-H^5), 3.63 (t, *J* = 5.9 Hz, 1.8H, *E*-H^5), 1.66 – 1.62 (m, 3H, H^8), 1.41 (s, 9H, H^4). **^{13}C NMR** (101 MHz, $CDCl_3$) δ 155.9 (C^2), 127.7 (C^6/C^7), 127.6 (C^6/C^7), 79.2 (C^3), 42.6 (C^5), 28.5 (C^4), 17.7 (C^8). **HRMS** (ESI-TOF) m/z: $[M + Na]^+$ Calcd for $C_9H_{17}NO_2Na$ 194.1151; Found 194.1157. Spectral data are in agreement with the literature.[197]

***tert*-Butyl (*E*)-hex-2-en-1-ylcarbamate (270)**[1]

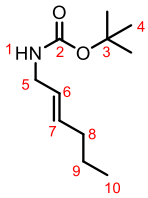

Reaction performed on 20.2 mmol scale following general procedure **2D** using *trans*-2-hexen-1-ol (2.38 mL, 20.2 mmol, 1.00 equiv.), **264** (4.82 g, 22.2 mmol, 1.10 equiv.), triphenylphosphine (5.82 g, 22.2 mmol, 1.10 equiv.) and DIAD (4.37 mL, 22.2 mmol, 1.10 equiv.) in anhydrous THF (155 mL), which was stirred for 17 h at 0 °C to room temperature. The reaction intermediate was redissolved in THF (65 mL) and H_2O (25 mL), and stirred with LiOH (2.42 g, 101 mmol, 5.00 equiv.) for 3 h at room temperature. Flash column chromatography (5−40% acetone/petroleum ether) gave **270** as a pale-yellow liquid (3.46 g, 17.4 mmol, 86% yield). **IR** (film) ν_{max} 3347, 2962, 2930, 1693, 1505, 1248, 1170, 968, 755 cm^{-1}. **^{1}H NMR** (400 MHz, $CDCl_3$) δ 5.58 (dtt, *J* = 15.3, 6.7, 1.3 Hz, 1H, H^7), 5.43 (dtt, *J* = 15.3, 6.0, 1.3 Hz, 1H, H^6), 4.50 (bs, 1H, H^1), 3.67 (t, *J* = 6.0 Hz, 2H, H^5), 2.02 – 1.94 (m, 2H, H^8), 1.44 (s, 9H, H^4), 1.37 (h, *J* = 7.4 Hz, 2H, H^9), 0.88 (t, *J* = 7.4 Hz, 3H, H^{10}). **^{13}C NMR** (101 MHz, $CDCl_3$) δ 155.9 (C^2), 133.1 (C^7), 126.6 (C^6), 79.3 (C^3), 42.8 (C^5), 34.4 (C^8), 28.6 (C^4), 22.4 (C^9), 13.8 (C^{10}). **HRMS** (ESI-TOF) m/z: $[M + Na]^+$ Calcd for $C_{11}H_{21}NO_2Na$ 222.1464; Found 222.1473. Spectral data are in agreement with the literature.[198]

***tert*-Butyl (*R*)-oct-1-en-3-ylcarbamate (271)**[1]

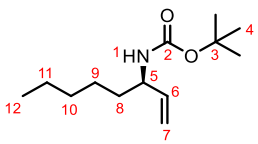

Reaction performed on 2.76 mmol scale following general procedure **2D** using (*S*)-1-octen-3-ol (420 µL, 2.76 mmol, 1.00 equiv.), **264** (660 mg, 3.04 mmol, 1.10 equiv.), triphenylphosphine (799 mg, 3.04 mmol, 1.10 equiv.) and DIAD (600 µL, 3.04 mmol, 1.10 equiv.) in anhydrous THF (21.2 mL), which

was stirred for 22 h at 0 °C to room temperature. The reaction intermediate was redissolved in THF (8.9 mL) and H_2O (3.5 mL), and stirred with LiOH (331 mg, 13.8 mmol, 5.00 equiv.) for 2 h at room temperature. Flash column chromatography (1−8% acetone/pentane) gave **271** as a yellow oil (424 mg, 1.86 mmol, 68% yield). $[\alpha]_D^{23} = -12$ (*c* = 1.08 in $CHCl_3$). **IR** (film) ν_{max} 3343, 2958, 2930, 1690, 1518, 1365, 1246, 1171, 773 cm^{-1}. **^{1}H NMR** (400 MHz, $CDCl_3$) δ 5.69 (ddd, *J* = 17.2, 10.4, 5.7 Hz, 1H, H^6), 5.09 (dt, *J* = 17.2, 1.3 Hz, 1H, H^7), 5.01 (dt, *J* = 10.4, 1.3 Hz, 1H, H^7), 4.48 (bs, 1H, H^1), 4.02 (bs, 1H, H^5), 1.52 – 1.41 (m, 2H, H^8), 1.40 (s, 9H, H^4), 1.33 – 1.19 (m, 6H, H^9 + H^{10} + H^{11}), 0.83 (t, *J* = 6.6 Hz, 3H, H^{12}). **^{13}C NMR** (101 MHz, $CDCl_3$) δ 155.5 (C^2), 139.3 (C^6), 114.2 (C^7), 79.2 (C^3), 52.9 (C^5), 35.2 (C^8), 31.7 (C^{10}), 28.5 (C^4), 25.4 (C^9), 22.6 (C^{11}), 14.0 (C^{12}). **HRMS** (ESI-TOF) m/z: $[M + Na]^+$ Calcd for $C_{13}H_{25}NO_2Na$ 250.1778; Found 250.1776. **HPLC** (OD-H, *i*-PrOH/*n*-hexane = 1/99, flow rate = 0.5 mL/min, λ = 205 nm) t_R = 8.79 min (major), 10.28 min (minor), ≥99:1 *er*.

***tert*-Butyl oct-1-en-3-ylcarbamate (±-271)**[1]

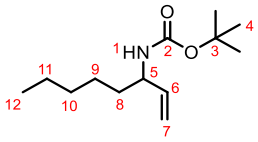

Reaction performed on 6.01 mmol scale following general procedure **2D** using 1-octen-3-ol (0.92 mL, 6.0 mmol, 1.0 equiv.), **264** (1.43 g, 6.60 mmol, 1.10 equiv.), triphenylphosphine (1.73 g, 6.60 mmol, 1.10 equiv.) and DIAD (1.30 mL, 6.60 mmol, 1.10 equiv.) in anhydrous THF (46.2 mL), which was stirred for 22 h at 0 °C to room temperature. The reaction intermediate was redissolved in THF (19.4 mL) and H_2O (7.5 mL), and stirred with LiOH (719 mg, 30.0 mmol, 5.00 equiv.) for 2 h at room temperature. Flash column chromatography (2−20% acetone/pentane) gave **±-271** as a pale-yellow oil (1.05 g, 4.62 mmol, 77% yield). **IR** (film) ν_{max} 3341, 2959, 2930, 2860, 1692, 1505, 1365, 1245, 1167, 917, 772 cm^{-1}. **^{1}H NMR** (400 MHz, $CDCl_3$) δ 5.74 (ddd, *J* = 17.2, 10.4, 5.6 Hz, 1H, H^6), 5.14 (dt, *J* = 17.2, 1.4 Hz, 1H, H^7), 5.07 (dt, *J* = 10.4, 1.4 Hz, 1H, H^7), 4.41 (bs, 1H, H^1), 4.07 (bs, 1H, H^5), 1.58 – 1.38 (m, 2H, H^8), 1.44 (s, 9H, H^4), 1.36 – 1.24 (m, 6H, H^9 + H^{10} + H^{11}), 0.88 (t, *J* = 6.7 Hz, 3H, H^{12}). **^{13}C NMR** (101 MHz, $CDCl_3$) δ 155.6 (C^2), 139.4 (C^6), 114.3 (C^7), 79.4 (C^3), 53.0 (C^5), 35.4 (C^8), 31.8 (C^{10}), 28.6 (C^4), 25.5 (C^9), 22.7 (C^{11}), 14.1 (C^{12}). **HRMS** (ESI-TOF) m/z: $[M + Na]^+$ Calcd for $C_{13}H_{25}NO_2Na$ 250.1778; Found 250.1784. **HPLC** (OD-H, *i*-PrOH/*n*-hexane = 1/99, flow rate = 0.5 mL/min, λ = 205 nm) t_R = 8.56 min (50.02%), 10.28 min (49.98%).

***tert*-Butyl (1-cyclohexylallyl)carbamate (272)**

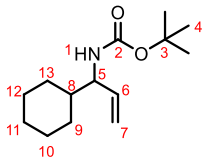

The starting reagent 1-cyclohexylprop-2-en-1-ol was synthesised by following a literature procedure[199] using cyclohexanecarboxaldehyde (2.42 mL, 20.0 mmol, 1.00 equiv.) and vinylmagnesium bromide (1M in THF; 24 mL, 24 mmol, 1.2 equiv.) in anhydrous THF (40 mL, 2 mL/mmol), which was stirred for 21 h at 0 ℃ to room temperature. Flash column chromatography (1−8% acetone/pentane followed by 2−11% EtOAc/CH_2Cl_2) gave 1-cyclohexylprop-2-en-1-ol as a pale-yellow oil (1.59 g, 11.4 mmol, 57% yield). **^{1}H NMR** (400 MHz, $CDCl_3$) δ 5.86 (ddd, *J* = 17.1, 10.4, 6.6 Hz, 1H), 5.23 – 5.12 (m, 2H), 3.85 (tt, *J* = 6.4, 1.2 Hz, 1H), 1.90 – 1.79 (m, 1H), 1.81 – 1.62 (m, 3H), 1.57 (s, 1H), 1.40 (tdt, *J* = 11.7, 6.4, 3.3 Hz, 1H), 1.30 – 1.07 (m, 3H), 1.06 – 0.93 (m, 2H). **^{13}C NMR** (101 MHz, $CDCl_3$) δ 140.0, 115.6, 77.9, 43.6, 28.9, 28.5, 26.7, 26.3, 26.2. Spectral data are in agreement with the literature.[199]

Reaction performed on 11.4 mmol scale following general procedure **2D** using 1-cyclohexylprop-2-en-1-ol (1.59 g, 11.4 mmol, 1.00 equiv.), **264** (2.72 g, 12.5 mmol, 1.10 equiv.), triphenylphosphine (3.28 g, 12.5 mmol, 1.10 equiv.) and DIAD (2.46 mL, 12.5 mmol, 1.10 equiv.) in anhydrous THF (87 mL), which was stirred for 18 h at 0 °C to room temperature. The reaction intermediate was redissolved in THF (37 mL) and H_2O (14 mL), and stirred with LiOH (1.36 g, 56.9 mmol, 5.00 equiv.) for 8 h at room temperature. Flash column chromatography (0−10% EtOAc/petroleum ether followed by 10−70% CH_2Cl_2/petroleum ether) gave **272** as a white solid (752 mg, 3.14 mmol, 28% yield). **MP** 71−72 °C. **IR** (film) ν_{max} 3342, 2978, 2925, 2853, 1693, 1502, 1365, 1246, 1171, 1009, 916 cm^{-1}. **^{1}H NMR** (400 MHz, $CDCl_3$) δ 5.73 (ddd, *J* = 16.8, 10.4, 6.0 Hz, 1H, H^6), 5.18 – 5.06 (m, 2H, H^7), 4.50 (bs, 1H, H^1), 3.96 (bs, 1H, H^5), 1.79 – 1.60 (m, 5H, H^9/H^{10}/H^{11}/H^{12}/H^{13}), 1.44 (s, 9H, H^4), 1.42 – 1.33 (m, 1H, H^8), 1.29 – 1.09 (m, 3H, H^9/H^{10}/H^{11}/H^{12}/H^{13}), 1.08 – 0.90 (m, 2H, H^9/H^{10}/H^{11}/H^{12}/H^{13}). **^{13}C NMR** (101 MHz, $CDCl_3$) δ 155.7 (C^2), 137.7 (C^6), 115.1 (C^7), 79.3 (C^3), 57.7 (C^5), 42.5 (C^8), 29.5 (C^9/C^{10}/C^{11}/C^{12}/C^{13}), 28.8 (C^9/C^{10}/C^{11}/C^{12}/C^{13}), 28.6 (C^4), 26.5 (C^9/C^{10}/C^{11}/C^{12}/C^{13}), 26.3 (C^9/C^{10}/C^{11}/C^{12}/C^{13}), 26.3 (C^9/C^{10}/C^{11}/C^{12}/C^{13}). **HRMS** (ESI-TOF) m/z: $[M + H]^+$ Calcd for $C_{14}H_{26}NO_2$ 240.1958; Found 240.1953. Analytical data are in agreement with the literature.[200]

***tert*-Butyl (2-cyclohexylallyl)carbamate (273)**

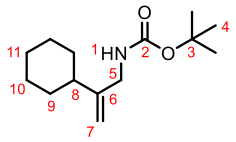

The starting reagent 2-cyclohexylprop-2-en-1-ol was synthesised by following a literature procedure[201] using propargyl alcohol (0.87 mL, 15 mmol, 1.0 equiv.), cyclohexylmagnesium chloride (1.3 M in toluene/THF; 34.6 mL, 45.0 mmol, 3.00 equiv.) and copper(I) iodide (1.43 g, 7.50 mmol, 0.500 equiv.) in anhydrous toluene (8.0 mL, 0.53 mL/mmol), which was stirred for 25.5 h at −78 °C to room temperature. Flash column chromatography (6−38% Et_2O/petroleum ether) gave 2-cyclohexylprop-2-en-1-ol as a yellow oil (531 mg, 3.79 mmol, 25% yield). **^{1}H NMR** (400 MHz, $CDCl_3$) δ 5.00 (q, *J* = 1.5 Hz, 1H), 4.87 (p, *J* = 1.1 Hz, 1H), 4.11 (t, *J* = 1.1 Hz, 2H), 1.95 (tt, *J* = 11.2, 3.0 Hz, 1H), 1.82 – 1.73 (m, 4H), 1.72 – 1.65 (m, 1H), 1.50 (bs, 1H), 1.35 – 1.10 (m, 5H). **^{13}C NMR** (101 MHz, $CDCl_3$) δ 154.7, 107.6, 65.4, 41.5, 32.6, 26.9, 26.4. Spectral data are in agreement with the literature.[201]

Reaction performed on 3.63 mmol scale following general procedure **2D** using 2-cyclohexylprop-2-en-1-ol (509 mg, 3.63 mmol, 1.00 equiv.), **264** (867 mg, 3.99 mmol, 1.10 equiv.), triphenylphosphine (1.05 g, 3.99 mmol, 1.10 equiv.) and DIAD (790 µL, 3.99 mmol, 1.10 equiv.) in anhydrous THF (28 mL), which was stirred for 16 h 0 °C to room temperature. The reaction intermediate was redissolved in THF (12 mL) and H_2O (5 mL), and stirred with LiOH (435 mg, 18.2 mmol, 5.00 equiv.) for 3 h at room temperature. Flash column chromatography (0−11% EtOAc/petroleum ether) gave **273** as pale-yellow oil (749 mg, 3.13 mmol, 86% yield). **IR** (film) ν_{max} 3349, 2978, 2931, 1692, 1511, 1366, 1247, 1163 cm^{-1}. **^{1}H NMR** (400 MHz, $CDCl_3$) δ 4.87 – 4.79 (m, 2H, H^7), 4.55 (bs, 1H, H^1), 3.71 (s, 2H, H^5), 1.86 (td, *J* = 11.2, 5.5 Hz, 1H, H^8), 1.81 – 1.72 (m, 4H, H^9 + H^{10}), 1.72 – 1.63 (m, 1H, H^{11}), 1.45 (s, 9H, H^4), 1.33 – 1.10 (m, 5H, H^9 + H^{10} + H^{11}). **^{13}C NMR** (101 MHz, $CDCl_3$) δ 156.1 (C^2), 152.1 (C^6), 107.9 (C^7), 79.4 (C^3), 44.4 (C^5), 42.4 (C^8), 32.5 (C^9), 28.6 (C^4), 26.9 (C^{10}), 26.4 (C^{11}). **HRMS** (ESI-TOF) m/z: [M + H – *t*-Bu]$^+$ Calcd for $C_{10}H_{17}NO_2$ 184.1332; Found 184.1328.

***tert*-Butyl (*E*)-(3-cyclohexylallyl)carbamate (274)**

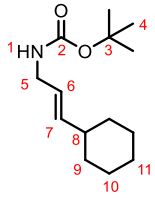

The starting reagent (*E*)-3-cyclohexylprop-2-enol was synthesised as followed:

Ethyl (*E*)-3-cyclohexylacrylate was synthesised by following a literature procedure[202] using triethyl phosphonoacetate (3.12 mL, 15.8 mmol, 1.05 equiv.) in anhydrous THF (53 mL, 3.33 mL/mmol), *n*-BuLi (1.60 M in hexane; 9.66 mL, 15.5 mmol, 1.03 equiv.) and cyclohexanecarbaldehyde (1.82 mL, 15.0 mmol, 1.00 equiv.), which was stirred for 5 min at −78 °C followed by 2.5 h at 0 °C. Flash column chromatography (1–14% Et_2O/pentane) gave ethyl (*E*)-3-cyclohexylacrylate (2.46 g, 13.5 mmol, 90% yield). **^{1}H NMR** (400 MHz, $CDCl_3$) δ 6.91 (dd, *J* = 15.8, 6.8 Hz, 1H), 5.75 (dd, *J* = 15.8, 1.5 Hz, 1H), 4.18 (q, *J* = 7.1 Hz, 2H), 2.17 – 2.07 (m, 1H), 1.80 – 1.71 (m, 3H), 1.70 – 1.63 (m, 2H), 1.28 (t, *J* = 7.1 Hz, 3H), 1.25 – 1.07 (m, 5H). **^{13}C NMR** (101 MHz, $CDCl_3$) δ 167.3, 154.4, 119.0, 60.3, 40.5, 31.8, 26.1, 25.9, 14.4. Spectral data agree with the literature.[202] Ethyl (*Z*)-3-cyclohexylacrylate was also afforded (79 mg, 0.43 mmol, 3% yield). **^{1}H NMR** (400 MHz, $CDCl_3$) δ 5.98 (dd, *J* = 11.6, 9.8 Hz, 1H), 5.61 (dd, *J* = 11.6, 1.1 Hz, 1H), 4.12 (q, *J* = 7.2 Hz, 2H), 3.32 – 3.21 (m, 1H), 1.73 – 1.59 (m, 5H), 1.37 – 1.27 (m, 2H), 1.25 (t, *J* = 7.1 Hz, 3H), 1.20 – 0.98 (m, 3H). **^{13}C NMR** (101 MHz, $CDCl_3$) δ 166.4, 155.6, 117.8, 59.8, 37.4, 32.4, 26.0, 25.6, 14.3. Spectral data are in agreement with the literature.[202]

Subsequently, following a literature procedure,[202] ethyl (*E*)-3-cyclohexylacrylate (2.43 g, 13.3 mmol, 1.00 equiv.) in anhydrous CH_2Cl_2 (13.3 mL, 1.00 mL/mmol) was reacted with DIBAL-H (1.00 M in CH_2Cl_2; 27.9 mL, 27.9 mmol, 2.10 equiv.), which was stirred for 2 h at 0 °C. (*E*)-3-cyclohexylprop-2-enol was afforded and used as crude (1.01 g, 7.20 mmol, 54% yield). **^{1}H NMR** (400 MHz, $CDCl_3$) δ 5.67 – 5.54 (m, 2H), 4.09 – 4.06 (m, 2H), 2.01 – 1.91 (m, 1H), 1.76 – 1.65 (m, 4H), 1.68 – 1.60 (m, 1H), 1.49 (bs, 1H), 1.32 – 1.01 (m, 5H). **^{13}C NMR** (101 MHz, $CDCl_3$) δ 139.3, 126.5, 64.1, 40.4, 32.9, 26.3, 26.1. Spectral data are in agreement with the literature.[202]

Reaction performed on 7.01 mmol scale following general procedure **2D** using (*E*)-3-cyclohexylprop-2-enol (984 mg, 7.01 mmol, 1.00 equiv.), **264** (1.70 g, 7.85 mmol, 1.12 equiv.), triphenylphosphine (2.02 g, 7.70 mmol, 1.10 equiv.) and DIAD (1.52 mL, 7.72 mmol, 1.10 equiv.) in anhydrous THF (54 mL), which was stirred for 21 h at 0 °C to room temperature. The reaction intermediate was redissolved in THF (23 mL) and H_2O (9 mL), and stirred with LiOH (838 mg, 35.0 mmol, 5.00 equiv.) for 2 h at room temperature. Flash column chromatography (1–8% EtOAc/petroleum ether) gave **274** as a pale-yellow oil (1.55 g, 6.49 mmol, 93% yield). **IR** (film) ν_{max} 3347, 2924, 2852, 1698, 1516, 1366, 1249, 1172, 969, 773 cm^{-1}. **^{1}H NMR** (400 MHz, $CDCl_3$) δ 5.52 (ddt, *J* = 15.5, 6.6, 1.1 Hz, 1H, H^7), 5.38 (dtd, *J* = 15.5, 6.0, 1.2 Hz, 1H, H^6), 4.47 (bs, 1H, H^1), 3.66 (d, *J* = 6.0 Hz, 2H, H^5), 1.98 – 1.87 (m, 1H, H^8), 1.75 – 1.66 (m, 4H, H^9 + H^{10}), 1.65 – 1.58 (m, 1H, H^{11}), 1.44 (s, 9H, H^4), 1.31 – 1.10 (m, 3H, H^{10} + H^{11}), 1.09 – 0.98 (m, 2H, H^9). **^{13}C NMR** (101 MHz, $CDCl_3$) δ 155.9 (C^2), 139.1 (C^7), 123.9 (C^6), 79.4 (C^3), 43.0 (C^5), 40.4 (C^8), 33.0 (C^9), 28.6 (C^4), 26.3 (C^{11}), 26.1 (C^{10}). **HRMS** (ESI-TOF) m/z: $[M + Na]^+$ Calcd for $C_{14}H_{25}NO_2Na$ 262.1778; Found 262.1778.

***tert*-Butyl (((1*R*,5*S*)-6,6-dimethylbicyclo[3.1.1]hept-2-en-2-yl)methyl)carbamate (275)**[1]

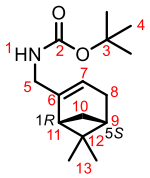

Reaction performed on 10.1 mmol scale following general procedure **2D** using (1*R*)-(–)-myrtenol (1.61 mL, 10.1 mmol, 1.00 equiv.), **264** (2.41 g, 11.1 mmol, 1.10 equiv.), triphenylphosphine (2.91 g, 11.1 mmol, 1.10 equiv.) and DIAD (2.19 mL, 11.1 mmol, 1.10 equiv.) in anhydrous THF (78 mL), which was stirred for 24 h at 0 °C to room temperature. The reaction intermediate was redissolved in THF (32.6 mL) and H_2O (12.6 mL), and stirred with LiOH (1.20 g, 50.0 mmol, 5.00 equiv.) for 2.5 h at room temperature. Flash column chromatography (1−12% acetone/petroleum ether) gave **275** as a white solid (2.23 g, 8.86 mmol, 88% yield). **MP** 57–58 °C. **IR** (film) ν_{max} 3354, 2987, 2914, 1694, 1504, 1365, 1257, 1162 cm^{-1}. **^{1}H NMR** (400 MHz, $CDCl_3$) δ 5.38 – 5.34 (m, 1H, H^7), 4.47 (bs, 1H, H^1), 3.61 (bs, 2H, H^5), 2.37 (dt, *J* = 8.6, 5.6 Hz, 1H, H^{10}), 2.31 – 2.16 (m, 2H, H^8), 2.11 – 2.03 (m, 2H, H^9 + H^{11}), 1.44 (s, 9H, H^4), 1.27 (s, 3H, H^{13}), 1.14 (d, *J* = 8.6 Hz, 1H, H^{10}), 0.82 (s, 3H, H^{13}). **^{13}C NMR** (101 MHz, $CDCl_3$) δ 156.1 (C^2), 145.2 (C^6), 118.2 (C^7), 79.3 (C^3), 45.6 (C^5), 44.1 (C^9/C^{11}), 41.0 (C^9/C^{11}), 38.1 (C^{12}), 31.7 (C^{10}), 31.2 (C^8), 28.6 (C^4), 26.3 (C^{13}), 21.2 (C^{13}). **HRMS** (ESI-TOF) m/z: $[M + Na]^+$ Calcd for $C_{15}H_{25}NO_2Na$ 274.1778; Found 274.1788.

***tert*-Butyl (*Z*)-(2-(1,3,3-trimethylbicyclo[2.2.1]heptan-2-ylidene)ethyl)carbamate (276)**

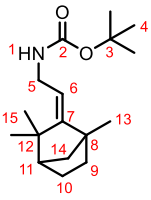

The starting reagent (*Z*)-2-(1,3,3-trimethylbicyclo[2.2.1]heptan-2-ylidene)ethan-1-ol was synthesised by following a literature procedure[203] using 1,3,3-trimethylbicyclo[2.2.1]heptan-2-one (0.96 mL, 6.0 mmol, 1.0 equiv.) in anhydrous Et_2O (2.7 mL, 0.45 mL/mmol), ethoxyacetylene (1.15 g, 6.56 mmol, 1.10 equiv.) in anhydrous Et_2O (13.4 mL, 2.04 mL/mmol) and *n*-BuLi (1.60 M in hexanes, 3.70 mL, 5.96 mmol), which was stirred for 23 h at −64 °C to −78 °C; concentrated H_2SO_4 (0.15 mL, 0.020 mL/mmol) in anhydrous THF (6.70 mL, 1.12 mL/mmol), which was stirred for 5 h at 0 °C to room temperature; KOH in H_2O (468 mg in 2.30 mL) in EtOH (6.7 mL, 1.1 mL/mmol), which was stirred for 3 h at reflux; thionyl chloride (0.87 mL, 12 mmol, 2.0 equiv.) in MeOH (3 mL, 0.5 mL/mmol), which was stirred for 2 h at room temperature to 60 °C under air; $LiAlH_4$ (2.39 g, 17.9 mmol, 3.00 equiv.) in anhydrous Et_2O (41 mL, 6.9 mL/mmol, which was stirred for 25 h at 0 °C to room temperature. Flash

column chromatography (5–40% EtOAc/petroleum ether) gave (*Z*)-2-(1,3,3-trimethylbicyclo[2.2.1]heptan-2-ylidene)ethan-1-ol as a yellow oil (439 mg, 2.43 mmol, 41% yield). **IR** (film) ν_{max} 3311, 2957, 2868, 1460, 1378, 1363, 1033, 1016, 1000, 978, 772 cm^{-1}. **^{1}H NMR** (400 MHz, $CDCl_3$) δ 5.15 (t, *J* = 7.3 Hz, 1H), 4.25 (d, *J* = 7.3 Hz, 2H), 1.80 – 1.67 (m, 2H), 1.56 (dq, *J* = 9.8, 2.1 Hz, 1H), 1.53 – 1.48 (m, 1H), 1.47 (d, *J* = 2.1 Hz, 1H), 1.22 (dd, *J* = 9.8, 1.5 Hz, 1H), 1.19 (s, 4H), 1.16 (s, 3H), 1.13 (s, 3H). **^{13}C NMR** (101 MHz, $CDCl_3$) δ 161.4, 114.6, 59.8, 50.7, 49.6, 44.1, 42.9, 35.7, 28.2, 26.1, 25.6, 19.1. **HRMS** (ESI-TOF) m/z: $[M + H - H_2O]^+$ Calcd for $C_{12}H_{20}O$ 163.1481; Found 163.1477.

Reaction performed on 2.58 mmol scale following general procedure **2D** using (*Z*)-2-(1,3,3-trimethylbicyclo[2.2.1]heptan-2-ylidene)ethan-1-ol (464 mg, 2.58 mmol, 1.00 equiv.), **264** (617 mg, 2.84 mmol, 1.10 equiv.), triphenylphosphine (745 mg, 2.84 mmol, 1.10 equiv.) and DIAD (560 µL, 2.84 mmol, 1.10 equiv.) in anhydrous THF (19.8 mL), which was stirred for 26 h at 0 °C to room temperature. The reaction intermediate was redissolved in THF (8.5 mL) and H_2O (3.2 mL), and stirred with LiOH (309 mg, 12.9 mmol, 5.00 equiv.) for 2 h at room temperature. Flash column chromatography (2–20% acetone/pentane) gave **276** as a pale-yellow oil (517 mg, 1.85 mmol, 72% yield). **IR** (film) ν_{max} 3350, 2960, 2928, 2868, 1706, 1500, 1461, 1391, 1365, 1248, 1172, 775, 770 cm^{-1}. **^{1}H NMR** (400 MHz, $CDCl_3$) δ 4.91 (t, *J* = 7.4 Hz, 1H, H^6), 4.39 (bs, 1H, H^1), 3.83 (t, *J* = 6.6 Hz, 2H, H^5), 1.76 – 1.68 (m, 2H, H^{10} + H^{11}), 1.56 – 1.46 (m, 3H, H^9 + H^{10} + H^{14}), 1.45 (s, 9H, H^4), 1.19 (s, 3H, H^{15}), 1.18 – 1.13 (m, 2H, H^9 + H^{14}), 1.12 (s, 3H, H^{15}), 1.12 (s, 3H, H^{13}). **^{13}C NMR** (101 MHz, $CDCl_3$) δ 161.1 (C^7), 155.9 (C^2), 111.8 (C^6), 79.3 (C^3), 50.7 (C^8), 49.7 (C^{11}), 44.1 (C^{14}), 42.7 (C^{12}), 38.8 (C^5), 35.8 (C^9), 28.6 (C^4), 27.8 (C^{13}), 25.8 (C^{15}), 25.6 (C^{10}), 19.2 (C^{15}). **HRMS** (ESI-TOF) m/z: $[M + H]^+$ Calcd for $C_{17}H_{30}NO_2$ 280.2271; Found 280.2273.

tert-Butyl (cyclohex-1-en-1-ylmethyl)carbamate (277)

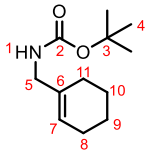

The starting reagent cyclohex-1-en-1-ylmethanol was synthesised by following a literature procedure[204] using 1-cyclohexene-1-carboxylic acid (760 mg, 6.03 mmol, 1.00 equiv.) in anhydrous Et_2O (30 mL, 5.0 mL/mmol) and lithium aluminium hydride (683 mg, 18.0 mmol, 3.00 equiv.) in anhydrous Et_2O (3.8 mL, 0.21 mL/mmol), which was stirred for 1 h at 0 °C. Crude yield: 61% (410 mg, 3.66 mmol). **^{1}H NMR** (400 MHz, $CDCl_3$) δ 5.72 – 5.64 (m, 1H), 3.98 (s, 2H), 2.06 – 1.98 (m, 4H), 1.70 – 1.60 (m, 2H), 1.63 – 1.53 (m, 2H), 1.36 (bs, 1H). **^{13}C NMR** (101 MHz, $CDCl_3$) δ 137.7, 123.2, 67.9, 25.8, 25.1, 22.7, 22.6. Spectral data are in agreement with the literature.[204]

Reaction performed on 3.55 mmol scale following general procedure **2D** using cyclohex-1-en-1-ylmethanol (398 mg, 3.55 mmol, 1.00 equiv.), **264** (849 mg, 3.91 mmol, 1.10 equiv.), triphenylphosphine (1.03 g, 3.91 mmol, 1.10 equiv.) and DIAD (0.77 mL, 3.9 mmol, 1.1 equiv.) in anhydrous THF (27 mL), which was stirred for 19 h at 0 °C to room temperature. The reaction intermediate was redissolved in THF (11.5 mL) and H_2O (4.4 mL), and stirred with LiOH (426 mg, 17.8 mmol, 5.00 equiv.) for 3 h at room temperature. Flash column chromatography (5−42% EtOAc/petroleum ether) gave **277** as a pale-yellow oil (565 mg, 2.67 mmol, 75% yield). **IR** (film) ν_{max} 3347, 2927, 1695, 1508, 1366, 1246, 1164, 772, 753, 666 cm^{-1}. **^{1}H NMR** (400 MHz, $CDCl_3$) δ 5.54 (tt, *J* = 3.7, 1.7 Hz, 1H, H^7), 4.52 (bs, 1H, H^1), 3.59 (d, *J* = 4.4 Hz, 2H, H^5), 2.03 – 1.96 (m, 2H, H^8), 1.96 – 1.88 (m, 2H, H^{11}), 1.66 – 1.58 (m, 2H, H^{10}), 1.58 – 1.51 (m, 2H, H^9), 1.44 (s, 9H, H^4). **^{13}C NMR** (101 MHz, $CDCl_3$) δ 156.2 (C^2), 135.1 (C^6), 122.7 (C^7), 79.3 (C^3), 46.8 (C^5), 28.6 (C^4), 26.5 (C^{11}), 25.1 (C^8), 22.7 (C^{10}), 22.5 (C^9). **HRMS** (ESI-TOF) m/z: $[M + H]^+$ Calcd for $C_{12}H_{22}NO_2$ 212.1645; Found 212.1643.

***tert*-Butyl cyclohex-2-en-1-ylcarbamate (278)**

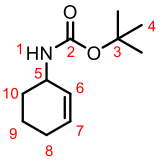

Reaction performed on 8.86 mmol scale following general procedure **2D** using 2-cyclohexene-1-ol (870 µL, 8.86 mmol, 1.00 equiv.), **264** (2.12 g, 9.75 mmol, 1.10 equiv.), triphenylphosphine (2.56 g, 9.75 mmol, 1.10 equiv.) and DIAD (1.92 mL, 9.75 mmol, 1.10 equiv.) in anhydrous THF (68.2 mL), which was stirred for 41 h at 0 °C to room temperature. The reaction intermediate was redissolved in THF (28.6 mL) and H_2O (11.1 mL), and stirred with LiOH (1.06 g, 44.3 mmol, 5.00 equiv.) for 2 h at room temperature. Flash column chromatography (10% EtOAc/petroleum ether) gave **278** as a white solid (1.02 g, 5.15 mmol, 58% yield). **MP** 52–53 °C. **IR** (film) ν_{max} 3337, 2977, 2931, 1693, 1516, 1501, 1366, 1220, 1167, 772 cm^{-1}. **^{1}H NMR** (400 MHz, $CDCl_3$) δ 5.82 – 5.73 (m, 1H, H^7), 5.62 – 5.53 (m, 1H, H^6), 4.53 (bs, 1H, H^1), 4.11 (bs, 1H, H^5), 2.04 – 1.89 (m, 2H, H^8), 1.93 – 1.80 (m, 1H, H^{10}), 1.67 – 1.54 (m, 2H, H^9), 1.53 – 1.45 (m, 1H, H^{10}), 1.42 (s, 9H, H^4). **^{13}C NMR** (101 MHz, $CDCl_3$) δ 155.3 (C^2), 130.5 (C^7), 128.3 (C^6), 79.2 (C^3), 45.9 (C^5), 29.9 (C^{10}), 28.5 (C^4), 24.9 (C^8), 19.8 (C^9). **HRMS** (ESI-TOF) m/z: $[M + Na]^+$ Calcd for $C_{11}H_{19}NO_2Na$ 220.1308; Found 220.1312. Analytical data are in agreement with the literature.[205]

***tert*-Butyl (3,5,5-trimethylcyclohexyl-2-en-1-yl)carbamate (279)**

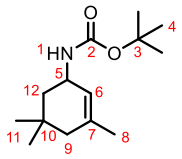

Reaction performed on 4.5 mmol scale following general procedure **2D** using 3,5,5-trimethyl-2-cyclohexene-1-ol (0.69 mL, 4.5 mmol, 1.0 equiv.), **264** (1.08 g, 4.95 mmol, 1.10 equiv.), triphenylphosphine (1.30 g, 4.95 mmol, 1.10 equiv.) and DIAD (970 µL, 4.95 mmol, 1.10 equiv.) in anhydrous THF (35 mL), which was stirred for 14 h at 0 °C to room temperature. The reaction intermediate was redissolved in THF (14.5 mL) and H_2O (5.6 mL), and stirred with LiOH (539 mg, 22.5 mmol, 5.00 equiv.) for 2 h at room temperature. Flash column chromatography (1−16% acetone/petroleum ether) gave **279** as a white/pale-yellow solid (474 mg, 1.98 mmol, 44% yield). **MP** 79–80 °C. **IR** (film) ν_{max} 3341, 2953, 2249, 1697, 1494, 1365, 1244, 1220, 1166, 1047, 1017, 909, 773, 731 cm^{-1}. **^{1}H NMR** (400 MHz, $CDCl_3$) δ 5.26 – 5.20 (m, 1H, H^6), 4.45 – 4.38 (m, 1H, H^1), 4.14 (bs, 1H, H^5), 1.80 – 1.73 (m, 1H, H^9), 1.73 – 1.68 (m, 1H, H^{12}), 1.65 – 1.58 (m, 3H, H^8), 1.60 – 1.50 (m, 1H, H^9), 1.41 (s, 9H, H^4), 1.01 (dd, *J* = 12.5, 10.2 Hz, 1H, H^{12}), 0.92 (s, 3H, H^{11}), 0.87 (s, 3H, H^{11}). **^{13}C NMR** (101 MHz, $CDCl_3$) δ 155.6 (C^2), 135.8 (C^7), 121.9 (C^6), 79.1 (C^3), 46.5 (C^5), 44.0 (C^9), 42.9 (C^{12}), 31.4 (C^{11}), 30.7 (C^{10}), 28.5 (C^4), 25.7 (C^{11}), 23.6 (C^8). **HRMS** (ESI-TOF) m/z: $[M + H]^+$ Calcd for $C_{14}H_{26}NO_2$ 240.1958; Found 240.1955.

***tert*-Butyl (2-phenylallyl)carbamate (280)**[1]

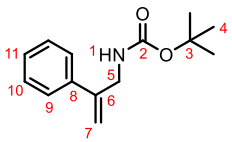

The starting reagent 2-phenylprop-2-en-1-ol was synthesised by following a literature procedure[206] using propargyl alcohol (1.34 mL, 23.0 mmol, 1.00 equiv.), phenylmagnesium bromide (2.60 M in Et_2O; 22.1 mL, 57.5 mmol, 2.50 equiv.) and copper(I) iodide (657 mg, 3.45 mmol, 0.150 equiv.) in anhydrous Et_2O (11.5 mL, 0.500 mL/mmol), which was stirred for 24 h at reflux. Flash column chromatography (7−60% acetone/petroleum ether) gave 2-phenylprop-2-en-1-ol as an orange liquid (quantitative). **^{1}H NMR** (400 MHz, $CDCl_3$) δ 7.48 – 7.43 (m, 2H), 7.39 – 7.28 (m, 3H), 5.48 (q, *J* = 1.0 Hz, 1H), 5.36 (q, *J* = 1.4 Hz, 1H), 4.55 (d, *J* = 5.9 Hz, 2H), 1.68 (t, *J* = 5.9 Hz, 1H). **^{13}C NMR** (101 MHz, $CDCl_3$) δ 147.4, 138.6, 128.6, 128.1, 126.2, 112.7, 65.2. Spectral data are in agreement with the literature.[206]

Reaction performed on 21.7 mmol scale following general procedure **2D** using 2-phenylprop-2-en-1-ol (2.92 g, 21.7 mmol, 1.00 equiv.), **264** (5.42 g, 24.9 mmol, 1.15 equiv.), triphenylphosphine (6.26 g, 23.9 mmol, 1.10 equiv.) and DIAD (4.70 mL, 23.9 mmol, 1.10 equiv.) in anhydrous THF (175 mL), which was stirred for 21 h at 0 °C to room temperature. The reaction intermediate was redissolved in THF (70 mL) and H_2O (27 mL), and stirred with LiOH (2.59 g, 109 mmol, 5.00 equiv.) for 3.5 h at room temperature. Flash column chromatography (3−24% EtOAc/petroleum ether) gave **280** as a yellow oil (3.91 g, 16.8 mmol, 77% yield). **IR** (film) ν_{max} 3347, 2977, 1693, 1496, 1365, 1246, 1164, 778, 702 cm^{-1}. **^{1}H NMR** (400 MHz, $CDCl_3$) δ 7.46 – 7.39 (m, 2H, H^{10}), 7.37 – 7.27 (m, 3H, H^9 + H^{11}), 5.42 (s, 1H, H^7), 5.23 (q, *J* = 1.4 Hz, 1H, H^7), 4.66 (bs, 1H, H^1), 4.19 (d, *J* = 3.7 Hz, 2H, H^5), 1.44 (s, 9H, H^4). **^{13}C NMR** (101 MHz, $CDCl_3$) δ 155.9 (C^2), 145.1 (C^8), 138.8 (C^6), 128.6 (C^9), 128.0 (C^{11}), 126.3 (C^{10}), 113.3 (C^7), 79.6 (C^3), 44.5 (C^5), 28.5 (C^4). **HRMS** (ESI-TOF) m/z: $[M + Na]^+$ Calcd for $C_{14}H_{19}NO_2Na$ 256.1308; Found 256.1305. Spectral data are in agreement with the literature.[207]

***tert*-Butyl (2-benzylallyl)carbamate (281)**

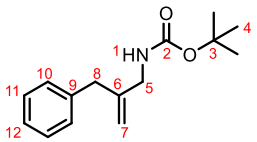

The starting reagent 2-benzylallyl alcohol was synthesised as followed:

2-Benzylacrylaldehyde was synthesised by following a literature procedure[208] using 3-phenylpropanal (2.66 mL, 20.0 mmol, 1.00 equiv.), aqueous formaldehyde (33 wt%; 1.49 mL, 20.0 mmol, 1.00 equiv.), pyrrolidine (0.17 mL, 2.0 mmol, 10 mol%) and propionic acid (0.15 mL, 2.0 mmol, 10 mol%) in *i*-PrOH (20 mL, 1.0 mL/mmol), which was stirred for 20 h at 45 °C. Flash column chromatography (0−6% EtOAc/petroleum ether) gave 2-benzylacrylaldehyde as a pale-yellow oil (2.37 g, 16.2 mmol, 81% yield). **^{1}H NMR** (400 MHz, $CDCl_3$) δ 9.61 (s, 1H), 7.33 – 7.27 (m, 2H), 7.25 – 7.20 (m, 1H), 7.20 – 7.16 (m, 2H), 6.12 – 6.09 (m, 1H), 6.07 (q, *J* = 0.9 Hz, 1H), 3.57 (s, 2H). **^{13}C NMR** (101 MHz, $CDCl_3$) δ 194.1, 149.9, 138.3, 135.3, 129.3, 128.7, 126.6, 34.3. Spectral data are in agreement with the literature.[208]

Subsequently, by following a literature procedure,[209] 2-benzylacrylaldehyde (2.32 g, 15.9 mmol, 1.00 equiv.) was reacted with $NaBH_4$ (632 mg, 16.7 mmol, 1.05 equiv.) in anhydrous MeOH (8 mL, 0.5 mL/mmol) for 30 min at 0 °C. Flash column chromatography (7−60% EtOAc/petroleum ether) gave 2-benzylallyl alcohol as a colourless oil (1.45 g, 9.76 mmol, 61% yield). **^{1}H NMR** (400 MHz, $CDCl_3$) δ 7.32 – 7.27 (m, 2H), 7.24 – 7.19 (m, 3H), 5.15 – 5.08 (m, 1H), 4.94 – 4.86 (m, 1H), 4.05 (d, *J* = 5.5 Hz, 2H), 3.42 (s, 2H). **^{13}C NMR** (101 MHz, $CDCl_3$) δ 148.3, 139.2, 129.1, 128.6, 126.4, 111.6, 65.5, 40.0. Spectral data are in agreement with the literature.[210]

Reaction performed on 12.0 mmol scale following general procedure **2D** using 2-benzylallyl alcohol (1.78 g, 12.0 mmol, 1.00 equiv.), **264** (2.86 g, 13.2 mmol, 1.10 equiv.), triphenylphosphine (3.46 g, 13.2 mmol, 1.10 equiv.) and DIAD (2.60 mL, 13.2 mmol, 1.10 equiv.) in anhydrous THF (92 mL), which was stirred for 17 h at 0 °C to room temperature. The reaction intermediate was redissolved in THF (39 mL) and H_2O (15 mL), and stirred with LiOH (1.43 g, 59.9 mmol, 5.00 equiv.) for 5 h at room temperature. Flash column chromatography (2−20% EtOAc/petroleum ether) gave **281** as a colourless oil (2.35 g, 9.49 mmol, 79% yield). **IR** (film) ν_{max} 3349, 2977, 1699, 1506, 1366, 1219, 1166, 778, 766, 699 cm^{-1}. **^{1}H NMR** (400 MHz, $CDCl_3$) δ 7.31 – 7.26 (m, 2H, H^{11}), 7.23 – 7.16 (m, 3H, H^{10} + H^{12}), 4.99 (s, 1H, H^7), 4.85 (s, 1H, H^7), 4.59 (bs, 1H, H^1), 3.67 (d, J = 5.2 Hz, 2H, H^5), 3.36 (s, 2H, H^8), 1.44 (s, 9H, H^4). **^{13}C NMR** (101 MHz, $CDCl_3$) δ 156.0 (C^2), 146.0 (C^6), 139.0 (C^9), 129.1 (C^{10}), 128.6 (C^{11}), 126.4 (C^{12}), 111.8 (C^7), 79.5 (C^3), 44.9 (C^5), 41.0 (C^8), 28.5 (C^4). **HRMS** (ESI-TOF) m/z: [M + H – *t*-Bu]$^+$ Calcd for $C_{11}H_{13}NO_2$ 191.0941; Found 191.0940. Spectral data are in agreement with the literature.[206]

***tert*-Butyl (1-phenylallyl)carbamate (282)**[1]

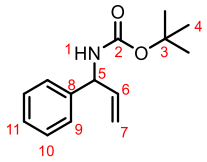

Reaction performed on 10.2 mmol scale following general procedure **2D** using α-vinylbenzyl alcohol (1.33 mL, 10.2 mmol, 1.00 equiv.), **264** (2.43 g, 11.2 mmol, 1.10 equiv.), triphenylphosphine (2.93 g, 11.2 mmol, 1.10 equiv.) and DIAD (2.20 mL, 11.2 mmol, 1.10 equiv.) in anhydrous THF (78 mL), which was stirred for 3.5 d at 0 °C to room temperature. The reaction intermediate was redissolved in THF (33 mL) and H_2O (13 mL), and stirred with LiOH (1.22 g, 50.8 mmol, 5.00 equiv.) for 4.5 h at room temperature. Flash column chromatography (2−20% EtOAc/petroleum ether) gave **282** as a white solid (428 mg, 1.83 mmol, 18% yield). **MP** 65–67 °C. **IR** (film) ν_{max} 3334, 2978, 1690, 1493, 1366, 1164, 698 cm^{-1}. **^{1}H NMR** (400 MHz, $CDCl_3$) δ 7.35 – 7.23 (m, 5H, H^9 + H^{10} + H^{11}), 5.98 (ddd, J = 15.5, 10.1, 5.4 Hz, 1H, H^6), 5.28 (bs, 1H, H^5), 5.24 – 5.17 (m, 2H, H^7), 4.96 (bs, 1H, H^1), 1.44 (s, 9H, H^4). **^{13}C NMR** (101 MHz, $CDCl_3$) δ 155.1 (C^2), 141.2 (C^8), 138.1 (C^6), 128.7 (C^9/C^{10}/C^{11}), 127.5 (C^9/C^{10}/C^{11}), 127.1 (C^9/C^{10}/C^{11}), 115.5 (C^7), 79.7 (C^3), 56.7 (C^5), 28.4 (C^4). **HRMS** (ESI-TOF) m/z: [M + Na]$^+$ Calcd for $C_{14}H_{19}NO_2Na$ 256.1308; Found 256.1301. Spectral data are in agreement with the literature.[211]

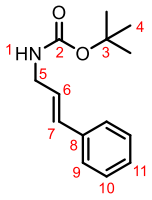

In addition, *tert*-butyl cinnamylcarbamate **283** was afforded as a white solid (520 mg, 2.23 mmol, 22% yield). **MP** 79–80 °C. **IR** (film) ν_{max} 3346, 2977, 1690, 1497, 1366, 1248, 1164, 743, 693 cm^{-1}. **^{1}H NMR** (400 MHz, $CDCl_3$) δ 7.38 – 7.34 (m, 2H, H^{10}), 7.33 – 7.28 (m, 2H, H^9), 7.25 – 7.21 (m, 1H, H^{11}), 6.50 (dt, *J* = 15.9, 1.6 Hz, 1H, H^7), 6.19 (dt, *J* = 15.9, 6.1 Hz, 1H, H^6), 4.71 (bs, 1H, H^1), 3.91 (t, *J* = 6.1 Hz, 2H, H^5), 1.47 (s, 9H, H^4). **^{13}C NMR** (101 MHz, $CDCl_3$) δ 155.9 (C^2), 136.8 (C^8), 131.5 (C^7), 128.7 (C^9), 127.7 (C^{11}), 126.5 (C^6), 126.5 (C^{10}), 79.6 (C^3), 42.8 (C^5), 28.5 (C^4). **HRMS** (ESI-TOF) m/z: $[M + Na]^+$ Calcd for $C_{14}H_{19}NO_2Na$ 256.1308; Found 256.1313. Spectral data agree with the literature.[212]

***tert*-Butyl penta-1,4-dien-3-ylcarbamate (284)**

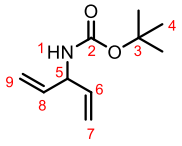

Reaction performed on 22.0 mmol scale following general procedure **2D** using 1,4-pentadien-3-ol (2.14 mL, 22.0 mmol, 1.00 equiv.), **264** (5.39 g, 24.8 mmol, 1.13 equiv.), triphenylphosphine (6.35 g, 24.2 mmol, 1.10 equiv.) and DIAD (4.76 mL, 24.2 mmol, 1.10 equiv.) in anhydrous THF (169 mL), which was stirred for 20 h at 0 °C to room temperature. The reaction intermediate was redissolved in THF (71 mL) and H_2O (28 mL), and stirred with LiOH (2.63 g, 110 mmol, 5.00 equiv.) for 22.5 h at room temperature. Flash column chromatography (2−16% EtOAc/petroleum ether) gave **284** as a yellow liquid (621 mg, 3.39 mmol, 15% yield). **IR** (film) ν_{max} 3336, 2979, 1690, 1514, 1366, 1244, 1164 1071 cm^{-1}. **^{1}H NMR** (400 MHz, $CDCl_3$) δ 5.82 (ddd, *J* = 17.2, 10.4, 5.4 Hz, 2H, H^6 + H^8), 5.23 – 5.13 (m, 4H, H^7 + H^9), 4.69 (bs, 1H, H^5), 4.56 (bs, 1H, H^1), 1.45 (s, 9H, H^4). **^{13}C NMR** (101 MHz, $CDCl_3$) δ 155.3 (C^2), 137.3 (C^6 + C^8), 115.6 (C^7 + C^9), 79.8 (C^3), 54.6 (C^5), 28.5 (C^4). **HRMS** (ESI-TOF) m/z: $[M + Na]^+$ Calcd for $C_{10}H_{17}NO_2Na$ 206.1151; Found 206.1156.

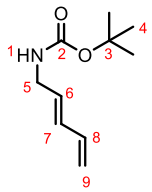

In addition, *tert*-butyl (*E*)-penta-2,4-dien-1-ylcarbamate **285** was afforded as a yellow liquid (1.02 g, 5.59 mmol, 25% yield). **IR** (film) ν_{max} 3347, 2977, 1690, 1513, 1366, 1249, 1165, 1005 cm^{-1}. **^{1}H NMR**

(400 MHz, $CDCl_3$) δ 6.31 (dt, *J* = 16.9, 10.2 Hz, 1H, H^8), 6.21 – 6.09 (m, 1H, H^7), 5.68 (dt, *J* = 15.1, 6.0 Hz, 1H, H^6), 5.21 – 5.14 (m, 1H, H^9), 5.09 – 5.04 (m, 1H, H^9), 4.57 (bs, 1H, H^1), 3.77 (d, *J* = 6.0 Hz, 2H, H^5), 1.45 (s, 9H, H^4). **^{13}C NMR** (101 MHz, $CDCl_3$) δ 155.9 (C^2), 136.3 (C^8), 132.3 (C^7), 130.5 (C^6), 117.4 (C^9), 79.6 (C^3), 42.4 (C^5), 28.5 (C^4). **HRMS** (ESI-TOF) m/z: $[M + Na]^+$ Calcd for $C_{10}H_{17}NO_2Na$ 206.1151; Found 206.1151. Spectral data are in agreement with the literature.[213]

***tert*-Butyl ((2*E*,4*E*)-hexa-2,4-dien-1-yl)carbamate (286)**[1]

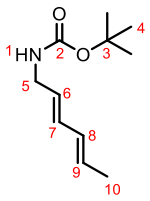

Reaction performed on 15.0 mmol scale following general procedure **2D** using *trans,trans*-2,4-hexadien-1-ol (1.69 mL, 15.0 mmol, 1.00 equiv.), **264** (3.55 g, 16.4 mmol, 1.09 equiv.), triphenylphosphine (4.33 g, 16.5 mmol, 1.10 equiv.) and DIAD (3.25 mL, 16.5 mmol, 1.10 equiv.) in anhydrous THF (115 mL), which was stirred for 15 h at 0 °C to room temperature. The reaction intermediate was redissolved in THF (48 mL) and H_2O (19 mL), and stirred with LiOH (1.79 g, 75.0 mmol, 5.00 equiv.) for 2 h at room temperature. Flash column chromatography (1−12% EtOAc/petroleum ether) gave **286** as a pale-yellow solid (2.24 g, 11.4 mmol, 76% yield; containing traces of isomeric products). **MP** 47–48 °C. **IR** (film) ν_{max} 3348, 2978, 1694, 1164, 987, 908, 730 cm^{-1}. **^{1}H NMR** (400 MHz, $CDCl_3$) (suspected mixture of *E,E* to *Z,Z*, *Z,E*, and *E,Z* in a 0.84:0.16 ratio; only major *E,E* shown) δ 6.10 – 5.86 (m, 2H, H^7 + H^8), 5.56 (dq, *J* = 13.6, 6.8 Hz, 1H, H^9), 5.43 (dt, *J* = 14.2, 6.4 Hz, 1H, H^6), 4.81 (bs, 1H, H^1), 3.64 (t, *J* = 6.4 Hz, 2H, H^5), 1.65 (d, *J* = 6.8 Hz, 3H, H^{10}), 1.35 (s, 9H, H^4). **^{13}C NMR** (101 MHz, $CDCl_3$) (suspected mixture of *E,E* to *Z,Z*, *Z,E*, and *E,Z* in a 0.84:0.16 ratio; only major *E,E* shown) δ 155.7 (C^2), 131.7 (C^7), 130.7 (C^8), 129.1 (C^9), 127.0 (C^6), 78.9 (C^3), 42.2 (C^5), 28.3 (C^4), 17.9 (C^{10}). **HRMS** (ESI-TOF) m/z: $[M + Na]^+$ Calcd for $C_{11}H_{19}NO_2Na$ 220.1308; Found 220.1305. Spectral data of the major product (*E,E*) are in agreement with the literature.[214]

***tert*-Butyl (2-methylenebut-3-en-1-yl)carbamate (287)**

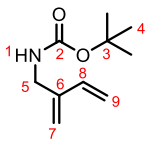

The starting reagent 2-methylenebut-3-en-1-ol was synthesised by following a literature procedure[215] using propargyl alcohol (0.58 mL, 10 mmol, 1.0 equiv.) and Cu(I)I (952 mg, 5.00 mmol, 0.500 equiv.)

in anhydrous toluene (13.3 mL, 1.33 mL/mmol) and vinylmagnesium bromide (1.0 M in THF; 30 mL, 30 mmol, 3.0 equiv.), which was stirred for 20.5 h at room temperature. The reagent was used crude in the next step. **^{1}H NMR** (400 MHz, CDCl3) δ 6.40 (dd, *J* = 17.9, 11.1 Hz, 1H), 5.38 – 5.24 (m, 2H), 5.23 – 5.09 (m, 2H), 4.35 (t, *J* = 1.2 Hz, 2H), 1.55 (bs, 1H). **^{13}C NMR** (101 MHz, $CDCl_3$) δ 145.4, 136.5, 115.8, 114.3, 62.8.

Reaction performed on 10 mmol scale following general procedure **2D** using 2-methylenebut-3-en-1-ol (10 mmol, 1.0 equiv.), **264** (2.41 g, 11.1 mmol, 1.11 equiv.), triphenylphosphine (2.89 g, 11.0 mmol, 1.10 equiv.) and DIAD (2.17 mL, 11.0 mmol, 1.10 equiv.) in anhydrous THF (77 mL), which was stirred for 22 h at 0 °C to room temperature. The reaction intermediate was redissolved in THF (32 mL) and H_2O (13 mL), and stirred with LiOH (1.20 g, 50.0 mmol, 5.00 equiv.) for 23 h at room temperature. Flash column chromatography (1−14% EtOAc/petroleum ether) gave **287** as a pale-yellow oil (716 mg, 3.91 mmol, 39% yield). **IR** (film) ν_{max} 3352, 2925, 1702, 1514, 1366, 1249, 1171 cm^{-1}. **^{1}H NMR** (400 MHz, $CDCl_3$) δ 6.38 (ddd, *J* = 17.8, 11.1, 0.4 Hz, 1H, H^8), 5.27 (d, *J* = 17.8 Hz, 1H, H^9), 5.16 – 5.09 (m, 3H, H^7 + H^9), 4.62 (bs, 1H, H^1), 3.94 (s, 2H, H^5), 1.45 (s, 9H, H^4). **^{13}C NMR** (101 MHz, $CDCl_3$) δ 155.9 (C^2), 143.1 (C^6), 136.9 (C^8), 116.4 (C^7), 114.4 (C^9), 79.6 (C^3), 41.7 (C^5), 28.5 (C^4). **HRMS** (ESI-TOF) m/z: $[M + H]^+$ Calcd for $C_{10}H_{18}NO_2$ 184.1332; Found 184.1330. Analytical data are in agreement with the literature.[216]

***tert*-Butyl (*E*)-(3-(trimethylsilyl)allyl)carbamate (288)**[1]

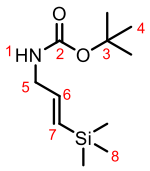

Reaction performed on 3.84 mmol scale following general procedure **2D** using *trans*-3-(trimethylsilyl)allyl alcohol (590 µL, 3.84 mmol, 1.00 equiv.), **264** (1.29 g, 5.94 mmol, 1.55 equiv.), triphenylphosphine (1.56 g, 5.94 mmol, 1.55 equiv.) and DIAD (1.17 mL, 5.94 mmol, 1.55 equiv.) in anhydrous THF (41 mL), which was stirred for 16 h at 0 °C to room temperature. The reaction intermediate was redissolved in THF (17.4 mL) and H_2O (6.8 mL), and stirred with LiOH (647 mg, 27.0 mmol, 5.00 equiv.) for 3 h at room temperature. Flash column chromatography (5−40% acetone/petroleum ether) gave **288** as a pale-yellow oil (830 mg, 3.62 mmol, 94% yield). **IR** (film) ν_{max} 3347, 2956, 2956, 1694, 1513, 1247, 1171, 851, 836 cm^{-1}. **^{1}H NMR** (400 MHz, $CDCl_3$) δ 6.00 (dt, *J* = 18.6, 4.8 Hz, 1H, H^6), 5.79 (dt, *J* = 18.6, 1.7 Hz, 1H, H^7), 4.60 (bs, 1H, H^1), 3.78 (bs, 2H, H^5), 1.45 (s, 9H, H^4), 0.05 (s, 9H, H^8). **^{13}C NMR** (101 MHz, $CDCl_3$) δ 155.9 (C^2), 142.4 (C^6), 130.6 (C^7), 79.5 (C^3), 45.2 (C^5), 28.5 (C^4), -1.2 (C^8). **HRMS** (ESI-TOF) m/z: $[M + Na]^+$ Calcd for $C_{11}H_{23}NO_2SiNa$ 252.1390; Found 252.1398. Spectral data are in agreement with the literature.[217]

***tert*-Butyl (*E*)-(4,4,4-trifluorobut-2-en-1-yl)carbamate (289)**[1]

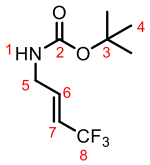

Reaction performed on 6.49 mmol scale following general procedure **2D** using (*E*)-4,4,4-trifluorobut-2-en-1-ol (660 µL, 6.49 mmol, 1.00 equiv.), **264** (1.56 g, 7.15 mmol, 1.10 equiv.), triphenylphosphine (1.88 g, 7.15 mmol, 1.10 equiv.) and DIAD (1.41 mL, 7.15 mmol, 1.10 equiv.) in anhydrous THF (50 mL), which was stirred for 23 h at 0 °C to room temperature. The reaction intermediate was redissolved in THF (21 mL) and H_2O (8 mL), and stirred with LiOH (778 mg, 32.5 mmol, 5.01 equiv.) for 3 h at room temperature. Flash column chromatography (4−32% EtOAc/petroleum ether) gave **289** as a yellow oil (1.33 g, 5.89 mmol, 91% yield; corrected for residual solvents present). **IR** (film) ν_{max} 3345, 2982, 1685, 1269, 1250, 1117 cm^{-1}. **^{1}H NMR** (400 MHz, $CDCl_3$) δ 6.43 – 6.30 (m, 1H, H^6), 5.74 (dqt, J = 15.7, 6.4, 1.8 Hz, 1H, H^7), 4.78 (bs, 1H, H^1), 3.86 (bs, 2H, H^5), 1.44 (s, 9H, H^4). **^{13}C NMR** (101 MHz, $CDCl_3$) δ 155.7 (C^2), 137.4 (q, J_F = 6.2 Hz, C^6), 123.1 (q, J_F = 269.0 Hz, C^8), 119.0 (q, J_F = 34.1 Hz, C^7), 80.2 (C^3), 40.8 (C^5), 28.4 (C^4). **^{19}F NMR** (377 MHz, $CDCl_3$): δ −64.1 (bs, 3F). **HRMS** (ESI-TOF) m/z: $[M + Na]^+$ Calcd for $C_9H_{14}NO_2F_3Na$ 248.0869; Found 248.0873.

***tert*-Butyl (5-((*tert*-butyldimethylsilyl)oxy)-2-methylenepentyl)carbamate (290)**

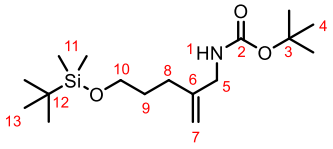

The starting reagent 5-((*tert*-butyldimethylsilyl)oxy)-2methylenepentan-1-ol was synthesised as followed:

tert-Butyldimethylsilyl 2-iodoethyl ether was synthesised by following a literature procedure[218] using 2-iodoethanol (1.95 mL, 25.0 mmol, 1.00 equiv.) and imidazole (2.55 g, 30.0 mmol, 1.20 equiv.) in anhydrous CH_2Cl_2 (86.0 mL, 3.45 mL/mmol) and *tert*-butyldimethylsilyl chloride (4.52 g, 30.0 mmol, 1.20 equiv.), which was stirred for 1 h at room temperature. Flash column chromatography (pentane) gave *tert*-butyldimethylsilyl 2-iodoethyl ether as a colourless liquid (quant.). **^{1}H NMR** (400 MHz, $CDCl_3$) δ 3.83 (t, J = 7.0 Hz, 2H), 3.20 (t, J = 7.0 Hz, 2H), 0.91 (s, 9H), 0.09 (s, 6H). **^{13}C NMR** (101 MHz, $CDCl_3$) δ 64.4, 26.0, 18.5, 7.2, -5.1. Spectral data are in agreement with literature.[218]

Subsequently, by following a literature procedure,[218] *tert*-butyldimethylsilyl 2-iodoethyl ether (7.06 g, 24.7 mmol, 1.00 equiv.) was reacted with *n*-BuLi (2.37 M in *n*-hexane; 26.4 mL, 62.5 mmol, 2.50

equiv.) in anhydrous Et_2O (40 mL, 0.64 mL/mmol), *N*,*N*,*N*,*N*-tetramethylethylenediamine (TMEDA; 9.37 mL, 62.5 mmol, 2.50 equiv.) and 2-methyl-2-propen-1-ol (2.63 mL, 31.3 mmol, 1.25 equiv.), which was stirred for a total of 34 h at −78 °C to room temperature. Flash column chromatography (0−10% acetone/petroleum ether) gave 5-((*tert*-butyldimethylsilyl)oxy)-2methylenepentan-1-ol as a pale-yellow oil (2.07 g, 8.98 mmol, 36% yield). **^{1}H NMR** (400 MHz, $CDCl_3$) δ 5.06 – 5.00 (m, 1H), 4.91 – 4.85 (m, 1H), 4.09 – 4.07 (m, 2H), 3.63 (t, *J* = 6.3 Hz, 2H), 2.17 (s, 2H), 2.13 (t, *J* = 7.7 Hz, 2H), 1.73 – 1.65 (m, 2H), 1.62 (bs, 1H), 0.89 (s, 9H), 0.05 (s, 6H). **^{13}C NMR** (101 MHz, $CDCl_3$) δ 148.9, 109.6, 66.2, 62.9, 31.1, 29.4, 26.1, 18.5, -5.2. Spectral data are in agreement with literature.[218]

Reaction performed on 8.95 mmol scale following general procedure **2D** using 5-((*tert*-butyldimethylsilyl)oxy)-2methylenepentan-1-ol (2.06 g, 8.95 mmol, 1.00 equiv.), **264** (2.14 g, 9.85 mmol, 1.10 equiv.), triphenylphosphine (2.58 g, 9.85 mmol, 1.10 equiv.) and DIAD (1.94 mL, 9.85 mmol, 1.10 equiv.) in anhydrous THF (69 mL), which was stirred for 16 h at 0 °C to room temperature. The reaction intermediate was redissolved in THF (29 mL) and H_2O (11 mL), and stirred with LiOH (1.07 g, 44.8 mmol, 5.00 equiv.) for 2 h at room temperature. Flash column chromatography (2−10% EtOAc/petroleum ether) gave **290** as a pale-yellow oil (2.53 g, 7.68 mmol, 86% yield). **IR** (film) ν_{max} 3352, 2954, 2929, 2857, 1700, 1511, 1366, 1251, 1169, 1101, 834, 774 cm^{-1}. **^{1}H NMR** (400 MHz, $CDCl_3$) δ 4.90 – 4.88 (m, 1H, H^7), 4.84 – 4.83 (m, 1H, H^7), 4.63 (bs, 1H, H^1), 3.69 (d, *J* = 6.0 Hz, 2H, H^5), 3.61 (t, *J* = 6.3 Hz, 2H, H^{10}), 2.08 (t, *J* = 7.5 Hz, 2H, H^8), 1.71 – 1.63 (m, 2H, H^9), 1.45 (s, 9H, H^4), 0.89 (s, 9H, H^{13}), 0.04 (s, 6H, H^{11}). **^{13}C NMR** (101 MHz, $CDCl_3$) δ 156.0 (C^2), 146.4 (C^6), 109.8 (C^7), 79.4 (C^3), 62.8 (C^{10}), 45.4 (C^5), 30.9 (C^9), 30.3 (C^8), 28.6 (C^4), 26.1 (C^{13}), 18.5 (C^{12}), -5.2 (C^{11}). **HRMS** (ESI-TOF) m/z: $[M + H]^+$ Calcd for $C_{17}H_{36}NO_3Si$ 330.2459; Found 330.2454.

***tert*-Butyl (2-methylenebut-3-yn-1-yl)carbamate (291)**

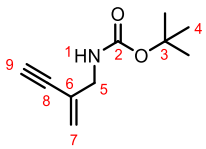

The starting reagent 2-methylene-4-(trimethylsilyl)but-3-yn-1-ol was synthesised as followed:

2-Iodoprop-2-en-1-ol was synthesised by following a literature procedure[219] using NaH (7.49 g, 50.0 mmol, 2.00 equiv.) in MeCN (40 mL, 1.6 mL/mmol) and H_2O (0.54 mL, 30 mmol, 1.2 equiv.), trimethylsilyl chloride (5.43 g, 50.0 mmol, 2.00 equiv.) and propargyl alcohol (1.46 mL, 25.0 mmol, 1.00 equiv.), which was stirred for 1.5 h at room temperature. Flash column chromatography (5−40% acetone/petroleum ether) gave 2-iodoprop-2-en-1-ol as a yellow liquid (1.86 g, 10.1 mmol, 40% yield). **^{1}H NMR** (400 MHz, $CDCl_3$) δ 6.39 (q, *J* = 1.7 Hz, 1H), 5.89 – 5.84 (m, 1H), 4.18 (t, *J* = 1.4 Hz, 2H),

1.99 (bs, 1H). **^{13}C NMR** (101 MHz, $CDCl_3$) δ 124.6, 110.6, 71.2. Spectral data are in agreement with the literature.[219]

Subsequently, by following a literature procedure,[220,221] 2-iodoprop-2-en-1-ol (1.84 g, 10.0 mmol, 1.00 equiv.) in anhydrous THF (20 mL, 2.0 mL/mmol) was reacted with Cu(I)I (133 mg, 0.698 mmol, 7 mol%) and $Pd(PPh_3)_4$ (347 mg, 0.300 mmol, 3 mol%) in anhydrous THF (32.0 mL, 45.5 mL/mmol), (trimethylsilyl)acetylene (1.80 mL, 13.0 mmol, 1.30 equiv.) and triethylamine (1.81 mL, 13.0 mmol, 1.30 equiv.), which was stirred for 19 h at room temperature. Flash column chromatography (5−40% acetone/petroleum ether) gave 2-methylene-4-(trimethylsilyl)but-3-yn-1-ol as a pale-yellow oil (925 mg, 5.99 mmol, 60% yield). **IR** (film) ν_{max} 3360, 2960, 2147, 1250, 1057, 839, 760 cm^{-1}. **^{1}H NMR** (400 MHz, $CDCl_3$) δ 5.54 (q, *J* = 1.6 Hz, 1H), 5.52 (q, *J* = 1.4 Hz, 1H), 4.13 (t, *J* = 1.5 Hz, 2H), 1.76 (bs, 1H), 0.20 (s, 9H). **^{13}C NMR** (101 MHz, $CDCl_3$) δ 131.4, 121.4, 102.8, 96.4, 65.3, 0.0. **HRMS** (ESI-TOF) m/z: $[M + H]^+$ Calcd for $C_8H_{15}OSi$ 154.0808; Found 154.0808. Analytical data are in agreement with the literature.[222]

Reaction performed on 5.92 mmol scale following general procedure **2D** using 2-methylene-4-(trimethylsilyl)but-3-yn-1-ol (913 mg, 5.92 mmol, 1.00 equiv.), **264** (1.41 g, 6.51 mmol, 1.10 equiv.), triphenylphosphine (1.71 g, 6.51 mmol, 1.10 equiv.) and DIAD (1.28 mL, 6.51 mmol, 1.10 equiv.) in anhydrous THF (46 mL), which was stirred for 18 h at 0 °C to room temperature. The reaction intermediate was redissolved in THF (19 mL) and H_2O (7.4 mL), and stirred with LiOH (709 mg, 29.6 mmol, 5.00 equiv.) for 4 h at room temperature. Flash column chromatography (3−28% EtOAc/petroleum ether) gave **291** as a pale-yellow oil (854 mg, 4.71 mmol, 80% yield). **IR** (film) ν_{max} 3298, 2978, 1696, 1510, 1366, 1283, 1250, 1168, 1051, 909, 641 cm^{-1}. **^{1}H NMR** (400 MHz, $CDCl_3$) δ 5.55 – 5.49 (m, 1H, H^7), 5.47 (bs, 1H, H^7), 4.79 (bs, 1H, H^1), 3.80 (d, *J* = 4.7 Hz, 2H, H^5), 2.93 (s, 1H, H^9), 1.44 (s, 9H, H^4). **^{13}C NMR** (101 MHz, $CDCl_3$) δ 155.7 (C^2), 128.1 (C^6), 123.0 (C^7), 82.1 (C^8), 79.8 (C^3), 78.6 (C^9), 45.3 (C^5), 28.5 (C^4). **HRMS** (ESI-TOF) m/z: $[M + H - t\text{-Bu}]^+$ Calcd for $C_6H_8NO_2$ 126.0550; Found 126.0547.

tert-Butyl (4-_tert_-butyldimethylsilyl)-2-methylenebut-3-yn-1-yl)carbamate (292)

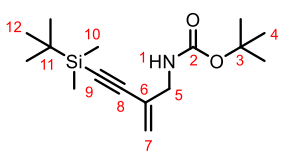

An oven-dried flask containing a magnetic stir bar was sealed with a suba seal, placed under anhydrous N_2, and charged with **291** (854 mg, 4.71 mmol, 1.00 equiv.) and anhydrous THF (28.0 mL, 6.25 mL/mmol). *n*-BuLi (1.60 M in *n*-hexane; 5.89 mL, 9.42 mmol, 2.00 equiv.) was then added dropwise at −70 °C, and the reaction mixture was stirred at −70 °C for 30 min. *tert*-Butyldimethylsilyl chloride

(1.56 g, 10.4 mmol, 2.21 equiv.) in anhydrous THF (2.6 mL, 0.25 mL/mmol) was added dropwise at −70 °C and the reaction mixture was stirred at −60 °C for 1 h. After warming the reaction mixture up to room temperature, acetic acid (0.25 M; 19 mL) was added and stirred for 1 h at room temperature. Then an aqueous solution of NH_4Cl, an aqueous solution of NaCl and EtOAc were added, and the organic phase was extracted. The aqueous phase was washed with EtOAc (2×) and then the organic phases were combined, dried over $MgSO_4$, filtered, and concentrated *in vacuo*. Flash column chromatography (0−10% Et_2O/petroleum ether) gave **292** as a white solid (759 mg, 2.57 mmol, 55% yield). **MP** 56−57 °C. **IR** (film) ν_{max} 3347, 2954, 2929, 2857, 2146, 1699, 1510, 1366, 1249, 1167, 837, 774, 680 cm^{-1}. **^{1}H NMR** (400 MHz, $CDCl_3$) δ 5.47 (q, *J* = 1.3 Hz, 1H, H^7), 5.40 (q, *J* = 1.5 Hz, 1H, H^7), 4.76 (bs, 1H, H^1), 3.79 (d, *J* = 5.8 Hz, 2H, H^5), 1.44 (s, 9H, H^4), 0.94 (s, 9H, H^{12}), 0.12 (s, 6H, H^{10}). **^{13}C NMR** (101 MHz, $CDCl_3$) δ 155.7 (C^2), 129.0 (C^6), 121.8 (C^7), 104.0 (C^8), 94.4 (C^9), 79.7 (C^3), 45.3 (C^5), 28.5 (C^4), 26.2 (C^{12}), 16.7 (C^{11}), -4.5 (C^{10}). **HRMS** (ESI-TOF) m/z: $[M + H]^+$ Calcd for $C_{16}H_{30}NO_2Si$ 296.2040; Found 296.2035.

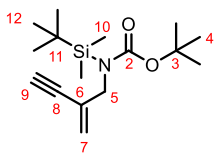

292-1

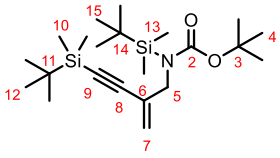

292-2

In addition, *tert*-butyl (*tert*-butyldimethylsilyl)(2-methylenebut-3-yn-1-yl)carbamate **292-1** and *tert*-butyl (*tert*-butyldimethylsilyl)(4-(*tert*-butyldimethylsilyl)-2-methylenebut-3-yn-1-yl)carbamate **292-2** were afforded in a mixture with a 0.25:1 ratio, as a pale-yellow oil (**292-1**: 27 mg, 0.091 mmol, 2% yield; **292-2**: 107 mg, 0.261 mmol, 6% yield). **IR** (film) ν_{max} 2955, 2930, 2858, 2146, 1690, 1366, 1251, 1162, 908, 838, 824, 775, 732 cm^{-1}. **^{1}H NMR** (400 MHz, $CDCl_3$) δ 5.52 (q, *J* = 1.7 Hz, 0.25H, $\underline{H^7}$), 5.46 (q, *J* = 1.7 Hz, 1H, H^7), 5.31 (q, *J* = 1.5 Hz, 0.25H, $\underline{H^7}$), 5.26 (q, *J* = 1.8 Hz, 1H, H^7), 3.81 (s, 0.50H, $\underline{H^5}$), 3.77 (s, 2H, H^5), 2.91 (s, 0.25H, $\underline{H^9}$), 1.46 (s, 11.25H, $\underline{H^4}$ + H^4), 0.94 – 0.93 (m, 20.25H, $\underline{H^{12}}$ + H^{12} + H^{15}), 0.26 (s, 6H, H^{10}), 0.26 (s, 1.5H, $\underline{H^{10}}$), 0.11 (s, 6H, H^{13}). **^{13}C NMR** (101 MHz, $CDCl_3$) δ 158.3 (C^2 + C^2), 120.9 ($\underline{C^7}$), 120.1 (C^7), 104.7 ($\underline{C^8}$ + C^8), 93.7 (C^9), 80.4 ($\underline{C^3}$ + C^3), 78.4 ($\underline{C^9}$), 49.6 (C^5), 49.5 ($\underline{C^5}$), 28.5 ($\underline{C^4}$ + C^4), 27.2 (C^{12}), 26.3 ($\underline{C^{12}}$ + C^{15}), 19.8 ($\underline{C^{11}}$ + C^{11}), 16.8 (C^{14}), -3.0 ($\underline{C^{10}}$ + C^{10}), -4.5 (C^{13}). **292-1**: **HRMS** (ESI-TOF) m/z: $[M + H - t\text{-Bu}]^+$ Calcd for $C_{12}H_{22}NO_2Si$ 240.1414; Found 240.1413. **292-2**: **HRMS** (ESI-TOF) m/z: $[M + H - t\text{-Bu}]^+$ Calcd for $C_{18}H_{36}NO_2Si$ 354.2279; Found 354.2279.

***tert*-Butyl (*E*)-(3-(4,4,5,5-tetramethyl-1,3,2-dioxaborolan-2-yl)allyl)carbamate (293)**

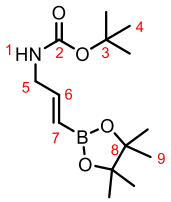

An oven-dried flask containing a magnetic stir bar was sealed with a suba seal, placed under anhydrous N_2, and charged with *trans*-2-chloromethylvinylboronic acid pinacol ester (680 µL, 3.45 mmol, 1.00 equiv.) and anhydrous DMF (5.80 mL, 1.67 mL/mmol). **264** (973 mg, 4.48 mmol, 1.30 equiv.) and KO*t*Bu (503 mg, 4.48 mmol, 1.30 equiv.) were added, and the reaction mixture was stirred for 4 h at 60 °C. After cooling down the reaction mixture to room temperature, CH_2Cl_2 (12 mL, 3.3 mL/mmol) was added and the organic layer was washed with H_2O (2×; 12 mL, 3.3 mL/mmol). The organic layer was dried over Na_2SO_4, filtered, and concentrated *in vacuo*. The reaction intermediate was redissolved in THF (11 mL, 3.2 mL/mmol) and H_2O (4.00 mL, 1.25 mL/mmol), and stirred with LiOH (413 mg, 17.3 mmol, 5.00 equiv.) for 2 h at room temperature. After addition of H_2O (41 mL; 12 mL/mmol) and EtOAc (41 mL; 12 mL/mmol), the organic phase was extracted. The aqueous phase was washed with EtOAc (3×; 21 mL; 6.0 mL/mmol) and then the organic phases were combined, dried over $MgSO_4$, filtered, and concentrated *in vacuo*. Flash column chromatography (6−48% EtOAc/petroleum ether) gave **293** as a pale-yellow oil (581 mg, 2.05 mmol, 59% yield). **IR** (film) ν_{max} 3356, 2977, 1696, 1648, 1520, 165, 1322, 1247, 1143, 971, 850 cm^{-1}. **^{1}H NMR** (400 MHz, $CDCl_3$) δ 6.58 (dt, *J* = 18.1, 4.7 Hz, 1H, H^6), 5.57 (dt, *J* = 18.1, 1.9 Hz, 1H, H^7), 4.63 (bs, 1H, H^1), 3.83 (s, 2H, H^5), 1.43 (s, 9H, H^4), 1.26 (s, 12H, H^9). **^{13}C NMR** (101 MHz, $CDCl_3$) δ 155.9 (C^2), 149.5 (C^6), 118.4 (broad, C^7), 83.4 (C^8), 79.5 (C^3), 44.1 (C^5), 28.5 (C^4), 24.9 (C^9). **HRMS** (ESI-TOF) m/z: $[M + Na]^+$ Calcd for $C_{14}H_{26}BNO_4Na$ 306.1850; Found 306.1859.[223]

***N*-Methyl-1-methylallylamine hydrochloride salt (294)**[1]

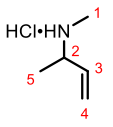

Reaction performed on 8.04 mmol scale following general procedure **2E** using **269** (1.38 g, 8.04 mmol, 1.00 equiv.), NaH (644 mg, 16.1 mmol, 2.00 equiv.) and iodomethane (2.00 mL, 32.2 mmol, 4.00 equiv.) in anhydrous THF (13.4 mL), which was stirred for 17 h at 0 °C to room temperature. The reaction intermediate was redissolved in CH_2Cl_2 (42.3 mL) and stirred with TFA (6.80 mL, 89.2 mmol, 11.1 equiv.) for 2.5 d at room temperature. The product was redissolved in MeOH (24.4 mL) and stirred with HCl (1.25 M in MeOH; 21.5 mL, 26.9 mmol, 3.35 equiv.) for 5 min at room temperature. Yield:

82% (804 mg, 6.61 mmol). White solid. **MP** 101–102 °C. **IR** (film) ν_{max} 3400, 2958, 2734, 1469, 751 cm^{-1}. **^{1}H NMR** (400 MHz, $MeOD_4$) δ 5.85 (ddd, *J* = 17.1, 10.3, 8.2 Hz, 1H, H^3), 5.56 – 5.44 (m, 2H, H^4), 3.75 (p, *J* = 7.0 Hz, 1H, H^2), 2.63 (s, 3H, H^1), 1.43 (d, *J* = 6.7 Hz, 3H, H^5). **^{13}C NMR** (101 MHz, $MeOD_4$) δ 134.5 (C^3), 122.8 (C^4), 59.1 (C^2), 31.0 (C^1), 17.9 (C^5). **HRMS** (APCI) m/z: $[M + H]^+$ Calcd for $C_5H_{12}N$ 86.0964; Found 86.0961.

N-Methyl-(2-methyl-2-propen-1-amine hydrochloride salt (295)[1]

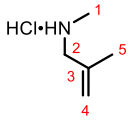

Reaction performed on 25.0 mmol scale following general procedure **2E** using **262** (4.27 g, 25.0 mmol, 1.00 equiv.), NaH (2.00 g, 50.0 mmol, 2.00 equiv.) and iodomethane (6.23 mL, 100 mmol, 4.00 equiv.) in anhydrous THF (42 mL), which was stirred for 3.5 h at 0 °C to room temperature. The reaction intermediate was redissolved in CH_2Cl_2 (132 mL) and stirred with TFA (21.0 mL, 278 mmol, 11.1 equiv.) for 13.5 h at room temperature. The product was redissolved in MeOH (76 mL) and stirred with HCl (1.25 M in MeOH; 67.0 mL, 84.0 mmol, 3.35 equiv.) for 5 min at room temperature. Yield: 90% (2.75 g, 22.6 mmol). White solid. **MP** 124–125 °C. **IR** (film) ν_{max} 3020, 1214, 744, 668 cm^{-1}. **^{1}H NMR** (400 MHz, $MeOD_4$) δ 5.20 – 5.18 (m, 1H, H^4), 5.15 – 5.12 (m, 1H, H^4), 3.60 (s, 2H, H^2), 2.71 (s, 3H, H^1), 1.87 (td, *J* = 1.0, 0.4 Hz, 3H, H^5). **^{13}C NMR** (101 MHz, $MeOD_4$) δ 137.8 (C^3), 117.9 (C^4), 55.1 (C^2), 33.3 (C^1), 20.7 (C^5). **HRMS** (APCI) m/z: $[M + H]^+$ Calcd for $C_5H_{12}N$ 86.0964; Found 86.0960.

N-Methylbut-2-en-1-amine hydrochloride salt (296)[1]

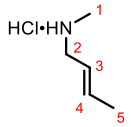

Reaction performed on 14.5 mmol scale following general procedure **2E** using **263** (2.48 g, 14.5 mmol, 1.00 equiv.), NaH (1.16 g, 29.0 mmol, 2.00 equiv.) and iodomethane (3.60 mL, 58.0 mmol, 4.00 equiv.) in anhydrous DMF (24 mL), which was stirred for 2 h at 0 °C to room temperature. The reaction intermediate was redissolved in CH_2Cl_2 (76 mL) and stirred with TFA (12.3 mL, 161 mmol, 11.1 equiv.) for 1 h at room temperature. The product was redissolved in MeOH (44 mL) and stirred with HCl (1.25 M in MeOH; 39.2 mL, 49.0 mmol, 3.35 equiv.) for 5 min at room temperature. Yield: 72% (1.27 g, 10.4 mmol). Pale-yellow solid. **MP** 66–67 °C. **IR** (film) ν_{max} 3365, 2484, 1220, 971, 775, 771 cm^{-1}. **^{1}H NMR** (400 MHz, $MeOD_4$) (suspected mixture of *E*:*Z* in a 0.95:0.05 ratio) δ 6.02 (dqt, *J* = 15.3, 6.6, 1.1 Hz, 1H, H^4), 5.57 (dtq, *J* = 15.3, 7.1, 1.7 Hz, 1H, H^3), 3.71 – 3.67 (m, 0.1H, *Z*-H^2), 3.55 (dt, *J* = 7.1, 1.1

Hz, 1.9H, *E*-H[2]), 2.68 (s, 0.1H, *Z*-H[1]), 2.65 (s, 2.9H, *E*-H[1]), 1.79 (ddt, *J* = 6.6, 1.7, 1.0 Hz, 2.9H, *E*-H[5]), 1.77 – 1.75 (m, 0.1H, *Z*-H[5]). **^{13}C NMR** (101 MHz, $MeOD_4$) δ 137.5 (C^4), 121.7 (C^3), 51.6 (C^2), 32.5 (C^1), 18.1 (C^5). **HRMS** (APCI) m/z: $[M + H]^+$ Calcd for $C_5H_{12}N$ 86.0964; Found 86.0960.

_N_-Methyl-(_E_)-hex-2-en-1-amine hydrochloride salt (297)[1]

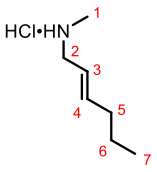

Reaction performed on 17.3 mmol scale following general procedure **2E** using **270** (3.45 g, 17.3 mmol, 1.00 equiv.), NaH (1.38 g, 34.6 mmol, 2.00 equiv.) and iodomethane (4.30 mL, 69.2 mmol, 4.00 equiv.) in anhydrous DMF (29 mL), which was stirred for 2 h at 0 °C to room temperature. The reaction intermediate was redissolved in CH_2Cl_2 (91 mL) and stirred with TFA (12.0 mL, 192 mmol, 11.1 equiv.) for 19.5 h at room temperature. The product was redissolved in MeOH (52 mL) and stirred with HCl (1.25 M in MeOH; 47.0 mL, 58.0 mmol, 3.35 equiv.) for 5 min at room temperature. Yield: 90% (2.32 g, 15.5 mmol). Off-white solid. **MP** 107–108 °C. **IR** (film) ν_{max} 3339, 2472, 2070, 1121, 973, 458 cm^{-1}. **^{1}H NMR** (400 MHz, $MeOD_4$) δ 6.01 (dtt, *J* = 15.0, 6.9, 1.2 Hz, 1H, H^4), 5.62 – 5.49 (m, 1H, H^3), 3.57 (d, *J* = 7.1 Hz, 2H, H^2), 2.65 (s, 3H, H^1), 2.11 (q, *J* = 7.1 Hz, 2H, H^5), 1.47 (h, *J* = 7.4 Hz, 2H, H^6), 0.94 (t, *J* = 7.4 Hz, 3H, H^7). **^{13}C NMR** (101 MHz, $MeOD_4$) δ 142.5 (C^4), 120.7 (C^3), 51.6 (C^2), 35.5 (C^5), 32.5 (C^1), 22.9 (C^6), 13.9 (C^7). **HRMS** (APCI) m/z: $[M + H]^+$ Calcd for $C_7H_{16}N$ 114.1277; Found 114.1272.

_N_-Methyl-(_R_)-oct-1-en-3-amine hydrochloride salt (298)[1]

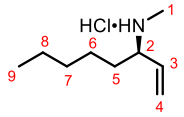

Reaction performed on 1.23 mmol scale following general procedure **2E** using **271** (279 mg, 1.23 mmol, 1.00 equiv.), NaH (98 mg, 2.5 mmol, 2.0 equiv.) and iodomethane (310 µL, 4.92 mmol, 4.00 equiv.) in anhydrous DMF (2.1 mL), which was stirred for 3 h at 0 °C to room temperature. The reaction intermediate was redissolved in CH_2Cl_2 (6.5 mL) and stirred with TFA (1.10 mL, 13.7 mmol, 11.1 equiv.) for 20 h at room temperature. The product was redissolved in MeOH (3.7 mL) and stirred with HCl (1.25 M in MeOH; 3.30 mL, 4.12 mmol, 3.35 equiv.) for 5 min at room temperature. Yield: 98% (215 mg, 1.21 mmol). Orange gum. $[\alpha]_D^{23} = +12$ (*c* = 0.96 in $CHCl_3$). **IR** (film) ν_{max} 3393, 2930, 2720, 1466, 772 cm^{-1}. **^{1}H NMR** (400 MHz, $MeOD_4$) δ 5.72 (ddd, *J* = 16.8, 10.3, 9.1 Hz, 1H, H^3), 5.58 – 5.50

(m, 2H, H^4), 3.56 (td, *J* = 9.6, 4.3 Hz, 1H, H^2), 2.62 (s, 3H, H^1), 1.87 – 1.77 (m, 1H, H^5), 1.70 – 1.59 (m, 1H, H^5), 1.42 – 1.28 (m, 6H, H^6 + H^7 + H^8), 0.91 (t, *J* = 6.6 Hz, 3H, H^9). **^{13}C NMR** (101 MHz, $MeOD_4$) δ 133.1 (C^3), 124.8 (C^4), 64.2 (C^2), 32.8 (C^5), 32.3 (C^7), 31.2 (C^1), 26.0 (C^6), 23.4 (C^8), 14.2 (C^9). **HRMS** (ESI-TOF) m/z: $[M + H]^+$ Calcd for $C_9H_{20}N$ 142.1590; Found 142.1586.

***N*-Methyl-(±)-oct-1-en-3-amine hydrochloride salt (±-298)**[1]

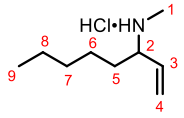

Reaction performed on 3.82 mmol scale following general procedure **2E** using **±-271** (869 mg, 3.82 mmol, 1.00 equiv.), NaH (306 mg, 7.65 mmol, 2.00 equiv.) and iodomethane (950 µL, 15.3 mmol, 4.00 equiv.) in anhydrous DMF (6.4 mL), which was stirred for 21.5 h at 0 °C to room temperature. The reaction intermediate was redissolved in CH_2Cl_2 (20.1 mL) and stirred with TFA (3.25 mL, 42.4 mmol, 11.1 equiv.) for 22 h at room temperature. The product was redissolved in MeOH (11.6 mL) and stirred with HCl (1.25 M in MeOH; 10.2 mL, 12.8 mmol, 3.35 equiv.) for 5 min at room temperature. Yield: 78% (532 mg, 2.99 mmol). Off-white solid. **MP** 94–95 °C. **IR** (film) ν_{max} 3404, 2956, 2931, 2861, 2723, 1465, 1022, 999, 935, 752 cm^{-1}. **^{1}H NMR** (400 MHz, $MeOD_4$) δ 5.76 (ddd, *J* = 16.6, 10.5, 9.2 Hz, 1H, H^3), 5.57 – 5.50 (m, 2H, H^4), 3.58 (td, *J* = 9.7, 4.3 Hz, 1H, H^2), 2.62 (s, 3H, H^1), 1.93 – 1.80 (m, 1H, H^5), 1.73 – 1.61 (m, 1H, H^5), 1.45 – 1.28 (m, 6H, H^6 + H^7 + H^8), 0.91 (t, *J* = 6.8 Hz, 3H, H^9). **^{13}C NMR** (101 MHz, $MeOD_4$) δ 133.2 (C^3), 124.7 (C^4), 64.2 (C^2), 32.8 (C^5), 32.3 (C^7), 31.2 (C^1), 26.0 (C^6), 23.4 (C^8), 14.3 (C^9). **HRMS** (ESI-TOF) m/z: $[M + H]^+$ Calcd for $C_9H_{20}N$ 142.1590; Found 142.1591.

***N*-Methyl-1-cyclohexyl-prop-2-en-1-amine hydrochloride salt (299)**

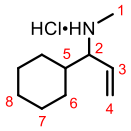

Reaction performed on 1.23 mmol scale following general procedure **2E** using **272** (295 mg, 1.23 mmol, 1.00 equiv.), NaH (98 mg, 2.5 mmol, 2.0 equiv.) and iodomethane (310 µL, 4.92 mmol, 4.00 equiv.) in anhydrous THF (2.1 mL), which was stirred for 46 h at 0 °C to room temperature. The reaction intermediate was redissolved in CH_2Cl_2 (6.5 mL) and stirred with TFA (1.05 mL, 13.7 mmol, 11.1 equiv.) for 31 h at room temperature. The product was redissolved in MeOH (3.7 mL) and stirred with HCl (1.25 M in MeOH; 3.30 mL, 4.12 mmol, 3.35 equiv.) for 5 min at room temperature. Yield: 70% (164 mg, 0.866 mmol). Brownish solid. **MP** 151−152 °C. **IR** (film) ν_{max} 3401, 2926, 2719, 1450, 1023, 1000, 937, 750 cm^{-1}. **^{1}H NMR** (400 MHz, $MeOD_4$) δ 5.77 (ddd, *J* = 16.9, 10.2, 9.5 Hz, 1H, H^3), 5.57

(dd, J = 10.2, 1.4 Hz, 1H, H^4), 5.49 (ddd, J = 16.9, 1.4, 0.5 Hz, 1H, H^4), 3.43 (dd, J = 9.5, 5.4 Hz, 1H, H^2), 2.62 (s, 3H, H^1), 1.85 – 1.73 (m, 4H, $H^5 + H^6 + H^7 + H^8$), 1.73 – 1.67 (m, 1H, H^7/H^8), 1.41 – 1.01 (m, 5H, $H^6 + H^7 + H^8$). **^{13}C NMR** (101 MHz, $MeOD_4$) δ 131.2 (C^3), 125.4 (C^4), 69.3 (C^2), 41.0 (C^5), 31.9 (C^1), 30.5 (C^6), 28.6 (C^6), 27.0 (C^7/C^8), 26.9 (C^7/C^8), 26.8 (C^7/C^8). **HRMS** (ESI-TOF) m/z: $[M + H]^+$ Calcd for $C_{10}H_{20}N$ 154.1590; Found 154.1587.

***N*-Methyl-2-cyclohexyl-prop-2-en-1-amine hydrochloride salt (300)**

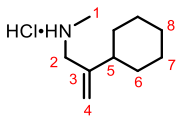

Reaction performed on 3.05 mmol scale following general procedure **2E** using **273** (730 mg, 3.05 mmol, 1.00 equiv.), NaH (244 mg, 6.10 mmol, 2.00 equiv.) and iodomethane (760 µL, 12.2 mmol, 4.00 equiv.) in anhydrous THF (5.1 mL), which was stirred for 4 h at 0 °C to room temperature. The reaction intermediate was redissolved in CH_2Cl_2 (16.1 mL) and stirred with TFA (2.60 mL, 33.9 mmol, 11.1 equiv.) for 15 h at room temperature. The product was redissolved in MeOH (9.2 mL) and stirred with HCl (1.25 M in MeOH; 8.20 mL, 10.2 mmol, 3.35 equiv.) for 5 min at room temperature. Yield: 86% (497 mg, 2.62 mmol). White solid. **MP** 169−170 °C. **IR** (film) ν_{max} 2924, 2774, 1219, 908, 772 cm^{-1}. **^{1}H NMR** (400 MHz, $MeOD_4$) δ 5.23 – 5.18 (m, 1H, H^4), 5.10 (t, J = 1.4 Hz, 1H, H^4), 3.65 – 3.60 (m, 2H, H^2), 2.71 (s, 3H, H^1), 1.97 (tt, J = 11.8, 2.4 Hz, 1H, H^5), 1.88 – 1.78 (m, 4H, $H^6 + H^7$), 1.79 – 1.68 (m, 1H, H^8), 1.45 – 1.29 (m, 2H, H^7), 1.30 – 1.14 (m, 3H, $H^6 + H^8$). **^{13}C NMR** (101 MHz, $MeOD_4$) δ 147.8 (C^3), 113.9 (C^4), 53.2 (C^2), 43.5 (C^5), 33.5 (C^1), 33.2 (C^6), 27.6 (C^7), 27.2 (C^8). **HRMS** (ESI-TOF) m/z: $[M + H]^+$ Calcd for $C_{10}H_{20}N$ 154.1590; Found 154.1594.

***N*-Methyl-(*E*)-3-cyclohexylprop-2-en-1-amine hydrochloride salt (301)**

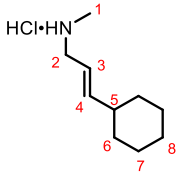

Reaction performed on 6.32 mmol scale following general procedure **2E** using **274** (1.51 g, 6.32 mmol, 1.00 equiv.), NaH (506 mg, 12.6 mmol, 2.00 equiv.) and iodomethane (1.57 mL, 25.3 mmol, 4.00 equiv.) in anhydrous THF (10.5 mL), which was stirred for 22 h at 0 °C to room temperature. The reaction intermediate was redissolved in CH_2Cl_2 (33.3 mL) and stirred with TFA (6.70 mL, 70.2 mmol, 11.1 equiv.) for 18 h at room temperature. The product was redissolved in MeOH (19 mL) and stirred with HCl (1.25 M in MeOH; 17.0 mL, 21.2 mmol, 3.35 equiv.) for 5 min at room temperature. Yield:

81% (976 mg, 5.15 mmol). White solid. **MP** 118–119 °C. **IR** (film) ν_{max} 3404, 2924, 2851, 2777, 2733, 2441, 1447, 1219, 971, 751 cm^{-1}. **^{1}H NMR** (400 MHz, $MeOD_4$) δ 5.95 (ddt, *J* = 15.5, 6.8, 1.0 Hz, 1H, H^4), 5.51 (dtd, *J* = 15.5, 7.1, 1.3 Hz, 1H, H^3), 3.55 (dt, *J* = 7.1, 1.0 Hz, 2H, H^2), 2.64 (s, 3H, H^1), 2.13 – 2.00 (m, 1H, H^5), 1.82 – 1.73 (m, 4H, H^6 + H^7), 1.72 – 1.64 (m, 1H, H^8), 1.40 – 1.08 (m, 5H, H^6 + H^7 + H^8). **^{13}C NMR** (101 MHz, $MeOD_4$) δ 148.1 (C^4), 118.1 (C^3), 51.8 (C^2), 41.9 (C^5), 33.5 (C^6), 32.5 (C^1), 27.1 (C^8), 26.9 (C^7). **HRMS** (nanospray) m/z: $[M + H]^+$ Calcd for $C_{10}H_{20}N$ 154.1596; Found 154.1600.

_N_-Methyl-1-((1_R_,5_S_)-6,6-dimethylbicyclo[3.1.1]hept-2-en-2-ylmethanamine hydrochloride salt (302)[1]

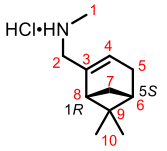

Reaction performed on 12.5 mmol scale following general procedure **2E** using **275** (3.15 g, 12.5 mmol, 1.00 equiv.), NaH (1.00 g, 25.1 mmol, 2.00 equiv.) and iodomethane (3.12 mL, 50.1 mmol, 4.00 equiv.) in anhydrous DMF (21 mL), which was stirred for 2 h at 0 °C to room temperature. The reaction intermediate was redissolved in CH_2Cl_2 (66 mL) and stirred with TFA (10.6 mL, 139 mmol, 11.1 equiv.) for 22 h at room temperature. The product was redissolved in MeOH (38 mL) and stirred with HCl (1.25 M in MeOH; 33.5 mL, 41.9 mmol, 3.35 equiv.) for 5 min at room temperature. Yield: 82% (2.07 g, 10.3 mmol). White solid. **MP** 215 – 216 °C. **IR** (film) ν_{max} 3339, 2945, 2490, 1024, 979 cm^{-1}. **^{1}H NMR** (400 MHz, $MeOD_4$) δ 5.81 – 5.77 (m, 1H, H^4), 3.53 (s, 2H, H^2), 2.67 (s, 3H, H^1), 2.53 (dt, *J* = 8.9, 5.6 Hz, 1H, H^5), 2.46 – 2.28 (m, 2H, H^5 + H^7), 2.24 (td, *J* = 5.6, 1.7 Hz, 1H, H^8), 2.15 (ttd, *J* = 5.6, 2.8, 1.2 Hz, 1H, H^6), 1.35 (s, 3H, H^{10}), 1.22 (d, *J* = 8.9 Hz, 1H, H^7), 0.89 (s, 3H, H^{10}). **^{13}C NMR** (101 MHz, $MeOD_4$) δ 140.4 (C^3), 127.3 (C^4), 54.5 (C^2), 45.3 (C^8), 41.7 (C^6), 39.1 (C^9), 33.2 (C^1), 32.5 (C^5/C^7), 32.4 (C^5/C^7), 26.3 (C^{10}), 21.4 (C^{10}). **HRMS** (APCI) m/z: $[M + H]^+$ Calcd for $C_{11}H_{20}N$ 166.1590; Found 166.1586.

***N*-Methyl-(*Z*)-2-(1,3,3-trimethylbicyclo[2.2.1]heptan-2-ylidene)ethan-1-amine hydrochloride salt (303)**

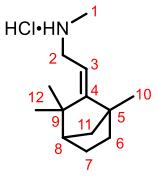

Reaction performed on 1.69 mmol scale following general procedure **2E** using **276** (472 mg, 1.69 mmol, 1.00 equiv.), NaH (135 mg, 3.38 mmol, 2.00 equiv.) and iodomethane (420 µL, 6.76 mmol, 4.00 equiv.) in anhydrous THF (2.8 mL), which was stirred for 2 h at 0 °C to room temperature. The reaction intermediate was redissolved in CH_2Cl_2 (9.0 mL) and stirred with TFA (1.44 mL, 18.8 mmol, 11.1 equiv.) for 16 h at room temperature. The product was redissolved in MeOH (5.1 mL) and stirred with HCl (1.25 M in MeOH; 4.50 mL, 5.66 mmol, 3.35 equiv.) for 5 min at room temperature. Yield: 64% (250 mg, 1.09 mmol). White solid. **MP** 273–274 °C. **IR** (film) ν_{max} 3339, 2468, 2244, 2212, 2070, 1121, 1092, 973, 772, 460 cm^{-1}. **^{1}H NMR** (400 MHz, $MeOD_4$) δ 5.03 (t, *J* = 7.3 Hz, 1H, H^3), 3.76 (d, *J* = 7.3 Hz, 2H, H^2), 2.69 (s, 3H, H^1), 1.84 – 1.77 (m, 2H, H^7 + H^8), 1.63 (dq, *J* = 9.9, 2.3 Hz, 1H, H^{11}), 1.60 – 1.53 (m, 2H, H^6 + H^7), 1.32 (dd, *J* = 9.9, 1.5 Hz, 1H, H^{11}), 1.26 (s, 3H, H^{12}), 1.26 – 1.22 (m, 1H, H^6), 1.21 (s, 3H, H^{10}), 1.19 (s, 3H, H^{12}). **^{13}C NMR** (101 MHz, $MeOD_4$) δ 167.9 (C^4), 106.3 (C^3), 52.3 (C^5), 50.8 (C^8), 48.1 (C^2), 44.7 (C^{11}), 44.0 (C^9), 36.5 (C^6), 32.8 (C^1), 27.8 (C^{12}), 26.2 (C^7), 25.9 (C^{12}), 19.2 (C^{10}). **HRMS** (ESI-TOF) m/z: $[M + H]^+$ Calcd for $C_{13}H_{24}N$ 194.1903; Found 194.1898.

***N*-Methyl-1-(cyclohex-1-en-1-yl)-methanamine hydrochloride salt (304)**

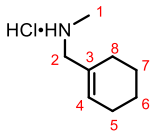

Reaction performed on 2.55 mmol scale following general procedure **2E** using **277** (540 mg, 2.55 mmol, 1.00 equiv.), NaH (204 mg, 5.10 mmol, 2.00 equiv.) and iodomethane (630 µL, 10.2 mmol, 4.00 equiv.) in anhydrous THF (4.3 mL), which was stirred for 4 h at 0 °C to room temperature. The reaction intermediate was redissolved in CH_2Cl_2 (13.5 mL) and stirred with TFA (2.20 mL, 28.3 mmol, 11.1 equiv.) for 15 h at room temperature. The product was redissolved in MeOH (7.7 mL) and stirred with HCl (1.25 M in MeOH; 6.80 mL, 8.54 mmol, 3.35 equiv.) for 5 min at room temperature. Yield: 90% (370 mg, 2.29 mmol). White solid. **MP** 135−136 °C. **IR** (film) ν_{max} 3351, 2478, 2071, 1121, 972, 772, 457 cm^{-1}. **^{1}H NMR** (400 MHz, $MeOD_4$) δ 5.94 – 5.90 (m, 1H, H^4), 3.49 (d, *J* = 0.7 Hz, 2H, H^2), 2.65 (s, 3H, H^1), 2.15 – 2.08 (m, 2H, H^5), 2.08 – 2.02 (m, 2H, H^8), 1.75 – 1.68 (m, 2H, H^7), 1.66 – 1.59 (m, 2H, H^6). **^{13}C NMR** (101 MHz, $MeOD_4$) δ 132.0 (C^3), 130.3 (C^4), 56.1 (C^2), 33.0 (C^1), 27.5 (C^8), 26.2

(C^5), 23.4 (C^7), 22.7 (C^6). **HRMS** (ESI-TOF) m/z: $[M + H]^+$ Calcd for $C_8H_{16}N$ 126.1277; Found 126.1279.

N-Methylcyclohex-2-en-1-amine hydrochloride salt (305)

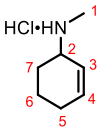

Reaction performed on 5.30 mmol scale following general procedure **2E** using **278** (1.05 g, 5.30 mmol, 1.00 equiv.), NaH (424 mg, 10.6 mmol, 2.00 equiv.) and iodomethane (1.32 mL, 21.2 mmol, 4.00 equiv.) in anhydrous THF (8.8 mL), which was stirred for 22 h at 0 °C to room temperature. The reaction intermediate was redissolved in CH_2Cl_2 (28 mL) and stirred with TFA (4.50 mL, 58.8 mmol, 11.1 equiv.) for 23 h at room temperature. The product was redissolved in MeOH (16 mL) and stirred with HCl (1.25 M in MeOH; 14.2 mL, 17.8 mmol, 3.35 equiv.) for 5 min at room temperature. Yield: 66% (514 mg, 3.48 mmol). Pale-yellow solid. **MP** 100–101 °C. **IR** (film) ν_{max} 3399, 2947, 2714, 1467, 1218, 1038, 924, 771, 744, 664 cm^{-1}. **^{1}H NMR** (400 MHz, $MeOD_4$) δ 6.22 – 6.13 (m, 1H, H^4), 5.81 – 5.72 (m, 1H, H^3), 3.79 – 3.70 (m, 1H, H^2), 2.70 (s, 3H, H^1), 2.17 – 2.08 (m, 3H, H^5 + H^7), 1.90 – 1.81 (m, 1H, H^6), 1.78 – 1.63 (m, 2H, H^6 + H^7). **^{13}C NMR** (101 MHz, $MeOD_4$) δ 136.8 (C^4), 122.3 (C^3), 55.6 (C^2), 30.5 (C^1), 26.1 (C^7), 25.6 (C^5), 20.1 (C^6). **HRMS** (nanospray) m/z: $[M + H]^+$ Calcd for $C_7H_{14}N$ 112.1126; Found 112.1128.

N-Methyl-2-phenylprop-2-en-1-amine hydrochloride salt (306)[1]

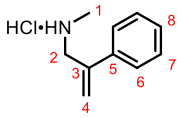

Reaction performed on 16.6 mmol scale following general procedure **2E** using **280** (3.86 g, 16.6 mmol, 1.00 equiv.), NaH (1.32 g, 33.1 mmol, 2.00 equiv.) and iodomethane (4.12 mL, 66.2 mmol, 4.00 equiv.) in anhydrous DMF (27.6 mL), which was stirred for 4.5 h at 0 °C to room temperature. The reaction intermediate was redissolved in CH_2Cl_2 (87 mL) and stirred with TFA (14.1 mL, 184 mmol, 11.1 equiv.) for 21.5 h at room temperature. The product was redissolved in MeOH (50 mL) and stirred with HCl (1.25 M in MeOH; 44.4 mL, 55.5 mmol, 3.35 equiv.) for 5 min at room temperature. Yield: 93% (2.82 g, 15.4 mmol). Greyish solid. **MP** 115–117 °C. **IR** (film) ν_{max} 3382, 2964, 2492, 1463, 973, 778, 766 cm^{-1}. **^{1}H NMR** (400 MHz, $MeOD_4$) δ 7.55 – 7.50 (m, 2H, H^6), 7.46 – 7.36 (m, 3H, H^7 + H^8), 5.72 (s, 1H, H^4), 5.53 (t, J = 1.2 Hz, 1H, H^4), 4.15 (s, 2H, H^2), 2.72 (s, 3H, H^1). **^{13}C NMR** (101 MHz, $MeOD_4$)

δ 141.4 (C^3), 138.5 (C^5), 130.1 (C^7), 130.0 (C^8), 127.4 (C^6), 119.8 (C^4), 53.0 (C^2), 33.4 (C^1). **HRMS** (ESI-TOF) m/z: $[M + H]^+$ Calcd for $C_{10}H_{14}N$ 148.1121; Found 148.1125.

***N*-Methyl-2-benzylprop-2-en-1-amine hydrochloride salt (307)**

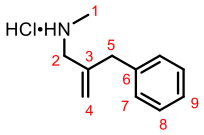

Reaction performed on 9.40 mmol scale following general procedure **2E** using **281** (2.33 g, 9.40 mmol, 1.00 equiv.), NaH (752 mg, 18.8 mmol, 2.00 equiv.) and iodomethane (2.34 mL, 37.6 mmol, 4.00 equiv.) in anhydrous THF (15.7 mL), which was stirred for 6 h at 0 °C to room temperature. The reaction intermediate was redissolved in CH_2Cl_2 (49.5 mL) and stirred with TFA (8.00 mL, 104 mmol, 11.1 equiv.) for 19 h at room temperature. The product was redissolved in MeOH (28.0 mL) and stirred with HCl (1.25 M in MeOH; 25.0 mL, 31.5 mmol, 3.35 equiv.) for 5 min at room temperature. Yield: 80% (1.49 g, 7.55 mmol). White solid. **MP** 102−103 °C. **IR** (film) ν_{max} 3339, 2468, 2070, 1121, 1092, 973, 771, 481 cm^{-1}. **^{1}H NMR** (400 MHz, $MeOD_4$) δ 7.37 – 7.26 (m, 2H, H^7), 7.30 – 7.18 (m, 3H, H^8 + H^9), 5.27 – 5.24 (m, 1H, H^4), 5.18 – 5.16 (m, 1H, H^4), 3.55 (dd, *J* = 1.3, 0.6 Hz, 2H, H^2), 3.49 (s, 2H, H^5), 2.70 (s, 3H, H^1). **^{13}C NMR** (101 MHz, $MeOD_4$) δ 141.8 (C^3), 138.9 (C^6), 130.2 (C^8), 129.7 (C^7), 127.8 (C^9), 117.8 (C^4), 53.2 (C^2), 41.8 (C^5), 33.5 (C^1). **HRMS** (ESI-TOF) m/z: $[M + H]^+$ Calcd for $C_{11}H_{16}N$ 162.1277; Found 162.1276.

***N*-Methyl-(*E*)-3-phenylprop-2-en-1-amine hydrochloride salt (308)**[1]

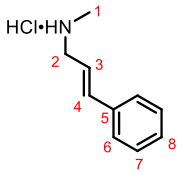

Reaction performed on 2.91 mmol scale following general procedure **2E** using **283** (678 mg, 2.91 mmol, 1.00 equiv.), NaH (232 mg, 5.80 mmol, 2.00 equiv.) and iodomethane (720 µL, 11.6 mmol, 4.00 equiv.) in anhydrous DMF (4.8 mL), which was stirred for 4.5 h at 0 °C to room temperature. The reaction intermediate was redissolved in CH_2Cl_2 (15.3 mL) and stirred with TFA (2.50 mL, 32.2 mmol, 11.1 equiv.) for 21.5 h at room temperature. The product was redissolved in MeOH (8.8 mL) and stirred with HCl (1.25 M in MeOH; 7.80 mL, 9.72 mmol, 3.35 equiv.) for 5 min at room temperature. Yield: 81% (430 mg, 2.34 mmol). Off-white solid. **MP** 141–142 °C. **IR** (film) ν_{max} 3392, 2958, 2751, 2513, 2138, 1449, 970, 740, 692 cm^{-1}. **^{1}H NMR** (400 MHz, $MeOD_4$) δ 7.50 – 7.45 (m, 2H, H^6), 7.36 – 7.25 (m, 3H,

H^7 + H^8), 6.88 (d, *J* = 15.8 Hz, 1H, H^4), 6.35 (dt, *J* = 15.8, 7.1 Hz, 1H, H^3), 3.78 (d, *J* = 7.1 Hz, 2H, H^2), 2.70 (s, 3H, H^1). **^{13}C NMR** (101 MHz, $MeOD_4$) δ 139.7 (C^4), 136.8 (C^5), 129.7 (C^7), 129.7 (C^8), 127.8 (C^6), 119.3 (C^3), 51.6 (C^2), 32.7 (C^1). **HRMS** (ESI-TOF) m/z: $[M + H]^+$ Calcd for $C_{10}H_{14}N$ 148.1121; Found 148.1125.

(*E*)-*N*-Methylpenta-2,4-dien-1-amine hydrochloride salt (309)

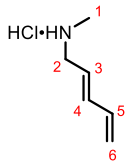

Reaction performed on 5.50 mmol scale following general procedure **2E** using **285** (1.01 g, 5.50 mmol, 1.00 equiv.), NaH (440 mg, 11.0 mmol, 2.00 equiv.) and iodomethane (1.37 mL, 22.0 mmol, 4.00 equiv.) in anhydrous THF (9.2 mL), which was stirred for 22 h at 0 °C to room temperature. The reaction intermediate was redissolved in CH_2Cl_2 (29 mL) and stirred with TFA (4.70 mL, 61.1 mmol, 11.1 equiv.) for 23.5 h at room temperature. The product was redissolved in MeOH (16.7 mL) and stirred with HCl (1.25 M in MeOH; 14.7 mL, 18.4 mmol, 3.35 equiv.) for 5 min at room temperature. Yield: 67% (491 mg, 3.69 mmol). Brown solid. **MP** 80−81 °C. **IR** (film) ν_{max} 3400, 2963, 2760, 1605, 1466, 1010, 919, 773 cm^{-1}. **^{1}H NMR** (400 MHz, $MeOD_4$) δ 6.51 (ddt, *J* = 14.2, 10.2, 1.0 Hz, 1H, H^4), 6.48 – 6.38 (m, 1H, H^5), 5.82 – 5.70 (m, 1H, H^3), 5.42 – 5.34 (m, 1H, H^6), 5.30 – 5.22 (m, 1H, H^6), 3.67 (dd, *J* = 7.2, 1.0 Hz, 2H, H^2), 2.67 (s, 3H, H^1). **^{13}C NMR** (101 MHz, $MeOD_4$) δ 140.5 (C^4), 136.7 (C^5), 123.1 (C^3), 121.0 (C^6), 51.3 (C^2), 32.7 (C^1). **HRMS** (APCI) m/z: $[M + H]^+$ Calcd for $C_6H_{12}N$ 98.0964; Found 98.0960.

***N*-Methyl-(2*E*,4*E*)-hexa-2,4-dien-1-amine hydrochloride salt (310)**[1]

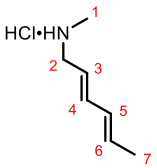

Reaction performed on 10.8 mmol scale following general procedure **2E** using **286** (2.12 g, 10.8 mmol, 1.00 equiv.), NaH (861 mg, 21.5 mmol, 2.00 equiv.) and iodomethane (2.68 mL, 43.0 mmol, 4.00 equiv.) in anhydrous DMF (18 mL), which was stirred for 2 h at 0 °C to room temperature. The reaction intermediate was redissolved in CH_2Cl_2 (57 mL) and stirred with TFA (9.10 mL, 119 mmol, 11.1 equiv.) for 22.5 h at room temperature. The product was redissolved in MeOH (33 mL) and stirred with HCl (1.25 M in MeOH; 28.8 mL, 36.1 mmol, 3.35 equiv.) for 5 min at room temperature. Yield: 66% (1.05

g, 7.13 mmol; containing traces of isomeric products); corrected for residual solvent present. Brown solid. **MP** 75–76 °C. **IR** (film) ν_{max} 3396, 2962, 2737, 2182, 1460, 993 cm^{-1}. **^{1}H NMR** (400 MHz, $MeOD_4$) δ 6.45 (dd, *J* = 15.2, 10.4 Hz, 1H, H^4), 6.14 (ddq, *J* = 15.0, 10.4, 1.2 Hz, 1H, H^5), 5.89 (dq, *J* = 15.0, 6.7 Hz, 1H, H^6), 5.58 (dt, *J* = 15.2, 7.2 Hz, 1H, H^3), 3.62 (d, *J* = 7.2 Hz, 2H, H^2), 2.65 (s, 3H, H^1), 1.78 (dd, *J* = 6.7, 1.2 Hz, 3H, H^7). **^{13}C NMR** (101 MHz, $MeOD_4$) δ 140.6 (C^4), 134.4 (C^6), 131.2 (C^5), 119.5 (C^3), 51.6 (C^2), 32.6 (C^1), 18.2 (C^7). **HRMS** (APCI) m/z: $[M + H]^+$ Calcd for $C_7H_{14}N$ 112.1121; Found 112.1116.

***N*-Methyl-2-methylenebut-3-en-1-amine hydrochloride salt (311)**

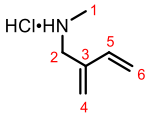

Reaction performed on 3.79 mmol scale following general procedure **2E** using **287** (695 mg, 3.79 mmol, 1.00 equiv.), NaH (303 mg, 7.58 mmol, 2.00 equiv.) and iodomethane (940 µL, 15.2 mmol, 4.00 equiv.) in anhydrous THF (6.3 mL), which was stirred for 23 h at 0 °C to room temperature. The reaction intermediate was redissolved in CH_2Cl_2 (20 mL) and stirred with TFA (3.20 mL, 42.1 mmol, 11.1 equiv.) for 7 h at room temperature. The product was redissolved in MeOH (11.5 mL) and stirred with HCl (1.25 M in MeOH; 10.2 mL, 12.7 mmol, 3.35 equiv.) for 5 min at room temperature. Yield: 59% (299 mg, 2.24 mmol). Brown solid. **MP** 105−106 °C. **IR** (film) ν_{max} 3398, 2962, 2756, 1600, 1466, 920, 772 cm^{-1}. **^{1}H NMR** (400 MHz, $MeOD_4$) δ 6.50 (dd, *J* = 17.9, 11.1 Hz, 1H, H^5), 5.51 (s, 1H, H^6), 5.47 – 5.40 (m, 2H, H^4 + H^6), 5.30 (ddd, *J* = 11.1, 1.4, 0.7 Hz, 1H, H^4), 3.87 (d, *J* = 1.1 Hz, 2H, H^2), 2.75 (s, 3H, H^1). **^{13}C NMR** (101 MHz, $MeOD_4$) δ 139.1 (C^3), 136.8 (C^5), 121.8 (C^6), 116.6 (C^4), 49.9 (C^2), 33.6 (C^1). **HRMS** (APCI) m/z: $[M + H]^+$ Calcd for $C_6H_{12}N$ 98.0964; Found 98.0960.

***N*-Methyl-(*E*)-3-(trimethylsilyl)prop-2-en-1-amine hydrochloride salt (312)**[1]

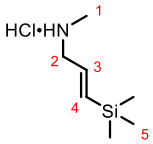

Reaction performed on 3.69 mmol scale following general procedure **2E** using **288** (848 mg, 3.69 mmol, 1.00 equiv.), NaH (296 mg, 7.39 mmol, 2.00 equiv.) and iodomethane (920 µL, 14.8 mmol, 4.00 equiv.) in anhydrous DMF (6.2 mL), which was stirred for 2 h at 0 °C to room temperature. The reaction intermediate was redissolved in CH_2Cl_2 (19.4 mL) and stirred with TFA (3.10 mL, 40.9 mmol, 11.1 equiv.) for 19 h at room temperature. The product was redissolved in MeOH (11.2 mL) and stirred with

HCl (1.25 M in MeOH; 9.90 mL, 12.4 mmol, 3.35 equiv.) for 5 min at room temperature. Yield: 73% (484 mg, 2.69 mmol). Off-white solid. **MP** 132–133 °C. **IR** (film) ν_{max} 3377, 2956, 2494, 2068, 1249, 977, 861, 837, 772 cm^{-1}. **^{1}H NMR** (400 MHz, $MeOD_4$) δ 6.24 (dt, *J* = 18.7, 0.8 Hz, 1H, H^4), 6.15 (dt, *J* = 18.7, 5.6 Hz, 1H, H^3), 3.68 (dd, *J* = 5.6, 0.8 Hz, 2H, H^2), 2.69 (s, 3H, H^1), 0.12 (s, 9H, H^5). **^{13}C NMR** (101 MHz, $MeOD_4$) δ 141.0 (C^4), 136.1 (C^3), 53.9 (C^2), 32.9 (C^1), -1.5 (C^5). **HRMS** (APCI) m/z: $[M + H]^+$ Calcd for $C_7H_{18}NSi$ 144.1203; Found 144.1196.

N-Methyl-4-(*tert*-butyldimethylsilyl)-2-methylenebut-3-yn-1-amine hydrochloride salt (313)

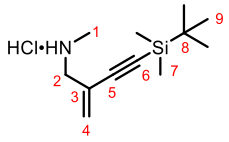

Reaction performed on 2.50 mmol scale following general procedure **2E** using **292** (738 mg, 2.50 mmol, 1.00 equiv.), NaH (200 mg, 5.00 mmol, 2.00 equiv.) and iodomethane (620 µL, 10.0 mmol, 4.00 equiv.) in anhydrous THF (4.2 mL), which was stirred for 3.5 h at 0 °C to room temperature. The reaction intermediate was redissolved in CH_2Cl_2 (13.2 mL) and stirred with TFA (2.13 mL, 27.8 mmol, 11.1 equiv.) for 15 h at room temperature. The product was redissolved in MeOH (7.6 mL) and stirred with HCl (1.25 M in MeOH; 6.70 mL, 8.40 mmol, 3.35 equiv.) for 5 min at room temperature. Yield: 68% (419 mg, 1.70 mmol). Pale-yellow solid. **MP** 139−140 °C. **IR** (film) ν_{max} 3357, 2475, 2227, 2071, 1120, 972, 823, 458 cm^{-1}. **^{1}H NMR** (400 MHz, $MeOD_4$) δ 5.82 (q, *J* = 0.6 Hz, 1H, H^4), 5.77 (td, *J* = 1.2, 0.6 Hz, 1H, H^4), 3.74 (dd, *J* = 1.2, 0.6 Hz, 2H, H^2), 2.76 (s, 3H, H^1), 0.98 (s, 9H, H^9), 0.17 (s, 6H, H^7). **^{13}C NMR** (101 MHz, $MeOD_4$) δ 129.8 (C^4), 124.0 (C^3), 103.2 (C^5), 97.3 (C^6), 53.5 (C^2), 33.5 (C^1), 26.5 (C^9), 17.4 (C^8), -4.7 (C^7). **HRMS** (ESI-TOF) m/z: $[M + H]^+$ Calcd for $C_{12}H_{24}NSi$ 210.1673; Found 210.1669.

N-Methyl-5-((*tert*-butyldimethylsilyl)oxy)-2-methylenepentan-1-amine hydrochloride salt (315)

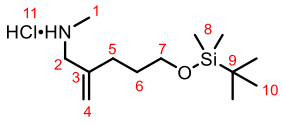

Reaction performed on 0.819 mmol scale following general procedure **2E** using **290** (270 mg, 0.819 mmol, 1.00 equiv.), NaH (66 mg, 1.7 mmol, 2.1 equiv.) and iodomethane (200 µL, 3.28 mmol, 4.00 equiv.) in anhydrous THF (1.4 mL), which was stirred for 1 h at 0 °C to room temperature. The reaction intermediate was redissolved in CH_2Cl_2 (4.3 mL) and stirred with TFA (700 µL, 1.50 mmol, 11.1 equiv.) for 20 h at room temperature. The product was redissolved in MeOH (2.5 mL) and stirred with HCl

(1.25 M in MeOH; 2.20 mL, 2.75 mmol, 3.35 equiv.) for 5 min at room temperature. During the Boc deprotection with TFA, the alcohol got deprotected, giving the unprotected version of the title compound as an orange oil. The compound was redissolved in anhydrous CH_2Cl_2 (2 mL), *tert*-butyldimethylsilyl chloride (301 mg, 2.00 mmol, 2.40 equiv.) and triethylamine (420 µL, 3.00 mmol, 3.70 equiv.) were added, and the reaction mixture was stirred for 17.5 h at room temperature. After concentrating *in vacuo*, filtering from Et_2O removed insoluble by-products and gave **315** as an orange gum (119 mg, 0.425 mmol, 52% yield). **IR** (film) ν_{max} 3401, 2953, 2929, 2857, 1677, 1472, 1254, 1202, 1099, 834, 775 cm^{-1}. **^{1}H NMR** (400 MHz, $CDCl_3$) δ 9.64 (s, 2H, H^{11}), 5.28 (s, 1H, H^4), 5.22 (t, J = 1.5 Hz, 1H, H^4), 3.62 (t, J = 6.3 Hz, 2H, H^7), 3.52 (s, 2H, H^2), 2.63 (s, 3H, H^1), 2.23 (t, J = 7.7 Hz, 2H, H^5), 1.72 – 1.64 (m, 2H, H^6), 0.88 (s, 9H, H^{10}), 0.04 (s, 6H, H^8). **^{13}C NMR** (101 MHz, $CDCl_3$) δ 139.1 (C^3), 117.8 (C^4), 62.2 (C^7), 52.7 (C^2), 32.0 (C^1), 30.6 (C^6), 30.5 (C^5), 26.1 (C^{10}), 18.4 (C^9), -5.2 (C^8). **HRMS** (ESI-TOF) m/z: $[M + H]^+$ Calcd for $C_{13}H_{30}NOSi$ 244.2091; Found 244.2084.

Ethyl 2-(3-allyl-3-methylureido)-2-oxoacetate (319)

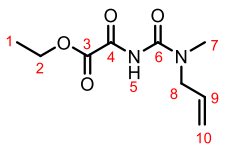

An oven-dried round bottom flask containing a magnetic stir bar was sealed with a suba seal, placed under N_2, and charged with ethyl oxamate (2.93 g, 25.0 mmol, 1.00 equiv.) and anhydrous DCE (7.4 mL, 0.29 mL/mmol). At 0 °C oxalyl chloride (2.54 mL, 30.0 mmol, 1.20 equiv.) was added dropwise, and then the reaction mixture was refluxed for 5 h. The reaction mixture was concentrated *in vacuo* (till 133 mbar) and the residue was redissolved in anhydrous CH_2Cl_2 (25 mL, 0.80 mL/mmol) and then *N*-allylmethylamine (2.80 mL, 28.8 mmol, 1.15 equiv.) and triethylamine (8.36 mL, 60.0 mmol, 2.40 equiv.) were added dropwise at 0 °C. The reaction mixture was stirred at room temperature for 5 h, concentrated *in vacuo*. Flash column chromatography (0.5–4% MeOH/CH_2Cl_2) gave **319** as a yellow oil (3.73 g, 17.4 mmol, 70% yield). **IR** (film) ν_{max} 3265, 2984, 1677, 1488, 1187, 753, 666 cm^{-1}. **^{1}H NMR** (400 MHz, $CDCl_3$) δ 8.79 (bs, 1H, H^5), 5.89 – 5.70 (m, 1H, H^9), 5.34 – 5.16 (m, 2H, H^{10}), 4.36 (q, J = 7.1 Hz, 2H, H^2), 3.97 – 3.91 (m, 2H, H^8), 2.98 (s, 3H, H^7), 1.37 (t, J = 7.1 Hz, 3H, H^1). **^{13}C NMR** (101 MHz, $CDCl_3$) δ 160.3 (C^3 + C^4), 151.7 (C^6), 132.0 (C^9), 118.3 (C^{10}), 63.6 (C^2), 50.9 (C^8), 35.1 (C^7), 14.0 (C^1). **HRMS** (ESI-TOF) m/z: $[M + Na]^+$ Calcd for $C_9H_{14}N_2O_4Na$ 237.0846; Found 237.0850.

1-Allyl-3-(but-3-en-2-yl)-1-methylurea (320)

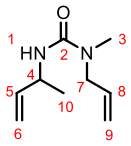

Reaction performed on 1.05 mmol scale following general procedure **2D** using 3-buten-2-ol (90.0 µL, 1.05 mmol, 1.00 equiv.), **319** (248 mg, 1.16 mmol, 1.10 equiv.), triphenylphosphine (304 mg, 1.16 mmol, 1.10 equiv.) and DIAD (230 µL, 1.16 mmol, 1.10 equiv.) in anhydrous THF (8 mL), which was stirred for 22 h at 0 °C to room temperature. The reaction intermediate was redissolved in THF (3.4 mL) and H_2O (1.3 mL), and stirred with LiOH (126 mg, 5.25 mmol, 5.00 equiv.) for 7 h at room temperature. Flash column chromatography (7−60% acetone/petroleum ether) gave **320** as a pale-yellow oil (14 mg, 0.083 mmol, 8% yield). **IR** (film) ν_{max} 3375, 2928, 1700, 1456, 1398, 1240, 1217, 1167, 1107, 992, 919, 770 cm^{-1}. **^{1}H NMR** (400 MHz, $CDCl_3$) δ 5.92 – 5.71 (m, 2H, H^5 + H^8), 5.33 – 5.06 (m, 5H, H^4 + H^6 + H^9), 3.87 (bs, 2H, H^7), 2.87 (s, 3H, H^3), 1.31 (d, J = 6.6 Hz, 3H, H^{10}). Due to degradation, the compound was not fully characterised.

1,3-Di(but-3-en-2-yl)-1,3-dimethylurea (232)

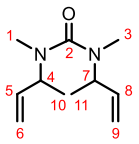

Reaction performed on 1.50 mmol scale following general procedure **2A** using **294** (182 mg, 1.50 mmol, 1.00 equiv.) in anhydrous CH_2Cl_2 (15 mL), triphosgene (267 mg, 0.900 mmol, 0.600 equiv.) in anhydrous CH_2Cl_2 (15 mL), anhydrous pyridine (240 µL, 3.00 mmol, 2.00 equiv.), which was stirred for 22 h at 0 °C to room temperature. Reaction intermediate was redissolved in anhydrous MeCN (21.4 mL) and stirred with **294** (237 mg, 1.95 mmol, 1.30 equiv.) and triethylamine (730 µL, 5.25 mmol, 3.50 equiv.) for 3 d at room temperature. Flash column chromatography (2−20% acetone/pentane) gave **232** as a yellow liquid (189 mg, 0.963 mmol, 64% yield). **IR** (film) ν_{max} 3458, 2973, 1634, 1485, 1447, 1380, 1331, 1102, 1084, 919, 772 cm^{-1}. **^{1}H NMR** (400 MHz, $CDCl_3$) δ 5.87 (dddd, J = 17.3, 10.6, 4.5, 3.3 Hz, 2H, H^5 + H^8), 5.17 – 5.09 (m, 4H, H^6 + H^9), 4.41 (qdt, J = 6.6, 4.2, 1.9 Hz, 2H, H^4 + H^7), 2.61 (s, 6H, H^1 + H^3), 1.22 (t, J = 7.0 Hz, 6H, H^{10} + H^{11}). **^{13}C NMR** (101 MHz, $CDCl_3$) δ 165.5 (C^2), 139.1 (C^5/C^8), 139.0 (C^5/C^8), 115.5 (C^6/C^9), 115.4 (C^6/C^9), 54.2 (C^4/C^7), 54.2 (C^4/C^7), 30.9 (C^1/C^3), 30.9 (C^1/C^3), 16.2 (C^{10}/C^{11}), 16.1 (C^{10}/C^{11}). **HRMS** (ESI-TOF) m/z: $[M + Na]^+$ Calcd for $C_{11}H_{20}N_2ONa$ 219.1468; Found 219.1469.

1,3-Dimethyl-1,3-bis(2-methylallyl)urea (230)

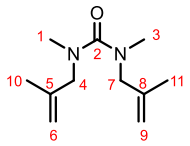

Reaction performed on 2.50 mmol scale following general procedure **2A** using **295** (304 mg, 2.50 mmol, 1.00 equiv.) in anhydrous CH_2Cl_2 (25 mL), triphosgene (445 mg, 1.50 mmol, 0.600 equiv.) in anhydrous CH_2Cl_2 (25 mL), anhydrous pyridine (0.61 mL, 7.5 mmol, 3.0 equiv.), which was stirred for 2 h at 0 °C to room temperature. Reaction intermediate was redissolved in anhydrous MeCN (36 mL) and stirred with **295** (399 mg, 3.28 mmol, 1.30 equiv.) and triethylamine (1.57 mL, 11.3 mmol, 4.50 equiv.) for 21.5 h at room temperature. Flash column chromatography (3−24% acetone/petroleum ether) gave **230** as a yellow liquid (109 mg, 0.554 mmol, 22% yield). **IR** (film) ν_{max} 2915, 1643, 1485, 1457, 1381, 1237, 1105, 895 cm^{-1}. **^{1}H NMR** (400 MHz, $CDCl_3$) δ 4.94 – 4.83 (m, 4H, H^6 + H^9), 3.67 (s, 4H, H^4 + H^7), 2.73 (s, 6H, H^1 + H^3), 1.67 (s, 6H, H^{10} + H^{11}). **^{13}C NMR** (101 MHz, $CDCl_3$) δ 165.7 (C^2), 141.7 (C^5 + C^8), 111.6 (C^6 + C^9), 56.8 (C^4 + C^7), 36.3 (C^1 + C^3), 20.1 (C^{10} + C^{11}). **HRMS** (ESI-TOF) m/z: $[M + H]^+$ Calcd for $C_{11}H_{21}N_2O$ 197.1648; Found 197.1652.

1,3-Di((*E*)-but-2-en-1-yl)-1,3-dimethylurea (228)

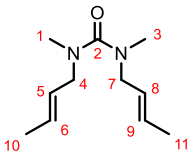

Reaction performed on 1.30 mmol scale following general procedure **2A** using **296** (158 mg, 1.30 mmol, 1.00 equiv.) in anhydrous CH_2Cl_2 (13 mL), triphosgene (231 mg, 0.780 mmol, 0.600 equiv.) in anhydrous CH_2Cl_2 (13 mL), anhydrous pyridine (0.21 mL, 2.6 mmol, 2.0 equiv.), which was stirred for 17 h at 0 °C to room temperature. Reaction intermediate was redissolved in anhydrous MeCN (19 mL) and stirred with **296** (206 mg, 1.69 mmol, 1.30 equiv.) and triethylamine (630 µL, 4.55 mmol, 3.50 equiv.) for 1 d at room temperature and 1 d at 45 °C. Flash column chromatography (5−40% acetone/petroleum ether) gave **228** as a yellow liquid (171 mg, 0.871 mmol, 67% yield). **IR** (film) ν_{max} 3389, 2918, 1634, 1486, 1448, 1385, 1222, 1092, 964, 915, 772, 752 cm^{-1}. **^{1}H NMR** (400 MHz, $CDCl_3$) δ 5.61 (dqt, *J* = 15.3, 6.4, 1.3 Hz, 2H, H^6 + H^9), 5.45 (dtq, *J* = 15.3, 6.1, 1.5 Hz, 2H, H^5 + H^8), 3.65 (dt, *J* = 6.1, 1.3 Hz, 4H, H^4 + H^7), 2.71 (s, 6H, H^1 + H^3), 1.70 (dq, *J* = 6.4, 1.5 Hz, 6H, H^{10} + H^{11}). **^{13}C NMR** (101 MHz, $CDCl_3$) δ 165.4 (C^2), 128.5 (C^6 + C^9), 127.1 (C^5 + C^8), 52.9 (C^4 + C^7), 35.9 (C^1 + C^3), 17.8 (C^{10} + C^{11}). **HRMS** (ESI-TOF) m/z: $[M + Na]^+$ Calcd for $C_{11}H_{20}N_2ONa$ 219.1468; Found 219.1478.

1,3-Di((*E*)-hex-2-en-1-yl)-1,3-dimethylurea (321)

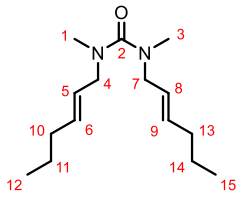

Reaction performed on 1.21 mmol scale following general procedure **2A** using **297** (181 mg, 1.21 mmol, 1.00 equiv.) in anhydrous CH_2Cl_2 (12 mL), triphosgene (214 mg, 0.720 mmol, 0.595 equiv.) in anhydrous CH_2Cl_2 (12 mL), anhydrous pyridine (190 µL, 2.42 mmol, 2.00 equiv.), which was stirred for 24 h at 0 °C to room temperature. Reaction intermediate was redissolved in anhydrous MeCN (17 mL) and stirred with **297** (234 mg, 1.56 mmol, 1.29 equiv.) and triethylamine (590 µL, 4.24 mmol, 3.50 equiv.) for 23.5 h at room temperature to 45 °C. Flash column chromatography (5−40% acetone/petroleum ether) gave **321** as a yellow liquid (133 mg, 0.526 mmol, 43% yield). **IR** (film) ν_{max} 2958, 2927, 1646, 1487, 1464, 1385, 1215, 1101, 971, 752 cm^{-1}. **^{1}H NMR** (400 MHz, $CDCl_3$) δ 5.59 (dtt, *J* = 15.3, 6.7, 1.3 Hz, 2H, $H^6 + H^9$), 5.43 (dtt, *J* = 15.3, 6.0, 1.4 Hz, 2H, $H^5 + H^8$), 3.66 (dd, *J* = 6.0, 1.1 Hz, 4H, $H^4 + H^7$), 2.72 (s, 6H, $H^1 + H^3$), 2.08 – 1.97 (m, 4H, $H^{10} + H^{13}$), 1.40 (h, *J* = 7.4 Hz, 4H, $H^{11} + H^{14}$), 0.90 (t, *J* = 7.4 Hz, 6H, $H^{12} + H^{15}$). **^{13}C NMR** (101 MHz, $CDCl_3$) δ 165.4 (C^2), 133.9 ($C^6 + C^9$), 126.0 ($C^5 + C^8$), 53.0 ($C^4 + C^7$), 35.8 ($C^1 + C^3$), 34.5 ($C^{10} + C^{13}$), 22.5 ($C^{11} + C^{14}$), 13.8 ($C^{12} + C^{15}$). **HRMS** (ESI-TOF) m/z: $[M + H]^+$ Calcd for $C_{15}H_{29}N_2O$ 253.2274; Found 253.2279.

1,3-Bis(2-cyclohexylallyl)-1,3-dimethylurea (322)

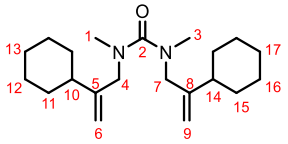

Reaction performed on 0.602 mmol scale following general procedure **2A** using **300** (114 mg, 0.602 mmol, 1.00 equiv.), triphosgene (107 mg, 0.360 mmol, 0.598 equiv.) in anhydrous CH_2Cl_2 (12 mL), anhydrous pyridine (0.10 mL, 1.2 mmol, 2.0 equiv.), which was stirred for 16 h at 0 °C to room temperature. Reaction intermediate was redissolved in anhydrous MeCN (8.6 mL) and stirred with **300** (148 mg, 0.780 mmol, 1.30 equiv.) and triethylamine (290 µL, 2.10 mmol, 3.50 equiv.) for 5.5 h at room temperature. Flash column chromatography (5−40% EtOAc/petroleum ether) gave **322** as a pale-yellow oil (152 mg, 0.458 mmol, 76% yield). **IR** (film) ν_{max} 2923, 2851, 1645, 1449, 1385, 1238, 1103, 890, 772 cm^{-1}. **^{1}H NMR** (400 MHz, $CDCl_3$) δ 4.91 – 4.85 (m, 4H, $H^6 + H^9$), 3.72 (t, *J* = 1.3 Hz, 4H, $H^4 + H^7$), 2.71 (s, 6H, $H^1 + H^3$), 1.81 – 1.71 (m, 10H, $H^{10} + H^{11} + H^{12} + H^{14} + H^{15} + H^{16}$), 1.71 – 1.64 (m, 2H, $H^{13} + H^{17}$), 1.33 – 1.09 (m, 10H, $H^{11} + H^{12} + H^{13} + H^{15} + H^{16} + H^{17}$). **^{13}C NMR** (101 MHz, $CDCl_3$) δ 165.8 (C^2), 150.6 ($C^5 + C^8$), 108.4 ($C^6 + C^9$), 54.9 ($C^4 + C^7$), 42.2 ($C^{10} + C^{14}$), 36.5 ($C^1 + C^3$), 32.6 (C^{11}

+ C^{15}/C^{12} + C^{16}), 26.9 (C^{11} + C^{15}/C^{12} + C^{16}), 26.5 (C^{13} + C^{17}). **HRMS** (ESI-TOF) m/z: $[M + H]^+$ Calcd for $C_{21}H_{37}N_2O$ 333.2900; Found 333.2897.

1,3-Bis((*E*)-3-cyclohexylallyl)-1,3-dimethylurea (323)

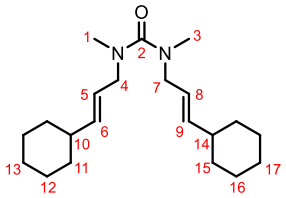

Reaction performed on 1.20 mmol scale following general procedure **2A** using **301** (228 mg, 1.20 mmol, 1.00 equiv.), triphosgene (214 mg, 0.720 mmol, 0.600 equiv.) in anhydrous CH_2Cl_2 (24 mL), anhydrous pyridine (0.19 mL, 2.4 mmol, 2.0 equiv.), which was stirred for 16 h at 0 °C to room temperature. Reaction intermediate was redissolved in anhydrous MeCN (17 mL) and stirred with **301** (296 mg, 1.56 mmol, 1.30 equiv.) and triethylamine (0.59 mL, 4.2 mmol, 3.5 equiv.) for 3 d at room temperature. Flash column chromatography (5−40% EtOAc/petroleum ether) gave **323** as a yellow oil (352 mg, 1.06 mmol, 88% yield). **IR** (film) ν_{max} 2921, 2850, 1645, 1448, 1384, 1219, 777, 775, 767 cm^{-1}. **^{1}H NMR** (400 MHz, $CDCl_3$) δ 5.54 (ddt, *J* = 15.5, 6.6, 1.3 Hz, 2H, H^6 + H^9), 5.37 (dtd, *J* = 15.5, 6.1, 1.2 Hz, 2H, H^5 + H^8), 3.65 (d, *J* = 6.1 Hz, 4H, H^4 + H^7), 2.70 (s, 6H, H^1 + H^3), 2.02 – 1.91 (m, 2H, H^{10} + H^{14}), 1.75 – 1.67 (m, 8H, H^{11} + H^{12} + H^{15} + H^{16}), 1.67 – 1.59 (m, 2H, H^{13} + H^{17}), 1.33 – 1.00 (m, 10H, H^{11} + H^{12} + H^{13} +H^{15} + H^{16} + H^{17}). **^{13}C NMR** (101 MHz, $CDCl_3$) δ 165.4 (C^2), 140.0 (C^6 + C^9), 123.2 (C^5 + C^8), 53.1 (C^4 + C^7), 40.5 (C^{10} + C^{14}), 35.7 (C^1 + C^3), 33.1 (C^{11} + C^{15}), 26.3 (C^{13} + C^{17}), 26.1 (C^{12} + C^{16}). **HRMS** (ESI-TOF) m/z: $[M + H]^+$ Calcd for $C_{21}H_{37}N_2O$ 333.2900; Found 333.2896.

1,3-Bis(((1*R*,5*S*)-6,6-dimethylbicyclo[3.1.1]hept-2-en-2-yl)methyl)-1,3-dimethylurea (324)

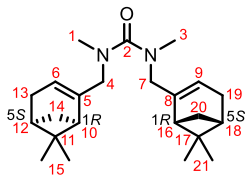

Reaction performed on 1.00 mmol scale following general procedure **2A** using **302** (202 mg, 1.00 mmol, 1.00 equiv.), triphosgene (178 mg, 0.600 mmol, 0.600 equiv.) in anhydrous CH_2Cl_2 (20 mL), anhydrous pyridine (0.16 mL, 2.0 mmol, 2.0 equiv.), which was stirred for 2 h at 0 °C to room temperature. Reaction intermediate was redissolved in anhydrous MeCN (14 mL) and stirred with **302** (262 mg, 1.30 mmol, 1.30 equiv. + 101 mg, 0.501 mmol, 0.501 equiv.) and triethylamine (0.49 mL, 3.5 mmol, 3.5 equiv. + 0.07 mL, 0.5 mmol, 0.5 equiv.) for 4 d at room temperature. Flash column chromatography

(4−32% EtOAc/pentane) gave **324** as a yellow solid (293 mg, 0.822 mmol, 82% yield). **MP** 50–51 °C. **IR** ν_{max} (film) 2921, 1625, 1216, 771, 759, 667 cm^{-1}. **^{1}H NMR** (400 MHz, $CDCl_3$) δ 5.42 – 5.34 (m, 2H, H^6 + H^9), 3.81 (dq, *J* = 15.9, 2.3 Hz, 2H, H^4 + H^7), 3.44 (dq, *J* = 15.9, 1.7 Hz, 2H, H^4 + H^7), 2.71 (s, 6H, H^1 + H^3), 2.37 (dt, *J* = 8.6, 5.6 Hz, 2H, H^{13} + H^{19}), 2.34 – 2.18 (m, 4H, H^{14} + H^{20}), 2.13 – 2.05 (m, 2H, H^{12} + H^{18}), 1.95 (td, *J* = 5.6, 1.5 Hz, 2H, H^{10} + H^{16}), 1.26 (s, 6H, H^{15} + H^{21}), 1.12 (d, *J* = 8.6 Hz, 2H, H^{13} + H^{19}), 0.82 (s, 6H, H^{15} + H^{21}). **^{13}C NMR** (101 MHz, $CDCl_3$) δ 165.7 (C^2), 144.9 (C^5 + C^8), 118.6 (C^6 + C^9), 55.7 (C^4 + C^7), 43.5 (C^{10} + C^{16}), 41.1 (C^{12} + C^{18}), 38.3 (C^{11} + C^{17}), 36.6 (C^1 + C^3), 31.7 (C^{13} + C^{19}), 31.4 (C^{14} + C^{20}), 26.4 (C^{15} + C^{21}), 21.1 (C^{15} + C^{21}). **HRMS** (ESI-TOF) m/z: $[M + H]^+$ Calcd for $C_{23}H_{37}N_2O$ 357.2900; Found 357.2899.

1,3-Di((2*E*,4*E*)-hexa-2,4-dien-1-yl)-1,3-dimethylurea (325)

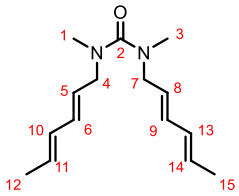

Reaction performed on 1.10 mmol scale following general procedure **2A** using **310** (162 mg, 1.10 mmol, 1.00 equiv.), triphosgene (196 mg, 0.660 mmol, 0.600 equiv.) in anhydrous CH_2Cl_2 (22 mL), anhydrous pyridine (0.18 mL, 2.2 mmol, 2.0 equiv.), which was stirred for 24 h at 0 °C to room temperature. Reaction intermediate was redissolved in anhydrous MeCN (16 mL) and stirred with **310** (211 mg, 1.43 mmol, 1.30 equiv.) and triethylamine (540 µL, 3.85 mmol, 3.50 equiv.) for 44 h at room temperature. Flash column chromatography (7−60% EtOAc/pentane) gave **325** as a yellow/orange oil (134 mg, 0.538 mmol, 49% yield). **IR** (film) ν_{max} 3018, 2915, 2852, 1640, 1486, 1460, 1382, 1354, 1103, 986, 775 cm^{-1}. **^{1}H NMR** (400 MHz, $CDCl_3$) δ 6.18 – 5.99 (m, 4H, H^6 + H^9 + H^{10} + H^{13}), 5.67 (dq, *J* = 13.4, 6.7 Hz, 2H, H^{11} + H^{14}), 5.52 (dt, *J* = 14.8, 6.3 Hz, 2H, H^5 + H^8), 3.72 (d, *J* = 6.3 Hz, 4H, H^4 + H^7), 2.72 (s, 6H, H^1 + H^3), 1.74 (d, *J* = 6.7 Hz, 6H, H^{12} + H^{15}). **^{13}C NMR** (101 MHz, $CDCl_3$) δ 165.2 (C^2), 133.0 (C^6 + C^9), 130.9 (C^{10} + C^{13}), 129.5 (C^{11} + C^{14}), 126.5 (C^5 + C^8), 52.8 (C^4 + C^7), 36.1 (C^1 + C^3), 18.2 (C^{12} + C^{15}). **HRMS** (ESI-TOF) m/z: $[M + H]^+$ Calcd for $C_{15}H_{25}N_2O$ 249.1961; Found 249.1962.

1-Allyl-3-(but-3-en-2-yl)-1,3-dimethylurea (237)

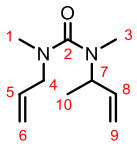

Reaction performed on 0.844 mmol scale following general procedure **2A** using **294** (103 mg, 0.844 mmol, 1.00 equiv.), triphosgene (151 mg, 0.507 mmol, 0.601 equiv.) in anhydrous CH_2Cl_2 (16.8 mL), anhydrous pyridine (140 µL, 1.68 mmol, 1.99 equiv.), which was stirred for 23 h at 0 °C to room temperature. Reaction intermediate was redissolved in anhydrous MeCN (12 mL) and stirred with *N*-allylmethylamine (0.10 mL, 1.1 mmol, 1.3 equiv.) and triethylamine (0.29 mL, 2.1 mmol, 2.5 equiv.) for 1 d at 40 °C and 1 d at 60 °C. Flash column chromatography (5−40% acetone/petroleum ether) gave **237** as a pale-yellow oil (104 mg, 0.572 mmol, 68% yield). **IR** (film) ν_{max} 2925, 1638, 1486, 1460, 1382, 1092, 920, 773 cm^{-1}. **^{1}H NMR** (400 MHz, $CDCl_3$) δ 5.92 – 5.76 (m, 2H, H^5 + H^8), 5.24 – 5.08 (m, 4H, H^6 + H^9), 4.46 (qdt, *J* = 6.9, 4.2, 1.9 Hz, 1H, H^7), 3.72 (dq, *J* = 5.6, 1.7 Hz, 2H, H^4), 2.74 (s, 3H, H^1), 2.63 (s, 3H, H^3), 1.23 (d, *J* = 6.9 Hz, 3H, H^{10}). **^{13}C NMR** (101 MHz, $CDCl_3$) δ 165.4 (C^2), 138.9 (C^8), 134.4 (C^5), 117.0 (C^6), 115.5 (C^9), 54.1 (C^7), 53.8 (C^4), 36.3 (C^1), 30.9 (C^3), 16.2 (C^{10}). **HRMS** (ESI-TOF) m/z: $[M + Na]^+$ Calcd for $C_{10}H_{18}N_2ONa$ 205.1311; Found 205.1311.

1-Allyl-1,3-dimethyl-3-(2-methylallyl)urea (243)

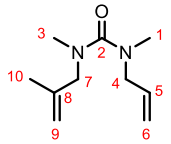

Reaction performed on 5.00 mmol scale following general procedure **2A** using **295** (608 mg, 5.00 mmol, 1.00 equiv.), triphosgene (890 mg, 3.00 mmol, 0.600 equiv.) in anhydrous CH_2Cl_2 (100 mL), anhydrous pyridine (0.81 mL, 10 mmol, 2.0 equiv.), which was stirred for 16.5 h at 0 °C to room temperature. Reaction intermediate was redissolved in anhydrous MeCN (43 mL) and stirred with *N*-allylmethylamine (0.62 mL, 6.5 mmol, 1.3 equiv.) and triethylamine (1.74 mL, 12.5 mmol, 2.50 equiv.) for 2 at room temperature. Flash column chromatography (5−19% acetone/petroleum ether) gave **243** as a pale-yellow liquid (851 mg, 4.17 mmol, 93% yield). **IR** (film) ν_{max} 3493, 3077, 2911, 1641, 1487, 1383, 1235, 922, 898, 772 cm^{-1}. **^{1}H NMR** (400 MHz, $CDCl_3$) δ 5.81 (ddt, *J* = 17.2, 10.3, 5.6 Hz, 1H, H^5), 5.25 – 5.13 (m, 2H, H^6), 4.93 – 4.83 (m, 2H, H^9), 3.72 (dt, *J* = 5.6, 1.6 Hz, 2H, H^4), 3.67 (s, 2H, H^7), 2.74 (s, 3H, H^1/H^3), 2.74 (s, 3H, H^1/H^3), 1.68 – 1.66 (m, 3H, H^{10}). **^{13}C NMR** (101 MHz, $CDCl_3$) δ 165.5 (C^2), 141.6 (C^8), 134.4 (C^5), 117.0 (C^6), 111.7 (C^9), 56.8 (C^7), 53.5 (C^4), 36.4 (C^3), 36.1 (C^1), 20.2 (C^{10}). **HRMS** (ESI-TOF) m/z: $[M + H]^+$ Calcd for $C_{10}H_{19}N_2O$ 183.1497; Found 183.1499.

(*E*)-1-Allyl-3-(but-2-en-1-yl)-1,3-dimethylurea (242)

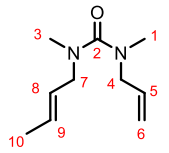

Reaction performed on 1.30 mmol scale following general procedure **2A** using **296** (158 mg, 1.30 mmol, 1.00 equiv.), triphosgene (231 mg, 0.780 mmol, 0.600 equiv.) in anhydrous CH_2Cl_2 (26 mL), anhydrous pyridine (0.21 mL, 2.6 mmol, 2.0 equiv.), which was stirred for 17 h at 0 °C to room temperature. Reaction intermediate was redissolved in anhydrous MeCN (19 mL) and stirred with *N*-allylmethylamine (160 µL, 1.69 mmol, 1.30 equiv.) and triethylamine (630 µL, 4.55 mmol, 2.50 equiv.) for 22 h at room temperature. Flash column chromatography (5−40% acetone/petroleum ether) gave **242** as a yellow liquid (211 mg, 1.16 mmol, 89% yield). **IR** (film) ν_{max} 3489, 2918, 1637, 1486, 1383, 1222, 1091, 967, 923, 773 cm^{-1}. **^{1}H NMR** (400 MHz, $CDCl_3$) δ 5.81 (ddt, *J* = 17.2, 10.2, 5.6 Hz, 1H, H^5), 5.61 (dqt, *J* = 15.4, 6.4, 1.4 Hz, 1H, H^9), 5.45 (dtq, *J* = 15.4, 6.1, 1.4 Hz, 1H, H^8), 5.22 – 5.14 (m, 2H, H^6), 3.72 (dt, *J* = 5.6, 1.6 Hz, 2H, H^4), 3.64 (dt, *J* = 6.1, 1.4 Hz, 2H, H^7), 2.74 (s, 3H, H^1), 2.71 (s, 3H, H^3), 1.69 (dq, *J* = 6.4, 1.4 Hz, 3H, H^{10}). **^{13}C NMR** (101 MHz, $CDCl_3$) δ 165.3 (C^2), 134.4 (C^5), 128.6 (C^9), 127.0 (C^8), 117.0 (C^6), 53.6 (C^4), 52.8 (C^7), 36.2 (C^1), 35.9 (C^3), 17.8 (C^{10}). **HRMS** (ESI-TOF) m/z: $[M + Na]^+$ Calcd for $C_{10}H_{18}N_2ONa$ 205.1311; Found 205.1315.

(*E*)-1-Allyl-3-(hex-2-en-1-yl)-1,3-dimethylurea (326)

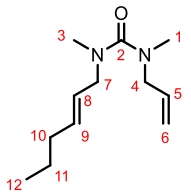

Reaction performed on 1.40 mmol scale following general procedure **2A** using **297** (210 mg, 1.40 mmol, 1.00 equiv.), triphosgene (249 mg, 0.840 mmol, 0.600 equiv.) in anhydrous CH_2Cl_2 (28 mL), anhydrous pyridine (0.23 mL, 2.8 mmol, 2.0 equiv.), which was stirred for 24.5 h at 0 °C to room temperature. Reaction intermediate was redissolved in anhydrous MeCN (20 mL) and stirred with *N*-allylmethylamine (170 µL, 1.82 mmol, 1.30 equiv.) and triethylamine (0.49 mL, 3.5 mmol, 2.5 equiv.) for 24 h at 45 °C. Flash column chromatography (5−40% acetone/petroleum ether) gave **326** as a yellow oil (214 mg, 1.02 mmol, 73% yield). **IR** (film) ν_{max} 2959, 2928, 1642, 1488, 1385, 1095, 972, 753 cm^{-1}. **^{1}H NMR** (400 MHz, $CDCl_3$) δ 5.81 (ddt, *J* = 17.2, 10.2, 5.7 Hz, 1H, H^5), 5.58 (dtt, *J* = 15.3, 6.6, 1.3 Hz, 1H, H^9), 5.42 (dtt, *J* = 15.3, 6.0, 1.4 Hz, 1H, H^8), 5.22 – 5.14 (m, 2H, H^6), 3.72 (dt, *J* = 5.7, 1.3 Hz, 2H, H^4), 3.66 (dd, *J* = 6.0, 0.7 Hz, 2H, H^7), 2.74 (s, 3H, H^1), 2.71 (s, 3H, H^3), 2.05 – 1.98 (m, 2H, H^{10}),

1.39 (h, *J* = 7.4 Hz, 2H, H^{11}), 0.88 (t, *J* = 7.4 Hz, 3H, H^{12}). **^{13}C NMR** (101 MHz, $CDCl_3$) δ 165.4 (C^2), 134.4 (C^5), 134.0 (C^9), 125.8 (C^8), 117.0 (C^6), 53.6 (C^4), 52.9 (C^7), 36.2 (C^1), 35.8 (C^3), 34.4 (C^{10}), 22.5 (C^{11}), 13.7 (C^{12}). **HRMS** (ESI-TOF) m/z: $[M + H]^+$ Calcd for $C_{12}H_{23}N_2O$ 211.1805; Found 211.1801.

(*E*)-1-(But-2-en-1-yl)-3-(but-3-en-2-yl)-1,3-dimethylurea (327)

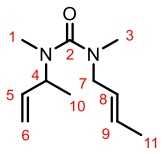

Reaction performed on 0.61 mmol scale following general procedure **2A** using **294** (74 mg, 0.61 mmol, 1.00 equiv.), triphosgene (152 mg, 0.511 mmol, 0.838 equiv.) in anhydrous CH_2Cl_2 (17 mL), anhydrous pyridine (0.14 mL, 1.7 mmol, 2.8 equiv.), which was stirred for 24 h at 0 °C to room temperature. Reaction intermediate was redissolved in anhydrous MeCN (9 mL) and stirred with **296** (96 mg, 0.79 mmol, 1.30 equiv.) and triethylamine (300 µL, 2.14 mmol, 3.50 equiv.) for 4 d at room temperature followed by 4 h at 45 °C. Flash column chromatography (3–28% EtOAc/petroleum ether) gave **327** as a yellow oil (53 mg, 0.27 mmol, 44% yield). **IR** (film) ν_{max} 2969, 2920, 1635, 1485, 1450, 1381, 1311, 1119, 1094, 965, 918, 779 cm^{-1}. **^{1}H NMR** (400 MHz, $CDCl_3$) δ 5.84 (ddd, *J* = 17.4, 10.6, 4.5 Hz, 1H, H^5), 5.59 (dqt, *J* = 15.3, 6.4, 1.4 Hz, 1H, H^9), 5.44 (dtq, *J* = 15.3, 6.1, 1.4 Hz, 1H, H^8), 5.18 – 5.05 (m, 2H, H^6), 4.49 – 4.37 (m, 1H, H^4), 3.63 – 3.60 (m, 2H, H^7), 2.69 (s, 3H, H^1), 2.61 (s, 3H, H^3), 1.68 (dq, *J* = 6.4, 1.4 Hz, 3H, H^{11}), 1.20 (d, *J* = 6.9 Hz, 3H, H^{10}). **^{13}C NMR** (101 MHz, $CDCl_3$) δ 165.4 (C^2), 139.0 (C^5), 128.5 (C^9), 127.0 (C^8), 115.4 (C^6), 54.0 (C^4), 53.0 (C^7), 35.9 (C^1), 30.8 (C^3), 17.8 (C^{11}), 16.1 (C^{10}). **HRMS** (ESI-TOF) m/z: $[M + Na]^+$ Calcd for $C_{11}H_{20}N_2ONa$ 219.1468; Found 219.1478.

(*E*)-1-(But-2-en-1-yl)-1,3-dimethyl-3-(2-methylallyl)urea (241)

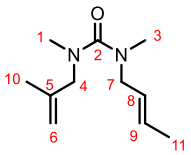

Reaction performed on 0.60 mmol scale following general procedure **2A** using **295** (73 mg, 0.60 mmol, 1.0 equiv.), triphosgene (112 mg, 0.388 mmol, 0.647 equiv.) in anhydrous CH_2Cl_2 (12 mL), anhydrous pyridine (0.10 mL, 1.2 mmol, 2.0 equiv.), which was stirred for 16 h at 0 °C to room temperature. Reaction intermediate was redissolved in anhydrous MeCN (8.6 mL) and stirred with **296** (95 mg, 0.78 mmol, 1.3 equiv.) and triethylamine (0.29 mL, 2.1 mmol, 3.5 equiv.) for 6.5 h at room temperature. Flash column chromatography (5–40% EtOAc/petroleum ether) gave **241** as a yellow oil (81 mg, 0.41

mmol, 69% yield). **IR** (film) ν_{max} 3418, 2919, 2519, 1698, 1628, 1489, 1448, 1386, 1245, 1096, 966, 898, 477 cm^{-1}. **^{1}H NMR** (400 MHz, $CDCl_3$) (suspected mixture of *E*:*Z* in a 0.7:0.3 ratio) δ 5.69 – 5.54 (m, 1H, H^9), 5.50 – 5.39 (m, 1H, H^8), 4.90 – 4.84 (m, 2H, H^6), 3.77 (d, *J* = 6.6 Hz, 0.6H, *Z*-H^7), 3.67 (s, 2H, H^4), 3.64 (dt, *J* = 6.1, 1.4 Hz, 1.4H, *E*-H^7), 2.73 (s, 0.9H, *Z*-H^3), 2.73 (s, 3H, H^1), 2.71 (s, 2.1H, *E*-H^3), 1.69 (dq, *J* = 6.4, 1.4 Hz, 2.1H, *E*-H^{11}), 1.68 – 1.63 (m, 3.9H, *Z*-H^{11} + H^{10}). **^{13}C NMR** (101 MHz, $CDCl_3$) δ 165.6 (*Z*-C^2), 165.5 (*E*-C^2), 141.6 (C^5), 128.5 (*E*-C^9), 127.5 (*Z*-C^9), 127.0 (*E*-C^8), 126.7 (*Z*-C^8), 111.8 (*Z*-C^6), 111.7 (*E*-C^6), 56.8 (C^4), 52.9 (*E*-C^7), 47.3 (*Z*-C^7), 36.4 (*E*-C^1), 36.4 (*Z*-C^1), 36.0 (*Z*-C^3), 35.8 (*E*-C^3), 20.1 (C^{10}), 17.8 (*E*-C^{11}), 13.0 (*Z*-C^{11}). **HRMS** (ESI-TOF) m/z: $[M + Na]^+$ Calcd for $C_{11}H_{21}N_2ONa$ 197.1648; Found 197.1643.

1,3-Dimethyl-3-(2-methylallyl)-1-(oct-1-en-3-yl)urea (328)

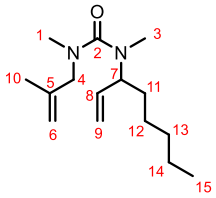

Reaction performed on 1.20 mmol scale following general procedure **2A** using **±-298** (214 mg, 1.20 mmol, 1.00 equiv.), triphosgene (214 mg, 0.720 mmol, 0.600 equiv.) in anhydrous CH_2Cl_2 (24 mL), anhydrous pyridine (0.19 mL, 2.4 mmol, 2.0 equiv.), which was stirred for 16 h at 0 ℃ to room temperature. Reaction intermediate was redissolved in anhydrous MeCN (17 mL) and stirred with **295** (190 mg, 1.56 mmol, 1.30 equiv.) and triethylamine (0.59 mL, 4.2 mmol, 3.5 equiv.) for 5.5 h at room temperature. Flash column chromatography (5−40% EtOAc/petroleum ether) gave **328** as a yellow oil (159 mg, 0.628 mmol, 52% yield). **IR** (film) ν_{max} 2929, 1640, 1456, 1380, 1099, 771 cm^{-1}. **^{1}H NMR** (400 MHz, $CDCl_3$) δ 5.83 (ddd, *J* = 17.3, 10.6, 5.1 Hz, 1H, H^8), 5.19 – 5.10 (m, 2H, H^9), 4.93 – 4.85 (m, 2H, H^6), 4.25 – 4.18 (m, 1H, H^7), 3.65 (AB q, *J* = 16.1 Hz, 2H, H^4), 2.71 (s, 3H, H^1), 2.64 (s, 3H, H^3), 1.67 (s, 3H, H^{10}), 1.63 – 1.48 (m, 2H, H^{11}), 1.35 – 1.21 (m, 6H, H^{12} + H^{13} + H^{14}), 0.87 (t, *J* = 6.7 Hz, 3H, H^{15}). **^{13}C NMR** (101 MHz, $CDCl_3$) δ 166.0 (C^2), 141.7 (C^5), 137.6 (C^8), 115.8 (C^9), 111.7 (C^6), 59.2 (C^7), 57.0 (C^4), 36.5 (C^1), 31.8 (C^{13}), 31.3 (C^{11}), 30.7 (C^3), 26.1 (C^{12}), 22.7 (C^{14}), 20.2 (C^{10}), 14.2 (C^{15}). **HRMS** (ESI-TOF) m/z: $[M + H]^+$ Calcd for $C_{15}H_{29}N_2O$ 253.2274; Found 253.2274.

1-(But-3-en-2-yl)-1,3-dimethyl-3-(2-methylallyl)urea (329)

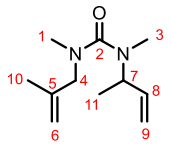

Reaction performed on 0.851 mmol scale following general procedure **2A** using **294** (104 mg, 0.851 mmol, 1.00 equiv.), triphosgene (152 mg, 0.511 mmol, 0.600 equiv.) in anhydrous CH_2Cl_2 (17 mL), anhydrous pyridine (0.14 mL, 1.7 mmol, 2.0 equiv.), which was stirred for 24 h at 0 °C to room temperature. Reaction intermediate was redissolved in anhydrous MeCN (12 mL) and stirred with **295** (134 mg, 1.11 mmol, 1.30 equiv.) and triethylamine (410 µL, 2.98 mmol, 3.50 equiv.) for 3 d at room temperature then 4 h at 45 °C. Flash column chromatography (3−28% EtOAc/petroleum ether) gave **329** as a pale-yellow oil (76 mg, 0.39 mmol, 45% yield). **IR** (film) ν_{max} 3482, 2971, 2922, 1635, 1485, 1456, 1380, 1289, 1102, 898 cm^{-1}. **^{1}H NMR** (400 MHz, $CDCl_3$) δ 5.86 (ddd, *J* = 17.4, 10.7, 4.5 Hz, 1H, H^8), 5.17 – 5.09 (m, 2H, H^9), 4.89 – 4.84 (m, 2H, H^6), 4.43 (qdt, *J* = 6.9, 4.5, 1.9 Hz, 1H, H^7), 3.65 (AB q, *J* = 16.1 Hz, 2H, H^4), 2.72 (s, 3H, H^1), 2.62 (s, 3H, H^3), 1.67 (dd, *J* = 1.4, 0.8 Hz, 3H, H^{10}), 1.22 (d, *J* = 6.9 Hz, 3H, H^{11}). **^{13}C NMR** (101 MHz, $CDCl_3$) δ 165.6 (C^2), 141.7 (C^5), 138.9 (C^8), 115.5 (C^9), 111.7 (C^6), 56.9 (C^4), 54.2 (C^7), 36.5 (C^1), 30.7 (C^3), 20.2 (C^{10}), 16.2 (C^{11}). **HRMS** (ESI-TOF) m/z: $[M + Na]^+$ Calcd for $C_{11}H_{20}N_2ONa$ 219.1468; Found 219.1471.

1-(1-Cyclohexylallyl)-1,3-dimethyl-3-(2-methylallyl)urea (330)

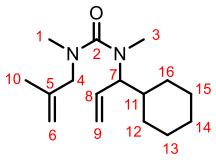

Reaction performed on 0.866 mmol scale following general procedure **2A** using **299** (164 mg, 0.866 mmol, 1.00 equiv.), triphosgene (154 mg, 0.520 mmol, 0.600 equiv.) in anhydrous CH_2Cl_2 (17.4 mL), anhydrous pyridine (140 µL, 1.74 mmol, 2.00 equiv.), which was stirred for 19 h at 0 °C to room temperature. Reaction intermediate was redissolved in anhydrous MeCN (12.4 mL) and stirred with **295** (153 mg, 1.13 mmol, 1.30 equiv.) and triethylamine (0.43 mL, 3.1 mmol, 3.5 equiv.) for 2 d at room temperature. Then **295** (77 mg, 0.57 mmol, 0.65 equiv.) and triethylamine (220 µL, 1.53 mmol, 1.75 equiv.) were added again and the reaction mixture was stirred for another 4 d at room temperature. Flash column chromatography (3−26% EtOAc/petroleum ether) gave **330** as a yellow oil (196 mg, 0.742 mmol, 85% yield). **IR** (film) ν_{max} 2926, 2853, 1711, 1636, 1451, 1385, 1220, 1101, 773 cm^{-1}. **^{1}H NMR** (400 MHz, $CDCl_3$) δ 5.87 (ddd, *J* = 17.2, 10.5, 7.3 Hz, 1H, H^8), 5.21 – 5.10 (m, 2H, H^9), 4.93 – 4.85 (m, 2H, H^6), 3.79 (ddt, *J* = 9.8, 7.3, 1.2 Hz, 1H, H^7), 3.62 (AB q, *J* = 16.1 Hz, 2H, H^4), 2.69 (s, 3H,

H^{1}), 2.68 (s, 3H, H^{3}), 1.77 – 1.60 (m, 5H, H^{12} + H^{13} + H^{14} + H^{15} + H^{16}), 1.67 (dd, *J* = 1.5, 0.8 Hz, 3H, H^{10}), 1.58 – 1.46 (m, 1H, H^{11}), 1.25 – 1.06 (m, 3H, H^{13} + H^{14} + H^{15}), 0.96 – 0.76 (m, 2H, H^{12} + H^{16}). **^{13}C NMR** (101 MHz, $CDCl_3$) δ 166.1 (C^{2}), 141.7 (C^{5}), 135.4 (C^{8}), 117.5 (C^{9}), 111.7 (C^{6}), 65.6 (C^{7}), 57.1 (C^{4}), 38.6 (C^{11}), 36.3 (C^{1}), 31.5 (C^{3}), 30.9 (C^{12}/C^{16}), 30.1 (C^{12}/C^{16}), 26.5 (C^{14}), 26.2 (C^{13}/C^{15}), 26.1 (C^{13}/C^{15}), 20.3 (C^{10}). **HRMS** (ESI-TOF) m/z: $[M + H]^+$ Calcd for $C_{16}H_{29}N_2O$ 265.2274; Found 265.2283.

1-(1-Cyclohexylallyl)-3-(2-cyclohexylallyl)-1,3-dimethylurea (331)

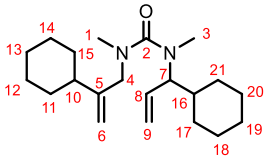

Reaction performed on 0.800 mmol scale following general procedure **2A** using **299** (152 mg, 0.800 mmol, 1.00 equiv.), triphosgene (142 mg, 0.480 mmol, 0.600 equiv.) in anhydrous CH_2Cl_2 (16 mL), anhydrous pyridine (0.13 mL, 1.6 mmol, 2.0 equiv.), which was stirred for 16 h at 0 °C to room temperature. Reaction intermediate was redissolved in anhydrous MeCN (12.4 mL) and stirred with **300** (197 mg, 1.04 mmol, 1.30 equiv.) and triethylamine (0.39 mL, 2.8 mmol, 3.5 equiv.) for 4 h at room temperature. Flash column chromatography (5−25% EtOAc/petroleum ether) gave **331** as a pale-yellow oil (217 mg, 0.651 mmol, 81% yield). **IR** (film) ν_{max} 3391, 2922, 2850, 1641, 1448, 1382, 1280, 1220, 1096, 889, 773 cm^{-1}. **^{1}H NMR** (400 MHz, $CDCl_3$) δ 5.86 (ddd, *J* = 17.2, 10.5, 7.1 Hz, 1H, H^{8}), 5.19 (ddd, *J* = 10.5, 1.8, 1.1 Hz, 1H, H^{9}), 5.13 (ddd, *J* = 17.2, 1.8, 1.4 Hz, 1H, H^{9}), 4.93 – 4.85 (m, 2H, H^{6}), 3.82 – 3.54 (m, 3H, H^{4} + H^{7}), 2.66 (s, 3H, H^{1}), 2.66 (s, 3H, H^{3}), 1.82 – 1.60 (m, 11H, H^{10} + H^{11} + H^{12} + H^{13} + H^{14} + H^{15} + H^{17} + H^{18} + H^{19} + H^{20} + H^{21}), 1.53 (qt, *J* = 10.9, 3.2 Hz, 1H, H^{16}), 1.30 – 1.06 (m, 8H, H^{11} + H^{12} + H^{13} + H^{14} + H^{15} + H^{18} + H^{19} + H^{20}), 0.95 – 0.77 (m, 2H, H^{17} + H^{21}). **^{13}C NMR** (101 MHz, $CDCl_3$) δ 166.1 (C^{2}), 150.7 (C^{5}), 135.3 (C^{8}), 117.3 (C^{9}), 108.6 (C^{6}), 65.6 (C^{7}), 55.3 (C^{4}), 42.0 (C^{10}), 38.6 (C^{16}), 36.5 (C^{1}), 32.7 (C^{11}/C^{15}), 32.5 (C^{11}/C^{15}), 31.4 (C^{3}), 30.9 (C^{17}/C^{21}), 30.0 (C^{17}/C^{21}), 26.9 (C^{13} + H^{19}), 26.5 (C^{12}/C^{14}), 26.4 (C^{12}/C^{14}), 26.2 (C^{18}/C^{20}), 26.1 (C^{18}/C^{20}). **HRMS** (ESI-TOF) m/z: $[M + H]^+$ Calcd for $C_{21}H_{37}N_2O$ 333.2900; Found 333.2893.

1-(2-Cyclohexylallyl)-1,3-dimethyl-3-(2-methylallyl)urea (332)

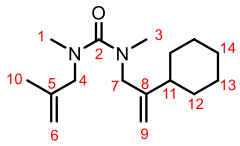

Reaction performed on 1.50 mmol scale following general procedure **2A** using **300** (285 mg, 1.50 mmol, 1.00 equiv.), triphosgene (267 mg, 0.900 mmol, 0.600 equiv.) in anhydrous CH_2Cl_2 (30 mL), anhydrous pyridine (0.24 mL, 3.0 mmol, 2.0 equiv.), which was stirred for 24 h at 0 °C to room temperature. Reaction intermediate was redissolved in anhydrous MeCN (21.4 mL) and stirred with **295** (237 mg, 1.95 mmol, 1.30 equiv.) and triethylamine (730 µL, 5.25 mmol, 3.50 equiv.) for 23 h at room temperature. Flash column chromatography (1−14% acetone/pentane) gave **332** as a yellow oil (347 mg, 1.31 mmol, 87% yield). **IR** (film) ν_{max} 2924, 2852, 1641, 1485, 1448, 1382, 1237, 1103, 891, 772, 751 cm^{-1}. **^{1}H NMR** (400 MHz, $CDCl_3$) δ 4.91 – 4.85 (m, 4H, H^6 + H^9), 3.72 (t, *J* = 1.5 Hz, 2H, H^7), 3.66 (s, 2H, H^4), 2.72 (s, 3H, H^1), 2.72 (s, 3H, H^3), 1.80 – 1.70 (m, 5H, H^{11} + H^{12} + H^{13}), 1.70 – 1.67 (m, 1H, H^{14}), 1.66 (dd, *J* = 1.5, 0.8 Hz, 3H, H^{10}), 1.31 – 1.09 (m, 5H, H^{12} + H^{13} + H^{14}). **^{13}C NMR** (101 MHz, $CDCl_3$) δ 165.7 (C^2), 150.7 (C^8), 141.7 (C^5), 111.7 (C^6), 108.4 (C^9), 56.7 (C^4), 55.0 (C^7), 42.1 (C^{11}), 36.5 (C^3), 36.3 (C^1), 32.5 (C^{12}/C^{13}), 26.9 (C^{12}/C^{13}), 26.4 (C^{14}), 20.2 (C^{10}). **HRMS** (ESI-TOF) m/z: $[M + H]^+$ Calcd for $C_{16}H_{29}N_2O$ 265.2274; Found 265.2276.

(*E*)-1-(3-Cyclohexylallyl)-1,3-dimethyl-3-(2-methylallyl)urea (333)

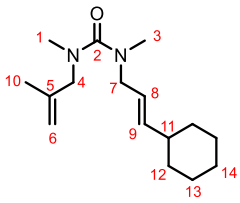

Reaction performed on 1.50 mmol scale following general procedure **2A** using **301** (285 mg, 1.50 mmol, 1.00 equiv.), triphosgene (267 mg, 0.900 mmol, 0.600 equiv.) in anhydrous CH_2Cl_2 (30 mL), anhydrous pyridine (0.24 mL, 3.0 mmol, 2.0 equiv.), which was stirred for 24 h at 0 °C to room temperature. Reaction intermediate was redissolved in anhydrous MeCN (21.4 mL) and stirred with **295** (237 mg, 1.95 mmol, 1.30 equiv.) and triethylamine (730 µL, 5.25 mmol, 3.50 equiv.) for 23 h at room temperature. Flash column chromatography (1−14% EtOAc/pentane) gave **333** as a yellow oil (308 mg, 1.16 mmol, 78% yield). **IR** (film) ν_{max} 2922, 2850, 1640, 1486, 1448, 1383, 1235, 1104, 971, 897, 772, 751 cm^{-1}. **^{1}H NMR** (400 MHz, $CDCl_3$) δ 5.54 (ddt, *J* = 15.5, 6.6, 1.4 Hz, 1H, H^9), 5.37 (dtd, *J* = 15.5, 6.0, 1.2 Hz, 1H, H^8), 4.90 – 4.84 (m, 2H, H^6), 3.67 (s, 2H, H^4), 3.65 (d, *J* = 6.0 Hz, 2H, H^7), 2.73 (s, 3H, H^1), 2.70 (s, 3H, H^3), 2.01 – 1.91 (m, 1H, H^{11}), 1.74 – 1.68 (m, 4H, H^{12} + H^{13}), 1.67 (dd, *J* = 1.4, 0.7

Hz, 3H, H^{10}), 1.66 – 1.60 (m, 1H, H^{14}), 1.31 – 1.01 (m, 5H, H^{12} + H^{13} + H^{14}). **^{13}C NMR** (101 MHz, $CDCl_3$) δ 165.6 (C^2), 141.7 (C^5), 140.0 (C^9), 123.1 (C^8), 111.7 (C^6), 56.8 (C^4), 53.1 (C^7), 40.6 (C^{11}), 36.4 (C^1), 35.6 (C^3), 33.1 (C^{12}), 26.3 (C^{14}), 26.1 (C^{13}), 20.2 (C^{10}). **HRMS** (ESI-TOF) m/z: $[M + H]^+$ Calcd for $C_{16}H_{29}N_2O$ 265.2274; Found 265.2285.

1-Allyl-3-(((1*R*,5*S*)-6,6-dimethylbicyclo[3.1.1]hept-2-en-2-yl)methyl)-1,3-dimethylurea (334)

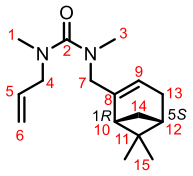

Reaction performed on 1.00 mmol scale following general procedure **2A** using **302** (202 mg, 1.00 mmol, 1.00 equiv.), triphosgene (178 mg, 0.600 mmol, 0.600 equiv.) in anhydrous CH_2Cl_2 (20 mL), anhydrous pyridine (0.16 mL, 2.0 mmol, 2.0 equiv.), which was stirred for 2 h at 0 °C to room temperature. Reaction intermediate was redissolved in anhydrous MeCN (14 mL) and stirred with *N*-allylmethylamine (0.12 mL, 1.3 mmol, 1.3 equiv.) and triethylamine (0.35 mL, 2.5 mmol, 2.5 equiv.) for 3.5 d at room temperature. Flash column chromatography (4−32% EtOAc/pentane) gave **334** as a pale-yellow oil (209 mg, 0.795 mmol, 79% yield). **IR** (film) ν_{max} 2916, 1646, 1485, 1382, 1231, 1094, 921, 774 cm^{-1}. **^{1}H NMR** (400 MHz, $CDCl_3$) δ 5.80 (ddt, *J* = 17.2, 10.2, 5.6 Hz, 1H, H^5), 5.42 – 5.35 (m, 1H, H^9), 5.23 – 5.12 (m, 2H, H^6), 3.79 – 3.64 (m, 3H, H^4 + H^7), 3.54 (dq, *J* = 16.0, 1.8 Hz, 1H, H^7), 2.73 (s, 3H, H^1/H^3), 2.73 (s, 3H, H^1/H^3), 2.37 (dt, *J* = 8.6, 5.6 Hz, 1H, H^{13}), 2.34 – 2.19 (m, 2H, H^{14}), 2.15 – 2.06 (m, 1H, H^{12}), 1.96 (td, *J* = 5.6, 1.5 Hz, 1H, H^{10}), 1.26 (s, 3H, H^{15}), 1.12 (d, *J* = 8.6 Hz, 1H, H^{13}), 0.83 (s, 3H, H^{15}). **^{13}C NMR** (101 MHz, $CDCl_3$) δ 165.5 (C^2), 144.7 (C^8), 134.4 (C^5), 118.5 (C^9), 117.0 (C^6), 55.6 (C^7), 53.6 (C^4), 43.6 (C^{10}), 41.1 (C^{12}), 38.2 (C^{11}), 36.6 (C^3), 36.1 (C^1), 31.7 (C^{13}), 31.3 (C^{14}), 26.3 (C^{15}), 21.2 (C^{15}). **HRMS** (ESI-TOF) m/z: $[M + H]^+$ Calcd for $C_{16}H_{27}N_2O$ 263.2118; Found 263.2117.

1-(((1*R*,5*S*)-6,6-Dimethylbicyclo[3.1.1]hept-2-en-2-yl)methyl)-1,3-dimethyl-3-(2-methylallyl)urea (335)

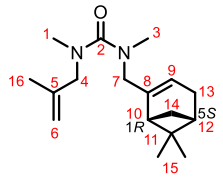

Reaction performed on 1.50 mmol scale following general procedure **2A** using **302** (303 mg, 1.50 mmol, 1.00 equiv.), triphosgene (272 mg, 0.916 mmol, 0.611 equiv.) in anhydrous CH_2Cl_2 (30 mL), anhydrous pyridine (0.24 mL, 3.0 mmol, 2.0 equiv.), which was stirred for 19 h at 0 °C to room temperature. Reaction intermediate was redissolved in anhydrous MeCN (21.4 mL) and stirred with **295** (264 mg, 1.95 mmol, 1.30 equiv.) and triethylamine (730 µL, 5.25 mmol, 3.50 equiv.) for 30 h at room temperature. Flash column chromatography (1−14% acetone/pentane) gave **335** as a pale-yellow oil (285 mg, 1.03 mmol, 69% yield). **IR** (film) ν_{max} 2915, 1646, 1486, 1382, 1233, 1221, 1105, 899, 772 cm^{-1}. **^{1}H NMR** (400 MHz, $CDCl_3$) δ 5.43 – 5.35 (m, 1H, H^9), 4.89 – 4.84 (m, 2H, H^6), 3.75 (dq, *J* = 16.1, 2.3 Hz, 1H, H^7), 3.67 (AB q, *J* = 16.0 Hz, 2H, H^4), 3.53 (dq, *J* = 16.1, 1.7 Hz, 1H, H^7), 2.72 (s, 3H, H^1/H^3), 2.71 (s, 3H, H^1/H^3), 2.37 (dt, *J* = 8.6, 5.6 Hz, 1H, H^{13}), 2.34 – 2.19 (m, 2H, H^{14}), 2.10 (ttd, *J* = 5.6, 2.9, 1.4 Hz, 1H, H^{12}), 1.97 (td, *J* = 5.6, 1.4 Hz, 1H, H^{10}), 1.66 (dd, *J* = 1.5, 0.8 Hz, 3H, H^{16}), 1.26 (s, 3H, H^{15}), 1.12 (d, *J* = 8.6 Hz, 1H, H^{13}), 0.82 (s, 3H, H^{15}). **^{13}C NMR** (101 MHz, $CDCl_3$) δ 165.7 (C^2), 144.8 (C^8), 141.6 (C^5), 118.6 (C^9), 111.8 (C^6), 56.8 (C^4), 55.7 (C^7), 43.6 (C^{10}), 41.1 (C^{12}), 38.2 (C^{11}), 36.5 (C^3), 36.4 (C^1), 31.7 (C^{13}), 31.3 (C^{14}), 26.3 (C^{15}), 21.1 (C^{15}), 20.2 (C^{16}). **HRMS** (ESI-TOF) m/z: $[M + H]^+$ Calcd for $C_{17}H_{29}N_2O$ 277.2274; Found 277.2268.

(*Z*)-1,3-Dimethyl-3-(2-methylallyl)-1-(2-(1,3,3-trimethylbicyclo[2.2.1]heptan-2-ylidene)ethyl)urea (336)

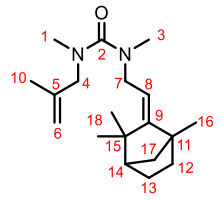

Reaction performed on 0.900 mmol scale following general procedure **2A** using **303** (207 mg, 0.900 mmol, 1.00 equiv.), triphosgene (160 mg, 0.540 mmol, 0.600 equiv.) in anhydrous CH_2Cl_2 (18 mL), anhydrous pyridine (0.15 mL, 1.8 mmol, 2.0 equiv.), which was stirred for 16 h at 0 °C to room temperature. Reaction intermediate was redissolved in anhydrous MeCN (13 mL) and stirred with **295** (142 mg, 1.17 mmol, 1.30 equiv.) and triethylamine (440 µL, 3.15 mmol, 3.50 equiv.) for 21.5 h at room temperature. Flash column chromatography (5−40% EtOAc/petroleum ether) gave **336** as a

yellow oil (243 mg, 0.799 mmol, 89% yield). **IR** (film) ν_{max} 2957, 1645, 1485, 1461, 1377, 1362, 1231, 1221, 1103, 908, 896, 772 cm^{-1}. **^{1}H NMR** (400 MHz, $CDCl_3$) δ 4.93 – 4.86 (m, 3H, H^6 + H^8), 3.86 (d, *J* = 6.6 Hz, 2H, H^7), 3.69 (s, 2H, H^4), 2.74 (s, 3H, H^1), 2.73 (s, 3H, H^3), 1.77 – 1.70 (m, 2H, H^{13} + H^{14}), 1.68 (s, 3H, H^{10}), 1.55 (dq, *J* = 9.6, 2.2 Hz, 1H, H^{17}), 1.55 – 1.38 (m, 2H, H^{12} + H^{13}), 1.24 – 1.17 (m, 2H, H^{12} + H^{17}), 1.19 (s, 3H, H^{18}), 1.14 (s, 3H, H^{16}), 1.12 (s, 3H, H^{18}). **^{13}C NMR** (101 MHz, $CDCl_3$) δ 165.6 (C^2), 160.5 (C^9), 141.7 (C^5), 112.5 (C^8), 111.8 (C^6), 56.9 (C^4), 50.8 (C^{11}), 49.7 (C^{14}), 48.5 (C^7), 44.1 (C^{17}), 42.7 (C^{15}), 36.5 (C^1), 36.1 (C^{12}), 35.8 (C^3), 27.4 (C^{18}), 25.7 (C^{13}), 25.5 (C^{18}), 20.2 (C^{10}), 19.3 (C^{16}). **HRMS** (ESI-TOF) m/z: $[M + H]^+$ Calcd for $C_{19}H_{33}N_2O$ 305.2587; Found 305.2583.

1-Allyl-3-(cyclohex-1-en-1-ylmethyl)-1,3-dimethylurea (337)

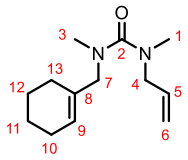

Reaction performed on 0.60 mmol scale following general procedure **2A** using **304** (97 mg, 0.60 mmol, 1.0 equiv.), triphosgene (107 mg, 0.360 mmol, 0.600 equiv.) in anhydrous CH_2Cl_2 (12 mL), anhydrous pyridine (0.10 mL, 1.2 mmol, 2.0 equiv.), which was stirred for 15 h at 0 °C to room temperature. Reaction intermediate was redissolved in anhydrous MeCN (8.6 mL) and stirred with *N*-allylmethylamine (70 μL, 0.78 mmol, 1.3 equiv.) and triethylamine (0.21 mL, 1.5 mmol, 2.5 equiv.) for 6 h at room temperature. Flash column chromatography (10−80% EtOAc/petroleum ether) gave **337** as a pale-yellow oil (114 mg, 0.512 mmol, 85% yield). **IR** (film) ν_{max} 2923, 1639, 1485, 1385, 1371, 1231, 1092, 920, 773 cm^{-1}. **^{1}H NMR** (400 MHz, $CDCl_3$) δ 5.81 (ddt, *J* = 17.1, 10.2, 5.6 Hz, 1H, H^5), 5.56 (tt, *J* = 3.7, 1.6 Hz, 1H, H^9), 5.23 – 5.13 (m, 2H, H^6), 3.71 (dt, *J* = 5.6, 1.6 Hz, 2H, H^4), 3.63 (s, 2H, H^7), 2.73 (s, 3H, H^1), 2.69 (s, 3H, H^3), 2.05 – 1.98 (m, 2H, H^{10}), 1.87 – 1.80 (m, 2H, H^{13}), 1.66 – 1.51 (m, 4H, H^{11} + H^{12}). **^{13}C NMR** (101 MHz, $CDCl_3$) δ 165.7 (C^2), 134.5 (C^5), 134.0 (C^8), 123.8 (C^9), 116.9 (C^6), 57.0 (C^7), 53.7 (C^4), 36.1 (C^1), 36.0 (C^3), 26.4 (C^{13}), 25.2 (C^{10}), 22.7 (C^{11}), 22.6 (C^{12}). **HRMS** (ESI-TOF) m/z: $[M + H]^+$ Calcd for $C_{13}H_{23}N_2O$ 223.1805; Found 223.1803.

1-(Cyclohex-2-en-1-yl)-1,3-dimethyl-3-(2-methylallyl)urea (338)

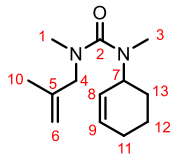

Reaction performed on 1.51 mmol scale following general procedure **2A** using **305** (223 mg, 1.51 mmol, 1.00 equiv.), triphosgene (267 mg, 0.900 mmol, 0.596 equiv.) in anhydrous CH_2Cl_2 (30 mL), anhydrous pyridine (0.24 mL, 3.0 mmol, 2.0 equiv.), which was stirred for 18 h at 0 °C to room temperature. Reaction intermediate was redissolved in anhydrous MeCN (21.4 mL) and stirred with **295** (264 mg, 1.95 mmol, 1.30 equiv.) and triethylamine (730 µL, 5.25 mmol, 3.50 equiv.) for 18 h at room temperature. Flash column chromatography (1−14% acetone/pentane) gave **338** as a yellow oil (299 mg, 1.34 mmol, 90% yield). **IR** (film) ν_{max} 3440, 2932, 1635, 1485, 1455, 1377, 1289, 1105, 895, 773 cm^{-1}. **^{1}H NMR** (400 MHz, $CDCl_3$) δ 5.90 – 5.80 (m, 1H, H^8), 5.55 – 5.46 (m, 1H, H^9), 4.91 – 4.83 (m, 2H, H^6), 4.44 – 4.33 (m, 1H, H^7), 3.66 (AB q, J = 16.0 Hz, 2H, H^4), 2.72 (s, 3H, H^1), 2.65 (s, 3H, H^3), 2.01 – 1.95 (m, 2H, H^{11}), 1.85 – 1.77 (m, 2H, H^{12} + H^{13}), 1.67 (s, 3H, H^{10}), 1.64 – 1.57 (m, 2H, H^{12} + H^{13}). **^{13}C NMR** (101 MHz, $CDCl_3$) δ 165.8 (C^2), 141.7 (C^5), 131.2 (C^8), 129.5 (C^9), 111.7 (C^6), 57.0 (C^4), 54.5 (C^7), 36.6 (C^1), 31.4 (C^3), 26.4 (C^{12}), 24.8 (C^{11}), 21.9 (C^{13}), 20.2 (C^{10}). **HRMS** (ESI-TOF) m/z: $[M + H]^+$ Calcd for $C_{13}H_{23}N_2O$ 223.1805; Found 223.1801.

***N*-Methyl-*N*-(2-methylallyl)-3,6-dihydropyridine-1(2*H*)-carboxamide (339)**

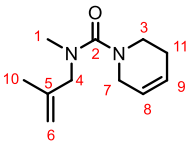

Reaction performed on 1.50 mmol scale following general procedure **2A** using **295** (210 mg, 1.50 mmol, 1.00 equiv.), triphosgene (267 mg, 0.900 mmol, 0.600 equiv.) in anhydrous CH_2Cl_2 (30 mL), and pyridine (0.24 mL, 3.0 mmol, 2.0 equiv.), which was stirred for 19 h at 0 °C to room temperature. Reaction intermediate was redissolved in anhydrous MeCN (21.4 mL), and stirred with 1,2,3,6-tetrahydropyridine (180 µL, 1.95 mmol, 1.30 equiv.) and triethylamine (520 µL, 3.75 mmol, 2.50 equiv.) for 6 h at room temperature. Flash column chromatography (5–29% acetone/pentane) gave **339** as a yellow oil (262 mg, 1.35 mmol, 90% yield). **IR** (film) ν_{max} 3359, 2916, 1635, 1538, 1485, 1447, 1398, 1386, 1239, 1075, 900, 771 cm^{-1}. **^{1}H NMR** (400 MHz, $CDCl_3$) δ 5.85 – 5.78 (m, 1H, H^9), 5.70 – 5.63 (m, 1H, H^8), 4.91 – 4.84 (m, 2H, H^6), 3.74 – 3.71 (m, 2H, H^7), 3.69 (s, 2H, H^4), 3.31 (t, J = 5.6 Hz, 2H, H^3), 2.75 (s, 3H, H^1), 2.21 – 2.15 (m, 2H, H^{11}), 1.68 (dd, J = 1.5, 0.8 Hz, 3H, H^{10}). **^{13}C NMR** (101 MHz, $CDCl_3$) δ 165.0 (C^2), 141.6 (C^5), 125.7 (C^9), 125.2 (C^8), 111.8 (C^6), 56.6 (C^4), 46.4 (C^7), 44.0 (C^3), 36.2

(C^1), 25.5 (C^{11}), 20.2 (C^{10}). **HRMS** (ESI-TOF) m/z: $[M + H]^+$ Calcd for $C_{11}H_{19}N_2O$ 195.1492; Found 195.1487.

1-Allyl-1,3-dimethyl-3-(2-phenylallyl)urea (340)

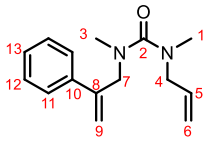

Reaction performed on 1.10 mmol scale following general procedure **2A** using **306** (202 mg, 1.10 mmol, 1 equiv.), triphosgene (196 mg, 0.660 mmol, 0.600 equiv.) in anhydrous CH_2Cl_2 (22 mL), anhydrous pyridine (0.18 mL, 2.2 mmol, 2.0 equiv.), which was stirred for 18 h at 0 °C to room temperature. Reaction intermediate was redissolved in anhydrous MeCN (16 mL) and stirred with *N*-allylmethylamine (140 µL, 1.43 mmol, 1.30 equiv.) and triethylamine (380 µL, 2.75 mmol, 2.50 equiv.) for 24 h at room temperature. Flash column chromatography (5−40% acetone/pentane) gave **340** as a yellow oil (226 mg, 0.923 mmol, 84% yield). **IR** (film) ν_{max} 2910, 2239, 1633, 1489, 1383, 1237, 1099, 907, 774, 728, 710, 645 cm^{-1}. **^{1}H NMR** (400 MHz, $CDCl_3$) δ 7.39 – 7.35 (m, 2H, H^{11}), 7.34 – 7.26 (m, 3H, H^{12} + H^{13}), 5.80 – 5.70 (m, 1H, H^5), 5.46 (q, *J* = 1.1 Hz, 1H, H^9), 5.23 (q, *J* = 1.5 Hz, 1H, H^9), 5.16 (dq, *J* = 7.1, 1.6 Hz, 1H, H^6), 5.13 (t, *J* = 1.6 Hz, 1H, H^6), 4.24 (t, *J* = 1.4 Hz, 2H, H^7), 3.61 (dt, *J* = 5.7, 1.6 Hz, 2H, H^4), 2.73 (s, 3H, H^3), 2.62 (s, 3H, H^1). **^{13}C NMR** (101 MHz, $CDCl_3$) δ 165.3 (C^2), 144.6 (C^{10}), 139.2 (C^8), 134.3 (C^5), 128.5 (C^{12}), 128.0 (C^{13}), 126.3 (C^{11}), 117.0 (C^6), 113.8 (C^9), 54.4 (C^7), 53.5 (C^4), 36.7 (C^3), 35.9 (C^1). **HRMS** (ESI-TOF) m/z: $[M + H]^+$ Calcd for $C_{15}H_{21}N_2O$ 245.1648; Found 245.1648.

1-Allyl-3-(2-benzylallyl)-1,3-dimethylurea (341)

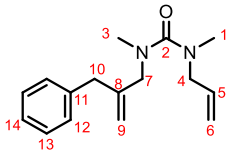

Reaction performed on 1.20 mmol scale following general procedure **2A** using **307** (237 mg, 1.20 mmol, 1.00 equiv.), triphosgene (214 mg, 0.720 mmol, 0.600 equiv.) in anhydrous CH_2Cl_2 (24 mL), anhydrous pyridine (0.19 mL, 2.4 mmol, 2.0 equiv.), which was stirred for 17 h at 0 °C to room temperature. Reaction intermediate was redissolved in anhydrous MeCN (17 mL) and stirred with *N*-allylmethylamine (150 µL, 1.56 mmol, 1.30 equiv.) and triethylamine (0.42 mL, 3.0 mmol, 2.5 equiv.) for 4 h at room temperature. Flash column chromatography (7−60% EtOAc/petroleum ether) gave **341** as an orange oil (294 mg, 1.14 mmol, 95% yield). **IR** (film) ν_{max} 2908, 1641, 1490, 1384, 1236, 1098,

914, 773, 741, 700 cm^{-1}. **^{1}H NMR** (400 MHz, $CDCl_3$) δ 7.31 – 7.26 (m, 2H, H^{12}), 7.23 – 7.19 (m, 1H, H^{14}), 7.19 – 7.14 (m, 2H, H^{13}), 5.71 (ddt, *J* = 17.8, 9.7, 5.6 Hz, 1H, H^{5}), 5.15 – 5.07 (m, 2H, H^{6}), 5.04 – 4.99 (m, 1H, H^{9}), 4.95 – 4.93 (m, 1H, H^{9}), 3.68 – 3.64 (m, 4H, H^{4} + H^{7}), 3.30 (s, 2H, H^{10}), 2.72 (s, 3H, H^{3}), 2.66 (s, 3H, H^{1}). **^{13}C NMR** (101 MHz, $CDCl_3$) δ 165.4 (C^{2}), 144.8 (C^{8}), 139.0 (C^{11}), 134.3 (C^{5}), 129.0 (C^{13}), 128.5 (C^{12}), 126.4 (C^{14}), 116.9 (C^{6}), 113.0 (C^{9}), 55.4 (C^{7}), 53.5 (C^{4}), 40.9 (C^{10}), 36.5 (C^{3}), 35.9 (C^{1}). **HRMS** (ESI-TOF) m/z: $[M + H]^+$ Calcd for $C_{16}H_{23}N_2O$ 259.1805; Found 259.1802.

1-Allyl-3-cinnamyl-1,3-dimethylurea (248)

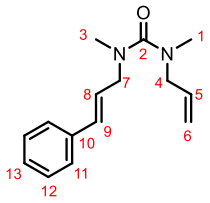

Reaction performed on 0.650 mmol scale following general procedure **2A** using **308** (119 mg, 0.650 mmol, 1.00 equiv.), triphosgene (116 mg, 0.390 mmol, 0.600 equiv.) in anhydrous CH_2Cl_2 (13 mL), anhydrous pyridine (0.11 mL, 1.3 mmol, 2.0 equiv.), which was stirred for 18 h at 0 °C to room temperature. Reaction intermediate was redissolved in anhydrous MeCN (9 mL) and stirred with *N*-allylmethylamine (80 µL, 0.85 mmol, 1.3 equiv.) and triethylamine (230 µL, 1.63 mmol, 2.51 equiv.) for 24 h at room temperature. Flash column chromatography (5−40% acetone/pentane) gave **248** as a yellow oil (149 mg, 0.611 mmol, 94% yield). **IR** (film) ν_{max} 2914, 1637, 1488, 1384, 1357, 773 cm^{-1}. **^{1}H NMR** (400 MHz, $CDCl_3$) δ 7.40 – 7.36 (m, 2H, H^{12}), 7.34 – 7.29 (m, 2H, H^{11}), 7.23 (tt, *J* = 7.2, 2.2 Hz, 1H, H^{13}), 6.53 (dt, *J* = 15.9, 1.5 Hz, 1H, H^{9}), 6.22 (dt, *J* = 15.9, 6.2 Hz, 1H, H^{8}), 5.84 (ddt, *J* = 17.2, 10.2, 5.6 Hz, 1H, H^{5}), 5.27 – 5.15 (m, 2H, H^{6}), 3.90 (dd, *J* = 6.2, 1.5 Hz, 2H, H^{7}), 3.77 (dt, *J* = 5.6, 1.6 Hz, 2H, H^{4}), 2.80 (s, 3H, H^{1}/H^{3}), 2.79 (s, 3H, H^{1}/H^{3}). **^{13}C NMR** (101 MHz, $CDCl_3$) δ 165.3 (C^{2}), 136.8 (C^{10}), 134.3 (C^{5}), 132.5 (C^{9}), 128.7 (C^{11}), 127.7 (C^{13}), 126.5 (C^{12}), 125.9 (C^{8}), 117.1 (C^{6}), 53.6 (C^{4}), 53.1 (C^{7}), 36.3 (C^{1}/C^{3}), 36.2 (C^{1}/C^{3}). **HRMS** (ESI-TOF) m/z: $[M + H]^+$ Calcd for $C_{15}H_{21}N_2O$ 245.1648; Found 245.1641.

(*E*)-1,3-Dimethyl-3-(2-methylallyl)-1-(penta-2,4-dien-1-yl)urea (342)

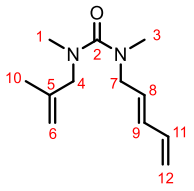

Reaction performed on 1.50 mmol scale following general procedure **2A** using **309** (200 mg, 1.50 mmol, 1.00 equiv.), triphosgene (267 mg, 0.900 mmol, 0.600 equiv.) in anhydrous CH_2Cl_2 (30 mL), anhydrous pyridine (0.24 mL, 3.0 mmol, 2.0 equiv.), which was stirred for 24 h at 0 °C to room temperature. Reaction intermediate was redissolved in anhydrous MeCN (21.4 mL) and stirred with **295** (237 mg, 1.95 mmol, 1.30 equiv.) and triethylamine (730 µL, 5.25 mmol, 3.50 equiv.) for 41 h at room temperature. Flash column chromatography (2−22% acetone/pentane) gave **342** as a pale-yellow liquid (180 mg, 0.866 mmol, 58% yield). **IR** (film) ν_{max} 2855, 1639, 1486, 1382, 1220, 1104, 1005, 899, 773 cm^{-1}. **^{1}H NMR** (400 MHz, $CDCl_3$) δ 6.34 (dt, *J* = 16.9, 10.3 Hz, 1H, H^{11}), 6.21 – 6.13 (m, 1H, H^9), 5.69 (dtd, *J* = 15.2, 6.1, 0.7 Hz, 1H, H^8), 5.21 – 5.15 (m, 1H, H^{12}), 5.09 – 5.04 (m, 1H, H^{12}), 4.91 – 4.85 (m, 2H, H^6), 3.76 (d, *J* = 6.1 Hz, 2H, H^7), 3.68 (s, 2H, H^4), 2.74 (s, 6H, H^1 + H^3), 1.67 (dd, *J* = 1.5, 0.8 Hz, 3H, H^{10}). **^{13}C NMR** (101 MHz, $CDCl_3$) δ 165.5 (C^2), 141.5 (C^5), 136.4 (C^{11}), 133.2 (C^9), 130.0 (C^8), 117.2 (C^{12}), 111.7 (C^6), 56.8 (C^4), 52.6 (C^7), 36.4 (C^1), 36.2 (C^3), 20.2 (C^{10}). **HRMS** (ESI-TOF) m/z: $[M + H]^+$ Calcd for $C_{12}H_{21}N_2O$ 209.1648; Found 209.1638.

1,3-Dimethyl-3-(2-methylallyl)-1-(2-methylenebut-3-en-1-yl)urea (343)

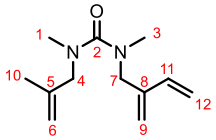

Reaction performed on 1.50 mmol scale following general procedure **2A** using **311** (200 mg, 1.50 mmol, 1.00 equiv.), triphosgene (267 mg, 0.900 mmol, 0.600 equiv.) in anhydrous CH_2Cl_2 (30 mL), anhydrous pyridine (0.24 mL, 3.0 mmol, 2.0 equiv.), which was stirred for 24 h at 0 °C to room temperature. Reaction intermediate was redissolved in anhydrous MeCN (21.4 mL) and stirred with **295** (166 mg, 1.37 mmol, 0.900 equiv.) and triethylamine (730 µL, 5.25 mmol, 3.50 equiv.) for 41 h at room temperature. Flash column chromatography (5−40% acetone/pentane) gave **343** as a yellow liquid (175 mg, 0.841 mmol, 56% yield; 72% yield BRSM). **IR** (film) ν_{max} 2860, 1643, 1487, 1383, 1237, 1106 cm^{-1}. **^{1}H NMR** (400 MHz, $CDCl_3$) δ 6.37 (dd, *J* = 17.8, 11.1 Hz, 1H, H^{11}), 5.22 – 5.04 (m, 4H, H^9 + H^{12}), 4.89 – 4.85 (m, 2H, H^6), 3.96 (s, 2H, H^7), 3.66 (s, 2H, H^4), 2.75 (s, 3H, H^3), 2.72 (s, 3H, H^1), 1.67 – 1.64 (m, 3H, H^{10}). **^{13}C NMR** (101 MHz, $CDCl_3$) δ 165.5 (C^2), 142.0 (C^8), 141.7 (C^5), 137.0 (C^{11}),

116.6 (C^{12}), 114.2 (C^{9}), 111.7 (C^{6}), 56.7 (C^{4}), 52.1 (C^{7}), 36.7 (C^{3}), 36.2 (C^{1}), 20.1 (C^{10}). **HRMS** (ESI-TOF) m/z: $[M + H]^+$ Calcd for $C_{12}H_{21}N_2O$ 209.1648; Found 209.1639.

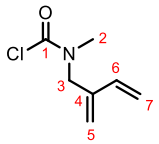

In addition, methyl(2-methylenebut-3-en-1-yl)carbamic chloride was recovered as a yellow oil (53 mg, 0.33 mmol, 22% yield). **IR** (film) ν_{max} 2935, 1727, 1382, 1195, 1074, 905, 772, 729, 667 cm^{-1}. **^{1}H NMR** (400 MHz, $CDCl_3$; rotameric ratio 0.57:0.43) δ 6.40 (ddd, *J* = 22.5, 17.8, 11.1 Hz, 1H, H^6), 5.33 – 5.03 (m, 4H, H^5 + H^7), 4.28 (s, 0.85H, minor H^3), 4.21 (s, 1.15H, major H^3), 3.06 (s, 1.72H, major H^2), 3.02 (s, 1.28H, minor H^2). **^{13}C NMR** (101 MHz, $CDCl_3$; rotameric ratio 0.57:0.43) δ 150.1 (C^1), 139.8 (major C^4), 139.3 (minor C^4), 136.4 (minor C^6), 136.0 (major C^6), 118.2 (major C^7), 116.3 (minor C^7), 115.5 (major C^5), 114.7 (minor C^5), 53.8 (minor C^3), 52.0 (major C^3), 37.7 (major C^2), 36.9 (minor C^2). **HRMS** (ESI-TOF) m/z: $[M + H]^+$ Calcd for $C_7H_{11}NOCl$ 160.0524; Found 160.0524.

1-Allyl-3-((2*E*,4*E*)-hexa-2,4-dien-1-yl)-1,3-dimethylurea (344)

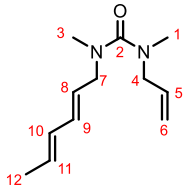

Reaction performed on 1.20 mmol scale following general procedure **2A** using **310** (177 mg, 1.20 mmol, 1.00 equiv.), triphosgene (214 mg, 0.720 mmol, 0.600 equiv.) in anhydrous CH_2Cl_2 (24 mL), anhydrous pyridine (0.19 mL, 2.4 mmol, 2.0 equiv.), which was stirred for 24 h at 0 °C to room temperature. Reaction intermediate was redissolved in anhydrous MeCN (17 mL) and stirred with *N*-allylmethylamine (150 µL, 1.56 mmol, 1.30 equiv.) and triethylamine (0.42 mL, 3.0 mmol, 3.5 equiv.) for 23.5 h at room temperature. Flash column chromatography (7−60% EtOAc/pentane) gave **344** as a yellow oil (167 mg, 0.802 mmol, 67% yield). **IR** (film) ν_{max} 3383, 2918, 1634, 1489, 1385, 1270, 1095, 991, 924, 754 cm^{-1}. **^{1}H NMR** (400 MHz, $CDCl_3$) δ 6.18 – 5.99 (m, 2H, H^9 + H^{10}), 5.81 (ddt, *J* = 17.2, 10.2, 5.6 Hz, 1H, H^5), 5.67 (dq, *J* = 13.5, 6.7 Hz, 1H, H^{11}), 5.53 (dt, *J* = 14.6, 6.2 Hz, 1H, H^8), 5.24 – 5.13 (m, 2H, H^6), 3.76 – 3.68 (m, 4H, H^4 + H^7), 2.74 (s, 3H, H^1), 2.72 (s, 3H, H^3), 1.74 (dd, *J* = 6.7, 0.9 Hz, 3H, H^{12}). **^{13}C NMR** (101 MHz, $CDCl_3$) δ 165.3 (C^2), 134.3 (C^5), 133.0 (C^9), 130.9 (C^{10}), 129.5 (C^{11}), 126.5 (C^8), 117.0 (C^6), 53.6 (C^4), 52.8 (C^7), 36.2 (C^1/C^3), 36.1 (C^1/C^3), 18.2 (C^{12}). **HRMS** (ESI-TOF) m/z: $[M + Na]^+$ Calcd for $C_{12}H_{20}N_2ONa$ 231.1468; Found 231.1468.

(*E*)-1,3-Dimethyl-3-(2-methylallyl)-1-(3-(trimethylsilyl)allyl)urea (345)

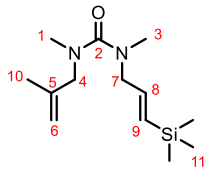

Reaction performed on 1.20 mmol scale following general procedure **2A** using **312** (216 mg, 1.20 mmol, 1.00 equiv.), triphosgene (214 mg, 0.720 mmol, 0.600 equiv.) in anhydrous CH_2Cl_2 (24 mL), anhydrous pyridine (0.19 mL, 2.4 mmol, 2.0 equiv.), which was stirred for 17 h at 0 °C to room temperature. Reaction intermediate was redissolved in anhydrous MeCN (17 mL) and stirred with **295** (190 mg, 1.56 mmol, 1.30 equiv. + 95 mg, 0.78 mmol, 0.65 equiv.) and triethylamine (0.59 mL, 4.2 mmol, 3.5 equiv.) for 1.5 d at room temperature. Flash column chromatography (5−40% EtOAc/petroleum ether) gave **345** as a yellow oil (265 mg, 1.04 mmol, 87% yield). **IR** (film) ν_{max} 2954, 2898, 1646, 1486, 1383, 1247, 1104, 865, 837 cm^{-1}. **^{1}H NMR** (400 MHz, $CDCl_3$) δ 5.97 (dt, *J* = 18.7, 4.7 Hz, 1H, H^8), 5.83 (dt, *J* = 18.7, 1.5 Hz, 1H, H^9), 4.91 – 4.84 (m, 2H, H^6), 3.75 (dd, *J* = 4.7, 1.5 Hz, 2H, H^7), 3.66 (s, 2H, H^4), 2.73 (s, 3H, H^1), 2.72 (s, 3H, H^3), 1.66 (dd, *J* = 1.4, 0.8 Hz, 3H, H^{10}), 0.06 (s, 9H, H^{11}). **^{13}C NMR** (101 MHz, $CDCl_3$) δ 165.6 (C^2), 141.8 (C^8), 141.6 (C^5), 132.2 (C^9), 111.6 (C^6), 56.8 (C^4), 55.9 (C^7), 36.4 (C^1), 36.1 (C^3), 20.2 (C^{10}), -1.2 (C^{11}). **HRMS** (ESI-TOF) m/z: $[M + H]^+$ Calcd for $C_{13}H_{27}N_2OSi$ 255.1887; Found 255.1885.

1-Allyl-3-(4-*tert*-butyldimethylsilyl)-2-methylenebut-3-yn-1-yl)-1,3-dimethylurea (346)

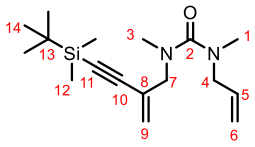

Reaction performed on 0.800 mmol scale following general procedure **2A** using **313** (197 mg, 0.800 mmol, 1.00 equiv.), triphosgene (142 mg, 0.480 mmol, 0.600 equiv.) in anhydrous CH_2Cl_2 (16 mL), anhydrous pyridine (0.13 mL, 1.6 mmol, 2.0 equiv.), which was stirred for 16 h at 0 °C to room temperature. Reaction intermediate was redissolved in anhydrous MeCN (11.4 mL) and stirred with *N*-allylmethylamine (280 µL, 1.04 mmol, 1.30 equiv.) and triethylamine (0.28 mL, 2.0 mmol, 2.5 equiv.) for 4 h at room temperature. Then, *N*-allylmethylamine (100 µL, 2.92 mmol, 3.60 equiv.) and triethylamine (0.28 mL, 2.0 mmol, 2.5 equiv.) were added again, and the reaction was stirred for 5 h at room temperature. Flash column chromatography (5−25% EtOAc/petroleum ether) gave **346** as a pale-yellow oil (221 mg, 0.722 mmol, 90% yield). **IR** (film) ν_{max} 2953, 2929, 2856, 2147, 1649, 1487, 1471, 1381, 1249, 915, 860, 837, 775 680 cm^{-1}. **^{1}H NMR** (400 MHz, $CDCl_3$) δ 5.81 (ddt, *J* = 17.2, 10.3, 5.6 Hz, 1H, H^5), 5.52 (q, *J* = 1.4 Hz, 1H, H^9), 5.41 (q, *J* = 1.6 Hz, 1H, H^9), 5.22 – 5.14 (m, 2H, H^6), 3.81 (t,

J = 1.5 Hz, 2H, H^7), 3.74 (dt, J = 5.6, 1.6 Hz, 2H, H^4), 2.78 (s, 3H, H^3), 2.75 (s, 3H, H^1), 0.92 (s, 9H, H^{14}), 0.09 (s, 6H, H^{12}). **^{13}C NMR** (101 MHz, $CDCl_3$) δ 165.1 (C^2), 134.2 (C^5), 128.3 (C^8), 122.9 (C^9), 117.1 (C^6), 104.3 (C^{10}), 93.9 (C^{11}), 55.6 (C^7), 53.6 (C^4), 36.8 (C^3), 36.1 (C^1), 26.2 (C^{14}), 16.7 (C^{13}), -4.6 (C^{12}). **HRMS** (ESI-TOF) m/z: $[M + H]^+$ Calcd for $C_{17}H_{31}N_2OSi$ 307.2200; Found 307.2193.

1-Allyl-3-(5-((*tert*-butyldimethylsilyl)oxy)-2-methylenepentyl)-1,3-dimethylurea (347)

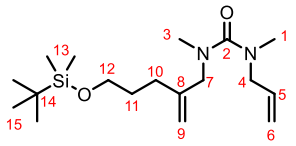

Reaction performed on 0.778 mmol scale following general procedure **2A** using **315** (218 mg, 0.778 mmol, 1.00 equiv.), triphosgene (142 mg, 0.480 mmol, 0.617 equiv.) in anhydrous CH_2Cl_2 (16 mL), anhydrous pyridine (0.13 mL, 1.6 mmol, 2.0 equiv.), which was stirred for 16 h at 0 °C to room temperature. Reaction intermediate was redissolved in anhydrous MeCN (11.4 mL) and stirred with *N*-allylmethylamine (100 µL, 1.04 mmol, 1.30 equiv.) and triethylamine (0.28 mL, 2.0 mmol, 2.5 equiv.) for 4 h at room temperature. Then, *N*-allylmethylamine (100 µL, 1.04 mmol, 1.30 equiv.) and triethylamine (0.28 mL, 2.0 mmol, 2.5 equiv.) were added again, and the reaction was stirred for 18.5 h at room temperature followed by 2 h 40 °C. Flash column chromatography (2−12% acetone/petroleum ether) gave **347** as a pale-yellow oil (155 mg, 0.454 mmol, 58% yield). **IR** (film) ν_{max} 2953, 2928, 2856, 1650, 1472, 1384, 1251, 1100, 835, 775 cm^{-1}. **^{1}H NMR** (400 MHz, $CDCl_3$) δ 5.81 (ddt, J = 17.1, 10.2, 5.6 Hz, 1H, H^5), 5.23 – 5.15 (m, 2H, H^6), 4.95 – 4.89 (m, 2H, H^9), 3.76 – 3.68 (m, 4H, H^4 + H^7), 3.61 (t, J = 6.3 Hz, 2H, H^{12}), 2.74 (s, 3H, H^1/H^3), 2.74 (s, 3H, H^1/H^3), 2.04 – 1.98 (m, 2H, H^{10}), 1.71 – 1.60 (m, 2H, H^{11}), 0.89 (s, 9H, H^{15}), 0.04 (s, 6H, H^{13}). **^{13}C NMR** (101 MHz, $CDCl_3$) δ 165.5 (C^2), 145.1 (C^8), 134.4 (C^5), 117.0 (C^6), 110.7 (C^9), 62.8 (C^{12}), 55.8 (C^7), 53.6 (C^4), 36.6 (C^3), 36.1 (C^1), 31.0 (C^{11}), 30.0 (C^{10}), 26.1 (C^{15}), 18.5 (C^{14}), -5.1 (C^{13}). **HRMS** (ESI-TOF) m/z: $[M + H]_+$ Calcd for $C_{18}H_{37}N_2O_2Si$ 341.2619; Found 341.2610.

5.3 N→C Vinyl Migration of Symmetrical and Unsymmetrical Diallyl Ureas

5.3.1 General Procedures

General Procedure 3A (LDA preparation):

An oven- or flame-dried round-bottom flask containing a magnetic stir bar was sealed with a suba seal and placed under anhydrous N_2. The flask was charged with distilled DIPA (1 equiv.) and anhydrous THF (6.67 mL/mmol in total with amount of THF used for General Procedure **3B**). At 0 °C *n*-BuLi (2.5 M in hexanes; 1 equiv.) was added and the reaction mixture was stirred for 5 min. before use.

General Procedure 3B (N→C vinyl migration using LDA):

An oven- or flame-dried round-bottom flask containing a magnetic stir bar was sealed with a suba seal and placed under anhydrous N_2. The flask was charged with the urea (1 equiv.) and anhydrous THF (6.67 mL/mmol in total with amount of THF used for General Procedure **3A**), and then cooled down to −78 °C. At −78 °C, freshly prepared LDA (x equiv.) was added dropwise. The reaction mixture was stirred at −78 °C, or as stated otherwise, for between 2 h and 5.5 h. The reaction mixture was quenched with MeOH (10 mL/mmol). A saturated aqueous solution of NH_4Cl (40 mL/mmol) and CH_2Cl_2 (40 mL/mmol) were added, and the organic phase was extracted. The aqueous phase was washed with CH_2Cl_2 (3×, 40 mL/mmol), and the organic phases were combined, dried over $MgSO_4$, filtered, and concentrated *in vacuo*. The crude product was then purified by normal-phase flash column chromatography.

In case of reverse addition, the flask was charged with freshly prepared LDA instead and the urea was then added dropwise.

General Procedure 3C (N→C vinyl migration using KHMDS and 18-crown-6):

An oven- or flame-dried round-bottom flask or microwave vial containing a magnetic stir bar was sealed with a suba seal and placed under anhydrous N_2. The flask was charged with the urea (1 equiv.), anhydrous THF (10 mL/mmol) and 18-crown-6 (2.2 equiv.). The reaction mixture was cooled down to −78 °C and KHMDS (1 M in THF; 2 equiv.) was added dropwise. After 1 h at −78 °C, the reaction mixture was gradually warmed up by setting the cryostat at 0 °C (or followed by putting the reaction mixture at room temperature) and stirred for between 18 h and 6.5 d. The reaction mixture was quenched with MeOH (10 mL/mmol), after which Et_2O (40 mL/mmol) and a saturated aqueous solution of NH_4Cl

(40 mL/mmol) were added. After extracting the organic phase, the aqueous phase was washed with Et_2O (3×, 40 mL/mmol). The organic phases were collected, dried over $MgSO_4$, filtered, and concentrated *in vacuo*. The crude product was then purified by normal-phase flash column chromatography.

5.3.2 Product Characterisation

1,3,5-Trimethyl-4-phenyltetrahydropyrimidin-2(1*H*)-one (349)

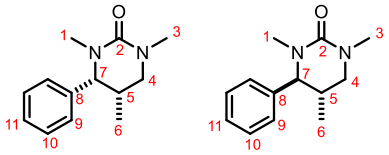

Reaction performed on 0.462 mmol scale following general procedure **3B** using **214** (101 mg, 0.462 mmol, 1.00 equiv.) in anhydrous THF (1.9 mL), LDA (prepared following general procedure **3A**; 0.458 M stock solution; 1.21 mL, 0.554 mmol, 1.20 equiv.), which was stirred for 3 h at –78 °C. Flash column chromatography (25–100% Et_2O/pentane) gave **349** as a white solid (52 mg, 0.24 mmol, 52% yield, **d.r.** 1.4:1 *cis*:*trans*). **MP** (*cis*) 150–151 °C. **MP** (*trans*) 107–108 °C. **IR** (film) ν_{max} 2919, 1625, 1510, 1277, 772 cm^{-1}. **^{1}H NMR** (400 MHz, $CDCl_3$; *cis* assigned by NOE analysis) δ 7.68 – 7.53 (m, 3H, H^{10} + H^{11}), 7.38 (d, *J* = 6.8 Hz, 2H, H^9), 4.50 (d, *J* = 5.1 Hz, 1H, H^7), 3.30 (s, 3H, H^3), 3.29 – 3.18 (m, 2H, H^4), 3.13 (s, 3H, H^1), 2.95 – 2.79 (m, 1H, H^5), 1.00 (d, *J* = 6.9 Hz, 3H, H^6). **^{13}C NMR** (101 MHz, $CDCl_3$; *cis*) δ 156.6 (C^2), 138.0 (C^8), 128.4 (C^{10}), 128.0 (C^9), 127.8 (C^{11}), 66.8 (C^7), 50.6 (C^4), 35.8 (C^3), 35.1 (C^1), 31.0 (C^5), 15.2 (C^6). **^{1}H NMR** (400 MHz, $CDCl_3$; *trans* assigned by NOE analysis) δ 7.67 – 7.53 (m, 3H, H^{10} + H^{11}), 7.45 (d, *J* = 7.0 Hz, 2H, H^9), 4.30 (d, *J* = 5.1 Hz, 1H, H^7), 3.48 (dd, *J* = 11.9, 4.1 Hz, 1H, H^4), 3.28 (s, 3H, H^3), 3.15 (dd, *J* = 11.9, 5.5 Hz, 1H, H^4), 3.09 (s, 3H, H^1), 2.42 – 2.25 (m, 1H, H^5), 1.38 (d, *J* = 6.8 Hz, 3H, H^6). **^{13}C NMR** (101 MHz, $CDCl_3$; *trans*) δ 156.9 (C^2), 141.8 (C^8), 128.8 (C^{10}), 127.6 (C^{11}), 126.6 (C^9), 68.5 (C^7), 51.0 (C^4), 36.2 (C^3), 35.0 (C^1), 34.7 (C^5), 17.4 (C^4). **HRMS** (ESI-TOF) m/z: $[M + H]^+$ Calcd for $C_{13}H_{19}N_2O$ 219.1492; Found 219.1483.

(*E*)-1,3-Dimethyl-1-(1-phenylbut-2-en-1-yl)urea (348)

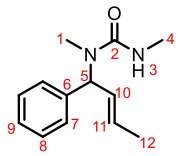

Reaction performed on 0.462 mmol scale following general procedure **3B** using **215** (101 mg, 0.462 mmol, 1.00 equiv.) in anhydrous THF (1.05 mL), LDA (freshly prepared following general procedure **3A**; 0.284 M stock solution; 1.95 mL, 0.554 mmol, 1.20 equiv.), which was stirred for 5 h at –78 °C. Flash column chromatography (12–100% EtOAc/petroleum ether) gave **348** as a white solid (82 mg, 0.38 mmol, 81% yield). **MP** 77–78 °C. **IR** (film) ν_{max} 3345, 2917, 1622, 1538, 1303, 971, 770, 702 cm^{-1}. **^{1}H NMR** (400 MHz, $(CD_3)_2CO$) δ 7.37 – 7.28 (m, 2H, H^7/H^8), 7.28 – 7.19 (m, 3H, H^7/H^8 + H^9), 6.08 (d, *J* = 6.8 Hz, 1H, H^5), 5.80 (ddq, *J* = 15.3, 6.8, 1.3 Hz, 1H, H^{10}), 5.67 (dqd, *J* = 15.3, 6.3, 1.1 Hz,

2H, H^3 + H^{11}), 2.73 (d, *J* = 4.5 Hz, 3H, H^4), 2.64 (s, 3H, H^1), 1.77 (dt, *J* = 6.3, 1.3 Hz, 3H, H^{12}). **^{13}C NMR** (101 MHz, $CDCl_3$) δ 159.2 (C^2), 140.5 (C^6), 129.3 (C^{10}/C^{11}), 128.3 (C^7/C^8), 127.9 (C^{10}/C^{11}), 127.6 (C^7/C^8), 127.1 (C^9), 59.4 (C^5), 30.1 (C^1), 27.7 (C^4), 17.9 (C^{12}). **HRMS** (ESI-TOF) m/z: $[M + H]^+$ Calcd for $C_{13}H_{19}N_2O$ 219.1492; Found 219.1487.

(*E*)-*N*,2-Dimethyl-3-oxo-*N*-(prop-1-en-1-yl)propanamide (353)

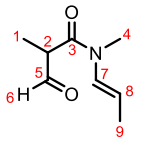

Reaction performed on 0.606 mmol scale following general procedure **3B** using **207** (102 mg, 0.606 mmol, 1.00 equiv.) in anhydrous THF (2.2 mL) and LDA (freshly prepared following general procedure **3A**; 1.83 mL, 0.727 mmol, 1.20 equiv.), which was stirred for 2 h at 0 °C to room temperature. Flash column chromatography (5−40% EtOAc/petroleum ether) gave **353** (29 mg, 0.19 mmol, 31% yield). **IR** (film) ν_{max} 3344, 2934, 1638, 1460, 1220, 772 cm^{-1}. **^{1}H NMR** (400 MHz, $CDCl_3$; suspected mixture of rotamers with a ratio of 1:0.5) δ 9.64 (d, *J* = 2.0 Hz, 1H, major rot. H^6), 9.63 (d, *J* = 2.0 Hz, 0.5H, minor rot. H^6), 7.26 (dq, *J* = 14.4, 1.7 Hz, 0.5H, minor rot. H^7), 6.55 (dq, *J* = 13.6, 1.7 Hz, 1H, major rot. H^7), 5.23 – 5.13 (m, 1H, major rot. H^8), 5.13 – 5.04 (m, 0.5H, minor rot. H^8), 3.66 (qd, *J* = 7.1, 2.0 Hz, 1H, major rot. H^2), 3.63 – 3.58 (m, 0.5H, minor rot. H^2), 3.09 (s, 4.5H, H^4), 1.74 – 1.70 (m, 4.5H, H^9), 1.40 – 1.36 (m, 4.5H, H^1). **^{13}C NMR** (101 MHz, $CDCl_3$; suspected mixture of rotamers with a ratio of 1:0.5) δ 198.3 (C^5), 168.7 (major rot. C^3), 168.1 (minor rot. C^3), 128.3 (major rot. C^7), 127.5 (minor rot. C^7), 110.6 (major rot. C^8), 108.0 (minor rot. C^8), 50.5 (minor rot. C^2), 50.0 (major rot. C^2), 32.7 (minor rot. C^4), 30.9 (major rot. C^4), 15.5 (major rot. C^9), 15.5 (minor rot. C^9), 12.0 (C^1). **HRMS** (ESI-TOF) m/z: $[M + H]^+$ Calcd for $C_8H_{14}N_2O$ 156.1019; Found 156.1016.

(*E*)-2-Cyano-*N*-methyl-*N*-(prop-1-en-1-yl)acetamide (357)

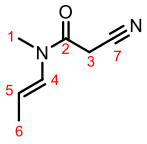

Reaction performed on 0.601 mmol scale following general procedure **3C** using **207** (101 mg, 0.601 mmol, 1.00 equiv.) in anhydrous THF (6 mL), 18-crown-6 (1.25 M in THF; 1.06 mL, 1.32 mmol, 2.20 equiv.) and KHMDS (1.00 M in THF; 1.20 mL, 1.20 mmol, 2.00 equiv.), which was stirred for 5.5 h at 0 °C to room temperature. Flash column chromatography (5−40% acetone/petroleum ether) gave **357** (56 mg, 0.33 mmol, 55% yield). **IR** (film) ν_{max} 2924, 2262, 1654, 1396, 1377, 1220, 1124, 927, 772

cm^{-1}. **^{1}H NMR** (400 MHz, $CDCl_3$; suspected mixture of rotamers with a ratio of 1:0.4) δ 7.17 (dq, *J* = 14.4, 1.7 Hz, 0.4H, minor rot. H^4), 6.35 (dq, *J* = 13.5, 1.6 Hz, 1H, major rot. H^4), 5.29 (dq, *J* = 13.5, 6.6 Hz, 1H, major rot. H^5), 5.15 (dq, *J* = 14.4, 6.6 Hz, 0.4H, minor rot. H^5), 3.59 (s, 0.8H, minor rot. H^3), 3.59 (s, 2H, major rot. H^3), 3.12 (s, 1.2H, minor rot. H^1), 3.11 (s, 3H, major rot. H^1), 1.77 – 1.73 (m, 4.2H, H^6). **^{13}C NMR** (101 MHz, $CDCl_3$) δ 160.2 (major rot. C^2), 159.8 (minor rot. C^2), 127.8 (major rot. C^4), 127.2 (minor rot. C^4), 113.7 (C^7), 113.5 (major rot. C^5), 109.1 (minor rot. C^5), 33.3 (minor rot. C^1), 31.8 (major rot. C^1), 26.0 (minor rot. C^3), 25.6 (major rot. C^3), 15.5 (major rot. C^6), 15.4 (minor rot. C^6). **HRMS** (ESI-TOF) m/z: $[M + H]^+$ Calcd for $C_7H_{10}N_2O$ 139.0866; Found 139.0860.

1,3,5-Trimethyl-4-vinyltetrahydropyrimidin-2(1*H*)-one (360)

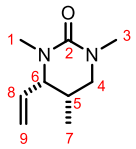

Reaction performed on 0.594 mmol scale following general procedure **3B** using **206** (100 mg, 0.594 mmol, 1.00 equiv.) in anhydrous THF (3.4 mL, 5.8 mL/mmol) and LDA (freshly prepared following general procedure **3A**; 1.26 mL, 0.297 mmol, 0.500 equiv.), which was stirred for 3.5 h at –78 °C. Flash column chromatography (40−55% EtOAc/pentane) gave **360** as a yellow/orange oil (19 mg, 0.11 mmol, 19% yield). **IR** (film) ν_{max} 3450, 2918, 1633, 1513, 773 cm^{-1}. **^{1}H NMR** (400 MHz, $CDCl_3$; assigned as $CH{=}CH_2$ *cis* to CH_3 following NOE analysis) δ 5.65 (ddd, *J* = 17.0, 10.3, 7.1 Hz, 1H, H^8), 5.28 (d, *J* = 10.3 Hz, 1H, H^9), 5.11 (dt, *J* = 17.0, 1.2 Hz, 1H, H^9), 3.54 (t, *J* = 5.9 Hz, 1H, H^6), 3.10 – 2.92 (m, 2H, H^4), 2.90 (s, 3H, H^3), 2.86 (s, 3H, H^1), 2.43 – 2.28 (m, 1H, H^5), 0.90 (d, *J* = 6.9 Hz, 3H, H^7). **^{13}C NMR** (101 MHz, $CDCl_3$) δ 156.2 (C^2), 133.0 (C^8), 118.7 (C^9), 65.0 (C^6), 51.4 (C^4), 35.7 (C^3), 34.6 (C^1), 30.5 (C^5), 14.8 (C^7). **HRMS** (ESI-TOF) m/z: $[M + H]^+$ Calcd for $C_9H_{17}N_2O$ 169.1335; Found 169.1325.

In addition, a mixture of 1,3-dimethyl-1,3-di((*Z*)-prop-1-en-1-yl)urea **364** (1 mg, 0.007 mmol, 1% yield) and (*Z*)-1-allyl-1,3-dimethyl-3-(prop-1-en-1-yl)urea **363** (9 mg, 0.05 mmol, 9% yield) was afforded, along with 4-ethylidene-1,3,5-trimethyltetrahydropyrimidin-2(1*H*)-one **361** (22 mg, 0.13 mmol, 22% yield) and (*Z*)-1-(hexa-1,4-dien-3-yl)-1,3-dimethylurea **358** (6 mg, 0.03 mmol, 6% yield). **206** was recovered in 11% yield (11 mg, 0.065 mmol).

4-Ethylidene-1,3,5-trimethyltetrahydropyrimidin-2(1*H*)-one (361)

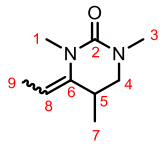

Reaction performed on 0.58 mmol scale following general procedure **3B** (reverse addition) using LDA (freshly prepared following general procedure **3A**; 2.69 mL, 1.27 mmol, 2.19 equiv.), **206** (98 mg, 0.58 mmol, 1.0 equiv.) in anhydrous THF (1.9 mL, 3.2 mL/mmol) and distilled DMPU (0.35 mL, 2.9 mmol, 5.0 equiv.), which was stirred for 5.5 h at –78 °C. Flash column chromatography (10−80% acetone/petroleum ether) gave **361** as a pale-yellow oil (52 mg, 0.31 mmol, 53% yield). **IR** (film) ν_{max} 2925, 1646, 1500, 1300, 772 cm^{-1}. **^{1}H NMR** (400 MHz, $CDCl_3$) δ 4.63 (q, *J* = 7.1 Hz, 1H, H^8), 3.23 (dd, *J* = 11.1, 5.2 Hz, 1H, H^4), 3.15 (s, 3H, H^1), 2.92 (s, 3H, H^3), 2.83 (dd, *J* = 11.1, 6.9 Hz, 1H, H^4), 2.47 (h, *J* = 6.3 Hz, 1H, H^5), 1.64 (d, *J* = 7.1 Hz, 3H, H^9), 1.06 (d, *J* = 6.7 Hz, 3H, H^7). **^{13}C NMR** (101 MHz, $CDCl_3$) δ 155.2 (C^2), 142.9 (C^6), 104.0 (C^8), 54.5 (C^4), 36.9 (C^1), 35.8 (C^3), 33.3 (C^5), 16.1 (C^7), 13.4 (C^9). **HRMS** (ESI-TOF) m/z: $[M + H]^+$ Calcd for $C_9H_{17}N_2O$ 169.1335; Found 169.1326.

In addition, **360** (8 mg, 0.04 mmol, 8% yield) and 1-((2*Z*,4*Z*)-hexa-2,4-dien-3-yl)-1,3-dimethylurea **359** (1 mg, 0.007 mmol, 1% yield) were afforded.

(*Z*)-1-(Hexa-1,4-dien-3-yl)-1,3-dimethylurea (358)

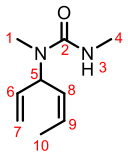

Reaction performed on 0.58 mmol scale following general procedure **3B** (reverse addition) using LDA (freshly prepared following general procedure **3A**; 2.63 mL, 1.17 mmol, 2.00 equiv.) and **206** (98 mg, 0.58 mmol, 1.0 equiv.) in anhydrous THF (1.4 mL, 2.4 mL/mmol), which was stirred for 2 h at –78 °C. Flash column chromatography (10−50% acetone/petroleum ether) gave **358** as a yellow oil (32 mg, 0.19 mmol, 33% yield). **IR** (film) ν_{max} 3345, 2925, 1626, 1539, 1411, 1378, 772 cm^{-1}. **^{1}H NMR** (400 MHz, $CDCl_3$) δ 5.81 (ddd, *J* = 17.3, 10.5, 4.1 Hz, 1H, H^6), 5.73 (dqd, *J* = 10.4, 6.9, 0.9, 1H, H^9), 5.64 – 5.57 (m, 1H, H^5), 5.40 (ddq, *J* = 10.4, 8.4, 1.8 Hz, 1H, H^8), 5.22 – 5.10 (m, 2H, H^7), 4.34 (bs, 1H, H^3), 2.82 (d, *J* = 4.6 Hz, 3H, H^4), 2.73 (s, 3H, H^1), 1.69 (dd, *J* = 6.9, 1.8 Hz, 3H, H^{10}). **^{13}C NMR** (101 MHz, $CDCl_3$) δ 158.8 (C^2), 137.7 (C^6), 128.9 (C^9), 126.4 (C^8), 116.2 (C^7), 53.5 (C^5), 29.8 (C^4), 27.8 (C^1), 13.6 (C^{10}). **HRMS** (ESI-TOF) m/z: $[M + H]^+$ Calcd for $C_9H_{17}N_2O$ 169.1335; Found 169.1336.

In addition, a mixture of **364** (20 mg, 0.12 mmol, 20% yield), **363** (8 mg, 0.05 mmol, 8% yield) and **206** (1 mg, 0.006 mmol, 1% yield) was afforded, along with **360** (6 mg, 0.04 mmol, 6% yield) and **361** (5 mg, 0.03 mmol, 5% yield).

1-((2*Z*,4*E*)-Hexa-2,4-dien-3-yl)-1,3-dimethylurea (362)

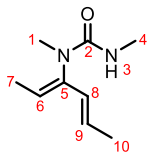

Reaction performed on 0.594 mmol scale following general procedure **3C** using **206** (100 mg, 0.594 mmol, 1.00 equiv.) in anhydrous THF (5.9 mL), 18-crown-6 (1.25 M in THF; 1.04 mL, 1.30 mmol, 2.19 equiv.) and KHMDS (1.00 M in THF; 1.19 mL, 1.19 mmol, 2.00 equiv.), which was stirred for 24 h at −78 °C to 0 °C. Flash column chromatography (10−80% acetone/petroleum ether) gave **362** as an orange oil (86 mg, 0.51 mmol, 86%). **IR** (film) ν_{max} 3352, 2920, 1642, 1524, 1330, 963, 771 cm^{-1}. **^{1}H NMR** (400 MHz, $CDCl_3$; *Z*,*E*-geometry assigned following NOE analysis) δ 5.86 (dq, *J* = 15.3, 1.6 Hz, 1H, H^8), 5.61 (q, *J* = 6.9 Hz, 1H, H^6), 5.58 – 5.50 (m, 1H, H^9), 4.44 (bs, 1H, H^3), 2.96 (s, 3H, H^1), 2.73 (d, *J* = 4.8 Hz, 3H, H^4), 1.74 (ddd, *J* = 6.8, 1.6, 0.9 Hz, 3H, H^{10}), 1.62 (d, *J* = 6.9 Hz, 3H, H^7). **^{13}C NMR** (101 MHz, $CDCl_3$) δ 157.7 (C^2), 140.8 (C^5), 127.8 (C^8), 125.9 (C^6), 125.8 (C^9), 34.1 (C^1), 27.6 (C^4), 17.8 (C^{10}), 12.7 (C^7). **HRMS** (ESI-TOF) m/z: $[M + H]^+$ Calcd for $C_9H_{17}N_2O$ 169.1335; Found 169.1333.

(*Z*)-1,3-Dimethyl-1-(1-phenylbut-1-en-1-yl)urea (367)

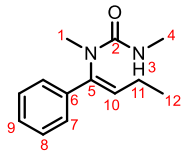

Reaction performed on 0.479 mmol scale following general procedure **3C** using **214** (105 mg, 0.479 mmol, 1.00 equiv.) in anhydrous THF (4.8 mL), 18-crown-6 (1.25 M in THF; 840 µL, 1.05 mmol, 2.19 equiv.) and KHMDS (1.0 M in THF; 0.96 mL, 0.96 mmol, 2.0 equiv.), which was stirred for 24 h at −78 °C to 0 °C. Flash column chromatography (10−80% acetone/petroleum ether) gave **367** as a dark orange oil (84 mg, 0.38 mmol, 80% yield). **IR** (film) ν_{max} 3452, 2967, 1637, 1521, 1330, 1205, 907, 726, 694 cm^{-1}. **^{1}H NMR** (400 MHz, $CDCl_3$; alkene geometry assigned by NOE analysis) δ 7.40 – 7.27 (m, 5H, H^7 + H^8 + H^9), 6.10 (t, *J* = 7.3 Hz, 1H, H^{10}), 4.66 (bs, 1H, H^3), 3.02 (s, 3H, H^1), 2.75 (d, *J* = 4.6 Hz, 3H, H^4), 2.27 – 2.18 (m, 2H, H^{11}), 1.08 (t, *J* = 7.5 Hz, 3H, H^{12}). **^{13}C NMR** (101 MHz, $CDCl_3$) δ 157.9 (C^2), 139.3 (C^5), 136.1 (C^6), 131.4 (C^{10}), 129.0 (C^7/C^8), 128.4 (C^9), 125.6 (C^7/C^8), 34.7 (C^1), 27.6

(C^4), 21.4 (C^{11}), 13.5 (C^{12}). **HRMS** (ESI-TOF) m/z: $[M + Na]^+$ Calcd for $C_{13}H_{18}N_2ONa$ 241.1311; Found 241.1319.

1-(2,5-Dimethylhexa-2,4-dien-3-yl)-1,3-dimethylurea (374)

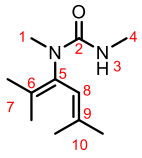

Reaction performed on 0.43 mmol scale following general procedure **3C** using **230** (84 mg, 0.43 mmol, 1.0 equiv.) in anhydrous THF (4.3 mL), 18-crown-6 (1.25 M in THF; 750 µL, 0.938 mmol, 2.18 equiv.) and KHMDS (1.0 M in THF; 0.86 mL, 0.86 mmol, 2.0 equiv.), which was stirred for 30 h at −78 °C to room temperature. Flash column chromatography (0−4% acetone/Et_2O) gave **374** as yellow oil (69 mg, 0.35 mmol, 82% yield). **IR** (film) ν_{max} 3352, 2911, 1637, 1517, 1325, 1193, 1089, 768 cm^{-1}. **^{1}H NMR** (400 MHz, $CDCl_3$) δ 5.54 (s, 1H, H^8), 4.53 (bs, 1H, H^3), 2.82 (s, 3H, H^1), 2.73 (d, J = 4.8 Hz, 3H, H^4), 1.76 (s, 3H, H^{10}), 1.67 (s, 3H, H^7), 1.64 (s, 3H, H^7), 1.57 (s, 3H, H^{10}). **^{13}C NMR** (101 MHz, $CDCl_3$) δ 157.7 (C^2), 137.0 (C^9), 132.8 (C^6), 132.3 (C^5), 118.9 (C^8), 33.3 (C^1), 27.5 (C^4), 26.5 (C^{10}), 20.4 (C^7), 19.3 (C^7), 19.1 (C^{10}). **HRMS** (ESI-TOF) m/z: $[M + Na]^+$ Calcd for $C_{11}H_{20}N_2ONa$ 219.1468; Found 219.1475.

4-(But-2-en-2-yl)-1,3,4,5-tetramethylimidazolidin-2-one (375, 376 and 377)

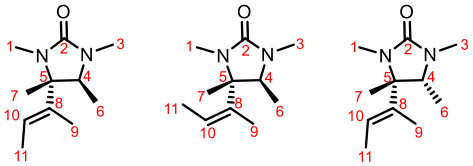

375 ***376*** **377**

Reaction performed on 0.37 mmol scale following general procedure **3C** using **232** (72 mg, 0.37 mmol, 1.00 equiv.) in anhydrous THF (3.7 mL), 18-crown-6 (214 mg, 0.810 mmol, 2.19 equiv.) and KHMDS (1.0 M in THF; 0.74 mL, 0.74 mmol, 2.0 equiv.), which was stirred for 26 h at −78 °C to room temperature. Flash column chromatography (1−8% *i*-PrOH/petroleum ether) gave **375**, ***376***, and **377** in a ratio of 1:0.3:0.3 as a pale-yellow oil (36 mg, 0.18 mmol, 50% yield). **IR** (film) ν_{max} 2922, 1687, 1436, 1391, 922, 767, 727, 644 cm^{-1}. **^{1}H NMR** (400 MHz, $CDCl_3$; diastereomeric ratio and alkene geometry assigned by NOE analysis) δ 5.55 – 5.43 (m, 1.3H, H^{10} + H^{10}), 5.37 (qq, J = 6.6, 1.2 Hz, 0.3H, H^{10}), 3.32 (q, J = 6.5 Hz, 0.3H, H^4), 3.14 (q, J = 6.6 Hz, 1H, H^4), 3.08 (q, J = 6.6 Hz, 0.3H, H^4), 2.69 (s, 0.9H, H^3), 2.68 (s, 3H, H^3), 2.67 (s, 0.9H, H^3), 2.59 (s, 0.9H, H^1), 2.56 (s, 0.9H, H^1), 2.50 (s, 3H, H^1), 1.68 (p, J = 1.5 Hz, 0.9H, H^9), 1.64 – 1.59 (m, 4.8H, H^{11} + H^{11} + H^{11}), 1.55 (p, J = 1.1 Hz, 3H, H^9), 1.46 (p, J =

1.2 Hz, 0.9H, H^9), 1.30 (s, 0.9H, H^7), 1.16 (s, 0.9H, *H^7*), 1.13 (d, *J* = 6.5 Hz, 0.9H, *H^6*), 1.11 (s, 3H, $\underline{H^7}$), 1.01 (d, *J* = 6.6 Hz, 3H, $\underline{H^6}$), 0.94 (d, *J* = 6.6 Hz, 0.9H, H^6). **^{13}C NMR** (101 MHz, $CDCl_3$) δ 161.5 (C^2), 161.3 ($\underline{C^2}$), 160.6 (*C^2*), 136.0 ($\underline{C^8}$ + C^8), 135.8 (*C^8*), 125.5 (*C^{10}*), 123.5 (C^{10}), 123.0 ($\underline{C^{10}}$), 65.8 ($\underline{C^5}$), 65.3 (C^5), 64.4 (*C^5*), 62.9 (C^4), 61.9 (*C^4*), 58.8 ($\underline{C^4}$), 29.5 (C^3), 29.4 ($\underline{C^3}$), 29.0 (*C^3*), 26.1 (C^1), 26.1 (*C^1*), 26.0 ($\underline{C^1}$), 24.3 (*C^9*), 23.7 (C^7), 16.3 (*H^7*), 14.7 ($\underline{C^7}$), 14.4 (*C^{11}*/C^{11}), 14.0 ($\underline{C^{11}}$ + *C^{11}*/C^{11}), 13.8 (C^9), 13.7 (C^6), 13.6 (*C^6*), 12.9 ($\underline{C^6}$), 12.3 ($\underline{C^9}$). **HRMS** (ESI-TOF) m/z: $[M + Na]^+$ Calcd for $C_{11}H_{20}N_2ONa$ 219.1468; Found 219.1477.

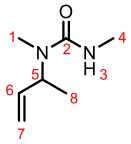

In addition, 1-(but-3-en-2-yl)-1,3-dimethylurea **378** was afforded as a pale-yellow oil (10 mg, 0.071 mmol, 19% yield). **IR** (film) ν_{max} 2973, 2922, 2865, 2240, 1687, 1436, 1391, 922, 767, 727, 644, 583 cm^{-1}. **^{1}H NMR** (400 MHz, $CDCl_3$) δ 5.78 (ddd, *J* = 17.4, 10.6, 4.2 Hz, 1H, H^6), 5.18 – 5.05 (m, 2H, H^7), 4.92 (qdt, *J* = 6.9, 4.2, 2.1 Hz, 1H, H^5), 4.43 (bs, 1H, H^3), 2.80 (d, *J* = 4.6 Hz, 3H, H^4), 2.65 (s, 3H, H^1), 1.18 (d, *J* = 6.9 Hz, 3H, H^8). **^{13}C NMR** (101 MHz, $CDCl_3$) δ 158.9 (C^2), 139.2 (C^6), 115.2 (C^7), 51.1 (C^5), 28.4 (C^1), 27.8 (C^4), 16.3 (C^8). **HRMS** (ESI-TOF) m/z: $[M + H]^+$ Calcd for $C_7H_{15}N_2O$ 143.1179; Found 143.1180.

1,3-Dimethyl-1-((5*E*)-octa-3,5-dien-4-yl)urea (379) and 1,3-dimethyl-1-((2*E*)-octa-2,4-dien-4-yl)urea (<u>380</u>)

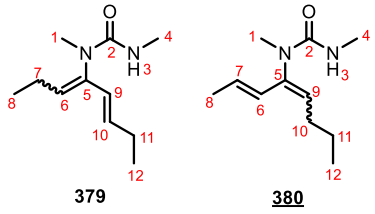

379 **<u>380</u>**

Reaction performed on 0.550 mmol scale following general procedure **3C** using **228** (108 mg, 0.550 mmol, 1.00 equiv.) in anhydrous THF (5.5 mL), 18-crown-6 (1.25 M in THF; 970 µL, 1.21 mmol, 2.20 equiv.) and KHMDS (1.00 M in THF; 1.10 mL, 1.10 mmol, 2.00 equiv.), which was stirred for 3 d at −78 °C to room temperature. Flash column chromatography (10−80% acetone/petroleum ether) gave a mixture of **379** and **<u>380</u>** as an orange oil (32 mg, 0.16 mmol, 30% yield; ratio of **379**:**<u>380</u>** is 0.5:1). **IR** (film) ν_{max} 3354, 2961, 1643, 1524, 1333, 1215, 964, 750 cm^{-1}. **^{1}H NMR** (400 MHz, $CDCl_3$; the squiggly bond in **379** and **<u>380</u>** means that the compound is a single isomer yet of unknown configuration) δ 5.85 (dq, *J* = 15.3, 1.6 Hz, 1H, $\underline{H^6}$), 5.83 (dt, *J* = 13.8, 1.6 Hz, 0.5H, H^9), 5.66 – 5.53 (m, 1.5H, H^{10} + $\underline{H^7}$), 5.46 (td, *J* = 7.5, 3.0 Hz, 1H, 1.5H, H^6 + $\underline{H^9}$), 4.45 (bs, 1.5H, H^3 + $\underline{H^3}$), 2.96 (s, 1.5H, H^1), 2.96 (s,

3H, H[1]), 2.71 (m, 4.5H, H[4] + H[4]), 2.13 – 1.96 (m, 4H, H[7] + H[11] + H[10]), 1.73 (ddd, *J* = 6.7, 1.6, 0.7 Hz, 3H, H[8]), 1.42 – 1.31 (m, 2H, H[11]), 0.96 (q, *J* = 7.5 Hz, 3H, H[8] + H[12]), 0.87 (t, *J* = 7.4 Hz, 3H, H[12]). **^{13}C NMR** (101 MHz, $CDCl_3$) δ 157.8 (C[2]), 157.8 (C[2]), 139.8 (C[5]), 139.3 (C[5]), 133.5 (C[6]), 132.9 (C[10]), 131.7 (C[9]), 127.9 (C[6]), 126.0 (C[7]), 125.4 (C[9]), 34.6 (C[1]), 34.6 (C[1]), 29.3 (C[10]), 27.5 (C[4] + C[4]), 25.3 (C[11]), 22.2 (C[11]), 20.7 (C[7]), 17.8 (C[8]), 14.1 (C[12]), 13.5 (C[8]/C[12]), 13.4 (C[8]/C[12]). **HRMS** (ESI-TOF) m/z: $[M + H]^+$ Calcd for $C_{11}H_{21}N_2O$ 197.1648; Found 197.1649.

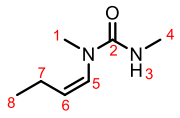

In addition, (*Z*)-1-(but-1-en-1-yl)-1,3-dimethylurea **381** was afforded as orange oil (20 mg, 0.14 mmol, 26% yield). **IR** (film) ν_{max} 3347, 2962, 2935, 2222, 1634, 1532, 1412, 1332, 1068, 771 cm^{-1}. **^{1}H NMR** (400 MHz, $CDCl_3$) δ 5.91 (dt, *J* = 7.7, 1.6 Hz, 1H, H[5]), 5.25 (q, *J* = 7.4 Hz, 1H, H[6]), 4.63 (bs, 1H, H[3]), 2.98 (s, 3H, H[1]), 2.77 (d, *J* = 4.7 Hz, 3H, H[4]), 2.05 (pd, *J* = 7.5, 1.6 Hz, 2H, H[7]), 0.98 (t, *J* = 7.6 Hz, 3H, H[8]). **^{13}C NMR** (101 MHz, $CDCl_3$) δ 157.9 (C[2]), 130.9 (C[6]), 128.1 (C[5]), 35.3 (C[1]), 27.6 (C[4]), 20.2 (C[7]), 13.6 (C[8]). **HRMS** (ESI-TOF) m/z: $[M + H]^+$ Calcd for $C_7H_{15}N_2O$ 143.1179; Found 143.1180.

1-((4*E*,6*Z*)-Dodeca-4,6-dien-6-yl)-1,3-dimethylurea (382) and 1-((5*Z*,7*E*)-dodeca-5,7-dien-6-yl)-1,3-dimethylurea (383)

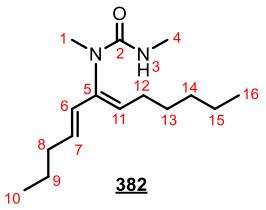

382

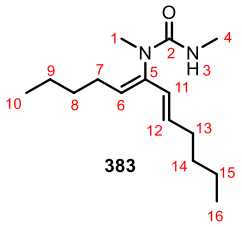

383

Reaction performed on 0.403 mmol scale following general procedure **3C** using **321** (102 mg, 0.403 mmol, 1.00 equiv.) in anhydrous THF (4 mL), 18-crown-6 (1.25 M in THF; 710 µL, 0.888 mmol, 2.20 equiv.) and KHMDS (1.0 M in THF; 0.81 mL, 0.81 mmol, 2.0 equiv.), which was stirred for 1.5 d at −78 °C to room temperature. Flash column chromatography (5−40% acetone/petroleum ether) gave a mixture of isomers **382** and **383** in a ratio of 1:1, as a pale-yellow oil (61 mg, 0.24 mmol, 60% yield). **IR** (film) ν_{max} 3366, 2956, 2926, 1645, 1520, 1466, 1410, 1329, 964, 767 cm^{-1}. **^{1}H NMR** (400 MHz, $CDCl_3$; alkene geometry assigned by NOE analysis) δ 5.81 (dq, *J* = 15.5, 1.7 Hz, 1H, H[6] + H[11]), 5.54 (dt, *J* = 15.5, 7.1 Hz, 1H, H[7] + H[12]), 5.45 (td, *J* = 7.4, 2.7 Hz, 1H, H[11] + H[6]), 4.44 (q, *J* = 4.7 Hz, 1H, H[3] + H[3]), 2.95 (s, 3H, H[1] + H[1]), 2.70 (d, *J* = 4.7 Hz, 3H, H[4] + H[4]), 2.09 – 1.97 (m, 4H, H[8] + H[12] + H[7] + H[13]), 1.42 – 1.19 (m, 8H, H[9] + H[13] + H[14] + H[15] + H[8] + H[9] + H[14] + H[15]), 0.90 – 0.80 (m, 6H, H[10] + H[16] + H[10] + H[16]). **^{13}C NMR** (101 MHz, $CDCl_3$) δ 157.8 (C[2] + C[2]), 139.6 (C[5]/C[5]), 139.6 (C[5]/C[5]), 132.2 (C[11]/C[6]),

132.1 (C[11]/C[6]), 131.5 (C[7]/C[12]), 131.2 (C[7]/C[12]), 126.5 (C[6]/C[11]), 126.3 (C[6]/C[11]), 34.5 (C[1] + C[1]), 34.3 (C[8]/C[13]), 31.9 (C[8]/C[13]), 31.7 (C[14]), 31.4 (C[14]/C[8]), 31.1 (C[14]/C[8]), 28.6 (C[13]), 27.4 (C[4] + C[4]), 27.3 (C[12]/C[7]), 27.0 (C[12]/C[7]), 22.6 (C[9]/C[15]/C[9]/C[15]), 22.5 (C[9]/C[15]/C[9]/C[15]), 22.4 (C[9]/C[15]/C[9]/C[15]), 22.2 (C[9]/C[15]/C[9]/C[15]), 14.0 (C[10]/C[16]), 14.0 (C[10]/C[16]), 13.7 (C[10]/C[16]). **HRMS** (ESI-TOF) m/z: $[M + H]^+$ Calcd for $C_{15}H_{29}N_2O$ 253.2274; Found 253.2280.

1-((2*Z*,4*E*)-2,5-Dicyclohexylhexa-2,4-dien-3-yl)-1,3-dimethylurea (384)

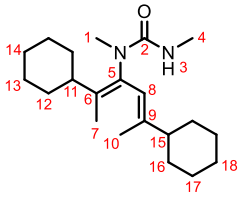

Reaction performed on 0.400 mmol scale following general procedure **3C** using **322** (133 mg, 0.400 mmol, 1.00 equiv.) in anhydrous THF (4 mL), 18-crown-6 (232 mg, 0.878 mmol, 2.20 equiv.) and KHMDS (1.0 M in THF; 0.80 mL, 0.80 mmol, 2.0 equiv.), which was stirred for 44 h at −78 °C to room temperature. Flash column chromatography (5−40% EtOAc/petroleum ether) gave **384** as a white solid (54 mg, 0.16 mmol, 41% yield). **MP** 106−107 °C. **IR** (film) ν_{max} 3362, 2924, 2851, 1644, 1519, 1448, 1327, 752 cm^{-1}. **^{1}H NMR** (400 MHz, $CDCl_3$; alkene geometry assigned by NOE analysis) δ 5.51 (q, *J* = 1.2 Hz, 1H, H[8]), 4.61 (q, *J* = 4.8 Hz, 1H, H[3]), 2.84 (s, 3H, H[1]), 2.75 (d, *J* = 4.8 Hz, 3H, H[4]), 2.59 – 2.47 (m, 1H, H[11]), 1.92 (tt, *J* = 11.4, 3.1 Hz, 1H, H[15]), 1.81 – 1.61 (m, 8H, H[12]/H[13]/H[14]/H[16]/H[17]/H[18]), 1.59 (d, *J* = 1.0 Hz, 3H, H[7]), 1.55 (d, *J* = 1.2 Hz, 3H, H[10]), 1.46 – 1.06 (m, 12H, H[12]/H[13]/H[14]/H[16]/H[17]/H[18]). **^{13}C NMR** (101 MHz, $CDCl_3$; coalescence of cyclohexyl carbons observed at 55 °C) δ 158.0 (C[2]), 146.6 (C[9]), 141.7 (C[6]), 131.1 (C[5]), 117.3 (C[8]), 48.1 (C[15]), 40.4 (C[11]), 33.9 (C[1]), 32.3 (C[12]/C[13]/C[14]/C[16]/C[17]/C[18]), 32.2 (C[12]/C[13]/C[14]/C[16]/C[17]/C[18]), 31.7 (C[12]/C[13]/C[14]/C[16]/C[17]/C[18]), 30.5 (C[12]/C[13]/C[14]/C[16]/C[17]/C[18]), 27.4 (C[4]), 26.8 (C[12]/C[13]/C[14]/C[16]/C[17]/C[18]), 26.7 (C[12]/C[13]/C[14]/C[16]/C[17]/C[18]), 26.4 (C[12]/C[13]/C[14]/C[16]/C[17]/C[18]), 26.4 (C[12]/C[13]/C[14]/C[16]/C[17]/C[18]), 26.3 (C[12]/C[13]/C[14]/C[16]/C[17]/C[18]), 26.2 (C[12]/C[13]/C[14]/C[16]/C[17]/C[18]), 15.8 (C[10]), 14.1 (C[7]). **HRMS** (ESI-TOF) m/z: $[M + H]^+$ Calcd for $C_{21}H_{37}N_2O$ 333.2900; Found 333.2896.

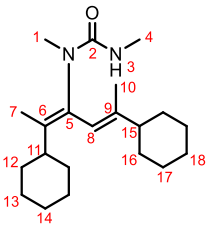

In addition, isomer 1-((2*E*,4*E*)-2,5-dicyclohexylhexa-2,4-dien-3-yl)-1,3-dimethylurea **385** was afforded as a pale-yellow oil (30 mg, 0.091 mmol, 23% yield). **IR** (film) ν_{max} 2923, 2851, 1645, 1514, 1447, 1325, 771, 751 cm^{-1}. **^{1}H NMR** (400 MHz, $CDCl_3$; alkene geometry assigned by NOE analysis)

δ 5.56 – 5.49 (m, 1H, H^8), 4.57 (q, *J* = 4.7 Hz, 1H, H^3), 2.82 (s, 3H, H^1), 2.75 (d, *J* = 4.7 Hz, 3H, H^4), 2.50 – 2.28 (m, 1H, H^{11}), 1.92 (tt, *J* = 11.3, 3.2 Hz, 1H, H^{15}), 1.82 – 1.63 (m, 8H, $H^{12}/H^{13}/H^{14}/H^{16}/H^{17}/H^{18}$), 1.59 (d, *J* = 1.3 Hz, 3H, H^{10}), 1.57 (d, *J* = 1.3 Hz, 3H, H^7), 1.56 – 1.38 (m, 2H, $H^{12}/H^{13}/H^{14}/H^{16}/H^{17}/H^{18}$), 1.38 – 1.07 (m, 10H, $H^{12}/H^{13}/H^{14}/H^{16}/H^{17}/H^{18}$). **^{13}C NMR** (101 MHz, $CDCl_3$; coalescence of cyclohexyl carbons observed at 55 °C) δ 157.7 (C^2), 146.3 (C^9), 141.2 (C^6), 131.4 (C^5), 116.6 (C^8), 48.3 (C^{15}), 41.5 (C^{11}), 33.1 (C^1), 32.2 ($C^{12}/C^{13}/C^{14}/C^{16}/C^{17}/C^{18}$), 32.0 ($C^{12}/C^{13}/C^{14}/C^{16}/C^{17}/C^{18}$), 31.3 ($C^{12}/C^{13}/C^{14}/C^{16}/C^{17}/C^{18}$), 30.1 ($C^{12}/C^{13}/C^{14}/C^{16}/C^{17}/C^{18}$), 27.6 ($C^4$), 26.8 ($C^{12}/C^{13}/C^{14}/C^{16}/C^{17}/C^{18}$), 26.8 ($C^{12}/C^{13}/C^{14}/C^{16}/C^{17}/C^{18}$), 26.8 ($C^{12}/C^{13}/C^{14}/C^{16}/C^{17}/C^{18}$), 26.7 ($C^{12}/C^{13}/C^{14}/C^{16}/C^{17}/C^{18}$), 26.4 ($C^{12}/C^{13}/C^{14}/C^{16}/C^{17}/C^{18}$), 26.2 ($C^{12}/C^{13}/C^{14}/C^{16}/C^{17}/C^{18}$), 15.7 ($C^{10}$), 12.6 ($C^7$). **HRMS** (ESI-TOF) m/z: $[M + H]^+$ Calcd for $C_{21}H_{37}N_2O$ 333.2900; Found 333.2896.

Two other isomers (5 mg, 0.01 mmol, 4% yield; 8 mg, 0.02 mmol, 6% yield) were observed, but unidentifiable due to the small amount formed and inability to separate them.

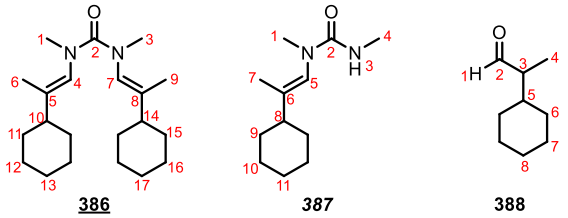

386 ***387*** 388

In addition, a mixture of 1,3-bis((*E*)-2-cyclohexylprop-1-en-1-yl)-1,3-dimethyl urea **386** (5 mg, 0.02 mmol, 4% yield), (*E*)-1-(2-cyclohexylprop-1-en-1-yl)-1,3-dimethylurea ***387*** (2 mg, 0.01 mmol, 3% yield) and 2-cyclohexylpropanal **388** (2 mg, 0.01 mmol, 4% yield) was afforded with a ratio of 1:0.50:0.43 as a yellow oil. **IR** (film) ν_{max} 3354, 2924, 2852, 1634, 1512, 1449, 1228, 1208, 1157, 1028, 771 cm^{-1}. **^{1}H NMR** (400 MHz, $CDCl_3$) δ 9.64 (d, *J* = 2.3 Hz, 0.4H, H^1), 5.77 (p, *J* = 1.4 Hz, 0.5H, H^5), 5.60 (p, *J* = 1.3 Hz, 2H, H^4 + H^7), 4.53 (bs, 0.5H, H^3), 2.93 (s, 1.5H, H^1), 2.88 (s, 6H, H^1 + H^3), 2.77 (d, *J* = 4.6 Hz, 1.5H, H^4), 2.24 – 2.15 (m, 0.4H, H^3), 1.99 – 1.87 (m, 1H, H^8), 1.85 – 1.60 (m, 16.9H, H^{10}–H^{17} + H^9–H^{11} + H^5–H^8), 1.59 (d, *J* = 1.3 Hz, 1.5H, H^7), 1.46 (d, *J* = 1.4 Hz, H^6 + H^9), 1.32 – 1.09 (m, 14.5H, H^{11}–H^{13} + H^{15}–H^{17} + H^9–H^{11} + H^6–H^8), 1.03 (d, *J* = 7.1 Hz, 1.2H, H^4). **^{13}C NMR** (101 MHz, $CDCl_3$) δ 206.0 (C^2), 161.5 (C^2), 158.3 (C^2), 144.7 (C^6), 136.1 (C^5+C^8), 126.7 (C^4+C^7), 123.3 (C^5), 52.0 (C^3), 44.7 (C^{10} + C^{14}), 44.5 (C^8), 38.7 (C^5), 37.2 (C^1+C^3), 35.1 (C^1), 32.0 (C^6), 31.9 (C^9), 31.8 (C^{11} + C^{15}), 27.6 (C^4), 26.7 (C^{12} + C^{16}), 26.6 (C^{13} + C^{17}), 26.5 (C^{11}), 26.4 (C^{10}), 26.4 (C^7), 26.2 (C^8), 13.8 (C^6 + C^9), 13.6 (C^7), 10.2 (C^4). **386**: **HRMS** (ESI-TOF) m/z: $[M + H]^+$ Calcd for $C_{21}H_{37}N_2O$ 333.2900; Found 333.2905. ***387***: **HRMS** (ESI-TOF) m/z: $[M + H]^+$ Calcd for $C_{12}H_{23}N_2O$ 211.1805; Found 211.1808.

1-((1*E*,2*E*)-1,2-Bis((1*R*,5*S*)-6,6-dimethylbicyclo[3.1.1]heptan-2-ylidene)ethyl)-1,3-dimethylurea (389)

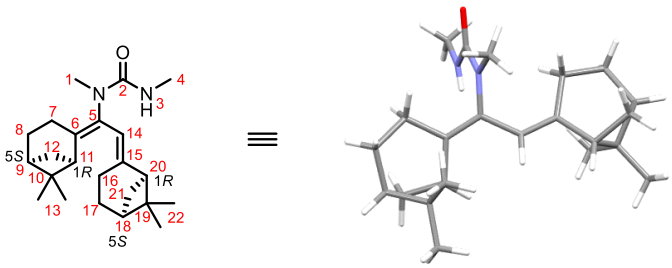

Reaction performed on 0.318 mmol scale following general procedure **3C** using **324** (114 mg, 0.318 mmol, 1.00 equiv.) in anhydrous THF (3.2 mL), 18-crown-6 (185 mg, 0.700 mmol, 2.20 equiv.) and KHMDS (1.0 M in THF; 0.64 mL, 0.64 mmol, 2.0 equiv.), which was stirred for 7 d at −78 °C to room temperature. Flash column chromatography (7−45% EtOAc/pentane) gave **389** as a yellow solid (26 mg, 0.073 mmol, 23% yield; contains minor impurities). **MP** 185–186 °C. **IR** (film) ν_{max} 2918, 1652, 1516, 1457, 1334, 752 cm^{-1}. **^{1}H NMR** (500 MHz, DMSO-d_6) δ 5.50 (s, 1H, H^{14}), 5.09 (bs, 1H, H^3), 2.81 (s, 3H, H^1/H^4), 2.62 (s, 3H, H^1/H^4), 2.42 (t, J = 5.6 Hz, 1H, H^{20}), 2.39 – 2.26 (m, 6H, H^7/H^8/H^{12}/H^{16}/H^{17}/H^{21}), 1.99 – 1.94 (m, 3H, H^9 + H^{11} + H^{18}), 1.91 – 1.81 (m, 4H, H^7/H^8/H^{12}/H^{16}/H^{17}/H^{21}), 1.44 – 1.31 (m, 2H, H^7/H^8/H^{12}/H^{16}/H^{17}/H^{21}), 1.29 (s, 3H, H^{13}/H^{22}), 1.28 (s, 3H, H^{13}/H^{22}), 0.78 (s, 3H, H^{13}/H^{22}), 0.72 (s, 3H, H^{13}/H^{22}). **^{13}C NMR** (126 MHz, DMSO-d_6, 95 °C) δ 156.3 (C^2), 144.0 (C^6 + C^{15}), 129.6 (C^5), 115.5 (C^{14}), 53.3 (C^{20}), 45.5 (C^{11}), 39.9 (C^9 + C^{18}), 33.0 (C^1/C^4), 30.9 (C^7/C^8/C^{12}/C^{16}/C^{17}/C^{21}), 30.6 (C^7/C^8/C^{12}/C^{16}/C^{17}/C^{21}), 26.7 (C^1/C^4), 25.6 (C^{13}/C^{22}), 25.6 (C^{13}/C^{22}), 23.2 (C^7/C^8/C^{12}/C^{16}/C^{17}/C^{21}), 22.9 (C^7/C^8/C^{12}/C^{16}/C^{17}/C^{21}), 21.3 (C^{13}/C^{22}), 21.0 (C^{13}/C^{22}), 19.1 (C^7/C^8/C^{12}/C^{16}/C^{17}/C^{21}), 18.9 (C^7/C^8/C^{12}/C^{16}/C^{17}/C^{21}). **HRMS** (ESI-TOF) m/z: [M + H]$^+$ Calcd for $C_{23}H_{37}N_2O$ 357.2900; Found 357.2898.

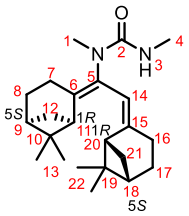

In addition, 1-((1*E*,2*Z*)-1,2-bis((1*R*,5*S*)-6,6-dimethylbicyclo[3.1.1]heptan-2-ylidene)ethyl)-1,3-dimethylurea **390** was afforded as a yellow oil (23 mg, 0.065 mmol, 20% yield). **IR** (film) ν_{max} 3360, 2923, 1710, 1641, 1536, 1462, 1220, 773 cm^{-1}. **^{1}H NMR** (500 MHz, DMSO-d_6, 95 °C; alkene geometry assigned by NOE analysis; C^5–C^6 alkene geometry based on the crystal structure of **389**) δ 5.63 (t, J = 2.3 Hz, 1H, H^{14}), 5.01 (bs, 1H, H^3), 2.74 (s, 3H, H^1/H^4), 2.63 – 2.57 (m, 1H, H^{11}), 2.57 (s, 3H, H^1/H^4), 2.48 – 2.41 (m, 3H, H^{20} + H^8/H^{12}/H^{17}/H^{21}), 2.40 – 2.27 (m, 5H, H^8/H^{12}/H^{16}/H^{17}/H^{21}), 2.02 – 1.94 (m, 2H, H^9 + H^{18}), 1.92 – 1.86 (m, 2H, H^8/H^{12}/H^{17}/H^{21}), 1.86 – 1.77 (m, 2H, H^8/H^{12}/H^{17}/H^{21}), 1.34 – 1.26 (m,

1H, $H^8/H^{12}/H^{17}/H^{21}$), 1.25 (s, 3H, H^{13}/H^{22}), 1.24 (s, 3H, H^{13}/H^{22}), 0.75 (s, 3H, H^{13}/H^{22}), 0.74 (s, 3H, H^{13}/H^{22}). **^{13}C NMR** (126 MHz, DMSO-d_6, 95 °C) δ 156.8 (C^2), 142.0 (C^6 + C^{15}), 129.5 (C^5), 115.8 (C^{14}), 53.8 (C^{20}), 45.0 (C^{11}), 39.9 (C^9 + C^{18}), 34.3 (C^1/C^4), 30.7 (C^7), 27.1 ($C^8/C^{12}/C^{17}/C^{21}$), 26.5 (C^1/C^4), 25.7 (C^{13}/C^{22}), 25.6 (C^{13}/C^{22}), 23.3 ($C^8/C^{12}/C^{17}/C^{21}$), 23.0 ($C^8/C^{12}/C^{17}/C^{21}$), 21.6 (C^{13}/C^{22}), 21.3 (C^{13}/C^{22}), 20.0 ($C^8/C^{12}/C^{17}/C^{21}$), 18.9 (C^{16}). **HRMS** (ESI-TOF) m/z: $[M + H]^+$ Calcd for $C_{23}H_{37}N_2O$ 357.2900; Found 357.2898.

1,3-Dimethyl-1-(3-methylbut-2-en-1-yl)urea (397)

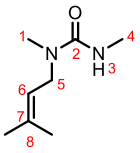

Reaction performed on 0.39 mmol scale following general procedure **3C** using **251** (88 mg, 0.39 mmol, 1.0 equiv.) in anhydrous THF (3.9 mL), 18-crown-6 (1.25 M in THF; 690 µL, 0.863 mmol, 2.21 equiv.) and KHMDS (1.0 M in THF; 0.78 mL, 0.78 mmol, 2.0 equiv.), which was stirred for 24 h at −78 °C to 0 °C. Flash column chromatography (2−20% acetone/CH_2Cl_2) gave **397** as a yellow oil (19 mg, 0.12 mmol, 31% yield). **IR** (film) ν_{max} 3342, 2920, 1627, 1536, 1375, 1273, 1238, 1149, 1086, 770 cm^{-1}. **^{1}H NMR** (400 MHz, $CDCl_3$) δ 5.11 (thept, J = 6.9, 1.3 Hz, 1H, H^6), 4.43 (bs, 1H, H^3), 3.81 (d, J = 6.9 Hz, 2H, H^5), 2.79 (s, 3H, H^1), 2.76 (d, J = 4.6 Hz, 3H, H^4), 1.70 – 1.69 (m, 3H, H^8), 1.65 (s, 3H, H^8). **^{13}C NMR** (101 MHz, $CDCl_3$) δ 159.1 (C^2), 135.4 (C^7), 120.7 (C^6), 46.4 (C^5), 33.9 (C^1), 27.7 (C^4), 25.8 (C^8), 17.8 (C^8). **HRMS** (ESI-TOF) m/z: $[M + H]^+$ Calcd for $C_8H_{17}N_2O$ 157.1335; Found 157.1334.

In addition, starting urea **251** was recovered as a yellow oil (25 mg, 0.11 mmol, 29% yield).

1,3-Dimethyl-1-((2*Z*,4*E*)-4-methylhexa-2,4-dien-3-yl)urea (401)

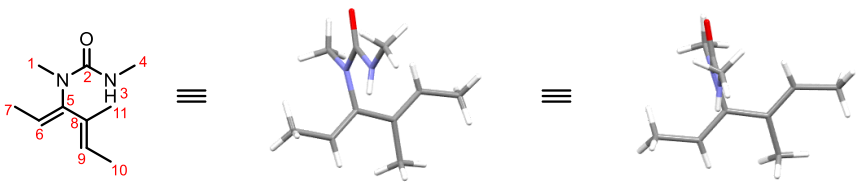

Reaction performed on 0.43 mmol scale following general procedure **3C** using **237** (78 mg, 0.43 mmol, 1.00 equiv.) in anhydrous THF (4.3 mL), 18-crown-6 (250 mg, 0.946 mmol, 2.20 equiv.) and KHMDS (1.0 M in THF; 0.86 mL, 0.86 mmol, 2.0 equiv.), which was stirred for 18 h at −78 °C to room temperature. Flash column chromatography (4−32% *i*-PrOH/pentane) gave **401** as a yellow sticky solid (34 mg, 0.19 mmol, 43% yield). **IR** (film) ν_{max} 3356, 2927, 1708, 1633, 1534, 1451, 1394, 1073, 772

cm^{-1}. **^{1}H NMR** (400 MHz, $CDCl_3$) δ 5.67 (q, *J* = 6.9 Hz, 1H, H^6), 5.57 (q, *J* = 7.1 Hz, 1H, H^9), 4.39 (bs, 1H, H^3), 2.92 (s, 3H, H^1), 2.71 (d, *J* = 4.8 Hz, 3H, H^4), 1.73 (p, *J* = 1.0 Hz, 3H, H^{11}), 1.69 (dq, *J* = 7.1, 1.0 Hz, 3H, H^{10}), 1.64 (d, *J* = 6.9 Hz, 3H, H^7). **^{13}C NMR** (101 MHz, $CDCl_3$) δ 157.9 (C^2), 143.4 (C^8), 130.0 (C^5), 122.6 (C^9), 122.0 (C^6), 34.4 (C^1), 27.6 (C^4), 14.0 (C^{10}), 13.3 (C^{11}), 13.1 (C^7). **HRMS** (ESI-TOF) m/z: $[M + H]^+$ Calcd for $C_{10}H_{19}N_2O$ 183.1492; Found 183.1491.

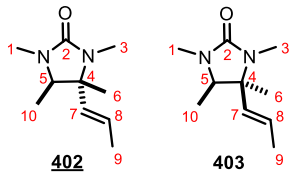

402 **403**

In addition, (*E*)-1,3,4,5-tetramethyl-4-(prop-1-en-1-yl)imidazolidin-2-one with a diastereomeric ratio of 0.65:0.35 for **402**:**403** was afforded as an orange oil (18 mg, 0.10 mmol, 23% yield). **IR** (film) ν_{max} 3317, 2971, 2922, 1700, 1439, 1393, 770 cm^{-1}. **^{1}H NMR** (400 MHz, $CDCl_3$; diastereomers assigned by NOE analysis) δ 5.63 (dq, *J* = 15.6, 6.5 Hz, 0.65H, $\underline{H^8}$), 5.52 (dq, *J* = 15.8, 6.4 Hz, 0.35H, H^8), 5.34 (dq, *J* = 15.6, 1.6 Hz, 0.65H, $\underline{H^7}$), 5.24 (dq, *J* = 15.8, 1.6 Hz, 0.35H, H^7), 3.07 – 3.01 (m, 1H, $\underline{H^5}$ + H^5), 2.70 (s, 3H, $\underline{H^1}$ + H^1), 2.61 (s, 1H, H^3), 2.60 (s, 2H, $\underline{H^3}$), 1.77 – 1.69 (m, 3H, $\underline{H^9}$ + H^9), 1.27 (s, 1H, H^6), 1.08 – 1.01 (m, 5H, $\underline{H^6}$ + $\underline{H^{10}}$ + H^{10}). **^{13}C NMR** (101 MHz, $CDCl_3$) δ 161.4 ($\underline{C^2}$ + C^2), 134.1 ($\underline{C^7}$), 129.4 (C^7), 128.0 (C^8), 128.0 ($\underline{C^8}$), 63.0 (C^5), 62.0 ($\underline{C^5}$), 29.4 ($\underline{C^1}$), 29.3 (C^1), 25.8 ($\underline{C^3}$ + C^3), 21.5 (C^6), 18.1 ($\underline{C^9}$), 18.0 (C^9), 14.2 ($\underline{C^6}$), 13.7 (C^{10}), 12.3 ($\underline{C^{10}}$). **HRMS** (ESI-TOF) m/z: $[M + H]^+$ Calcd for $C_{10}H_{19}N_2O$ 183.1492; Found 183.1494.

1-((2*E*)-Hepta-2,4-dien-4-yl)-1,3-dimethylurea (<u>404</u>) and **1-((4*E*)-hepta-2,4-dien-4-yl)-1,3-dimethylurea (405)**

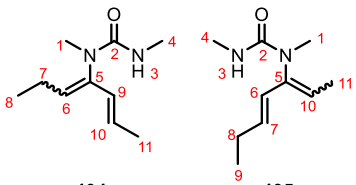

<u>404</u> **405**

Reaction performed on 0.560 mmol scale following general procedure **3C** using **242** (102 mg, 0.560 mmol, 1.00 equiv.) in anhydrous THF (5.6 mL), 18-crown-6 (1.25 M in THF; 990 µL, 1.23 mmol, 2.20 equiv.) and KHMDS (1.00 M in THF; 1.12 mL, 1.12 mmol, 2.00 equiv.), which was stirred for 3 d at −78 °C to room temperature. Flash column chromatography (10−80% acetone/petroleum ether) gave **<u>404</u>** and **405** in a ratio of 0.65:0.35 as a yellow oil (25 mg, 0.14 mmol, 24% yield). **IR** (film) ν_{max} 3359, 2963, 1640, 1524, 1410, 1332, 963, 772 cm^{-1}. **^{1}H NMR** (400 MHz, $CDCl_3$) δ 5.84 (dq, *J* = 15.6, 1.5 Hz, 0.65H, $\underline{H^9}$), 5.84 (dt, *J* = 15.5, 1.5 Hz, 0.35H, H^6), 5.66 – 5.52 (m, 1.35H, $\underline{H^{10}}$ + H^7 + H^{10}), 5.44 (t, *J* = 7.5 Hz, 0.65H, $\underline{H^6}$), 4.45 (bs, 1H, $\underline{H^3}$ + H^3), 2.96 (s, 1.05H, H^1), 2.96 (s, 1.95H, $\underline{H^1}$), 2.72 (d, *J* = 4.8

Hz, 1.05H, H^4), 2.71 (d, *J* = 4.8 Hz, 1.95H, H^4), 2.14 – 1.97 (m, 2H, H^7 + H^8), 1.75 – 1.71 (m, 1.95H, H^{11}), 1.62 (d, *J* = 7.1 Hz, 1.05H, H^{11}), 0.97 (t, *J* = 7.4 Hz, 1.05H, H^9), 0.95 (t, *J* = 7.5 Hz, 1.95H, H^8). **^{13}C NMR** (101 MHz, $CDCl_3$) δ 157.8 (C^2), 157.7 (C^2), 140.8 (C^5), 139.2 (C^5), 133.2 (C^6), 132.7 (C^7), 127.8 (C^9), 126.1 (C^{10}), 126.0 (C^{10}), 125.3 (C^6), 34.6 (C^1), 34.1 (C^1), 27.5 (C^4), 27.5 (C^4), 25.3 (C^8), 20.6 (C^7), 17.8 (C^{11}), 13.5 (C^9), 13.4 (C^8), 12.8 (C^{11}). **HRMS** (ESI-TOF) m/z: $[M + Na]^+$ Calcd for $C_{10}H_{18}N_2ONa$ 205.1311; Found 205.1313.

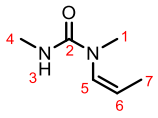

In addition, (*Z*)-1,3-dimethyl-1-(prop-1-en-1-yl)urea **366** was afforded as an orange oil (8 mg, 0.08 mmol, 14% yield). **IR** (film) ν_{max} 3340, 2922, 1635, 1525, 1411, 1329, 770, 743, 534 cm^{-1}. **^{1}H NMR** (400 MHz, $CDCl_3$) δ 5.96 (dq, *J* = 7.7, 1.7 Hz, 1H, H^5), 5.34 (dq, *J* = 7.7, 6.9 Hz, 1H, H^6), 4.62 (bs, 1H, H^3), 2.97 (s, 3H, H^1), 2.77 (d, *J* = 4.8 Hz, 3H, H^4), 1.61 (dd, *J* = 6.9, 1.7 Hz, 3H, H^7). **^{13}C NMR** (101 MHz, $CDCl_3$) δ 157.8 (C^2), 129.8 (C^5), 123.4 (C^6), 35.0 (C^1), 27.5 (C^4), 12.4 (C^7). **HRMS** (ESI-TOF) m/z: $[M + H]^+$ Calcd for $C_6H_{13}N_2O$ 129.1022; Found 129.1021.

1,3-Dimethyl-1-((2*Z*,4*E*)-nona-2,4-dien-3-yl)urea (406)

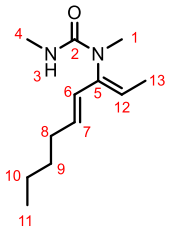

Reaction performed on 0.511 mmol scale following general procedure **3C** using **326** (108 mg, 0.511 mmol, 1.00 equiv.) in anhydrous THF (5.1 mL), 18-crown-6 (1.25 M in THF; 900 µL, 1.12 mmol, 2.19 equiv.) and KHMDS (1.00 M in THF; 1.02 mL, 1.02 mmol, 2.00 equiv.), which was stirred for 39 h at −78 °C to room temperature. Flash column chromatography (5−30% acetone/petroleum ether followed by 0−8% *i*-PrOH/petroleum ether) gave **406** as a yellow oil (12 mg, 0.057 mmol, 11% yield). **IR** (film) ν_{max} 3350, 2926, 1646, 1524, 1330, 965, 772 cm^{-1}. **^{1}H NMR** (400 MHz, $CDCl_3$; alkene geometry assigned by NOE analysis) δ 5.85 (dt, *J* = 15.5, 1.5 Hz, 1H, H^6), 5.63 – 5.53 (m, 2H, H^7 + H^{12}), 4.48 – 4.42 (m, 1H, H^3), 2.99 (s, 3H, H^1), 2.75 (d, *J* = 4.8 Hz, 3H, H^4), 2.09 (q, *J* = 7.1 Hz, 2H, H^8), 1.65 (d, *J* = 6.9 Hz, 3H, H^{13}), 1.44 – 1.22 (m, 4H, H^9 + H^{10}), 0.89 (t, *J* = 7.1 Hz, 3H, H^{11}). **^{13}C NMR** (101 MHz, $CDCl_3$) δ 157.8 (C^2), 140.9 (C^5), 131.4 (C^7), 126.3 (C^6), 126.1 (C^{12}), 34.1 (C^1), 32.0 (C^8), 31.5 (C^9), 27.6 (C^4), 22.3 (C^{10}), 14.0 (C^{11}), 12.8 (C^{13}). **HRMS** (ESI-TOF) m/z: $[M + H]^+$ Calcd for $C_{12}H_{23}N_2O$ 211.1805; Found 211.1808.

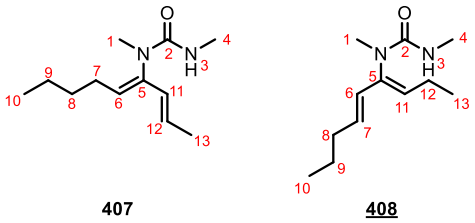

407 **408**

In addition, a mixture of 1,3-dimethyl-1-((2*E*,4*Z*)-nona-2,4-dien-4-yl)urea **407** and 1,3-dimethyl-1-((3*Z*,5*E*)-nona-3,5-dien-4-yl)urea **408** was afforded in a ratio of 1:1 as a yellow oil (31 mg, 0.15 mmol, 29% yield). **IR** (film) ν_{max} 3350, 2958, 2929, 1645, 1520, 1330, 962, 766, 730 cm^{-1}. **^{1}H NMR** (400 MHz, $CDCl_3$; alkene geometry assigned by NOE analysis) δ 5.86 (dq, *J* = 15.4, 1.6 Hz, 1H, H^{11}), 5.83 (dt, *J* = 15.5, 1.5 Hz, 1H, H^{6}), 5.66 – 5.52 (m, 2H, H^{12} + H^{7}), 5.46 (td, *J* = 7.5, 2.8 Hz, 2H, H^{6} + H^{11}), 4.50 – 4.41 (m, 2H, H^{3} + H^{3}), 2.98 (s, 3H, H^{1}/H^{1}), 2.97 (s, 3H, H^{1}/H^{1}), 2.73 (d, *J* = 4.7 Hz, 6H, H^{4} + H^{4}), 2.12 – 1.97 (m, 6H, H^{7} + H^{8} + H^{12}), 1.75 (ddd, *J* = 6.8, 1.6, 0.6 Hz, 3H, H^{13}), 1.46 – 1.33 (m, 2H, H^{9}), 1.35 – 1.23 (m, 4H, H^{8} + H^{9}), 0.97 (t, *J* = 7.5 Hz, 3H, H^{13}), 0.87 (t, *J* = 7.1 Hz, 3H, H^{10}/H^{10}), 0.87 (t, *J* = 7.4 Hz, 3H, H^{10}/H^{10}). **^{13}C NMR** (101 MHz, $CDCl_3$) δ 157.8 (C^{2}/C^{2}), 157.8 (C^{2}/C^{2}), 139.7 (C^{5}), 139.3 (C^{5}), 133.5 (C^{6}), 132.0 (C^{11}), 131.4 (C^{7}), 127.9 (C^{11}), 126.5 (C^{6}), 125.9 (C^{12}), 34.6 (C^{1}/C^{1}), 34.6 (C^{1}/C^{1}), 34.3 (C^{8}), 31.1 (C^{8}), 27.5 (C^{4}/C^{4}), 27.5 (C^{4}/C^{4}), 27.0 (C^{7}), 22.6 (C^{9}), 22.5 (C^{9}), 20.7 (C^{12}), 17.8 (C^{13}), 14.0 (C^{10}/C^{10}), 13.7 (C^{10}/C^{10}), 13.4 (C^{13}). **HRMS** (ESI-TOF) m/z: $[M + H]^+$ Calcd for $C_{12}H_{23}N_2O$ 211.1805; Found 211.1808.

(*E*)-4-(But-2-en-1-yl)-1,3,4,5-tetramethylimidazolidin-2-one (409)

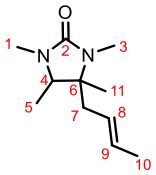

Reaction performed on 0.24 mmol scale following general procedure **3C** using **327** (47 mg, 0.24 mmol, 1.0 equiv.) in anhydrous THF (2.4 mL), 18-crown-6 (139 mg, 0.526 mmol, 2.19 equiv.) and KHMDS (1.0 M in THF; 0.48 mL, 0.48 mmol, 2.0 equiv.), which was stirred for 5 d at −78 °C to room temperature. Then KHMDS (1.0 M in THF; 0.48 mL, 0.48 mmol, 2.0 equiv.) and 18-crown-6 (139 mg, 0.526 mmol, 2.19 equiv.) were added again, and the reaction was stirred for 1 d at room temperature. Flash column chromatography (6−48% acetone/pentane) gave **409** as a yellow oil (6 mg, 0.03 mmol, 13% yield). **IR** (film) ν_{max} 3450, 2922, 1689, 1485, 1439, 1391, 1261, 1051, 970, 801, 764, 584 cm^{-1}. **^{1}H NMR** (400 MHz, $CDCl_3$) δ 5.54 – 5.43 (m, 1H, H^{9}), 5.37 – 5.24 (m, 1H, H^{8}), 3.18 (q, *J* = 6.5 Hz, 1H, H^{4}), 2.70 (s, 3H, H^{1}/H^{3}), 2.68 (s, 3H, H^{1}/H^{3}), 2.30 – 2.18 (m, 1H, H^{7}), 2.17 – 2.07 (m, 1H, H^{7}), 1.66 (dd, *J* = 6.3, 1.3 Hz, 3H, H^{10}), 1.07 (d, *J* = 6.5 Hz, 3H, H^{5}), 1.01 (s, 3H, H^{11}). **^{13}C NMR** (101 MHz, $CDCl_3$) δ 160.9 (C^{2}), 129.4 (C^{9}), 125.4 (C^{8}), 60.8 (C^{6}), 58.4 (C^{4}), 40.7 (C^{7}), 29.1 (C^{1}/C^{3}), 25.2 (C^{1}/C^{3}),

18.2 (C^{10}), 17.3 (C^{11}), 13.2 (C^{5}). **HRMS** (ESI-TOF) m/z: $[M + H]^+$ Calcd for $C_{11}H_{21}N_2O$ 197.1648; Found 197.1645.

1-(1-(Cyclohex-1-en-1-yl)but-1-en-1-yl)-1,3-dimethylurea (410)

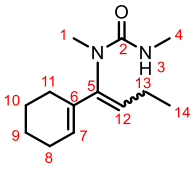

Reaction performed on 0.40 mmol scale following general procedure **3C** using **337** (89 mg, 0.40 mmol, 1.0 equiv.) in anhydrous THF (4 mL), 18-crown-6 (232 mg, 0.878 mmol, 2.20 equiv.) and KHMDS (1.0 M in THF; 0.80 mL, 0.80 mmol, 2.0 equiv.), which was stirred for 46 h at −78 °C to room temperature. Flash column chromatography (5−42% EtOAc/petroleum ether) gave **410** as an orange oil (59 mg, 0.27 mmol, 66% yield). **IR** (film) ν_{max} 3348, 2930, 1634, 1525, 1448, 1410, 1334, 772 cm^{-1}. **^{1}H NMR** (400 MHz, $CDCl_3$) δ 5.76 (t, *J* = 3.5 Hz, 1H, H^7), 5.54 (t, *J* = 7.3 Hz, 1H, H^{12}), 4.42 (q, *J* = 4.8 Hz, 1H, H^3), 2.94 (s, 3H, H^1), 2.73 (d, *J* = 4.8 Hz, 3H, H^4), 2.17 – 2.00 (m, 6H, H^8 + H^{11} + H^{13}), 1.72 – 1.50 (m, 4H, H^9 + H^{10}), 0.98 (t, *J* = 7.5 Hz, 3H, H^{14}). **^{13}C NMR** (101 MHz, $CDCl_3$) δ 158.1 (C^2), 141.3 (C^5), 131.1 (C^6), 128.5 (C^{12}), 125.7 (C^7), 35.0 (C^1), 27.5 (C^4), 25.7 (C^8), 25.5 (C^{11}), 22.8 (C^{10}), 22.3 (C^9), 20.9 (C^{13}), 13.7 (C^{14}). **HRMS** (ESI-TOF) m/z: $[M + H]^+$ Calcd for $C_{13}H_{23}N_2O$ 223.1805; Found 223.1800.

(*E*)-1,3-Dimethyl-1-(2-methylhexa-2,4-dien-3-yl)urea (411)

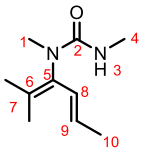

Reaction performed on 0.740 mmol scale following general procedure **3C** using **243** (135 mg, 0.740 mmol, 1.00 equiv.) in anhydrous THF (7.4 mL), 18-crown-6 (1.25 M in THF; 1.30 mL, 1.63 mmol, 2.20 equiv.) and KHMDS (1.00 M in THF; 1.48 mL, 1.48 mmol, 2.00 equiv.), which was stirred for 28 h at −78 °C to room temperature. Flash column chromatography (7−60% acetone/petroleum ether) gave **411** as a yellow oil (95 mg, 0.52 mmol, 70% yield). **IR** (film) ν_{max} 3355, 2920, 1638, 1523, 1336, 1216, 960, 749, 665 cm^{-1}. **^{1}H NMR** (400 MHz, $CDCl_3$) δ 6.19 (dq, *J* = 15.3, 1.6 Hz, 1H, H^8), 5.57 (dq, *J* = 15.3, 6.7 Hz, 1H, H^9), 4.39 (bs, 1H, H^3), 2.93 (s, 3H, H^1), 2.73 (d, *J* = 4.8 Hz, 3H, H^4), 1.83 (s, 3H, H^7), 1.78 (d, *J* = 6.7 Hz, 3H, H^{10}), 1.68 (s, 3H, H^7). **^{13}C NMR** (101 MHz, $CDCl_3$) δ 158.2 (C^2), 133.7 (C^5),

132.9 (C^6), 126.1 (C^9), 123.4 (C^8), 34.1 (C^1), 27.6 (C^4), 20.1 (C^7), 19.4 (C^7), 18.2 (C^{10}). **HRMS** (ESI-TOF) m/z: $[M + Na]^+$ Calcd for $C_{10}H_{18}N_2ONa$ 205.1311; Found 205.1318.

(*Z*)-1-(2,4-Dimethylhexa-2,4-dien-3-yl)-1,3-dimethylurea (412) and **(*E*)-1-(2,4-dimethylhexa-2,4-dien-3-yl)-1,3-dimethylurea (413)**

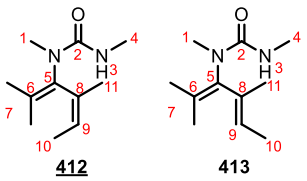

412 **413**

Reaction performed on 0.36 mmol scale following general procedure **3C** using **329** (70 mg, 0.36 mmol, 1.0 equiv.) in anhydrous THF (3.6 mL), 18-crown-6 (207 mg, 0.784 mmol, 2.18 equiv.) and KHMDS (1.0 M in THF; 0.71 mL, 0.71 mmol, 2.0 equiv.), which was stirred for 5 d at −78 °C to room temperature. Flash column chromatography (5−40% acetone/pentane) gave a mixture of isomers **412** and **413** in a ratio of 1:0.6 as a yellow oil (51 mg, 0.26 mmol, 72% yield). **IR** (film) ν_{max} 3368, 2913, 1638, 1516, 1442, 1408, 1325, 1088, 769, 753 cm^{-1}. **^{1}H NMR** (400 MHz, $CDCl_3$) δ 5.44 (qq, *J* = 6.8, 1.5 Hz, 1H, H^9), 5.36 (qq, *J* = 6.8, 1.5 Hz, 0.6H, H^9), 4.60 (bs, 1.6H, H^3 + H^3), 2.81 (s, 1.8H, H^1), 2.78 (s, 3H, H^1), 2.73 – 2.69 (m, 4.8H, H^4 + H^4), 1.71 (s, 1.8H, H^7), 1.65 – 1.63 (m, 1.8H, H^{10}), 1.62 (s, 3H, H^7), 1.60 (p, *J* = 1.5 Hz, 3H, H^{11}), 1.58 (s, 4.8H, H^7 + H^7), 1.52 (p, *J* = 1.2 Hz, 1.8H, H^{11}), 1.45 (dq, *J* = 6.8, 1.5 Hz, 3H, H^{10}). **^{13}C NMR** (101 MHz, $CDCl_3$) δ 158.0 (C^2 + C^2), 138.3 (C^5), 133.0 (C^5), 131.7 (C^8), 131.5 (C^8), 131.5 (C^6), 130.3 (C^6), 127.5 (C^9), 125.9 (C^9), 33.7 (C^1), 32.9 (C^1), 27.5 (C^4 + C^4), 21.6 (C^{11}), 21.2 (C^7), 20.3 (C^7), 19.8 (C^7), 19.1 (C^7), 14.9 (C^{10}), 14.3 (C^{11}), 13.6 (C^{10}). **HRMS** (ESI-TOF) m/z: $[M + H]^+$ Calcd for $C_{11}H_{21}N_2O$ 197.1648; Found 197.1647.

(*E*)-1,3-Dimethyl-1-(2-methylhepta-2,4-dien-3-yl)urea (414)

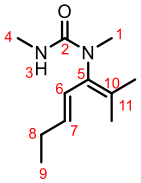

Reaction performed on 0.540 mmol scale following general procedure **3C** using **241** (106 mg, 0.540 mmol, 1.00 equiv.) in anhydrous THF (5.4 mL), 18-crown-6 (1.25 M in THF; 950 µL, 1.19 mmol, 2.20 equiv.) and KHMDS (1.00 M in THF; 1.08 mL, 1.08 mmol, 2.00 equiv.), which was stirred for 20 h at −78 °C to room temperature. A lot of the reaction intermediate was visible by TLC, thus 18-crown-6 (1.25 M in THF; 950 µL, 1.19 mmol, 2.20 equiv.) and KHMDS (1.00 M in THF; 1.08 mL, 1.08 mmol,

2.00 equiv.) were added again to then stir another 30 h at room temperature. Flash column chromatography (20% acetone/pentane) gave **414** as a brown/orange oil (18 mg, 0.091 mmol, 17% yield). **IR** (film) ν_{max} 3348, 2929, 1642, 1523, 1409, 1333, 1153, 961, 772 cm^{-1}. **^{1}H NMR** (400 MHz, $CDCl_3$) δ 6.15 (dt, *J* = 15.3, 1.6 Hz, 1H, H^6), 5.60 (dt, *J* = 15.3, 6.6 Hz, 1H, H^7), 4.39 (bs, 1H, H^3), 2.93 (s, 3H, H^1), 2.73 (d, *J* = 4.8 Hz, 3H, H^4), 2.12 (p, *J* = 7.1 Hz, 2H, H^8), 1.83 (s, 3H, H^{11}), 1.68 (s, 3H, H^{11}), 0.99 (t, *J* = 7.5 Hz, 3H, H^9). **^{13}C NMR** (101 MHz, $CDCl_3$) δ 158.2 (C^2), 133.7 (C^5), 133.2 (C^{10}), 133.1 (C^7), 121.0 (C^6), 34.1 (C^1), 27.6 (C^4), 25.8 (C^8), 20.2 (C^{11}), 19.5 (C^{11}), 13.8 (C^9). **HRMS** (ESI-TOF) m/z: $[M + Na]^+$ Calcd for $C_{11}H_{20}N_2ONa$ 219.1468; Found 219.1473.

In addition, the following compounds were afforded.

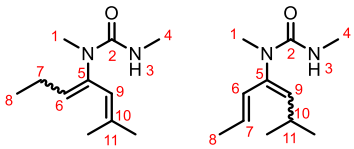

415 **416**

A mixture of 1,3-dimethyl-1-(2-methylhepta-2,4-dien-4-yl)urea **415** and 1,3-dimethyl-1-((2*E*)-6-methylhepta-2,4-dien-4-yl)urea **416** with a ratio of 0.59:0.41 was afforded as brown/orange oil (26 mg, 0.13 mmol, 24% yield). **IR** (film) ν_{max} 3358, 2961, 1641, 1520, 1448, 1410, 1329, 1190, 963, 771 cm^{-1}. **^{1}H NMR** (400 MHz, $CDCl_3$) δ 5.83 (dq, *J* = 15.3, 1.6 Hz, 0.41H, H^6), 5.64 – 5.57 (m, 0.41H, H^7), 5.57 – 5.54 (m, 0.59H, $\underline{H^9}$), 5.39 (t, *J* = 7.5 Hz, 0.59H, $\underline{H^6}$), 5.27 (d, *J* = 10.2 Hz, 0.41H, H^9), 4.57 (bs, 0.59H, $\underline{H^3}$), 4.47 (bs, 0.41H, H^3), 2.98 (s, 1.23H, H^1), 2.92 (s, 1.77H, $\underline{H^1}$), 2.75 (d, *J* = 4.7 Hz, 1.77H, $\underline{H^4}$), 2.73 (d, *J* = 4.7 Hz, 1.23H, H^4), 2.58 – 2.48 (m, 0.41H, H^{10}), 2.05 (p, *J* = 7.5 Hz, 1.18H, $\underline{H^7}$), 1.78 (s, 1.77H, $\underline{H^{11}}$), 1.74 (ddd, *J* = 6.7, 1.6, 0.6 Hz, 1.23H, H^8), 1.72 (s, 1.77H, $\underline{H^{11}}$), 0.97 (t, *J* = 7.5 Hz, 1.77H, $\underline{H^8}$), 0.94 (dd, *J* = 10.2, 6.6 Hz, 2.46H, H^{11}). **^{13}C NMR** (101 MHz, $CDCl_3$) δ 157.9 (C^2), 157.5 ($\underline{C^2}$), 138.9 (C^9), 137.8 ($\underline{C^5}$), 137.5 (C^5), 136.2 ($\underline{C^{10}}$), 133.9 ($\underline{C^6}$), 127.9 (C^6), 126.1 (C^7), 121.9 ($\underline{C^9}$), 35.0 (C^1), 34.3 ($\underline{C^1}$), 27.6 ($\underline{C^{11}}$), 27.5 ($\underline{C^4}$), 27.5 (C^4), 26.9 (C^{10}), 22.7 (C^{11}), 20.6 (C^{11}), 18.5 ($\underline{C^{11}}$), 17.8 (C^8), 13.7 ($\underline{C^8}$). **HRMS** (ESI-TOF) m/z: $[M + H]^+$ Calcd for $C_{11}H_{21}N_2O$ 197.1648; Found 197.1648.

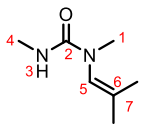

1,3-Dimethyl-1-(2-methylprop-1-en-1-yl)urea **417** was afforded as a brown/orange oil (20 mg, 0.14 mmol, 27% yield). **IR** (film) ν_{max} 3339, 2937, 2917, 1637, 1520, 1409, 1323, 1089, 834, 770 cm^{-1}. **^{1}H NMR** (400 MHz, $CDCl_3$) δ 5.72 (hept, *J* = 1.4 Hz, 1H, H^5), 4.58 (bs, 1H, H^3), 2.93 (s, 3H, H^1), 2.76 (d, *J* = 4.8 Hz, 3H, H^4), 1.71 (d, *J* = 1.4 Hz, 3H, H^7), 1.62 (d, *J* = 1.4 Hz, 3H, H^7). **^{13}C NMR** (101 MHz, $CDCl_3$) δ 158.3 (C^2), 135.7 (C^6), 124.3 (C^5), 35.0 (C^1), 27.6 (C^4), 22.0 (C^7), 17.4 (C^7). **HRMS** (ESI-TOF) m/z: $[M + H]^+$ Calcd for $C_7H_{15}N_2O$ 143.1179; Found 143.1175.

1-((*E*)-3,7-Dimethylocta-2,6-dien-1-yl)-1,3-dimethyl-3-((*Z*)-prop-1-en-1-yl)urea (418)

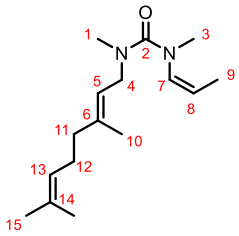

Reaction performed on 0.415 mmol scale following general procedure **3C** using **240** (104 mg, 0.415 mmol, 1.00 equiv.) in anhydrous THF (4.1 mL), 18-crown-6 (1.25 M in THF; 730 μL, 0.913 mmol, 2.20 equiv.) and KHMDS (1.0 M in THF; 0.83 mL, 0.83 mmol, 2.0 equiv.), which was stirred for 5 d at −78 °C to room temperature. Flash column chromatography (5−40% acetone/petroleum ether) gave **418** as a pale-yellow oil (22 mg, 0.086 mmol, 20% yield). **IR** (film) ν_{max} 2923, 1637, 1449, 1376, 1284, 1109, 1070, 930, 769 cm^{-1}. **^{1}H NMR** (400 MHz, $CDCl_3$) δ 5.93 (dq, *J* = 8.1, 1.7 Hz, 1H, H^7), 5.16 (tq, *J* = 6.9, 1.2 Hz, 1H, H^5), 5.11 – 5.01 (m, 1H, H^{13}), 4.99 (dq, *J* = 8.1, 7.0 Hz, 1H, H^8), 3.77 (d, *J* = 6.9 Hz, 2H, H^4), 2.96 (s, 3H, H^3), 2.69 (s, 3H, H^1), 2.14 – 1.97 (m, 4H, H^{11} + H^{12}), 1.66 (d, *J* = 1.0 Hz, 3H, H^{15}), 1.63 (s, 3H, H^{15}), 1.61 – 1.58 (m, 6H, H^9 + H^{10}). **^{13}C NMR** (101 MHz, $CDCl_3$) δ 162.9 (C^2), 139.1 (C^6), 133.1 (C^7), 131.7 (C^{14}), 124.1 (C^{13}), 120.7 (C^5), 114.6 (C^8), 48.0 (C^4), 39.8 (C^{11}), 36.9 (C^3), 35.6 (C^1), 26.5 (C^{12}), 25.8 (C^{15}), 17.8 (C^{15}), 16.2 (C^{10}), 12.6 (C^9). **HRMS** (ESI-TOF) m/z: [M + H]$^+$ Calcd for $C_{16}H_{29}N_2O$ 265.2274; Found 265.2274.

In addition, (*Z*)-1,3-dimethyl-1-(prop-1-en-1-yl)urea **366** was afforded (31 mg, 0.24 mmol, 58% yield).

(*Z*)-1-(4-Ethylidene-2-methylnon-2-en-3-yl)-1,3-dimethylurea (<u>419</u>) and **(*E*)-1-(4-ethylidene-2-methylnon-2-en-3-yl)-1,3-dimethylurea (420)**

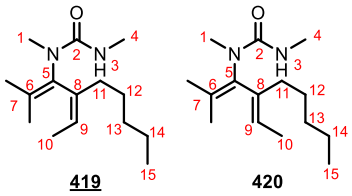

Reaction performed on 0.400 mmol scale following general procedure **3C** using **328** (101 mg, 0.400 mmol, 1.00 equiv.) in anhydrous THF (4 mL), 18-crown-6 (232 mg, 0.878 mmol, 2.20 equiv.) and KHMDS (1.0 M in THF; 0.80 mL, 0.80 mmol, 2.0 equiv.), which was stirred for 3 d at −78 °C to room temperature. Flash column chromatography (1−12% *i*-PrOH/petroleum ether) gave a mixture of isomers **<u>419</u>** and **420** in a ratio of 1:0.3 as a yellow oil (87 mg, 0.34 mmol, 86% yield). **IR** (film) ν_{max} 3384, 2927, 1641, 1515, 1448, 1324, 1089, 772 cm^{-1}. **^{1}H NMR** (400 MHz, $CDCl_3$; alkene geometry assigned by NOE analysis) δ 5.50 (qt, *J* = 6.8, 1.1 Hz, 1H, <u>H^9</u>), 5.37 (q, *J* = 6.8 Hz, 0.3H, H^9), 4.60 (bs,

1.3H, $\underline{H^3}$ + H^3), 2.86 (s, 0.9H, H^1), 2.83 (s, 3H, $\underline{H^1}$), 2.78 – 2.74 (m, 3.9H, $\underline{H^4}$ + H^4), 1.97 – 1.81 (m, 2.6H, $\underline{H^{11}}$ + H^{11}), 1.76 (s, 0.9H, H^7), 1.71 – 1.68 (m, 3.9H, $\underline{H^7}$ + H^{10}), 1.65 (s, 0.9H, H^7), 1.63 (s, 3H, $\underline{H^7}$), 1.52 (dt, *J* = 6.8, 1.0 Hz, 3H, $\underline{H^{10}}$), 1.35 – 1.19 (m, 7.8H, $\underline{H^{12}}$ + $\underline{H^{13}}$ + $\underline{H^{14}}$ + H^{12} + H^{13} + H^{14}), 0.89 – 0.82 (m, 3.9H, $\underline{H^{15}}$ + H^{15}). **^{13}C NMR** (101 MHz, $CDCl_3$) δ 158.1 (C^2), 158.1 ($\underline{C^2}$), 137.9 (C^5), 136.9 (C^8), 136.4 ($\underline{C^8}$), 132.4 ($\underline{C^6}$), 132.4 ($\underline{C^5}$), 131.5 (C^6), 127.8 (C^9), 125.4 ($\underline{C^9}$), 35.2 ($\underline{C^{11}}$), 34.1 (C^1), 33.2 (broad, $\underline{C^1}$), 32.1 (C^{13}), 31.8 ($\underline{C^{13}}$), 28.7 ($\underline{C^{12}}$), 28.4 (C^{12}), 28.0 (C^{11}), 27.6 ($\underline{C^4}$), 27.5 (C^4), 22.6 ($\underline{C^{14}}$), 22.6 (C^{14}), 21.4 (C^7), 20.5 ($\underline{C^7}$), 20.0 (C^7), 19.3 ($\underline{C^7}$), 14.9 ($\underline{C^{10}}$), 14.2 ($\underline{C^{15}}$ + C^{15}), 13.6 (C^{10}). **HRMS** (ESI-TOF) m/z: $[M + H]^+$ Calcd for $C_{15}H_{29}N_2O$ 253.2274; Found 253.2280.

(*Z*)-1-(4-Cyclohexyl-2-methylhexa-2,4-dien-3-yl)-1,3-dimethylurea (421)

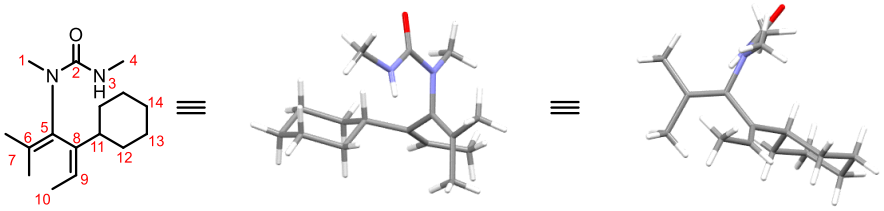

Reaction performed on 0.400 mmol scale following general procedure **3C** using **330** (106 mg, 0.400 mmol, 1.00 equiv.) in anhydrous THF (4 mL), 18-crown-6 (232 mg, 0.878 mmol, 2.20 equiv.) and KHMDS (1.0 M in THF; 0.80 mL, 0.80 mmol, 2.0 equiv.), which was stirred for 27 h at −78 °C to room temperature, followed by 19 h at 40 °C. Then 18-crown-6 (116 mg, 0.440 mmol, 1.10 equiv.) and KHMDS (1.0 M in THF; 0.40 mL, 0.40 mmol, 1.0 equiv.) were added again and the reaction mixture was stirred for 8 h at room temperature, followed by another addition of 18-crown-6 (232 mg, 0.878 mmol, 2.20 equiv.) and KHMDS (1.0 M in THF; 0.80 mL, 0.80 mmol, 2.0 equiv.), which was stirred for 15.5 h at room temperature. Flash column chromatography (3−40% acetone/pentane) gave **421** as a pale-yellow solid (86 mg, 0.33 mmol, 81% yield). **MP** 126–127 °C. **IR** (film) ν_{max} 3391, 2922, 2851, 1639, 1512, 1446, 1407, 1321, 1088 cm^{-1}. **^{1}H NMR** (400 MHz, $CDCl_3$) δ 5.48 (qd, *J* = 6.8, 1.1 Hz, 1H, H^9), 4.65 (bs, 1H, H^3), 2.85 – 2.73 (m, 6H, H^1 + H^4), 1.80 – 1.70 (m, 3H, H^{11} + H^{12}/H^{13}/H^{14}), 1.68 (s, 3H, H^7), 1.67 – 1.61 (m, 3H, H^{12}/H^{13}/H^{14}), 1.60 (s, 3H, H^7), 1.52 (d, *J* = 6.8 Hz, 3H, H^{10}), 1.29 – 0.94 (m, 5H, H^{12}/H^{13}/H^{14}). **^{13}C NMR** (101 MHz, $CDCl_3$) δ 158.2 (C^2), 141.3 (broad, C^5), 132.4 (C^8), 132.3 (broad, C^6), 122.4 (broad, C^9), 41.4 (C^{11}), 34.3 (broad, C^1), 32.0 (broad, C^{12}/C^{13}/C^{14}), 27.6 (C^4), 27.1 (C^{12}/C^{13}/C^{14}), 26.9 (C^{12}/C^{13}/C^{14}), 26.5 (C^{12}/C^{13}/C^{14}), 20.6 (C^7), 19.4 (C^7), 14.8 (C^{10}). **HRMS** (ESI-TOF) m/z: $[M + H]^+$ Calcd for $C_{16}H_{29}N_2O$ 265.2274; Found 265.2277.

1-((2*E*,4*Z*)-2,4-Dicyclohexylhexa-2,4-dien-3-yl)-1,3-dimethylurea (422) and **1-((2*E*,4E)-2,4-dicyclohexylhexa-2,4-dien-3-yl)-1,3-dimethylurea (423)**

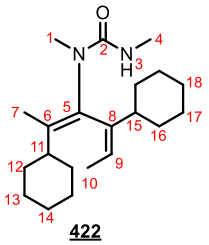

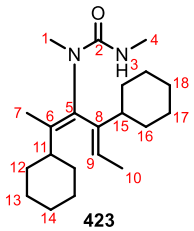

Reaction performed on 0.400 mmol scale following general procedure **3C** using **331** (133 mg, 0.400 mmol, 1.00 equiv.) in anhydrous THF (4 mL), 18-crown-6 (232 mg, 0.878 mmol, 2.20 equiv.) and KHMDS (1.0 M in THF; 0.80 mL, 0.80 mmol, 2.0 equiv.), which was stirred for 6 d at −78 °C to room temperature. Flash column chromatography (8−60% EtOAc/petroleum ether) gave a mixture of isomers **422** and **423** in a ratio of 1:0.3 as a yellow oil (22 mg, 0.066 mmol, 17% yield). **IR** (film) ν_{max} 2923, 2851, 1652, 1512, 1446, 1319, 772, 730 cm^{-1}. **^{1}H NMR** (500 MHz, toluene-d_8; alkene geometry tentatively assigned by NOE analysis) δ 5.40 (q, J = 6.8 Hz, 1H, H^9), 5.22 (q, J = 6.9 Hz, 0.3H, H^9), 4.64 (bs, 1.3H, H^3 + H^3), 2.95 (bs, 0.9H, H^1), 2.88 (bs, 3H, H^1), 2.82 – 2.77 (m, 3.9H, H^4 + H^4), 2.51 – 2.39 (m, 0.6H, H^{11} + H^{15}), 2.32 – 2.25 (m, 1H, H^{11}), 1.87 (t, J = 11.3 Hz, 1H, H^{15}), 1.79 – 1.61 (m, 10H, $H^{12}/H^{13}/H^{14}/H^{16}/H^{17}/H^{18}$ + $H^{12}/H^{13}/H^{14}/H^{16}/H^{17}/H^{18}$), 1.59 (d, J = 6.9 Hz, 0.9H, H^{10}), 1.55 (s, 3H, H^7), 1.48 (s, 3H, H^{10}), 1.46 (s, 0.9H, H^7), 1.43 – 1.28 (m, 3H, $H^{12}/H^{13}/H^{14}/H^{16}/H^{17}/H^{18}$ + $H^{12}/H^{13}/H^{14}/H^{16}/H^{17}/H^{18}$), 1.25 – 1.00 (m, 13H, $H^{12}/H^{13}/H^{14}/H^{16}/H^{17}/H^{18}$ + $H^{12}/H^{13}/H^{14}/H^{16}/H^{17}/H^{18}$). **^{13}C NMR** (126 MHz, toluene-d_8, 55 °C; unable to assign all peaks due to complexity and overlapping signals) δ 157.4 (C^2), 156.8 (C^2), 142.3 (C^5/C^5), 142.1 (C^5/C^5), 139.7 (C^6), 138.9 (C^8), 138.8 (C^6), 132.6 (C^8), 126.7 (C^9), 122.6 (C^9), 43.0 (C^{11}), 42.6 (C^{11}), 42.6 (C^{15}), 40.7 (C^{15}), 34.4, 33.0, 31.8, 31.6, 31.3, 30.3, 27.6, 27.0, 26.9, 26.9, 26.8, 26.6, 26.5, 15.5 (C^{10}), 13.5 (C^{10}), 13.0 (C^7), 12.5 (C^7). **HRMS** (ESI-TOF) m/z: $[M + H]^+$ Calcd for $C_{21}H_{36}N_2O$ 333.2900; Found 333.2906.

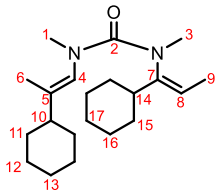

In addition, the reaction intermediate 1-((*E*)-2-cyclohexylprop-1-en-1-yl)-3-((*Z*)-1-cyclohexylprop-1-en-1-yl)-1,3-dimethylurea **424** was afforded as a pale-yellow oil (74 mg, 0.22 mmol, 55% yield). **IR** (film) ν_{max} 3370, 2925, 2853, 1709, 1634, 1520, 1448, 1338, 771 cm^{-1}. **^{1}H NMR** (400 MHz, $CDCl_3$; alkene geometry assigned by NOE analysis) δ 5.67 (p, J = 1.3 Hz, 1H, H^4), 4.97 (qd, J = 6.8, 1.3 Hz, 1H, H^8), 2.97 (s, 3H, H^3), 2.94 (s, 3H, H^1), 2.04 – 1.94 (m, 1H, H^{14}), 1.79 – 1.68 (m, 8H, H^{10} + $H^{11}/H^{12}/H^{13}/H^{15}/H^{16}/H^{17}$), 1.66 – 1.61 (m, 3H, $H^{11}/H^{12}/H^{13}/H^{15}/H^{16}/H^{17}$), 1.59 (dd, J = 6.8, 1.5 Hz, 3H,

H^9), 1.55 (d, J = 1.3 Hz, 3H, H^6), 1.30 – 1.05 (m, 8H, $H^{11}/H^{12}/H^{13}/H^{15}/H^{16}/H^{17}$), 1.05 – 0.93 (m, 2H, $H^{11}/H^{12}/H^{13}/H^{15}/H^{16}/H^{17}$). **^{13}C NMR** (101 MHz, $CDCl_3$) δ 160.6 (C^2), 149.9 (C^7), 133.7 (C^5), 126.5 (C^4), 115.1 (C^8), 44.7 (C^{10}), 42.2 (C^{14}), 40.1 (C^3), 37.8 (C^1), 31.8 (broad, $C^{11}/C^{12}/C^{13}/C^{15}/C^{16}/C^{17}$), 31.6 ($C^{11}/C^{12}/C^{13}/C^{15}/C^{16}/C^{17}$), 26.8 ($C^{11}/C^{12}/C^{13}/C^{15}/C^{16}/C^{17}$), 26.8 ($C^{11}/C^{12}/C^{13}/C^{15}/C^{16}/C^{17}$), 26.6 ($C^{11}/C^{12}/C^{13}/C^{15}/C^{16}/C^{17}$), 26.4 ($C^{11}/C^{12}/C^{13}/C^{15}/C^{16}/C^{17}$), 14.4 ($C^6$), 13.5 ($C^9$). **HRMS** (ESI-TOF) m/z: $[M + H]^+$ Calcd for $C_{21}H_{36}N_2O$ 333.2900; Found 333.2905.

(*E*)-1-(5-Cyclohexyl-2-methylhexa-2,4-dien-3-yl)-1,3-dimethylurea (425)

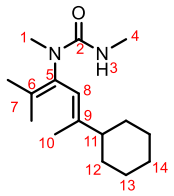

Reaction performed on 0.400 mmol scale following general procedure **3C** using **332** (106 mg, 0.400 mmol, 1.00 equiv.) in anhydrous THF (4 mL), 18-crown-6 (232 mg, 0.878 mmol, 2.20 equiv.) and KHMDS (1.0 M in THF; 0.80 mL, 0.80 mmol, 2.0 equiv.), which was stirred for 29 h at −78 °C to room temperature. Flash column chromatography (5−42% acetone/pentane followed by 1-8% *i*-PrOH/pentane) gave **425** as a pale-yellow oil (43 mg, 0.16 mmol, 41% yield). **IR** (film) ν_{max} 3353, 2923, 2851, 1637, 1516, 1448, 1327, 1088 cm^{-1}. **^{1}H NMR** (400 MHz, $CDCl_3$; alkene geometry assigned by NOE analysis) δ 5.55 – 5.49 (m, 1H, H^8), 4.57 (q, J = 4.7 Hz, 1H, H^3), 2.84 (s, 3H, H^1), 2.76 (d, J = 4.7 Hz, 3H, H^4), 1.92 (tt, J = 10.9, 3.1 Hz, 1H, H^{11}), 1.85 – 1.69 (m, 5H, $H^{12}/H^{13}/H^{14}$), 1.69 – 1.64 (m, 6H, H^7), 1.56 (d, J = 1.3 Hz, 3H, H^{10}), 1.35 – 1.09 (m, 5H, $H^{12}/H^{13}/H^{14}$). **^{13}C NMR** (101 MHz, $CDCl_3$; cyclohexyl peaks of 32.3 and 32.1 ppm, and 26.8 and 26.8 ppm coalesced at 55 °C) δ 157.8 (C^2), 146.7 (C^9), 132.7 (C^6), 132.5 (C^5), 117.0 (C^8), 48.0 (C^{11}), 33.3 (C^1), 32.3 (C^{12}/C^{13}), 32.1 (C^{12}/C^{13}), 27.6 (C^4), 26.8 (C^{12}/C^{13}), 26.8 (C^{12}/C^{13}), 26.4 (C^{14}), 20.6 (C^7), 19.3 (C^7), 15.9 (C^{10}). **HRMS** (ESI-TOF) m/z: $[M + H]^+$ Calcd for $C_{16}H_{29}N_2O$ 265.2274; Found 265.2279.

In addition, migration products (*E*)-1-(2-cyclohexyl-5-methylhexa-2,4-dien-3-yl)-1,3-dimethylurea **426** and (*Z*)-1-(2-cyclohexyl-5-methylhexa-2,4-dien-3-yl)-1,3-dimethylurea **427** were afforded, along with reaction intermediate (*E*)-1-(2-cyclohexylprop-1-en-1-yl)-1,3-dimethyl-3-(2-methylprop-1-en-1-yl)urea **428**.

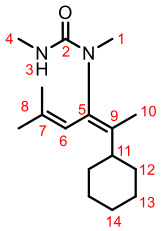

426 was afforded as pale-yellow oil (19 mg, 0.072 mmol, 18% yield). **IR** (film) ν_{max} 3377, 2925, 2852, 1645, 1516, 1448, 13334, 1193, 772 cm^{-1}. **^{1}H NMR** (400 MHz, $CDCl_3$; alkene geometry assigned by NOE analysis) δ 5.64 – 5.61 (m, 1H, H^6), 4.59 – 4.51 (m, 1H, H^3), 2.84 (s, 3H, H^1), 2.76 (d, *J* = 4.8 Hz, 3H, H^4), 2.47 – 2.35 (m, 1H, H^{11}), 1.81 (d, *J* = 1.3 Hz, 3H, H^8), 1.80 – 1.66 (m, 4H, $H^{12}/H^{13}/H^{14}$), 1.64 (d, *J* = 1.3 Hz, 3H, H^8), 1.58 (s, 3H, H^{10}), 1.57 – 1.53 (m, 1H, $H^{12}/H^{13}/H^{14}$), 1.50 – 1.40 (m, 1H, $H^{12}/H^{13}/H^{14}$), 1.40 – 1.21 (m, 4H, $H^{12}/H^{13}/H^{14}$). **^{13}C NMR** (101 MHz, $CDCl_3$; cyclohexyl peaks of 26.6 and 26.6 ppm coalesced at 55 °C) δ 157.7 (C^2), 141.5 (C^9), 136.9 (C^7), 131.5 (C^5), 118.5 (C^6), 41.3 (C^{11}), 33.3 (C^1), 31.2 ($C^{12}/C^{13}/C^{14}$), 30.2 ($C^{12}/C^{13}/C^{14}$), 27.6 (C^4), 27.0 (C^8), 26.6 ($C^{12}/C^{13}/C^{14}$), 26.6 ($C^{12}/C^{13}/C^{14}$), 26.2 ($C^{12}/C^{13}/C^{14}$), 19.0 (C^8), 12.6 (C^{10}). **HRMS** (ESI-TOF) m/z: $[M + H]^+$ Calcd for $C_{16}H_{29}N_2O$ 265.2274; Found 265.2280.

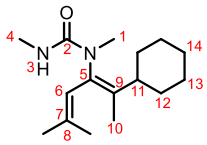

427 was afforded as pale-yellow oil (15 mg, 0.057 mmol, 14% yield). **IR** (film) ν_{max} 3359, 2925, 2852, 1751, 1645, 1523, 1448, 772 cm^{-1}. **^{1}H NMR** (400 MHz, $CDCl_3$; alkene geometry assigned by NOE analysis) δ 5.57 (q, *J* = 1.3 Hz, 1H, H^6), 4.62 – 4.53 (m, 1H, H^3), 2.86 (s, 3H, H^1), 2.75 (d, *J* = 4.9 Hz, 3H, H^4), 2.57 – 2.48 (m, 1H, H^{11}), 1.80 (d, *J* = 1.3 Hz, 3H, H^8), 1.78 – 1.65 (m, 2H, $H^{12}/H^{13}/H^{14}$), 1.62 (s, 3H, H^{10}), 1.60 (d, *J* = 1.3 Hz, 3H, H^8), 1.45 – 1.09 (m, 8H, $H^{12}/H^{13}/H^{14}$). **^{13}C NMR** (101 MHz, $CDCl_3$; cyclohexyl peaks of 26.3 and 26.3 ppm coalesced at 55 °C) δ 158.0 (C^2), 141.9 (C^9), 137.1 (C^7), 131.1 (C^5), 119.3 (C^6), 40.4 (C^{11}), 34.1 (C^1), 31.6 ($C^{12}/C^{13}/C^{14}$), 30.5 ($C^{12}/C^{13}/C^{14}$), 27.5 (C^4), 26.5 (C^8), 26.4 ($C^{12}/C^{13}/C^{14}$), 26.3 ($C^{12}/C^{13}/C^{14}$), 26.3 ($C^{12}/C^{13}/C^{14}$), 19.2 (C^8), 14.1 (C^{10}). **HRMS** (ESI-TOF) m/z: $[M + H]^+$ Calcd for $C_{16}H_{29}N_2O$ 265.2274; Found 265.2280.

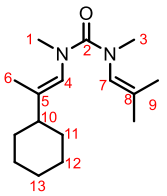

428 was afforded as a yellow oil (16 mg, 0.061 mmol, 15% yield). **^{1}H NMR** (400 MHz, $CDCl_3$) δ 5.59 (p, *J* = 1.3 Hz, 1H, H^4), 5.56 (hept, *J* = 1.3 Hz, 1H, H^7), 2.89 (s, 3H, H^1/H^3), 2.88 (s, 3H, H^1/H^3), 1.87 – 1.60 (m, 6H, H^{10} + $H^{11}/H^{12}/H^{13}$), 1.59 (d, *J* = 1.3 Hz, 3H, H^9), 1.51 (d, *J* = 1.3 Hz, 3H, H^9), 1.47 (d, *J* =

1.3 Hz, 3H, H^6), 1.32 – 1.09 (m, 5H, $H^{11}/H^{12}/H^{13}$). **^{13}C NMR** (101 MHz, $CDCl_3$) δ 161.5 (C^2), 136.9 (C^5), 127.7 (C^7), 127.4 (C^8), 126.5 (C^4), 44.5 (C^{10}), 37.2 (C^1/C^3), 37.1 (C^1/C^3), 31.9 (C^{11}/C^{12}), 26.7 (C^{11}/C^{12}), 26.4 (C^{13}), 22.1 (C^9), 17.5 (C^9), 13.7 (C^6). No full characterisation was afforded as the compound had decomposed in $CDCl_3$.

1-((*Z*)-1-((1*R*,5*S*)-6,6-Dimethylbicyclo[3.1.1]heptan-2-ylidene)-3-methylbut-2-en-2-yl)-1,3-dimethylurea (429) and **1-((*E*)-1-((1*R*,5*S*)-6,6-dimethylbicyclo[3.1.1]heptan-2-ylidene)-3-methylbut-2-en-2-yl)-1,3-dimethylurea (430)**

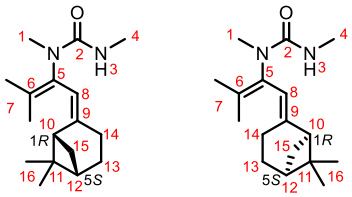

429 **430**

Reaction performed on 0.402 mmol scale following general procedure **3C** using **335** (111 mg, 0.402 mmol, 1.00 equiv.) in anhydrous THF (4 mL), 18-crown-6 (232 mg, 0.878 mmol, 2.18 equiv.) and KHMDS (1.0 M in THF; 0.80 mL, 0.80 mmol, 2.0 equiv.), which was stirred for 3 d at −78 °C to room temperature. Flash column chromatography (20% EtOAc/pentane) gave a mixture of isomers **429** and **430** in a ratio of 1:0.8 as a yellow oil (32 mg, 0.12 mmol, 29% yield). **IR** (film) ν_{max} 3352, 2922, 1637, 1524, 1454, 1338, 772, 729 cm^{-1}. **^{1}H NMR** (400 MHz, $CDCl_3$; doubling of all peaks assumed to be due to restricted/slow rotation of the N–C^5 or C^5–C^8; alkene geometry assigned by NOE analysis) δ 5.73 (t, *J* = 1.4 Hz, 0.5H, H^8), 5.72 (t, *J* = 1.5 Hz, 0.5H, H^8), 5.61 – 5.55 (m, 0.4H, H^8), 5.57 – 5.51 (m, 0.4H, H^8), 4.75 – 4.70 (m, 0.4H, H^3), 4.66 – 4.60 (m, 0.4H, H^3), 4.54 – 4.49 (m, 0.5H, H^3), 4.48 – 4.42 (m, 0.5H, H^3), 2.90 (s, 1.2H, H^1), 2.85 (s, 1.2H, H^1), 2.83 (s, 1.5H, H^1), 2.81 (s, 1.5H, H^1), 2.78 – 2.70 (m, 7.2H, H^4 + H^4 + H^{12} + H^{12}), 2.46 – 2.29 (m, 7.2H, H^{13} + H^{13} + H^{15} + H^{15}), 2.01 – 1.96 (m, 1.8H, H^{10} + H^{10}), 1.95 – 1.83 (m, 3.6H, H^{14} + H^{14}), 1.80 (d, *J* = 1.4 Hz, 3H, H^7), 1.76 (bs, 2.4H, H^7), 1.65 (d, *J* = 1.3 Hz, 1.5H, H^7), 1.64 (d, *J* = 1.3 Hz, 1.5H, H^7), 1.61 (d, *J* = 1.3 Hz, 1.2H, H^7), 1.58 (d, *J* = 1.3 Hz, 1.2H, H^7), 1.28 (s, 1.2H, H^{16}), 1.27 (s, 1.2H, H^{16}), 1.24 (s, 1.5H, H^{16}), 1.22 (s, 1.5H, H^{16}), 0.77 (s, 1.2H, H^{16}), 0.76 (s, 1.2H, H^{16}), 0.75 (s, 1.5H, H^{16}), 0.74 (s, 1.5H, H^{16}). **^{13}C NMR** (101 MHz, $CDCl_3$; doubling of peaks assumed to be due to restricted/slow rotation of the N–C^5 or C^5–C^8 bond) δ 158.2 (C^2), 158.2 (C^2), 157.7 (C^2), 157.5 (C^2), 144.8 (C^9), 144.2 (C^9), 144.1 (C^9), 144.0 (C^9), 135.9 (C^6), 135.4 (C^6), 135.0 (C^6), 134.8 (C^6), 130.2 (C^5), 130.2 (C^5), 130.0 (C^5), 129.9 (C^5), 118.2 (C^8), 118.1 (C^8), 118.0 (C^8), 117.9 (C^8), 46.3 (C^{12}), 46.0 (C^{12}), 45.6 (C^{12}), 45.5 (C^{12}), 41.4 (C^{11}), 41.1 (C^{11}), 40.8 (C^{11}), 40.6 (C^{11}), 40.6 (C^{10}), 40.5 (C^{10}), 35.1 (C^1), 34.6 (C^1), 33.5 (C^1), 33.0 (C^1), 28.0 (C^7), 27.9 (C^7), 27.6 (C^{15}), 27.5 (C^4 + C^{15}), 27.5 (C^4 + C^{15}), 27.4 (C^4 + C^{15}), 27.4 (C^4), 27.2 (C^7), 27.0 (C^7), 26.6 (C^{16}), 26.4 (C^{16}), 26.3 (C^{16}), 26.2 (C^{16}), 23.8 (C^{14}), 23.7 (C^{14}), 23.6 (C^{14}), 22.6 (C^{16}), 22.5 (C^{16}), 22.2 (C^{16}), 21.8 (C^{16}), 21.0 (C^{13}), 20.9

($\underline{C}^{13}$), 19.9 (C^{13}), 19.7 (C^{13}), 18.9 (C^{7}), 18.8 (C^{7}), 18.7 ($\underline{C}^{7}$), 18.6 ($\underline{C}^{7}$). **HRMS** (ESI-TOF) m/z: $[M + H]^+$ Calcd for $C_{17}H_{29}N_2O$ 277.2274; Found 277.2273.

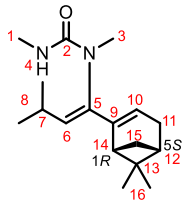

In addition, 1-((*Z*)-1-((1*R*,5*S*)-6,6-dimethylbicyclo[3.1.1]hept-2-en-2-yl)-3-methylbut-1-en-1-yl)-1,3-dimethylurea **431** was afforded as a pale-yellow oil (17 mg, 0.062 mmol, 15% yield). **IR** (film) ν_{max} 3347, 2956, 2926, 1653, 1533, 1465, 1220, 775, 731 cm^{-1}. **^{1}H NMR** (400 MHz, $CDCl_3$; doubling of all peaks assumed to be due to restricted/slow rotation of the N–C^5 or C^5–C^9; alkene geometry assigned by NOE) δ 5.56 (q, *J* = 3.5 Hz, 1H, H^{10}), 5.38 (s, 0.5H, H^6), 5.35 (s, 0.5H, H^6), 4.46 – 4.40 (m, 0.5H, H^4), 4.40 – 4.34 (m, 0.5H, H^4), 2.99 (s, 1.5H, H^3), 2.98 (s, 1.5H, H^3), 2.74 (d, *J* = 4.7 Hz, 1.5H, H^1), 2.72 (d, *J* = 4.8 Hz, 1.5H, H^1), 2.62 – 2.48 (m, 1H, H^7), 2.46 – 2.39 (m, 2H, H^{14} + H^{15}), 2.38 – 2.23 (m, 2H, H^{11}), 2.16 – 2.09 (m, 1H, H^{12}), 1.34 (s, 1.5H, H^{16}), 1.32 (s, 1.5H, H^{16}), 1.16 – 1.09 (m, 1H, H^{15}), 0.98 (d, *J* = 2.8 Hz, 1.5H, H^8), 0.96 (d, *J* = 2.7 Hz, 1.5H, H^8), 0.95 (s, 1.5H, H^8), 0.93 (s, 1.5H, H^8), 0.80 (s, 3H, H^{16}). **^{13}C NMR** (101 MHz, $CDCl_3$; doubling of peaks assumed to be due to restricted/slow rotation of the N–C^5 or C^5–C^9 bond) δ 158.1 (C^2), 158.1 (C^2) 142.4 (C^9), 138.4 (C^5), 138.4 (C^5), 134.1 (C^6), 134.0 (C^6), 121.2 (C^{10}), 121.1 (C^{10}), 42.1 (C^{14}), 42.0 (C^{14}), 40.9 (C^{12}), 40.8 (C^{12}), 38.2 (C^{13}), 37.9 (C^{13}), 35.7 (C^3), 35.5 (C^3), 31.7 (C^{11}), 31.4 (C^{15}), 27.5 (C^1), 27.5 (C^1), 27.2 (C^7), 26.5 (C^{16}), 26.5 (C^{16}), 23.0 (C^8), 23.0 (C^8), 22.5 (C^8), 22.4 (C^8), 20.8 (C^{16}), 20.7 (C^{16}). **HRMS** (ESI-TOF) m/z: $[M + H]^+$ Calcd for $C_{17}H_{29}N_2O$ 277.2274; Found 277.2273.

(*E*)-1-(3-Cyclohexylallyl)-1,3-dimethyl-3-(2-methylprop-1-en-1-yl)urea (432)

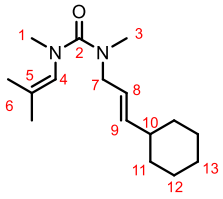

Reaction performed on 0.405 mmol scale following general procedure **3C** using **333** (107 mg, 0.405 mmol, 1.00 equiv.) in anhydrous THF (3.9 mL), 18-crown-6 (232 mg, 0.878 mmol, 2.17 equiv.) and KHMDS (0.91 M in THF; 0.88 mL, 0.80 mmol, 2.0 equiv.), which was stirred for 2 d at −78 °C to room temperature. Flash column chromatography (3–30% EtOAc/pentane) gave **432** as a yellow oil (97 mg, 0.37 mmol, 91% yield). **IR** (film) ν_{max} 2922, 2851, 1645, 1480, 1449, 1384, 1374, 1104, 972, 773 cm^{-1}. **^{1}H NMR** (400 MHz, $CDCl_3$) δ 5.74 (hept, *J* = 1.4 Hz, 1H, H^4), 5.50 (ddt, *J* = 15.5, 6.5, 1.3 Hz, 1H, H^9),

5.31 (dtd, *J* = 15.5, 6.3, 1.3 Hz, 1H, H^8), 3.65 (dt, *J* = 6.3, 1.0 Hz, 2H, H^7), 2.88 (s, 3H, H^1), 2.67 (s, 3H, H^3), 2.01 – 1.88 (m, 1H, H^9), 1.74 – 1.70 (m, 4H, H^{11} + H^{12}), 1.68 (d, *J* = 1.5 Hz, 3H, H^6), 1.67 – 1.60 (m, 1H, H^{13}), 1.58 (d, *J* = 1.3 Hz, 3H, H^6), 1.34 – 0.98 (m, 5H, H^{11} + H^{12} + H^{13}). **^{13}C NMR** (101 MHz, $CDCl_3$) δ 163.1 (C^2), 140.1 (C^9), 128.1 (C^4), 127.3 (C^5), 123.3 (C^8), 52.9 (C^7), 40.5 (C^{10}), 37.4 (C^1), 35.2 (C^3), 33.1 (C^{11}), 26.3 (C^{13}), 26.1 (C^{12}), 22.1 (C^6), 17.6 (C^6). **HRMS** (ESI-TOF) m/z: $[M + H]^+$ Calcd for $C_{16}H_{29}N_2O$ 265.2274; Found 265.2265.

1-(Cyclohex-2-en-1-yl)-1,3-dimethyl-3-(2-methylprop-1-en-1-yl)urea (435)

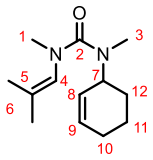

Reaction performed on 0.40 mmol scale following general procedure **3C** using **338** (90 mg, 0.40 mmol, 1.0 equiv.) in anhydrous THF (4 mL), 18-crown-6 (232 mg, 0.878 mmol, 2.20 equiv.) and KHMDS (1.0 M in THF; 0.80 mL, 0.80 mmol, 2.0 equiv.), which was stirred for 4 d at −78 °C to room temperature. Flash column chromatography with neutralised silica (8% acetone/pentane) gave **435** as a pale-yellow oil (84 mg, 0.38 mmol, 95% yield). **IR** (film) ν_{max} 2930, 1637, 1479, 1446, 1373, 1319, 1105, 772 cm^{-1}. **^{1}H NMR** (400 MHz, $CDCl_3$) δ 5.85 – 5.75 (m, 1H, H^8), 5.69 (hept, *J* = 1.4 Hz, 1H, H^4), 5.45 – 5.36 (m, 1H, H^9), 4.53 – 4.44 (m, 1H, H^7), 2.84 (s, 3H, H^1), 2.57 (s, 3H, H^3), 2.01 – 1.88 (m, 2H, H^{10}), 1.82 – 1.71 (m, 2H, H^{11} + H^{12}), 1.65 (d, *J* = 1.4 Hz, 3H, H^6), 1.55 (d, *J* = 1.4 Hz, 3H, H^6), 1.55 – 1.49 (m, 2H, H^{11} + H^{12}). **^{13}C NMR** (101 MHz, $CDCl_3$) δ 163.2 (C^2), 130.8 (C^8), 129.7 (C^9), 127.9 (C^4), 127.6 (C^5), 54.2 (C^7), 37.3 (C^1), 31.1 (C^3), 26.7 (C^{11}), 24.7 (C^{10}), 22.0 (C^6), 21.8 (C^{12}), 17.4 (C^6). **HRMS** (ESI-TOF) m/z: $[M + H]^+$ Calcd for $C_{13}H_{23}N_2O$ 223.1805; Found 223.1801.

(*E*)-1,3,4,4-Tetramethyl-6-((1,3,3-trimethylbicyclo[2.2.1]heptan-2-yl)methylene)tetrahydropyrimidin-2(1*H*)-one (437)

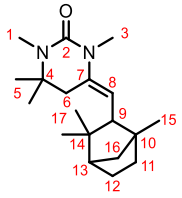

Reaction performed on 0.401 mmol scale following general procedure **3C** using **336** (122 mg, 0.401 mmol, 1.00 equiv.) in anhydrous THF (4 mL), 18-crown-6 (232 mg, 0.878 mmol, 2.19 equiv.) and KHMDS (1.0 M in THF; 0.80 mL, 0.80 mmol, 2.0 equiv.), which was stirred for 2 d at −78 °C to room

temperature. Then, as TLC showed only the presence of the reaction intermediate, 18-crown-6 (232 mg, 0.878 mmol, 2.19 equiv.) and KHMDS (1.0 M in THF; 0.80 mL, 0.80 mmol, 2.0 equiv.) were added again at 0 °C, after which the reaction was stirred for another 3 d at room temperature followed by 24 h at reflux. Flash column chromatography (3−28% EtOAc/petroleum ether) gave **437** as a yellow oil (20 mg, 0.066 mmol, 16% yield). **IR** (film) ν_{max} 2951, 1625, 1480, 1435, 1363, 1103, 750, 665 cm^{-1}. **^{1}H NMR** (400 MHz, $CDCl_3$; alkene geometry analysed by NOE analysis; suspected mixture of rotamers with a 1:0.6 ratio – major rotamer is underlined) δ 4.70 (d, *J* = 11.0 Hz, 1H, $\underline{H^{8}}$), 4.55 (d, *J* = 11.3 Hz, 0.6H, H^{8}), 3.18 (s, 3H, $\underline{H^{3}}$), 3.17 (s, 1.8H, H^{3}), 2.92 – 2.89 (m, 4.8H, $\underline{H^{1}}$ + H^{1}), 2.42 (d, *J* = 0.6 Hz, 2H, $\underline{H^{6}}$), 2.39 (dd, *J* = 6.5, 1.2 Hz, 1.2H, H^{6}), 1.89 (dd, *J* = 11.0, 1.9 Hz, 1H, $\underline{H^{9}}$), 1.77 – 1.62 (m, 5.6H, H^{9} + $\underline{H^{13}}$ + H^{13} + $\underline{H^{11}}$/$\underline{H^{12}}$/$\underline{H^{16}}$ + H^{11}/H^{12}/H^{16}), 1.59 – 1.53 (m, 1.6H, $\underline{H^{11}}$/$\underline{H^{12}}$/$\underline{H^{16}}$ + H^{11}/H^{12}/H^{16}), 1.50 – 1.36 (m, 4H, $\underline{H^{11}}$/$\underline{H^{12}}$/$\underline{H^{16}}$ + H^{11}/H^{12}/H^{16}), 1.20 – 1.18 (m, 9.6H, $\underline{H^{5}}$ + H^{5}), 0.97 (s, 1.8H, H^{17}), 0.94 (s, 3H, $\underline{H^{17}}$), 0.90 (s, 3H, $\underline{H^{15}}$), 0.88 (s, 1.8H, H^{15}), 0.79 (s, 1.8H, H^{17}), 0.76 (s, 3H, $\underline{H^{17}}$). **^{13}C NMR** (101 MHz, $CDCl_3$; suspected mixture of rotamers with a 1:0.6 ratio – major rotamer is underlined) δ 154.3 (C^{2}), 154.2 ($\underline{C^{2}}$), 135.9 ($\underline{C^{7}}$), 133.6 (C^{7}), 107.5 (C^{8}), 103.5 ($\underline{C^{8}}$), 56.2 (C^{9}), 54.5 ($\underline{C^{9}}$), 52.9 (C^{4}), 52.8 ($\underline{C^{4}}$), 49.7 ($\underline{C^{10}}$), 48.8 ($\underline{C^{13}}$ + C^{13}), 48.6 (C^{10}), 44.9 ($\underline{C^{11}}$/$\underline{C^{12}}$/$\underline{C^{16}}$), 43.0 (C^{14}), 42.4 (C^{11}/C^{12}/C^{16}), 40.4 ($\underline{C^{14}}$), 38.3 (C^{11}/C^{12}/C^{16}), 38.0 ($\underline{C^{6}}$), 37.8 (C^{6}), 32.2 ($\underline{C^{17}}$), 32.0 ($\underline{C^{3}}$), 31.8 (C^{3}), 28.7 ($\underline{C^{1}}$ + C^{1}), 28.0 (C^{17}), 27.9 ($\underline{C^{11}}$/$\underline{C^{12}}$/$\underline{C^{16}}$), 26.6 (C^{17}), 26.4 ($\underline{C^{11}}$/$\underline{C^{12}}$/$\underline{C^{16}}$), 26.1 (C^{5}), 26.0 ($\underline{C^{5}}$ + C^{5}), 25.9 (C^{11}/C^{12}/C^{16}), 23.0 ($\underline{C^{17}}$), 20.9 ($\underline{C^{15}}$), 19.6 (C^{15}). **HRMS** (ESI-TOF) m/z: $[M + H]^{+}$ Calcd for $C_{19}H_{33}N_2O$ 305.2587; Found 305.2584.

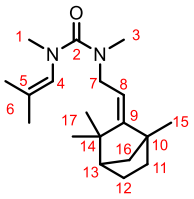

In addition, (*Z*)-1,3-dimethyl-3-(2-methylprop-1-en-1-yl)-1-(2-(1,3,3-trimethylbicyclo[2.2.1]heptan-2-ylidene)ethyl)urea **436** was afforded as a yellow oil (37 mg, 0.12 mmol, 30% yield). **IR** (film) ν_{max} 2957, 2868, 1642, 1480, 1462, 1384, 1374, 1362, 1104, 772 cm^{-1}. **^{1}H NMR** (400 MHz, $CDCl_3$) δ 5.72 (hept, *J* = 1.4 Hz, 1H, H^{4}), 4.83 (t, *J* = 6.6 Hz, 1H, H^{8}), 3.85 (d, *J* = 6.6 Hz, 2H, H^{7}), 2.87 (s, 3H, H^{1}), 2.69 (s, 3H, H^{3}), 1.74 – 1.68 (m, 2H, H^{12} + H^{13}), 1.67 (d, *J* = 1.4 Hz, 3H, H^{6}), 1.56 (d, *J* = 1.4 Hz, 3H, H^{6}), 1.55 – 1.40 (m, 3H, H^{11} + H^{12} + H^{16}), 1.21 – 1.17 (m, 2H, H^{11} + H^{16}), 1.16 (s, 3H, H^{17}), 1.12 (s, 3H, H^{15}), 1.09 (s, 3H, H^{17}). **^{13}C NMR** (101 MHz, $CDCl_3$) δ 163.1 (C^{2}), 159.9 (C^{9}), 128.0 (C^{4}), 127.3 (C^{5}), 112.7 (C^{8}), 50.7 (C^{10}), 49.7 (C^{13}), 48.2 (C^{7}), 44.0 (C^{16}), 42.6 (C^{14}), 37.3 (C^{1}), 36.0 (C^{11}), 35.3 (C^{3}), 27.3 (C^{17}), 25.6 (C^{12}), 25.5 (C^{17}), 22.1 (C^{6}), 19.3 (C^{15}), 17.5 (C^{6}). **HRMS** (ESI-TOF) m/z: $[M + H]^{+}$ Calcd for $C_{19}H_{33}N_2O$ 305.2587; Found 305.2586.

(*E*)-5-Benzyl-1,3-dimethyl-4-(2-phenylethylidene)tetrahydropyrimidin-2(1*H*)-one (440)

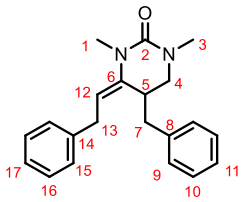

Reaction performed on 0.31 mmol scale following general procedure **3C** using **249** (98 mg, 0.31 mmol, 1.0 equiv.) in anhydrous THF (3.1 mL), 18-crown-6 (1.25 M in THF; 540 μL, 0.675 mmol, 2.18 equiv.) and KHMDS (1.0 M in THF; 0.61 mL, 0.61 mmol, 2.0 equiv.), which was stirred for 24 h at −78 °C to 0 °C. Flash column chromatography (10−80% acetone/petroleum ether) gave **440** as a yellow oil (42 mg, 0.13 mmol, 42% yield). **IR** (film) ν_{max} 3025, 2923, 1664, 1637, 1493, 1306, 752, 700 cm^{-1}. **^{1}H NMR** (400 MHz, $CDCl_3$; alkene geometry assigned by NOE analysis) δ 7.33 – 7.25 (m, 4H, H^{10} + H^{16}), 7.25 – 7.16 (m, 2H, H^{11} + H^{17}), 7.15 – 7.09 (m, 4H, H^{9} + H^{15}), 4.80 (t, *J* = 7.5 Hz, 1H, H^{12}), 3.38 – 3.27 (m, 2H, H^{4} + H^{13}), 3.19 (s, 3H, H^{1}), 3.17 – 3.12 (m, 1H, H^{13}), 3.09 (dddd, *J* = 7.9, 5.6, 3.7, 1.9 Hz, 1H, H^{5}), 3.00 (s, 3H, H^{3}), 2.92 (dd, *J* = 12.0, 1.9 Hz, 1H, H^{4}), 2.81 (d, *J* = 7.9 Hz, 2H, H^{7}). **^{13}C NMR** (101 MHz, $CDCl_3$) δ 154.3 (C^{2}), 141.4 (C^{14}), 140.4 (C^{6}), 139.2 (C^{8}), 129.3 (C^{9}), 128.7 (C^{10}/C^{16}), 128.6 (C^{10}/C^{16}), 128.2 (C^{15}), 126.7 (C^{11}/C^{17}), 126.2 (C^{11}/C^{17}), 103.4 (C^{12}), 48.6 (C^{4}), 37.7 (C^{7}), 36.5 (C^{3}), 35.4 (C^{5}), 32.7 (C^{13}), 31.7 (C^{1}). **HRMS** (ESI-TOF) m/z: $[M + H]^+$ Calcd for $C_{21}H_{24}N_2O$ 321.1961; Found 321.1965.

1,3-Dimethyl-1,3-bis((*E*)-3-phenylprop-1-en-1-yl)urea (443)

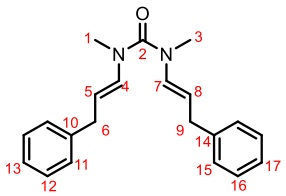

Reaction performed on 0.499 mmol scale following general procedure **2B** using **249** (160 mg, 0.499 mmol, 1.00 equiv.) and $[Ph_3P]_3Ru(CO)(Cl)H$ (48 mg, 0.050 mmol, 10 mol%) in anhydrous THF (5 mL), which was stirred for 16 h at reflux. Flash column chromatography (2−20% acetone/petroleum ether) gave **443** as a yellow oil (56 mg, 0.17 mmol, 35% yield). **IR** (film) ν_{max} 3029, 2917, 1648, 1380, 1104, 773 cm^{-1}. **^{1}H NMR** (400 MHz, $CDCl_3$) δ 7.32 – 7.27 (m, 4H, H^{11} + H^{15}), 7.23 – 7.17 (m, 6H, H^{12} + H^{13} + H^{16} + H^{17}), 6.63 (dt, *J* = 14.0, 1.3 Hz, 2H, H^{4} + H^{7}), 4.99 (dt, *J* = 14.0, 7.2 Hz, 2H, H^{5} + H^{8}), 3.38 (d, *J* = 7.2 Hz, 4H, H^{6} + H^{9}), 3.03 (s, 6H, H^{1} + H^{3}). **^{13}C NMR** (101 MHz, $CDCl_3$) δ 159.5 (C^{2}), 141.3 (C^{10} + C^{14}), 132.2 (C^{4} + C^{7}), 128.6 (C^{11} + C^{15}), 128.5 (C^{12} + C^{16}), 126.3 (C^{13} + C^{17}), 107.6 (C^{5} + C^{8}), 36.7

(C^6 + C^9), 34.0 (C^1 + C^3). **HRMS** (ESI-TOF) m/z: $[M + H]^+$ Calcd for $C_{21}H_{24}N_2O$ 321.1961; Found 321.1962.

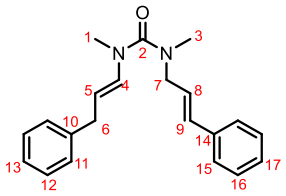

In addition, 1-cinnamyl-1,3-dimethyl-3-((*E*)-3-phenylprop-1-en-1-yl)urea was afforded as a yellow oil (75 mg, 0.23 mmol, 47% yield). **IR** (film) ν_{max} 3026, 2917, 1644, 1383, 773 cm^{-1}. **^{1}H NMR** (400 MHz, $CDCl_3$) δ 7.41 – 7.27 (m, 6H, H^{11} + H^{12} + H^{15} + H^{16}), 7.26 – 7.16 (m, 4H, H^{11} + H^{12}/H^{16} + H^{13} + H^{17}), 6.63 (dt, *J* = 14.0, 1.3 Hz, 1H, H^4), 6.55 (dt, *J* = 15.8, 1.6 Hz, 1H, H^9), 6.20 (dt, *J* = 15.8, 6.3 Hz, 1H, H^8), 4.94 (dt, *J* = 14.0, 7.1 Hz, 1H, H^5), 3.94 (dd, *J* = 6.3, 1.6 Hz, 2H, H^7), 3.37 (dd, *J* = 7.1, 1.3 Hz, 2H, H^6), 3.02 (s, 3H, H^1), 2.83 (s, 3H, H^3). **^{13}C NMR** (101 MHz, $CDCl_3$) δ 162.3 (C^2), 141.5 (C^{10}), 136.7 (C^{14}), 133.2 (C^8), 132.7 (C^4), 128.7 (C^{12}/C^{16}), 128.6 (C^{12}/C^{16}), 128.5 (C^{11}), 127.9 (C^{13}/C^{17}), 126.6 (C^{15}), 126.2 (C^{13}/C^{17}), 125.2 (C^9), 106.4 (C^5), 53.3 (C^7), 36.8 (C^6), 36.4 (C^3), 33.8 (C^1). **HRMS** (ESI-TOF) m/z: $[M + H]^+$ Calcd for $C_{21}H_{24}N_2O$ 321.1961; Found 321.1965.

Starting urea **249** was recovered as a brownish oil (22 mg, 0.069 mmol, 14% yield).

4-Benzyl-1,3-dimethyl-5-propyl-1,3-dihydro-2*H*-imidazol-2-one (450)

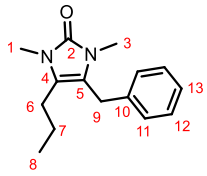

Reaction performed on 0.38 mmol scale following general procedure **3C** using **248** (93 mg, 0.38 mmol, 1.0 equiv.) in anhydrous THF (3.8 mL), 18-crown-6 (221 mg, 0.837 mmol, 2.20 equiv.) and KHMDS (1.0 M in THF; 0.76 mL, 0.76 mmol, 2.0 equiv.), which was stirred for 24 h at −78 °C to 0 °C. Flash column chromatography (14−80% acetone/pentane) gave **450** as a yellow oil (38 mg, 0.16 mmol, 41% yield). **IR** (film) ν_{max} 3363, 2958, 2929, 1674, 1651, 1455, 1396, 746, 707, 693 cm^{-1}. **^{1}H NMR** (400 MHz, $CDCl_3$) δ 7.32 – 7.23 (m, 2H, H^{12}), 7.23 – 7.18 (m, 1H, H^{13}), 7.11 – 7.08 (m, 2H, H^{11}), 3.77 (s, 2H, H^9), 3.23 (s, 3H, H^1), 2.96 (s, 3H, H^3), 2.39 (t, *J* = 7.5 Hz, 2H, H^6), 1.49 (h, *J* = 7.5 Hz, 2H, H^7), 0.92 (t, *J* = 7.5 Hz, 3H, H^8). **^{13}C NMR** (101 MHz, $CDCl_3$) δ 153.8 (C^2), 138.3 (C^{10}), 128.8 (C^{12}), 127.9 (C^{11}), 126.7 (C^{13}), 119.6 (C^4), 115.8 (C^5), 29.2 (C^9), 27.7 (C^3), 27.7 (C^1), 25.3 (C^6), 23.1 (C^7), 13.8 (C^8). **HRMS** (ESI-TOF) m/z: $[M + H]^+$ Calcd for $C_{15}H_{21}N_2O$ 245.1648; Found 245.1651.

1,3-Dimethyl-1-((*E*)-3-phenylprop-1-en-1-yl)-3-((*E*)-prop-1-en-1-yl)urea (452)

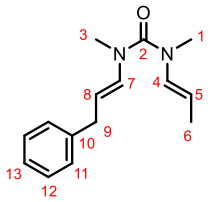

Reaction performed on 0.499 mmol scale following general procedure **2B** using **248** (122 mg, 0.499 mmol, 1.00 equiv.) and $[Ph_3P]_3Ru(CO)(Cl)H$ (48 mg, 0.050 mmol, 10 mol%) in anhydrous THF (5 mL), which was stirred for 16 h at reflux. Flash column chromatography (5−40% acetone/petroleum ether) gave **452** as a pale-yellow oil (33 mg, 0.14 mmol, 27% yield). **IR** (film) ν_{max} 3026, 2924, 1647, 1372, 772 cm^{-1}. **^{1}H NMR** (400 MHz, $CDCl_3$) δ 7.33 – 7.27 (m, 2H, H^{11}), 7.24 – 7.17 (m, 3H, H^{12} + H^{13}), 6.60 (dt, *J* = 14.0, 1.3 Hz, 1H, H^7), 6.50 (dq, *J* = 14.0, 1.5 Hz, 1H, H^4), 4.97 (dt, *J* = 14.0, 7.2 Hz, 1H, H^8), 4.84 (dq, *J* = 14.0, 6.6 Hz, 1H, H^5), 3.37 (d, *J* = 7.2 Hz, 2H, H^9), 3.01 (s, 3H, H^3), 3.00 (s, 3H, H^1), 1.71 (dd, *J* = 6.6, 1.5 Hz, 3H, H^6). **^{13}C NMR** (101 MHz, $CDCl_3$) δ 159.5 (C^2), 141.4 (C^{10}), 132.4 (C^7), 131.7 (C^4), 128.6 (C^{11}/C^{12}), 128.5 (C^{11}/C^{12}), 126.2 (C^{13}), 107.2 (C^8), 103.4 (C^5), 36.7 (C^9), 34.0 (C^3), 33.9 (C^1), 15.5 (C^6). **HRMS** (ESI-TOF) m/z: $[M + H]^+$ Calcd for $C_{15}H_{21}N_2O$ 245.1648; Found 245.1651.

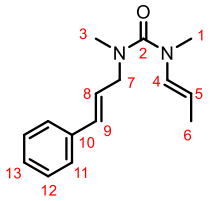

In addition, 1-cinnamyl-1,3-dimethyl-3-((*E*)-prop-1-en-1-yl)urea **451** was afforded as a pale-yellow oil (57 mg, 0.23 mmol, 47% yield). **IR** (film) ν_{max} 3033, 2920, 1640, 1372, 1110, 772 cm^{-1}. **^{1}H NMR** (400 MHz, $CDCl_3$) δ 7.33 – 7.28 (m, 2H, H^{12}), 7.26 – 7.21 (m, 2H, H^{11}), 7.19 – 7.14 (m, 1H, H^{13}), 6.51 – 6.40 (m, 2H, H^4 + H^9), 6.15 (dt, *J* = 15.8, 6.3 Hz, 1H, H^8), 4.70 (dq, *J* = 14.1, 6.6 Hz, 1H, H^5), 3.84 (dd, *J* = 6.3, 1.5 Hz, 2H, H^7), 2.92 (s, 3H, H^1), 2.75 (s, 3H, H^3), 1.61 (dd, *J* = 6.6, 1.6 Hz, 3H, H^6). **^{13}C NMR** (101 MHz, $CDCl_3$) δ 162.3 (C^2), 136.7 (C^{10}), 133.0 (C^4), 132.1 (C^9), 128.7 (C^{11}), 127.8 (C^{13}), 126.5 (C^{12}), 125.3 (C^8), 102.1 (C^5), 53.2 (C^7), 36.3 (C^3), 33.7 (C^1), 15.5 (C^6). **HRMS** (ESI-TOF) m/z: $[M + H]^+$ Calcd for $C_{15}H_{21}N_2O$ 245.1648; Found 245.1650.

1,3-Dimethyl-1-((2*Z*,4*E*)-2-phenylhexa-2,4-dien-3-yl)urea (453)

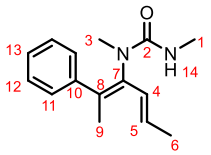

Reaction performed on 0.438 mmol scale following general procedure **3C** using **340** (107 mg, 0.438 mmol, 1.00 equiv.) in anhydrous THF (4.4 mL), 18-crown-6 (254 mg, 0.962 mmol, 2.20 equiv.) and KHMDS (1.0 M in THF; 0.88 mL, 0.88 mmol, 2.0 equiv.), which was stirred for 24 h at −78 °C to 0 °C. Flash column chromatography (14−60% acetone/pentane) gave **453** as a yellow oil (13 mg, 0.053 mmol, 12% yield) with minor impurities. **IR** (film) ν_{max} 3362, 2924, 1648, 1524, 1445, 1338, 769, 702 cm^{-1}. **^{1}H NMR** (400 MHz, $CDCl_3$) δ 7.41 – 7.35 (m, 2H, H^{11}/H^{12}), 7.34 – 7.28 (m, 1H, H^{13}), 7.23 – 7.19 (m, 2H, H^{11}/H^{12}), 5.94 (dq, *J* = 15.3, 1.6 Hz, 1H, H^{4}), 5.65 (dq, *J* = 15.3, 6.7 Hz, 1H, H^{5}), 4.57 – 4.49 (m, 1H, H^{14}), 3.06 (s, 3H, H^{3}), 2.80 (d, *J* = 4.8 Hz, 3H, H^{1}), 2.00 (s, 3H, H^{9}), 1.68 (dd, *J* = 6.7, 1.6 Hz, 3H, H^{6}). **^{13}C NMR** (101 MHz, $CDCl_3$) δ 158.0 (C^{2}), 141.1 (C^{8}/C^{10}), 137.3 (C^{8}/C^{10}), 135.8 (C^{7}), 128.5 (C^{11}/C^{12}), 128.4 (C^{11}/C^{12}), 127.6 (C^{13}), 127.4 (C^{5}), 124.8 (C^{4}), 34.3 (C^{3}), 27.8 (C^{1}), 20.4 (C^{9}), 18.1 (C^{6}). **HRMS** (ESI-TOF) m/z: $[M + H]^+$ Calcd for $C_{15}H_{21}N_2O$ 245.1648; Found 245.1649.

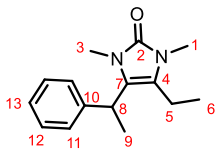

In addition, 4-ethyl-1,3-dimethyl-5-(1-phenylethyl)-1,3-dihydro-2*H*-imidazol-2-one **454** was afforded as an orange oil (77 mg, 0.32 mmol, 72% yield). **IR** (film) ν_{max} 3358, 2970, 1675, 1451, 1397, 1027, 748, 701, 594 cm^{-1}. **^{1}H NMR** (400 MHz, $CDCl_3$) δ 7.34 – 7.26 (m, 2H, H^{12}), 7.23 – 7.17 (m, 3H, H^{11} + H^{13}), 4.12 (q, *J* = 7.4 Hz, 1H, H^{8}), 3.22 (s, 3H, H^{1}), 2.88 (s, 3H, H^{3}), 2.43 (qd, *J* = 7.5, 1.3 Hz, 2H, H^{5}), 1.62 (d, *J* = 7.4 Hz, 3H, H^{9}), 1.08 (t, *J* = 7.5 Hz, 3H, H^{6}). **^{13}C NMR** (101 MHz, $CDCl_3$) δ 153.8 (C^{2}), 142.7 (C^{10}), 128.6 (C^{12}), 127.0 (C^{11}), 126.5 (C^{13}), 120.3 (C^{4}), 120.2 (C^{7}), 34.1 (C^{8}), 28.3 (C^{3}), 27.4 (C^{1}), 19.5 (C^{9}), 16.7 (C^{5}), 14.9 (C^{6}). **HRMS** (ESI-TOF) m/z: $[M + H]^+$ Calcd for $C_{15}H_{21}N_2O$ 245.1648; Found 245.1642.

(*Z*)-4-Ethyl-1,3-dimethyl-5-(1-phenylpropan-2-ylidene)imidazolidin-2-one (457)

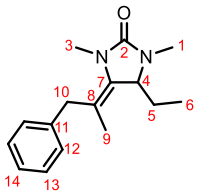

Reaction performed on 0.399 mmol scale following general procedure **3C** using **341** (103 mg, 0.399 mmol, 1.00 equiv.) in anhydrous THF (4 mL), 18-crown-6 (232 mg, 0.878 mmol, 2.20 equiv.) and KHMDS (1.0 M in THF; 0.80 mL, 0.80 mmol, 2.0 equiv.), which was stirred for 23 h at −78 °C to 0 °C. Flash column chromatography (1−20% acetone/CH_2Cl_2) gave **457** as a yellow oil (67 mg, 0.26 mmol, 65% yield). **IR** (film) ν_{max} 3316, 2932, 1709, 1669, 1453, 1390, 1081, 701 cm^{-1}. **^{1}H NMR** (400 MHz, $CDCl_3$; alkene geometry assigned following NOE analysis) δ 7.23 – 7.13 (m, 3H, H^{13} + H^{14}), 7.06 – 7.00 (m, 2H, H^{12}), 4.24 (t, *J* = 7.7 Hz, 1H, H^4), 2.96 (s, 2H, H^{10}), 2.86 (s, 3H, H^3), 2.54 (s, 3H, H^1), 2.37 – 2.21 (m, 2H, H^5), 1.55 (s, 3H, H^9), 1.09 (t, *J* = 7.4 Hz, 3H, H^6). **^{13}C NMR** (101 MHz, $CDCl_3$) δ 156.8 (C^2), 141.5 (C^8), 136.2 (C^{11}), 129.5 (C^{12}), 128.0 (C^{13}), 126.8 (C^{14}), 99.5 (C^4), 63.4 (C^7), 41.5 (C^{10}), 26.4 (C^1), 24.5 (C^3), 23.6 (C^9), 20.3 (C^5), 15.9 (C^6). **HRMS** (ESI-TOF) m/z: $[M + H]^+$ Calcd for $C_{16}H_{23}N_2O$ 259.1805; Found 259.1803.

(*E*)-4-(But-2-en-1-yl)-1,3-dimethylimidazolidin-2-one (476)

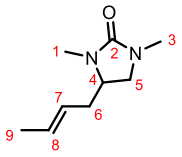

Reaction performed on 0.459 mmol scale following general procedure **3C** using **325** (114 mg, 0.459 mmol, 1.00 equiv.) in anhydrous THF (4.6 mL), 18-crown-6 (266 mg, 1.01 mmol, 2.19 equiv.) and KHMDS (1.0 M in THF; 0.92 mL, 0.92 mmol, 2.0 equiv.), which was stirred for 24 h at −78 °C to 0 °C. Flash column chromatography (20% EtOAc/pentane) gave **476** as a pale-yellow oil (12 mg, 0.071 mmol, 16% yield). **^{1}H NMR** (400 MHz, $CDCl_3$) δ 5.55 (dqt, *J* = 15.1, 6.5, 1.1 Hz, 1H, H^8), 5.31 (dtq, *J* = 15.1, 7.0, 1.4 Hz, 1H, H^7), 3.43 – 3.34 (m, 1H, H^4), 3.33 (d, *J* = 8.4 Hz, 1H, H^5), 2.91 (dd, *J* = 8.4, 7.3 Hz, 1H, H^5), 2.75 (s, 3H, H^3), 2.74 (s, 3H, H^1), 2.43 – 2.34 (m, 1H, H^6), 2.18 – 2.09 (m, 1H, H^6), 1.66 (dq, *J* = 6.5, 1.4 Hz, 3H, H^9). **^{13}C NMR** (101 MHz, $CDCl_3$) δ 161.9 (C^2), 129.3 (C^8), 125.1 (C^7), 55.4 (C^4), 50.5 (C^5), 35.5 (C^6), 31.3 (C^3), 29.5 (C^1), 18.2 (C^9).

(*E*)-1,3-Dimethyl-4-(pent-2-en-1-yl)-5-vinylimidazolidin-2-one (481)

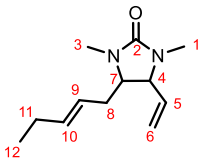

Reaction performed on 0.634 mmol scale following general procedure **3C** using **344** (132 mg, 0.634 mmol, 1.00 equiv.) in anhydrous THF (6.3 mL), 18-crown-6 (368 mg, 1.39 mmol, 2.19 equiv.) and KHMDS (1.00 M in THF; 1.27 mL, 1.27 mmol, 2.00 equiv.), which was stirred for 24 h at −78 °C to 0 °C. Flash column chromatography (20% EtOAc/pentane) gave **481** as a yellow oil (11 mg, 0.053 mmol, 8% yield; contains minor impurities). **IR** (film) ν_{max} 3379, 2962, 2929, 1699, 1440, 1392, 1220, 970, 772, 584 cm^{-1}. **^{1}H NMR** (400 MHz, $CDCl_3$) δ 5.73 – 5.52 (m, 2H, H^5 + H^{10}), 5.37 – 5.28 (m, 1H, H^9), 5.28 – 5.23 (m, 2H, H^6), 3.44 (dd, *J* = 8.4, 7.8 Hz, 1H, H^4), 3.07 (dt, *J* = 7.8, 5.1 Hz, 1H, H^7), 2.76 (s, 3H, H^3), 2.66 (s, 3H, H^1), 2.30 (ddq, *J* = 7.5, 5.1, 1.1 Hz, 2H, H^8), 2.06 – 1.97 (m, 2H, H^{11}), 0.96 (t, *J* = 7.5 Hz, 3H, H^{12}). **^{13}C NMR** (101 MHz, $CDCl_3$) δ 161.3 (C^2), 136.7 (C^5), 136.4 (C^{10}), 123.1 (C^9), 119.7 (C^6), 64.4 (C^4), 61.7 (C^7), 34.2 (C^8), 29.6 (C^3), 29.4 (C^1), 25.8 (C^{11}), 13.8 (C^{12}). **HRMS** (ESI-TOF) m/z: $[M + H]^+$ Calcd for $C_{12}H_{21}N_2O$ 209.1648; Found 209.1647.

In addition, (*Z*)-1,3-dimethyl-1-(prop-1-en-1-yl)urea **366** was afforded as a yellow oil (23 mg, 0.18 mmol, 28% yield).

(*E*)-4-(But-1-en-1-yl)-1,3-dimethyl-5-(prop-1-en-2-yl)imidazolidine-2-one (484)

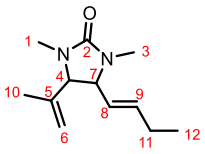

Reaction performed on 0.41 mmol scale following general procedure **3C** using **342** (85 mg, 0.41 mmol, 1.0 equiv.) in anhydrous THF (3.9 mL), 18-crown-6 (232 mg, 0.878 mmol, 2.14 equiv.) and KHMDS (0.91 M in THF; 0.88 mL, 0.80 mmol, 2.0 equiv.), which was stirred for 25 h at −78 °C to 0 °C. Flash column chromatography (5−42% EtOAc/pentane) gave **484** as a yellow oil (6 mg, 0.03 mmol, 7% yield; based on NMR ratio) mixed with an unidentifiable compound. **^{1}H NMR** (400 MHz, $CDCl_3$) δ 5.70 (dt, *J* = 15.3, 6.4 Hz, 1H, H^9), 5.30 – 5.20 (m, 1H, H^8), 4.99 – 4.93 (m, 2H, H^6), 3.41 (d, *J* = 1.3 Hz, 1H, H^4/H^7), 3.40 (d, *J* = 0.9 Hz, 1H, H^4/H^7), 2.67 (s, 3H, H^3), 2.64 (s, 3H, H^1), 2.11 – 2.05 (m, 2H, H^{11}), 1.65 (dd, *J* = 1.5, 0.9 Hz, 3H, H^{10}), 0.99 (t, *J* = 7.5 Hz, 3H, H^{12}). **^{13}C NMR** (101 MHz, $CDCl_3$) δ 161.5 (C^2), 141.2 (C^5), 138.6 (C^9), 127.0 (C^8), 115.8 (C^6), 69.5 (C^4), 63.8 (C^7), 29.7 (C^1), 29.4 (C^3), 25.4 (C^{11}), 17.4 (C^{10}), 13.6 (C^{12}). **HRMS** (ESI-TOF) m/z: $[M + Na]^+$ Calcd for $C_{12}H_{20}N_2ONa$ 231.1468; Found 231.1478.

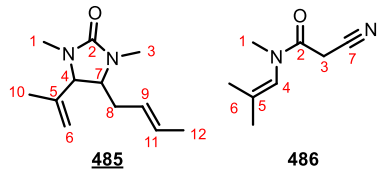

485 **486**

In addition, (*E*)-4-(but-2-en-1-yl)-1,3-dimethyl-5-(prop-1-en-2-yl)imidazolidine-2-one **485** was afforded as a yellow oil (23 mg, 0.11 mmol, 27% yield; based on NMR ratio) mixed with 2-cyano-*N*-(2-methylprop-1-en-1-yl)acetamide **486** (14 mg, 0.092 mmol, 22% yield; based on NMR ratio). **^{1}H NMR** (400 MHz, $CDCl_3$) δ 5.91 (hept, *J* = 1.5 Hz, 0.7H, H^4), 5.52 (dqt, *J* = 15.2, 6.4, 1.3 Hz, 1H, H^{11}), 5.29 (dtq, *J* = 15.2, 7.4, 1.5 Hz, 1H, H^9), 4.96 – 4.91 (m, 2H, H^6), 3.48 (dd, *J* = 7.2, 0.6 Hz, 1H, H^4), 3.35 (s, 1.4H, H^3), 3.10 (ddd, *J* = 7.2, 5.8, 4.2 Hz, 1H, H^7), 2.99 (s, 2.1H, H^1), 2.74 (s, 3H, H^3), 2.61 (s, 3H, H^1), 2.30 – 2.20 (m, 2H, H^8), 1.75 (d, *J* = 1.5 Hz, 2.1H, H^6), 1.65 (d, *J* = 1.5 Hz, 3H, H^{12}), 1.64 – 1.63 (m, 2.1H, H^6), 1.60 (dd, *J* = 1.5, 0.9 Hz, 3H, H^{10}). **^{13}C NMR** (101 MHz, $CDCl_3$) δ 162.1 (C^2), 161.1 (C^2), 142.2 (C^5), 138.8 (C^5), 129.3 (C^{11}), 125.1 (C^9), 123.9 (C^4), 115.8 (C^6), 114.1 (C^7), 66.9 (C^4), 59.4 (C^7), 35.5 (C^1), 34.7 (C^8), 29.4 (C^3), 29.2 (C^1), 25.3 (C^3), 21.8 (C^6), 18.1 (C^{12}), 17.4 (C^6), 16.9 (C^{10}). **485**: **HRMS** (ESI-TOF) m/z: $[M + Na]^+$ Calcd for $C_{12}H_{20}N_2ONa$ 231.1468; Found 231.1471. **486**: **HRMS** (ESI-TOF) m/z: $[M + Na]^+$ Calcd for $C_8H_{12}N_2ONa$ 175.0842; Found 175.0837.

(4*SR*,5*SR*)-(*Z*)-4-(But-2-en-2-yl)-1,3-dimethyl-5-(prop-1-en-2-yl)imidazolidine-2-one (489)

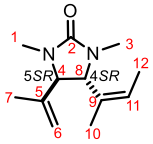

Reaction performed on 0.40 mmol scale following general procedure **3C** using **343** (84 mg, 0.40 mmol, 1.0 equiv.) in anhydrous THF (3.9 mL), 18-crown-6 (232 mg, 0.878 mmol, 2.20 equiv.) and KHMDS (0.91 M in THF; 0.88 mL, 0.80 mmol, 2.0 equiv.), which was stirred for 25 h at −78 °C to 0 °C. Flash column chromatography (5−42% EtOAc/pentane) gave **489** as an orange oil (72 mg, 0.35 mmol, 86% yield). **IR** (film) ν_{max} 2918, 2864, 2238, 1689, 1440, 1391, 1220, 1025, 907, 771, 727, 645 cm^{-1}. **^{1}H NMR** (400 MHz, $CDCl_3$; *anti*-conformation and alkene geometry assigned by NOE analysis) δ 5.50 – 5.40 (m, 1H, H^{11}), 4.94 (p, *J* = 1.5 Hz, 1H, H^6), 4.92 – 4.86 (m, 1H, H^6), 3.48 (d, *J* = 7.8 Hz, 1H, H^4), 3.43 (d, *J* = 7.8 Hz, 1H, H^8), 2.65 (s, 3H), 2.61 (s, 3H), 1.66 – 1.62 (m, 6H, H^7 + H^{12}), 1.53 (p, *J* = 1.1 Hz, 3H, H^{10}). **^{13}C NMR** (101 MHz, $CDCl_3$) δ 161.4 (C^2), 142.1 (C^5), 132.4 (C^9), 125.3 (C^{11}), 115.4 (C^6), 68.9 (C^8), 66.8 (C^4), 29.5 (C^1), 29.2 (C^3), 17.2 (C^7), 13.5 (C^{12}), 10.9 (C^{10}). **HRMS** (ESI-TOF) m/z: $[M + H]^+$ Calcd for $C_{12}H_{21}N_2O$ 209.1648; Found 209.1647.

1-Methyl-1,3,3-tri((*Z*)-prop-1-en-1-yl)urea (506)

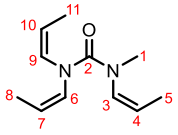

Reaction performed on 0.38 mmol scale following general procedure **3C** using **222** (74 mg, 0.38 mmol, 1.0 equiv.) in anhydrous THF (3.8 mL), 18-crown-6 (220 mg, 0.833 mmol, 2.19 equiv.) and KHMDS (1.0 M in THF; 0.76 mL, 0.76 mmol, 2.0 equiv.), which was stirred for 22 h at −78 °C to room temperature. Flash column chromatography (4−6% EtOAc/pentane) gave **506** as a yellow oil (3 mg, 0.02 mmol, 4% yield). **^{1}H NMR** (400 MHz, $CDCl_3$) δ 5.91 (dq, *J* = 7.9, 1.7 Hz, 3H, H^3 + H^6 + H^9), 5.12 – 5.03 (m, 3H, H^4 + H^7 + H^{10}), 3.04 (s, 3H, H^1), 1.59 (dd, *J* = 7.0, 1.7 Hz, 3H, H^5), 1.52 (dd, *J* = 7.0, 1.7 Hz, 6H, H^8 + H^{11}). **^{13}C NMR** (101 MHz, $CDCl_3$) δ 158.8 (C^2), 131.9 (C^3), 129.6 (C^6 + C^9), 117.2 (C^4), 115.4 (C^7 + C^{10}), 37.2 (C^1), 12.8 (C^8 + C^{11}), 12.6 (C^5). Full characterisation data was not obtained as the compound had decomposed in $CDCl_3$.

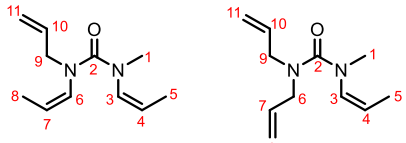

507 **508**

In addition, a mixture of 1-allyl-3-methyl-1,3-di((*Z*)-prop-1-en-1-yl)urea **507** and (*Z*)-1,1-diallyl-3-methyl-3-(prop-1-en-1-yl)urea **508** and with a ratio of 1:0.7 was afforded as a yellow oil (23 mg, 0.12 mmol, 31% yield). **^{1}H NMR** (400 MHz, $CDCl_3$) δ 6.00 (dq, *J* = 8.1, 1.7 Hz, 0.7H, $\underline{H^3}$), 5.93 – 5.72 (m, 3.4H, $\underline{H^7}$ + $\underline{H^{10}}$ + H^3 + H^{10}), 5.69 (dq, *J* = 8.0, 1.7 Hz, 1H, H^6), 5.16 – 5.07 (m, 5.8H, $\underline{H^8}$ + $\underline{H^{11}}$ + H^7 + H^{11}), 5.07 – 4.92 (m, 1.7H, $\underline{H^4}$ + H^4), 3.94 (dt, *J* = 6.1, 1.4 Hz, 1H, H^9), 3.75 (dt, *J* = 6.1, 1.4 Hz, 2.8H, $\underline{H^6}$ + $\underline{H^9}$), 3.00 (s, 3H, H^1), 2.97 (s, 2.1H, $\underline{H^1}$), 1.62 (dd, *J* = 7.1, 1.7 Hz, 2.1H, $\underline{H^5}$), 1.55 (dd, *J* = 7.0, 1.8 Hz, 3H, H^5), 1.49 (dd, *J* = 7.0, 1.7 Hz, 1H, H^8). **^{13}C NMR** (101 MHz, $CDCl_3$) δ 162.6 ($\underline{C^2}$), 160.4 (C^2), 134.5 (C^{10}), 134.3 ($\underline{C^7}$ + $\underline{C^{10}}$), 133.3 ($\underline{C^3}$), 132.3 (C^3), 130.5 (C^6), 118.0 (C^7), 117.5 ($\underline{C^8}$ + $\underline{C^{11}}$), 116.9 (C^{11}), 115.8 (C^4), 115.4 ($\underline{C^4}$), 52.1 (C^9), 50.1 ($\underline{C^6}$ + $\underline{C^9}$), 37.0 ($\underline{C^1}$), 36.9 (C^1) 12.8 ($\underline{C^5}$), 12.6 (C^5/C^8), 12.6 (C^5/C^8). Full characterisation data was not obtained as the compound had decomposed in $CDCl_3$.

(*E*)-4-Allyl-1,3,4-trimethyl-5-propylideneimidazolidin-2-one (511)

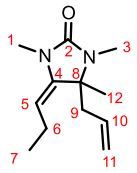

Reaction performed on 0.399 mmol scale following general procedure **3C** using **347** (136 mg, 0.399 mmol, 1.00 equiv.) in anhydrous THF (4 mL), 18-crown-6 (232 mg, 0.878 mmol, 2.20 equiv.) and KHMDS (1.0 M in THF; 0.80 mL, 0.80 mmol, 2.0 equiv.), which was stirred for 66 h at −78 °C to room temperature. Flash column chromatography (0−40% EtOAc/petroleum ether) gave **511** as a yellow oil (6 mg, 0.03 mmol, 7% yield). **IR** (film) ν_{max} 3429, 2933, 1706, 1464, 1393, 1220, 772 cm^{-1}. **^{1}H NMR** (400 MHz, $CDCl_3$) δ 5.50 (dddd, *J* = 16.8, 10.2, 7.6, 6.5 Hz, 1H, H^{10}), 5.09 – 4.97 (m, 2H, H^{11}), 4.30 (t, *J* = 7.8 Hz, 1H, H^{5}), 2.84 (s, 3H, H^{1}), 2.76 (s, 3H, H^{3}), 2.55 – 2.42 (m, 2H, H^{9}), 2.23 – 2.13 (m, 2H, H^{6}), 1.42 (s, 3H, H^{12}), 1.03 (t, *J* = 7.4 Hz, 3H, H^{7}). **^{13}C NMR** (101 MHz, $CDCl_3$) δ 157.1 (C^{2}), 141.5 (C^{4}), 132.6 (C^{10}), 118.6 (C^{11}), 99.1 (C^{5}), 62.3 (C^{8}), 40.4 (C^{9}), 26.7 (C^{1}), 24.0 (C^{3}), 23.6 (C^{12}), 20.0 (C^{6}), 15.9 (C^{7}). **HRMS** (ESI-TOF) m/z: $[M + H]^+$ Calcd for $C_{12}H_{21}N_2O$ 209.1648; Found 209.1644.

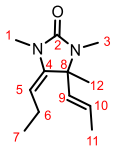

In addition, (*E*)-1,3,4-trimethyl-4-((*E*)-prop-1-en-1-yl)-5-propylideneimidazolidin-2-one **512** was afforded as a yellow oil (37 mg, 0.18 mmol, 45% yield). **IR** (film) ν_{max} 2949, 1707, 1668, 1445, 1220, 906, 773, 726, 647 cm^{-1}. **^{1}H NMR** (400 MHz, $CDCl_3$; alkene geometry assigned by NOE analysis) δ 5.67 (dq, *J* = 15.1, 6.5 Hz, 1H, H^{10}), 5.36 (dq, *J* = 15.5, 1.7 Hz, 1H, H^{9}), 4.23 (t, *J* = 7.4 Hz, 1H, H^{5}), 2.83 (s, 3H, H^{1}), 2.63 (s, 3H, H^{3}), 2.09 – 1.96 (m, 2H, H^{6}), 1.71 (dd, *J* = 6.5, 1.7 Hz, 3H, H^{11}), 1.41 (s, 3H, H^{12}), 0.91 (t, *J* = 7.4 Hz, 3H, H^{7}). **^{13}C NMR** (101 MHz, $CDCl_3$) δ 156.7 (C^{2}), 142.8 (C^{4}), 131.3 (C^{9}), 127.3 (C^{10}), 99.2 (C^{5}), 62.2 (C^{8}), 26.7 (C^{1}), 24.3 (C^{3}), 20.9 (C^{12}), 19.4 (C^{6}), 17.7 (C^{11}), 15.6 (C^{7}). **HRMS** (ESI-TOF) m/z: $[M + H]^+$ Calcd for $C_{12}H_{21}N_2O$ 209.1648; Found 209.1645.

4-Ethylidene-1,3,6-trimethyl-3,4-dihydropyrimidin-2(1*H*)-one (521)

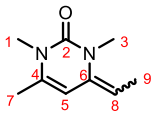

Reaction performed on 0.36 mmol scale following general procedure **3C** using **250** (89 mg, 0.36 mmol, 1.0 equiv.) in anhydrous THF (0.58 mL, 1.6 mL/mmol), 18-crown-6 (1.25 M in THF; 630 µL, 0.788

mmol, 2.19 equiv.) and KHMDS (1.0 M in THF; 0.72 mL, 0.72 mmol, 2.0 equiv.), which was stirred for 4 h at 0 ℃. Flash column chromatography (40−80% acetone/pentane) gave **521** (58% NMR yield, using 1,2,4-trimethoxybenzene as internal standard) as a yellow oil (53 mg, 0.32 mmol, 89% yield; contains a significant amount of grease). **IR** (film) ν_{max} 3358, 2924, 1672, 1439, 1393, 957, 744, 592 cm^{-1}. **^{1}H NMR** (400 MHz, $CDCl_3$) δ 5.99 – 5.89 (m, 1H, H^5), 5.74 (dq, *J* = 16.0, 6.5 Hz, 1H, H^8), 3.19 (s, 3H, H^1/H^3), 3.14 (s, 3H), 2.03 (s, 3H, H^7), 1.81 (dd, *J* = 6.6, 1.7 Hz, 3H, H^9). **^{13}C NMR** (101 MHz, $CDCl_3$) δ 153.3 (C^2), 126.3 (C^8), 117.7 (C^5), 117.4 (C^4/C^6), 115.6 (C^4/C^6), 28.6 (C^1/C^3), 27.4 (C^1/C^3), 19.0 (C^9), 9.3 (C^7). **HRMS** (ESI-TOF) m/z: $[M + H]^+$ Calcd for $C_9H_{15}N_2O$ 167.1179; Found 167.1182.

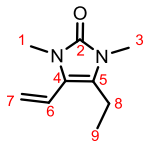

In addition, 4-ethyl-1,3-dimethyl-5-vinyl-1,3-dihydro-2*H*-imidazol-2-one **522** (18% NMR yield, using 1,2,4-trimethoxybenzene as internal standard) was afforded as a yellow oil (13 mg, 0.078 mmol, 22% yield; contains a significant amount of grease). **IR** (film) ν_{max} 3358, 2925, 1682, 1454, 1394, 1060, 748, 592 cm^{-1}. **^{1}H NMR** (400 MHz, $CDCl_3$) δ 6.33 (dd, *J* = 17.8, 11.9 Hz, 1H, H^6), 5.31 (dd, *J* = 17.8, 1.0 Hz, 1H, H^7), 5.10 (dd, *J* = 11.9, 1.0 Hz, 1H, H^7), 3.31 (s, 3H, H^1), 3.22 (s, 3H, H^3), 2.50 (q, *J* = 7.5 Hz, 2H, H^8), 1.13 (t, *J* = 7.5 Hz, 3H, H^9). **^{13}C NMR** (101 MHz, $CDCl_3$) δ 153.7 (C^2), 123.9 (C^5), 123.3 (C^6), 117.2 (C^4), 112.2 (C^7), 29.0 (C^1), 27.5 (C^3), 17.0 (C^8), 14.1 (C^9). **HRMS** (ESI-TOF) m/z: $[M + H]^+$ Calcd for $C_9H_{15}N_2O$ 167.1179; Found 167.1181.

N-Methyl-6-propylidene-3,6-dihydropyridine-1(2*H*)-carboxamide (529)

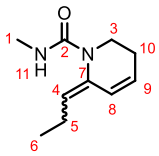

Reaction performed on 0.594 mmol scale following general procedure **3C** using **220** (107 mg, 0.594 mmol, 1.00 equiv.) in anhydrous THF (5.9 mL), 18-crown-6 (1.25 M in THF; 1.04 mL, 1.30 mmol, 2.19 equiv.) and KHMDS (1.00 M in THF; 1.19 mL, 1.19 mmol, 2.00 equiv.), which was stirred for 24 h at −78 °C to 0 °C. Flash column chromatography (5−40% acetone/petroleum ether) gave **529** (16% NMR yield, using 1,2,4-trimethoxybenzene as internal standard) as a pale-yellow oil (19 mg, 0.11 mmol, 18% yield; contains minor impurities). **IR** (film) ν_{max} 3344, 2927, 1710, 1636, 1489, 1453, 1220, 772 cm^{-1}. **^{1}H NMR** (400 MHz, $CDCl_3$) δ 6.00 (dt, *J* = 9.9, 2.0 Hz, 1H, H^8), 5.82 (dt, *J* = 9.9, 4.2 Hz, 1H, H^9), 5.19 (t, *J* = 7.5 Hz, 1H, H^4), 4.84 (bs, 1H, H^{11}), 3.86 – 3.60 (m, 2H, H^3), 2.79 (d, *J* = 4.8 Hz, 3H, H^1), 2.19 – 2.11 (m, 2H, H^{10}), 2.09 (p, *J* = 7.5 Hz, 2H, H^5), 0.99 (t, *J* = 7.5 Hz, 3H, H^6). ^{13}C NMR and

NOE were not obtained as the compound had decomposed in $CDCl_3$. **HRMS** (ESI-TOF) m/z: $[M + H]^+$ Calcd for $C_{10}H_{17}N_2O$ 181.1335; Found 181.1337.

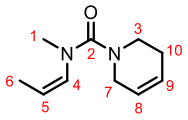

In addition, (*Z*)-*N*-methyl-*N*-(prop-1-en-1-yl)-3,6-dihydropyridine-1(2*H*)-carboxamide **530** (40% NMR yield, using 1,2,4-trimethoxybenzene as internal standard) was obtained as a pale-yellow oil (43 mg, 0.24 mmol, 40% yield; contains internal standard as minor impurity). **IR** (film) ν_{max} 2926, 1637, 142 1370, 1352, 1259, 1039, 995, 734, 455 cm^{-1}. **^{1}H NMR** (400 MHz, acetone-d_6) δ 6.49 (dt, *J* = 8.4, 2.0 Hz, 1H, H^8), 5.99 (dq, *J* = 8.1, 1.8 Hz, 1H, H^4), 5.07 (dq, *J* = 8.1, 7.0 Hz, 1H, H^5), 4.72 (dt, *J* = 8.4, 3.8 Hz, 1H, H^9), 3.44 – 3.37 (m, 2H, H^7), 2.91 (s, 3H, H^1), 2.01 (tdd, *J* = 6.2, 3.8, 2.0 Hz, 2H, H^{10}), 1.82 – 1.76 (m, 2H, H^3), 1.54 (dd, *J* = 7.0, 1.8 Hz, 3H, H^6). **^{13}C NMR** (101 MHz, acetone-d_6) δ 159.2 (C^2), 133.3 (C^4), 128.7 (C^8), 116.1 (C^5), 104.2 (C^9), 44.9 (C^7), 37.0 (C^1), 23.2 (C^3), 22.4 (C^{10}), 12.4 (C^6). **HRMS** (ESI-TOF) m/z: $[M + H]^+$ Calcd for $C_{10}H_{17}N_2O$ 181.1335; Found 181.1339.

Dimethyl 4-(1,3-dimethylureido)-3,6-dimethylcyclohexa-1,3-diene-1,2-dicarboxylate (532)

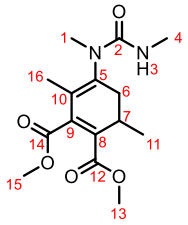

An oven-dried microwave vial containing a magnetic stir bar was sealed with a suba seal and placed under anhydrous N_2. The flask was charged with **362** (68 mg, 0.40 mmol, 1.0 equiv.), dimethyl acetylenedicarboxylate (60 µL, 0.49 mmol, 1.2 equiv.) and anhydrous toluene (0.67 mL, 1.7 mL/mmol). The microwave vial was capped, and the reaction mixture was then stirred for 1h45 at room temperature followed by 18 h at 50 °C. No significant conversion was observed by TLC; thus, the reaction mixture was stirred for 24 h more at 80 °C. Stirring the reaction mixture another 9h30 at 120 °C did not show by TLC to improve the conversion. Therefore, the reaction was cooled down and concentrated *in vacuo*. Flash column chromatography (10−40% acetone/petroleum ether followed by 3−22% *i*-PrOH/pentane) gave **532** as a yellow oil (40 mg, 0.13 mmol, 32% yield). **IR** (film) ν_{max} 3385, 2956, 1712, 1645, 1520, 1435, 1235, 1138, 1113, 1045, 729 cm^{-1}. **^{1}H NMR** (400 MHz, $CDCl_3$) δ 4.41 (q, *J* = 4.6 Hz, 1H, H^3), 3.83 (s, 3H, H^{13}/H^{15}), 3.75 (s, 3H, H^{13}/H^{15}), 2.96 (s, 3H, H^1), 2.96 – 2.90 (m, 1H, H^7), 2.77 (d, *J* = 4.6 Hz, 3H, H^4), 2.75 – 2.67 (m, 1H, H^6), 2.02 (dq, *J* = 17.6, 1.1 Hz, 1H, H^6), 1.68 (dd, *J* = 2.8, 1.0 Hz, 3H, H^{16}), 1.08 (d, *J* = 7.0 Hz, 3H, H^{11}). **^{13}C NMR** (101 MHz, $CDCl_3$) δ 168.8 (C^{12}/C^{14}), 166.0 (C^{12}/C^{14}),

156.5 (C^2), 140.3 (C^9), 138.5 (C^5), 129.3 (C^8), 125.1 (C^{10}), 52.5 (C^{13}/C^{15}), 52.4 (C^{13}/C^{15}), 33.1 (C^1), 32.7 (C^6), 27.7 (C^4), 27.6 (C^7), 17.8 (C^{11}), 13.2 (C^{16}). **HRMS** (ESI-TOF) m/z: $[M + H]^+$ Calcd for $C_{15}H_{23}N_2O_5$ 311.1601; Found 311.1609.

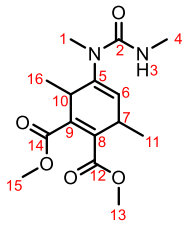

Dimethyl 4-(1,3-dimethylureido)-3,6-dimethylcyclohexa-1,4-diene-1,2-dicarboxylate **531** was also afforded as a yellow oil (13 mg, 0.042 mmol, 10% yield). **IR** (film) ν_{max} 3408, 2953, 1721, 1644, 1520, 1435, 1248, 1043, 754 cm^{-1}. **^{1}H NMR** (400 MHz, $CDCl_3$) δ 5.72 (d, *J* = 4.8 Hz, 1H, H^6), 4.59 (q, *J* = 4.7 Hz, 1H, H^3), 3.81 (s, 3H, H^{13}/H^{15}), 3.80 (s, 3H, H^{13}/H^{15}), 3.37 – 3.20 (m, 2H, H^7 + H^{10}), 3.06 (s, 3H, H^1), 2.77 (d, *J* = 4.7 Hz, 3H, H^4), 1.33 – 1.26 (m, 6H, H^{11} + H^{16}). **^{13}C NMR** (101 MHz, $CDCl_3$) δ 168.1 (C^{12}/C^{14}), 167.5 (C^{12}/C^{14}), 157.7 (C^2), 142.0 (C^5), 137.9 (C^8), 137.2 (C^9), 127.7 (C^6), 52.5 (C^{13}/C^{15}), 52.5 (C^{13}/C^{15}), 35.9 (C^1), 34.6 (C^7/C^{10}), 34.0 (C^7/C^{10}), 27.7 (C^4), 21.7 (C^{11}/C^{16}), 20.8 (C^{11}/C^{16}). **HRMS** (ESI-TOF) m/z: $[M + H]^+$ Calcd for $C_{15}H_{23}N_2O_5$ 311.1601; Found 311.1607.

In addition, starting urea **362** was recovered in a yield of 7% (5 mg, 0.03 mmol).

1-((3a*RS*,7*SR*,7a*RS*)-4,7-Dimethyl-1,3-dioxo-1,3,3a,6,7,7a-hexahydroisobenzofuran-5-yl)-1,3-dimethylurea (533)

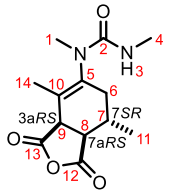

An oven-dried microwave vial containing a magnetic stir bar was sealed with a suba seal and placed under anhydrous N_2. The flask was charged with **362** (67 mg, 0.40 mmol, 1.0 equiv.) and anhydrous toluene (0.67 mL, 1.7 mL/mmol), to which maleic anhydride (47 mg, 0.48 mmol, 1.2 equiv.) was added. The microwave vial was capped, and the reaction mixture was first stirred for 2h45 at room temperature, followed by 18h45 at 50 °C. After stirring the reaction another 9 h at 80 °C, no significant further conversion was observed by TLC. The reaction was cooled down and concentrated *in vacuo*. By ^{1}H NMR using 1,2,4-trimethoxybenzene as an internal standard a crude NMR yield of 57% was determined for **533**. Flash column chromatography (10−80% acetone/pentane) turned out to decompose the compound. When the compound was dissolved in a small amount of CH_2Cl_2 and Et_2O, trituration with petroleum ether gave **533** as a white solid (46 mg, 0.17 mmol, 43% yield). **MP** 86–87 °C. **IR** (film) ν_{max}

3435, 3347, 2936, 1777, 1639, 1527, 1204, 919 761 cm^{-1}. **^{1}H NMR** (400 MHz, $CDCl_3$; major *exo*-product/major rotamer) δ 4.46 – 4.21 (m, 1H, H^3), 3.66 (d, *J* = 8.6 Hz, 1H, H^9), 3.36 (dd, *J* = 8.6, 5.2 Hz, 1H, H^8), 2.89 (s, 3H, H^1), 2.73 (d, *J* = 4.6 Hz, 3H, H^4), 2.30 – 2.20 (m, 2H, H^6 + H^7), 2.07 – 1.95 (m, 1H, H^6), 1.85 (s, 3H, H^{14}), 1.27 (d, *J* = 6.8 Hz, 3H, H^{11}). **^{13}C NMR** (101 MHz, $CDCl_3$; major *exo*-product/major rotamer) δ 170.9 (C^{13}), 169.6 (C^{12}), 156.7 (C^2), 137.6 (C^5), 125.0 (C^{10}), 47.0 (C^9), 45.0 (C^8), 33.5 (C^1), 31.8 (C^6), 29.0 (C^7), 27.7 (C^4), 16.8 (C^{11}), 15.7 (C^{14}). **HRMS** (ESI-TOF) m/z: $[M + H]^+$ Calcd for $C_{13}H_{19}N_2O_4$ 267.1339; Found 267.1346.

In addition, starting urea **362** was recovered in a yield of 6% (4 mg, 0.02 mmol).

1-(Hexan-3-yl)-1,3-dimethylurea (535)

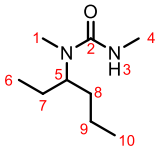

An oven-dried flask containing a magnetic stir bar was sealed with a suba seal and placed under anhydrous N_2. The flask was charged with **362** (67 mg, 0.40 mmol, 1.0 equiv.) and anhydrous MeOH (4.0 mL, 10 mL/mmol), to which then palladium on carbon (10 wt.%; 43 mg, 0.040 mmol, 10 mol%) was added. The nitrogen was exhausted by H_2, and the reaction mixture was stirred under H_2 (1 atm) for 5 h at room temperature. The reaction mixture was filtered through celite, washed with MeOH, and concentrated *in vacuo*. By ^{1}H NMR using 1,2,4-trimethoxybenzene as an internal standard a crude NMR yield of 71% was determined for **535**. Flash column chromatography (2−15% acetone/CH_2Cl_2) gave **535** as a pale-yellow oil (46 mg, 0.27 mmol, 67% yield), **IR** (film) ν_{max} 3343, 2959, 1625, 1532, 1331, 1193, 1101, 769 cm^{-1}. **^{1}H NMR** (400 MHz, $CDCl_3$) δ 4.30 (bs, 1H, H^3), 4.10 (bs, 1H, H^5), 2.81 (d, *J* = 4.7 Hz, 3H, H^4), 2.62 (s, 3H, H^1), 1.47 – 1.31 (m, 4H, H^7 + H^8), 1.30 – 1.20 (m, 2H, H^9), 0.89 (t, *J* = 7.2 Hz, 3H, H^{10}), 0.83 (t, *J* = 7.4 Hz, 3H, H^6). **^{13}C NMR** (101 MHz, $CDCl_3$) δ 159.7 (C^2), 55.5 (C^5), 35.2 (C^8), 27.8 (C^4), 27.0 (C^1), 26.0 (C^7), 19.8 (C^9), 14.2 (C^{10}), 11.1 (C^6). **HRMS** (ESI-TOF) m/z: $[M + H]^+$ Calcd for $C_9H_{21}N_2O$ 173.1648; Found 173.1650.

***N*-Methylhexan-3-amine hydrochloride salt (536)**

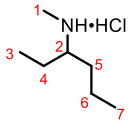

A microwave vial containing a magnetic stir bar was charged with **535** (38 mg, 0.22 mmol, 1.0 equiv.) and EtOH (1.11 mL, 5.05 mL/mmol), to which an aqueous solution of NaOH (2.00 M; 1.11 mL, 2.22

mmol, 10.0 equiv.) was added. The microwave vial was capped, and the reaction mixture was stirred for 4 h at 150 °C in the microwave. The reaction was cooled down to room temperature; then, while vigorously stirring, an excess of HCl (1.25 M in MeOH; 12.0 mL) was added rapidly, and after 5 min the reaction mixture was concentrated *in vacuo*. Filtration from acetone followed by MeOH removed insoluble white solids and gave **536** as an orange oil (32 mg, 0.21 mmol, 96% yield). **IR** (film) ν_{max} 3392, 2962, 2728, 1464, 748 cm^{-1}. **^{1}H NMR** (400 MHz, $MeOD_4$) δ 3.08 (p, *J* = 6.2 Hz, 1H, H^2), 2.68 (s, 3H, H^1), 1.79 – 1.70 (m, 2H, H^4), 1.69 – 1.61 (m, 2H, H^5), 1.49 – 1.35 (m, 2H, H^6), 1.03 – 0.97 (m, 6H, H^3 + H^7). **^{13}C NMR** (101 MHz, $MeOD_4$) δ 61.5 (C^2), 32.5 (C^5), 30.9 (C^1), 23.5 (C^4), 19.2 (C^6), 14.2 (C^7), 9.3 (C^3). **HRMS** (ESI-TOF) m/z: $[M + H]^+$ Calcd for $C_7H_{18}N$ 116.1434; Found 116.1431.

(*E*)-Hex-4-en-3-one (537)

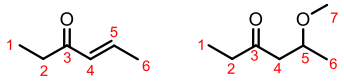

537 **538**

A microwave vial containing a magnetic stir bar was charged with **362** (63 mg, 0.38 mmol, 1.0 equiv.) and MeOH (0.19 mL, 0.50 mL/mmol), to which an aqueous solution of HCl (1.00 M; 1.69 mL, 1.69 mmol, 4.45 equiv.) was added. The microwave vial was capped, and the reaction mixture was stirred for 3 h at 50 °C. The reaction was cooled down to room temperature and then Et_2O was added to extract the reaction mixture. After extracting the organic phase, the aqueous phase was washed with Et_2O (3×). The organic phases were collected, and cautiously concentrated *in vacuo* at room temperature. Flash column chromatography (2−18% *i*-PrOH/petroleum ether) gave **537** (1 mg, 0.01 mmol, 3% yield) mixed with 5-methoxyhexan-3-one **538** (3 mg, 0.02 mmol, 6% yield) in a ratio of 0.6:1 as a pale-yellow oil. **^{1}H NMR** (400 MHz, $CDCl_3$) δ 6.84 (dq, *J* = 15.8, 6.8 Hz, 0.6H, $\underline{H^5}$), 6.12 (dq, *J* = 15.8, 1.7 Hz, 0.6H, $\underline{H^4}$), 3.83 – 3.76 (m, 1H, H^5), 3.29 (s, 3H, H^7), 2.69 (dd, *J* = 15.7, 7.3 Hz, 1H, H^4), 2.54 (q, *J* = 7.3 Hz, 1.2H, $\underline{H^2}$), 2.45 (qd, *J* = 7.3, 1.8 Hz, 2H, H^2), 2.38 (dd, *J* = 15.7, 5.4 Hz, 1H, H^4), 1.88 (dd, *J* = 6.8, 1.7 Hz, 1.8H, $\underline{H^6}$), 1.16 (d, *J* = 6.2 Hz, 3H, H^6), 1.08 (t, *J* = 7.3 Hz, 1.8H, $\underline{H^1}$), 1.04 (t, *J* = 7.3 Hz, 3H, H^1). **^{13}C NMR** (101 MHz, $CDCl_3$) δ 210.1 (C^3), 142.3 ($\underline{C^5}$), 131.8 ($\underline{C^4}$), 73.4 (C^5), 56.4 (C^7), 49.4 (C^4), 37.2 (C^2), 33.2 ($\underline{C^2}$), 19.4 (C^6), 18.3 ($\underline{C^6}$), 8.3 ($\underline{C^1}$), 7.7 (C^1). Spectral data are in agreement with literature.[224,225]

1-Allyl-3-((2*Z*,4*E*)-hexa-2,4-dien-3-yl)-1,3-dimethylurea (539)

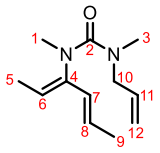

An oven-dried flask containing a magnetic stir bar was sealed with a suba seal and placed under anhydrous N_2. The flask was charged with **362** (64 mg, 0.38 mmol, 1.0 equiv.) and anhydrous DMF (0.63 mL, 1.7 mL/mmol), to which then sodium hydride (30 mg, 0.75 mmol, 2.0 equiv.) was added at 0 °C. After stirring the reaction mixture for 5 min at 0 °C, allyl bromide (130 µL, 1.52 mmol, 4.00 equiv.) was added and the reaction mixture was then stirred for 2 h at room temperature. The reaction was quenched with a saturated aqueous solution of NH_4Cl, and after extracting the organic phase, the aqueous phase was washed with EtOAc (3×). The organic phases were collected, dried over $MgSO_4$, filtered, and concentrated *in vacuo*. Flash column chromatography (0−30% acetone/petroleum ether) gave **539** as a yellow oil (52 mg, 0.25 mmol, 66% yield). **IR** (film) ν_{max} 3478, 2914, 1635, 1480, 1416, 1381, 1299, 1277, 1089, 966, 920, 793 cm^{-1}. **^{1}H NMR** (400 MHz, $CDCl_3$) δ 5.83 (dq, *J* = 15.4, 1.6 Hz, 1H, H^7), 5.77 – 5.61 (m, 2H, H^8 + H^{11}), 5.30 (q, *J* = 7.1 Hz, 1H, H^6), 5.14 – 5.05 (m, 2H, H^{12}), 3.74 (d, *J* = 6.3 Hz, 2H, H^{10}), 2.87 (s, 3H, H^1), 2.64 (s, 3H, H^3), 1.77 – 1.72 (m, 3H, H^9), 1.55 (d, *J* = 7.1 Hz, 3H, H^5). **^{13}C NMR** (101 MHz, $CDCl_3$) δ 162.3 (C^2), 142.6 (C^4), 134.5 (C^{11}), 129.3 (C^7), 125.0 (C^8), 122.2 (C^6), 117.0 (C^{12}), 52.9 (C^{10}), 36.8 (C^1), 35.1 (C^3), 17.9 (C^9), 12.8 (C^5). **HRMS** (ESI-TOF) m/z: $[M + H]^+$ Calcd for $C_{12}H_{21}N_2O$ 209.1648; Found 209.1649.

4-Ethyl-5-ethylidene-1,3-dimethyl-4-((*E*)-prop-1-en-1-yl)imidazolidin-2-one (543)

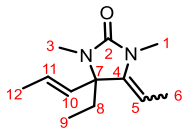

Reaction performed on 0.24 mmol scale following general procedure **3C** using **539** (50 mg, 0.24 mmol, 1.0 equiv.) in anhydrous THF (2.4 mL), 18-crown-6 (140 mg, 0.530 mmol, 2.21 equiv.) and KHMDS (1.0 M in THF; 0.48 mL, 0.48 mmol, 2.0 equiv.), which was stirred for 46 h at −78 °C to room temperature. Flash column chromatography (1−14% acetone/petroleum ether) gave **543** as a yellow oil (5 mg, 0.02 mmol, 10% yield). **IR** (film) ν_{max} 2923, 1717, 1673, 1439, 1378, 1079, 772 cm^{-1}. **^{1}H NMR** (400 MHz, $CDCl_3$) δ 5.69 (dq, *J* = 15.7, 6.5 Hz, 1H, H^{11}), 5.44 (dq, *J* = 15.7, 1.6 Hz, 1H, H^{10}), 4.41 (q, *J* = 7.2 Hz, 1H, H^5), 2.85 (s, 3H, H^1), 2.64 (s, 3H, H^3), 1.96 – 1.76 (m, 2H, H^8), 1.74 (dd, *J* = 6.5, 1.6 Hz, 3H, H^{12}), 1.62 (d, *J* = 7.2 Hz, 3H, H^6), 0.72 (t, *J* = 7.3 Hz, 3H, H^9). **^{13}C NMR** (101 MHz, $CDCl_3$) δ 157.5 (C^2), 141.4 (C^4), 131.0 (C^{10}), 127.4 (C^{11}), 91.2 (C^5), 65.9 (C^7), 26.7 (C^1), 24.9 (C^8), 24.2 (C^3),

17.9 (C^{12}), 11.3 (C^{6}), 7.4 (C^{9}). **HRMS** (ESI-TOF) m/z: $[M + H]^+$ Calcd for $C_{12}H_{21}N_2O$ 209.1648; Found 209.1650.

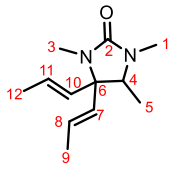

In addition, 1,3,5-trimethyl-4,4-di((*E*)-prop-1-en-1-yl)imidazolidine-2-one **544** was afforded as a yellow oil (17 mg, 0.082 mmol, 34% yield). **IR** (film) ν_{max} 2919, 1688, 1436, 1390, 975, 922, 765, 728 cm^{-1}. **^{1}H NMR** (400 MHz, $CDCl_3$) δ 5.66 (dq, *J* = 15.7, 6.4 Hz, 1H, H^8/H^{11}), 5.56 – 5.38 (m, 2H, H^7/H^{10} + H^8/H^{11}), 5.27 (dq, *J* = 15.7, 1.6 Hz, 1H, H^7/H^{10}), 3.13 (q, *J* = 6.6 Hz, 1H, H^4), 2.68 (s, 3H, H^1), 2.59 (s, 3H, H^3), 1.75 (dd, *J* = 6.4, 2.8, 1.6 Hz, 6H, H^9 + H^{12}), 1.04 (d, *J* = 6.6 Hz, 3H, H^5). **^{13}C NMR** (101 MHz, $CDCl_3$) δ 161.8 (C^2), 131.4 (C^7/C^{10}), 129.0 (C^8/C^{11}), 128.7 (C^8/C^{11}), 126.8 (C^7/C^{10}), 66.4 (C^6), 63.6 (C^4), 29.2 (C^1), 27.0 (C^3), 18.2 (C^9/C^{12}), 18.0 (C^9/C^{12}), 13.4 (C^5). **HRMS** (ESI-TOF) m/z: $[M + H]_+$ Calcd for $C_{12}H_{21}N_2O$ 209.1648; Found 209.1652.

The rest of the recovered material (in total 11 mg) was unidentifiable.

5.3.3 Mechanistic Studies

5.3.3.1 Product Characterisation

1,3-Dimethyl-1,3-di((*Z*)-prop-1-en-1-yl)urea (364)

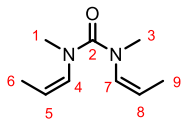

Reaction performed on 5.08 mmol scale following general procedure **3C** using **206** (855 mg, 5.08 mmol, 1.00 equiv.) in anhydrous THF (50 mL), 18-crown-6 (2.91 g, 11.0 mmol, 2.17 equiv.) and KHMDS (0.91 M in THF; 11 mL, 10 mmol, 2.0 equiv.), which was stirred for 1 h at −78 °C and then gradually warmed up to −20 °C over 2 h. Flash column chromatography (2−22% acetone/petroleum ether) gave **364** as pale-yellow liquid (783 mg, 4.65 mmol, 92% yield). **IR** (film) ν_{max} 2944, 1639, 1440, 1346, 1301, 1106, 1023, 771, 735, 724, 470 cm^{-1}. **^{1}H NMR** (400 MHz, $CDCl_3$) δ 5.86 (dq, *J* = 8.1, 1.7 Hz, 2H, H^4 + H^7), 4.98 (dq, *J* = 8.1, 7.0 Hz, 2H, H^5 + H^8), 2.99 (s, 6H, H^1 + H^3), 1.56 (dd, *J* = 7.0, 1.7 Hz, 6H, H^6 + H^9). **^{13}C NMR** (101 MHz, $CDCl_3$) δ 161.1 (C^2), 132.4 (C^4 + C^7), 115.9 (C^5 + C^8), 37.0 (C^1 + C^3), 12.5 (C^6 + C^9). **HRMS** (ESI-TOF) m/z: $[M + H]^+$ Calcd for $C_9H_{17}N_2O$ 169.1335; Found 169.1332.

In addition, 1-((2*Z*,4*E*)-hexa-2,4-dien-3-yl)-1,3-dimethylurea **362** was afforded as a pale-yellow oil (70 mg, 0.42 mmol, 8%).

(*E*)-*N*-Methyl-2,5-dioxo-*N*-(prop-1-en-1-yl)pyrrolidine-1-carboxamide (555)

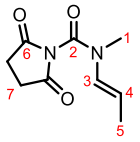

The starting reagent *N*-allyl-*N*-methyl-2,5-dioxopyrrolidine-1-carboxamide was prepared as followed: an oven-dried round-bottom flask containing a magnetic stir bar was sealed with a suba seal and placed under anhydrous N_2. The flask was charged with anhydrous MeCN (10 mL, 10 mL/mmol), *N*-methylallylamine (0.10 mL, 1.0 mmol, 1.0 equiv.) and anhydrous pyridine (0.15 mL, 1.8 mmol, 1.8 equiv.). *N*,*N*'-Disuccinimidyl carbonate (384 mg, 1.50 mmol, 1.50 equiv.) was added and the reaction mixture was stirred at room temperature for 5 h. The reaction mixture was concentrated *in vacuo* and *N*-allyl-*N*-methyl-2,5-dioxopyrrolidine-1-carboxamide was used as crude in the next step.

Reaction performed on 1.32 mmol scale following general procedure **2B** using *N*-allyl-*N*-methyl-2,5-dioxopyrrolidine-1-carboxamide (280 mg, 1.32 mmol, 1.00 equiv.) and $[Ph_3P]_3Ru(CO)(Cl)H$ (126 mg, 0.132 mmol, 10 mol%) in anhydrous THF (13.2 mL), which was stirred for 18 h at reflux. Flash column chromatography (20–100% EtOAc/petroleum ether) gave **555** as a white solid (238 mg, 1.12 mmol, 85% yield). **^{1}H NMR** (400 MHz, $CDCl_3$) (mixture of rotamers with a 1:0.8 ratio) δ 6.84 (d, *J* = 14.0 Hz, 1H, major rot. H^3), 6.70 (d, *J* = 14.3 Hz, 0.8H, minor rot. H^3), 5.16 – 5.03 (m, 1.8H, H^4), 3.13 (s, 2.4H, minor rot. H^1), 3.07 (s, 3H, major rot. H^1), 2.77 (s, 7.2H, H^7), 1.65 (d, *J* = 6.7 Hz, 5.4H, H^5). **^{13}C NMR** (101 MHz, $CDCl_3$) δ 169.6 (C^6), 149.7 (minor rot. C^2), 149.3 (major rot. C^2), 128.3 (minor rot. C^3), 126.9 (major rot. C^3), 108.8 (major rot. C^4), 108.4 (minor rot. C^4), 33.1 (major rot. C^1), 31.7 (minor rot. C^1), 25.6 (C^7), 15.3 (major rot. C^5), 15.2 (minor rot. C^5). **HRMS** (APCI) m/z: $[M + H]^+$ Calcd for $C_9H_{13}N_2O_4$ 213.0870; Found 213.0873.

(*E*)-*N*^{1}-Allyl-*N*^{1}-methyl-*N*^{4}-((methyl(prop-1-en-1-yl)carbamoyl)oxa)succinamide (556)

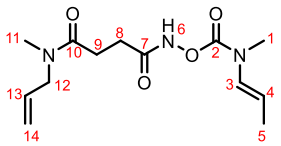

An oven-dried round-bottom flask containing a magnetic stir bar was sealed with a suba seal and placed under anhydrous N_2. The flask was charged with **555** (229 mg, 1.08 mmol, 1.00 equiv.) and anhydrous MeCN (15.4 mL, 14.3 mL/mmol). *N*-Methylallylamine (130 μL, 1.35 mmol, 1.25 equiv.) and triethylamine (380 μL, 2.73 mmol, 2.53 equiv.) were added, and the reaction mixture was stirred for 19 h at room temperature. A saturated aqueous solution of $NaHCO_3$ (15.4 mL, 14.3 mL/mmol) was added, and the organic phase was extracted. The aqueous phase was extracted with CH_2Cl_2 (3×), and the organic phases were collected, dried over $MgSO_4$, filtered, and concentrated *in vacuo*. Flash column chromatography (0.5–4% MeOH/CH_2Cl_2) gave **556** as an orange oil (153 mg, 0.540 mmol, 50% yield). **^{1}H NMR** (400 MHz, $CDCl_3$; suspected mixture of rotamers with a 1:0.8 ratio) δ 9.96 (s, 1H, H^6), 6.85 (d, *J* = 14.1 Hz, 1H, H^3), 5.83 – 5.65 (m, 1H, H^{13}), 5.26 – 5.09 (m, 2H, H^{14}), 5.02 – 4.90 (m, 1H, H^4), 4.02 – 3.89 (m, 2H, H^{12}), 3.08 (bs, 3H, H^1), 2.95 (s, 1.7H, major rot. H^{11}), 2.94 (m, 3H, minor rot. 1.3H, H^{11}), 2.75 – 2.66 (m, 2H, H^8/H^9), 2.66 – 2.56 (m, 2H, H^8/H^9), 1.69 (d, *J* = 6.6 Hz, 3H, H^5). **^{13}C NMR** (101 MHz, $CDCl_3$) δ 172.2 (major rot. C^7 + C^{10}), 171.8 (minor rot. C^7 + C^{10}), 132.8 (major rot. C^{13}), 132.0 (minor rot. C^{13}), 128.7 (minor rot. C^3), 127.6 (major rot. C^3), 117.6 (C^{14}), 117.1 (C^{14}), 106.5 (minor rot. C^4), 106.4 (major rot. C^4), 52.2 (C^{12}), 50.5 (C^{12}), 34.7 (major rot. C^{11}), 34.1 (minor rot. C^{11}), 32.2 (broad, C^1), 28.7 (C^8 + C^9), 15.3 (C^5). Full characterisation data was not obtained as the compound had decomposed in $CDCl_3$.

In addition, a mixture of starting material **555** (40 mg, 0.20 mmol, 19% yield) and desired product **554** (30 mg, 0.18 mmol, 17% yield) was afforded.

Phenyl (*E*)-methyl(prop-1-en-1-yl)carbamate (557)

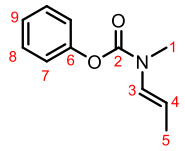

The starting reagent phenyl allyl(methyl)carbamate was prepared as followed: an oven-dried round-bottom flask containing a magnetic stir bar was sealed with a suba seal and placed under anhydrous N_2. The flask was charged with anhydrous CH_2Cl_2 (5.6 mL, 5.6 mL/mmol) and *N*-methylallylamine (100 µL, 1.04 mmol, 1.00 equiv.). At 0 °C, triethylamine (200 µL, 1.43 mmol, 1.38 equiv.). was added, followed by the dropwise addition of phenyl chloroformate (140 µL, 1.12 mmol, 1.08 equiv.), and the reaction mixture was stirred at room temperature for 1.5 h. A saturated aqueous solution of $NaHCO_3$ was added, and the organic phase was extracted. The aqueous phase was extracted with CH_2Cl_2 (3×), and the organic phases were collected, dried over $MgSO_4$, filtered, and concentrated *in vacuo*. Flash column chromatography (5–40% EtOAc/petroleum ether) gave phenyl allyl(methyl)carbamate, which was immediately used in the next step.

Reaction performed on 1.04 mmol scale following general procedure **2B** using phenyl allyl(methyl)carbamate (1.04 mmol, 1.00 equiv.) and $[Ph_3P]_3Ru(CO)(Cl)H$ (95 mg, 0.10 mmol, 10 mol%) in anhydrous THF (10 mL), which was stirred for 16.5 h at reflux. Flash column chromatography (5–40% EtOAc/petroleum ether) gave **557** as a pale-yellow oil (191 mg, 0.999 mmol, 96% yield). **IR** (film) ν_{max} 3378, 1645, 1568, 1408, 1220, 772 cm^{-1}. **^{1}H NMR** (400 MHz, $CDCl_3$; suspected mixture of rotamers with a 1:0.8 ratio) δ 7.38 (t, *J* = 7.8 Hz, 2H, H^8), 7.22 (t, *J* = 7.4 Hz, 1H, H^9), 7.13 (d, *J* = 7.8 Hz, 2H, H^7), 7.07 (d, *J* = 14.4 Hz, 0.6H, major rot. H^3), 7.02 (d, *J* = 14.4 Hz, 0.4H, minor rot. H^3), 5.07 – 4.92 (m, 1H, H^4), 3.22 (s, 1.2H, minor rot. H^1), 3.15 (s, 1.8H, major rot. H^1), 1.76 (d, *J* = 6.1 Hz, 3H, H^5). **^{13}C NMR** (101 MHz, $CDCl_3$) δ 152.5 (minor rot. C^2), 151.4 (major rot. C^2), 151.2 (C^6), 129.5 (C^8), 129.0 (minor rot. C^3), 128.4 (major rot. C^3), 125.7 (C^9), 121.8 (major rot. C^7), 121.8 (minor rot. C^7), 105.5 (minor rot. C^4), 105.4 (major rot. C^4), 31.7 (minor rot. C^1), 31.6 (major rot. C^1), 15.4 (major rot. C^5), 15.4 (minor rot. C^5). Mass not found by HRMS.

4-Nitrophenyl (*E*)-1-allyl(methyl)carbamate (558)

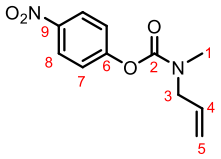

An oven-dried flask containing a magnetic stir bar was sealed with a suba seal and placed under anhydrous N_2. The flask was charged with anhydrous CH_2Cl_2 (167 mL, 5.56 mL/mmol), *N*-allyl methylamine (2.88 mL, 30.0 mmol, 1.00 equiv.) and triethylamine (5.85 mL, 42.0 mmol, 1.40 equiv.), and the reaction mixture was cooled to 0 °C. 4-Nitrophenyl chloroformate (6.65 g, 33.0 mmol, 1.10 equiv.) was added portion wise and the reaction mixture was warmed to room temperature and stirred for 3.5 h. A saturated aqueous solution of $NaHCO_3$ was added, and the organic phase was extracted. The aqueous phase was washed with CH_2Cl_2 (3×) and then the organic phases were combined, dried over $MgSO_4$, filtered, and concentrated *in vacuo*. Purification by flash column chromatography (2−10% acetone/petroleum ether) gave **558** as a pale-yellow oil (6.96 g, 29.5 mmol, 98% yield). **IR** (film) ν_{max} 3084, 2932, 1720, 1519, 1396, 1343, 1204, 1148, 1011, 864, 748, 494 cm^{-1}. **^{1}H NMR** (400 MHz, $CDCl_3$; suspected mixture of rotamers A and B with a 1:1 ratio) δ 8.24 (d, *J* = 8.8 Hz, 2H, H^8/H^7), 7.34 – 7.27 (m, 2H, H^7/H^8), 5.94 – 5.76 (m, 1H, H^4), 5.30 – 5.21 (m, 2H, H^5), 4.04 (d, *J* = 5.5 Hz, 1H, rot. B H^3), 3.98 (d, *J* = 6.0 Hz, 1H, rot. A H^3), 3.07 (s, 1.5H, rot. A H^1), 3.01 (s, 1.5H, rot. B H^1). **^{13}C NMR** (101 MHz, $CDCl_3$; suspected mixture of rotamers A and B with a 1:1 ratio) δ 156.5 (C^6), 153.4 (rot. A C^2), 153.4 (rot. B C^2), 144.9 (C^9), 132.6 (rot. B C^4), 132.4 (rot. A C^4), 125.2 (C^8/C^7), 122.4 (C^7/C^8), 118.3 (rot. A C^5), 117.4 (rot. B C^5), 52.1 (rot. A C^3), 52.0 (rot. B C^3), 34.9 (rot. B C^1), 34.2 (rot. A C^1). **HRMS** (ESI-TOF) m/z: $[M + H]^+$ Calcd for $C_{11}H_{13}N_2O_4$ 237.0875; Found 237.0878.

4-Nitrophenyl (*E*)-methyl(prop-1-en-1-yl)carbamate (559)

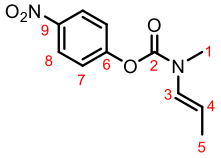

Reaction performed on 5.01 mmol scale following general procedure **2B** using **558** (1.18 g, 5.01 mmol, 1.00 equiv.) in anhydrous THF (50 mL) and carbonylchlorohydridotris(triphenylphosphine)ruthenium(II) (476 mg, 0.500 mmol, 10 mol%), which was stirred for 3.5 h at reflux. Flash column chromatography (2−12% EtOAc/petroleum ether) gave **559** as a pale-yellow solid (1.11 g, 4.68 mmol, 93% yield). **MP** 87−88 °C. **IR** (film) ν_{max} 3384, 2922, 1722, 1666, 1520, 1344, 1329, 1210, 1129, 940, 865, 751, 715 cm^{-1}. **^{1}H NMR** (400 MHz, $CDCl_3$; suspected mixture of rotamers with a 1:1.5 ratio) δ 8.28 – 8.24 (m, 2H, H^8/H^7), 7.35 – 7.30 (m, 2H,

H^7/H^8), 6.98 (ddq, *J* = 14.4, 12.8, 1.6 Hz, 1H, H^3), 5.14 – 5.00 (m, 1H, H^4), 3.23 (s, 1.2H, minor rot. H^1), 3.16 (s, 1.8H, major rot. H^1), 1.76 (dd, *J* = 6.8, 1.6 Hz, 3H, H^5). **^{13}C NMR** (101 MHz, $CDCl_3$; suspected mixture of rotamers with a 1:1.5 ratio) δ 156.1 (major rot. C^6), 156.0 (minor rot. C^6), 151.6 (minor rot. C^2), 151.2 (major rot. C^2), 145.2 (C^9), 128.4 (minor rot. C^3), 127.8 (major rot. C^3), 125.3 (C^8/C^7), 122.5 (major rot. C^7/C^8), 122.4 (minor rot. C^7/C^8), 107.1 (minor rot. C^4), 107.0 (major rot. C^4), 31.9 (major rot. C^1), 31.9 (minor rot. C^1), 15.4 (major rot. C^5), 15.4 (minor rot. C^5). **HRMS** (APCI) m/z: $[M + H]^+$ Calcd for $C_{11}H_{13}N_2O_4$ 237.0870; Found 237.0868.

(*E*)-1-Allyl-1,3-dimethyl-3-(prop-1-en-1-yl) (554)

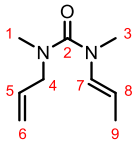

An oven-dried microwave vial containing a magnetic stir bar was sealed with a suba seal and placed under anhydrous N_2. The flask was charged with **559** (508 mg, 2.15 mmol, 1.00 equiv.), anhydrous DMF (7.5 mL, 2.5 mL/mmol), *N*-allylmethylamine (0.35 mL, 3.6 mmol, 1.7 equiv.) and K_2CO_3 (1.33 g, 9.62 mmol, 4.48 equiv.), and the reaction mixture was stirred in the microwave at 130 °C for 3.5 h. H_2O was added and the reaction mixture was extracted with CH_2Cl_2, after which the aqueous phase was washed with CH_2Cl_2 (2×). The combined organic phases were dried over $MgSO_4$, filtered, and concentrated *in vacuo*. Flash column chromatography with neutralised silica (0−4% EtOAc/petroleum ether) gave **554** as a pale-yellow liquid (337 mg, 2.00 mmol, 93% yield). **IR** (film) ν_{max} 3495, 2922, 1644, 1483, 1455, 1389, 1371, 1290, 1262, 1112, 1088, 947, 771 cm^{-1}. **^{1}H NMR** (400 MHz, toluene-d_8) δ 6.53 (dq, *J* = 14.1, 1.5 Hz, 1H, H^7), 5.63 (ddt, *J* = 17.8, 9.7, 5.7 Hz, 1H, H^5), 4.99 – 4.97 (m, 2H, H^6), 4.47 (dq, *J* = 14.1, 6.5 Hz, 1H, H^8), 3.47 (dt, *J* = 5.7, 1.5 Hz, 2H, H^4), 2.78 (s, 3H, H^3), 2.51 (s, 3H, H^1), 1.57 (dd, *J* = 6.5, 1.5 Hz, 3H, H^9). **^{13}C NMR** (101 MHz, toluene-d_8) δ 161.6 (C^2), 134.6 (C^5), 132.9 (C^7), 116.8 (C^6), 100.6 (C^8), 53.7 (C^4), 35.8 (C^1), 33.2 (C^3), 15.4 (C^9). **HRMS** (ESI-TOF) m/z: $[M + H]^+$ Calcd for $C_9H_{17}N_2O$ 169.1335; Found 169.1337.

1,3-Dimethyl-3-(((*E*)-1-(hexaprop-1-en-1-yl)-1-((*Z*)-prop-1-en-1-yl)urea (560)

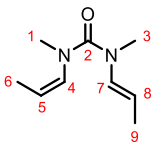

Reaction performed on 0.80 mmol scale following general procedure **3C** using **554** (135 mg, 0.802 mmol, 1.00 equiv.) in anhydrous THF (8 mL), 18-crown-6 (465 mg, 1.76 mmol, 2.20 equiv.) and

KHMDS (1.00 M in THF; 1.60 mL, 1.60 mmol, 2.00 equiv.), which was stirred for 2 h at −78 °C. Flash column chromatography with neutralised silica (0−5% acetone/petroleum ether) gave **560** as a yellow oil (119 mg, 0.707 mmol, 88% yield). **IR** (film) ν_{max} 3458, 2920, 1642, 1478, 1435, 1357, 1112, 943, 767, 745 cm^{-1}. **^{1}H NMR** (400 MHz, toluene-d_8) δ 6.75 (dq, J = 14.1, 1.6 Hz, 1H, H^{7}), 5.60 (dq, J = 8.1, 1.7 Hz, 1H, H^{4}), 4.70 (dq, J = 8.1, 7.1 Hz, 1H, H^{5}), 4.47 (dq, J = 14.1, 6.5 Hz, 1H, H^{8}), 2.81 (s, 3H, H^{1}), 2.73 (s, 3H, H^{3}), 1.57 (dd, J = 6.5, 1.6 Hz, 3H, H^{9}), 1.31 (dd, J = 7.1, 1.7 Hz, 3H, H^{6}). **^{13}C NMR** (101 MHz, toluene-d_8) δ 159.4 (C^{2}), 132.9 (C^{4}), 132.3 (C^{7}), 115.0 (C^{5}), 100.6 (C^{8}), 36.8 (C^{1}), 33.2 (C^{3}), 15.4 (C^{9}), 12.0 (C^{6}). **HRMS** (ESI-TOF) m/z: [M + H]$^{+}$ Calcd for $C_9H_{17}N_2O$ 169.1335; Found 169.1338.

(*E*)-1-(Hexa-1,4-dien-3-yl)-1,3-dimethylurea (352)

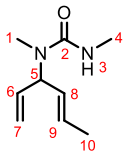

Reaction performed on 0.40 mmol scale following general procedure **3B** using **554** (68 mg, 0.40 mmol, 1.0 equiv.) in anhydrous THF (1.87 mL, total of 10.0 mL/mmol) and LDA (freshly prepared following general procedure **3A**; 2.13 mL, 0.808 mmol, 2.02 equiv.), which was stirred for 2.5 h at −78 °C. Flash column chromatography with neutralised silica (7−40% acetone/petroleum ether) gave **352** as a yellow oil (29 mg, 0.17 mmol, 43% yield). **IR** (film) ν_{max} 3340, 2938, 1623, 1532, 1482, 1411, 1371, 1304, 971, 925 cm^{-1}. **^{1}H NMR** (400 MHz, $CDCl_3$) δ 5.82 (ddd, J = 17.4, 10.5, 4.9 Hz, 1H, H^{6}), 5.62 (dqd, J = 15.4, 6.4, 1.4 Hz, 1H, H^{9}), 5.46 (ddq, J = 15.4, 5.9, 1.4 Hz, 1H, H^{8}), 5.28 – 5.19 (m, 1H, H^{5}), 5.23 – 5.09 (m, 2H, H^{7}), 4.40 (bs, 1H, H^{3}), 2.81 (d, J = 4.4 Hz, 3H, H^{4}), 2.71 (s, 3H, H^{1}), 1.71 (dt, J = 6.4, 1.4 Hz, 3H, H^{10}). **^{13}C NMR** (101 MHz, $CDCl_3$) δ 159.0 (C^{2}), 136.8 (C^{6}), 128.9 (C^{9}), 128.3 (C^{8}), 116.7 (C^{7}), 58.4 (C^{5}), 30.1 (C^{1}), 27.8 (C^{4}), 18.0 (C^{10}). **HRMS** (ESI-TOF) m/z: [M + H]$^{+}$ Calcd for $C_9H_{17}N_2O$ 169.1335; Found 169.1337.

In addition, 1-((2*Z*,4*E*)-hexa-2,4-dien-3-yl)-1,3-dimethylurea **362** was afforded as a yellow oil (13 mg, 0.077 mmol, 19% yield).

4-Nitrophenyl (*E*)-methyl(prop-1-en-1-yl-1,2,3,3-*d*$_4$)carbamate (559-D)

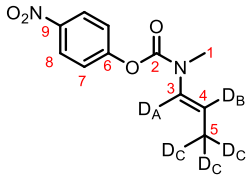

An oven-dried flask containing a magnetic stir bar was sealed with a suba seal and placed under anhydrous N_2. The flask was charged with **558** (923 mg, 3.91 mmol, 1.00 equiv.), anhydrous 1,4-dioxane (7.8 mL, 2.0 mL/mmol), carbonylchlorohydridotris(triphenylphosphine)ruthenium(II) (372 mg, 0.391 mmol, 10 mol%) and D_2O (0.96 mL, 53 mmol, 14 equiv.), and the reaction mixture was refluxed at 100 °C for 24 h. Note: the reaction had fallen dry overnight. The reaction mixture was extracted with Et_2O, and the aqueous phase was washed with Et_2O (2×). The combined organic phases were dried over $MgSO_4$, filtered, and concentrated *in vacuo*. Purification by flash column chromatography with neutralised silica (4−40% EtOAc/petroleum ether) gave **559-D** as a pale-yellow solid (763 mg, 3.16 mmol, 81% yield; deuterium incorporation: D_A = 64%, D_B = 62%, D_C = 64%). **^{1}H NMR** (400 MHz, $CDCl_3$; suspected mixture of rotamers with a 1:1.5 ratio) δ 8.28 – 8.23 (m, 2H, H^8/H^7), 7.36 – 7.28 (m, 2H, H^7/H^8), 7.02 – 6.93 (m, 0.36H, H^3), 5.12 – 4.99 (m, 0.34H, H^4), 3.23 (s, 1.2H, minor rot. H^1), 3.16 (s, 1.8H, major rot. H^1), 1.79 – 1.68 (m, 1.07H, H^5). **^{13}C NMR** (101 MHz, $CDCl_3$; suspected mixture of rotamers with a 1:1.5 ratio) δ 156.1 (major rot. C^6), 156.0 (minor rot. C^6), 151.6 (minor rot. C^2), 151.1 (major rot. C^2), 145.2 (C^9), 128.4 (broad, minor rot. C^3), 127.8 (broad, major rot. C^3), 125.3 (C^8/C^7), 122.5 (major rot. C^7/C^8), 122.4 (minor rot. C^7/C^8), 106.7 (broad, C^4), 31.9 (minor rot. C^1), 31.9 (major rot. C^1), 14.7 (broad, C^5). **HRMS** (APCI) m/z: $[M + H]^+$ Calcd for $C_{11}H_9D_4N_2O_4$ 241.1121; Found 241.1120. The spectral data agrees with compound **559** and the deuterium incorporation is confirmed by HRMS.

When the reaction was repeated, **559-D** was afforded in a yield of 85% (1.03 g, 4.27 mmol) with higher deuterium incorporation (D_A = 91%, D_B = 81%, D_C = 81%). This material was used for the synthesis of **568-D**.

(*E*)-1-Allyl-1,3-dimethyl-3-(prop-1-en-1-yl-1,2,3,3-*d*$_4$)urea (554-D)

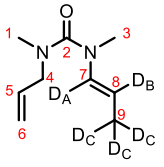

An oven-dried microwave vial containing a magnetic stir bar was sealed with a suba seal and placed under anhydrous N_2. The flask was charged with **559-D** (683 mg, 2.84 mmol, 1.00 equiv.), anhydrous

DMF (7.1 mL, 2.5 mL/mmol), *N*-allylmethylamine (330 µL, 3.42 mmol, 1.20 equiv.) and K_2CO_3 (1.26 g, 9.12 mmol, 3.21 equiv.), and the reaction mixture was stirred in the microwave at 130 °C for 2 h. H_2O was added and the reaction mixture was extracted with CH_2Cl_2, after which the aqueous phase was washed with CH_2Cl_2 (2×). The combined organic phases were dried over $MgSO_4$, filtered, and concentrated *in vacuo*. Flash column chromatography with neutralised silica (0−4% EtOAc/petroleum ether) gave **554-D** as a pale-yellow oil (429 mg, 2.49 mmol, 88% yield; deuterium incorporation: D_A = 67%, D_B = 66%, D_C = 67%). Caution: avoid using $CDCl_3$ as **554-D** then decomposes very rapidly in the NMR tube! **^{1}H NMR** (400 MHz, toluene-d_8) δ 6.57 – 6.50 (m, 0.33H, H^7), 5.69 – 5.55 (m, 1H, H^5), 5.01 – 4.89 (m, 2H, H^6), 4.51 – 4.42 (m, 0.34H, H^8), 3.47 (dt, *J* = 5.8, 1.6 Hz, 2H, H^4), 2.78 (s, 3H, H^3), 2.50 (s, 3H, H^1), 1.60 – 1.51 (m, 1H, H^9). **^{13}C NMR** (126 MHz, toluene-d_8) δ 161.6 (C^2), 134.5 (C^5), 132.8 (broad, C^7), 116.8 (C^6), 100.3 (broad, H^8), 53.7 (C^4), 35.8 (C^1), 33.1 (C^3), 14.9 (broad, C^9). **HRMS** (ESI-TOF) m/z: $[M + Na]^+$ Calcd for $C_9H_{12}D_4N_2ONa$ 195.1411; Found 195.1414. The spectral data agrees with compound **554** and the deuterium incorporation is confirmed by HRMS.

1,3-Dimethyl-1-((*E*)-prop-1-en-1-yl-1,2,3,3-*d*$_4$)-3-((*Z*)-prop-1-en-1-yl)urea (560-D)

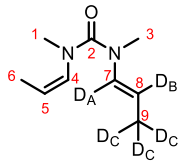

Reaction performed on 1.38 mmol scale following general procedure **3C** using **554-D** (237 mg, 1.38 mmol, 1.00 equiv.) in anhydrous THF (13.9 mL), 18-crown-6 (808 mg, 3.06 mmol, 2.22 equiv.) and KHMDS (1.00 M in THF; 2.78 mL, 2.78 mmol, 2.01 equiv.), which was stirred for 1.5 h at −78 °C. Flash column chromatography with neutralised silica (0−5% acetone/petroleum ether) gave **560-D** as a pale-yellow oil (208 mg, 1.21 mmol, 88% yield; deuterium incorporation: D_A = 66%, D_B = 63%, D_C = 66%). Caution: avoid using $CDCl_3$ as **560-D** then decomposes very rapidly in the NMR tube! **^{1}H NMR** (400 MHz, toluene-d_8) δ 6.80 – 6.71 (m, 0.34H, H^7), 5.60 (dq, *J* = 8.2, 1.7 Hz, 1H, H^4), 4.70 (dq, *J* = 8.2, 7.0 Hz, 1H, H^5), 4.54 – 4.43 (m, 0.37H, H^8), 2.81 (s, 3H, H^1), 2.73 (s, 3H, H^3), 1.59 – 1.50 (m, 1.02H, H^9), 1.31 (dd, *J* = 7.0, 1.7 Hz, 3H, H^6). **^{13}C NMR** (101 MHz, toluene-d_8) δ 159.4 (C^2), 132.9 (C^4), 132.2 (broad, C^7), 115.0 (C^5), 100.3 (broad, C^8), 36.8 (C^1), 33.2 (C^3), 15.1 (broad, C^9), 12.0 (C^6). **HRMS** (ESI-TOF) m/z: $[M + H]^+$ Calcd for $C_9H_{13}D_4N_2O$ 173.1592; Found 173.1588. The spectral data agrees with compound **560** and the deuterium incorporation is confirmed by HRMS.

(*E*)-1-(Hexa-1,4-dien-3-yl-4,5,6,6-*d*$_4$)-1,3-dimethylurea (352-D)

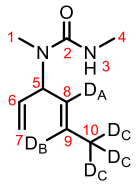

Reaction performed on 0.40 mmol scale following general procedure **3B** using **554-D** (68 mg, 0.40 mmol, 1.0 equiv.) in anhydrous THF (1.87 mL, total of 10.0 mL/mmol) and LDA (freshly prepared following general procedure **3A**; 2.13 mL, 0.800 mmol, 2.00 equiv.), which was stirred for 2.5 h at −78 °C. Flash column chromatography with neutralised silica (5−40% acetone/petroleum ether) gave **352-D** as a pale-yellow oil (38 mg, 0.22 mmol, 55% yield; deuterium incorporation: D_A = 64%, D_B = 66%, D_C = 66%). **^{1}H NMR** (400 MHz, $CDCl_3$) δ 5.79 (ddd, *J* = 17.3, 10.5, 4.9 Hz, 1H, H^6), 5.62 – 5.53 (m, 0.36H, H^9), 5.46 – 5.40 (m, 0.34H, H^8), 5.25 – 5.18 (m, 1H, H^5), 5.18 – 5.06 (m, 2H, H^7), 4.52 (bs, 1H, H^3), 2.77 (d, *J* = 3.2 Hz, 3H, H^4), 2.68 (s, 3H, H^1), 1.71 – 1.61 (m, 1.01H, H^{10}). **^{13}C NMR** (101 MHz, $CDCl_3$) δ 159.0 (C^2), 136.7 (C^6), 128.6 (broad, C^9), 128.2 (broad, C^8), 116.6 (C^7), 58.2 (broad, C^5), 30.0 (C^1), 27.7 (C^4), 17.3 (broad, C^{10}). **HRMS** (ESI-TOF) m/z: $[M + H]^+$ Calcd for $C_9H_{13}D_4N_2O$ 173.1586; Found 173.1586. The spectral data agrees with compound **352** and the deuterium incorporation is confirmed by HRMS.

In addition, 1-((2*Z*,4*E*)-hexa-2,4-dien-3-yl-4,5,6,6-*d*$_4$)-1,3-dimethylurea **362-D** was afforded as a pale-yellow oil (16 mg, 0.093 mmol, 23% yield; deuterium incorporation: D_A = 66%, D_B = 62%, D_C = 65%).

1-((2*Z*,4*E*)-Hexa-2,4-dien-3-yl-4,5,6,6-*d*$_4$)-1,3-dimethylurea (362-D)

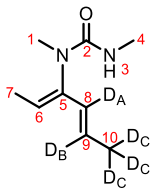

Reaction performed on 0.39 mmol scale following general procedure **3C** using **554-D** (68 mg, 0.39 mmol, 1.0 equiv.) in anhydrous THF (4 mL), 18-crown-6 (232 mg, 0.878 mmol, 2.25 equiv.) and KHMDS (1.0 M in THF; 0.80 mL, 0.80 mmol, 2.1 equiv.), which was stirred for 24 h at −78 °C to 0 °C. Flash column chromatography with neutralised silica (0−25% acetone/petroleum ether) gave **362-D** as a pale-yellow oil (32 mg, 0.19 mmol, 48% yield; deuterium incorporation: D_A = 60%, D_B = 51%, D_C = 61%). **^{1}H NMR** (400 MHz, $CDCl_3$) δ 5.87 – 5.81 (m, 0.40H, H^8), 5.63 – 5.54 (m, 0.49H, H^9), 5.52 (q, *J* = 7.0 Hz, 1H, H^6), 4.44 (bs, 1H, H^3), 2.94 (s, 3H, H^1), 2.71 (d, *J* = 4.6 Hz, 3H, H^4), 1.76 – 1.65 (m, 1.16H, H^{10}), 1.60 (d, *J* = 7.0 Hz, 3H, H^7). **^{13}C NMR** (101 MHz, $CDCl_3$) δ 157.7 (C^2), 140.7 (broad, C^5), 127.7 (broad, C^8), 125.8 (broad, C^6), 125.5 (broad, C^9), 34.1 (C^1), 27.5 (C^4), 17.7 (broad, C^{10}), 12.7 (C^7).

HRMS (ESI-TOF) m/z: $[M + H]^+$ Calcd for $C_9H_{13}D_4N_2O$ 173.1586; Found 173.1582. The spectral data agrees with compound **362** and the deuterium incorporation is confirmed by HRMS.

In addition, 1,3-dimethyl-1-((*E*)-prop-1-en-1-yl-1,2,3,3-d_4)-3-((*Z*)-prop-1-en-1-yl)urea **560-D** (pale-yellow oil; 18 mg, 0.10 mmol, 27% yield; deuterium incorporation: D_A = 59%, D_B = 56%, D_C = 68%) and 1,3-dimethyl-3-((*E*)-prop-1-en-1-yl)-1-((*E*)-prop-1-en-1-yl-1,2,3,3-d_4)urea **207-D** were afforded.

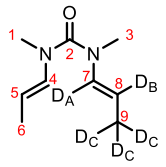

207-D was afforded as a pale-yellow oil (9 mg, 0.05 mmol, 14% yield; deuterium incorporation: D_A = 81%, D_B = 41%, D_C = 78%). **^{1}H NMR** (400 MHz, toluene-d_8) δ 6.51 (dq, *J* = 14.0, 1.5 Hz, 1.19H, H^4 + H^7), 4.52 – 4.42 (m, 1.59H, H^5 + H^8), 2.72 (s, 6H, H^1 + H^3), 1.52 (dd, *J* = 6.6, 1.5 Hz, 3H, H^6), 1.51 – 1.46 (m, 0.66H, H^9). **^{13}C NMR** (101 MHz, toluene-d_8) δ 158.7 (C^2), 132.5 (C^4 + C^7), 101.7 (C^5 + C^8), 33.5 (C^1 + C^3), 15.3 (C^6 + C^9). **HRMS** (ESI-TOF) m/z: $[M + H]^+$ Calcd for $C_9H_{13}D_4N_2O$ 173.1592; Found 173.1584. The spectral data agrees with compound **207** and the deuterium incorporation is confirmed by HRMS.

(*Z*)-1,3-Dimethyl-3-(2-methylprop-1-en-1-yl)-1-(prop-1-en-1-yl)urea (565)

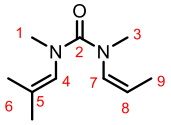

Reaction performed on 1.03 mmol scale following general procedure **3C** using **243** (188 mg, 1.03 mmol, 1.00 equiv.) in anhydrous THF (10 mL), 18-crown-6 (599 mg, 2.27 mmol, 2.20 equiv.) and KHMDS (1.00 M in THF; 2.06 mL, 2.06 mmol, 2.00 equiv.), which was stirred for 4 h at −78 °C to −20 °C. Flash column chromatography with neutralised silica (0−40% acetone/petroleum ether) gave **565** as a yellow oil (112 mg, 0.614 mmol, 60% yield). **IR** (film) ν_{max} 3357, 2941, 1631, 1571, 1458, 1412, 1277, 1052, 767 cm^{-1}. Caution: avoid using $CDCl_3$ as **565** then decomposes very rapidly in the NMR tube! **^{1}H NMR** (400 MHz, toluene-d_8) δ 5.73 (dq, *J* = 8.1, 1.7 Hz, 1H, H^7), 5.44 (hept, *J* = 1.4 Hz, 1H, H^4), 4.67 (dq, *J* = 8.1, 7.0 Hz, 1H, H^8), 2.91 (s, 3H, H^3), 2.85 (s, 3H, H^1), 1.41 (d, *J* = 1.4 Hz, 3H, H^6), 1.38 (d, *J* = 1.7 Hz, 1.5H, H^9), 1.37 (d, *J* = 1.7 Hz, 4.5H, H^6 + H^9). **^{13}C NMR** (101 MHz, toluene-d_8) δ 160.7 (C^2), 133.3 (C^7), 128.1 (C^4), 127.3 (C^5), 113.9 (C^8), 37.0 (C^1), 36.8 (C^3), 21.7 (C^6), 17.1 (C^6), 12.3 (C^9). **HRMS** (ESI-TOF) m/z: $[M + H]^+$ Calcd for $C_{10}H_{19}N_2O$ 183.1497; Found 183.1499.

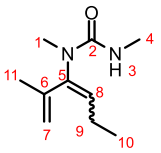

566

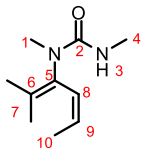

(*Z*)-411

In addition, a mixture of 1,3-dimethyl-1-(2-methylhexa-1,3-dien-3-yl)urea **566** and (*Z*)-1,3-dimethyl-1-(2-methylhexa-2,4-dien-3-yl)urea **(*Z*)-411** was afforded as a sticky yellow solid (ratio of 0.2:0.8, 35 mg, 0.19 mmol, 19% yield). **IR** (film) ν_{max} 3349, 2914, 1643, 1524, 1337, 1219, 772 cm^{-1}. **^{1}H NMR** (400 MHz, $CDCl_3$) δ 5.92 – 5.84 (m, 1H, H^8), 5.72 (t, *J* = 7.3 Hz, 0.23H, H^8), 5.59 (dq, *J* = 11.7, 7.3 Hz, 1H, H^9), 4.98 (d, *J* = 9.1 Hz, 0.46H, H^7), 4.52 (bs, 1H, H^3), 4.38 (bs, 0.23H, H^3), 2.97 (s, 0.69H, H^1), 2.89 (s, 3H, H^1), 2.77 (bs, 3H, H^4), 2.73 (bs, 0.69H, H^4), 2.15 – 2.05 (m, 0.46H, H^9), 1.90 (dd, *J* = 1.4, 0.7 Hz, 0.69H, H^{11}), 1.77 (s, 3H, H^7), 1.70 (s, 3H, H^7), 1.63 (dd, *J* = 7.3, 1.8 Hz, 3H, H^{10}), 1.01 (t, *J* = 7.6 Hz, 0.69H, H^{10}). **^{13}C NMR** (101 MHz, $CDCl_3$) δ 157.7 (C^2 + C^2), 141.0 (C^5), 137.9 (C^6), 134.9 (C^6), 132.6 (C^8), 132.2 (C^5), 127.7 (C^9), 123.2 (C^8), 113.8 (C^7), 34.9 (C^1), 33.7 (C^1), 27.6 (C^4), 27.6 (C^4), 21.2 (C^9), 20.3 (C^7), 20.1 (C^{11}), 19.5 (C^7), 14.0 (C^{10}), 13.4 (C^{10}). **HRMS** (ESI-TOF) m/z: $[M + H]^+$ Calcd for $C_{10}H_{19}N_2O$ 183.1497; Found 183.1496.

(*E*)-1,3-Dimethyl-1-(2-methylallyl)-3-(prop-1-en-1-yl-1,2,3,3-*d*$_4$)urea (568-D)

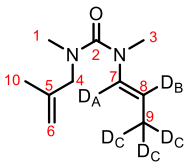

An oven-dried microwave vial containing a magnetic stir bar was sealed with a suba seal and placed under anhydrous N_2. The flask was charged with **559-D** (724 g, 3.00 mmol, 1.00 equiv.), anhydrous DMF (7.3 mL, 2.4 mL/mmol), **295** (438 mg, 3.60 mmol, 1.20 equiv.) and K_2CO_3 (1.82 g, 13.2 mmol, 4.40 equiv.), and the reaction mixture was stirred in the microwave at 130 °C for 4 h. H_2O was added and the reaction mixture was extracted with CH_2Cl_2, after which the aqueous phase was washed with CH_2Cl_2 (2×). The combined organic phases were dried over $MgSO_4$, filtered, and concentrated *in vacuo*. Flash column chromatography with neutralised silica (0−2% EtOAc/petroleum ether) gave **568-D** as a yellow oil (413 mg, 2.22 mmol, 74% yield). **^{1}H NMR** (400 MHz, toluene-*d*$_8$; deuterium incorporation: D_A = 84%, D_B = 80%, D_C = 81%) δ 6.60 – 6.55 (m, 0.16H, H^7), 4.79 – 4.72 (m, 2H, H^6), 4.52 – 4.43 (m, 0.20H, H^8), 3.46 (s, 2H, H^4), 2.79 (s, 3H, H^3), 2.53 (s, 3H, H^1), 1.58 – 1.51 (m, 0.58H, H^9), 1.47 (dd, *J* = 1.5, 0.8 Hz, 3H, H^{10}). **^{13}C NMR** (101 MHz, toluene-*d*$_8$) δ 161.8 (C^2), 141.9 (C^5), 132.7 (broad, C^7), 112.0 (C^6), 100.2 (broad, C^8), 56.9 (C^4), 35.9 (C^1), 33.1 (C^3), 19.9 (C^{10}), 14.7 (broad, C^9). **HRMS** (ESI-TOF) m/z: $[M + H]^+$ Calcd for $C_{10}H_{15}D_4N_2O$ 187.1743; Found 187.1746. The spectral data agrees with compound **568** and the deuterium incorporation is confirmed by HRMS.

(*E*)-1,3-Dimethyl-1-(2-methylallyl)-3-(prop-1-en-1-yl)urea (568)

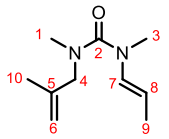

An oven-dried microwave vial containing a magnetic stir bar was sealed with a suba seal and placed under anhydrous N_2. The flask was charged with **559** (509 mg, 2.15 mmol, 1.00 equiv.), anhydrous DMF (5.2 mL, 2.4 mL/mmol), **295** (314 mg, 2.58 mmol, 1.20 equiv.) and K_2CO_3 (1.31 g, 9.46 mmol, 4.40 equiv.), and the reaction mixture was stirred in the microwave at 130 °C for 4 h. H_2O was added and the reaction mixture was extracted with CH_2Cl_2, after which the aqueous phase was washed with CH_2Cl_2 (2×). The combined organic phases were dried over $MgSO_4$, filtered, and concentrated *in vacuo*. Flash column chromatography with neutralised silica (0−4% EtOAc/petroleum ether) gave **568** as a yellow oil (316 mg, 1.73 mmol, 81% yield). **IR** (film) ν_{max} 2921, 1645, 1452, 1389, 1371, 1290, 1263, 111, 1090, 946, 899, 771 cm^{-1}. **^{1}H NMR** (400 MHz, toluene-d_8) δ 6.57 (dq, J = 14.0, 1.5 Hz, 1H, H^7), 4.77 – 4.73 (m, 2H, H^6), 4.48 (dq, J = 14.0, 6.5 Hz, 1H, H^8), 3.47 (s, 2H, H^4), 2.79 (s, 3H, H^3), 2.53 (s, 3H, H^1), 1.58 (dd, J = 6.5, 1.5 Hz, 3H, H^9), 1.47 (dd, J = 1.5, 0.8 Hz, 3H, H^{10}). **^{13}C NMR** (101 MHz, toluene-d_8) δ 161.8 (C^2), 141.9 (C^5), 132.8 (C^7), 112.0 (C^6), 100.6 (C^8), 56.9 (C^4), 35.9 (C^1), 33.2 (C^3), 19.9 (C^{10}), 15.4 (C^9). **HRMS** (ESI-TOF) m/z: $[M + H]^+$ Calcd for $C_{10}H_{19}N_2O$ 183.1492; Found 183.1495.

5.3.3.2 Deuterium Kinetic Isotope Effect Studies

Reaction set-up:

An oven-dried round-bottom flask containing a magnetic stir bar was sealed with a suba seal and placed under anhydrous N_2. The flask was charged with **568-D** (122 mg, 0.655 mmol, 1.00 equiv.), anhydrous THF (6.5 mL, 10 mL/mmol), 18-crown-6 (378 mg, 1.43 mmol, 2.18 equiv.) and 1,3,5-trimethoxybenzene (37 mg, 0.22 mmol, 0.34 equiv.). The reaction mixture was cooled down to −78 °C and KHMDS (1.00 M in THF; 1.30 mL, 1.30 mmol, 1.98 equiv.) was added dropwise. After 1 h at −78 °C, the reaction mixture was gradually warmed up by setting the cryostat at 0 °C. Once the temperature reached 0 °C (after 2 h), the flask was placed at room temperature and the first aliquot (0.26 mL – contains about 5 mg of reaction intermediate/product) was taken directly. The aliquot was quenched with MeOH, concentrated *in vacuo*, and dissolved in 0.5 mL of deuterated toluene; a crude ^{1}H NMR was taken immediately. Over a time period of almost 6 hours, 22 aliquots were taken at room temperature and analysed by crude ^{1}H NMR.

NMR preparation and parameters:

The NMR samples were prepared by dissolving the crude reaction mixture in 0.5 mL of toluene-d_8. The ^{1}H NMR spectra were recorded at 500 MHz employing a Bruker Avance III HD Spectrometer (500 MHz) equipped with a 5mm DCH CryoProbe. The following NMR parameters were applied to record the spectra: $\pi/2$ pulse, 8 scans, 40 s relaxation delay. For each NMR sample the FID was processed using the same settings: 128K zero filling, apodization stanning 8.0, phase correction regions, Whittaker smoother multipoint baseline correction (smooth 5) and peak picking via qGSD (7 rounds). Integrations (edited sum) were applied manually with a total width of 0.09 ppm for each peak. The peak at 6.13 ppm, belonging to the CHs of the internal standard 1,3,5-trimethoxybenzene, was set to an integration of 1000.0.

Formulae for the yield and deuterium incorporation calculations:

Yield = (((integration average non-deuterated signals*mmol IS)/(integration CHs IS/3))/mmol starting material)*100

= (((integration average non-deuterated signals *0.22)/(1000.0/3))/0.65)*100

Stdev = (Stdev of integration/integration average non-deuterated signals)*yield

α-Deuterium incorporation = (1-(integration H8/integration average of non-deuterated signals))*100

Stdev = (Stdev of integration/integration average non-deuterated signals)*α-deuterium incorporation

β-Deuterium incorporation = (1-(integration H9/integration average of non-deuterated signals))*100

Stdev = (Stdev of integration/integration average non-deuterated signals)*β-deuterium incorporation

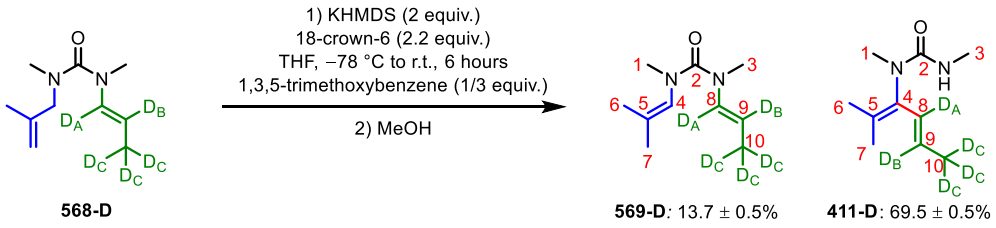

568-D **569-D**: 13.7 ± 0.5% **411-D**: 69.5 ± 0.5%

By ^{1}H NMR analysis, yields of 69.5 ± 0.5% and 13.7 ± 0.5% for product **411-D** and reaction intermediate **569-D**, respectively, were determined with the use of the internal standard – 1,3,5-trimethoxybenzene. The following output tables were used to make the graphs for the yield and

deuterium incorporation of reaction intermediate **569-D** and product **411-D** over the course of the reaction.

Output data:

Time Points (min)	Total Time (min)	^{1}H NMR integration of non-deuterated signals – reaction intermediate 569-D							Yield (%)	Stdev
		H4 (5.40 ppm)	H3 (2.79 ppm)	H1 (2.73 ppm)	H6 (1.39 ppm)	H7 (1.32 ppm)	Average	Stdev		
0	0	935.0	902.8	936.0	942.4	974.8	938.2	22.9	95.3	2.3
16	16	849.0	862.4	843.9	855.8	856.0	853.4	6.4	86.7	0.6
14	30	730.5	752.3	735.5	746.0	759.8	744.8	10.7	75.6	1.1
10	40	662.4	680.2	675.2	682.8	689.3	678.0	9.0	68.8	0.9
10	50	619.7	627.7	612.5	624.2	620.9	621.0	5.1	63.1	0.5
10	60	568.1	560.0	564.0	568.4	561.5	564.4	3.4	57.3	0.3
12	72	523.0	520.0	519.9	528.7	530.3	524.4	4.4	53.2	0.4
10	82	481.9	490.2	484.7	496.7	516.5	494.0	12.3	50.2	1.3
13	95	443.3	449.3	442.9	441.6	405.5	436.5	15.8	44.3	1.6
10	105	419.5	419.0	409.1	429.1	432.2	421.8	8.2	42.8	0.8
22	127	367.9	364.1	357.3	374.5	385.2	369.8	9.5	37.5	1.0
10	137	345.5	344.9	342.1	351.3	320.8	340.9	10.5	34.6	1.1
10	147	320.4	323.8	316.7	342.9	338.2	328.4	10.3	33.3	1.0
10	157	310.0	307.4	302.6	303.6	306.3	306.0	2.7	31.1	0.3
10	167	295.0	292.9	288.8	304.5	314.8	299.2	9.4	30.4	0.9
22	189	273.1	269.1	267.6	277.6	279.3	273.3	4.6	27.8	0.5
13	202	254.8	246.2	239	245.6	255.0	248.1	6.1	25.2	0.6
21	223	221.8	214.5	211.5	217.0	201.6	213.3	6.8	21.7	0.7
30	253	201.7	192.3	191.2	194.2	202.4	196.4	4.7	19.9	0.5
20	273	177.1	168.0	191.3	178.1	163.9	175.7	9.5	17.8	1.0
36	309	164.0	153.8	153.8	173.7	171.6	163.4	8.4	16.6	0.9
44	353	141.0	130.7	131.8	n.d.	n.d.	134.5	4.6	13.7	0.5

Time Points (min)	Total Time (min)	^{1}H NMR integration of deuterated signals – reaction intermediate 569-D					
		H8 (6.76 ppm)	α-Deuterium Incorporation (%)	Stdev	H9 (4.44 ppm)	β-Deuterium Incorporation (%)	Stdev
0	0	149.8	84.0	2.1	194.1	79.3	1.9
16	16	136.5	84.0	0.6	170.7	80.0	0.6
14	30	112.8	84.9	1.2	145.1	80.5	1.2
10	40	104.0	84.7	1.1	128.8	81.0	1.1
10	50	95.6	84.6	0.7	117.8	81.0	0.7
10	60	88.1	84.4	0.5	105.3	81.3	0.5
12	72	n.d.	n.d.	n.d.	98.3	81.3	0.7
10	82	n.d.	n.d.	n.d.	88.8	82.0	2.0
13	95	66.5	84.8	3.1	80.9	81.5	2.9
10	105	63.4	85.0	1.7	74.7	82.3	1.6
22	127	57.0	84.6	2.2	66.1	82.1	2.1
10	137	53.9	84.2	2.6	60.1	82.4	2.5
10	147	49.4	85.0	2.7	57.2	82.6	2.6
10	157	46.9	84.7	0.7	56.0	81.7	0.7
10	167	45.1	84.9	2.7	50.6	83.1	2.6
22	189	n.d.	n.d.	n.d.	44.6	83.7	1.4
13	202	n.d.	n.d.	n.d.	40.9	83.5	2.0
21	223	n.d.	n.d.	n.d.	36.2	83.0	2.6
30	253	30.2	84.6	2.0	31.6	83.9	2.0
20	273	27.1	84.6	4.6	29.2	83.4	4.5
36	309	25.3	84.5	4.4	29.3	82.1	4.2
44	353	19.8	85.3	2.9	20.1	85.1	2.9

Time Points (min)	Total Time (min)	^{1}H NMR integration of non-deuterated signals – product 411-D							
		H1 (2.79 ppm)	H3 (2.73 ppm)	H6 (1.39 ppm)	H7 (1.32 ppm)	Average	Stdev	Yield (%)	Stdev
0	0	0.0	0.0	0.0	0.0	0.0	0.0	0.0	0
16	16	89.0	88.1	n.d.	87.0	88.0	0.8	8.9	0.1
14	30	203.9	206.8	n.d.	209.6	206.8	2.3	21.0	0.2
10	40	266.4	264.5	n.d.	255.0	262.0	5.0	26.6	0.5
10	50	320.6	319.8	n.d.	312.5	317.6	3.6	32.3	0.4
10	60	361.2	361.5	n.d.	331.3	351.3	14.1	35.7	1.4
12	72	413.4	383.2	n.d.	415.1	403.9	14.6	41.0	1.5
10	82	442.8	422.8	444.5	440.1	437.5	8.7	44.4	0.9
13	95	475.6	449.2	473.4	465.6	466.0	10.4	47.3	1.1
10	105	501.4	474.3	504.0	474.7	488.6	14.1	49.6	1.4
22	127	544.4	519.8	533.7	508.1	526.5	13.7	53.5	1.4
10	137	561.3	556.9	566.5	526.2	552.7	15.7	56.1	1.6
10	147	585.6	548.4	556.2	559.2	562.3	14.0	57.1	1.4
10	157	601.1	590.3	573.1	568.1	583.1	13.2	59.2	1.3
10	167	612.3	577.2	593.0	573.3	589.0	15.4	59.8	1.6
22	189	662.8	619.3	624.7	642.3	637.3	17.0	64.7	1.7
13	202	653.2	620.6	652.2	579.8	626.5	29.9	63.6	3.0
21	223	666.8	660.2	646.4	662.9	659.1	7.7	66.9	0.8
30	253	672.6	669.5	615.9	686.8	661.2	27.0	67.1	2.7
20	273	710.0	701.2	640.0	674.1	681.3	27.3	69.2	2.8
36	309	709.2	684.2	633.6	688.2	678.8	27.8	68.9	2.8
44	353	690.2	679.7	n.d.	n.d.	685.0	5.2	69.5	0.5

Time Points (min)	Total Time (min)	^{1}H NMR integration of deuterated signals – product 411-D					
		H8 (6.08 ppm)	α-Deuterium Incorporation (%)	Stdev	H9 (5.40 ppm)	β-Deuterium Incorporation (%)	Stdev
0	0	0.0	0	n.d.	0.0	0	n.d.
16	16	25.2	71.4	0.7	27.0	69.3	0.7
14	30	42.8	79.3	0.9	54.0	73.9	0.8
10	40	61.3	76.6	1.5	69.0	73.7	1.4
10	50	58.1	81.7	0.9	83.8	73.6	0.8
10	60	75.1	78.6	3.2	94.8	73.0	2.9
12	72	59.4	85.3	3.1	110.0	72.8	2.6
10	82	76.8	82.4	1.6	123.4	71.8	1.4
13	95	81.3	82.6	1.8	134.3	71.2	1.6
10	105	85.1	82.6	2.4	144.1	70.5	2.0
22	127	111.7	78.8	2.1	164.7	68.7	1.8
10	137	118.0	78.7	2.2	170.1	69.2	2.0
10	147	102.6	81.8	2.0	181.2	67.8	1.7
10	157	128.6	77.9	1.8	188.8	67.6	1.5
10	167	111.0	81.2	2.1	201.5	65.8	1.7
22	189	99.1	84.4	2.3	223.8	64.9	1.7
13	202	113.4	81.9	3.9	230.4	63.2	3.0
21	223	105.3	84.0	1.0	296.1	55.1	0.6
30	253	131.0	80.2	3.3	274.4	58.5	2.4
20	273	124.8	81.7	3.3	280.6	58.8	2.4
36	309	144.8	78.7	3.2	303.2	55.3	2.3
44	353	190.7	72.2	0.6	303.4	55.7	0.4

Graphs of output data:

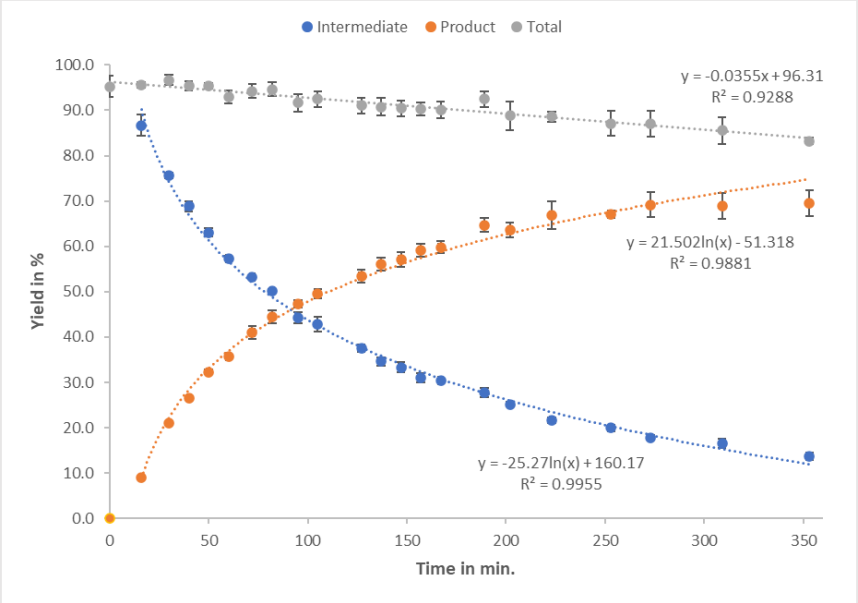

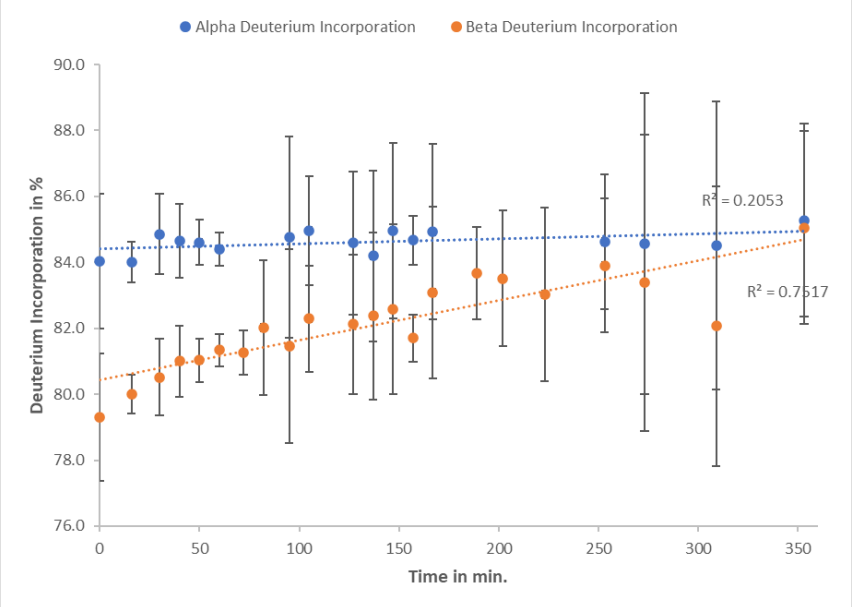

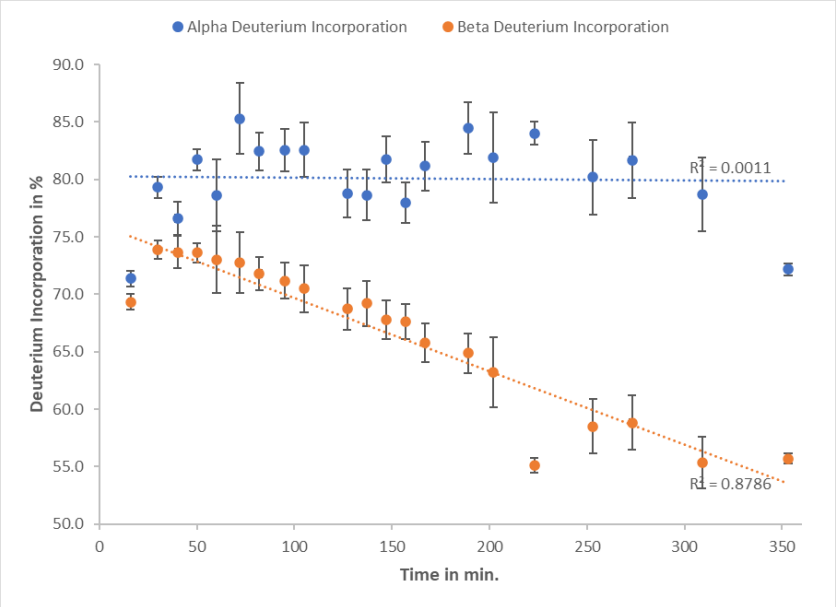

5.3.3.3 Natural Abundance ^{13}C Kinetic Isotope Effect Determination

Reaction set-up:

Run 1: An oven-dried round-bottom flask containing a magnetic stir bar was sealed with a suba seal and placed under anhydrous N_2. The flask was charged with **568** (73 mg, 0.40 mmol, 1.0 equiv.), anhydrous THF (4.0 mL, 10 mL/mmol), 18-crown-6 (232 mg, 0.878 mmol, 2.20 equiv.) and 1,3,5-trimethoxybenzene (21.6 mg, 0.128 mmol, 0.320 equiv.). The reaction mixture was cooled down to −78 °C and KHMDS (1.0 M in THF; 0.80 mL, 0.80 mmol, 2.0 equiv.) was added dropwise. After 1 h at −78 °C, the reaction mixture was gradually warmed up by setting the cryostat at 0 °C. Once the temperature reached 0 °C (after 2 h), the flask was placed at room temperature and stirred for 1.75 h. The reaction mixture was then quenched with MeOH and concentrated *in vacuo*.

For run 2, the same procedure was followed with **568** (71 mg, 0.39 mmol, 1.0 equiv.), anhydrous THF (3.9 mL, 10 mL/mmol), 18-crown-6 (227 mg, 0.859 mmol, 2.20 equiv.), 1,3,5-trimethoxybenzene (22 mg, 0.13 mmol, 0.34 equiv.) and KHMDS (1 M in THF; 0.78 mL, 0.78 mmol, 2 equiv.).

NMR preparation and parameters:

The two NMR samples (one from run 1 and one from run 2) were prepared by dissolving the crude reaction mixture in 0.5 mL of toluene-d_8. The ^{13}C NMR spectra were recorded at 126 MHz employing a Bruker Avance III HD Spectrometer (500 MHz) equipped with a 5mm DCH CryoProbe and using inverse gated decoupling. The following NMR parameters were applied to record the spectra: $\pi/6$ pulse,

128 scans for run 1 and 200 and 250 scans for run 2, 60 s relaxation delay. For each NMR sample a total of six spectra were recorded and their FIDs were processed at the same time applying the same settings: 256K zero filling, apodization stanning 8.0, phase correction regions, Whittaker smoother baseline correction (filter: 31; smooth factor: 65536) and peak picking via qGSD (7 rounds). Integrations (edited sum) were applied manually with a total width of 0.4 ppm for each peak. The peak at 93.3 ppm, belonging to the CHs of the internal standard 1,3,5-trimethoxybenzene, was set to an integration of 1000.0.

Formulae for the ^{13}C KIE calculations by Singleton:[181]

F = conversion of starting material **568** to product **411**.

R/R$_0$ = proportion of the minor isotopic component in "changed" carbons (at the reaction centre – C8, C9 and C10) compared to the "unchanged" carbons (not participating in the mechanism – C1, C2, C3, C6 and C7) in reaction intermediate **569**

Δ(R/R$_0$) = $R/R_0((\Delta R/R)^2 + (\Delta R_0/R_0)^2)^{1/2}$

KIE = $\frac{\ln(1-F)}{\ln(1-F)R/R_0}$

ΔKIE$_R$ = $\frac{-\ln(1-F)}{(R/R_0)ln^2[(1-F)R/R_0]}\Delta(R/R_0)$

ΔKIE$_F$ = $\frac{-\ln(R/R_0)}{(1-F)ln^2[(1-F)R/R_0]}\Delta F$

ΔKIE = $KIE*((\Delta KIE_R/KIE)^2 + (\Delta KIE_F/KIE)^2)^{1/2}$

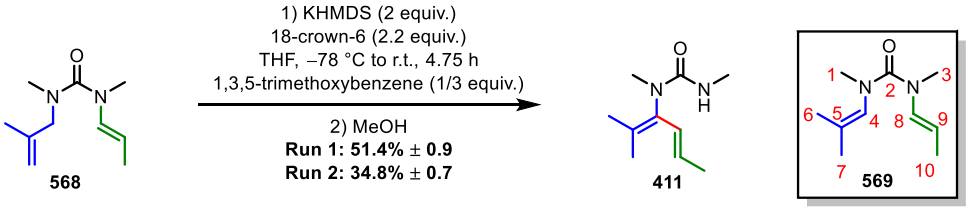

By ^{13}C NMR analysis, for the first and second run a conversion of 51.4 ± 0.9% and 34.8 ± 0.7%, respectively, was determined with the use of the internal standard – 1,3,5-trimethoxybenzene.

Output data first run:

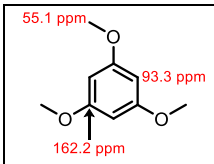	^{13}C NMR integration of internal standard (IS)							
ppm peaks	**fid1**	**fid2**	**fid3**	**fid4**	**fid5**	**fid6**	**IS**	**ΔIS**
162.2	1091.9	1099.2	1115.8	1100.4	1075.9	1099.8	1097.2	11.9
93.3	1000.0	1000.0	1000.0	1000.0	1000.0	1000.0	1000.0	0
55.1	959.8	1006.6	1007.3	1010.8	980.9	1018.7	997.4	20.4

Conversion (F)							
fid1	**fid2**	**fid3**	**fid4**	**fid5**	**fid6**	**F**	**ΔF**
50.8	51.7	51.3	50.2	53.0	51.1	51.4	0.9

^{13}C NMR integration of "unchanged" carbons (R_0)								
ppm peaks	**fid1**	**fid2**	**fid3**	**fid4**	**fid5**	**fid6**	**R_0**	**ΔR_0**
159.7 (C2)	399.3	399.3	404.8	407.7	391.9	401.6	400.8	5.0
37.2 (C1)	323.4	338.7	333.5	311.1	318.9	337.4	327.2	10.2
33.4 (C3)	372.4	347.6	359.6	341.5	345.1	350.3	352.8	10.4
21.7 (C6)	352.6	353.8	355.8	351.7	338.0	363.1	352.5	7.5
17.0 (C7)	359.2	357.8	362.1	354.6	355.3	349.7	356.5	3.9

^{13}C NMR integration of "changed" carbons (R)								
ppm peaks	**fid1**	**fid2**	**fid3**	**fid4**	**fid5**	**fid6**	**R**	**ΔR**
132.0 (C8)	377.8	402.2	394.9	399.1	374.0	388.9	389.5	10.5
100.4 (C9)	383.5	391.6	388.0	381.6	381.8	393.5	386.7	4.7
15.4 (C10)	367.4	370.8	320.7	352.0	360.1	354.2	354.2	16.4

Determination of ^{13}C KIEs						
ppm peaks	**R/R_0**	**$\Delta(R/R_0)$**	**ΔKIE_F**	**ΔKIE_R**	**KIE**	**ΔKIE**
132.0 (C8)	1.088155	0.032640	-0.003771	0.053342	1.132631	0.053475
100.4 (C9)	1.080286	0.019393	-0.003370	0.031201	1.119872	0.031383
15.4 (C10)	0.989579	0.047624	0.000354	0.064803	0.985702	0.064804

Output		
C	**KIE**	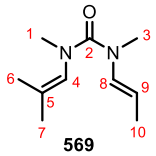
α (C8)	1.133 ± 0.053	
β (C9)	1.120 ± 0.031	
γ (C10)	0.986 ± 0.065	

569

Output data second run:

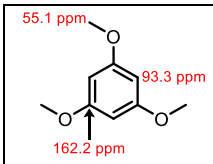

^{13}C NMR integration of internal standard (IS)								
ppm peaks	**fid1**	**fid2**	**fid3**	**fid4**	**fid5**	**fid6**	**IS**	**ΔIS**
162.2	1122.9	1105.5	1118.3	1119.0	1111.5	1144.4	1120.3	12.2
93.3	1000.0	1000.0	1000.0	1000.0	1000.0	1000.0	1000.0	0
55.1	1018.1	1015.0	995.2	998.4	987.1	989.6	1000.6	11.9

Conversion (F)							
fid1	**fid2**	**fid3**	**fid4**	**fid5**	**fid6**	**F**	**ΔF**
35.6	34.6	34.8	35.7	34.7	33.7	34.8	0.7

^{13}C NMR integration of "unchanged" carbons (R_0)								
ppm peaks	**fid1**	**fid2**	**fid3**	**fid4**	**fid5**	**fid6**	**R_0**	**ΔR_0**
159.7 (C2)	447.8	440.5	448.1	455.2	439.5	451.8	447.2	5.6
37.2 (C1)	394.6	380.7	374.6	376.2	360.5	369.6	376.0	10.4
33.4 (C3)	412.8	436.9	422.2	424.5	406.7	406.9	418.3	10.8
21.7 (C6)	412.0	401.8	410.7	397.3	396.4	391.9	401.7	7.4
17.0 (C7)	421.5	413.6	413.4	408.5	400.2	408.2	410.9	6.5

^{13}C NMR integration of "changed" carbons (R)								
ppm peaks	**fid1**	**fid2**	**fid3**	**fid4**	**fid5**	**fid6**	**R**	**ΔR**
132.0 (C8)	457.0	442.3	455.1	440.4	438.2	465.8	449.8	10.1
100.4 (C9)	451.0	459.4	441.7	449.5	431.6	427.2	443.4	11.2
15.4 (C10)	430.3	428.1	423.1	403.5	414.9	424.5	420.7	9.1

Determination of ^{13}C KIEs						
ppm peaks	**R/R_0**	**$\Delta(R/R_0)$**	**ΔKIE_F**	**ΔKIE_R**	**KIE**	**ΔKIE**
132.0 (C8)	1.094883	0.029132	-0.008136	0.100167	1.268935	0.100497
100.4 (C9)	1.079305	0.031313	-0.006302	0.100496	1.217184	0.100693
15.4 (C10)	1.024131	0.026485	-0.001491	0.067814	1.059039	0.067830

Output		
C	**KIE**	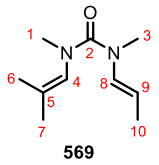
α (C8)	1.269 ± 0.100	
β (C9)	1.217 ± 0.101	
γ (C10)	1.059 ± 0.068	

569

6.0 Appendix: NOE Analysis and VT NMR

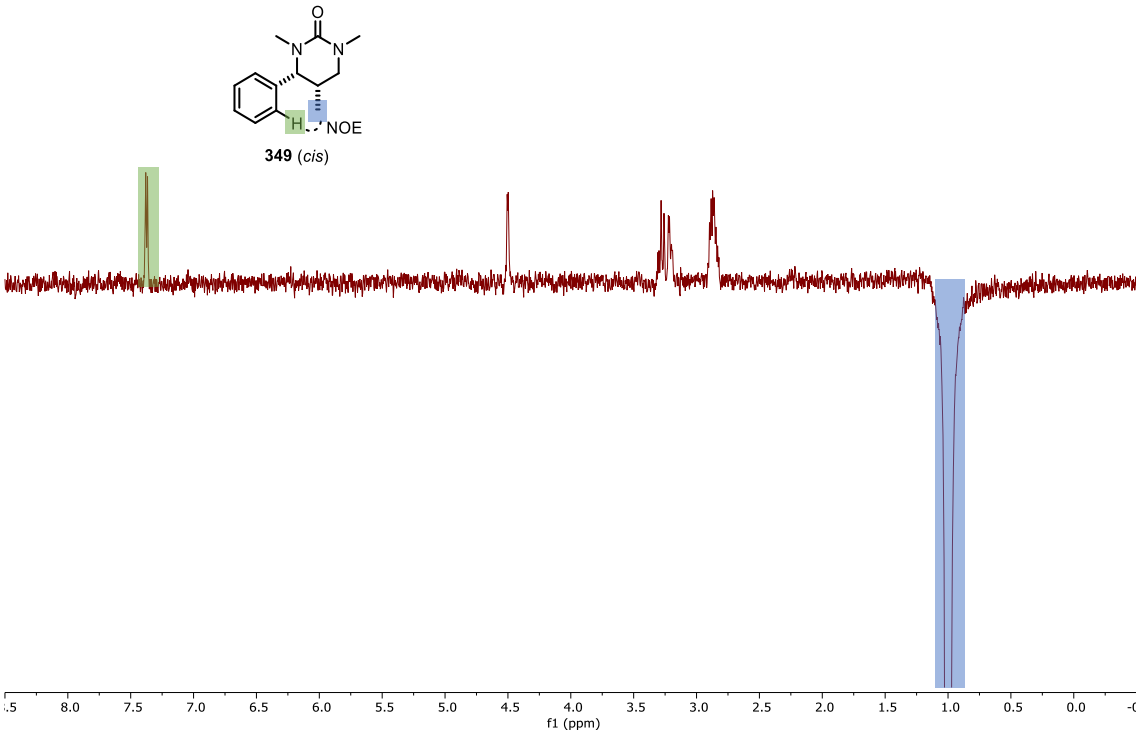

Figure A1. 1D NOESY (500 MHz, $CDCl_3$) of 349 (*cis*) (the methyl in blue was irradiated).

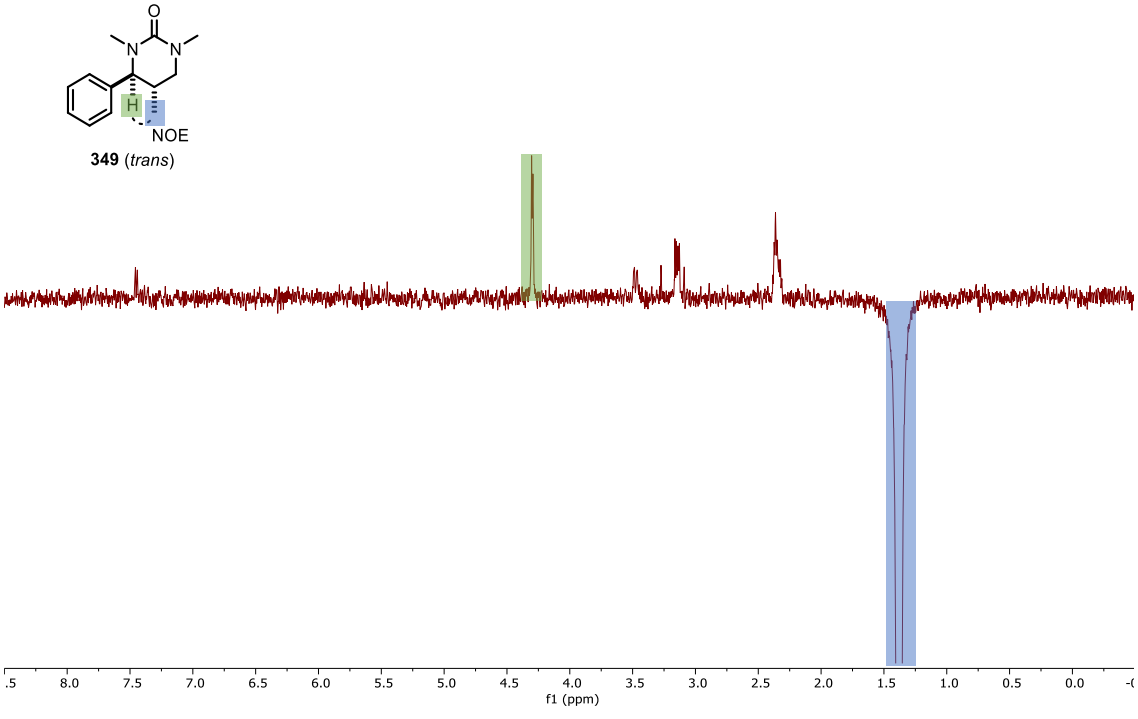

Figure A2. 1D NOESY (500 MHz, $CDCl_3$) of 349 (*trans*) (the methyl in blue was irradiated).

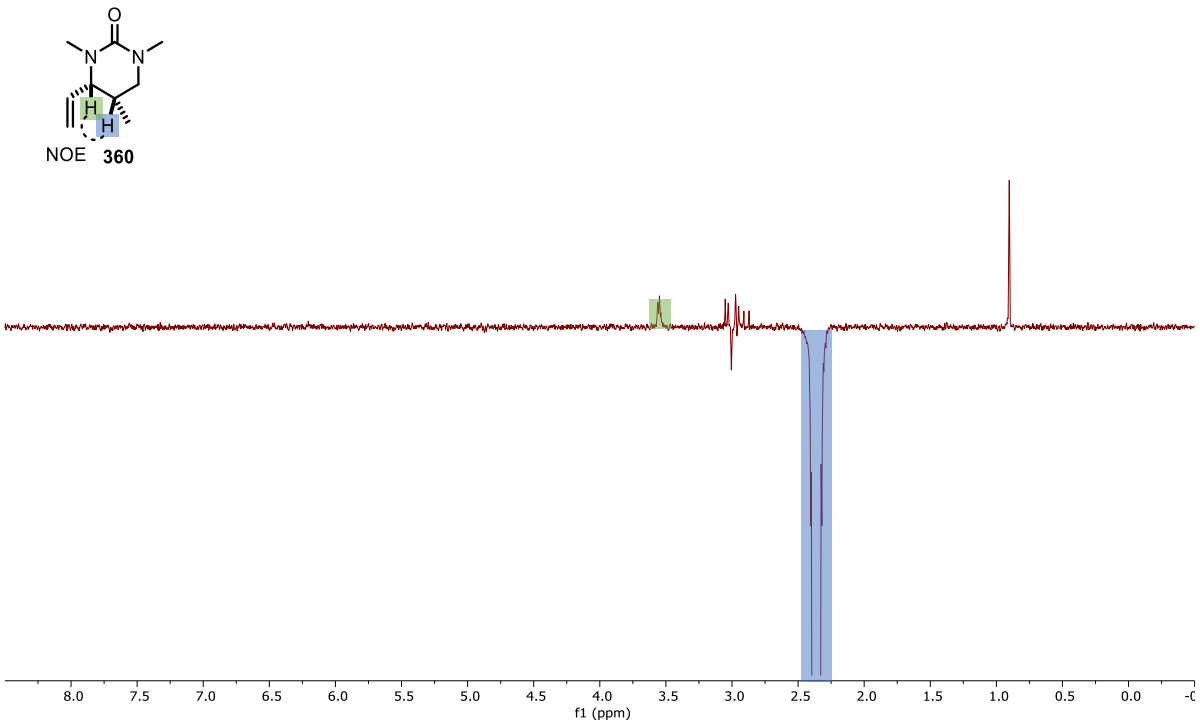

Figure A3. 1D NOESY (500 MHz, $CDCl_3$) of 360 (the proton in blue was irradiated).

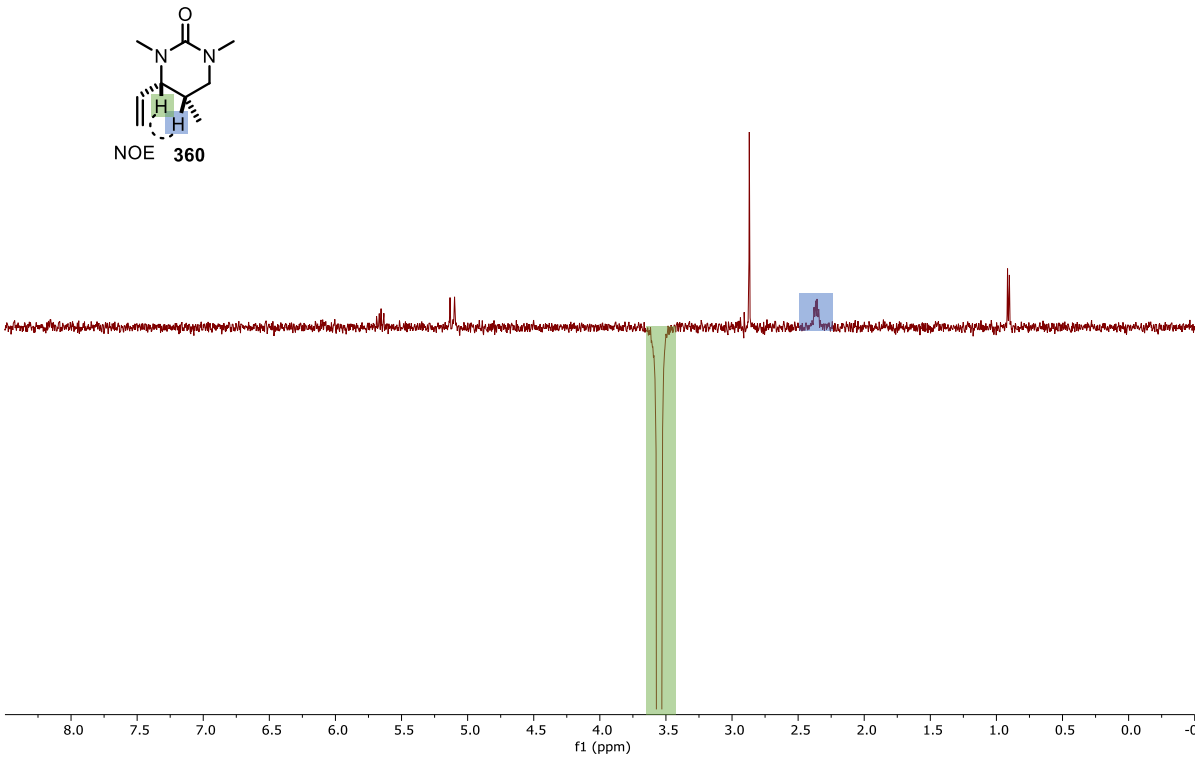

Figure A4. 1D NOESY (500 MHz, $CDCl_3$) of 360 (the proton in green was irradiated).

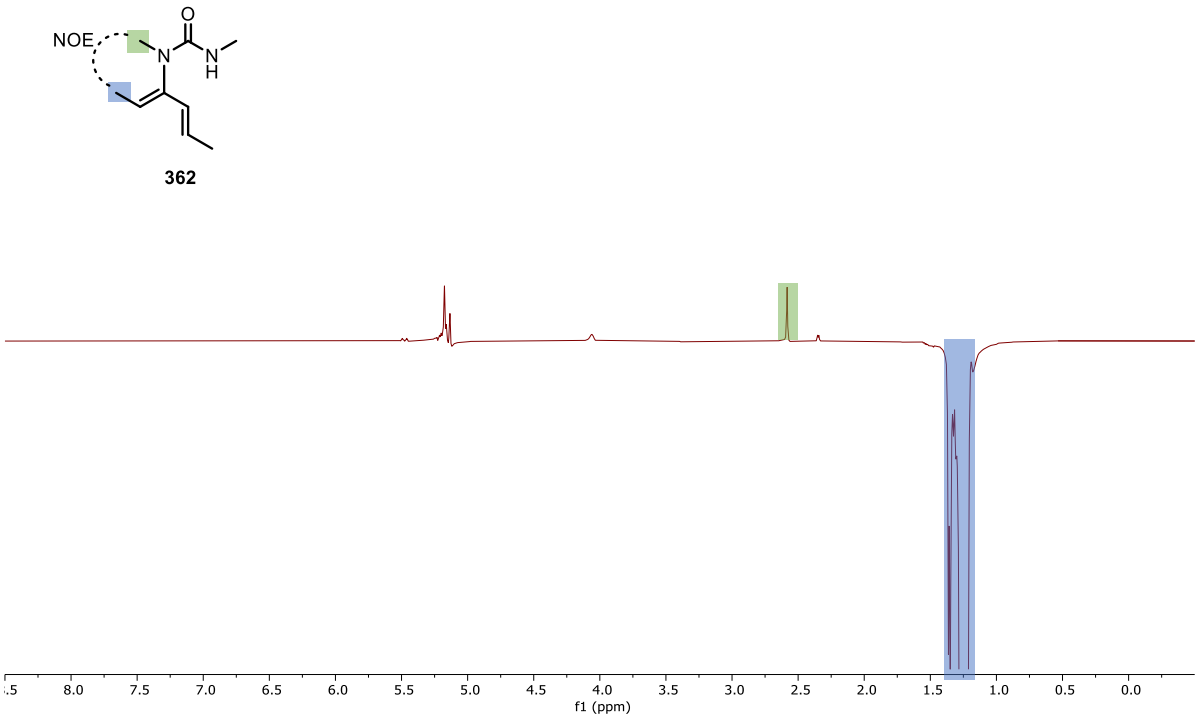

Figure A5. 1D NOESY (500 MHz, toluene-d_8) of 362 (the methyl in blue was irradiated).

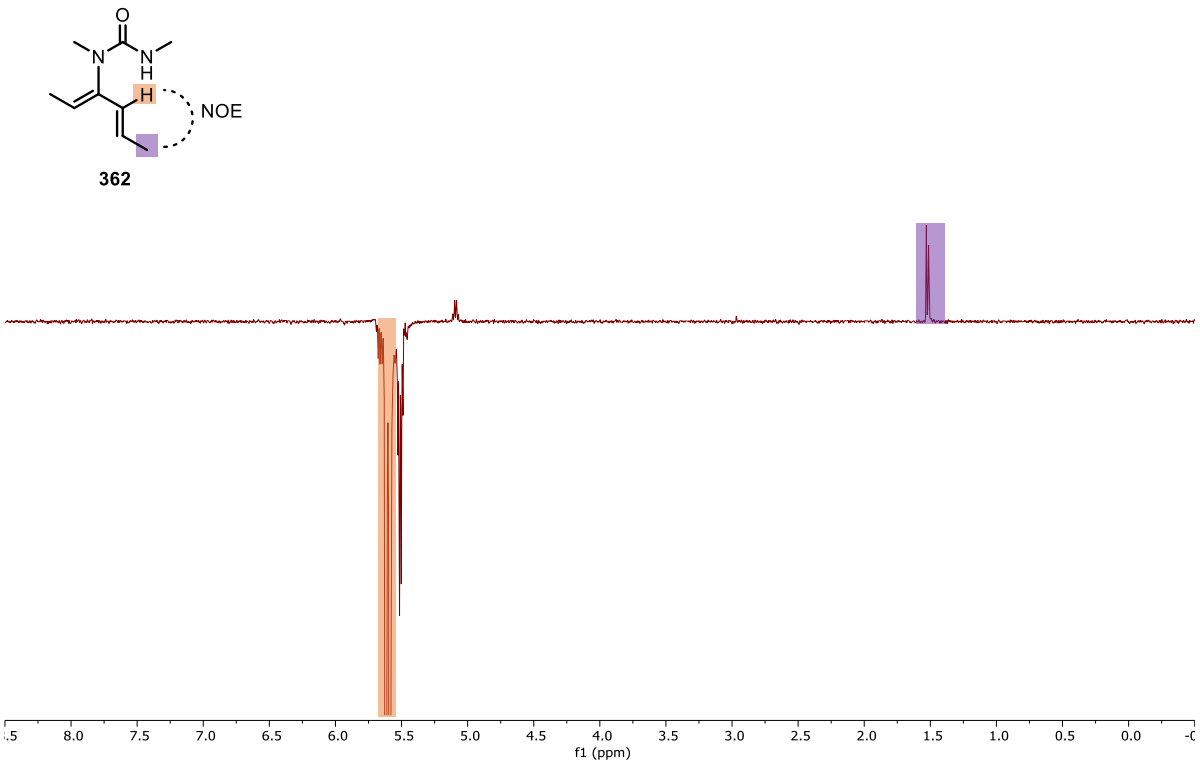

Figure A6. 1D NOESY (500 MHz, toluene-d_8) of 362 (the proton in orange was irradiated).

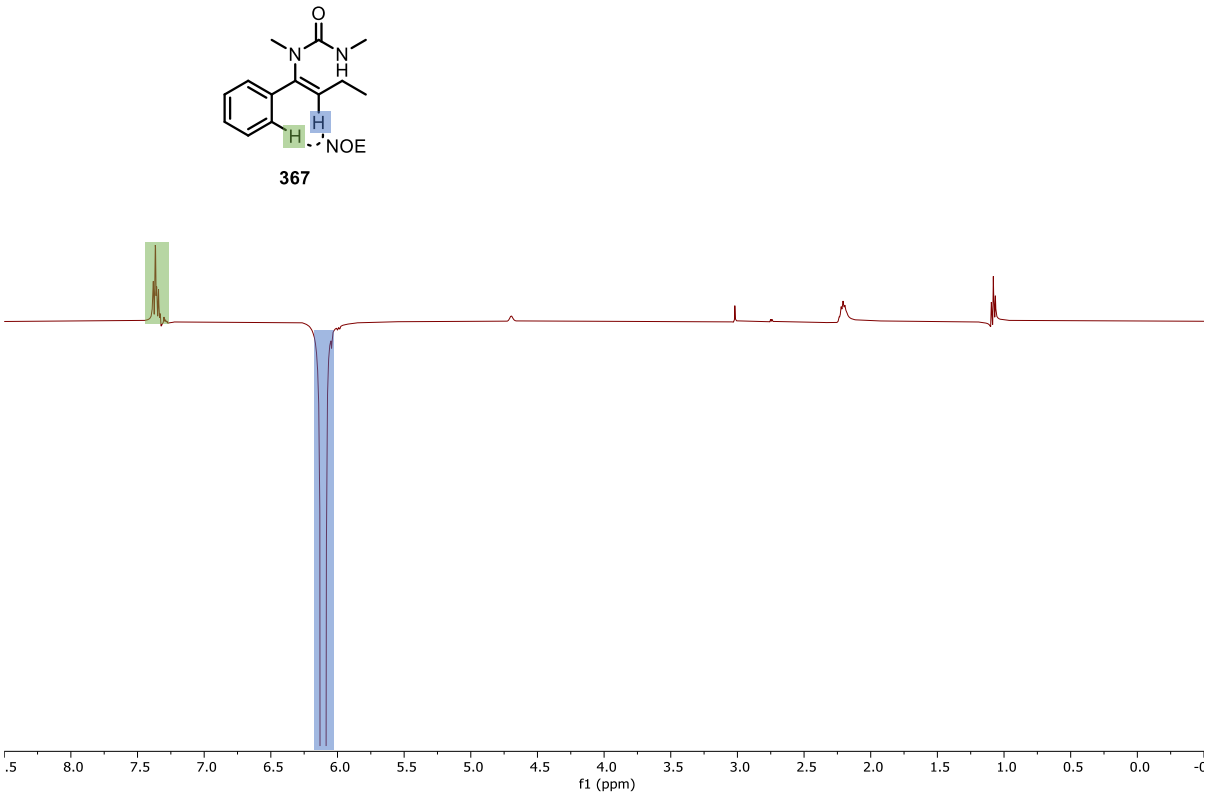

Figure A7. 1D NOESY (500 MHz, $CDCl_3$) of 367 (the proton in blue was irradiated).

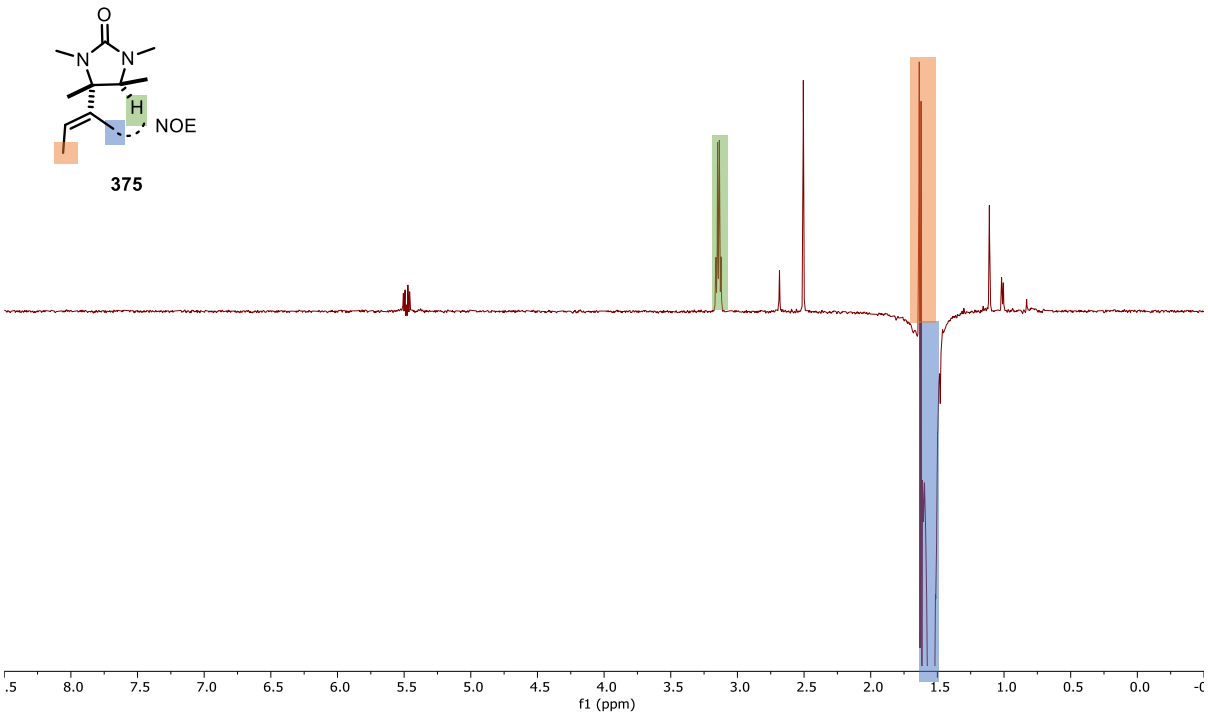

Figure A8. 1D NOESY (500 MHz, $CDCl_3$) of 375 (the methyl in blue was irradiated).

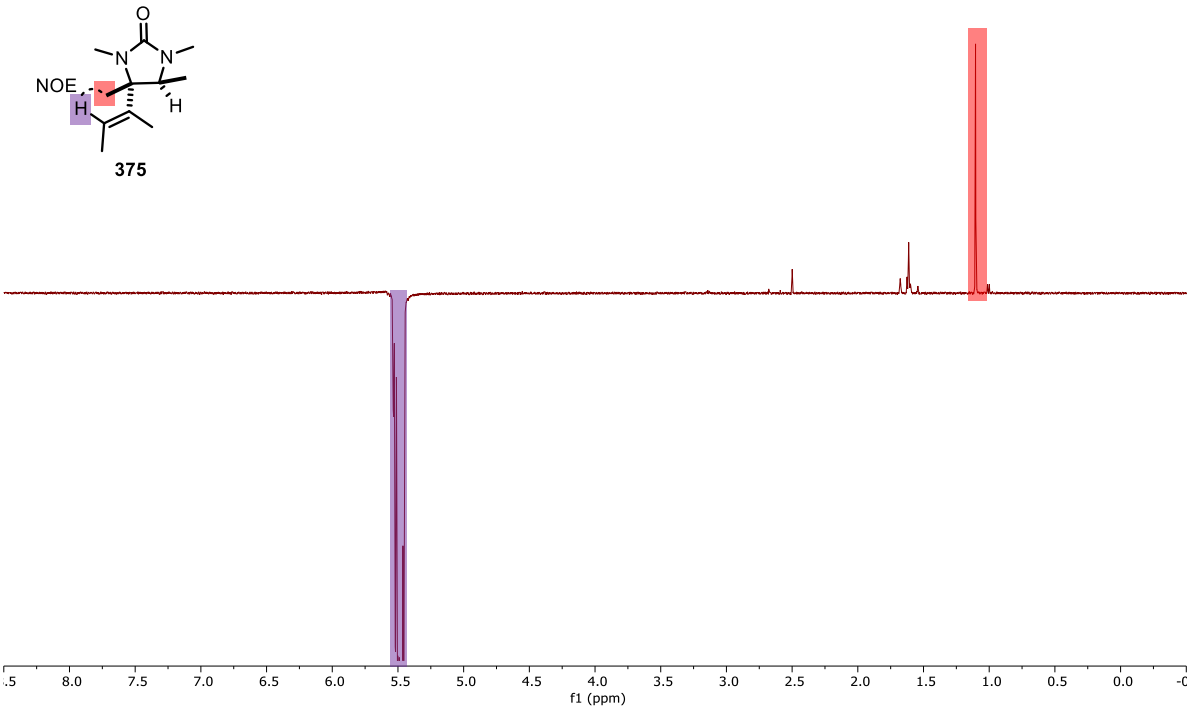

Figure A9. 1D NOESY (500 MHz, $CDCl_3$) of 375 (the proton in purple was irradiated).

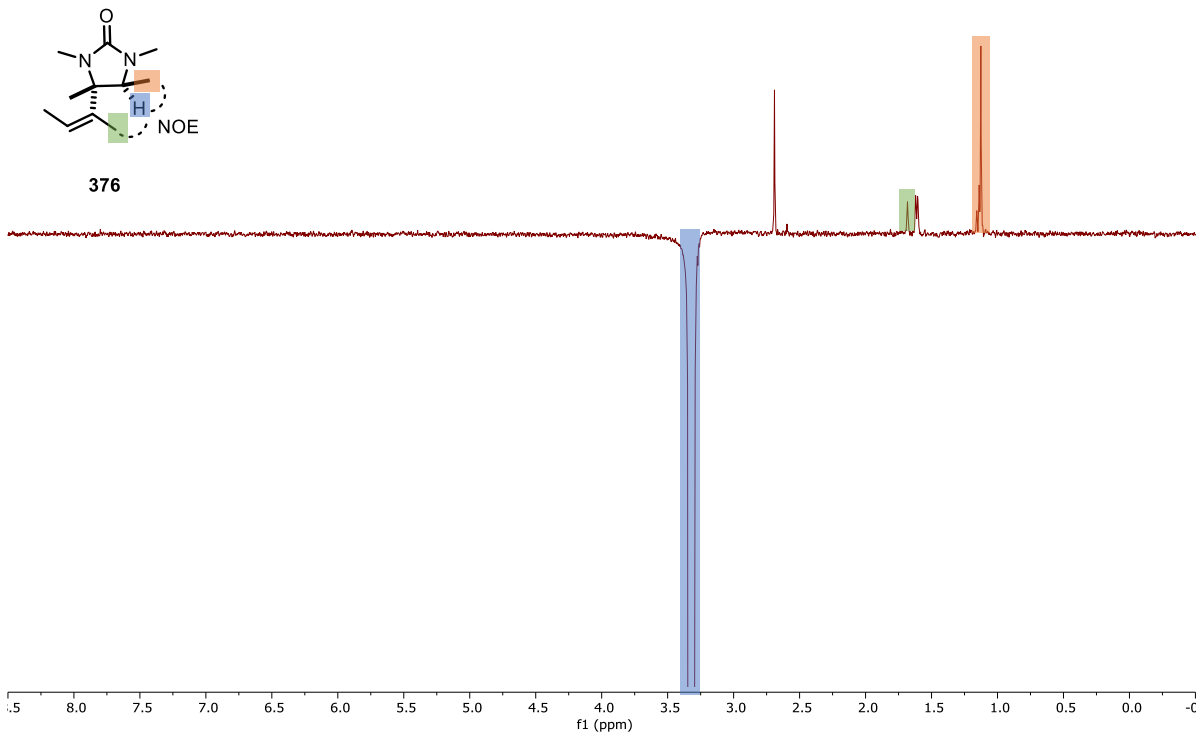

Figure A10. 1D NOESY (500 MHz, $CDCl_3$) of 376 (the proton in blue was irradiated).

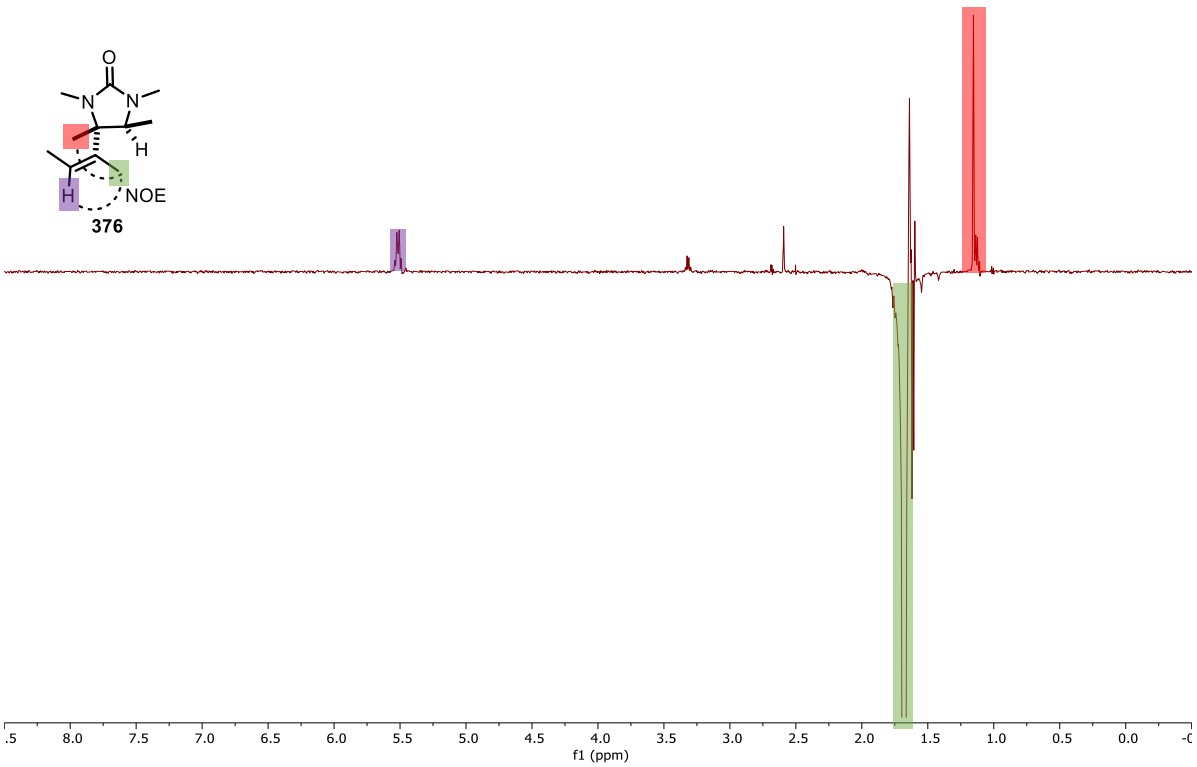

Figure A11. 1D NOESY (500 MHz, $CDCl_3$) of 376 (the methyl in green was irradiated).

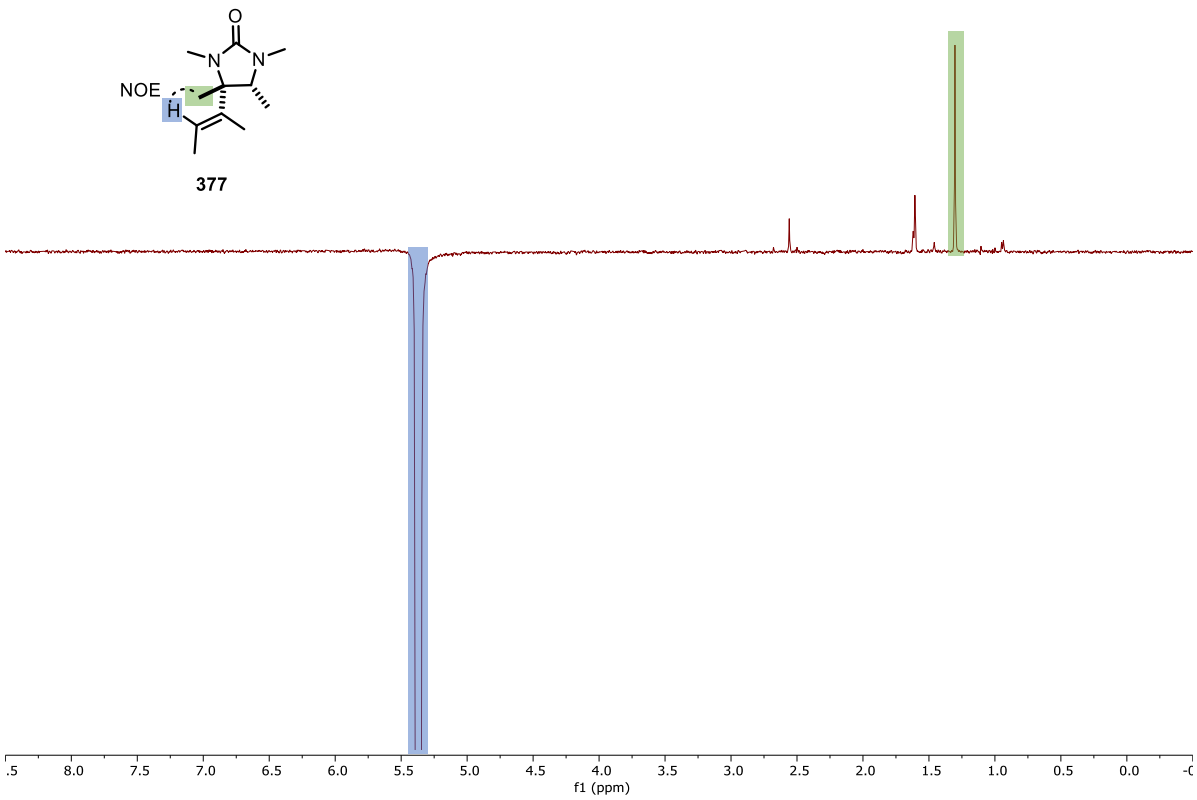

Figure A12. 1D NOESY (500 MHz, $CDCl_3$) of 377 (the proton in blue was irradiated).

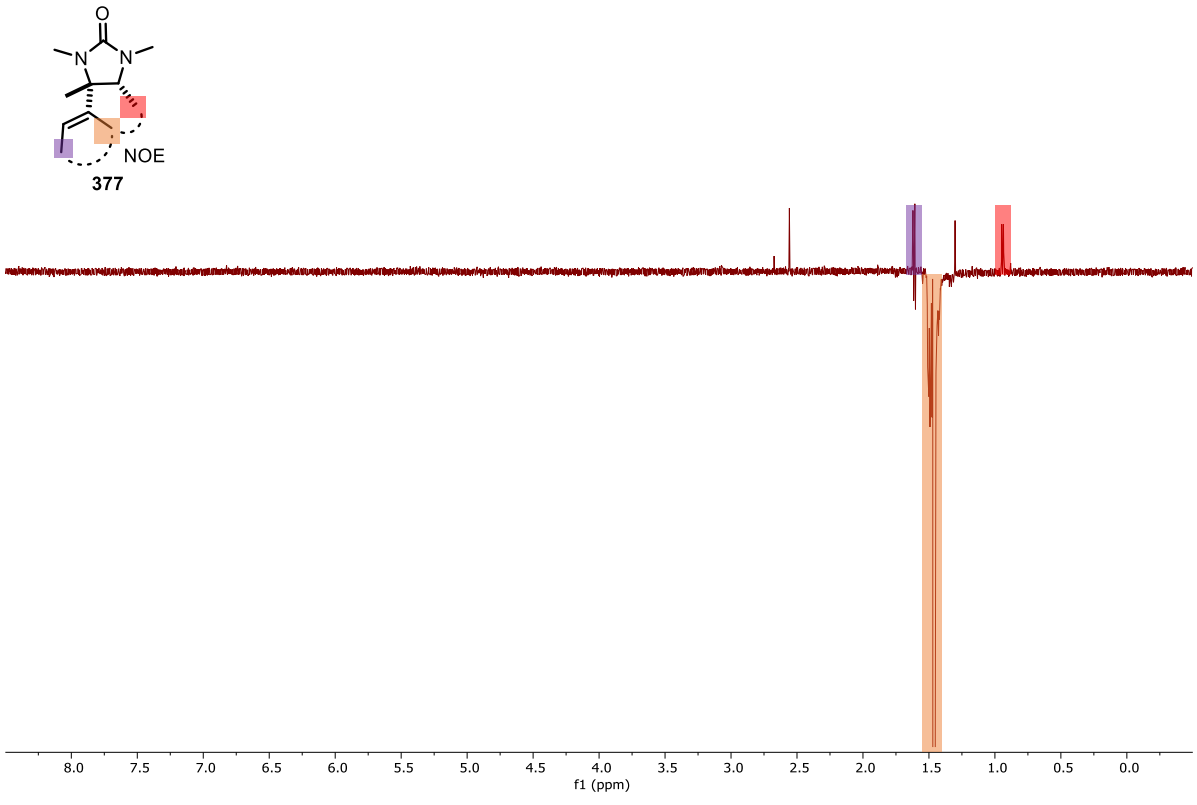

Figure A13. 1D NOESY (500 MHz, $CDCl_3$) of 377 (the methyl in orange was irradiated).

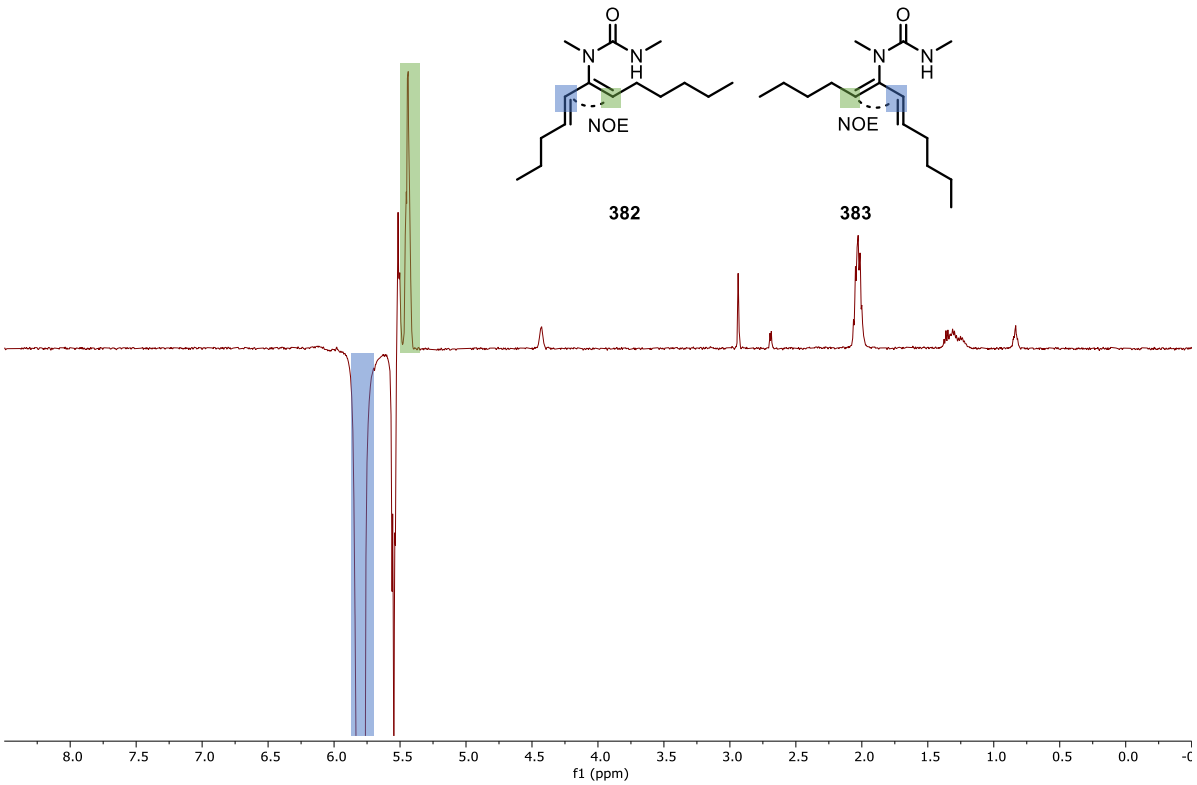

Figure A14. 1D NOESY (500 MHz, $CDCl_3$) of 382 and 383 (the proton in blue was irradiated).

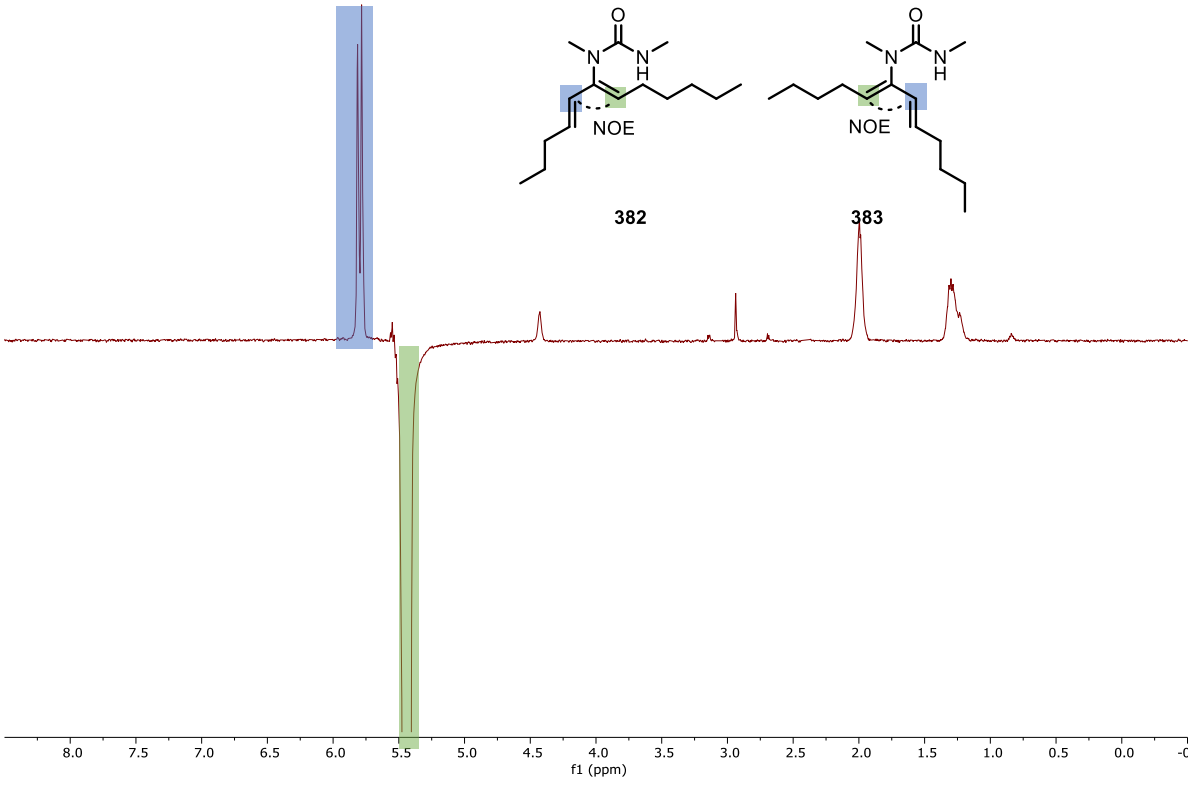

Figure A15. 1D NOESY (500 MHz, $CDCl_3$) of 382 and 383 (the proton in green was irradiated).

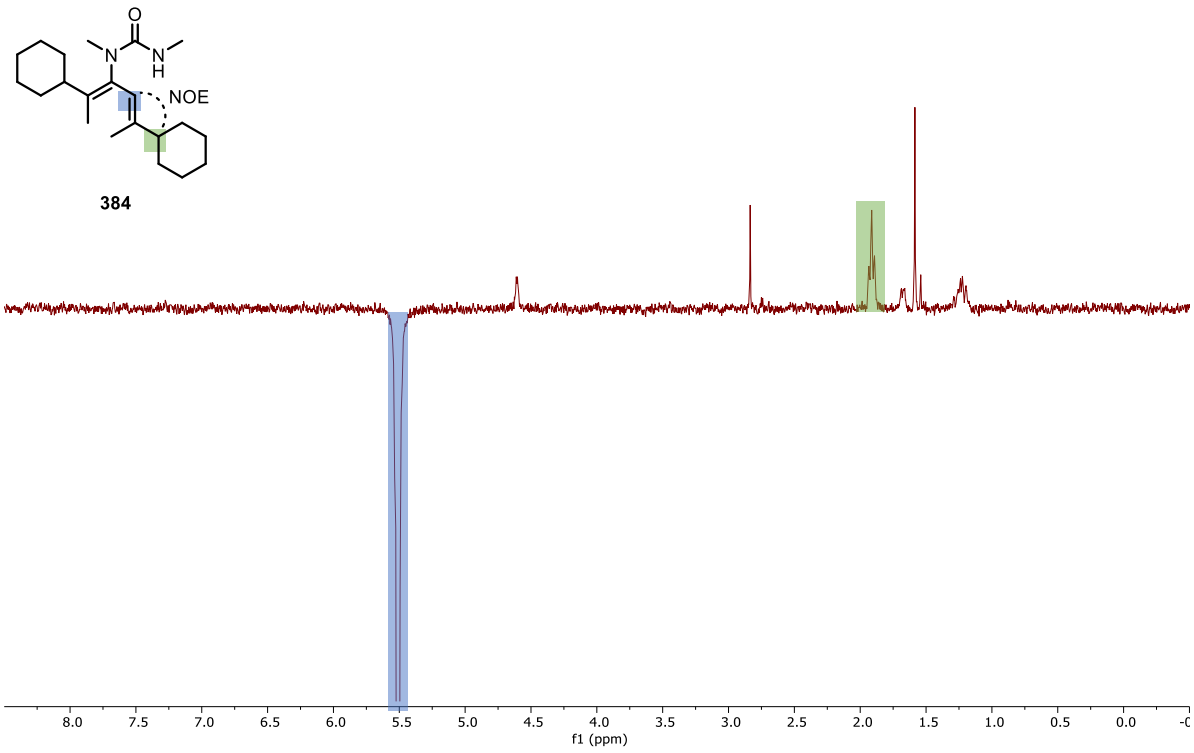

Figure A16. 1D NOESY (500 MHz, $CDCl_3$) of 384 (the proton in blue was irradiated).

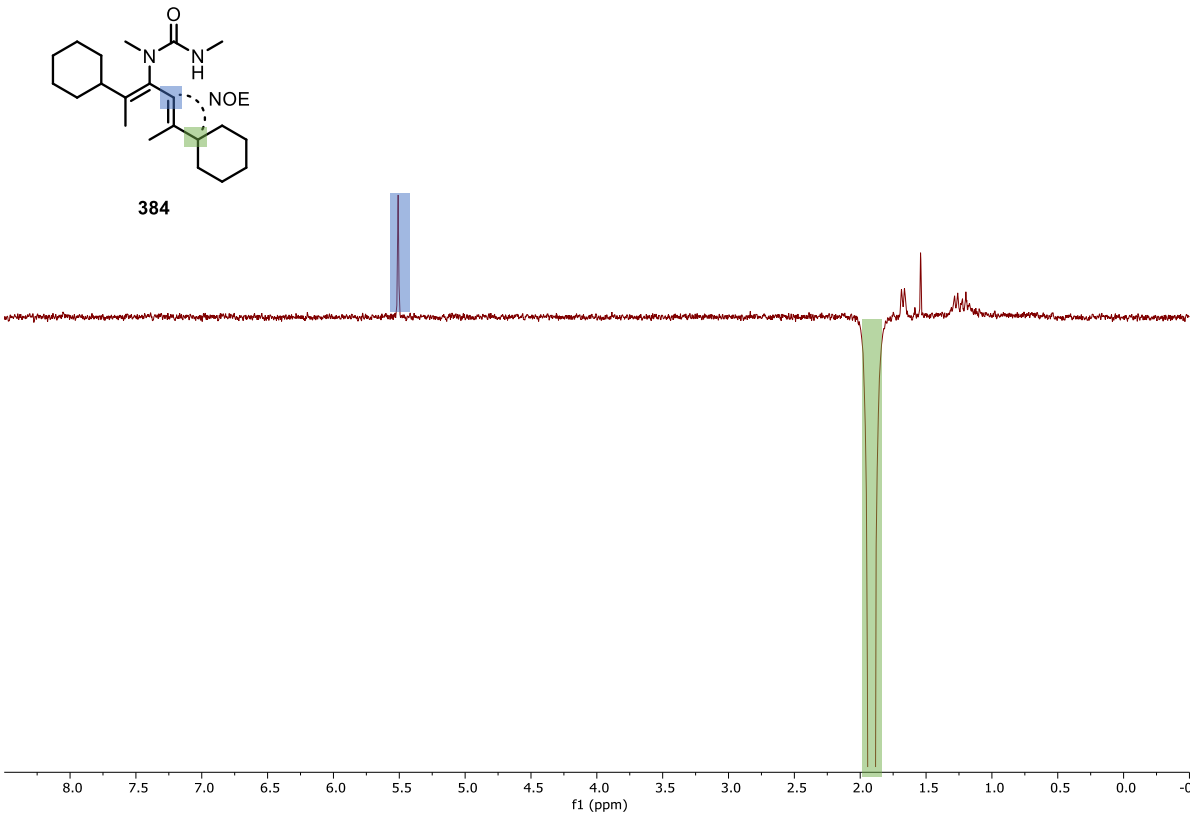

Figure A17. 1D NOESY (500 MHz, $CDCl_3$) of 384 (the proton in green was irradiated).

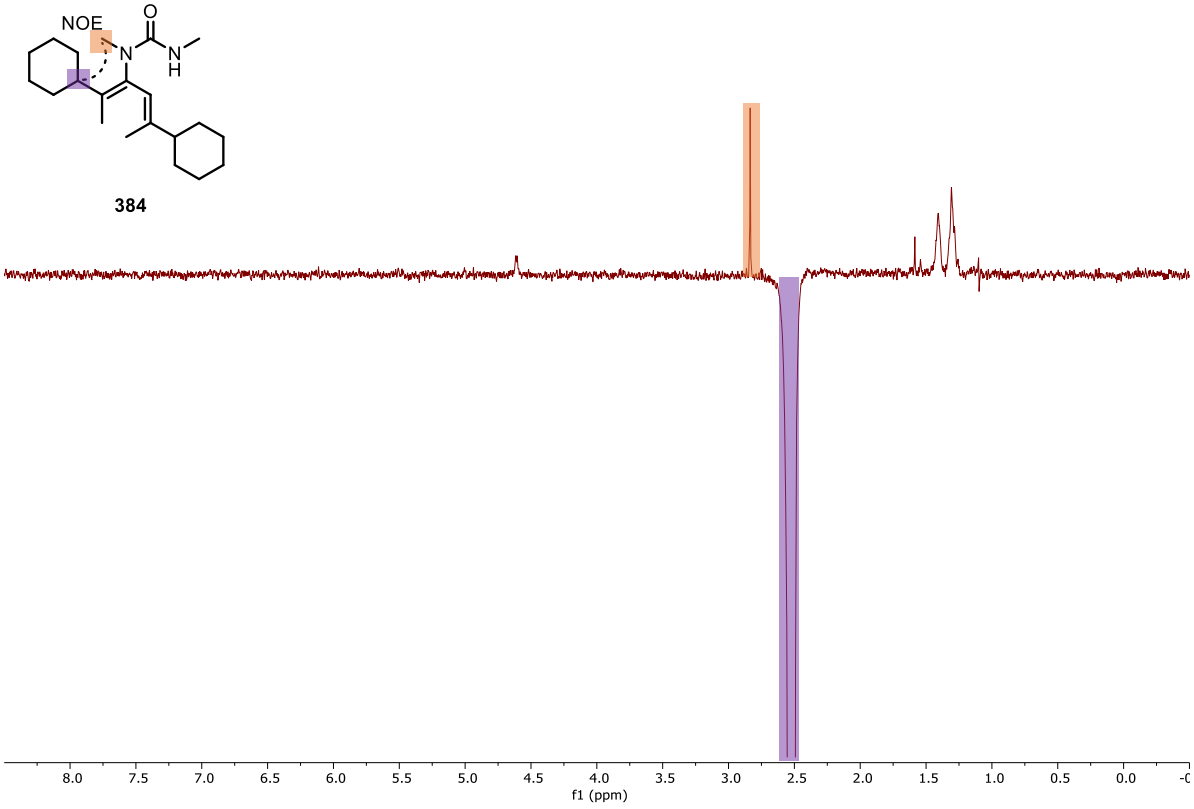

Figure A18. 1D NOESY (500 MHz, $CDCl_3$) of 384 (the proton in purple was irradiated).

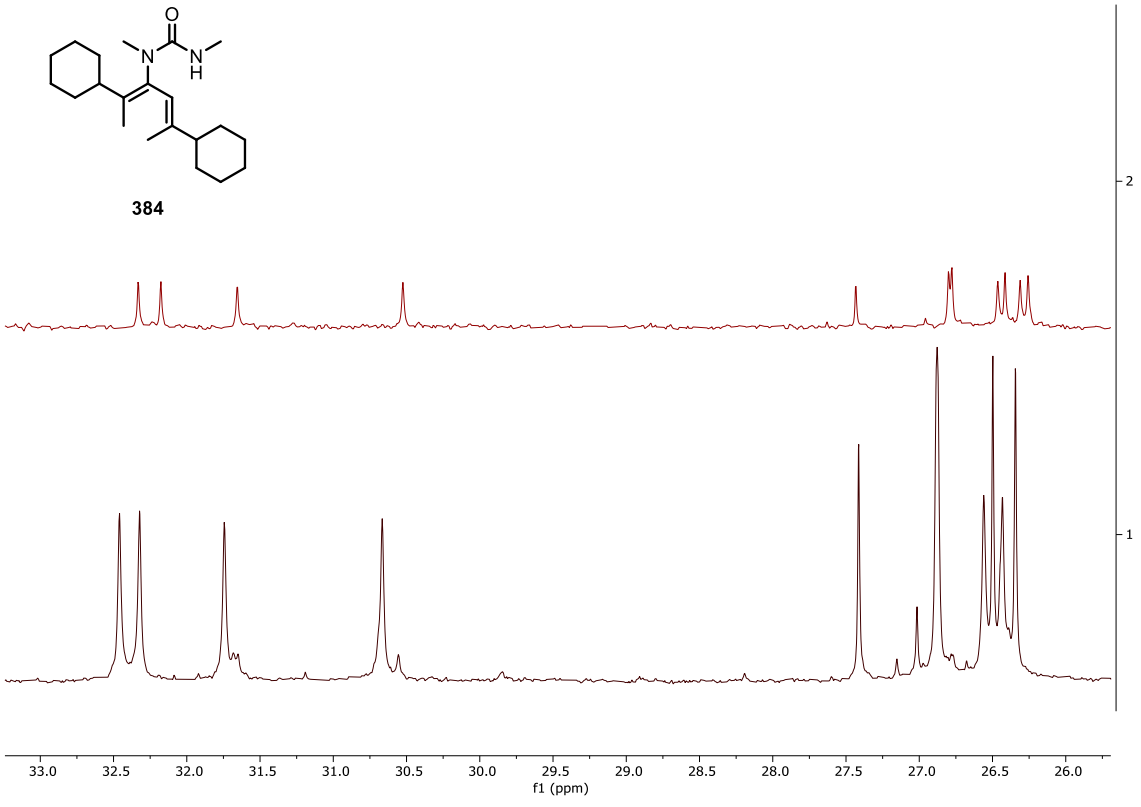

Figure A19. VT ^{13}C NMR of 384 (top was recorded at room temperature; bottom was recorded at 55 °C).

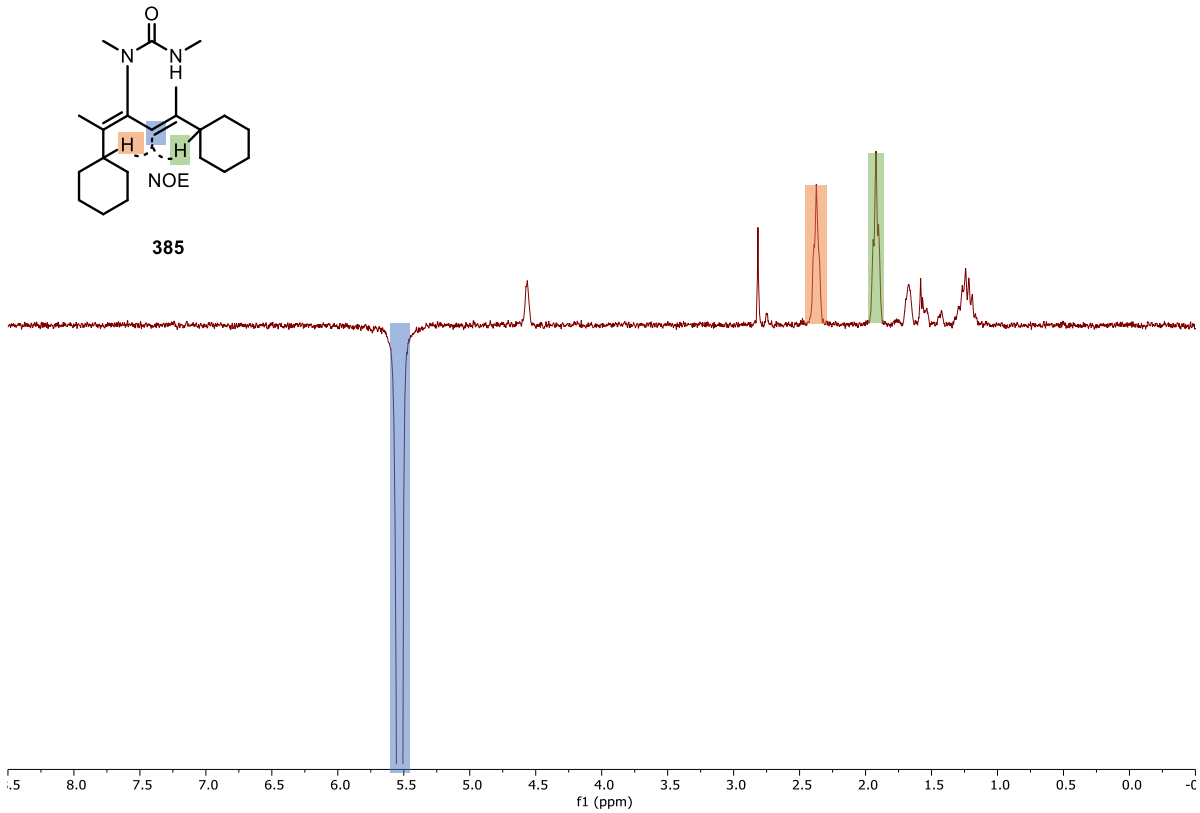

Figure A20. 1D NOESY (500 MHz, $CDCl_3$) of 385 (the proton in blue was irradiated).

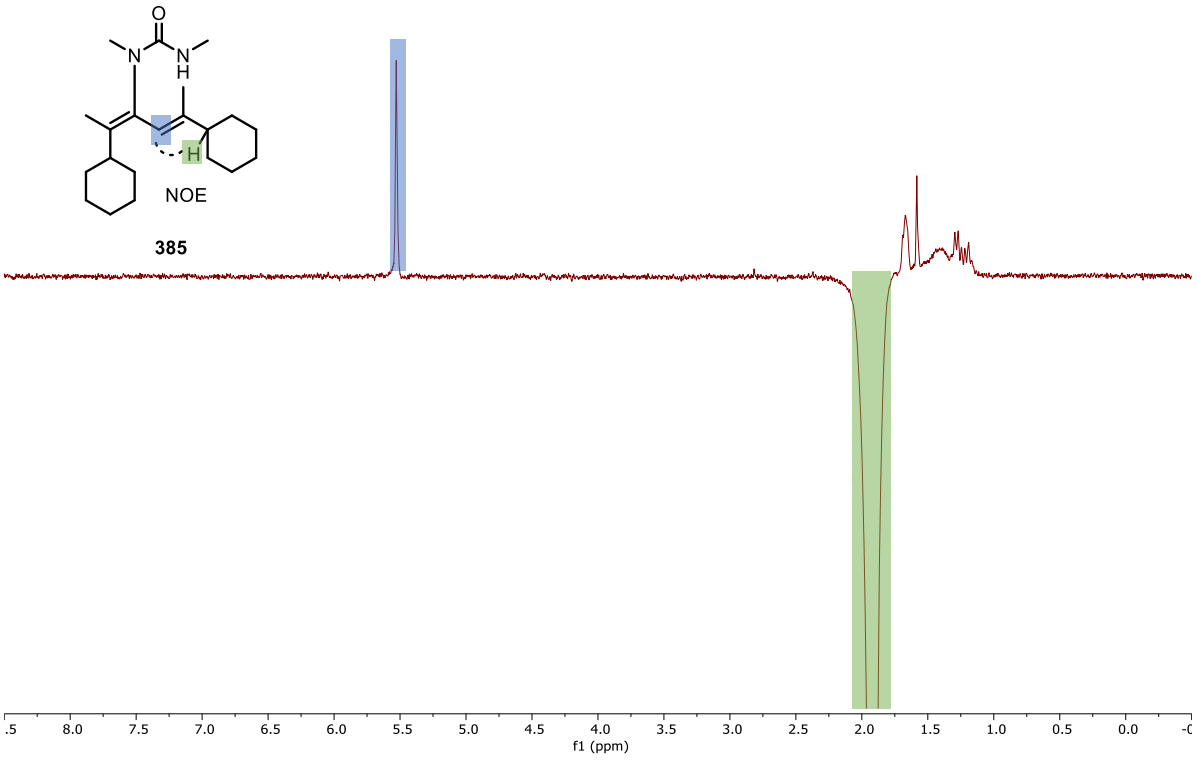

Figure A21. 1D NOESY (500 MHz, $CDCl_3$) of 385 (the proton in green was irradiated).

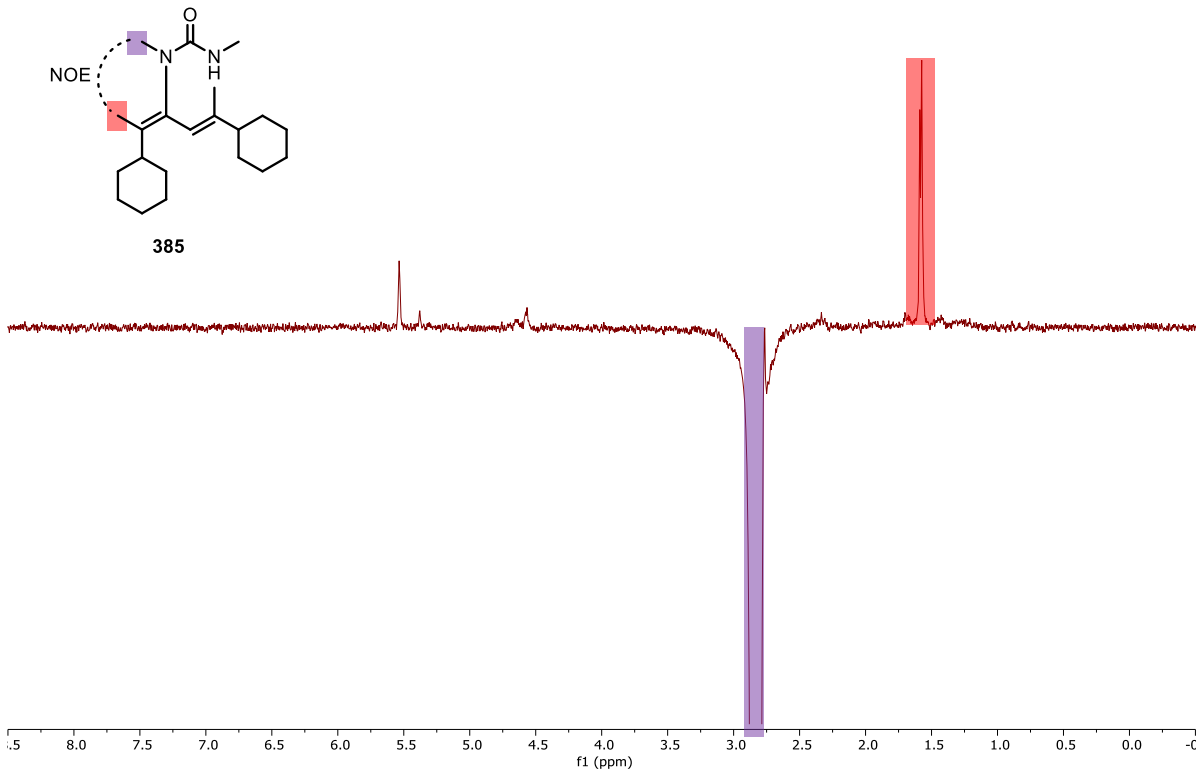

Figure A22. 1D NOESY (500 MHz, $CDCl_3$) of 385 (the methyl in purple was irradiated).

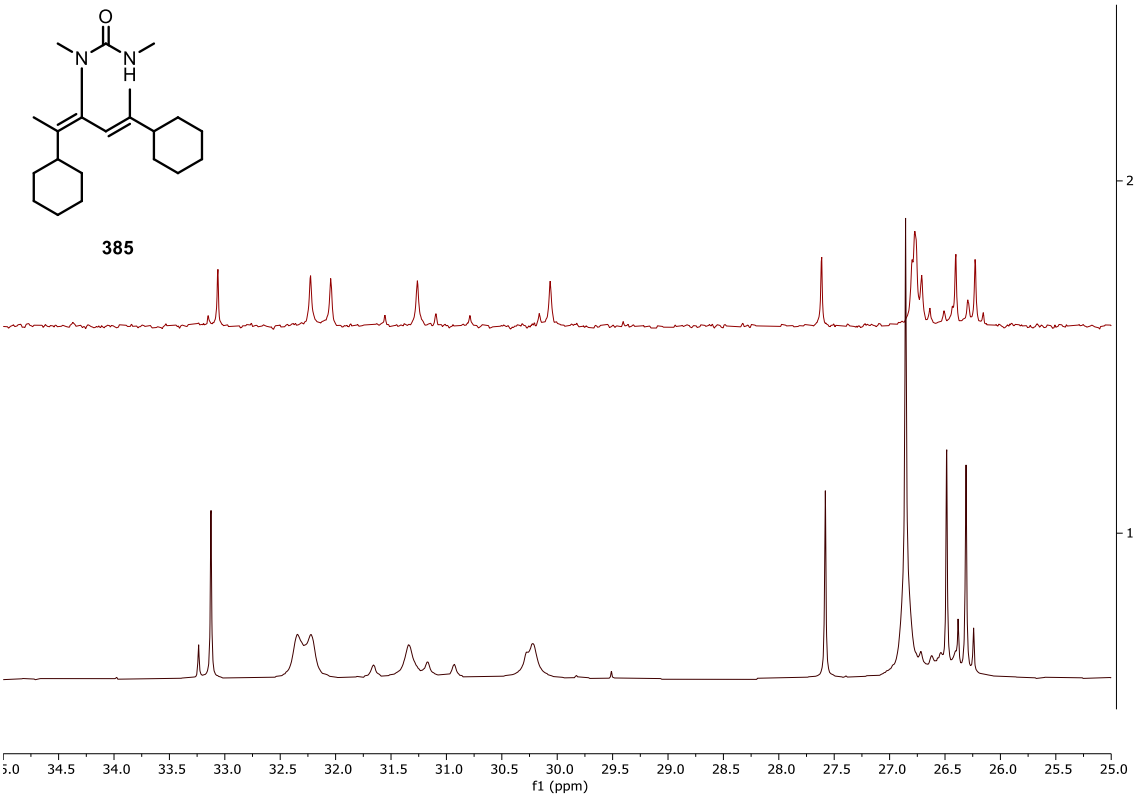

Figure A23. VT ^{13}C NMR of 385 (top was recorded at room temperature; bottom was recorded at 55 °C).

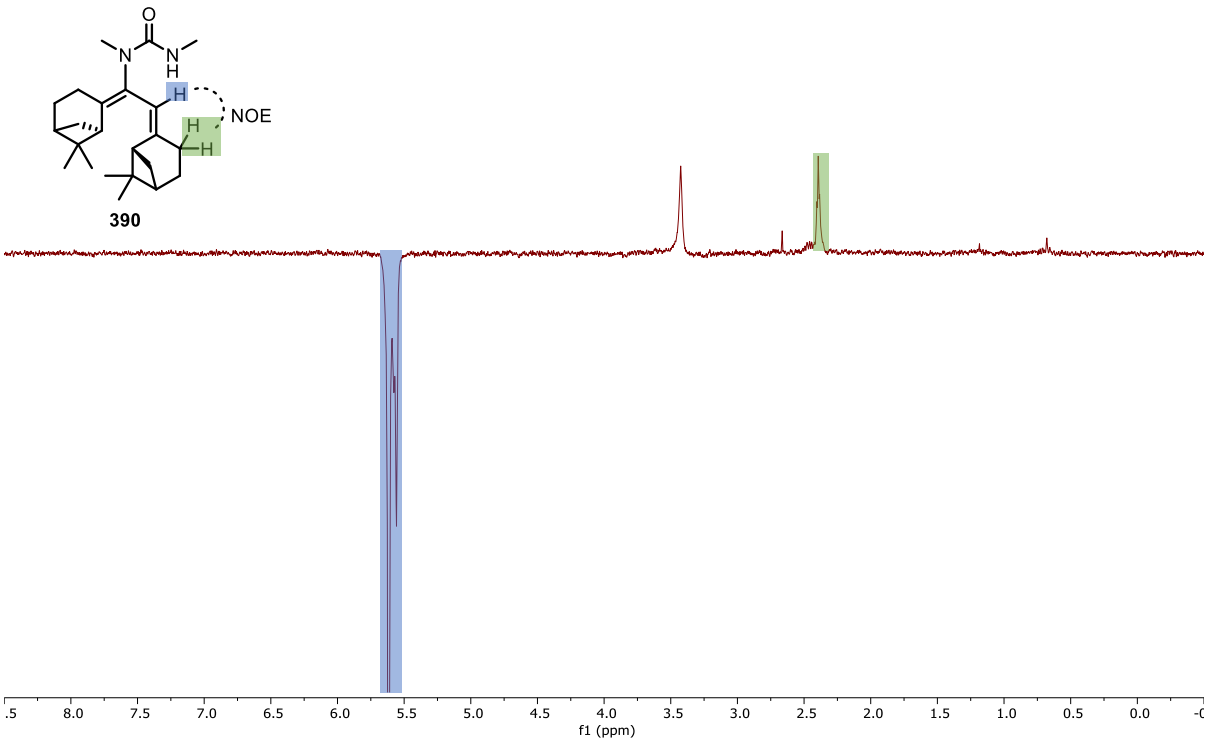

Figure A24. 1D NOESY (500 MHz, $CDCl_3$) of 390 (the proton in blue was irradiated).

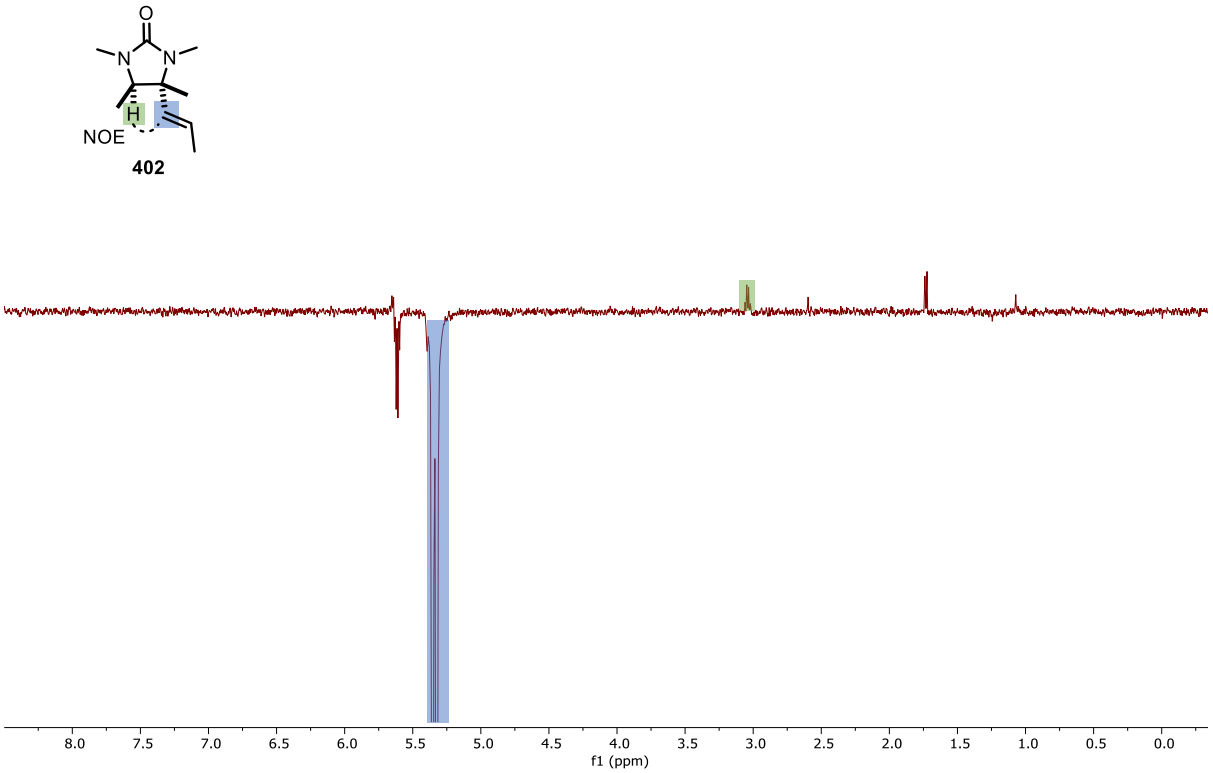

Figure A25. 1D NOESY (500 MHz, $CDCl_3$) of 402 (the proton in blue was irradiated).

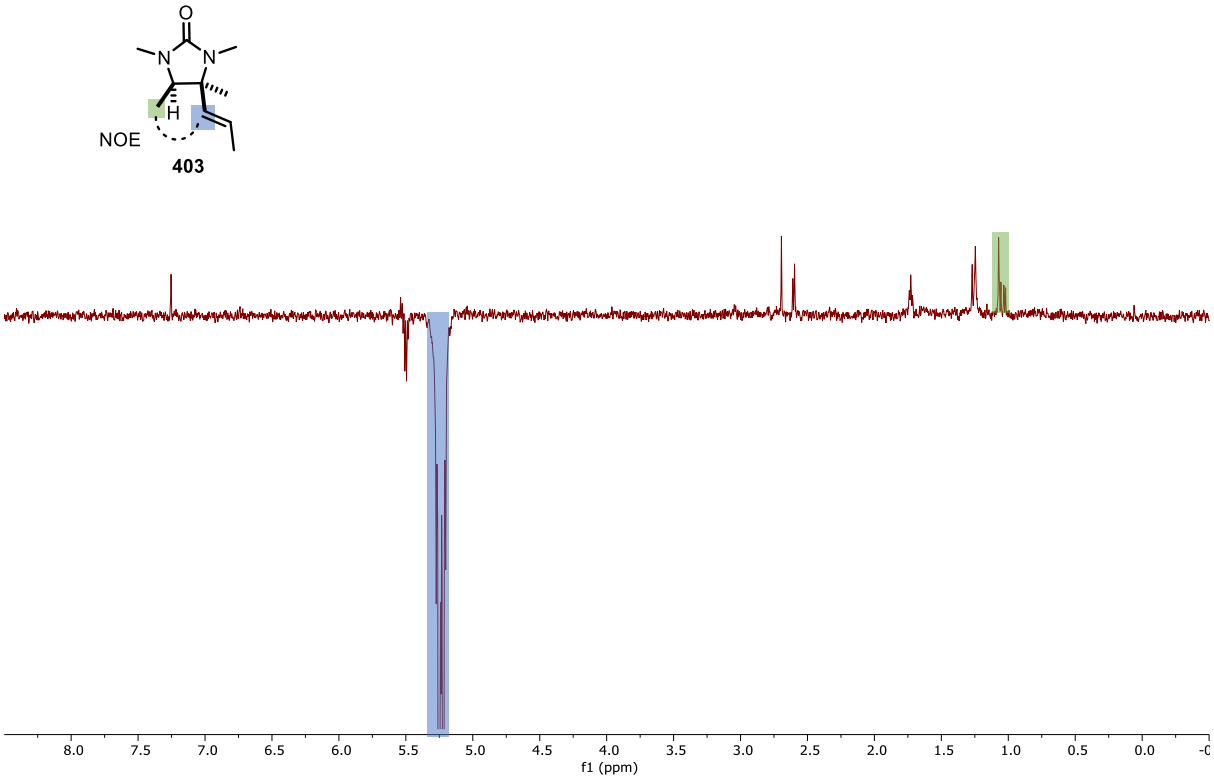

Figure A26. 1D NOESY (500 MHz, $CDCl_3$) of 403 (the proton in blue was irradiated).

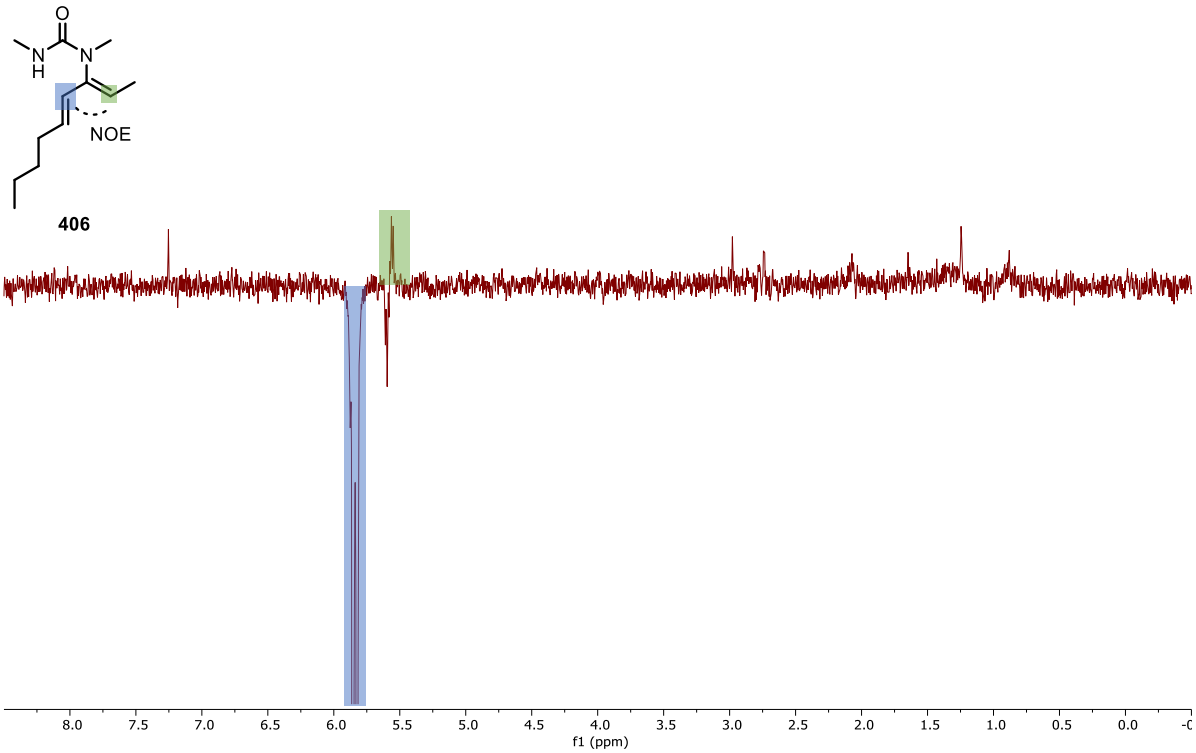

Figure A27. 1D NOESY (500 MHz, $CDCl_3$) of 406 (the proton in blue was irradiated).

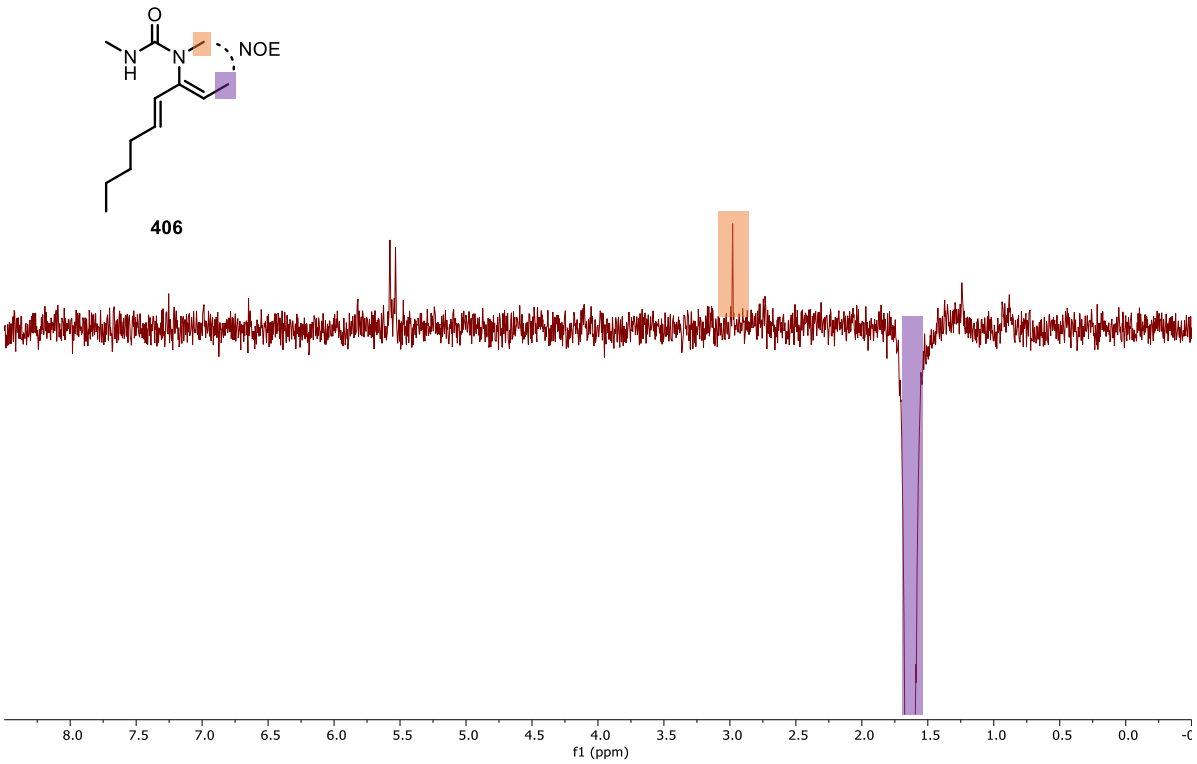

Figure A28. 1D NOESY (500 MHz, $CDCl_3$) of 406 (the methyl in purple was irradiated).

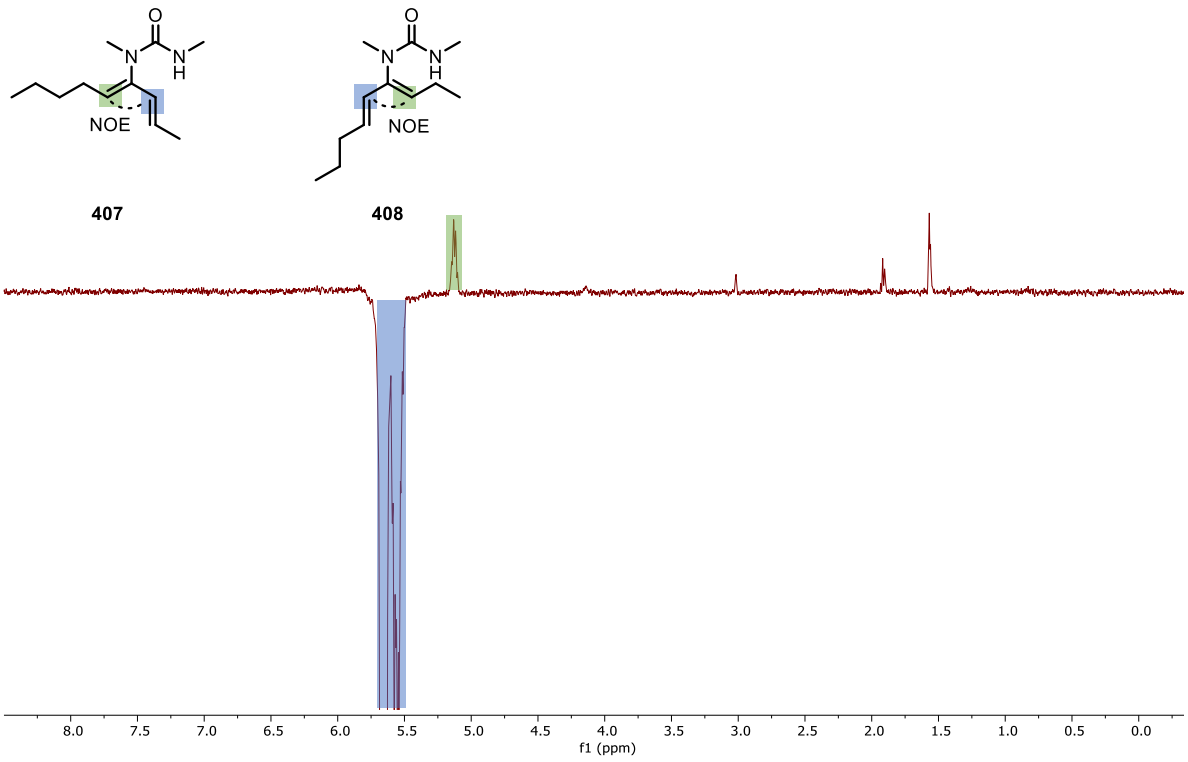

Figure A29. 1D NOESY (500 MHz, $CDCl_3$) of 407 and 408 (the proton in blue was irradiated).

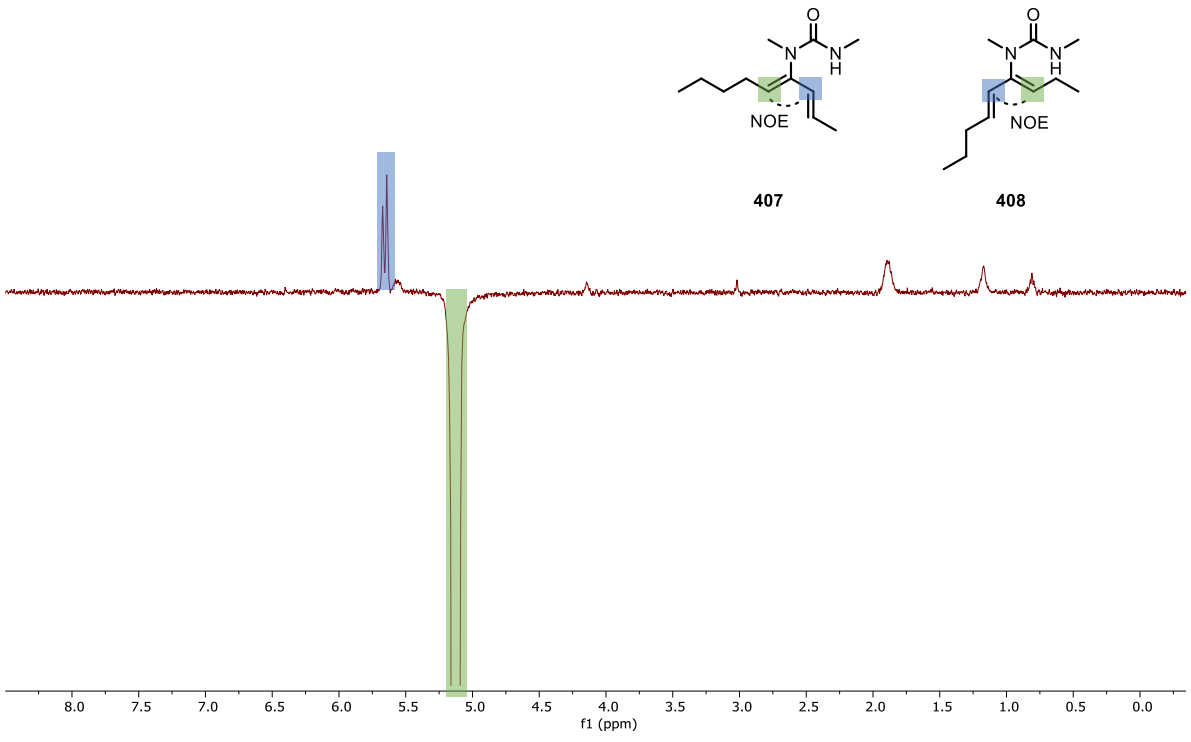

Figure A30. 1D NOESY (500 MHz, $CDCl_3$) of 407 and 408 (the proton in green was irradiated).

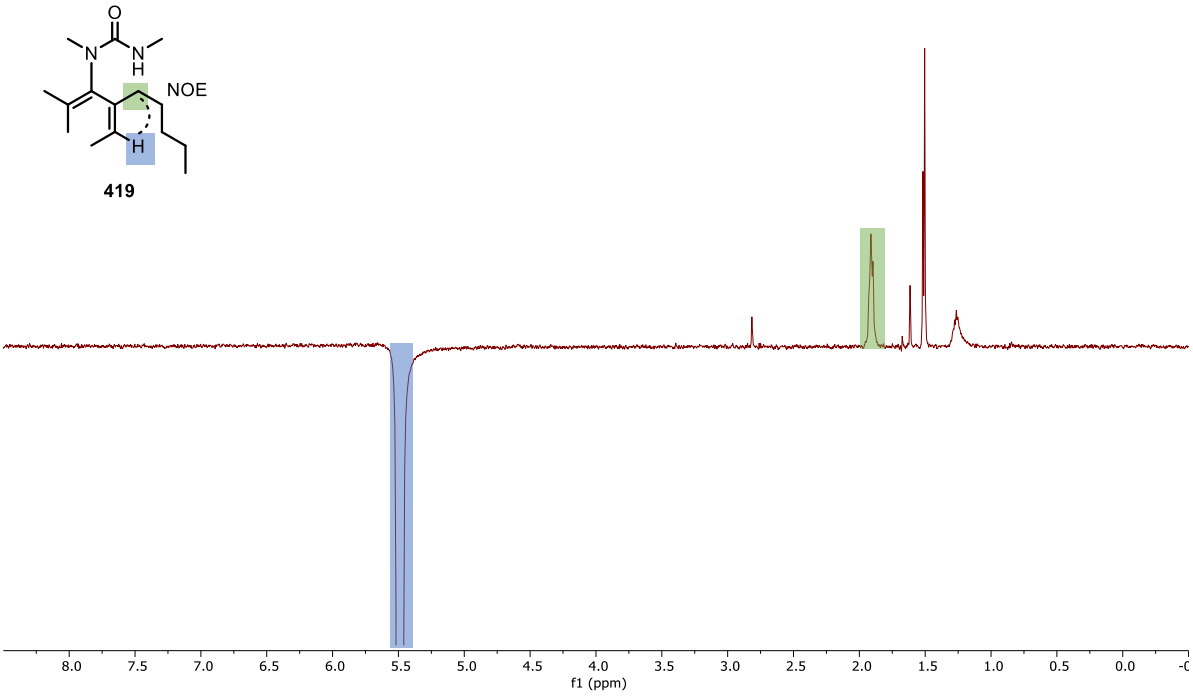

Figure A31. 1D NOESY (500 MHz, $CDCl_3$) of 419 (the proton in blue was irradiated).

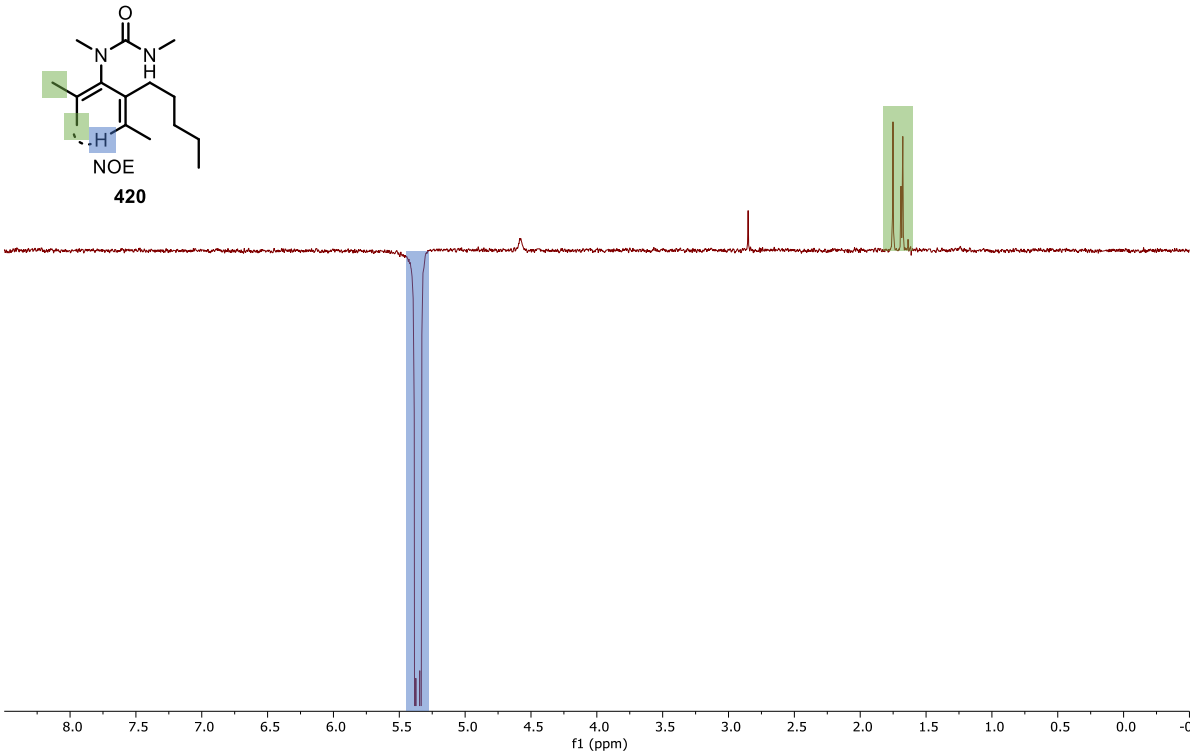

Figure A32. 1D NOESY (500 MHz, $CDCl_3$) of 420 (the proton in blue was irradiated).

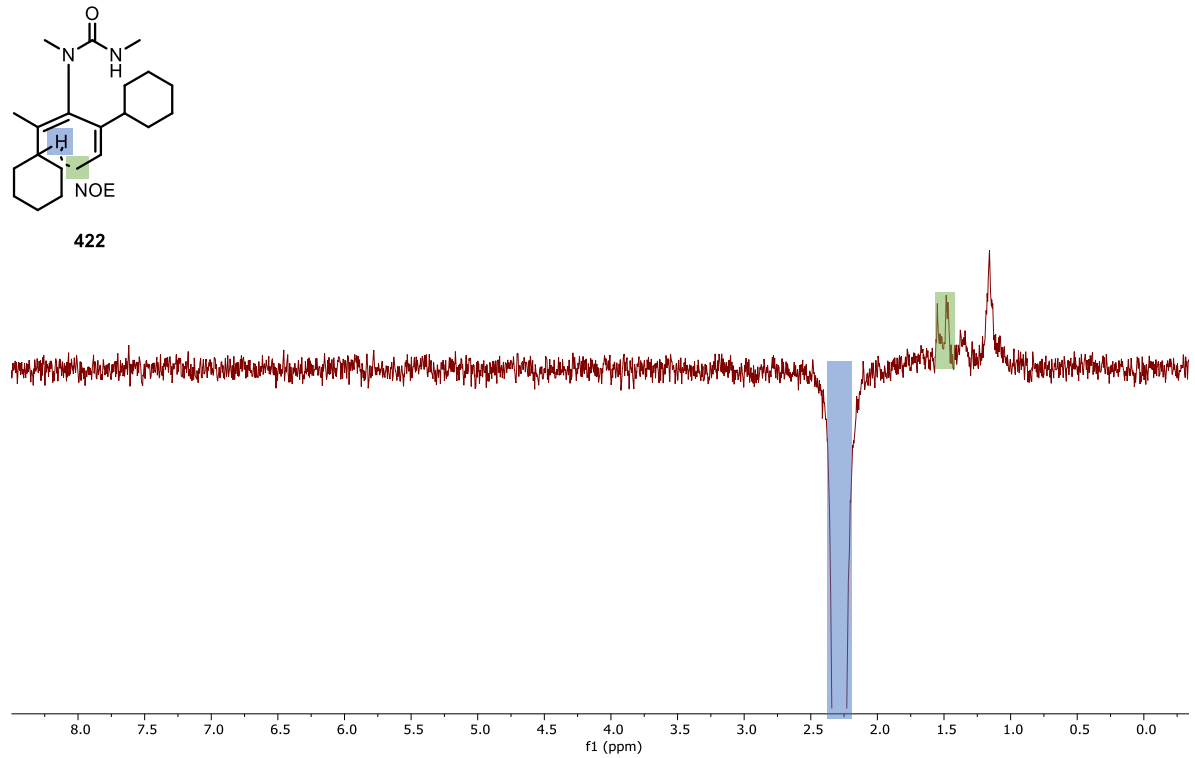

Figure A33. 1D NOESY (500 MHz, $CDCl_3$) of 422 (the proton in blue was irradiated).

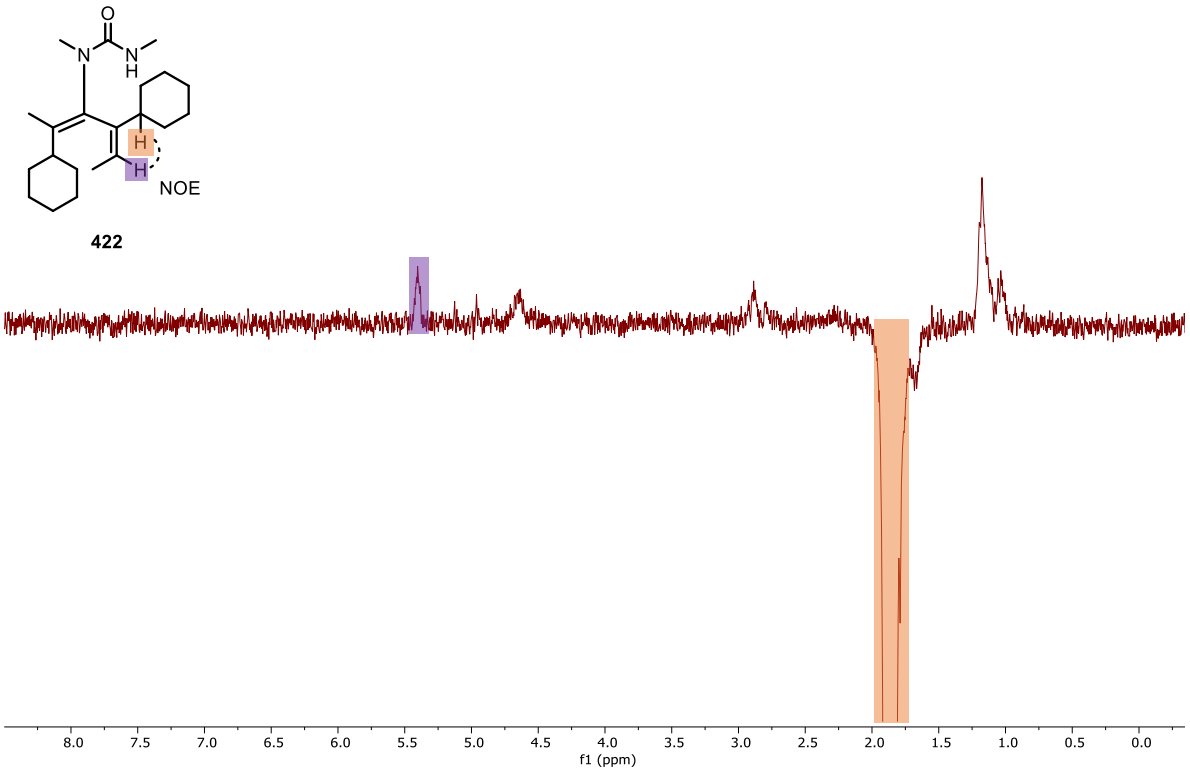

Figure A34. 1D NOESY (500 MHz, $CDCl_3$) of 422 (the proton in orange was irradiated).

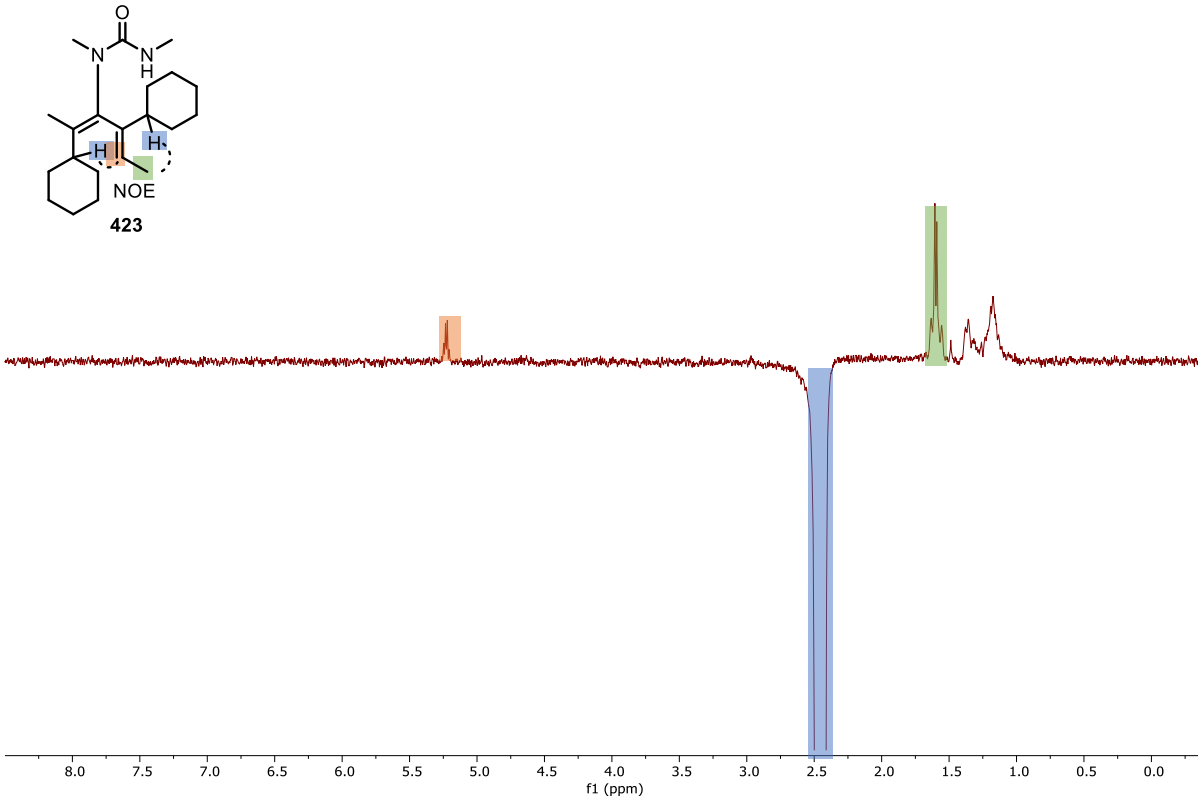

Figure A35. 1D NOESY (500 MHz, $CDCl_3$) of 423 (the protons in blue were irradiated).

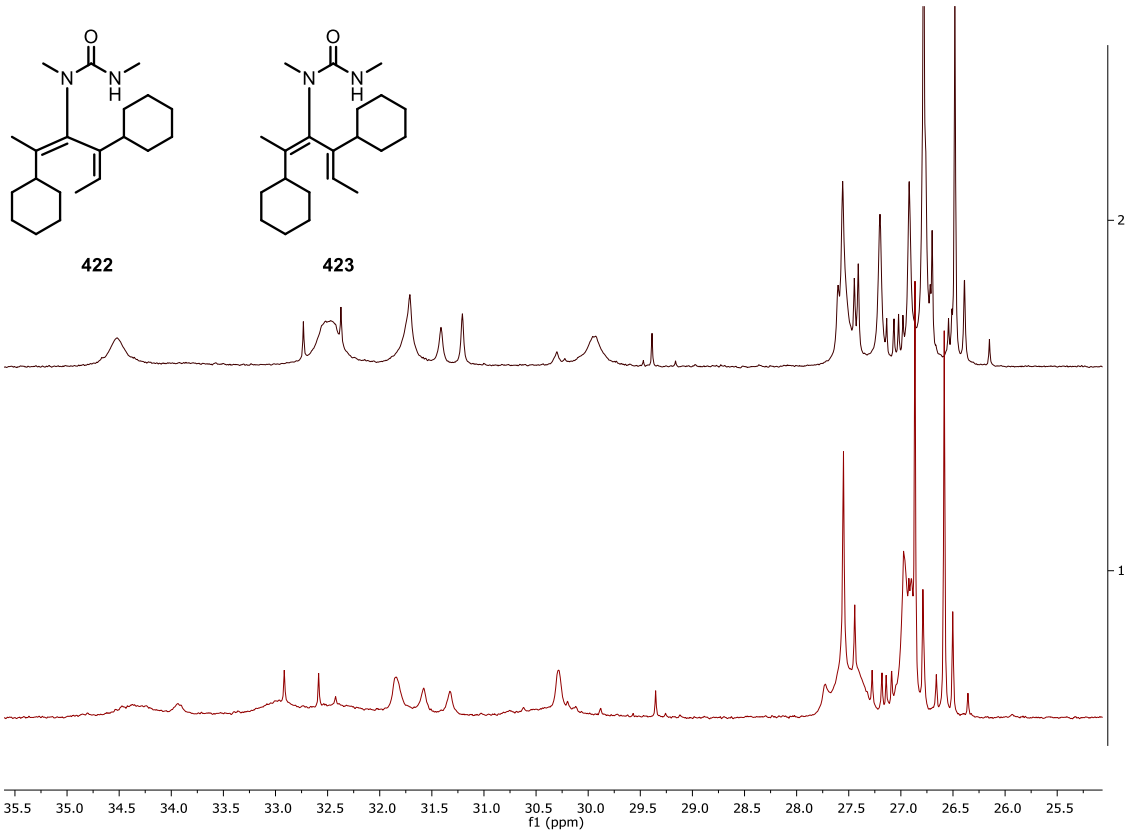

Figure A36. VT ^{13}C NMR of 422 and 423 (top was recorded at room temperature; bottom was recorded at 55 °C).

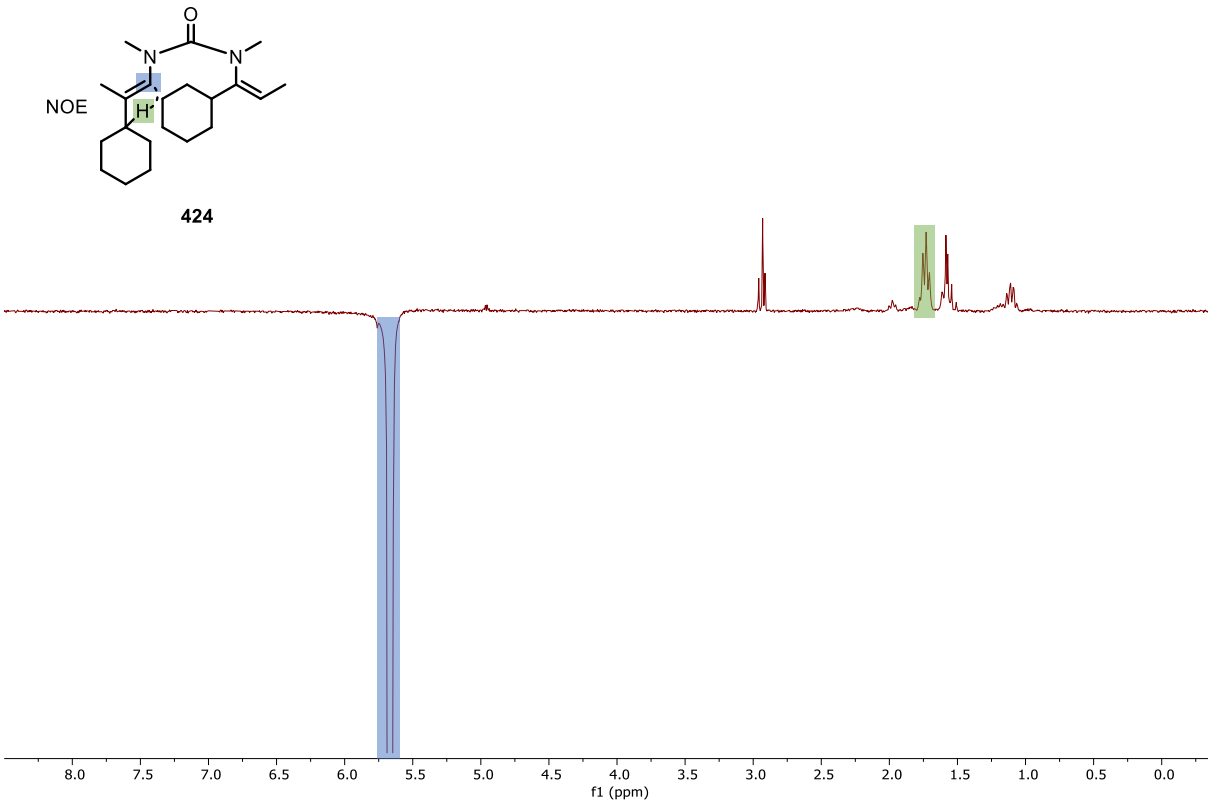

Figure A37. 1D NOESY (500 MHz, $CDCl_3$) of 424 (the proton in blue was irradiated).

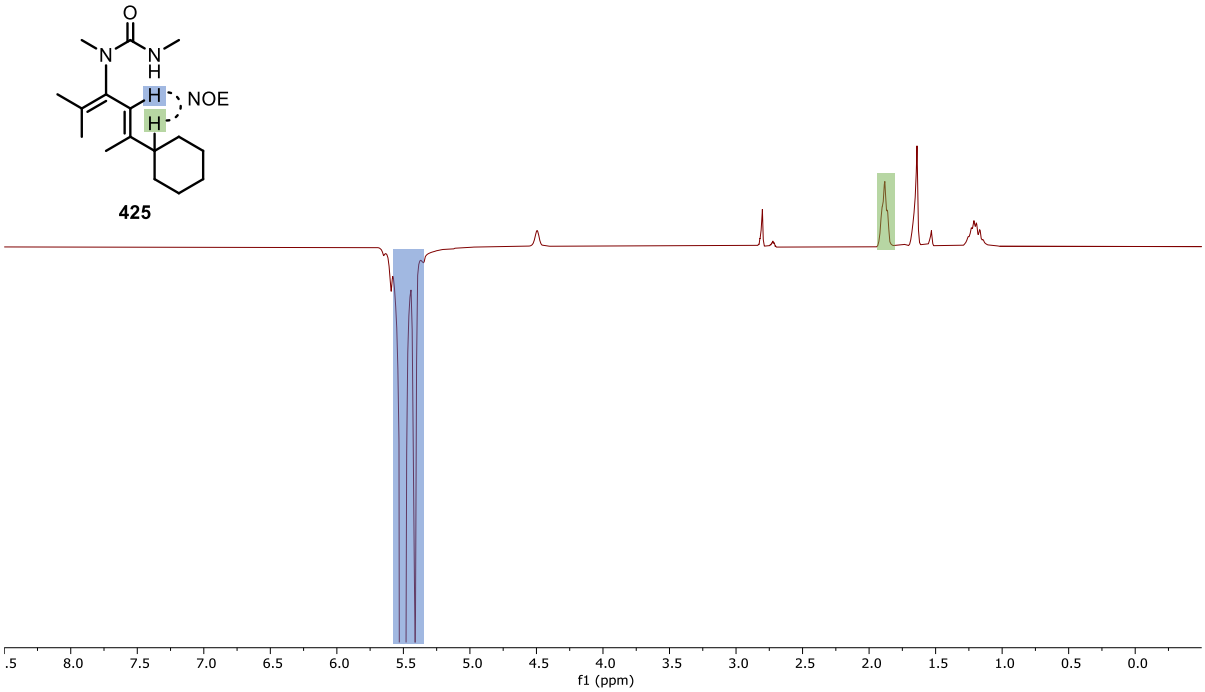

Figure A38. 1D NOESY (500 MHz, $CDCl_3$) of 425 (the proton in blue was irradiated).

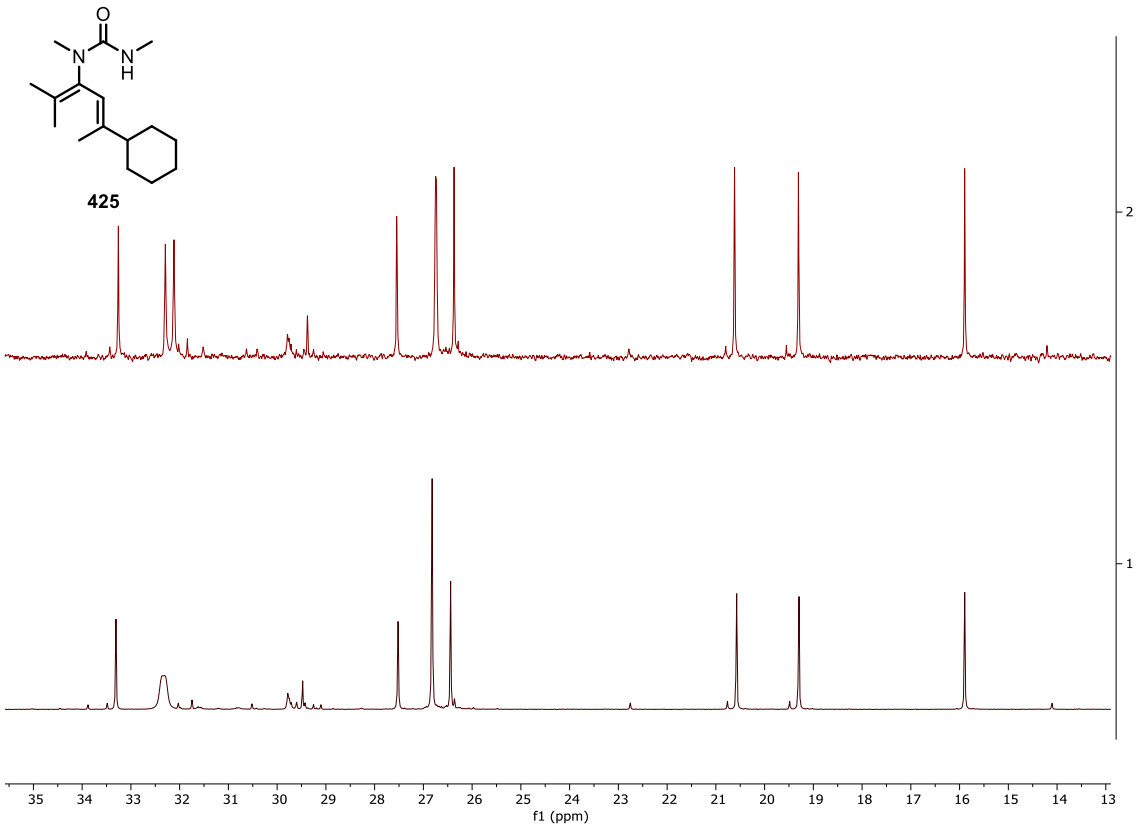

Figure A39. VT ^{13}C NMR of 425 (top was recorded at room temperature; bottom was recorded at 55 °C).

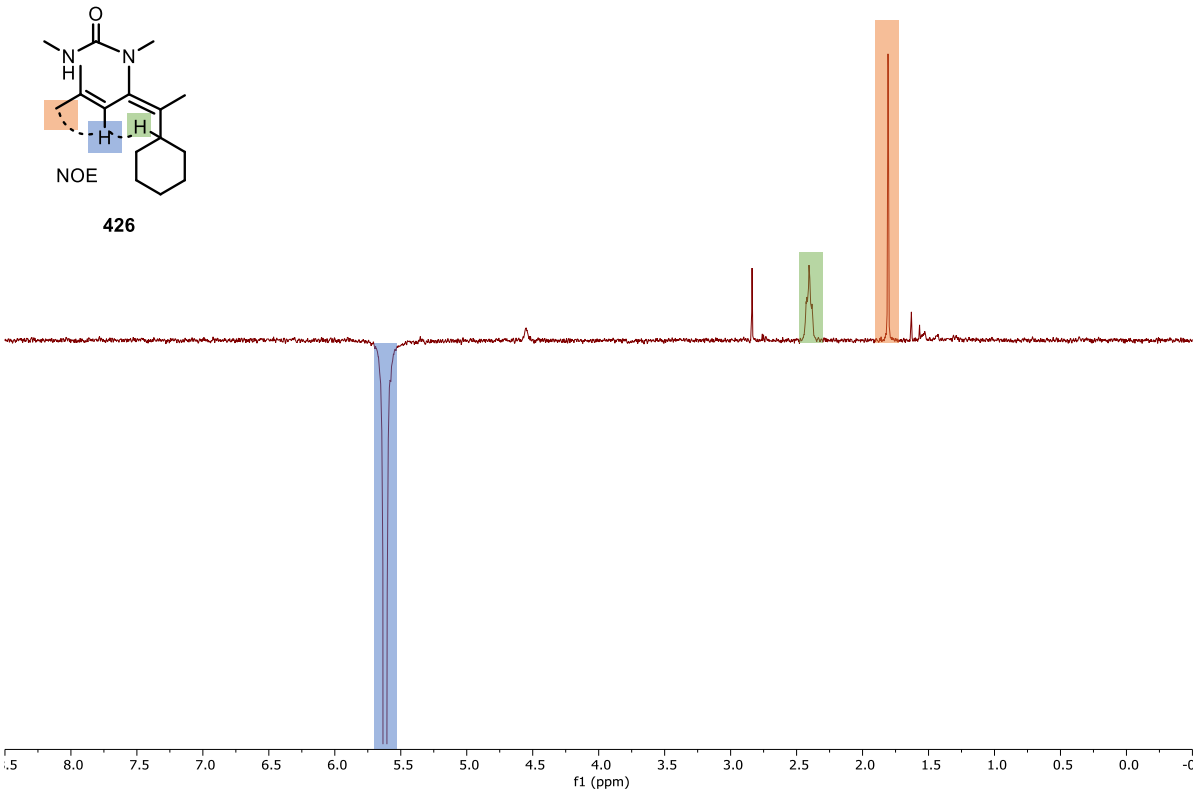

Figure A40. 1D NOESY (500 MHz, $CDCl_3$) of 426 (the proton in blue was irradiated).

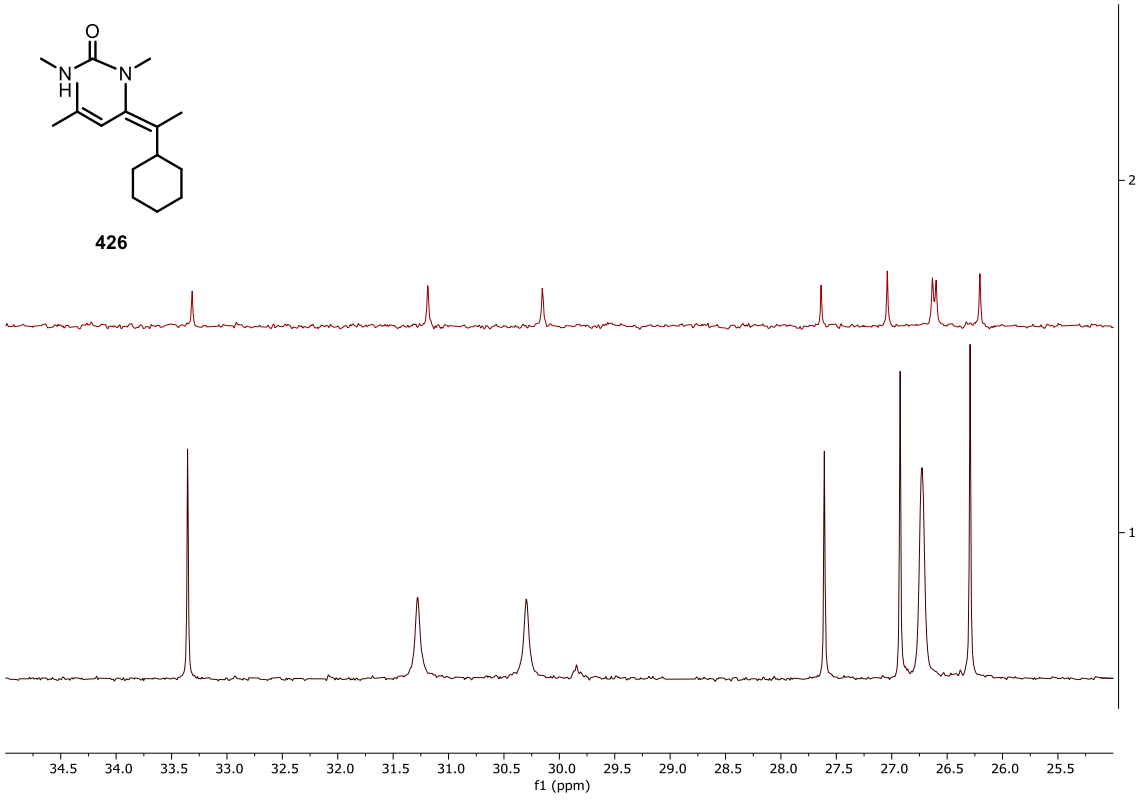

Figure A41. VT ^{13}C NMR of 426 (top was recorded at room temperature; bottom was recorded at 55 °C).

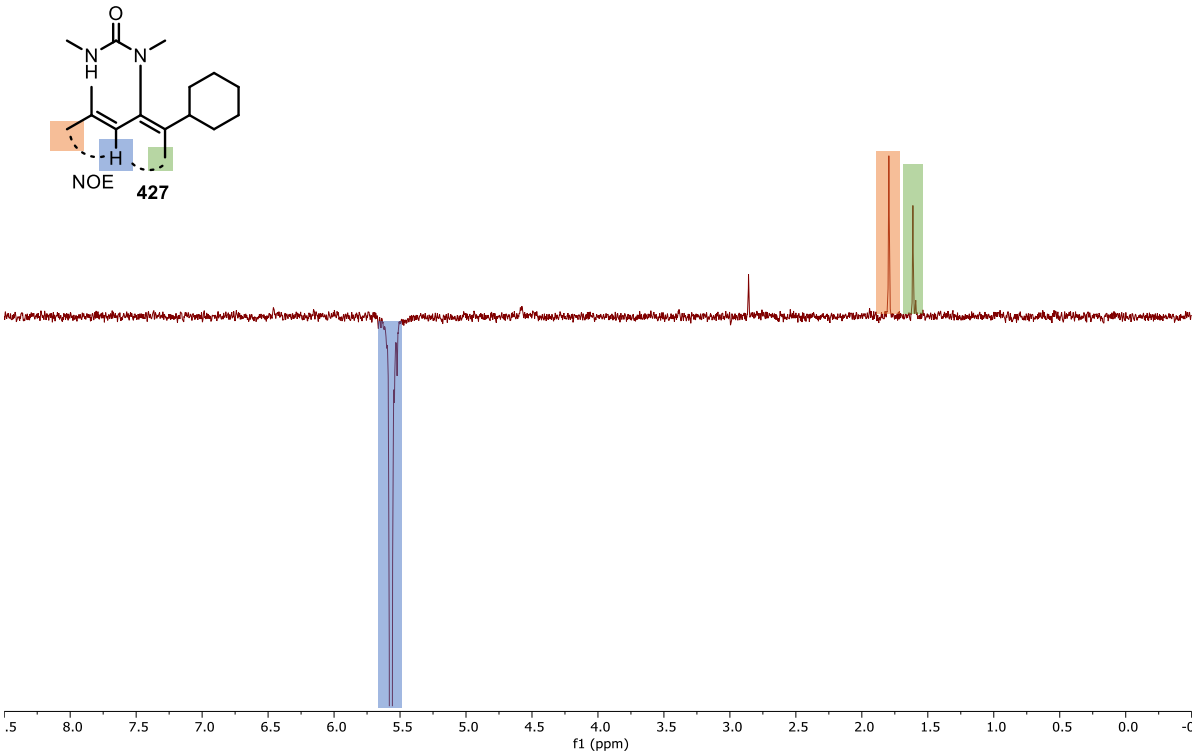

Figure A42. 1D NOESY (500 MHz, $CDCl_3$) of 427 (the proton in blue was irradiated).

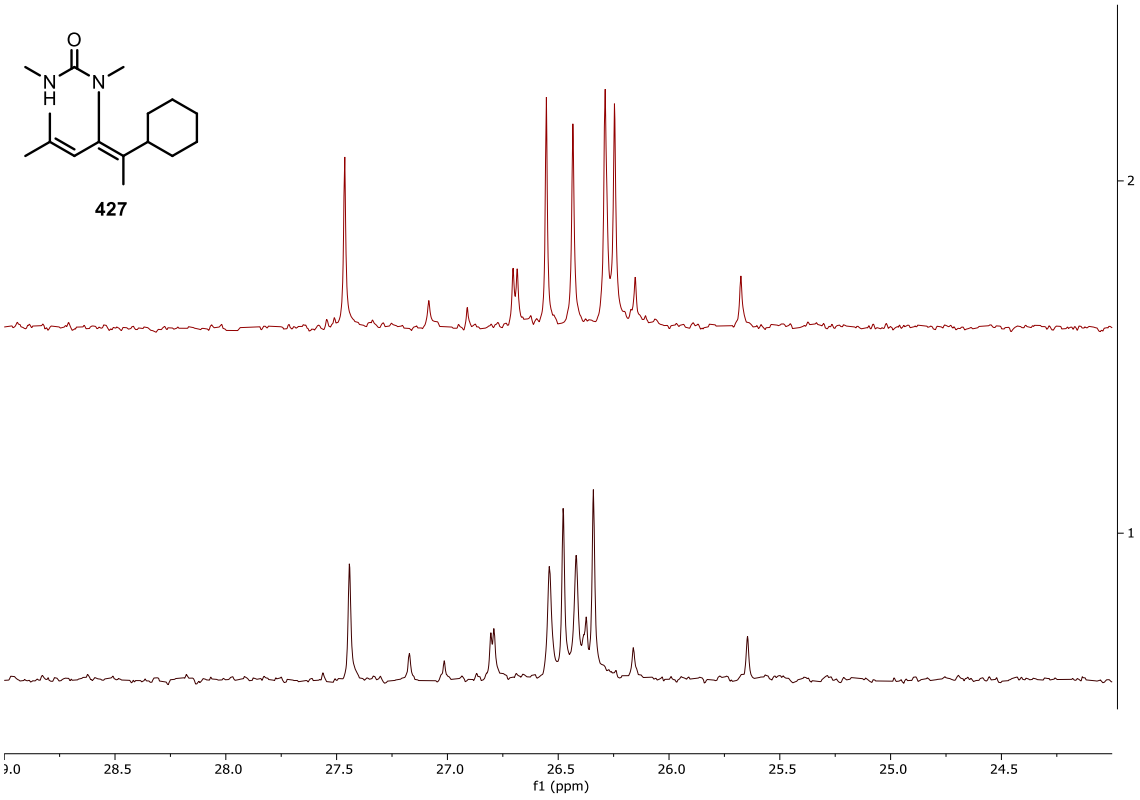

Figure A43. VT ^{13}C NMR of 427 (top was recorded at room temperature; bottom was recorded at 55 °C).

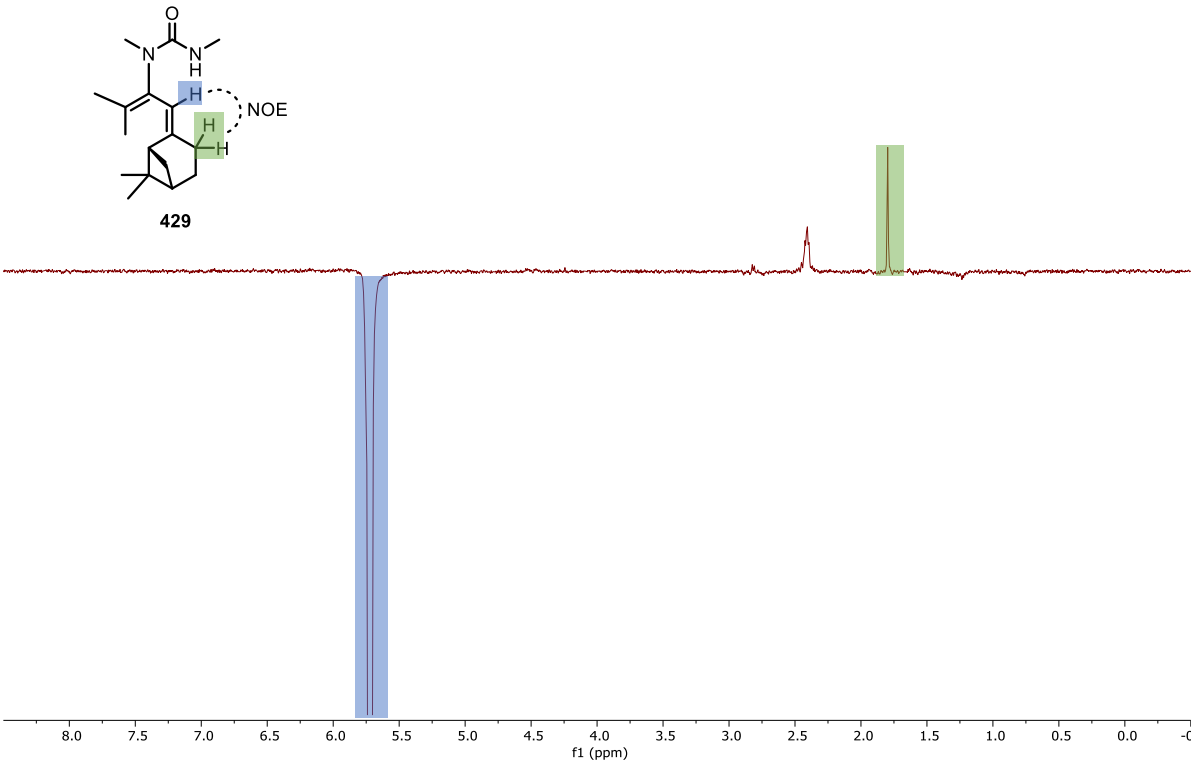

Figure A44. 1D NOESY (500 MHz, $CDCl_3$) of 429 (the proton in blue was irradiated).

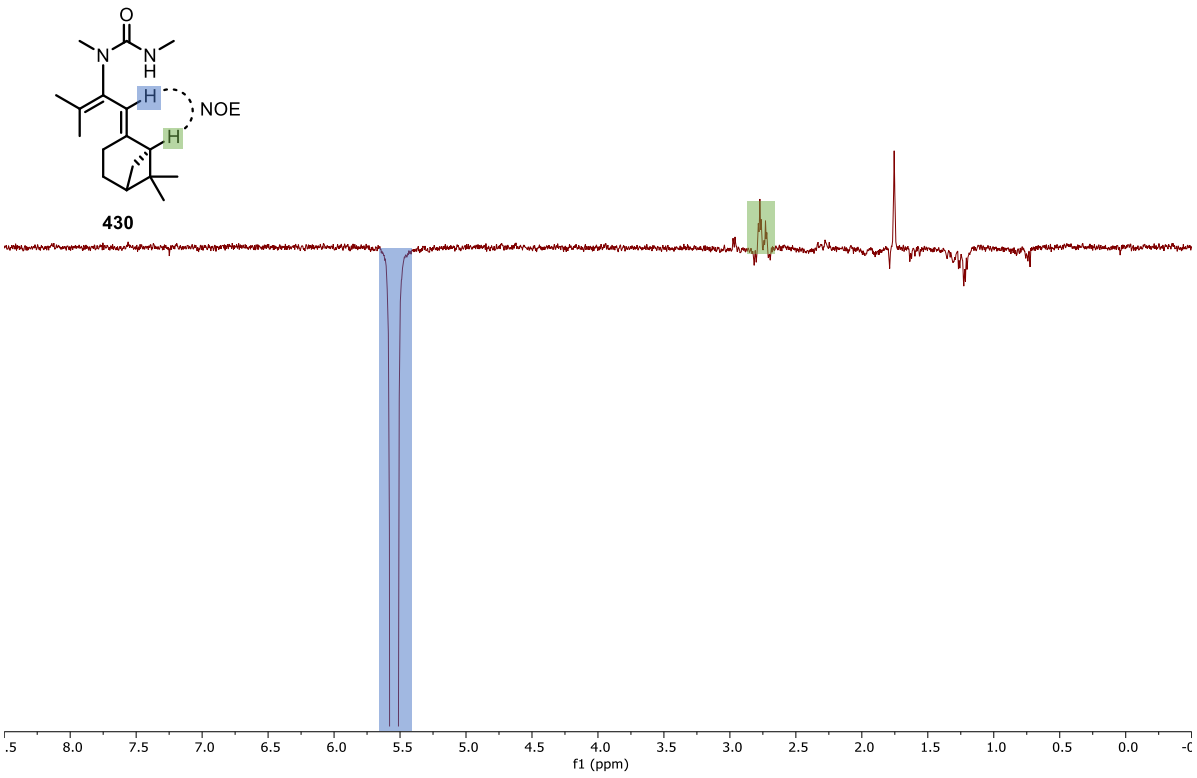

Figure A45. 1D NOESY (500 MHz, $CDCl_3$) of 430 (the proton in blue was irradiated).

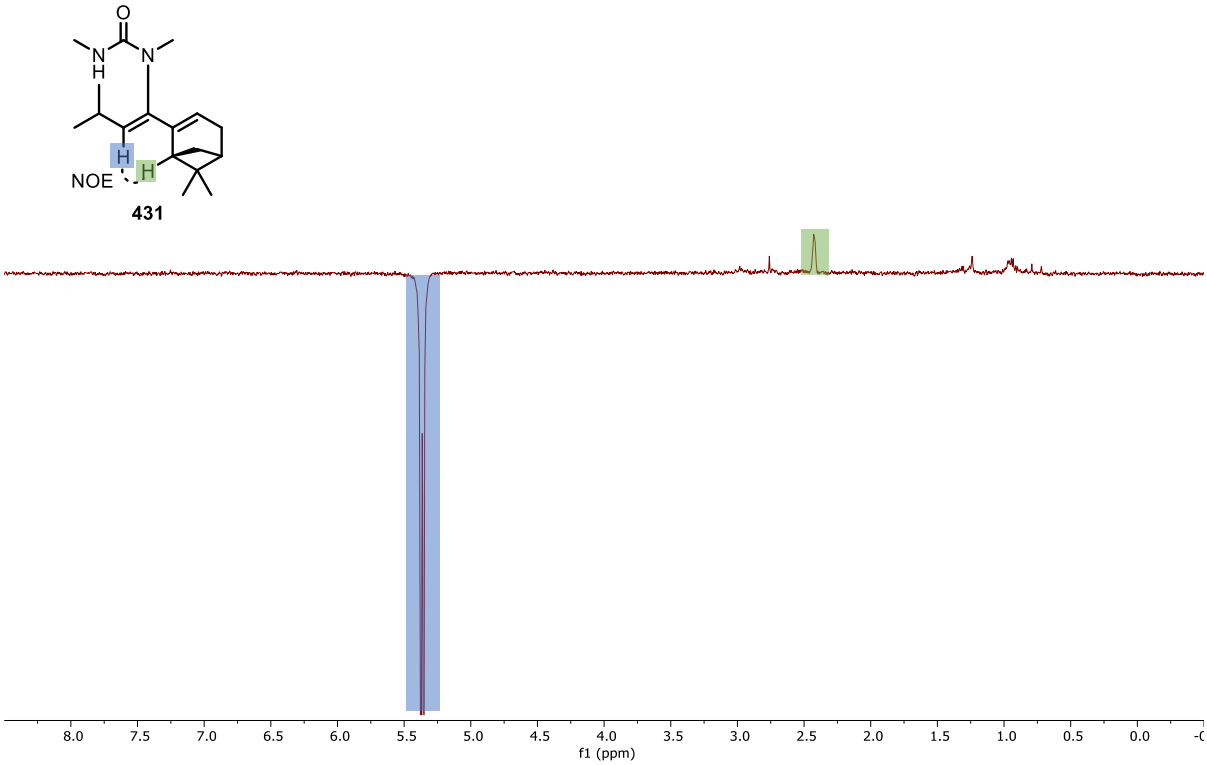

Figure A46. 1D NOESY (500 MHz, $CDCl_3$) of 431 (the proton in blue was irradiated).

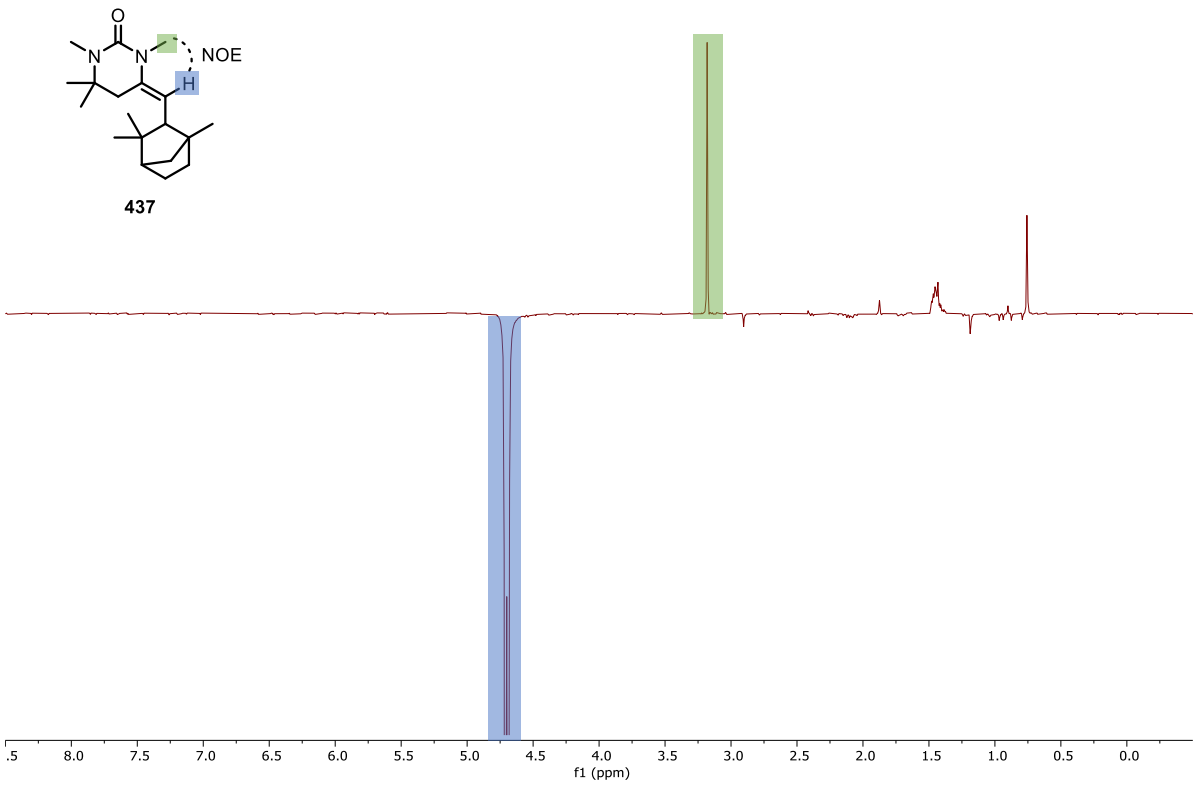

Figure A47. 1D NOESY (500 MHz, $CDCl_3$) of 437 (the proton in blue was irradiated).

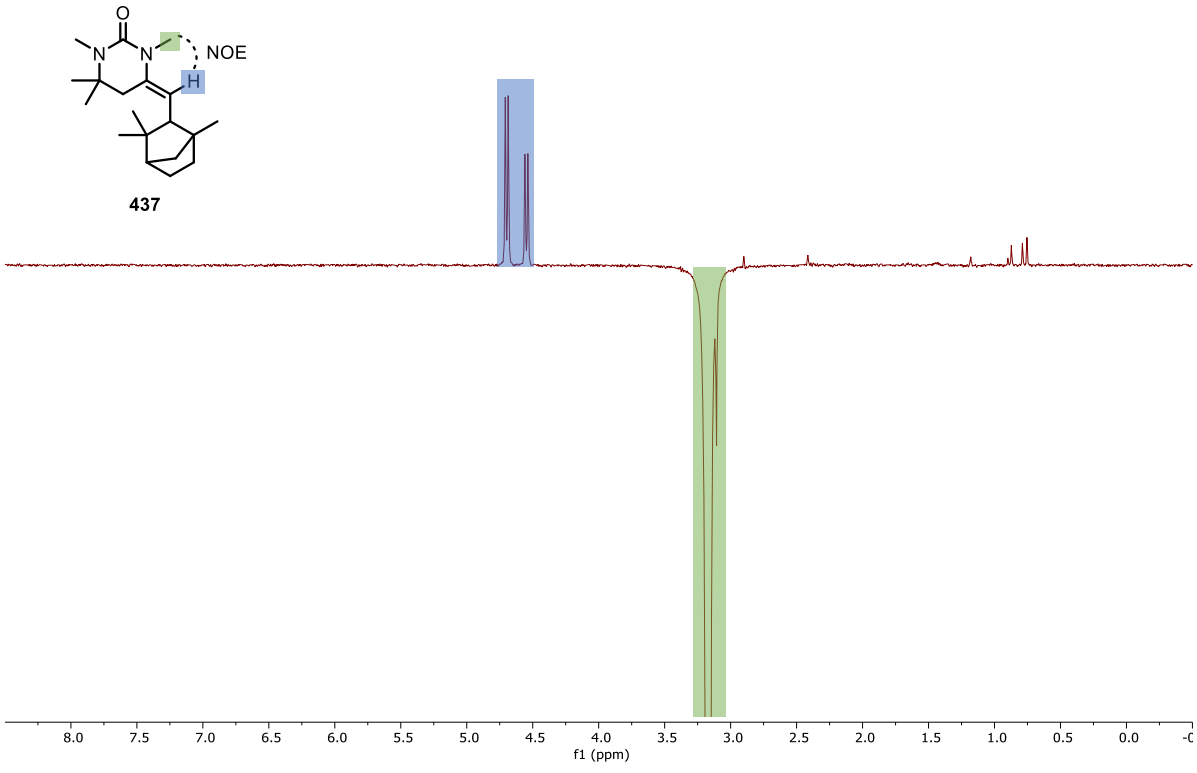

Figure A48. 1D NOESY (500 MHz, $CDCl_3$) of 437 (the methyl in green was irradiated).

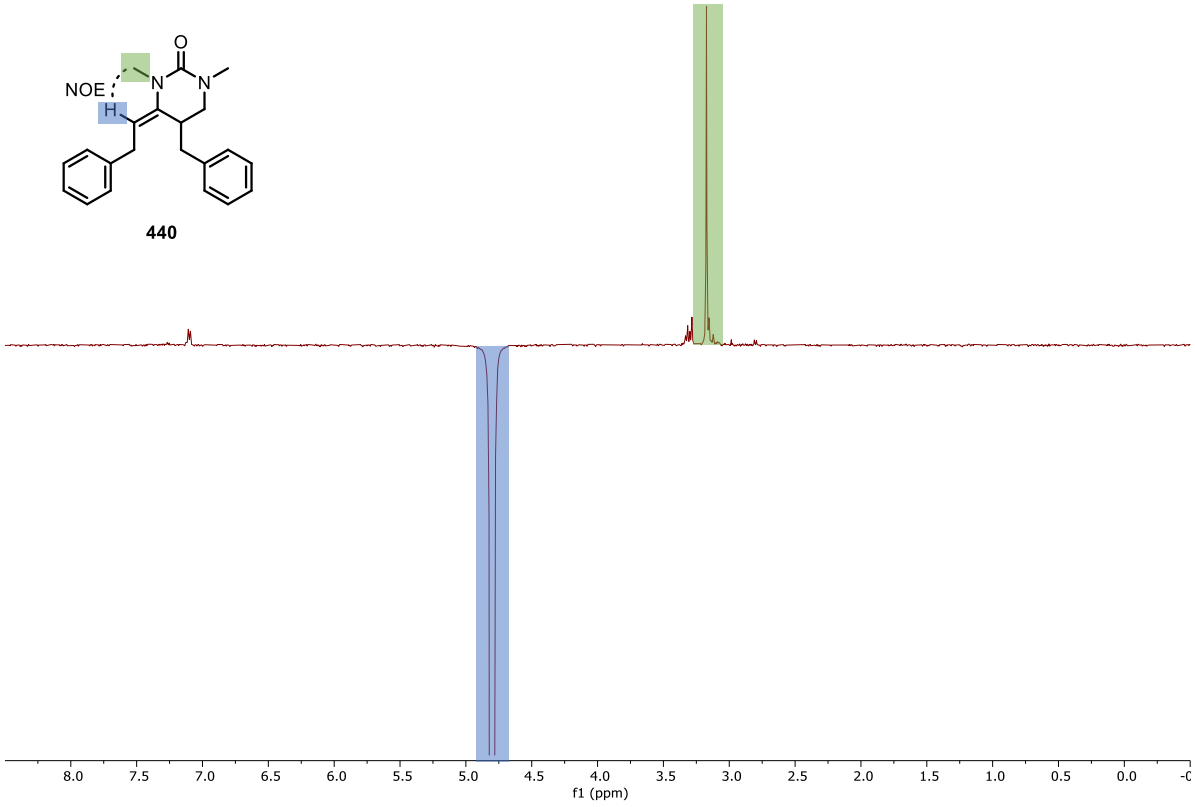

Figure A49. 1D NOESY (500 MHz, $CDCl_3$) of 440 (the proton in blue was irradiated).

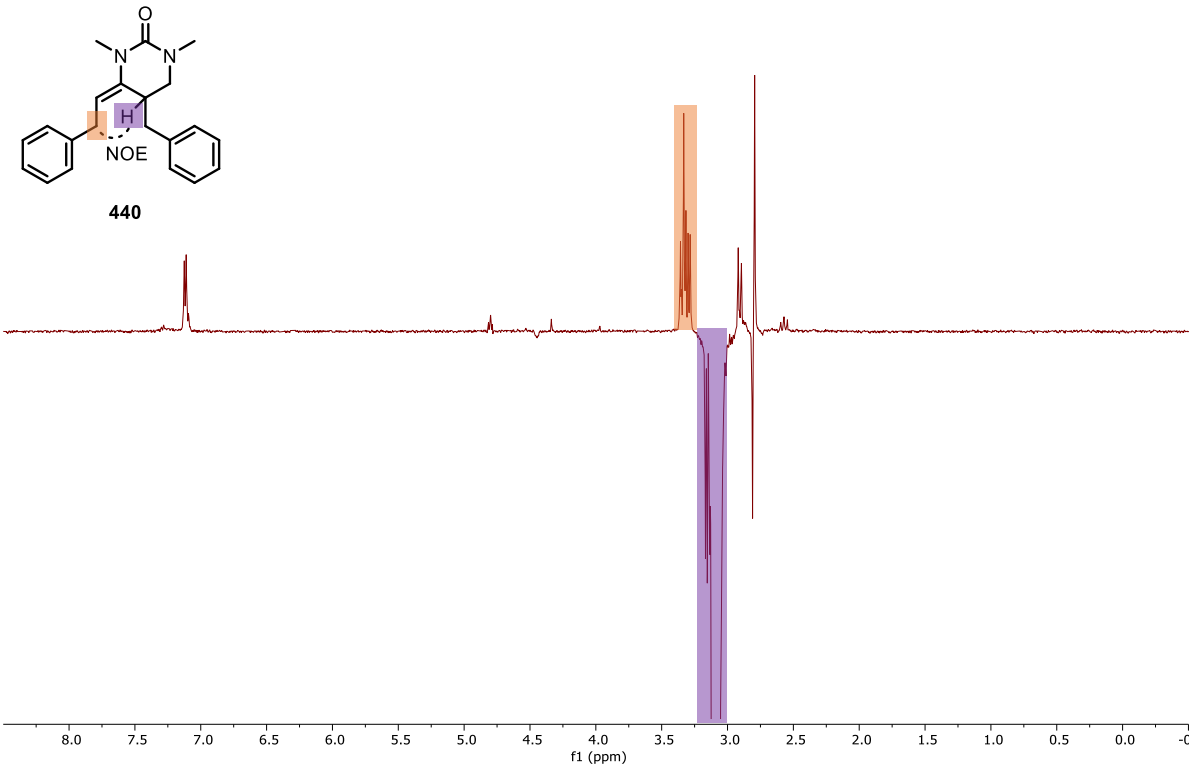

Figure A50. 1D NOESY (500 MHz, $CDCl_3$) of 440 (the proton in purple was irradiated).

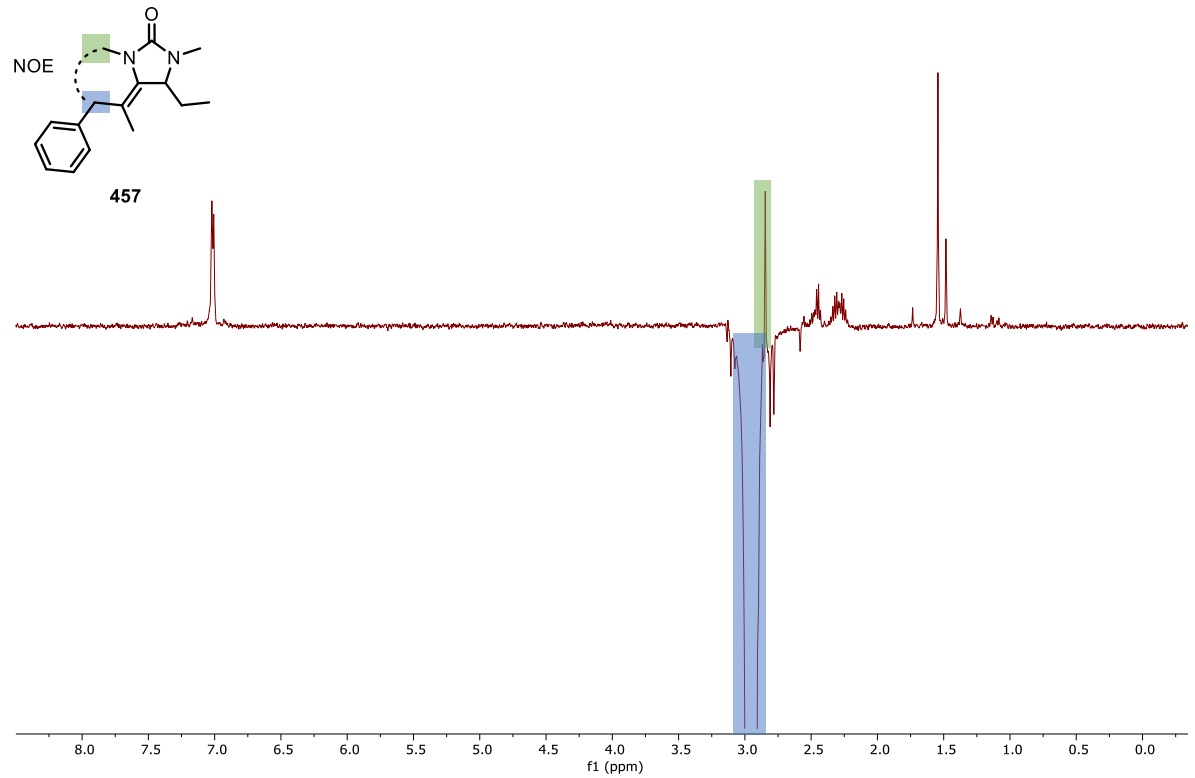

Figure A51. 1D NOESY (500 MHz, $CDCl_3$) of 457 (the methylene in blue was irradiated).

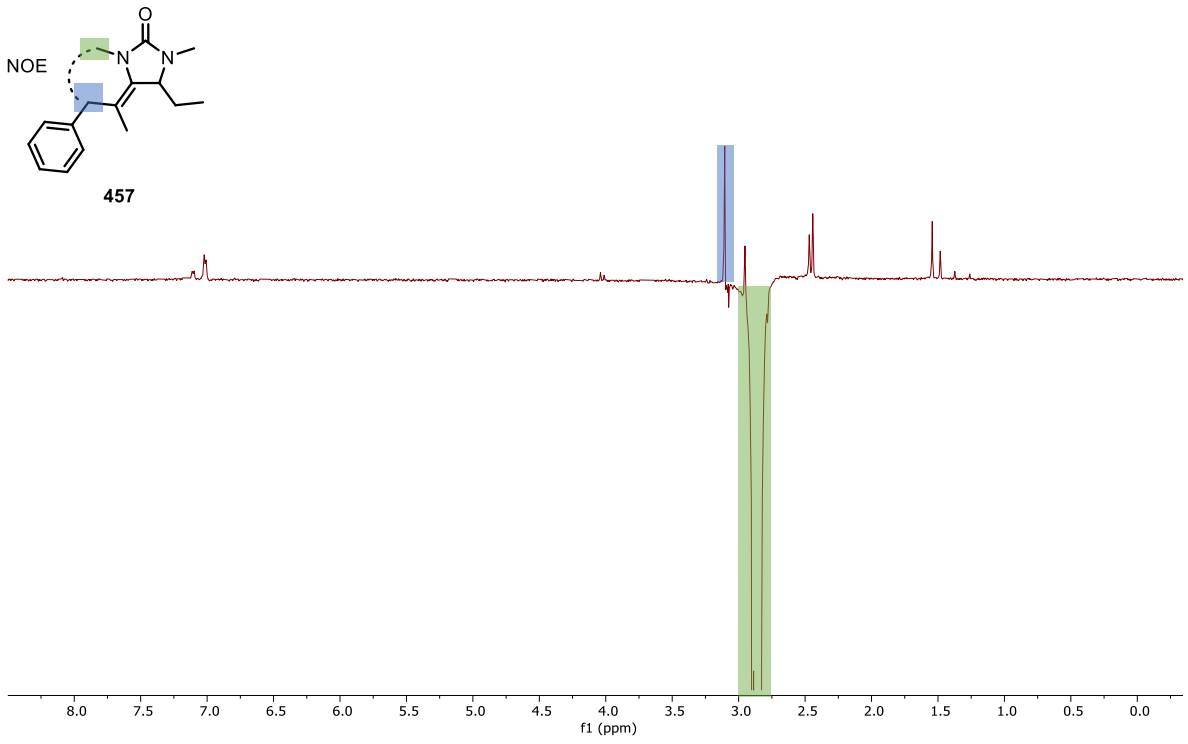

Figure A52. 1D NOESY (500 MHz, $CDCl_3$) of 457 (the methyl in green was irradiated).

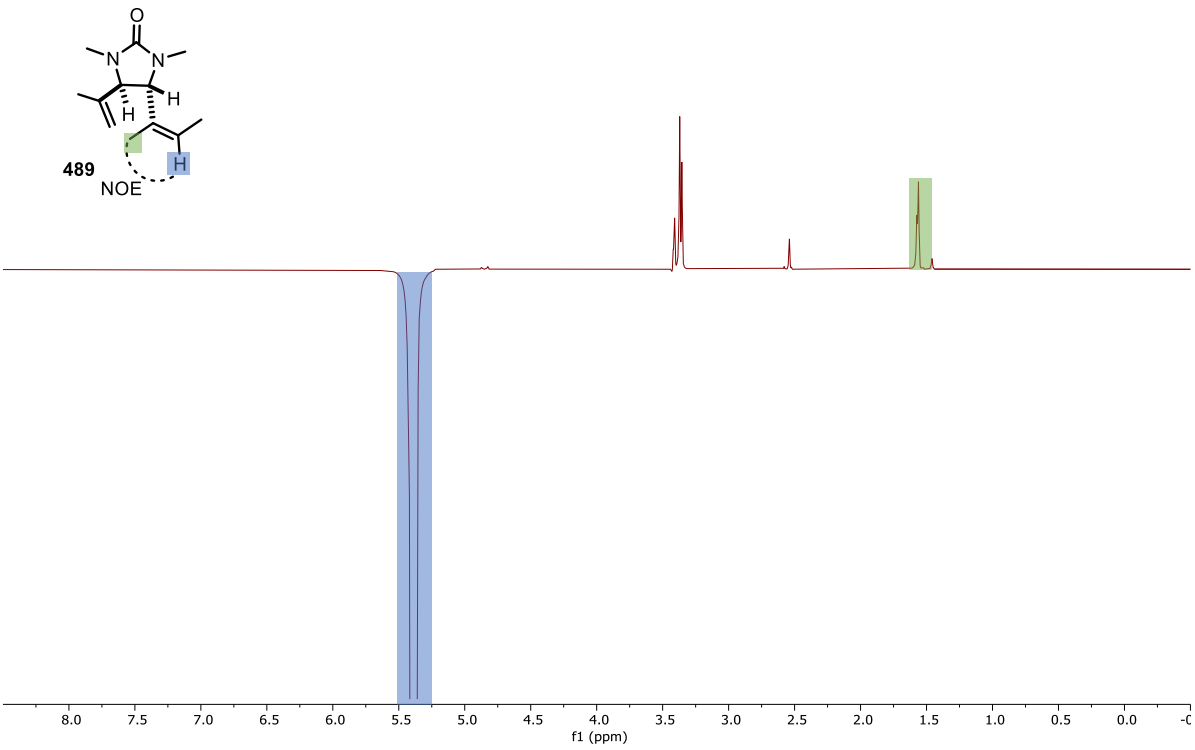

Figure A53. 1D NOESY (500 MHz, $CDCl_3$) of 489 (the proton in blue was irradiated).

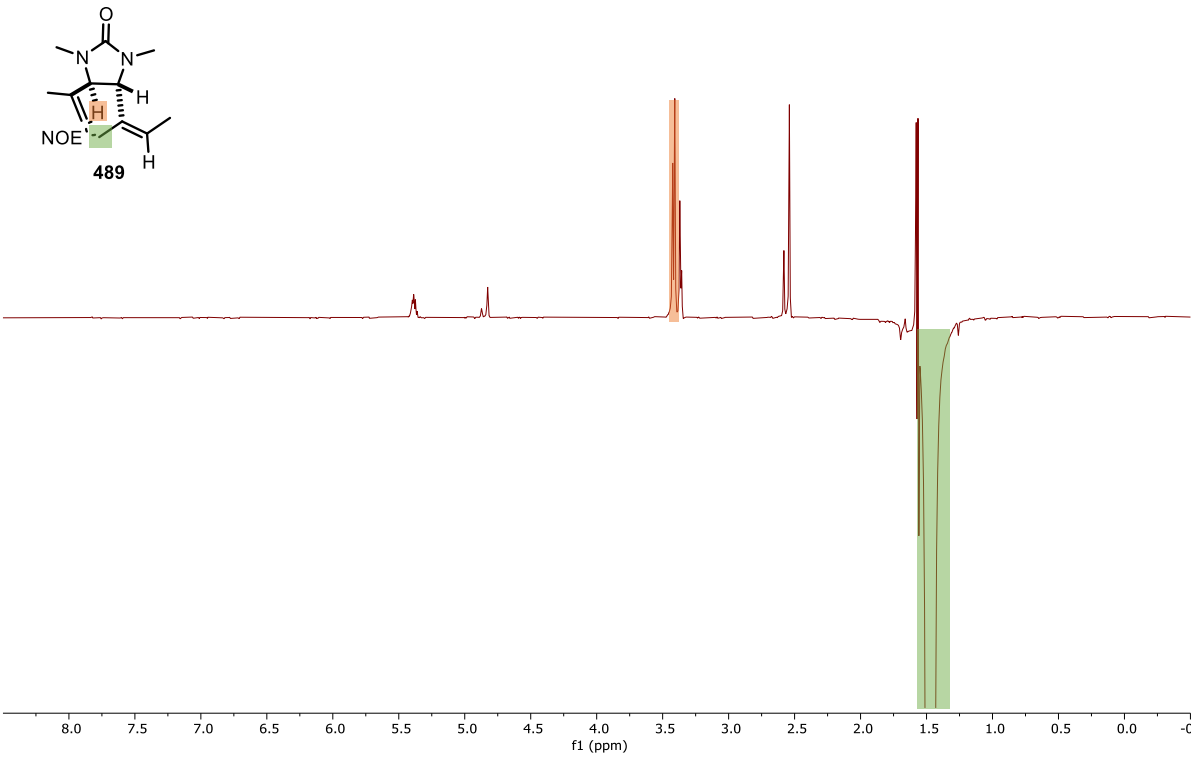

Figure A54. 1D NOESY (500 MHz, $CDCl_3$) of 489 (the methyl in green was irradiated).

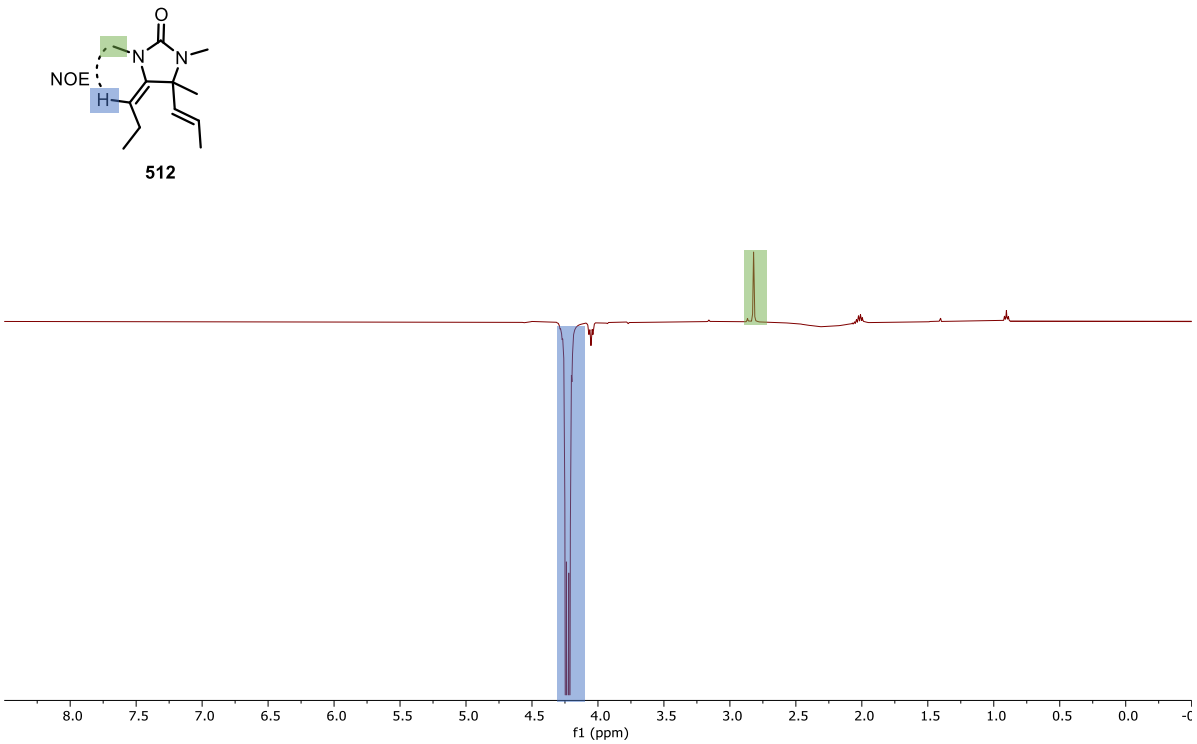

Figure A55. 1D NOESY (500 MHz, $CDCl_3$) of 512 (the proton in blue was irradiated).

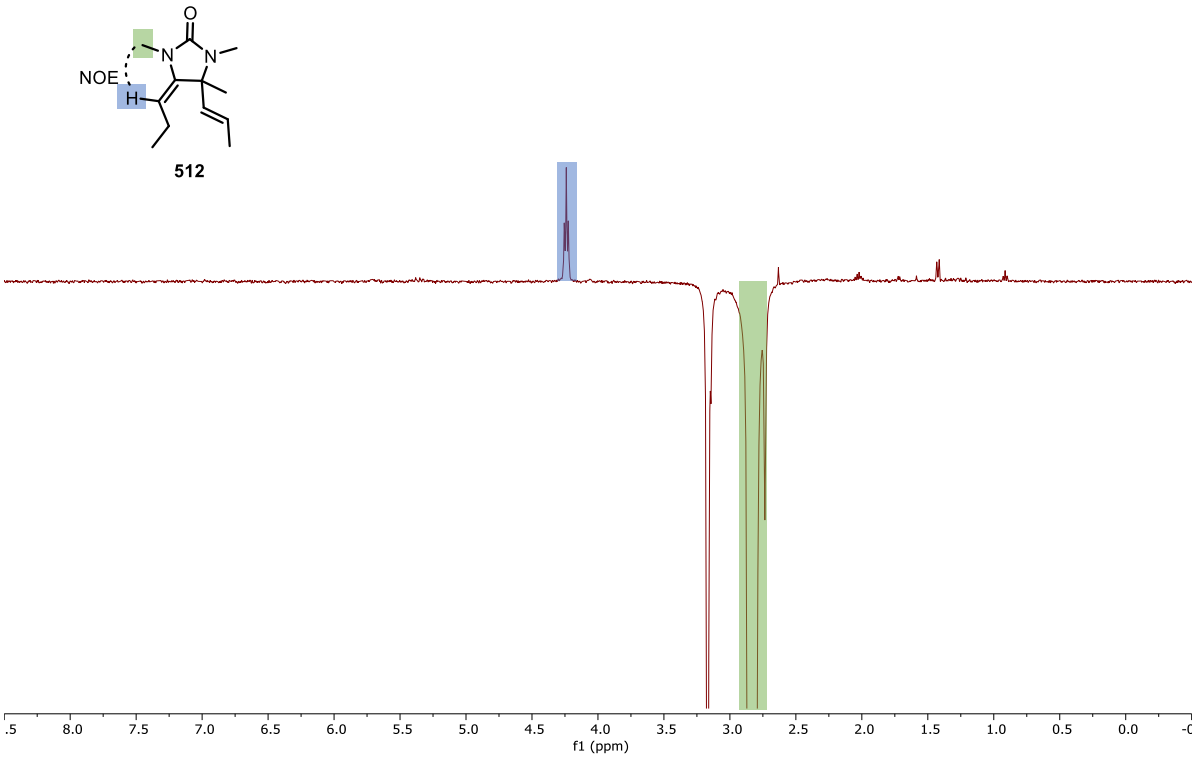

Figure A56. 1D NOESY (500 MHz, $CDCl_3$) of 512 (the methyl in green was irradiated).

7.0 References

[1] B. C. Van Veen, S. M. Wales, J. Clayden, *J. Org. Chem.* **2021**, *86*, 8538–8543.

[2] R. Bruckner, in *Adv. Org. Chem.* (Ed.: R. Bruckner), Academic Press, San Diego, **2002**, pp. 43–83.

[3] S. Rohrbach, A. J. Smith, J. H. Pang, D. L. Poole, T. Tuttle, S. Chiba, J. A. Murphy, *Angew. Chem. Int. Ed.* **2019**, *58*, 16368–16388.

[4] J. F. Bunnett, R. E. Zahler, *Chem. Rev.* **1951**, *49*, 273–412.

[5] Z. Rappoport, *Adv. Phys. Org. Chem.* **1969**, *7*, 1–114.

[6] G. Modena, *Acc. Chem. Res.* **1971**, *4*, 73–80.

[7] Z. Rappoport, *Recl. Trav. Chim. Pays-Bas* **1985**, *104*, 309–349.

[8] V. Lucchini, G. Modena, L. Pasquato, *J. Am. Chem. Soc.* **1995**, *117*, 2297–2300.

[9] I. Fernández, F. M. Bickelhaupt, E. Uggerud, *J. Org. Chem.* **2013**, *78*, 8574–8584.

[10] R. D. Bach, G. J. Wolber, *J. Am. Chem. Soc.* **1984**, *106*, 1401–1409.

[11] C. F. Bernasconi, Z. Rappoport, *Acc. Chem. Res.* **2009**, *42*, 993–1003.

[12] Z. Rappoport, *Acc. Chem. Res.* **1992**, *25*, 474–479.

[13] S. I. Miller, *Tetrahedron* **1977**, *33*, 1211–1218.

[14] Z. Rappoport, B. Avramovitch, *J. Org. Chem.* **1982**, *47*, 1397–1408.

[15] Z. Rappoport, *Acc. Chem. Res.* **1981**, *14*, 7–15.

[16] B. A. Shainyan, *Russ. Chem. Rev.* **1986**, *55*, 511–530.

[17] M. N. Glukhovtsev, A. Pross, L. Radom, *J. Am. Chem. Soc.* **1994**, *116*, 5961–5962.

[18] R. D. Bach, A. G. Baboul, H. B. Schlegel, *J. Am. Chem. Soc.* **2001**, *123*, 5787–5793.

[19] C. K. Kim, K. H. Hyun, C. K. Kim, I. Lee, *J. Am. Chem. Soc.* **2000**, *122*, 2294–2299.

[20] I. Lee, *Int. Rev. Phys. Chem.* **2003**, *22*, 263–283.

[21] T. Okuyama, G. Lodder, in *Adv. Phys. Org. Chem.* (Eds.: T.T. Tidwell, J.P. Richard), Elsevier Science Ltd., Amsterdam, The Netherlands, **2002**, pp. 1–56.

[22] M. Ochiai, *J. Organomet. Chem.* **2000**, *611*, 494–508.

[23] T. Okuyama, T. Takino, K. Sato, M. Ochiai, *J. Am. Chem. Soc.* **1998**, *120*, 2275–2282.

[24] K. Miyamoto, T. Okubo, M. Hirobe, M. Kunishima, M. Ochiai, *Tetrahedron* **2010**, *66*, 5819–5826.

[25] M. Ochiai, K. Oshima, Y. Masaki, *J. Am. Chem. Soc.* **1991**, *113*, 7059–7061.

[26] T. Okuyama, T. Takino, K. Sato, K. Oshima, S. Imamura, H. Yamataka, T. Asano, M. Ochiai, *Bull. Chem. Soc. Jpn.* **1998**, *71*, 243–257.

[27] M. Ochiai, Y. Nishi, M. Hirobe, *Tetrahedron Lett.* **2005**, *46*, 1863–1866.

[28] M. Ochiai, S. Yamamoto, K. Sato, *Chem. Commun.* **1999**, 1363–1364.

[29] J. Yan, Z. C. Chen, *Tetrahedron Lett.* **1999**, *40*, 5757–5758.

[30] J. Yan, Z. C. Chen, *Synth. Commun.* **1999**, *29*, 2867–2874.

[31] M. Ochiai, S. Yamamoto, T. Suefuji, D. W. Chen, *Org. Lett.* **2001**, *3*, 2753–2756.

[32] M. Ochiai, S. Yamamoto, *Chem. Commun.* **2002**, 2802–2803.

[33] M. Ochiai, T. Okubo, K. Miyamoto, *J. Am. Chem. Soc.* **2011**, *133*, 3342–3344.

[34] M. Ochiai, K. Oshima, Y. Masaki, *Tetrahedron Lett.* **1991**, *32*, 7711–7714.

[35] M. Ochiai, K. Oshima, Y. Masaki, M. Kunishima, S. Tani, *Tetrahedron Lett.* **1993**, *34*, 4829–4830.

[36] C. Wang, Y. Fan, Y. Yao, W. Chen, X. Cui, G. Zhu, W. Zhou, L. Tang, *ChemistrySelect* **2018**, *3*, 29–33.

[37] T. B. Poulsen, L. Bernardi, M. Bell, K. A. Jørgensen, *Angew. Chem. Int. Ed.* **2006**, *45*, 6551–6554.

[38] Q. Jin, C. Zheng, G. Zhao, G. Zou, *J. Org. Chem.* **2017**, *82*, 4840–4850.

[39] M. Bell, T. B. Poulsen, K. A. Jørgensen, *J. Org. Chem.* **2007**, *72*, 3053–3056.

[40] Y. Watanabe, T. Takagi, K. Miyamoto, J. Kanazawa, M. Uchiyama, *Org. Lett.* **2020**, *22*, 3469–3473.

[41] K. P. Park, H. J. Ha, *Bull. Chem. Soc. Jpn.* **1990**, *63*, 3006–3009.

[42] K. P. Park, H. J. Ha, P. G. Williard, *J. Org. Chem.* **1991**, *56*, 6725–6727.

[43] K. P. Park, I. Yi, C. O, *J. Org. Chem.* **1994**, *59*, 1053–1057.

[44] H. Zhang, Y. Liu, R. Chen, J. Xue, Y. Li, Y. Tang, *Asian J. Org. Chem.* **2013**, *2*, 307–310.

[45] C. Vila, S. Slack, G. Blay, M. C. Muñoz, J. R. Pedro, *Adv. Synth. Catal.* **2019**, *361*, 1902–1907.

[46] C. Vila, N. R. Dharmaraj, A. Faubel, G. Blay, M. L. Cardona, M. C. Muñoz, J. R. Pedro, *Eur. J. Org. Chem.* **2019**, 3040–3044.

[47] S. Morand, P. Jubault, J. P. Bouillon, S. Couve-Bonnaire, *Chem. Eur. J.* **2021**, *27*, 17273–17292.

[48] Y. Xiong, X. Zhang, T. Huang, S. Cao, *J. Org. Chem.* **2014**, *79*, 6395–6402.

[49] G. Jin, J. Zhang, W. Wu, S. Cao, *J. Fluor. Chem.* **2014**, *168*, 240–246.

[50] T. Huang, X. Zhao, X. Ji, W. Wu, S. Cao, *J. Fluor. Chem.* **2016**, *182*, 61–68.

[51] J. Zhang, C. Xu, W. Wu, S. Cao, *Chem. Eur. J.* **2016**, *22*, 9902–9908.

[52] Q. Q. Zhang, S. Y. Chen, E. Lin, H. Wang, Q. Li, *Org. Lett.* **2019**, *21*, 3123–3126.

[53] L. F. Jiang, B. T. Ren, B. Li, G. Y. Zhang, Y. Peng, Z. Y. Guan, Q. H. Deng, *J. Org. Chem.* **2019**, *84*, 6557–6564.

[54] Y. Peng, X. Zhang, X. Qi, Q. He, B. Zhang, J. Hao, C. Yang, *Eur. J. Org. Chem.* **2019**, 1170–1177.

[55] Y. Li, X. Li, X. Li, D. Shi, *J. Org. Chem.* **2021**, *86*, 6983–6993.

[56] M. Wang, F. Liang, Y. Xiong, S. Cao, *RSC Adv.* **2015**, *5*, 11996–11999.

[57] X. Zhang, Y. Lin, J. Zhang, S. Cao, *RSC Adv.* **2015**, *5*, 7905–7908.

[58] Y. Zong, Q. Ma, G. C. Tsui, *Org. Lett.* **2021**, *23*, 6169–6173.

[59] Y. Wang, Y. Tang, Y. Zong, G. C. Tsui, *Org. Lett.* **2022**, *24*, 4087–4092.

[60] J. Ichikawa, Y. Wada, M. Fujiwara, K. Sakoda, *Synthesis* **2002**, *13*, 1917–1936.

[61] J. E. Baldwin, *J. Chem. Soc., Chem. Commun.* **1976**, 734–736.

[62] J. E. Baldwin, J. Cutting, W. Dupont, L. Kruse, L. Silberman, R. C. Thomas, *J. Chem. Soc., Chem. Commun.* **1976**, 736–738.

[63] J. Ichikawa, Y. Wada, T. Okauchi, T. Minami, *Chem. Commun.* **1997**, 1537–1538.

[64] R. Morioka, T. Fujita, J. Ichikawa, *Helv. Chim. Acta* **2020**, *103*, e2000159.

[65] Y. Wada, J. Ichikawa, T. Katsume, T. Nohiro, T. Okauchi, T. Minami, *Bull. Chem. Soc. Jpn.* **2001**, *74*, 971–977.

[66] Z. Sun, L. Zhou, *J. Org. Chem.* **2022**, *87*, 4801–4812.

[67] C. Li, H. Li, G. Yao, X. Liang, C. Zhao, H. Xu, H. Jiang, C. Zhu, *Org. Chem. Front.* **2022**, *9*, 4692–4698.

[68] J. Ichikawa, M. Fujiwara, Y. Wada, T. Okauchi, T. Minami, *Chem. Commun.* **2000**, 1887–1888.

[69] J. Ichikawa, K. Sakoda, Y. Wada, *Chem. Lett.* **2002**, *31*, 282–283.

[70] K. Ando, *J. Org. Chem.* **2004**, *69*, 4203–4209.

[71] H. Miyauchi, S. Chiba, K. Fukamizu, K. Ando, K. Narasaka, *Tetrahedron* **2007**, *63*, 5940–5953.

[72] K. Ando, M. Kitamura, K. Miura, K. Narasaka, *Org. Lett.* **2004**, *6*, 2461–2463.

[73] S. Chiba, K. Ando, K. Narasaka, *Synlett* **2009**, *16*, 2549–2564.

[74] M. Y. Lei, Y. J. Xiao, W. M. Liu, K. Fukamizu, S. Chiba, K. Ando, K. Narasaka, *Tetrahedron* **2009**, *65*, 6888–6902.

[75] S. S. Shen, M. Y. Lei, Y. X. Wong, M. L. Tong, P. L. Y. Teo, S. Chiba, K. Narasaka, *Tetrahedron Lett.* **2009**, *50*, 3161–3163.

[76] S. Shen, Y. Liu, *Chin. J. Chem.* **2014**, *32*, 1107–1110.

[77] M. Y. Lei, K. Fukamizu, Y. J. Xiao, W. M. Liu, S. Twiddy, S. Chiba, K. Ando, K. Narasaka, *Tetrahedron Lett.* **2008**, *49*, 4125–4129.

[78] H. Yanagisawa, K. Miura, M. Kitamura, K. Narasaka, K. Ando, *Bull. Chem. Soc. Jpn.* **2003**, *76*, 2009–2026.

[79] N. Volz, J. Clayden, *Angew. Chem. Int. Ed.* **2011**, *50*, 12148–12155.

[80] A. K. Ghosh, M. Brindisi, *J. Med. Chem.* **2020**, *63*, 2751–2788.

[81] P. Ganis, G. Avitabile, E. Benedetti, C. Pedone, M. Goodman, *Proc. Natl. Acad. Sci.* **1970**, *67*, 426–433.

[82] J. Clayden, U. Hennecke, M. A. Vincent, I. H. Hillier, M. Helliwell, *Phys. Chem. Chem. Phys.* **2010**, *12*, 15056–15064.

[83] J. F. Galan, E. Germany, A. Pawlowski, L. Strickland, M. G. I. Galinato, *J. Phys. Chem. A* **2014**, *118*, 5304–5315.

[84] J. Clayden, H. Turner, M. Pickworth, T. Adler, *Org. Lett.* **2005**, *7*, 3147–3150.

[85] J. Clayden, J. Dufour, *Tetrahedron Lett.* **2006**, *47*, 6945–6946.

[86] J. Clayden, J. Dufour, D. M. Grainger, M. Helliwell, *J. Am. Chem. Soc.* **2007**, *129*, 7488–7489.

[87] S. M. Wales, R. K. Saunthwal, J. Clayden, *Acc. Chem. Res.* **2022**, *55*, 1731–1747.

[88] A. Ahmed, J. Clayden, S. A. Yasin, *Chem. Commun.* **1999**, 231–232.

[89] J. Clayden, F. E. Knowles, C. J. Menet, *Synlett* **2003**, *11*, 1701–1703.

[90] J. Clayden, in *Organolithiums Sel. Synth.* (Eds.: J.E. Baldwin, R.M. Williams), Elsevier, Amsterdam, The Netherlands, **2002**, pp. 193–194.

[91] M. A. Vincent, J. Maury, I. H. Hillier, J. Clayden, *Eur. J. Org. Chem.* **2015**, 953–959.

[92] D. M. Grainger, A. Campbell Smith, M. A. Vincent, I. H. Hillier, A. E. H. Wheatley, J. Clayden, *Eur. J. Org. Chem.* **2012**, 731–743.

[93] J. Clayden, U. Hennecke, *Org. Lett.* **2008**, *10*, 3567–3570.

[94] J. Maury, W. Zawodny, J. Clayden, *Org. Lett.* **2017**, *19*, 472–475.

[95] R. Bach, J. Clayden, U. Hennecke, *Synlett* **2009**, *3*, 421–424.

[96] J. E. Hall, J. V. Matlock, J. W. Ward, K. V. Gray, J. Clayden, *Angew. Chem. Int. Ed.* **2016**, *55*, 11153–11157.

[97] P. MacLellan, J. Clayden, *Chem. Commun.* **2011**, *47*, 3395–3397.

[98] J. Clayden, W. Farnaby, D. M. Grainger, U. Hennecke, M. Mancinelli, D. J. Tetlow, I. H. Hillier, M. A. Vincent, *J. Am. Chem. Soc.* **2009**, *131*, 3410–3411.

[99] R. C. Atkinson, D. J. Leonard, J. Maury, D. Castagnolo, N. Volz, J. Clayden, *Chem. Commun.* **2013**, *49*, 9734–9736.

[100] M. J. Millward, E. Ellis, J. W. Ward, J. Clayden, *Chem. Sci.* **2021**, *12*, 2091–2096.

[101] R. C. Atkinson, F. Fernández-Nieto, J. Mas Rosellõ, J. Clayden, *Angew. Chem. Int. Ed.* **2015**, *54*, 8961–8965.

[102] R. K. Saunthwal, M. T. Cornall, R. Abrams, J. W. Ward, J. Clayden, *Chem. Sci.* **2019**, *10*, 3408–3412.

[103] J. Mas-Roselló, M. Okoh, J. Clayden, *Chem. Commun.* **2018**, *54*, 10985–10988.

[104] J. Maury, J. Clayden, *J. Org. Chem.* **2015**, *80*, 10757–10768.

[105] D. J. Leonard, J. W. Ward, J. Clayden, *Nature* **2018**, *562*, 105–109.

[106] D. J. Tetlow, U. Hennecke, J. Raftery, M. J. Waring, D. S. Clarke, J. Clayden, *Org. Lett.* **2010**, *12*, 5442–5445.

[107] D. R. Carbery, *Org. Biomol. Chem.* **2008**, *6*, 3455–3460.

[108] J. Lefranc, D. J. Tetlow, M. Donnard, A. Minassi, E. Galvez, J. Clayden, *Org. Lett.* **2011**, *13*, 296–299.

[109] J. Clayden, M. Donnard, J. Lefranc, A. Minassi, D. J. Tetlow, *J. Am. Chem. Soc.* **2010**, *132*, 6624–6625.

[110] M. Tait, M. Donnard, A. Minassi, J. Lefranc, B. Bechi, G. Carbone, P. O'Brien, J. Clayden, *Org. Lett.* **2013**, *15*, 34–37.

[111] M. Tait, M. Donnard, A. Minassi, J. Lefranc, B. Bechi, G. Carbone, P. O'Brien, J. Clayden, *Org. Lett.* **2013**, *15*, 974–976.

[112] J. Lefranc, A. M. Fournier, G. Mingat, S. Herbert, T. Marcelli, J. Clayden, *J. Am. Chem. Soc.* **2012**, *134*, 7286–7289.

[113] J. Mas-Roselló, S. Hachisu, J. Clayden, *Angew. Chem. Int. Ed.* **2017**, *56*, 10750–10754.

[114] H. Abas, J. Mas-roselló, M. M. Amer, D. J. Durand, R. R. Groleau, N. Fey, J. Clayden, *Angew. Chem. Int. Ed.* **2019**, *58*, 2418–2422.

[115] S. Kumar, V. Kumar, S. P. Singh, in *Pericyclic React.*, Elsevier Academic Press, London, UK, **2016**, pp. 145–229.

[116] J. P. Chupp, E. R. Weiss, *J. Org. Chem.* **1968**, *33*, 2357–2361.

[117] M. B. Tait, S. Butterworth, J. Clayden, *Org. Lett.* **2015**, *17*, 1236–1239.

[118] D. V. McGrath, R. H. Grubbs, *Organometallics* **1994**, *13*, 224–235.

[119] B. Alcaide, P. Almendros, J. M. Alonso, *Chem. Eur. J.* **2006**, *12*, 2874–2879.

[120] S. Krompiec, M. Pigulla, N. Kuźnik, M. Krompiec, B. Marciniec, D. Chadyniak, J. Kasperczyk, *J. Mol. Catal. A Chem.* **2005**, *225*, 91–101.

[121] M. Johannsen, K. A. Jørgensen, *Chem. Rev.* **1998**, *98*, 1689–1708.

[122] R. B. Cheikh, R. Chaabouni, A. Laurent, P. Mison, A. Nafti, *Synthesis* **1983**, 685–699.

[123] J. Muzart, *Eur. J. Org. Chem.* **2007**, 3077–3089.

[124] H. Lei, T. Rovis, *J. Am. Chem. Soc.* **2019**, *141*, 2268–2273.

[125] Q. Cheng, J. Chen, S. Lin, T. Ritter, *J. Am. Chem. Soc.* **2020**, *142*, 17287–17293.

[126] W. K. Walker, D. L. Anderson, R. W. Stokes, S. J. Smith, D. J. Michaelis, *Org. Lett.* **2015**, *17*, 752–755.

[127] S. Ghorai, S. S. Chirke, W. B. Xu, J. F. Chen, C. Li, *J. Am. Chem. Soc.* **2019**, *141*, 11430–11434.

[128] M. S. Gibson, R. W. Bradshaw, *Angew. Chem. Int. Ed.* **1968**, *7*, 919–930.

[129] J. Osby, M. G. Martin, B. Ganem, *Tetrahedron Lett.* **1984**, *25*, 2093–2096.

[130] A. Zwierzak, S. Pilichowska, *Synthesis* **1982**, *11*, 922–924.

[131] L. E. Overman, C. E. Owen, M. M. Pavan, C. J. Richards, *Org. Lett.* **2003**, *5*, 1809–1812.

[132] C. E. Anderson, L. E. Overman, *J. Am. Chem. Soc.* **2003**, *125*, 12412–12413.

[133] R. A. Fernandes, P. Kattanguru, S. P. Gholap, D. A. Chaudhari, *Org. Biomol. Chem.* **2017**, *15*, 2672–2710.

[134] L. E. Overman, N. E. Carpenter, *Org. React.* **2005**, *66*, 1–107.

[135] L. Guandalini, M. Norcini, K. Varani, M. Pistolozzi, C. Gotti, C. Bazzicalupi, E. Martini, S. Dei, D. Manetti, S. Scapecchi, et al., *J. Med. Chem.* **2007**, *50*, 4993–5002.

[136] M. S. Estevão, F. J. S. Duarte, E. Fernandes, A. G. Santos, M. M. B. Marques, *Tetrahedron Lett.* **2012**, *53*, 2132–2136.

[137] R. J. P. Corriu, B. Geng, J. J. E. Moreau, *J. Org. Chem.* **1993**, *58*, 1443–1448.

[138] T. N. Mitchell, R. Wickenkamp, A. Amamria, R. Dicke, U. Schneider, *J. Org. Chem.* **1987**, *52*, 4868–4874.

[139] W. G. Young, R. A. Clement, C. H. Shih, *J. Am. Chem. Soc.* **1955**, *77*, 3061–3067.

[140] A. W. Weston, A. W. Ruddy, C. M. Suter, *J. Am. Chem. Soc.* **1943**, *65*, 674–677.

[141] P. A. Donets, E. V. Van der Eycken, *Synthesis* **2011**, *13*, 2147–2153.

[142] R. Guo, J. Huang, H. Huang, X. Zhao, *Org. Lett.* **2016**, *18*, 504–507.

[143] O. Mitsunobu, *Synthesis* **1981**, 1–28.

[144] S. Fletcher, *Org. Chem. Front.* **2015**, *2*, 739–752.

[145] U. Ragnarsson, L. Grehn, *Acc. Chem. Res.* **1991**, *24*, 285–289.

[146] F. Berrée, G. Michelot, M. Le Corre, *Tetrahedron Lett.* **1998**, *39*, 8275–8276.

[147] J. A. Gómez-Vidal, R. B. Silverman, *Org. Lett.* **2001**, *3*, 2481–2484.

[148] J. D. Firth, P. G. E. Craven, M. Lilburn, A. Pahl, S. P. Marsden, A. Nelson, *Chem. Commun.* **2016**, *52*, 9837–9840.

[149] P. Craven, A. Aimon, M. Dow, N. Fleury-Bregeot, R. Guilleux, R. Morgentin, D. Roche, T. Kalliokoski, R. Foster, S. P. Marsden, et al., *Bioorganic Med. Chem.* **2015**, *23*, 2629–2635.

[150] Y. Lee, R. B. Silverman, *Tetrahedron* **2001**, *57*, 5339–5352.

[151] T. Y. S. But, P. H. Toy, *Chem. Asian J.* **2007**, *2*, 1340–1355.

[152] F. Berrée, J. P. Bazureau, G. Michelot, M. Le Cone, *Synth. Commun.* **1999**, *29*, 2685–2693.

[153] Y. Pan, K. Calvert, R. B. Silverman, *Bioorganic Med. Chem.* **2004**, *12*, 5719–5725.

[154] B. P. Corbet, J. V. Matlock, J. Mas-Roselló, J. Clayden, *C. R. Chim.* **2017**, *20*, 634–642.

[155] L. Gupta, A. C. Hoepker, K. J. Singh, D. B. Collum, *J. Org. Chem.* **2009**, *74*, 2231–2233.

[156] D. Seebach, H. Bossler, H. Grundler, S. Shoda, R. Wenger, *Helv. Chim. Acta* **1991**, *74*, 197–224.

[157] C. Riche, C. Pascard-Billly, C. Cambillau, G. Bram, *J. Chem. Soc., Chem. Commun.* **1977**, 183–184.

[158] C. J. Pedersen, H. K. Frensdorff, *Angew. Chem. Int. Ed.* **1972**, *11*, 16–25.

[159] H. J. Reich, *Chem. Rev.* **2013**, *113*, 7130–7178.

[160] R. R. Fraser, M. Bresse, T. S. Mansour, *J. Chem. Soc., Chem. Commun.* **1983**, 620–621.

[161] R. R. Fraser, M. Bresse, T. S. Mansour, *J. Am. Chem. Soc.* **1983**, *105*, 7790–7791.

[162] R. R. Fraser, T. S. Mansour, S. Savard, *J. Org. Chem.* **1985**, *50*, 3232–3234.

[163] P. Beak, B. Lee, *J. Org. Chem.* **1989**, *54*, 458–464.

[164] B. A. Shainyan, Y. S. Danilevich, *Russ. J. Org. Chem.* **2013**, *49*, 1112–1116.

[165] O. Diels, K. Alder, *Justus Liebigs Ann. Chem.* **1928**, *460*, 98–122.

[166] K. C. Nicolaou, S. A. Snyder, T. Montagnon, G. Vassilikogiannakis, *Angew. Chem. Int. Ed.* **2002**, *41*, 1668–1698.

[167] M. W. Wright, M. E. Welker, *J. Org. Chem.* **1996**, *61*, 133–141.

[168] K. Alder, G. Stein, *Justus Liebigs Ann. Chem.* **1934**, *514*, 1–33.

[169] K. Alder, G. Stein, *Angew. Chem.* **1937**, *50*, 510–519.

[170] R. Hoffmann, R. B. Woodward, *J. Am. Chem. Soc.* **1965**, *87*, 4388–4389.

[171] C. S. Wannere, A. Paul, R. Herges, K. N. Houk, H. F. Schaefer, P. Von Rague Schleyer, *J. Comput. Chem.* **2006**, *28*, 344–361.

[172] J. I. Garcia, J. A. Mayoral, L. Salvatella, *Acc. Chem. Res.* **2000**, *33*, 658–664.

[173] I. Fernandez, F. M. Bickelhaupt, *J. Comput. Chem.* **2014**, *35*, 371–376.

[174] K. Sakata, H. Fujimoto, *Eur. J. Org. Chem.* **2016**, 4275–4278.

[175] W. J. Lording, T. Fallon, M. S. Sherburn, M. N. Paddon-Row, *Chem. Sci.* **2020**, *11*, 11915–11926.

[176] S. K. S. Tse, P. Xue, Z. Lin, G. Jia, *Adv. Synth. Catal.* **2010**, *352*, 1512–1522.

[177] F. H. Westheimer, *Chem. Rev.* **1961**, *61*, 265–273.

[178] K. B. Wiberg, *Chem. Rev.* **1955**, *55*, 713–743.

[179] M. Gomez-Gallego, M. A. Sierra, *Chem. Rev.* **2011**, *111*, 4857–4963.

[180] A. V. Salin, *ChemistrySelect* **2017**, *2*, 6984–6990.

[181] D. A. Singleton, A. A. Thomas, *J. Am. Chem. Soc.* **1995**, *117*, 9357–9358.

[182] J. S. Bandar, G. S. Sauer, W. D. Wulff, T. H. Lambert, M. J. Vetticatt, *J. Am. Chem. Soc.* **2014**, *136*, 10700–10707.

[183] N. Yoshikai, H. Matsuda, E. Nakamura, *J. Am. Chem. Soc.* **2009**, *131*, 9590–9599.

[184] D. A. Singleton, C. Hang, M. J. Szymanski, M. P. Meyer, A. G. Leach, K. T. Kuwata, J. S. Chen, A. Greer, C. S. Foote, K. N. Houk, *J. Am. Chem. Soc.* **2003**, *125*, 1319–1328.

[185] M. P. Meyer, *Adv. Phys. Org. Chem.* **2012**, *46*, 57–120.

[186] N. Yoshikai, E. Nakamura, *J. Am. Chem. Soc.* **2004**, *126*, 12264–12265.

[187] E. E. Kwan, Y. Zeng, H. A. Besser, E. N. Jacobsen, *Nat. Chem.* **2018**, *10*, 917–923.

[188] P. Cooper, G. E. M. Crisenza, L. J. Feron, J. F. Bower, *Angew. Chem. Int. Ed.* **2018**, *57*, 14198–14202.

[189] S. Grélaud, P. Cooper, L. J. Feron, J. F. Bower, *J. Am. Chem. Soc.* **2018**, *140*, 9351–9356.

[190] Y. Cao, J. G. Yang, Y. Deng, S. Wang, Q. Liu, C. Shen, W. Lu, C. M. Che, Y. Chen, L. He, *Angew. Chem. Int. Ed.* **2020**, *59*, 2080–2084.

[191] R. Pajkert, T. Böttcher, M. Ponomarenko, M. Bremer, G. V. Röschenthaler, *Tetrahedron* **2013**, *69*, 8943–8951.

[192] D. Kaiser, V. Tona, C. R. Gonçalves, S. Shaaban, A. Oppedisano, N. Maulide, *Angew. Chem. Int. Ed.* **2019**, *58*, 14639–14643.

[193] M. P. Doyle, A. V Kalinin, *J. Org. Chem.* **1996**, *61*, 2179–2184.

[194] Y. Yoshida, Y. Sakakura, N. Aso, S. Okada, Y. Tanabe, *Tetrahedron* **1999**, *55*, 2183–2192.

[195] M. K. Majhail, P. M. Ylioja, M. C. Willis, *Chem. Eur. J.* **2016**, *22*, 7879–7884.

[196] S. P. Chavan, A. B. Pathak, A. N. Dhawane, U. R. Kalkote, *Synth. Commun.* **2007**, *37*, 1503–1510.

[197] E. C. Taylor, B. Liu, *J. Org. Chem.* **2001**, *66*, 3726–3738.

[198] E. Richmond, I. U. Khan, J. Moran, *Chem. Eur. J.* **2016**, *22*, 12274–12277.

[199] S. C. Bergmeier, D. M. Stanchina, *J. Org. Chem.* **1997**, *62*, 4449–4456.

[200] D. J. Weix, D. Markovic, M. Ueda, J. F. Hartwig, *Org. Lett.* **2009**, *11*, 2944–2947.

[201] S. M. Smith, G. L. Hoang, R. Pal, M. O. B. Khaled, L. S. W. Pelter, X. C. Zeng, J. M. Takacs, *Chem. Commun.* **2012**, *48*, 12180–12182.

[202] E. S. M. Persson, J.-E. Backvall, *Acta Chem. Scand.* **1995**, *49*, 899–906.

[203] S. M. Reddy, V. L. Goedken, H. M. Walborsky, *J. Am. Chem. Soc.* **1986**, *108*, 2691–2699.

[204] P. S. M. Amado, L. M. T. Frija, J. A. S. Coelho, P. M. O'Neill, M. L. S. Cristiano, *J. Org. Chem.* **2021**, *86*, 10608–10620.

[205] D. W. Tay, I. T. Tsoi, J. C. Er, G. Y. C. Leung, Y.-Y. Yeung, *Org. Lett.* **2013**, *15*, 1310–1313.

[206] A. Garzan, A. Jaganathan, N. S. Marzijarani, R. Yousefi, D. C. Whitehead, J. E. Jackson, B. Borhan, *Chem. Eur. J.* **2013**, *19*, 9015–9021.

[207] P. A. Horn, R. K. Braun, V. G. Isoppo, J. S. da Costa, D. S. Lüdtke, A. V. Moro, *Adv. Synth. Catal.* **2017**, *359*, 2322–2328.

[208] A. Erkkila, P. M. Pihko, *J. Org. Chem.* **2006**, *71*, 2538–2541.

[209] B. T. Jones, J. Garcia-Carceles, L. Caiger, I. R. Hazelden, R. J. Lewis, T. Langer, J. F. Bower, *J. Am. Chem. Soc.* **2021**, *143*, 15593–15598.

[210] L. Nielsen, T. Skrydstrup, *J. Am. Chem. Soc.* **2008**, *130*, 13145–13151.

[211] B. Weiner, A. Baeza, T. Jerphagnon, B. L. Feringa, *J. Am. Chem. Soc.* **2009**, *131*, 9473–9474.

[212] C. Chen, S. Jin, Z. Zhang, B. Wei, H. Wang, K. Zhang, H. Lv, X. Q. Dong, X. Zhang, *J. Am. Chem. Soc.* **2016**, *138*, 9017–9020.

[213] G. Reginato, F. Gaggini, A. Mordini, M. Valacchi, *Tetrahedron* **2005**, *61*, 6791–6800.

[214] R. D. Connell, T. Rein, B. Åkermark, P. Helquist, *J. Org. Chem.* **1988**, *53*, 3845–3849.

[215] K. J. Schwarz, C. M. Pearson, G. A. Cintron-Rosado, P. Liu, T. N. Snaddon, *Angew. Chem. Int. Ed.* **2018**, *57*, 7800–7803.

[216] S. Domeyer, M. Bjerregaard, H. Johansson, D. S. Pedersen, *Beilstein J. Org. Chem.* **2017**, *13*, 644–647.

[217] D. Alvisi, E. Blart, B. F. Bonini, G. Mazzanti, A. Ricci, P. Zani, *J. Org. Chem.* **1996**, *61*, 7139–7146.

[218] Y. Kitabayashi, S. Yokoshima, To. Fukuyama, *Org. Lett.* **2014**, *16*, 2862–2864.

[219] P. Wollnitzke, S. Essig, J. P. Gölz, K. Von Schwarzenberg, D. Menche, *Org. Lett.* **2020**, *22*, 6344–6348.

[220] C. Thongsornkleeb, R. L. Danheiser, *J. Org. Chem.* **2005**, *70*, 2364–2367.

[221] K. C. Nicolaou, K. Koide, *Tetrahedron Lett.* **1997**, *38*, 3667–3670.

[222] M. Ito, A. Mera, T. Mashimo, T. Seki, S. Karanjit, E. Ohashi, A. Nakayama, K. Kitamura, T. Hamura, H. Ito, et al., *Chem. Eur. J.* **2018**, *24*, 17727–17733.

[223] J. Jia, T. Wu, Y. Fu, Z. Hu, H. Tang, Y. Pan, F. Huang, *Adv. Synth. Catal.* **2022**, *364*, 1873–1878.

[224] S. H. Guo, S. Z. Xing, S. Mao, Y. R. Gao, W. L. Chen, Y. Q. Wang, *Tetrahedron Lett.* **2014**, *55*, 6718–6720.

[225] D. A. Oare, M. A. Henderson, M. A. Sanner, C. H. Heathcock, *J. Org. Chem.* **1990**, *55*, 132–157.